MAR 18 1982

1051-A-11

Y 3. N88: 25/2333/v. 1

NUREG/CR-2333
BNL-NUREG-51458
Vol. 1

COMPLETED

430

ORIGINAL

Nuclear Waste Management Technical Support in the Development of Nuclear Waste Form Criteria for the NRC

Task 1
Waste Package Overview

Prepared by R. Dayal, B. S. Lee, R. J. Wilke, K. J. Swyler,
P. Soo, T. M. Ahn, N. S. McIntyre, E. Veakis

Brookhaven National Laboratory

Prepared for
U.S. Nuclear Regulatory
Commission

I

NOTICE

This report was prepared as an account of work sponsored by an agency of the United States Government. Neither the United States Government nor any agency thereof, or any of their employees, makes any warranty, expressed or implied, or assumes any legal liability of responsibility for any third party's use, or the results of such use, of any information, apparatus, product or process disclosed in this report, or represents that its use by such third party would not infringe privately owned rights.

The views expressed in this report are not necessarily those of the U.S. Nuclear Regulatory Commission.

Availability of Reference Materials Cited in NRC Publications

Most documents cited in NRC publications will be available from one of the following sources:

1. The NRC Public Document Room, 1717 H Street, N.W.
   Washington, DC 20555
2. The NRC/GPO Sales Program, U.S. Nuclear Regulatory Commission,
   Washington, DC 20555
3. The National Technical Information Service, Springfield, VA 22161

Although the listing that follows represents the majority of documents cited in NRC publications, it is not intended to be exhaustive.

Referenced documents available for inspection and copying for a fee from the NRC Public Document Room include NRC correspondence and internal NRC memoranda; NRC Office of Inspection and Enforcement bulletins, circulars, information notices, inspection and investigation notices; Licensee Event Reports; vendor reports and correspondence; Commission papers; and applicant and licensee documents and correspondence.

The following documents in the NUREG series are available for purchase from the NRC/GPO Sales Program: formal NRC staff and contractor reports, NRC-sponsored conference proceedings, and NRC booklets and brochures. Also available are Regulatory Guides, NRC regulations in the *Code of Federal Regulations*, and *Nuclear Regulatory Commission Issuances*.

Documents available from the National Technical Information Service include NUREG series reports and technical reports prepared by other federal agencies and reports prepared by the Atomic Energy Commission, forerunner agency to the Nuclear Regulatory Commission.

Documents available from public and special technical libraries include all open literature items, such as books, journal and periodical articles, and transactions. *Federal Register* notices, federal and state legislation, and congressional reports can usually be obtained from these libraries.

Documents such as theses, dissertations, foreign reports and translations, and non-NRC conference proceedings are available for purchase from the organization sponsoring the publication cited.

Single copies of NRC draft reports are available free upon written request to the Division of Technical Information and Document Control, U.S. Nuclear Regulatory Commission, Washington, DC 20555.

Copies of industry codes and standards used in a substantive manner in the NRC regulatory process are maintained at the NRC Library, 7920 Norfolk Avenue, Bethesda, Maryland, and are available there for reference use by the public. Codes and standards are usually copyrighted and may be purchased from the originating organization or, if they are American National Standards, from the American National Standards Institute, 1430 Broadway, New York, NY 10018.

GPO Printed copy price: $9.50

NUREG/CR-2333
BNL-NUREG-51458
Vol. 1

Nuclear Waste Management Technical Support in the Development of Nuclear Waste Form Criteria for the NRC

Task 1
Waste Package Overview

Manuscript Completed: September 1981
Date Published: February 1982

Prepared by
R. Dayal, B. S. Lee, R. J. Wilke, K. J. Swyler,
P. Soo, T. M. Ahn, N. S. McIntyre, E. Veakis

Department of Nuclear Energy
Brookhaven National Laboratory
Upton, NY 11973

Prepared for
Division of Waste Management
Office of Nuclear Material Safety and Safeguards
U.S. Nuclear Regulatory Commission
Washington, D.C. 20555
NRC FIN A3158

IMPORTANT NOTICE

All references made to the BNL interim reports, "NRC Nuclear Waste Management Technical Support in the Development of Nuclear Waste Form Criteria," Tasks 1-5, should be disregarded. The following references should be inserted in their places, as applicable.

R. Dayal, et al., "Nuclear Waste Management Technical Support in the Development of Nuclear Waste Form Criteria for the NRC, Task 1: Waste Package Overview," NUREG/CR-2333, Vol. 1, BNL-NUREG-51458, February 1982.

G. Bida, et al., "Nuclear Waste Management Technical Support in the Development of Nuclear Waste Form Criteria for the NRC, Task 2: Alternative TRU Technologies," NUREG/CR-2333, Vol. 2, BNL-NUREG-51458, February 1982.

D. Majumdar, et al., "Nuclear Waste Management Technical Support in the Development of Nuclear Waste Form Criteria for the NRC, Task 3: Waste Inventory Review," NUREG/CR-2333, Vol. 3, BNL-NUREG-51458, February 1982.

T.M. Ahn, et al., "Nuclear Waste Management Technical Support in the Development of Nuclear Waste Form Criteria for the NRC, Task 4: Test Development Review," NUREG/CR-2333, Vol. 4, BNL-NUREG-51458, February 1982.

M.S. Davis, "Nuclear Waste Management Technical Support in the Development of Nuclear Waste Form Criteria for the NRC, Task 5: National Waste Package Program," NUREG/CR-2333, Vol. 5, BNL-NUREG-51458, February 1982.

ABSTRACT

In this report we have assessed the current state of waste package development for high level waste, transuranic waste, and spent fuel in the U.S. and abroad. Specifically, we have reviewed recent and on-going research on various waste forms, container materials and backfills and tentatively identified those which are likely to perform most satisfactorily in the repository environment. Radiation effects on the waste package components have been reviewed and the magnitude of these effects has been identified. Areas requiring further research have been identified. The important variables affecting radionuclide release from the waste package have been described and an evaluation of regulatory criteria for high level waste and spent fuel is presented. Finally, for spent fuel, high level, and TRU waste, we have attempted to describe and identify components which could be used to construct a waste package having potential to meet NRC performance requirements.

CONTENTS

ABSTRACT . . . iii
FIGURES . . . ix
TABLES . . . xii
ACKNOWLEDGEMENTS . . . xix
EXECUTIVE SUMMARY . . . xxi

1. INTRODUCTION . . . 1
  1.1 Waste Package Definition . . . 1
  1.2 Functions of Waste Package Components . . . 1
  1.3 Performance Criteria . . . 3
  1.4 References . . . 4

2. EVALUATION OF WASTE FORMS . . . 6
  2.1 Glassy Forms . . . 11
    2.1.1 Borosilicate Glass . . . 11
    2.1.2 Glass Burial Field Experiment . . . 21
    2.1.3 Porous Glass Matrix Composite Glass . . . 23
  2.2 Glass Ceramics . . . 27
  2.3 Crystalline Forms . . . 30
    2.3.1 Supercalcine Ceramic . . . 31
    2.3.2 SYNROC . . . 32
      2.3.2.1 SYNROC Mineralogy and Composition . . . 33
    2.3.3 Titanate Ceramic . . . 40
    2.3.4 High Alumina Ceramic . . . 45
  2.4 Metal Matrices . . . 47
  2.5 Coated Particles . . . 56
  2.6 Comparative Evaluation of Waste Forms . . . 65
    2.6.1 Chemical Durability . . . 65
      2.6.1.1 Borosilicate Glass . . . 65
      2.6.1.2 Porous Glass Matrix . . . 67
      2.6.1.3 Glass Ceramics . . . 68
      2.6.1.4 Crystalline Ceramics . . . 68
        A. SYNROC . . . 71
        B. High Alumina Ceramic . . . 75
      2.6.1.5 Metal Matrices . . . 75
      2.6.1.6 Coated Particles . . . 77
    2.6.2 Thermal Properties . . . 80
      2.6.2.1 Glasses . . . 80
      2.6.2.2 Crystalline Ceramics . . . 85
      2.6.2.3 Metal Matrices and Coated Particles . . . 85
    2.6.3 Mechanical Properties . . . 89
  2.7 TRU Waste Forms . . . 94
  2.8 Spent Fuel as a Waste Form . . . 95
    2.8.1 Degradation of Spent Fuel Cladding . . . 95
    2.8.2 Cracking of Fuel Pellets . . . 95
    2.8.3 Fission Gas Release . . . 95
    2.8.4 Leaching Studies . . . 95
      2.8.4.1 Spent Fuel Leaching . . . 95
      2.8.4.2 Dissolution Studies of UO_2 . . . 96
      2.8.4.3 Electrochemical Studies . . . 99

CONTENTS, Continued

2.9 Conclusions for HLW Forms 101
2.10 Recommendations for HLW Forms 106
2.11 Conclusions for TRU Waste Forms 110
2.12 Recommendations for TRU Waste Forms 111
2.13 Conclusions and Recommendations for Spent Fuel. 112
2.14 References. 112

3. EVALUATION OF CONTAINER MATERIALS 122
3.1 Introduction. 122
3.2 Candidate Metallic Container Materials. 122
3.3 Temperature of Containers 124
3.4 Corrosion of Metallic Container Materials 124
  3.4.1 Corrosion Before Flooding. 125
    3.4.1.1 Bedded Salt Repository. 125
    3.4.1.2 Clay Repository 130
  3.4.2 Corrosion After Flooding 130
    3.4.2.1 Groundwater Chemistry 130
    3.4.2.2 General Corrosion 135
      A. Bedded Salt Repository. 135
      B. Basalt Repository 140
      C. Clay Repository 148
      D. Granite Repository. 153
      E. Summary 153
    3.4.2.3 Pitting Corrosion 154
      A. Stainless Steels. 154
      B. Copper. 158
      C. Titanium and Its Alloys 160
      D. Lead. 163
      E. Nickel Alloys 163
    3.4.2.4 Crevice Corrosion 163
      A. Stainless Steel 163
      B. Titanium and Its Alloys 164
      C. Lead. 167
      D. Copper. 167
      E. Nickel Alloys 167
    3.4.2.5 Stress Corrosion Cracking (SCC) 167
      A. Stainless Steel 169
      B. Copper and Copper Alloys. 173
      C. Titanium and Zirconium Alloys 175
      D. High Nickel Alloys. 178
      E. Lead. 181
      F. Stress Corrosion Cracking in Non-Chloride Environments 182
    3.4.2.6 Hydrogen Effects. 182
3.5 Assessment of Container Durability from Archeological Data. . 186
3.6 Non-Metallic Materials. 188
3.7 Strength and Ductility Requirements for Containers. 189
3.8 Weldability and Fabricability of Containers 189
3.9 Conclusions 190

CONTENTS, Continued

3.10 Recommendations 191
3.11 References. 193

4. EVALUATION OF BACKFILL MATERIALS. 201
4.1 Backfill Purposes and Properties. 201
4.2 Candidate Backfill Materials. 203
4.3 Backfill Evaluation 207
4.3.1 Swelling Properties and Permeability 207
4.3.2 Thermal Conductivity and Stability 211
4.3.3 Backfill Sorptive Properties 215
4.3.4 Radionuclide Diffusivity and Retention 224
4.4 Conclusions 230
4.5 Recommendations 231
4.6 References. 233

5. RADIATION EFFECTS ON WASTE PACKAGE COMPONENTS 237
5.1 General Considerations. 237
5.2 Radiation Effects in Waste Forms. 241
5.2.1 Glassy Waste Forms 241
5.2.1.1 Swelling. 243
5.2.1.2 Leach Resistance. 246
5.2.1.3 Helium Buildup. 250
5.2.1.4 Stored Energy 252
5.2.1.5 Transmutations. 252
5.2.1.6 Other Effects 254
5.2.2 Crystalline Waste Forms. 254
5.2.2.1 Metamictization 254
5.2.2.2 Swelling. 258
5.2.2.3 Leach Resistance. 262
5.2.2.4 Helium Buildup. 262
5.2.2.5 Transmutations. 262
5.2.2.6 Other Effects 263
5.2.3 Glass-Ceramic Waste Forms. 263
5.2.4 Multibarrier Waste Forms 264
5.2.4.1 Radiation Effects on Coating Materials. 264
5.2.5 TRU Waste Forms. 265
5.2.5.1 Traditional Waste Forms 265
5.2.5.2 Newly Developed Waste Forms 267
5.2.6 Spent Fuel 267
5.2.6.1 Radiation Effects in Fuel Pellets 267
5.2.6.2 Radiation Effects on the Cladding 268
5.3 Radiation Effects on Waste Containers 268
5.3.1 Displacement Damage. 268
5.3.2 Radiolysis 269
5.3.2.1 Radiation Corrosion 271
5.3.2.2 Hydrogen Embrittlement. 273
5.3.3 Other Effects. 273
5.4 Radiation Effects on Overpack Materials 274
5.5 Radiation Effects on Geomedia 276

CONTENTS, Continued

5.5.1 Rock Salt 276
5.5.1.1 Radiation Damage Formation 276
5.5.1.2 Effects on Materials Properties 277
5.5.2 Other Host Rocks 278
5.6 Summary and Conclusion 278
5.6.1 Radiation Durability of Waste Forms 279
5.6.2 Radiation Durability of Containers 281
5.6.3 Radiation Durability of Backfill 282
5.6.4 Performance Assessment 282
5.6.5 Outstanding Questions and Recommendations for Further Study 284
5.6.6 Conclusions 287
5.7 References 287

6. IDENTIFICATION OF VARIABLES AFFECTING RADIONUCLIDE RELEASE FROM THE WASTE PACKAGE 297
6.1 Waste Package Components 297
6.1.1 Waste Form 297
6.1.2 Container 299
6.1.3 Backfill 300
6.1.4 Waste Package 301
6.2 Repository Conditions 302
6.2.1 Repository Thermal Environment 302
6.2.2 Basalt Repository 303
6.2.3 Groundwater Flow Rates 303
6.2.4 Groundwater Chemistry 304
6.3 References 306

7. EVALUATION OF REGULATORY CRITERIA FOR HIGH LEVEL WASTE, SPENT FUEL, AND TRU WASTE 308
7.1 Containment of Radionuclides for a Specific Time Period . . . 308
7.2 Controlled Release of Radionuclides 309
7.3 Retrievability of Waste 313
7.4 Conclusions 314
7.5 Recommendations 314
7.6 References 315

8. REASONABLY ACHIEVABLE WASTE PACKAGES 316
8.1 Waste Forms 316
8.2 Containers 317
8.3 Overpack/Backfill Systems 318
8.4 Achievable Limits for Engineered Barriers 319
8.5 Retrievability of Waste 319
8.6 Conclusions 320
8.7 References 321

APPENDIX A A1
APPENDIX B B1

FIGURES

1.1 Stylized high level waste package configuration 2

2.1 Comparison of leach rates: (a) Leach Rates of Alkali and Alkaline-Earth Elements from Various Waste Products; (b) Leach Rates of Rare Earths and Actinide Elements from Various Waste Products 9

2.2 Canadian waste glass laboratory test and field burial results . . 22

2.3 Porous glass matrix process: (a) High Silica Glass Process, (b) Schematic Representation of Porous Glass Matrix Process 24

2.4 Phase diagrams depicting the stability fields of titanate phases in SYNROC 37

2.5 Leach rates of SYNROC and borosilicate glass. 43

2.6 Leach rates of PyC coated gel-derived ceramic particles 64

2.7 Cumulative silicon released versus time at 90°C 66

2.8 Cumulative quantities of cesium and strontium leached from SYNROC and borosilicate glasses. 73

2.9 Effect of temperature on initial leach rate of SYNROC and borosilicate glass (PNL 73-2) containing 10 Wt. % simulated radwaste. 74

2.10 Stability fields of sphene, perovskite, and rutile in terms of H^+, Ca^{2+} and silica activities. 76

2.11 Heat generated from a typical in-canister borosilicate glass having a waste loading of 25% by weight. Dimensions of glass cylinders are 300 cm (length) x 30 cm (diameter) 81

2.12 Long-term cesium leach rates of glasses PNL 77-107 and 77-260 as a function of temperature for a 2-month heat treatment 82

2.13 Long-term cesium leach rates of glasses PNL 72-68 and 76-68 as a function of temperature for a 2-month heat treatment 83

2.14 Leach rate of phosphate glass increases as heat treatment causes devitrification. 83

2.15 Ingrowth of Zn_2SiO_4 and $SrMoO_4$ as a function of temperature for glass PNL 72-68 heat-treated for 2 months 84

FIGURES, Continued

2.16 Glass leach rate as a function of heat treatment and temperature holding time for borosilicate glass IPM PW-4m: there is little change in leach rate as heat treatment devitrifies this borosilicate glass 84

2.17 Temperature difference between centerline and wall of cylindrical glass blocks and vitromets of equal heat generation per metal length as a function of time after reactor discharge. 86

2.18 Cs^+ retention in tailored ceramic nuclear waste forms 88

2.19 Canister centerline temperatures for CVD-coated supercalcine in various matrices 90

2.20 Leach rate of 28,000 MWd/MTU spent fuel in deionized water at 25°C based on selected elements. 97

2.21 Oxidation and dissolution mechanisms for a UO_2 surface. 100

3.1 Calculated temperature profiles for a salt repository 125

3.2 Potential/pH diagram for iron in chloride solutions (10^{-2}-10^{-3} mol Cl) at room temperature. 156

3.3 Effect of chloride concentration on pit initiation in tables 316L and 317L stainless steel and hastelloy G 159

3.4 Copper pit in cold brussels water 159

3.5 Influence of temperature, chloride content and pH value on crevice corrosion and pitting of unalloyed titanium. . . 161

3.6 Effect of temperature on pitting potential of CP titanium in 0.6 to 1 M halide solutions 162

3.7 Crevice corrosion of TiCode-12 (Ti-0.3 Mo-0.8 Ni) and pure Ti (Grade 2) in saturated NaCl solution. 165

3.8 Swedish lead-titanium canister design 168

3.9 Effect of temperature and chloride level on the time-for-cracking of type 304 stainless steel in aqueous NaCl solution . . 170

3.10 Relationship between chloride and oxygen content of alkaline-phosphate treated boiler water, and susceptibility to stress corrosion of austenitic stainless steel exposed to the steam phase with intermittent wetting. . . . 171

FIGURES, Continued

3.11 Onset of sensitization in 18-8 stainless steels as a function of carbon as determined by the strauss test 174

3.12 Effect of increasing the nickel content on the susceptibility of Fe-Cr-Ni wires in boiling 42% $MgCl_2$ 180

3.13 Schematic illustration showing the mechanism of hydrogen blistering. 184

3.14 Delayed fracture times and minimum stress for cracking of 0.4% C steel as a function of hydrogen content. . . . 184

4.1 Swelling pressure as a function of bulk density for sodium bentonite at 100% saturation 209

4.2 Range of empirically derived coefficients of permeability of sodium bentonite as a function of bulk density 209

4.3 The influence of various cations upon the swelling volume of montmorillonite clay 210

4.4 The thermal conductivity of an 85% graded silica-15% illite backfill as a function of moisture content. . . 213

4.5 Gel strength as a function of the number of wet/dry cycles for montmorillonitic clays 216

5.1 Volume changes in glass 244

5.2 Effect of gamma radiation on glass density 245

5.3 Effect of dose rate on stored energy in ^{244}Cm-doped PNL 72-68 HLW glass 253

5.4 Effects of internal alpha decay on various crystal structures 257

7.1 Radionuclide composition of SRP waste 310

7.2 Radioactive decay of PWR spent fuel 311

TABLES

1.1 Package Component Functions of a Stylized Waste Package Concept for HLW 3

2.1 Candidate High Level Waste Forms. 6

2.2 Major U.S. High Level Waste Form Developers 7

2.3 Comparison of Defense and Commercial High Level Waste 10

2.4 Composition of the Most Representative Borosilicate Waste Glass 13

2.5 Leach Rates of the Most Representative Borosilicate Waste Glasses in the Temperature Range of 70°C to 150°C 14

2.6 Leach Rates of the Most Representative Borosilicate Waste Glasses at Room Temperature. 18

2.7 Leach Rates of Typical Borosilicate Waste Glasses Under Hydrothermal Conditions 19

2.8 PGM Glass Analysis. 25

2.9 Comparison of Leach Rates of Glass at 70°C. 26

2.10 Silica Saturation Levels at Low Flow Rates. 26

2.11 Composition of Phosphate and Borosilicate Glasses and Glass Ceramics 28

2.12 Compositions and Crystal Phases of PNC Glass Ceramics 29

2.13 Leach Resistance of Basalt Glass Ceramic in Deionized Water at 90°C. 30

2.14 Primary Containment Phases in Current Supercalcine-Ceramics . . . 32

2.15 Overview of Current SYNROC Research 33

2.16 Typical SYNROC Compositions for B and C Formulations. 35

2.17 Summary of Distribution of Radwaste Elements Among SYNROC B Phases 36

2.18 Microprobe Analysis of SYNROC C (Weight Percent). 36

2.19 Distribution of Principal HLW Elements Between Coexisting Phases of SYNROC-D (Electron Probe Microanalysis). . . 38

TABLES, Continued

2.20 Microprobe Analysis of SYNROC D (Weight Percent). 39

2.21 Composition of SYNROC Waste, Matrix, and Product. 41

2.22 Lawrence Livermore Laboratory SYNROC-C and D Leach Rates. 42

2.23 ORNL Sol-Gel Particle Leach Rates 42

2.24 Primary Containment Phases Identified in Sandia Titanate-Ceramics. 44

2.25 Mineralogy and Waste Element Distribution 46

2.26 Tailored Ceramic Formulations for SRP Waste Compositions. 47

2.27 Leach Rates of High Alumina Ceramic and 76-68 Glass 48

2.28 Dissolution Rates of Individual Phases in High Alumina Ceramic 48

2.29 Laboratory Scale Matrix Test Sample Configuration 50

2.30 Phase Characterization Data for Matrix Waste Forms. 51

2.31 Radionuclide Containment for Matrix Waste Forms 52

2.32 Multibarrier Waste Form Development One Liter Demonstration 52

2.33 Process Related Cermet Characteristics. 52

2.34 Typical Cermet Property Ranges. 53

2.35 Matrix Encapsulated Waste Form Leach Rates. 54

2.36 Estimated Matrix Material Corrosion Rates from Composite Leach Tests. 55

2.37 Thermal Conductivity of Matrix Waste Forms. 55

2.38 Coatings Applied in Fluidized Bed to Particles in the 200 μm Range. 57

2.39 Duplex Coatings Applied in a Fluidized Bed to Particles in the 200 μm Range 57

2.40 Conditions for PyC and Al_2O_3 Coating of Supercalcine. 58

TABLES, Continued

2.41 Typical Kernel Diameters and Coating Thicknesses. 60

2.42 Leach Test Results for Coated and Uncoated Particles. 61

2.43 Leach Rates of Uncoated and Coated Supercalcine Pellets and Glass Marbles 62

2.44 Corrosion Rates of Metal Coatings 63

2.45 Fractional Waste Material Loss at 70°C. 67

2.46 Reactivity of Waste Forms in Silicate Groundwater 69

2.47 Hydrothermal Reactivity Trends in Bittern Brine 69

2.48 Hydrothermal Stability Tests on Crystalline Waste Forms 70

2.49 Matrix Alteration and Cs Solubility After Leaching of Copper Borosilicate Glass, Supercalcine, and Titanate Ceramic . . 72

2.50 Corrosion Rates of Lead Alloys in Dry ASSE Salt and an Aqueous Solution Saturated with the ASSE Salt. 78

2.51 Leaching Behavior of Coated Supercalcine Multibarrier Waste Forms 79

2.52 Summary of Some Important Thermophysical Properties of SYNROC 87

2.53 Thermal Properties of Glass and Supercalcine in Various Matrices. 91

2.54 Impact Data 92

2.55 Mechanical Impact Behavior of Metal Matrix Forms. 93

2.56 Tensile Strength for Various Waste Forms. 93

2.57 UO_2 Matrix Dissolution Rates. 98

3.1 Candidate HLW Package Materials 123

3.2 Repository Isolation Environments for High Level Waste. 126

3.3 Nominal Compositions of Alloys Used in Salt Exposure Studies. . . 128

3.4 Corrosion of Various Metals Under Conditions Simulating Salt Mine Storage of Fixed Wastes 129

TABLES, Continued

3.5 Compositions of Seawater (Sea Bed) and Brine (WIPP) 131

3.6 Shale Groundwater Chemistry 132

3.7 Flood Basalt Groundwater Chemistry. 132

3.8 Groundwater Chemistry of Jackass Flats Tuffs. 133

3.9 Groundwater Chemistry of Sierra Nevada Granite. 133

3.10 Groundwater Chemistry of Swedish Granite. 134

3.11 Maximum Corrosion Rates and Macroscopic Appearance of Materials Tested in Salton Sea Brine. 136

3.12 Nominal Chemical Composition of U.S. Candidate Canister Materials. 137

3.13 Corrosion Rates of U.S. Candidate Alloys in Deoxygenated Solutions. 138

3.14 Corrosion Rates of U.S. Candidate Alloys in Oxygenated Solutions. 138

3.15 Effect of Temperature on the Uniform Corrosion Rate of Titanium Alloys in Deoxygenated Brine A 139

3.16 Effect of Dissloved Oxygen on the Uniform Corrosion Rate of Titanium Alloys at 250°C. 139

3.17 Environmental Specifications. 141

3.18 Corrosion Rates for Titanium in Environment 1; Baltic Sea Water with 10 ppm F^-, pH 4.5, 8 ppm O_2 142

3.19 Corrosion Rates for Titanium Environment 2; Baltic Sea Water with 10 ppm F^-, pH 4.5, Less than 0.01 ppm O_2 143

3.20 Brine Solution Composition. 144

3.21 Corrosion of Samples in $MgCl_2$-NaCl Brine at 250°C 145

3.22 Synthetic Hanford Groundwater Formulations. 146

3.23 Corrosion of Samples in Simulated Hanford Groundwater at 250°C. 147

3.24 Simulated Grande Ronde Basalt Groundwater 149

TABLES, Continued

3.25 Weight Change of 250°C Screening Corrosion Test Specimens 149

3.26 Analysis of Groundwater Used in Corrosion Tests 150

3.27 Corrosion of Candidate Container Materials in Groundwater as a Function of Temperature and Time. 151

3.28 Estimated Thickness Changes (cm) of Lead Alloys After Exposure to Different Environments at 49°C for 1000 Years 152

3.29 Estimated Thickness Changes of Metals After 1000 Years at 250°C. 155

3.30 Pitting in Stainless Steels After Eight Years' Immersion in Seawater 157

3.31 Pitting in Stainless Steels After Eight Years' Exposure to a Sea Shore Atmosphere. 157

3.32 Results of Controlled Potential Crevice Corrosion Test in 1 N NaCl Cell on Ferritic Stainless Steels. . . 164

3.33 Titanium Crevice Specimens Exposed in Hanford Groundwater at 250°C 166

3.34 Effect of Seawater on the Fracture Strength of Titanium and Some Alloys. 176

3.35 Classification of Titanium Alloys Susceptible to Stress Corrosion Cracking in Seawater. 176

3.36 Fracture Characteristics of Titanium and Titanium-5 Al-2.5 Sn Alloy in Various Chloride Media at Room Temperature . . 177

3.37 Nominal Chemical Compositions of Titanium Alloys in Sandia Container Corrosion Program. 178

3.38 Effect of Alcohol/Chloride Environment on the Stress Corrosion Cracking of Titanium and Zirconium After Stressing for 470 h at Room Temperature 179

3.39 Results of Chloride Stress Corrosion Tests for Materials with Different Nickel Contents. 181

3.40 General Mechanisms of Hydrogen-Enhanced Cracking of Metals (Modified from Fidelle, Brouduer and Clauss). 185

3.41 Examples of Metal Archeological Artifacts 187

TABLES, Continued

4.1 The Functions and Properties of Backfill Materials. 202

4.2 Candidate Backfill Materials. 204

4.3 Cation Exchange Capacities of Some Clay Minerals and Zeolites. 205

4.4 Some Proposed Backfill Designs. 208

4.5 The Thermal Conductivity of Candidate Buffer/Backfills. 212

4.6 Effect of Hydrothermal Treatment on Cesium Sorption by Candidate Overpack Materials. 214

4.7 Variables Influencing Distribution Coefficients 217

4.8 K_d Values for Secondary Smectite in Basaltic Groundwater at 600°C. 218

4.9 Fraction of Radiotracers Sorbed on Various Sulfides 220

4.10 Sorption Characteristics of Potential Backfill Components for Salt Repositories 221

4.11 Sorption Characteristics of Various Minerals for Several Fission Product Ions 222

4.12 Sorption Characteristics of Various Mineral Mixtures for Certain Fission Product Ions 223

4.13 Experimentally Determined Diffusivities of Various Dissolved Species in Backfill. 225

4.14 Radionuclide Retardation Factors and Retention Times for One-Meter Thick Backfill Barriers 226

4.15 Calculated Retention Times for Various Backfill Compositions Assuming Diffusion Controlled Transport . . 228

4.16 Estimated Radionuclide Retention Times in One-Meter Thick Backfill Bed. 229

5.1 Radiation Environment in HLW Waste Glass. 238

5.2 Cumulative Alpha-Decay Dose in Glasses and SYNROC 242

5.3 Leach Rates for Some Glasses Doped with Alpha Emitters. 247

5.4 Sensitivity of Various Glasses to Alpha-Recoil Aging as Simulated by Ion-Implantation 248

TABLES, Continued

5.5 Dosimetry Equivalence Between External Ion Bombardment and Internal Alpha Decay. 248

5.6 Fractional Leach Rates for Glass and Supercalcine Without Gamma-Irradiation. 249

5.7 Effect of Gamma Irradiation on Glass Leaching 251

5.8 Saturation Behavior in Stored Energy Buildup. 253

5.9 Structural Damage in Ceramics for Internal Alpha Decay and Internal Fission 256

5.10 Inorganic Solids in Which Internal Radiolysis is Known to Occur 259

5.11 Density Changes in Neutron Irradiated SYNROC and SYNROC Minerals 261

5.12 Radiation Conditions in TRU Waste Forms 266

5.13 Shielding Properties of Waste Canister Materials. 269

5.14 External Radiation Conditions for Glass Waste Forms 270

5.15 Summary of Conclusions Regarding Identities of Species Appearing Around a Waste Can and Regarding Maximum Rate of Appearance. 272

5.16 Radiation Effects in Inorganic Ion-Exchange Media 275

5.17 Effect of Radiation on the Yield Strength of Rock Salt. 278

6.1 Thermal Characteristics of Reference Repositories 302

6.2 Reference Peak Near Field Temperatures (°C) 303

6.3 Basalt Repository Conditions. 304

6.4 Hydrologic Parameters for Host Rock Types (Based on Generic Stratigraphic Sections) 305

7.1 Relationship Between Release Time and Total Releases From the Engineering Repository. 312

ACKNOWLEDGEMENTS

The authors are grateful to their scientific colleagues for providing information, both published and unpublished, and stimulating discussions. They also wish to acknowledge the help and comments of the Nuclear Waste Management Division staff in preparing this report. We are particularily indebted to Katherine Becker, Cheryll Christie, Sharon Moore, Grace Searles, and Cathy Van Noy, for their skill and patience in the typing and preparation of this report.

EXECUTIVE SUMMARY

In this final report we present an assessment of the current state of waste package development for high level waste, transuranic waste, and spent fuel in the U.S. and abroad. The evaluation is based on a review of recent and ongoing research and development efforts on the principal components of the waste package. The main objective of the report is to identify for the NRC the types of information on the waste package which will be required for licensing.

In the evaluation of the waste package, the package components which are likely to perform most satisfactorily in the repository environment are identified. A description of the various high level waste forms, transuranic waste forms, and spent fuel is presented, followed by a comparative evaluation based on their chemical, physical, and mechanical properties. The potential contribution of the waste form to the performance of both the waste package and the engineered system is considered. For this purpose, the candidate waste forms are evaluated in terms of the 1000-year containment and the one part in 10^5 annual controlled release criteria. Waste forms that have the potential to meet the performance objectives are discussed. Areas requiring further research on waste form development have been identified.

The container evaluation consists of an in-depth analysis of corrosion data for various candidate materials. A discussion of corrosion resistant materials that have the potential to last for 1000 years under repository conditions is presented. Detailed recommendations for further corrosion research on candidate container materials are given.

A section on backfill evaluation and performance is also given. Both discrete and non-discrete backfills are considered and evaluated in terms of the 1000-year and the one part in 10^5 annual controlled release criteria for the waste package and the engineered system, respectively. The feasibility of using highly sorptive synthetic materials such as zeolites as backfill in a HLW repository has also been evaluated. The evaluation is presented in Appendix A of the report.

Effects of radiation on the properties of candidate waste package components have been identified and discussed. Emphasis is placed on the properties which most directly affect the ability of the waste package to retain radionuclides. Outstanding questions and recommendations for further study are discussed.

Many variables exist within the waste package/repository environment and some are critically important in determining whether the NRC performance objectives can be met. A short discussion is given on the principal variables which must be well understood in order to limit radionuclide release from a waste package or an engineered system.

The applicability and usefulness of the NRC performance requirements on the waste package and engineered system are evaluated. Based on our evaluation, the NRC performance objectives are reasonable and defensible as interim criteria.

Finally, for spent fuel, high level, and TRU wastes, we have attempted to describe and identify components which could be used to construct a waste package having optimum potential to meet NRC performance requirements.

1. INTRODUCTION

The proposed strategy adopted by the Nuclear Regulatory Commission (NRC) for regulating and licensing the disposal of high level radioactive wastes in geologic repositories involves a conservative multibarrier approach. The principal barrier in such a repository is the waste package, emplaced in an engineered repository structure which, in turn, is surrounded by the geologic site and its environs.

The purpose of this report is to assess the current state of waste package development for high level waste, transuranic waste, and spent fuel in the U.S. and abroad. Specifically, we have reviewed recent and on-going research on various waste forms, container materials and backfills and tentatively identified those which are likely to perform most satisfactorily in the repository environment. Radiation effects on the waste package components have been reviewed and the magnitude of these effects has been identified. Areas requiring further research have been identified. The important variables affecting radionuclide release from the waste package have been identified and an evaluation of regulatory criteria for high level waste and spent fuel is presented. Finally, for spent fuel, high level, and TRU waste, we have attempted to describe and identify components which could be used to construct a waste package having potential to meet NRC performance requirements.

1.1 Waste Package Definition

As outlined in the National Waste Terminal Storage (NWTS) Waste Package Program Plan,[1] the waste package is defined to "include everything that will be placed into the host rock, from the waste form to the boundary of the emplacement region. It includes any tailored emplacement hole backfill, but excludes the natural host rock itself." Figure 1.1 depicts a conceptual waste package for high level waste.[1]

In contrast to the DOE definition of the waste package described above, the NRC waste package consists of the solid waste form, its container and any ancillary enclosures, including its shielding, packaging, and overpack.[2] The most recent NRC definition considers discrete backfill an integral part of the waste package.[3] Since backfill as a barrier appears to have a great potential in contributing to the overall performance of the waste package, we have included a section on backfill evaluation and performance in this report.

1.2 Functions of Waste Package Components

The purpose of the waste package is to provide radionuclide containment in the repository, provide for the safe handling of waste at the repository and

BEST DOCUMENT AVAILABLE

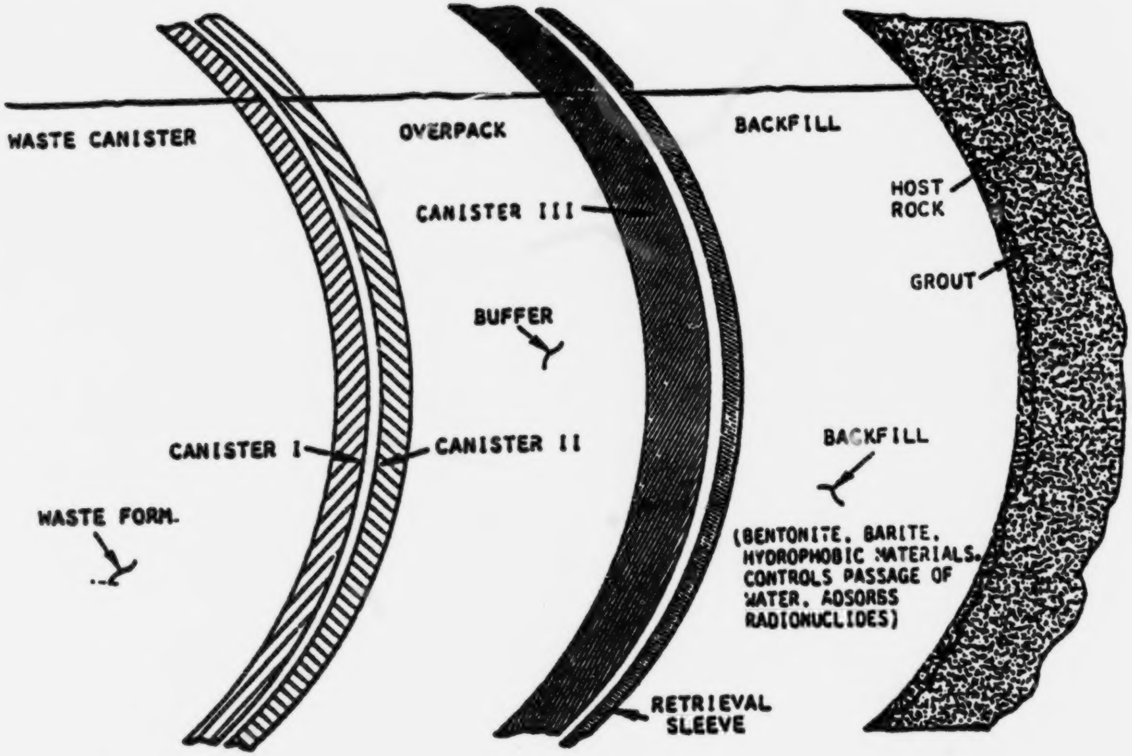
WASTE CANISTER
OVERPACK
BACKFILL
HOST ROCK
CANISTER III
GROUT
BUFFER
CANISTER I
CANISTER II
BACKFILL
WASTE FORM
(BENTONITE, BARITE, HYDROPHOBIC MATERIALS. CONTROLS PASSAGE OF WATER, ADSORBS RADIONUCLIDES)
RETRIEVAL SLEEVE

Figure 1.1 Stylized high level waste package configuration.[1]

during transportation, and preserve the ability to retrieve the waste safely throughout the retrieval period. Specific functions of the primary components of a waste package for high level waste, as described in the NWTS Waste Package Program Plan,[1] are outlined in Table 1.1.

Table 1.1[1]

Package Component Functions of a Stylized
Waste Package Concept for HLW

Component	Functions
Waste Form	Immobilizies the radioactive materials, resists leaching, powdering, cracking, and other modes of degradation
Canister	Contains the waste form during production, sealing, handling and retrieval, and serves as a transport vessel; serves as a barrier against waste form leaching and nuclide migration
Overpack	Applied as a second canister, it provides a radionuclide release barrier, in the event the integrity of the first canister is suspect; provides additional corrosion or structural resistance, or additional radiation shielding, if required
Sleeve	Acts as a hole liner into which the (overpacked) canister is to be placed to ease canister retrievability, provides structural support and, potentially, corrosion resistance
Backfill	Placed into the emplacement hole around the (overpacked) canister; acts as a sorptive medium, heat transfer agent, and plastic stress adjustment medium; it may contain oxygen-getters or chemical conditioning agents; it includes a migration retardant

1.3 Performance Criteria

The four main performance criteria for high level waste, spent fuel, and TRU waste specified by the NRC in 10 CFR 60* are outlined below:[2]

---

*The proposed rule (published in the Federal Register, July 8, 1981[3]) includes some changes from the May 13, 1980 draft[2] (referenced during preparation of the report) in definition of the waste package and the statement of the performance objectives.

(a) For the waste package there shall be containment of all radionuclides for the first 1000 years after decommissioning of the geologic repository operations area and as long thereafter as is reasonably achievable, assuming expected events and processes and that some of the waste dissolves soon after decommissioning.

(b) Starting 1000 years after decommissioning of the geologic repository operations area, the radionuclides present in HLW will be released from the underground facility at an annual rate that is as low as reasonably achievable and is in no case greater than an annual rate of one part in one hundred thousand of the total activity present in HLW within the underground facility 1000 years after decommissioning, assuming expected processes and events.

(c) Starting at decommissioning radionuclides present in TRU waste will be released at a rate that is as low as reasonably achievable and is in no case greater than one part in one hundred thousand of the total activity present in TRU waste within the underground facility, assuming expected processes and events.

(d) The repository area shall be designed so that radioactive waste stored there can be retrieved for a period of 50 years after termination of waste emplacement operations, if the geologic repository operations area has not been decommissioned. If during this period a decision is made to retrieve the wastes the Department shall insure that wastes could be retrieved in compliance with 10 CFR (Part 20) and in about the same period of time as that during which they were emplaced.

The 1000 year zero release criterion is designed to contain fission products species, such as Cs and Sr, which decay by beta/gamma processes and effectively become extinct as dangerous radionuclides after about 600 years. Any waste form or canister which can limit fission product migration from the waste package to near zero for 1000 years will, therefore, prevent hazard to the public from this type of radioactivity.

Actinide elements and the long-lived fission products, on the other hand, lose their radioactivity extremely slowly and remain hazardous for times of tens of millions of years. Any waste form or waste package which can provide regulated release of radioactivity sufficiently slow that the annual release does not exceed 10^{-5}/yr will, therefore, pose no health hazard to the biosphere.

1.4 References

1. NWTS Waste Package Program Plan, Vol 1, ONWI-96, 1980.

2. Code of Federal Regulations, 10 CFR 60, Technical Criteria for Regulating Geological Disposal of High Level Radioactive Waste. Advance notice of proposed rule making, May 13, 1980.

3. Code of Federal Regulations, 10 CFR 60, Technical Criteria for Regulating Geological Disposal of High Level Radioactive Waste. Advance notice of proposed rule making, July 8, 1981.

2.0 EVALUATION OF WASTE FORMS

The waste form represents the innermost and one of the potentially most effective barriers of the waste package system as well as the underground facility. Various waste form options for the immobilization of commercial and defense high level wastes are being considered in the U.S. and abroad (Table 2.1).[1] Currently, the major waste form research and development efforts are centered on glass. Borosilicate glass has been adopted by most foreign national programs involved in HLW immobilization research as the reference HLW form. In addition to the development of glass as a potential waste form, the U.S. is actively involved in the development and characterization of alternate waste forms such as crystalline ceramics, porous glass matrix, metal matrices, coated particles, etc. A list of the major participants involved in the U.S. High Level Waste Form development is given in Table 2.2.[2]

Table 2.1

Candidate High Level Waste Forms*

Category	Waste Form
Glass	Borosilicate Aluminosilicate Porous glass matrix
Glass Ceramics	Celsian glass ceramic Recrystallized fusion melts Basalt glass ceramic
Ceramics	Supercalcine Sandia titanate High alumina SYNROC
Coatings	Pyrolytic carbon Al_2O_3 SiC Nickel Glass
Metal Matrix	Glass marbles in metal matrix Sintered ceramic cores in metal matrix Cermets Coated glass marbles in metal matrix Coated ceramic cores in metal matrix

*Adapted from Rusin[1]

Table 2.2

Major U.S. High Level Waste Form Developers*

Waste Form	Developer
Glass Ceramics	PNL, Rockwell
Porous Glass Matrix	Catholic Univ.
Borosilicate Glass	PNL, SRL
Supercalcine Ceramic	Rockwell, PSU
SYNROC	LLL, ANL
Titanate Ion Exchangers	Sandia
Supercalcine Coating and Matrices	PNL
Glass-Marble/Metal Matrices	ANL, PNL
Cermets	ORNL
Coated Particles	ORNL, PNL
High Alumina Ceramic	Rockwell, PSU

*Adapted from Crandall[2]

Regulatory criteria, outlining the waste form requirements established by the NRC, are as follows:[3]

(1) Solidification. All liquid radioactive wastes must have been converted to a dry solid and placed in a sealed container before transfer to the repository.

(2) Stabilization. Finely divided waste forms must have been stabilized (for example, by incorporation into an encapsulating matrix) to limit the production and availability of respirable fines during any accident condition to a level as low as is reasonably achievable.

(3) Free Liquids. The waste package must contain no free liquids.

(4) Combustibles. All combustible radioactive waste must have been reduced to a noncombustible form unless the associated packaging is such that a fire involving a single package will not

i. Compromise the integrity of other packages,

ii. Result in radiation exposures or releases of radioactive materials in excess of permissible levels, and

iii. Adversely affect any safety related structures, systems, or components.

(5) Explosive, pyrophoric, and toxic materals. The Department shall insure that there are no explosive or pyrophoric materials in the radioactive waste, nor are there chemically toxic wastes that could compromise either the operation or performance of the repository or adversely affect operator safety.

Based on the requirements outlined above, the waste form should exhibit low dispersibility and good impact resistance in accident situations during transport and storage. In addition, radionuclide volatility should be low in the event of fires.

At this time, the NRC 1000-yr containment and controlled release criteria apply to the waste package and the underground facility, respectively.[3] There is no specific radionuclide release criterion on the waste form. However, since the waste form is a component of and represents the source term for both the waste package and the underground facility, it is important to evaluate its potential contribution to the performance of the waste package and the underground facility. For this purpose, we have attempted to evaluate the potential waste forms in terms of the NRC 1000-yr containment and 10^{-5}/yr controlled release criteria and, thereafter, identify those that are likely to meet these performance objectives.

It should be mentioned, however, that for the actinides and the rare earths, differences in leach rates for the various waste forms do not appear to be significant (Figure 2.1)[4]. In contrast, the leach rates expressed in terms of the alkali and alkaline earths for the same waste forms do exhibit significant differences (Figure 2.1)[4]. It appears that the lack of variation in the leach rates observed for the actinide and rare earth elements is due to the known solubility constraints on their chemical behavior. Considering that the actinides predominate during the post-1000-year containment period, we believe that their release will be determined by their solubility behavior rather than the rate of waste form dissolution. Therefore, actinide release may not be continuous and controlled over a period of time but episodic, primarily determined by a shift in local saturation equilibrium resulting from changing repository conditions. Considering these factors, the validity of evaluating the 10^{-5}/yr actinide-controlled release criterion using mainly fission product or rare earth or actinide leach rates based on short-term laboratory experiments is open to question.

In this review, both commercial and high level defense waste forms have been covered. A comparison of commercial and defense high level waste in terms of heat output and radionuclide content is given in Table 2.3.[5] It is important to point out that commercial HLW has a higher content of fission products and actinides, resulting in a greater heat output per canister. Among the HLW, the SRP wastes have the highest content of fission products and actinides. In addition, the SRP wastes contain high concentrations of non-radioactive contaminants such as iron and aluminum.

In the sections below, we present a description of the various high level waste forms, TRU waste forms, and spent fuel, and a discussion of their properties, followed by a comparative evaluation based on their chemical, physical, and mechanical properties. The comparative evaluation of the various waste forms was attempted to identify those waste forms that have the potential to meet the NRC criteria independently. The major conclusions and recommendations for further research are presented in the following sections.

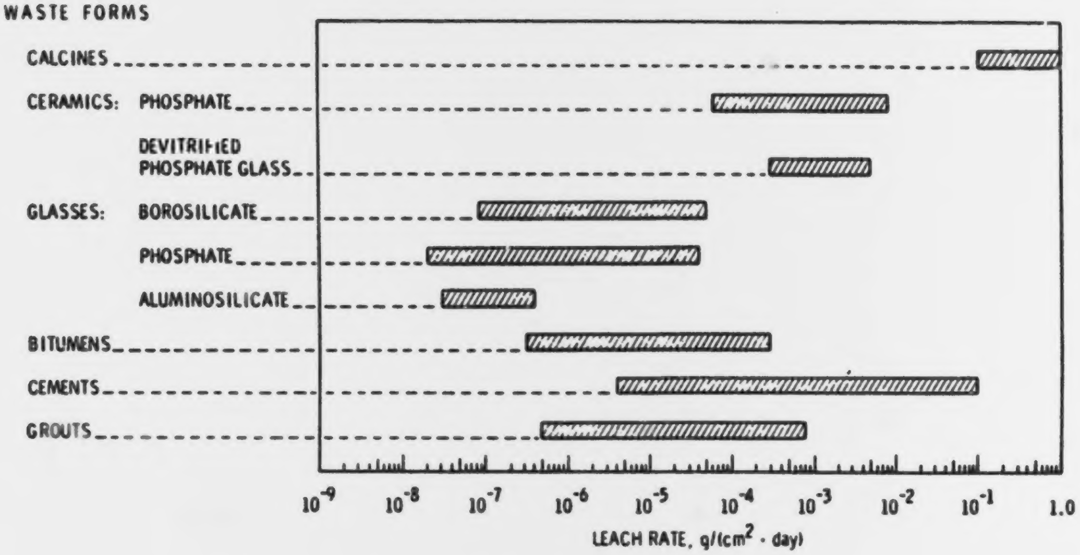

(a) Leach Rates of Alkali and Alkaline-Earth Elements from Various Waste Products

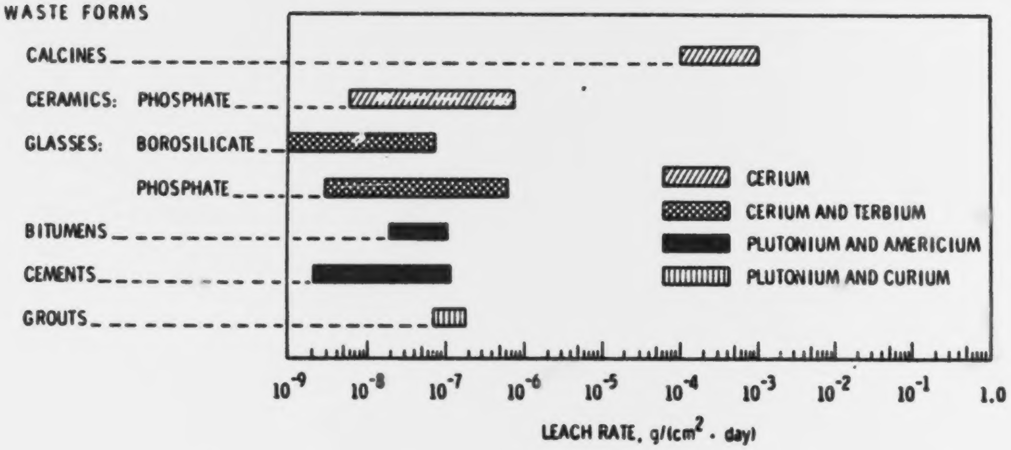

(b) Leach Rates of Rare Earths and Actinide Elements from Various Waste Products

Figure 2.1 Comparison of leach rates.[4]

BEST DOCUMENT AVAILABLE

Table 2.3

Comparison of Defense and Commercial High Level Waste

	Canisters Required	Heat Output kW/Canister(a)	Radionuclide Content, Ci/Canister(a)					
			^{90}SR	^{137}CS	^{238}Pu	^{239}PU	^{241}Am	^{244}Cm
Defense HLW(b)								
• Savannah River	8.0×10^{3}	0.2	1.5×10^{4}	1.5×10^{4}	1.4×10^{2}	2.9	8.2	8.2
• Idaho Falls	1.2×10^{4}	0.09	7.3×10^{3}	7.4×10^{3}	4×10^{1}	4×10^{-1}	6.0×10^{-1}	3.1×10^{-1}
• Hanford	2.6×10^{4}	0.06	5.2×10^{3}	4.8×10^{3}	2×10^{-2}	9.2×10^{-1}	6.5	5.4×10^{-1}
Total	4.6×10^{4}							
Commercial HLW(c)	1.0×10^{5} to 2.8×10^{5}	3.2 to 1.2	1.4×10^{5} to 5.0×10^{4}	2.0×10^{5} to 7.1×10^{4}	1.8×10^{2} to 6.5×10^{1}	4.3 to 1.5	1.7×10^{3} to 6.1×10^{2}	1.4×10^{4} to 5.1×10^{3}

(a) Nominal values, assuming uniform distribution of waste radionuclides among the canisters.

(b) Estimated data for the year 1990. Treated waste volumes (assuming a waste form having a 25% loading of waste oxides) and radionuclide contents supplied by J. L. Crandall and W. R. Cornman of the High Level Waste Lead Office at Savannah River. Canister requirements based on 0.6-m-diameter x 3-m-long canisters, 80% full of treated waste. Heat outputs based on the contained radionuclides.

(c) Data from this statement for the reprocessing of spent fuel containing 2.4×10^{5} MTHM (Case 3) and radioactivity at 6.5 years after reactor discharge. Canister requirement dictated by the heat output allowed by the disposal system.

2.1 Glassy Forms

The most common immobilization procedure advocated by a number of countries is to incorporate the radioactive waste calcine into a glassy matrix. Glasses are products obtained by melting waste oxides together with additives such as SiO_2, B_2O_3, Al_2O_3, P_2O_3, Na_2O_5, and CaO. Upon solidification, the melt forms a glass. Some of the glass compositions being studied in the U.S. and abroad include nepheline syenite, alkali borosilicate, zinc borosilicate, phosphoaluminosilicate, phosphate, etc. Concentrations of fission products in these glass formulations range from 2 to 30% by weight, the total waste loading being as high as 60%. Phosphate glasses are reported to be very corrosive to almost all container materials and were rejected in the U.S. in the 1960's. The most recent developments in the glass waste forms include the high silica porous glass matrix.

2.1.1 Borosilicate Glass

The alkali borosilicate system appears to be the most thoroughly studied among the various glass formulations. It is the most developed waste form and has received considerable attention in the U.S.,[1] the European community, Canada,[9] and Japan.[10] Typically a borosilicate waste glass might consist of about 20 to 30% waste oxides, 30 to 40% silica, 5 to 10% boron oxide and 10 to 15% alkali oxides, plus other additives. Domestic research and development efforts on borosilicate glass are primarily focused on the commerical and defense HLW glasses. PNL glasses belong to the former category while SRL, RHO, and ICPP glasses are the latter types. The amount of fission products and actinides are larger in the commercial HLW glasses, resulting in a temperature difference in the range of 100°C for 20-year seasoned wastes in rock salt.[5,11] The major concern for the performance assessment of glass is its chemical stability. Thermal, mechanical, and radiation stability are also important factors. In this section, the various types of borosilicate glass are briefly reviewed and their important features of chemical, mechanical, and thermal stability are summarized.

A variety of borosilicate-base waste glasses have been reported in the literature.[4,6-10,12,13] The compositional range of typical U. S. borosilicate waste glasses in terms of the three end components-the glass formers (SiO_2, B_2O_3, Al_2O_3), the modifiers (CaO, MgO, Na_2O), and the intermediates (ZnO, TiO_2, Cr_2O_3, Fe_2O_3, NiO)-are described elsewhere.[14] RHO defense glass has a higher content of formers while SRL defense glasses lie in the modifiers region. Domestic glasses are divided into two basic groups: commercial HLW glass and defense HLW glass. The commercial HLW glasses are the various types of PNL glasses: PNL 72-68 and PNL 76-68 glasses have been most widely characterized. PNL 76-68 is a typical waste borosilicate glass while PNL72-68 glass is a low silica glass developed earlier. The chemical composition of these glasses are given in Table 2.4. Variations of these glasses include 73-1, 76-183, 76-260, 77-107, 77-260, 78-157, 79-417, 79-418 formulations, zinc borosilicate glass and Sandia copper-titanium borosilicate glass.

Defense HLW glasses are divided into three basic groups, depending on the type of waste used: SRL or SRP glasses, RHO glasses and ICPP glasses. The most representative examples of each group are given in Table 2.4. Several other variations of these formulations have been reported. Examples are TDS 79-339, TDS-211, SRL-131, SRL-C411, SRL-T411, SRL-T211 for SRL glasses; RHO-Res.Liq. and RHO-$BiPO_4$ for RHO glasses; and ICPP-Zr13, ICPP-Zr51 for ICPP glasses. Representative foreign glasses, shown in Table 2.4, include the chemical compositions of glasses studied in Canada, the U.K., Germany, France, Italy, and Japan. Generally, the waste loading is lower in these glasses than in the domestic glasses.

Canadian borosilicate glasses were selected for development as matrices for the high- and medium-level wastes. Three categories of borosilicate glass products were tested: waste-Na_2O-B_2O_3-SiO_2, waste-Na_2O-CaO-B_2O_3-SiO_2 and waste-Na_2O-ZrO-B_2O_3-SiO_2. All initial work has been non-radioactive loading. Many glasses were examined in the U.K. for the immobilization of early wastes from reactors and defense wastes. They preferred a borosilicate composition optimized for a waste composition which consisted of 45.8% of fission product mixed oxides. French efforts have centered on sodium borosilicate and sodium aluminoborosilicate glasses as final materials for the solidification of HLW. Specific activity of these glasses are in the range of 1000 Ci/liter. In the German glasses, the waste loading is in the range of 15% and the variation of compositions has been made in SiO_2, MgO, Al_2O_3, and Na_2O. Italian glass is one of the glasses normally considered in Europe for scoping experiments to define the general mechanism of leaching over a long term. Japanese glass has high waste loading and is characterized by molybdate phase separation.

Tables 2.5, 2.6, and 2.7 are tabulations of laboratory leach rates at 70-150°C, at room temperature, and at elevated temperatures and pressures. An important parameter affecting the glass leach rate is temperature. More than an order of magnitude increase in leach rate is observed with a temperature increase of 100°C.[4,16,24]

Groundwater flow rates can affect glass leach rates. At high flow rates in the range of 2-70 m/y[18], the leach rates increase by one to two orders of magnitude. The effects of flow rates or glass leach rates are also a function of the isotope studied.[25] However, in flow conditions of less than 1 m/y, the leach rate does not change more than an order of magnitude. Some data from flow tests and Soxhlet tests are given as examples in Tables 2.5, 2.6, and 2.7.

Various vitrification processes and subsequent radiation, thermal and mechanical effects induce glass cracking, resulting in an increase in exposed surface area. This increased area will increase the fractional release rate by the direct contribution of cracked area to mass release[30] or by the shift in solution pH.[31] Initial processing and subsequent glass cracking may increase the surface area by one to two orders of magnitude.[32] The resulting mass release can be significant, changing the leach rate an order of magnitude.

Table 2.4

Composition of the Most Representative Borosilicate Waste Glass

Glass Type	Weight Percent											
	SiO_2	B_2O_3	Al_2O_3	CaO	MgO	Na_2O	ZnO	TiO_2	Fe_2O_3	Other	Waste Loading	Ref.
PNL 72-68	27.3	11.1		1.5		4.0	21.3			19.6	26.3	4
PNL 76-68	40.0	9.5		2.0		7.5	5.0	3.0			33.0	1
SRL	40.4	7.2		4.5		16.2		7.2		2.9	21.6	15
SRP-TDS-3A/131	39.8	10.4			1.4	12.0		0.7			30.9	15
ICPP	44.2	5.04				16.1				1.3	max 33.0	1
RHO-Purex	53.2	7.7				9.1					30.0	1
RHO-Redox	55.5	8.0				9.5				2.0	25.0	1
Canada	37.4 -64.7	10.7 -18.4		0.0 -10.0		10.0 -25.0	0.0 -10.0			balance	6.8-16.9	1
U.K.189	41.5	21.9				7.7				3.7	25.3	16
GP 98/12-German	48.2	10.5	2.2	3.5	1.8	14.9		3.9			15.0	17
France-Marcoule	47.6	18.6				12.4			6.4		15.0	1
Italy	48.0	15.0	5.0			12.0					20.0	8
Japan	38.1 -59.3	8.3 -15.5	5.3 -13.6	2.6 -5.1	0.0 -7.5	0.0 -4.8				balance	21.3-31.0	10

Table 2.5 (Cont'd.)

Leach Rates of the Most Representative Borosilicate Waste Glasses in the Temperature Range of 70°C to 150°

Glass Type	Element	Leach Rate (g/cm^2-day)	Temperature (C°)	Test Method	Time (day)	Solution Matrix	Other Variables	Reference
PNL 76-68	Si	5×10^{-5}	90	Static	28	DI Water	SA/V= 10^{-1}/cm	4
Sandia 75-32	Weight Loss	$4 \times 10^{-7}-10^{-5}$	Boiling Water	Soxhlet	730	DI Water		19
PNL 79-417, 418	Si	4×10^{-6}	90	Static	28	DI Water	SA/V= 10^{-1}/cm	4
SRP- (72 wt% Frit 21)	Cs, Sr, Pu	$10^{-9}-10^{-8}$	99	Soxhlet	100	DI Water, Silicate Water		20
SRP-TDS-3A/131	Cs, Sr	$2 \times 10^{-6}-10^{-4}$	90	MCC-1	28	DI Water		12
SRL	Cs	6×10^{-8}	90	Static	60	Brine		15
"	Cs, Sr	$(2-3) \times 10^{-5}$	90	MCC-1	28	DI Water		18
SRL 211	Eu, Ce	$5 \times 10^{-6}-10^{-5}$	90	MCC-1	28	DI Water		20
"	Cs, Sr	$10^{-4}-2 \times 10^{-3}$	90	MCC-1	40-100	DI Water		20
SRL 211, RV1, RV2, RV3	Weight Loss	$4 \times 10^{-8}-5 \times 10^{-7}$	100	Soxhlet	28	DI Water		21

Table 2.5 (Cont'd.)

Leach Rates of the Most Representative Borosilicate
Waste Glasses in the Temperature Range of 70°C to 150°

Glass Type	Element	Leach Rate (g/cm^2-day)	Temperature (C°)	Test Method	Time (day)	Solution Matrix	Other Variables	Reference
PNL 76-68	Si	$5x10^{-5}$	90	Static	28	DI Water	SA/V= 10^{-1}/cm	4
Sandia 75-32	Weight Loss	$4x10^{-7}-10^{-5}$	Boiling Water	Soxhlet	730	DI Water		19
PNL 79-417, 418	Si	$4x10^{-6}$	90	Static	28	DI Water	SA/V= 10^{-1}/cm	4
SRP- (72 wt% Frit 21)	Cs, Sr, Pu	$10^{-9}-10^{-8}$	99	Soxhlet	100	DI Water, Silicate Water		20
SRP-TDS-3A/131	Cs, Sr	$2x10^{-6}-10^{-4}$	90	MCC-1	28	DI Water		12
SRL	Cs	$6x10^{-8}$	90	Static	60	Brine		15
"	Cs, Sr	$(2-3)x10^{-5}$	90	MCC-1	28	DI Water		18
SRL 211	Eu, Ce	$5x10^{-6}-10^{-5}$	90	MCC-1	28	DI Water		20
"	Cs, Sr	$10^{-4}-2x10^{-3}$	90	MCC-1	40-100	DI Water		20
SRL 211, RV1, RV2, RV3	Weight Loss	$4x10^{-8}-5x10^{-7}$	100	Soxhlet	28	DI Water		21

Table 2.5 (Cont'd.)

Leach Rates of the Most Representative Borosilicate Waste Glasses in the Temperature Range of 70°C to 150°C

Glass Type	Element	Leach Rate (g/cm^2-day)	Temperature (°C)	Test Method	Time (days)	Solution Matrix	Other Varibles	Reference
SRL	SiO_2	$7x10^{-6}$	70	Flow Test	28		Flow Rate= 2 m/y	18
SRL	SiO_2	$3x10^{-5}$	70	Flow Test	28		Flow Rate= 70 m/y	18
TDS 211	Si	$3x10^{-5}$	90	Static	28	DI Water	SA/V= 10^{-1}/cm	4
TDS 79-339	Si	$4x10^{-6}$	90	Static	28	DI Water	SA/V= 10^{-1}/cm	4
RHO-Purex	Cs	10^{-5}-$4x10^{-4}$	100	Soxhlet			Powder	1
RHO-Res. Liq.	Si	$4x10^{-6}$	90	Static	28	DI Water	SA/V= 10^{-1}/cm	4
ICCP	Cs	$4x10^{-4}$	95	Soxhlet	14	D Water		13
"	Cs	$3x10^{-5}$	95	Static	28	D Water		13

Table 2.5 (Cont'd.)

Leach Rates of the Most Representative Borosilicate Waste Glasses in the Temperature Range of 70°C to 150°C

Glass Type	Element	Leach Rate (g/cm^2-day)	Temperature (°C)	Test Method	Time (days)	Solution Matrix	Other Variables	Reference
Canada	Na	10^{-5}-10^{-3}	100	IAEA	60			9
U.K.(189/209)	Weight Loss	10^{-4}-$2x10^{-4}$	100	Soxhlet		D Water Granite Water		26
Germany- (GP 98 112, 98/18, 98/26)	Weight Loss	10^{-4}	70	Soxhlet	15	D Water		17
France	Cs, Sr	$2x10^{-5}$	100		80			27
Italy	Over All	$3x10^{-2}$	80	Soxhlet	417	D Water		28
Japan	Cs, Sr	10^{-7}-10^{-6}	94	Soxhlet	2-4	D Water		10

DI Water: Deionized Water.
D Water: Distilled Water.
SA/V: The Ratio of Sample Surface Area to Solution Volume.
ND: Non-Detectable.
There is no difference between SRL glass and SRP glass.

Table 2.6

Leach Rates of the Most Representative Borosilicate Waste Glasses at Room Temperature

Glass Type	Element	Leach-Rate (g/cm^2-day)	Test Method	Time (days)	Solution Matrix	Other Variables	Reference
72-68	Cs, Sr	$10^{-4}-10^{-5}$	Soxhlet	1000			1
	Pu	10^{-6}	Soxhlet	1000			1
	Cm	10^{-7}	Soxhlet	1000			1
76-68	Np	$10^{-5}-10^{-7}$	IAEA	420	DI Water Brine		25
	Pu	$10^{-6}-10^{-9}$	IAEA	420	DI Water Brine		21
	Cs	$8x10^{-7}-2x10^{-6}$		7	DI Water		24
	Eu	$3x10^{-7}$		7	DI Water		24
SRL	Cs, Sr	$(3-4)x10^{-7}$	MCC-1		DI Water		29
	Pu	$(0.4-3)x10^{-5}$	MCC-1		DI Water	pH=4	29
SRL	Cs	10^{-9}	Static	365	Brine		15
	Cs	$10^{-7}-10^{-8}$	MCC-1	700	DI Water	pH=7-9	15
	Sr	$10^{-4}-10^{-8}$	MCC-1	700	DI Water	pH=4-7	15
SRP-TDS-3A/131	Pu	$5x10^{-8}$		1000	DI Water	SA/V= 10^{-1}/cm	12
	Cs, Sr	$2x10^{-7}$		1000	DI Water	SA/V= 10^{-1}/cm	12
Canada	Cs	10^{-5}		600	Granite Water		9
France	Cs, Sr	$5x10^{-7}$		80			27
U.K.-(189,209)	Weight Loss	$10^{-6}-10^{-7}$	Soxhlet		Granite Water		26

Table 2.7

Leach Rates of Typical Borosilicate Waste Glasses under Hydrothermal Conditions

Glass Type	Element	Leach-Rate (g/cm^2-day)	Test Method	Time (days)	Solution Matrix	Other Variables	Reference
76-68	Cs	$(2-4)x10^{-3}$		7	DI Water	286°C	24
	Eu	$3x10^{-6}$		7	DI Water	286°C	24
U.K.-(189,209)	Weight Loss	$(1-2)x10^{-3}$	Soxhlet		D Water, Granite Water	200°C, 60 MPa	26

Solution chemistry also affects glass chemical durability. In brine solutions, the leach rates are generally lower than in DI water and silicate water. Likewise alkaline elements released will enhance the durability because of resultant salinity increases. Cs and Mg, however, have an adverse effect. These changes, though, are well within an order of magnitude. The solution pH also affects the durability. In the pH range of 5 to 9, the leach rates are almost constant. Above and below this range, the leach resistance decreases drastically.[12,16,34,35] Although repository conditions may not exhibit such wide pH excursions, attention should be paid to extreme pH shifts which can result from accummulation of leached alkali and silica in the vicinity of the waste form. It is quite difficult to assess this pH effect quantitatively at the moment.

Glass composition can also affect the chemical durability. Although there is a general trend for this effect,[36,37] the change in leach rate does not appear to be significant, as shown in Tables 2.5, 2.6, and 2.7. No data on the effect of phase separation on the chemical durability have been reported. Further details are given elsewhere.* However, a study of commercial glass indicates that the heat treatment should be done carefully to avoid an easily leachable microstructure.[38] Other effects such as crystallization effects may not be significant.[39] With regard to weathering properties, ancient glass may be indicative of long term glass durability. Although the composition of ancient glasses is quite different from that of nuclear waste glass, there is some evidence for over a thousand years' durability.[38,39]

During transport and handling of the waste form package, accident situations may occur which will deliver high impact energy to the package. Several laboratory tests[12,22,40] indicate that impact resistance of glasses, especially waste borosilicate glass, is comparable to that of other waste forms. SRL 131 glass produced only 0.14 wt% respirable fines, less than 10 microns upon 10 joules/cm^3 impact energy, which is better than SYNROC, High silica glass, Pyrex or FUETAP.[14,27] PNL tests on 72-68 glass show the consequent effects of impact. At impact velocities of 7.6 m/sec and 36 m/s, the surface area increased by factors of 1.3 to 3 and 10 to 150, respectively.[41] Since there are no data on relative accident situations, it is difficult to assess these effects at this moment.

More important than analysis of accidents expected during transportation is the assessment of mechanical degradation of the waste form under repository conditions over long geological times. For this purpose, tensile strengths are informative. The tensile strength of 76-68 glass in 51.4 MPa, which is slightly higher than that of ceramic or glass ceramics waste forms.[4] On the other hand, compressive strength may not be important since the compressive strength is greater than the tensile strength by an order of magnitude. This could lead to frequent fracture of the waste form by tensile stresses, not only by the application of a tensile force, but also by the development of tensile stresses at certain portions of the waste form during general compression. Static fatigue is also known to be a very important mode of disintegration of glass in water. This is particulary important under repository conditions since cracks developed under static fatigue will increase the exposed surface area, leading to significant material releases. It is important to know that static fatigue limits exist below which static fatigue does not develop. However, no data are available on waste glasses. Detailed information on generic borosilicate glasses is contained in a separate BNL report.*

---

*T. M. Ahn and E. Veakis, "Glass Corrosion - A Review", Draft Informal Report, Brookhaven National Laboratory, Upton, NY, 1981.

It is important to consider the self-heating effects of waste glasses due to radioactive decay of fission products. The important consequences of self-heating include an increase in glass solubility and leach rate upon devitrification and subsequent cracking by stress generation.

Phase crystallization can be introduced during the vitrification process as well from by self-heating during storage. Typical crystal phases observed are molybdate, platinum group metal oxides (RuO_2), refractory oxides [Ce, RE^{3+}) O_2-x] and complex silicate or phosphate phases. This will often lead to a change in the leach rates either by direct change of leachability introduced by crystal phases or in an indirect way such as microstructure change or stress generation. The change in leach rates, though, is not significant for borosilicate glass. The variation is within an order of magnitude;[4,34] in some cases it is negligible. There is an unknown area, however, where differential thermal and radiation expansion may lead to microfracture, resulting in an increase in the exposed surface area. No data are available for this effect except general thermal expansion data on borosilicate glass which does not differ from that of other waste forms.[4]

2.1.2 Glass Burial Field Experiment

Glass blocks consisting of 85% nepheline syenite plus 15% lime and fission product solution were fabricated at the Chalk River Nuclear Laboratories (CRNL) in Ontario, Canada.[42,43] Each glass block contained 12 Ci of fission products. In 1960, twenty-five glass hemispheres were buried in sand (water flow was $\approx$10 cm/yr) on the CRNL site. After a year, no activity was detected in the surrounding soil. A second set of 25 blocks with slightly higher solubility and higher fission product loading (42 Ci) was prepared and placed in a tighter matrix. This time activity was detected in the soil and was monitored intermittently over the following 18 years.

From 1960 to 1967, the ^{90}Sr released from the blocks has remained constant at a leaching rate of 5×10^{-11} g/cm^2-d. The amount of glass being leached daily was calculated from the ^{90}Sr values for both the burial test results and laboratory test results as shown in Figure 2.2. In both cases, the leach rate decreases with time.

The CRNL glass block leaching study is of considerable importance to the waste management effort, since it has been the only long-term in situ leaching test with realistic flow conditions. It is the closest approach to a real repository situation. The substantially lower leaching rates observed in such

---

*T. M. Ahn and E. Veakis, "Glass Corrosion - A Review", Draft Informal Report, Brookhaven National Laboratory, Upton, NY, 1981.

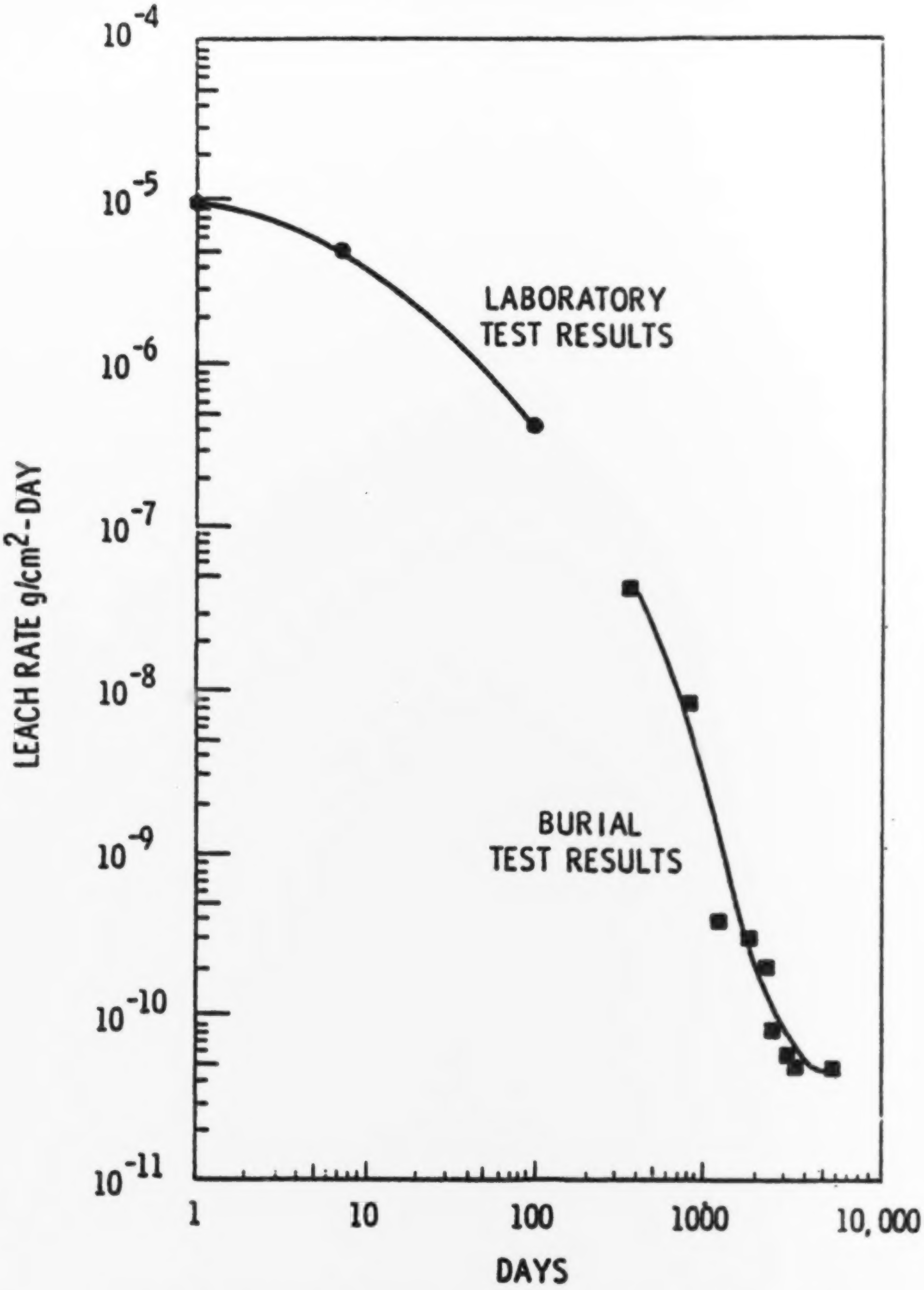

Figure 2.2 Canadian waste glass laboratory test and field burial test results.[42]

BEST DOCUMENT AVAILABLE

a situation may be the result of groundwater conditioning by the surrounding soil or due to saturation conditions resulting from low flow rates. It is important to note that bench-scale field tests did not show unexpectedly high leach rates compared to laboratory test results, indicating laboratory results may be scaled up and extrapolated without a major problem.

2.1.3 Porous Glass Matrix Composite Glass

One of the recent developments in glassy waste forms is the Porous Glass Matrix (PGM) process developed at Catholic University of America (CUA). The PGM glass is a composite vitrified solid consisting of a glass core loaded with up to 30% waste components and encapsulated in a waste-free protective glass envelope. The protective glass cladding is designed to delay leaching of the underlying core for a period beyond the thermal spike of the repository so that leaching under hydrothermal conditions is avoided. The presence of a large residual compressive strength in the cladding region provides high structural stability and prevents breakage and delayed fracture of the core, which are normally induced by the development of tensile stress during storage. Several recent papers have reported on the research and development efforts, characterization, and the testing of the PGM composite glass.[18,44-50]

The PGM process involves the use of a high silica porous glass which is prepared by heat treating an alkali borosilicate glass to induce phase separation into a high silica and a low silica phase and selectively dissolving the latter by leaching in an acid solution. This preferential acid leaching results in a high silica porous glass structure, having interconnected pores ranging in size from 100 to 500 Å, and consisting of 96% SiO_2 and 4% B_2O_3 (Figure 2.3a, Steps 1 to 3). The resultant high silica porous matrix is dried and crushed into a fine powder and subsequently mixed with the high level liquid wastes and solid precipitates. The liquid penetrates into the pores and deposits any dissolved wastes present in the liquid, while the solid precipitates are deposited between the grains of the powder (Figure 2.3b). Drying and heating allow the pores to collapse, thus trapping the dissolved wastes in the grain matrix. The mixture is then heated inside a high silica glass tube with a sealed end. After the powder sinters and traps the intergranular solids, the tube itself collapses on the porous glass and waste mixture. The collapsing temperature depends upon the specific composition of the encapsulating glass tube; it ranges from 900°C to 1300°C. The latter temperature is high due to the present use of commercial Vycor tubes. Lower temperatures can be readily obtained by using modified Phasil tubes.

Because of the great complexity of the glass tube melting process described above, the Catholic University researchers reported that an intermediate processing alternative which does not use the protective glass envelope has been developed. This alternative uses a spray calcine and in-can melter, equipment already developed and hot-tested for the borosilicate glass. Although the alternative process is relatively less complex, the resultant product does not possess a sacrificial cladding region to protect the underlying core from groundwater attack.

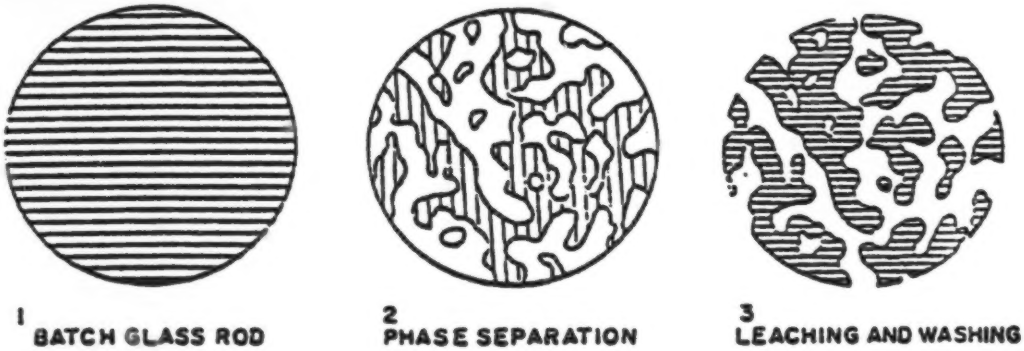
1 BATCH GLASS ROD
2 PHASE SEPARATION
3 LEACHING AND WASHING

(a) High silica glass process.

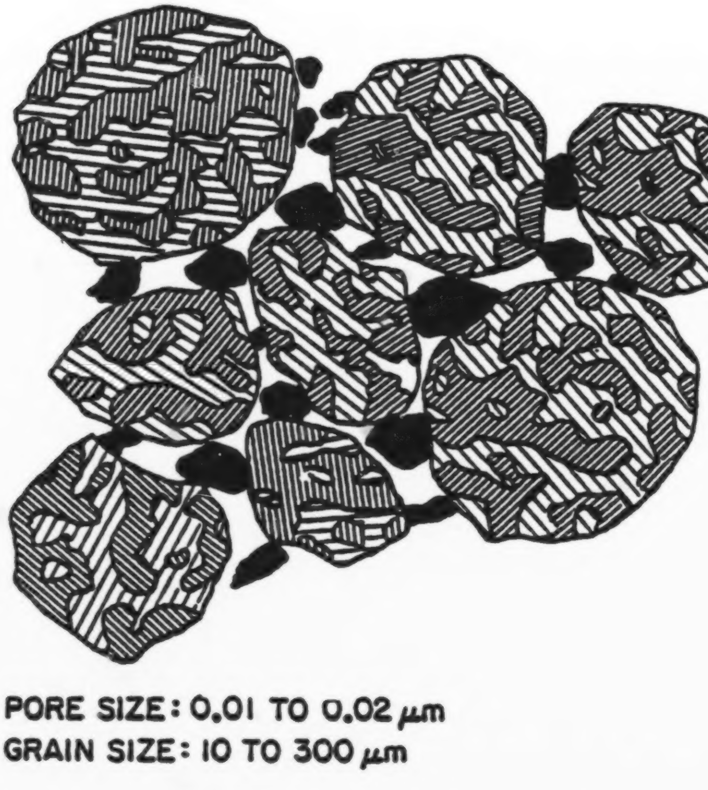
PORE SIZE: 0.01 TO 0.02 μm
GRAIN SIZE: 10 TO 300 μm

(b) Schematic representation of porous glass matrix process: The large grains represent the porous glass powder, ▨ with dissolved waste, ▧, in the pores. The waste solids, ■ are located interstitially between the grains.

Figure 2.3 Porous glass matrix process.[50]

BEST DOCUMENT AVAILABLE

At a recent meeting in Atlanta, it was reported that both composite core-clad glasses and core-only glasses have been produced in the laboratory.[18] Core-only glasses have been fabricated as cylinders (2" dia. x 4" long) using the three SRL sludges: 30% composite, 30% high-alumina, and 25% high iron. Samples containing U and fully loaded samples containing ^{37}Cs, ^{90}Sr, ^{60}Co, and U have also been produced. Compositional analysis of the PGM glasses produced from the three SRL sludges is given in Table 2.8.

Table 2.8[18]

PGM Glass Analysis

Oxide	Composite %	High Al_2O_3 %	High Fe_2O_3 %
SiO_2	56.4	62.6	56.4
B_2O_3	3.3	3.9	4.6
P_2O_5	5.8	5.3	5.3
Fe_2O_3	15.8	4.6	14.2
Al_2O_3	8.4	16.4	10.5
MnO	4.4	3.9	1.0
Cs_2O	.14	.14	.12
SrO	.10	.14	.09
U_3O_8	1.5	1.3	3.5
Na_2O	2.2	1.4	1.2
CaO	1.0	.43	.48
NiO	2.0	.67	2.7
ZrO_2	--	--	1.0
CeO_2	.40	.37	.30
Nd_2O_3	.33	.36	.24
Total	101.8	101.5	101.6

[a] SRP defense wastes.

Leach tests have been conducted under a range of conditions such as varying flow rates, solution matrices, temperatures, and time periods.[18] For comparison purposes, PNL and SRL glasses have also been tested under identical conditions. Phase characterization of the composite glasses is under way. Tests for mechanical strength and thermal stability are being conducted. Radiation effects have not yet been addressed.

Leach rates for PGM High Alumina and PGM Composite core glasses, PNL 76-78, and SRL borosilicate glass at 70°C for a range of flow rates are given in Table 2.9. At high and intermediate flow rates, the PGM core glasses are one to two orders of magnitude more leach resistant than the PNL 76-78 and SRL glasses. At low flow rates, reflecting nearly stagnant repository conditions, the glass dissolution rates are controlled by silica saturation levels. As shown in Table 2.10, the silica saturation levels are, in turn, controlled by the saturation pH of the system. Since PGM core glasses do not exhibit a wide pH excursion, apparently controlled by the addition of P_2O_5 to the glass matrix, their leach resistance is greater than that of the other glasses.

Table 2.9

Comparison of Leach Rates of Glass at 70°C (mg/m^2-day)

Core Glass	High Flow Rates F = 1,000 m/y	Intermediate Flow Rates F=70 m/y	Intermediate Flow Rates F=2 m/y	Low Flow Rates F = 0.1 m/y
PGM-High Alumina	0.8	2.0	0.5	--
PGM Composite	2.0	5.0	0.9	0.9
PNL 76-78	88	495	62	6.6
SRL	548	276	72	10.0

Table 2.10

Silica Saturation Levels at Low Flow Rates

Core Glass	Saturation pH	SiO_2 Saturation Level (mg/L)
PGM Composite	7.8	80
SRL	11.2	600
PNL 76-68	9.9	400

Preliminary results of leach tests on PGM cladding glasses show that, at high flow rates, the leach rates are more than an order of magnitude lower than those of the core glasses. It was reported that the following time periods would be required to dissolve a 4 mm thick protective jacket of PGM cladding glass: 12 x 10^6 years at 10°C; 12 x 10^4 years at 70°C; and 12 x 10^3 years at 100°C.[18]

Fully radioactive PGM composite core-clad glasses have been produced. Leach rates, based on core isotopes, are reported to be lower than 10^{-8} $g/m^2 \cdot d$. Estimated leach rates based on core exposure by fracture are 500 times lower than the leach rates for the bare core.

2.2 Glass Ceramics

Glass ceramics, being hydrid waste forms, can be formed by either glass or ceramic processes. The common types of glass ceramics are formed by partial devitrification of waste glass under controlled conditions. Most of the developmental work and evaluation of glass ceramic waste forms is being conducted at Hahn Meitner Institute (HMI), Berlin.[51-54] Domestic research and development is being done at PNL,[55,56] in collaboration with the Hahn Meitner Institute. The potential of glass ceramics as a waste form for immobilizing HLW is also being investigated in Japan.[57,58]

The glass ceramic waste form typically consists of one major and several minor crystalline phases in a glassy matrix. The crystallites vary in size from 0.5 to 1 m. The crystalline phases host the fission products and the actinides. The composition and mineralogy of the celsian- and the fresnoite-type glass ceramic waste forms developed at the Hahn Meitner Institute are given in Table 2.11. For comparison purposes, the compositions of phosphate and borosilicate glasses are also included in Table 2.11. Since boron is present in the residual glass matrix, the higher boron content results in a waste form having lower leach resistance. Based on their boron contents, the fresnoite glass ceramic has lower leachability than the celsian type. Further, the HMI group concluded that compared to glass systems the glass ceramic waste forms exhibit improved mechanical and thermal properties. There was no improvement, however, in the leach resistance.

The Power Reactor and Nuclear Fuel Development Corporation (PNC) in Japan has studied a number of glass ceramics for potential waste forms.[56,58] The composition and mineralogy of the various PNC glass ceramic waste forms are listed in Table 2.12. D-62 and D-210 are diposide-based, C-27 is celsian-based, P-50 is perovskite-based, E-63 is spodumene-based, and P-71 is based on sphene. Their studies show that the most promising form appears to be the formulation based on diopside.

Recent work at PNL on glass ceramic waste forms has focused on basalt-based glass ceramics. The formulation is composed of Hanford basalt as the raw material and 20% PW-9 simulated waste calcine. The mineral assemblage of PNL basalt glass ceramic, as reported by Rusin,[56] consists of augite [(Ca,Mg,Fe) SiO_3], powellite [(Ca,Sr) MoO_4], and a spinel phase (Ni,Fe_2O_4).

Leach resistance data for basalt glass ceramics are reported in Table 2.13. For comparison purposes, leach data for basalt rock and basalt glass with and without calcine are also given in Table 2.13. According to Rusin,[56] the leach rates for basalt glass and glass ceramic are not significantly different, in that they are within an order of magnitude. Scanning electron micrographs reveal that the residual glass phase is

Table 2.11

Composition of Phosphate and Borosilicate Glasses and Glass Ceramics

	Phosphate Glasses wt.%	Borosilicate Glasses wt.%	Glass Ceramic Celsian-Types wt.%	Glass Ceramic Fresnoite-Types wt.%
P_2O_5	30 - 60	--	--	--
Fe_2O_3	5 - 40	--	--	--
SiO_2	0 - 20	27 - 50	28 - 38	22 - 28
Al_2O_3	5 - 41	0 - 1	10 - 13	0 - 2
B_2O_3	0 - 17	9 - 22	2 - 7	0 - 3
CaO	--	0 - 4	0 - 6	0 - 4
BaO	--	--	13 - 16	28 - 36
Na_2O	0 - 30	4 - 20	0 - 2	--
Li_2O	--	0 - 4	1 - 3	--
TiO_2	--	0 - 6	3 - 4	14 - 23
ZnO	0 - 5	0 - 22	3 - 5	0 - 6
PbO	0 - 30	--	0 - 3	--
Waste oxides	≤ 40	20 - 30	20	20
Crystal phases	Fe-phosphate Na-Zr-Phosphate	Ru-Oxide, Pd, Ce-Oxide, spinel Zn-Silicate Sr-Molybdate Gd-Titanate Ca-RE-Silicate Gd-Ca-Phosphate and others	Cymrit or h-Celsian m-Celsian (Ba) $BaAl_2Si_2O_8$ RE-Titanate (RE,An,Sr) $RE_2Ti_2O_7$ Ba-Molybdate (Mo, Ba) $BaMoO_4$ Pollucite (Cs,Rb) $(Cs,Na)AlSi_2O_6$	Fresnoite (Ba,Sr) $Ba_2TiSi_2O_8$ Priderite (Ba) $K_2Fe_2Ti_6O_{16}$ RE-Titanate (RE,An,Sr) $RE_2Ti_2O_7$ Ba-Molybdate (Ba,Mo) $BaMoO_4$

Table 2.12

Compositions and Crystal Phases of PNC Glass Ceramics

Composition	Sample Number					
	D-62	C-27	P-50	E-63	D-210	P-71
SiO_2	47.5	35.0	30.0	50.0	41.02	40.0
Al_2O_3	6.8	15.0	10.0	12.5	8.20	6.5
B_2O_3		5.0	5.0		3.50	3.5
Fe_2O_3	9.5				8.70	
TiO_2	2.7	5.0	10.0	6.0	3.20	10.0
CaO	6.8	4.0	25.0		4.10	10.0
MgO	6.8				1.37	
BaO		13.0				
ZnO		2.7		4.0		
Li_2O				7.5		
HLW	20.0	20.0	20.0	20.0	30.0	30.0
Total	100.0	100.0	100.0	100.0	100.0	100.0
Crystal Phases	(a) Fe_3O_4 $CaMoO_4$ $CaTiO_3$	(b) $CaMoO_4$ $CaTiO_3$	(c) $CaSiO_3$ $CaMoO_4$ Sphene	(d) Li_2SiO_3	(a) $CaMoO_4$ Fe_3O_4 $CaTiO_3$	(e) $CaMoO_4$
Heat Treatment	1000°C 1 hr	850°C 1 hr	900°C 3 hr	800°C 2 hr	900°C 1 hr	900°C 1 hr

(a) Diopside ($CaO \cdot MgO \cdot 2SiO_2$)
(b) hexa-Celsian ($BaO \cdot Al_2O_3 \cdot 2SiO_3$)
(c) Perovskite ($CaTiO_3$)
(d) β-Spondumene ($Li_2O \cdot Al_2O_3 \cdot 4SiO_2$)
(e) sphene ($CaO \cdot TiO_2 \cdot SiO_2$)

preferentially leached in the glass ceramic. Rusin has reported that the residual glass content is the limiting factor in glass ceramic waste forms with respect to their chemical durability.

Basalt glass ceramic prepared using PW-46-7 and PW-80-2 are presently being characterized at PNL. It is reported that basalt glass ceramics appear to be able to accept wide compositional variations in waste streams. Basalt glass ceramic is also being investigated as a potential TRU waste form. This is discussed in detail in the Task 2 Report. Further details on the compositions, processing conditions, and product characterization of typical and commercial glass ceramics are discussed elsewhere.[56]

Table 2.13

Leach Resistance of Basalt Glass Ceramics in Deionized Water at 90°C[a]

	Element in Solution, g/m^2 [b]							
Wasteform	Al	Ca	Mg	Si	Na	Mo	Sr	Cs
Basalt	--[c]	2.72	2.45	3.73	--	--	--	--
Basalt Glass	--	0.30	0.19	0.22	--	--	--	--
Basalt Glass/ PW-9	0.38	2.46	1.89	1.89	--	3.27	2.08	2.84
Basalt Glass Ceramic/PW-9	--	0.75	0.23	1.04	--	1.86	1.91	1.97

[a] 9 days, SA/SV = 14 m^{-1}.
[b] Normalized g/m^2
[c] Solution concentration below detection limit.

2.3 Crystalline Forms

Presently the high-fired crystalline ceramics are being actively investigated as high level waste forms for both commercial and defense waste streams. The production of these ceramics involves a high-temperature firing step (>800°C), resulting in a water-free product of almost theoretical density. In contrast, concrete- and clay-based waste forms such as FUETAP and clay ceramics are produced at relatively lower temperatures. These low temperature ceramics are reported to retain some chemically bound water and bulk interstitial water and, as a result, are not suitable as high level waste forms.

The high-fired crystalline waste forms are characterized by several stable, mineral-like phases hosting the radionuclides and inert contaminants. The synthetic crystalline phases are analogues of natural minerals which are known to be stable under varying geologic conditions for long time periods. The concept inherent to this group of waste forms is the incorporation of radioactive waste ions as dilute solid solutions in the constituent mineral phases. Depending upon the composition of the host matrix and the inert additives, there are basically three types of polycrystalline ceramics being presently studied for the immobilization of commercial and defense high level wastes: silicate/ phosphate-based (supercalcine ceramics), alumina-based (high alumina ceramic) and titanate-based (SYNROC and Swedish and Sandia titanate ceramics). Zirconia-based ceramics are also being investigated.

2.3.1 Supercalcine Ceramic

The supercalcine ceramic, developed at Pennsylvania State University (PSU),[59,60] consists of an assemblage of high-integrity crystalline phases obtained by modifying the high level waste composition with inert chemical additives. On a weight basis, the supercalcine formulation consists of 50% radioactive waste and 50% inert additives such as the oxides of Si, Ca, Al, and Sr. Various processes used for the production of supercalcine ceramics are described by Ross et al.[61]

Table 2.14 gives a list of structure types present in supercalcine ceramics as reported by McCarthy.[59] Information on solid solution and partitioning of waste radionuclides is also given in Table 2.14. The lanthanides and actinides are incorporated in apatite-, monazite-, and fluorite-type phases; the fission products Cs, Ba, and Sr in pollucite and scheelite; and the inert contaminants such as Fe, Ni, and Cr in the spinel and corundum phases. The additive ions were Al, Si, and Ca. For high Na wastes the sodalite phase, (Ca,Sr,Ba) $[NaAlSiO_4]_6$ is formed instead of Na-pollucite and scheelite.

The domestic research and development effort on supercalcine ceramic is being primarily conducted at PSU and PNL. At PNL, simulated PUREX-type wastes having waste loadings of up to 80% have been processed into supercalcine ceramics. Current work includes development of Thorex-process ceramics formulations.

Two supercalcine ceramic compositions (SPC-2 and SPC-4) have been developed for use as core materials in multibarrier waste forms. Both formulations contain the simulated PW-7 waste composition. Disc pelletizing technique is used to obtain spherical pellets (1 to 7 mm in diam.) from powders. Rusin[1] reported that the leach rates for hot pressed supercalcine, based on soxhlet tests at pH 4 and 9, vary from 10^{-5} to 10^{-7} g/cm^2·d. Density varies from 2.2 to 4.8 g/cm^3 and waste loadings from 65 to 80%. Supercalcine ceramic has also been tested under hydrothermal conditions.

Table 2.14[59]

Primary Containment Phases in Current Supercalcine-Ceramics

HLW Ions	Primary Containment Phases	Structure Type
Sr, Ln[b]	$(\underline{Ca},Sr)_2Ln_8(\underline{Si}O_4)_6O_2$[c]	Apatite
Ln, $[PO_4]$	$LnPO_4$	Monazite
Cs, Rb, Na	$(Cs,Rb,Na)\underline{AlSi_2}O_6$	Pollucite
Sr, Ba	$(\underline{Ca},Sr,Ba)MoO_4$	Scheelite
U, Ce, Zr	$(U,Ce,Zr...)O_{2+x}$	Fluorite
Zr, Ce, U	$(Zr,Ce,U...)O_{2+x}$	Tetragonal-Fluorite
Fe, Ni, Cr	$(Ni,Fe)(Fe,Cr)_2O_4$ and $(Fe,Cr)_2O_3$	Spinel Corundum
Ru	RuO_2	Rutile

[a] Te, Pd, Rh, Tc, Pm, Np, Pu, Am, Cm were not induded in the simulated waste.
[b] Ln = La, Pr, Nd, Sm, Eu, Gd, Y.
[c] Additive ions are underlined.

2.3.2 SYNROC

An alternative method of high level radioactive waste immobilization in crystalline materials has been developed by Ringwood.[62] This method is based on the incorporation of radioactive waste ions as dilute solid solutions in the constituent titanate minerals. It differs from supercalcine ceramics in having lower waste loadings and a titanate-based mineralogy.

During the past couple of years, a considerable amount of data has been generated on SYNROC. Current SYNROC research efforts are listed in Table 2.15.[63] In the U.S., the LLL is almost exclusively involved in research on SYNROC D, a formulation for defense waste. At ORNL, application of sol-gel techniques to SYNROC fabrication is being investigated. Work at North Carolina State University (NCSU) involves SYNROC synthesis, characterization,

Table 2.15

Overview of Current SYNROC Research*

Institution	Research Area
Australian Atomic Energy Commission	Waste Form Synthesis, Leaching, Radiation Effects
Australian National Univ.	Waste Form "Optimization", Radiation Effects, Production Technology, Repository Design
Argonne National Laboratory	Single Phase Synthesis, Leaching, Radiation Effects
Idaho Chem. Proc. Plant	Waste Form Application
Los Alamos Scientific Lab.	Single Phase Synthesis, Radiation Effects
North Carolina State Univ.	Rate-Controlled Sintering, Characterization Leaching
Oak Ridge National Lab.	Production Technology (Sol-Gel), Waste Form Synthesis
Lawrence Livermore Nat'l. Lab.	Waste Form Synthesis, Leaching, Radiation Effects, Production Technology

*Adapted from Tewhey et al.[63]

and leaching studies. Work at ANL is investigating single-phase synthesis of hollandite, zirconolite, and perovskite as well as SYNROC C. The Australian National University and the Australian Atomic Energy Commission are actively involved in SYNROC synthesis, characterization, leaching studies, studies of radiation effects, and production technology. Research at the University of Western Ontario is investigating sphene, a calcium silico-titanate, for a potential high level waste form.

2.3.2.1 SYNROC Mineralogy and Composition

There are basically three SYNROC formulations being presently investigated:

- SYNROC B: The basic SYNROC formulation without HLW. The principal phases are "hollandite", perovskite, and zirconolite in the TiO_2-Al_2O_3-ZrO_2-CaO system.

- SYNROC C: C = commercial high level waste. Same mineralogy as SYNROC B except that radioactive waste elements are included in solid solution.

- SYNROC D: D = defense high level waste. This SYNROC formulation incorporates up to 70% defense waste sludge. The principal phases are "hollandite," zirconolite, perovskite, spinels, and nepheline.

Durham et al.[64] reported that the stoichiometries of perovskite and zirconolite in SYNROC are the same as those found in their natural analogues. The hollandite-type phase, however, has a different stoichiometry from that of the natural mineral. Pseudobrookite ($AlTiO_5$), rutile (TiO_2), and corundum (Al_2O_3) can occur as accessory minerals when excess alumina and titania are present in the formulation. Small amounts of nickel, present in SYNROC B formulation, are reported to control the redox conditions during synthesis. Since the SYNROC titanate minerals are known to exhibit extensive solid solution, the SYNROC process is extremely flexible in terms of accepting variable waste composition.

Typical SYNROC compositions for the B and C formulations are given in Table 2.16.[65]. Phase diagrams depicting the stability fields of "hollandite", perovskite, and zirconolite in the quaternary system Al_2O_3-TiO_2-ZrO_2-CaO and of zirconolite and perovskite in the ternary system CaO-TiO_2-ZrO_2 are shown in Figure 2.4.[63]

Experimental data presented by Ringwood et al.[62] show that nearly all the waste radionuclides enter and form homogeneous solid solutions with SYNROC minerals. Table 2.17 shows the partitioning of high level waste elements in the primary mineral phases of SYNROC B. "Hollandite" is the key component in SYNROC B because of its ability to bind very large atoms such as Cs, K, Na, and Ba in its tunnel structure. Other elements such as those listed in Table 2.17 can substitute isomorphously for Al and Ti present in the octahedral sites of the "hollandite" structure. As shown in Table 2.18 perovskite is also capable of incorporating a wide range of elements, including all rare earths, in its structure. When zirconolite is present, the actinide elements and rare earths preferentially enter this phase. In the absence of zirconolite, they can be accommodated by perovskite. The fission products, Cs, Ba, and Sr are present in hollandite and perovskite phases, respectively.

SYNROC D formulation consists of up to 70% of defense waste (SRP sludges) and 30% inert additives composed of SYNROC B components (TiO_2, B_2O, ZrO_2, and CaO). The mineral assemblage is composed of the principal SYNROC titanate phases plus large amounts of Al-Fe-Mn bearing spinels and other inert phases. For sludge containing a Na_2O content of 4-5%, the SYNROC D mineralogy consists of perovskite, zirconolite, nepheline ($NaAlSiO_4$), spinel and ilmenite. For washed sludge compositions with <1.5% Na_2O, nepheline is absent and replaced by "hollandite".

Distribution of principal HLW elements among the coexisting SYNROC D phases is given in Table 2.19.[66] Most of the inert cotaminants are present in the spinel phases, while the rare earths and the actinides are partitioned between zirconolite and perovskite. "Hollandite" is the principal host for Cs. However, in the absence of "hollandite" for a sludge composition of low

Table 2.16[65]

Typical SYNROC Compositions for B and C Formulations

SYNROC B		SYNROC C	
Component	(wt.%)	Component	(wt.%)
TiO_2	59.5	SYNROC B	85
ZrO_2	11.4	Simulated Radwaste	10
Al_2O_3	6.0	Additional TiO_2[b]	4
BaO[a]	7.2	Additional Al_2O_3	1
CaO[a]	15.9		

Simulated Radwaste

Component	(wt.%)	Component	(wt.%)
CeO_2	9.7	ZrO_2	24.3
Nd_2O_3	28.3	Cs_2O	8.4
Eu_2O_3	4.4	ZrO	6.2
FeO	9.6	NiO	2.8
MoO^2	26.3		
		Total =	100.0

---

[a] Added as carbonates.
[b] Recently, up to 10% additional TiO_2 has been used.

Table 2.17[64]

Summary of Distribution of Radwaste Elements Among SYNROC B Phases

"Hollandite"	Zirconolite	Perovskite
Mo^{4+}	U^{4+}	U^{4+}
Tc^{+}	Th^{4+}	Th^{4+}
Cr^{3+}	Pu^{4+}	Cm^{4+}
Ni^{2+}	Cm^{4+}	Pu^{4+}
Fe^{2+}	Am^{4+}	Am^{3+}
K^{+}	Y^{3+}	Y^{3+}
Cs^{+}	REE^{3+}	REE^{3+}
Rb^{+}	Na^{+}	Sr^{2+}
Na^{+}		Na^{+}

Table 2.18[65]

Microprobe Analysis of SYNROC C[a] (Weight Percent)

	"Hollandite"	Perovskite	Zirconolite	Pseudobrookite
TiO_2	68.2	54.5	47.4	52.6
Al_2O_3	10.4	1.2	3.6	47.4
CaO	0.3	33.7	14.6	0.8
ZrO_2	0.4	0.6	23.4	0.4
BaO	20.8	1.3	0.2	2.4
NiO	0.2	--	--	--
Cs_2O	1.0	--	--	--
SrO	--	2.0	1.0	--
UO_2	0.2	2.8	3.8	--
REE	--	2.0	2.0	--
	101.5	98.1	97.0	103.6

[a] Sample was hot pressed in graphite dies at 13000°C for one hour; starting material was made by coprecipitation from a molten urea solution. Powder was calcined at 600°C for 38 hours. Cs_2O, SrO and REE determined by EDS.

BEST DOCUMENT AVAILABLE

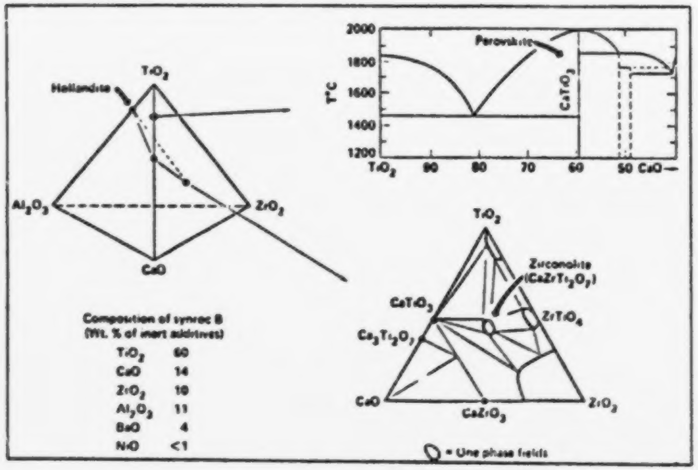
TiO2
Hollandite
Al2O3
ZrO2
CaO
2000
1800
1600
1400
1200
T°C
Perovskite
CaTiO3
TiO2
90
80
70
60
50 CaO —
TiO2
Zirconolite
(CaZrTi2O7)
CaTiO3
ZrTiO4
Ca3Ti2O7
CaO
CaZrO3
ZrO2
= One phase fields

Composition of synroc B
(Wt. % of inert additives)

TiO_2	60
CaO	14
ZrO_2	10
Al_2O_3	11
BaO	4
NiO	<1

Figure 2.4 Phase diagrams depicting the stability fields of titanate phases in SYNROC.[63]

Table 2.19[66]

Distribution of Principal HLW Elements Between Coexisting Phasis of SYNROC-D (Electron Probe Microanalysis)

Zirconolite	Perovskite	Spinel	Nepheline	Hollandite
U^{4+}	Na^{+}	Fe^{2+}	Na^{+}	Cs^{+}
Th^{4+}	Sr^{2+}	Ni^{2+}	K^{+}	Rb^{+}
Pu^{4+}	Pu^{3+}	Mn^{2+}	Rb^{+}	K^{+}
Cm^{4+}	Am^{3+}	Fe^{3+}	Ba^{2+}	Ba^{2+}
Am^{4+}	Cm^{3+}	Mn^{3+}	Cs^{+}	--
Np^{4+}	Np^{3+}	Al^{3+}	--	--
(ACT^{3+})[a]	REE^{3+}	Cr^{3+}	--	--
(REE^{3+})	(ACT^{4+})[a]	--	--	--
(Sr^{2+})	--	--	--	--

[a] ACT^{+3} = trivalent actinides.
ACT^{+4} = quadrivalent actinides.

Na_2O content, nepheline is the principal host phase for Cs which enters into solid solution with Na. Microprobe analysis of a SYNROC D formulation for a low Na composite sludge is given in Table 2.20.[64]

SYNROC D has been reported to exhibit wide flexibility with respect to the compositional variability of SRP sludges. For example, the stoichiometries of the principal titanate phases do not differ significantly, even though the three sludge compositions are appreciably different from one another. It is the spinel phase which accomodates an order of magnitude variation in the inert contaminants such as FeO, Al_2O_3 and NiO present in the three SRP sludge compositions.

Various processes are being employed for SYNROC fabrication. SYNROC can be produced by melting (1600°C), hot isostatic pressing (1100-1350°C) and by hot sintering (1000-1200°C). Of particular interest is the application of sol-gel technology developed for reactor fuel fabrication to SYNROC production. SYNROC microspheres and pellets of both B and D formulations have been prepared by the sol-gel process at ORNL.[67,68]

Table 2.20[64]

Microprobe Analysis of SYNROC D (Weight Percent)

	Hollandite	Perovskite	Zirconolite	Spinel
TiO_2	66.1	53.2	49.2	2.8
Al_2O_3	7.7	1.1	2.1	58.3
BaO	0.7	0.7	0.1	--
FeO	7.1	1.9	24.9	13.3
ZrO_2	3.1	0.3	24.9	--
CaO	4.1	32.9	11.4	0.1
MnO	2.7	1.4	1.1	4.5
Na_2O	0.1	0.2	--	--
NiO	3.2	0.2	0.5	21.0
UO_2	0.7	1.7	3.5	--
Cs_2O	1.0	--	--	--
SrO	--	2.5	1.0	--
REE	--	2.0	2.0	--
	96.5	98.1	97.2	100.0

SYNROC D samples have been prepared at LLL with SRP waste sludge ranging from 50 to 70% by weight. These samples have been tested for thermal and mechanical properties. Leach tests have been conducted on both monoliths and crushed material using static and dynamic methods. Effects of radiation damage on both natural and synthetic SYNROC titanate minerals have been studied. Preliminary data resulting from these investigations at LLL were presented at a recent meeting in Atlanta.[66]

Work on fabrication, characterization, and evaluation of SYNROC B and its constituent phases underway at ANL was also reported at the Atlanta meeting.[69]

Gel-derived spheres of SYNROC D consisting of up to 70% composite SRP sludge without Al removal have been synthesized at ORNL.[67,68] Compositions of SYNROC-B and SYNROC-D formulations, as reported at the Atlanta meeting,[68] are given in Table 2.21. Phase characterization data are being obtained. Leach data based on MCC-1 test have been reported. Tests to study mechanical strength and radiation stability have not been carried out yet. It should be pointed out that the main objective of ORNL group is to apply the sol-gel process to waste form development and the CVD technology to coat these waste forms with inert coatings. Since the external coatings determine the leach resistance, there is not much emphasis on characterization of the core material at this time.

Leach rates of SYNROC C and D fabricated at LLL, based on MCC-4 test at 75°C for both crushed and monolith samples, are presented in Table 2.22.[66] The discrepancy in the leach rates of crushed and monolith samples has been attributed to the differences in their reactive surface areas, not accounted for in normalizing leach data. The results are based on a 28-day test. Although the initial leach rates are not presented in Table 2.22, it has been reported that the leach rates generally decrease by more than an order of magnitude over the leach periods used ($\approx$30 days).

Comparison of leach rates of SYNROC C and borosilicate glass containing simulated high level commercial waste is displayed in Figure 2.5.[66] The results show that the SYNROC leach rates drop by more than an order of magnitude over a period of 20 days. In contrast, the glass leach rates remain constant over time. The long-term SYNROC leach rates are lower by two to three orders of magnitude as compared with those of glass.

Leach rates for gel-derived ORNL SYNROC B and D formulations, based on MCC-1 tests for 3 days, are given in Table 2.23.[68] For SYNROC B, all elements leached are below the analytical detection limits. In the case of SYNROC D, the leach rates vary in the range of 10^{-1} to 10^{-4} $g/m^2 \cdot d$.

2.3.3 Titanate Ceramic

This waste form was developed independently at Sandia Laboratories[70,71] and the Royal Institute of Technology in Sweden.[72] The immobilization process involves using sodium titanate based gels as inorganic ion exchangers for HLW dissolved ions. The loaded titanate ion exchanger is dried and isostatically hot-pressed into a largely crystalline dense ceramic. The waste radionuclides react with the titanate during hot-pressing to form low-solubility, mineral-like titanate and oxide phases, embedded in a rutile-form titania matrix. The highly resistant rutile-like matrix provides microstructural isolation of the radioactive phases. The primary containment of the waste radionuclides is provided by the titanate minerals. Table 2.24 gives a list of phases identified in the titanate ceramic produced at Sandia Laboratories. It is interesting to note that the rutile matrix occupies $\approx$50% of the volume of the waste form. In contrast, the other mineral phases occupy individually less than 10% of the overall sample volume.

Preliminary leach tests indicated that the silicate phase was selectively leached from the waste form. Current efforts at Sandia[73] focus on the elimination of silicate phases and on process simplification.

Table 2.21

Composition of Waste, Matrix, and Product*

Component	Synroc-B Product (wt %)	SRP[a] Waste (wt %)	SYNROC-D[b] Matrix (wt %)	SYNROC-D[b] Product (wt %)
Fe_2O_3	--	49.9	--	27.4
Al_2O_3	10.9	9.8	33.6	20.6
MnO_2	--	13.7	--	7.5
U_3O_8	--	4.5	--	2.5
CaO	13.8	3.7	10.3	6.7
NiO	--	6.3	--	3.4
SiO_2	--	1.2	15.8	7.8
Na_2O	--	7.0	--	3.8
Na_2SO_4	--	1.3	--	0.7
Ce_2O_3	--	1.1	--	0.6
Nd_2O_3	0.3	1.1	--	0.6
SrO	0.2	0.5	--	0.3
TiO_2	59.7	--	31.8	14.3
ZrO_2	9.8	--	8.5	3.8
BaO	4.2	--	--	--
Mo_2O_3	0.3	--	--	--
Ru_2O_3	0.3	--	--	--
Cs_2O	0.5	--	--	--

[a] Composite SRP waste with aluminum removal normalized to compensate for removal of zeolite and addition of Ce_2O_3, SrO, and Nd_2O_3.

[b] SYNROC-D (~70% wt % composite SRP waste without aluminum removal plus 30 wt % additives).

NOTE: Compositions based on assumption of complete recovery of all materials during gelation process.

*Adapted from Angelini et al.[68]

Table 2.22[66]

Lawrence Livermore Laboratory SYNROC-C and D Leach Rates ($g/m^2 \cdot d$)[a]

	SYNROC C		SYNROC D	
Element	Crushed[b]	Monolith	Crushed[b]	Monolith
Cs	3.4×10^{-1}	2.5×10^{-1}	1.2×10^{-2}	6.6×10^{-1}
Sr	2.6×10^{-2}	4.4×10^{-2}	5.4×10^{-2}	2.8×10^{-1}
Ca	1.0×10^{-2}	1.9×10^{-2}	1.9×10^{-2}	9.7×10^{-2}
Al	--	--	--	1.7×10^{-2}

[a] MCC-1, deionized water, 75°C, for 28 days.
[b] 150-300 μm.

Table 2.23[68]

ORNL Sol-Gel Particle Leach Rates ($g/m^2 \cdot d$)[a]

Element	SYNROC B	SYNROC D
U	--	4×10^{-3}
Zr	$<1 \times 10^{-3}$	3×10^{-3}
Cr	--	5×10^{-3}
Ti	$<1 \times 10^{-4}$	2×10^{-4}
Sr	$<5 \times 10^{-3}$	5×10^{-1}
Ca	$<5 \times 10^{-3}$	2×10^{-2}

[a] Based on MCC-1 tests: deionized water, 90°C, 3 days.

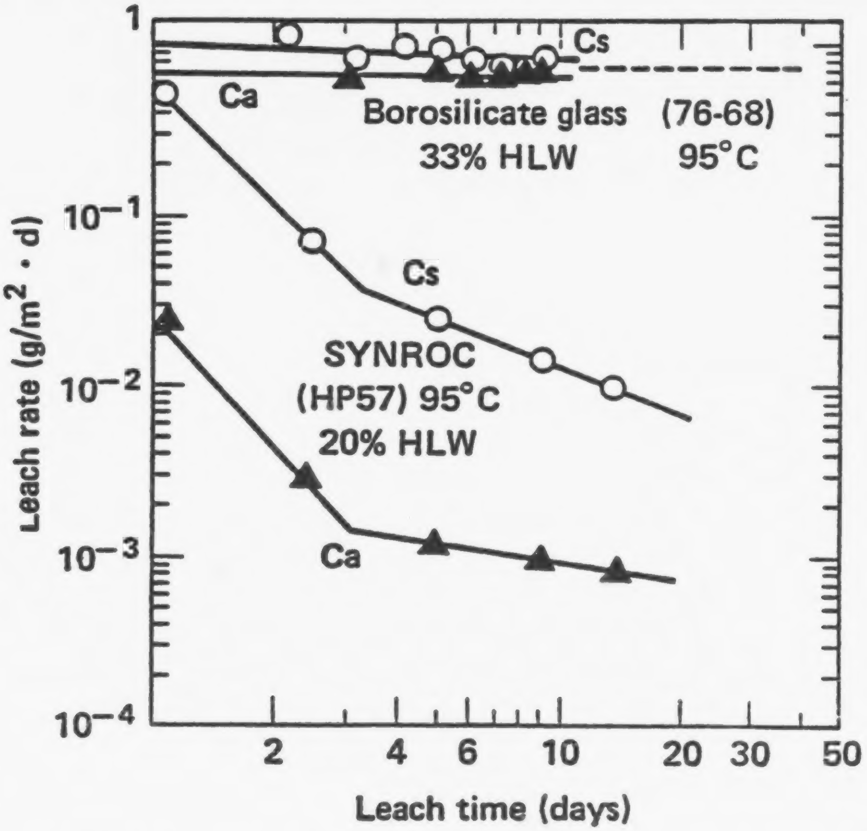

Figure 2.5 Leach rates of SYNROC and borosilicate glass.[66]

BEST DOCUMENT AVAILABLE

Table 2.24[71]

Primary Containment Phases Identified[a] in Sandia Titanate-Ceramics

Phase	Energy Dispersive Elemental Analysis	Volume Fraction
TiO_2 (Rutile)	Ti	50%
Amorphous Silica (SiO_2)	Si (Trace U,Ti,Al,Na)	5%
$Cs_2O \cdot Al_2O_3 \cdot 4SiO_2$ (dehydrated pollucite)	Si,Al,Ca (Trace Ti,Rb)	1%
$Gd_2Ti_2O_7$	Ti,Gd (Some U,Nd) (Trace Zr,Y)	10%
Elemental Mo	Mo (Trace Fe,Ti)	5%
Elemental Pd	Pd (Some Te and Ti) (Trace Fe,Mo)	2%
Cubic-ZrO_2	Zr (Trace U,Si)	5%
Amorphous Zeolite, (Na,Cs) Alumino-Silicate	Na,Cs,Al,Si (Trace Ti,U,Fe,Mo, Gd,Sr)	10%

[a] At least eight more distinct phases have been detected by electron diffraction and/or x-ray energy dispersive analysis. These have not been identified, but most appear to be titanates.

The modified titanate process involves reacting an acid simulant of the high level waste solution with a calcium titanate ion exchanger which fixes the waste nuclides. The product is then calcined at 600-800°C, followed by hot pressing at 1275°C and 1000 psi to give a dense titanate ceramic. The resultant end product is reported to contain five generic mineral phases: rutile (40-50%), zirconolite (15-20%), perovskite (about 30%), metallic solid solutions, and a multi-cation titanate phase isostructural with hollandite. Although the mineral assemblage of this titanate ceramic is remarkably similar to that of SYNROC formulations for commercial wastes, the Sandia process is relatively straightforward as compared with the complex SYNROC process proposed by Ringwood. Lower processing temperatures have been achieved by the addition of boron. The Fe-FeO equilibrium is used to control the oxygen fugacity during atmospheric pressure sintering.

2.3.4 High Alumina Ceramic

Like the Swedish and Sandia titanate ceramics, the high alumina ceramic consists of radionuclide containing phases which are protected from groundwater attack by highly inert, impermeable, encapsulating phases, free of radionuclides.

In contrast to the SYNROC and supercalcine ceramic processes where additives are used to alter the waste composition so that a specific mineral assemblage is obtained to host the fission products and actinides, the high alumina ceramic process takes advantage of the existing chemical composition of the waste to minimize the required tailoring and hence reduce the number of processing steps. Based on alumina tailoring, this ceramic process utilizes the high concentrations of alumina present in the defense nuclear wastes and is specifically developed for the immobilization of SRP defense wastes at Rockwell International Organizations.[74,75,76]

The high alumina ceramic is fabricated by reactive hot pressing at 1200-1300°C and consists principally of four crystalline phases: corundum, spinel, magnetoplumbite, and uraninite. The magnetoplumbite phase is known to have diverse crystal chemistry to accommodate most of the radionuclides in the SRP wastes while the uraninite phase hosts U, Th, and Zr. The highly leach resistant corundum and spinel phases, forming the bulk of the ceramic waste form, provide microstructural isolation of both radionuclide containing phases, uraninite and magnetoplumbite. The mineralogical composition and the waste element distributions among the various minerals in the waste form as determined by x-ray spectroscopy are given in Table 2.25.[74,75] Almost all the inert contaminants are present in spinel and magnetoplumbite phases while the waste radionuclides are incorporated in uraninite and magnetoplumbite. Since the principal host phase, magnetoplumbite, is known to exhibit a wide range of solid solution, the high alumina ceramic process offers great flexibility in terms of immobilizing high alumina defense wastes of variable composition.

The tailoring step involves addition of sufficient rare earths and alumina to the waste to obtain spinels and magnetoplumbite. The presence of reducing conditions, provided by graphite dies during hot pressing, results in the formation of uraninite. Addition of alumina to the system, in excess of the amount required for the formation of spinel and magnetoplumbite, results in the crystallization of corundum which together with spinel serves as an encapsulating matrix phase. The nature and amounts of inert encapsulating phases in the resultant waste form are a function of such variables as the waste composition, the inert additives, the waste loading and the consolidation process. For example, addition of titania, together with alumina, leads to the formation of pseudobrookite $(Fe, Al)_2 TiO_5$, a highly leach resistant, encapsulating phase compatible with magnetoplumbite, spinel, uraninite, and corundum.

Table 2.25[74,75]

Mineralogy and Waste Element Distribution

	Nominal Composition	Elements Detected
Principal Phases		
Spinel	(Mg, Fe, Ni, Mn) (Al, Fe_2O_4)	Al, Mn, Fe, Ni, Ti, Trace Mo, Si
Uraninite	UO_2	U, Trace Zr, Th
Magnetoplumbite	$XY_{12}O_{19}$ where X = Ca, Sr, Ba, $RE_{0.5} + Na_{0.5}$, etc. Y = Al, Fe, Ti, Si, Mn	Al, Mn, Fe, Ni, La Na, Ca, Ti, Trace Sr,Cs,Ba,Si,Mo, Ce, K
Phases Present With Excess Tailoring		
Corundum (Excess Al_2O_3)	Al_2O_3	Al, Trace Fe, Ti
Perovskite (Excess REO)	RE(Al, Fe)O_3	La, Al, Fe, Trace Ca, Na, Ce
Pseudobrookite (Excess TiO_2)	$(Fe, Ti, Al)_2TiO_5$	Fe, Ti, Al

Titania has been reported to be a useful sintering aid in alumina systems, providing a 100-150°C reduction in reactive hot pressing temperature. In the presence of high Na content in SRP sludge, the silica is included in the tailoring additives so that nepheline is formed, serving as an inert matrix phase. Further details of the tailoring additives for the three SRP waste compositions are given in Table 2.26.[77]

The natural analogues of the minerals present in high alumina ceramic waste form are known to be highly resistant to weathering under extreme geologic conditions as evidenced by occurrences of natural placer deposits consisting of an analogous alumina-spinel-hibonite (magnetoplumbite-thoria) assemblage in Fort Dauphin, Malagasy.[74,76]

At present, research at Pennsylvania State University and Rockwell Energy System is directed at optimizing the tailoring formulation for high waste loading in SRP sludge. The current SRP Defense Waste Processing Facility (DWPF) plan is to concentrate Cs^+ present in the HLW supernate on a zeolite. The loaded zeolite, when reduced to the proper size, can be readily incorporated into the ceramic waste form such as high alumina ceramic.[76]

Table 2.26[77]

Tailored Ceramic Formulations
for SRP Waste Compositions (wt %)

Components	High Fe		Composite		High Al
● Waste Calcines	25.0	50.0	30.0	65.0	90.0
● Tailoring Additives					
● Alumina	66.5	44.0	60.5	28.9	--
● Rare Earth Oxides	6.7	0.3	8.2	0.3	7.5
● Silica	--	4.1	--	5.3	--
● Zirconia	0.8	1.6	0.3	0.5	0.5
● Titania	1.0	--	1.0	--	2.0

Leaching studies, tests for radiation and thermal stability, phase characterization, and process assessment have been conducted. Preliminary data resulting from these studies have been reported.[77]

Comparison of leach rates of high alumina ceramic with 76-78 borosilicate glass is given in Table 2.27.[77] The leach rates are based on MCC-1 tests, lasting for a period of 28 days. Relative to glass, the ceramic leach rates are 10 to 100 times lower. Except U and Na, the elements measured are all below their analytical detection limits. Na release has been attributed to the dissolution of nepheline in the ceramic and is comparable to the Na release for glass. Leach rates of the constituent phases of high alumina ceramic are given in Table 2.28. Thermal tests showed the ceramic to be stable up to a temperature of 1200°C.[77]

2.4 Metal Matrices

Most waste forms can be embedded in a metal matrix to increase thermal conductivity, decrease leachability, and to reduce dispersability. Encapsulation of solid radioactive wastes in a continuous metal matrix has been described in detail.[78] A Belgian group at Mol was the first to develop this waste form and the process.[79] They were successful in embedding both crystalline and glassy beads in the lead matrix, where the metal phase occupies the void spece between the solid waste particles. A joint Belgian-German program, under way at Eurochemic/Mol, Belgium, involved a pilot-scale demonstration of encapsulation of phosphate glass beads in a lead alloy.[80]

Table 2.27[77]

Leach Rates of High Alumina Ceramic and 76-68 Glass ($g/m^2 \cdot d$)

Element	76-78 Borosilicate Glass	High Alumina Ceramic
Cs	1.8 - 3.6	$<1.0 \times 10^{-1}$
Sr	1.8×10^{-1}	$<3.5 \times 10^{-3}$
U	--	7.8×10^{-3}
REE	7.0×10^{-4}	$<3.5 \times 10^{-4}$
Al	--	$<3.5 \times 10^{-3}$
Fe	7.0×10^{-4}	$<3.5 \times 10^{-4}$
Na	2.4	2.3
Si	4.6×10^{-1}	--

[1] Based on MCC-1 test: static, deionized water, 90°C, 28 days.

Table 2.28[77]

Dissolution Rates of Individual Phases in High Alumina Ceramic

Phase	Leach Rate ($g/m^2 \cdot d$)
Spinel	$<10^{-3}$
Magnetoplumbite (Ion Exchange Mechanism)	$<10^{-1}$ Cs^+; $<10^{-4}$ Structural Elements
Corundum	$<10^{-3}$
Uraninite	8×10^{-3}
Nepheline	10^{-1}
Pollucite	5×10^{-2}

Embedding methods of solidified waste in metal matrices developed in Austria have been described by Neumann.[81] Domestic research and development efforts on metal encapsulation have been done at Idaho National Engineering Laboratory (INEL), Pacific Northwest Laboratories (PNL), and Argonne National Laboratory (ANL). Penetration of molten metal into the interstitial void space is achieved using the vacuum casting technique. Further details of the metal encapsulation process are given elsewhere.[78]

Wald et al. summarized the PNL research and development efforts on metal matrix encapsulation of waste forms at a recent HLW Technical Review meeting in Atlanta.[82] The various materials being studied at PNL for encapsulating glass beads and pelletized supercalcine ceramic are listed in Table 2.29. Phase characterization data for matrix waste forms are given in Table 2.30. The waste types and loadings considered in the PNL study of glass and supercalcine ceramic encapsulation in metal matrices are given in Table 2.31.

Leach resistance data for matrix encapsulated glass and supercalcine ceramic, based on MCC-1 test, have been reported.[82] Radiation and thermal stability and mechanical impact behavior have also been studied.

Encapsulation of coated and uncoated glass and supercalcine ceramic in metal matrices on a one-liter scale has been demonstrated at PNL (see Table 2.32).[83] Direct casting of glass marbles in a lead matrix has been achieved at ANL on a 2" diameter x 2' high canister scale.[84]

A process, developed at Oak Ridge National Laboratory, is designed to immobilize commercial and defense high level wastes as micron-size particles of oxides or crystalline host phases uniformly dispersed in a Fe-Ni base alloy matrix.[85] The metal matrix is composed of hydrogen-reducible metals already present in the waste or added to formulate an alloy composition. The resultant cermet waste form is reported to possess high thermal conductivity which permits relatively high waste loadings. Kobisk et al.[86] have reported that the cermet process has significant advantages over other waste fixation processes in that it uses existing technology; most of the steps involved in the process have been conducted in hot cell facilities; the urea treatment offers a very little loss of radionuclides during processing.

Actual Thorex waste from Nuclear Fuel Services and real sludge and acid wastes for the SRP are reported to have been successfully converted to cermets using in-cell batch processing. In addition, INEL calcines have been immobilized as cermet bodies. The maximum processing temperature is about 1100°C.

The waste loadings in cermet formulations have varied from 2 to 75% by weight. The ceramic and metal phase loadings vary from 20 to 50 wt % and 50 to 80 wt %, respectively. The metal matrix is composed of 70% Fe, 20% Ni, 5% Cu, and 5% other reducible metals derived from the waste such as technetium, ruthenium, and Pt metals. Process related cermet characteristics are listed in Table 2.33. The existing DOE contaminated stockpiles of 1600-2600 metric tons of nickel have been proposed as a possible source for nickel additive required in the ceramic formulation.[87]

Table 2.29[82]

Laboratory Scale Matrix Test Sample Configuration

Waste Form
● 76-68 Glass Beads: 6 mm Dia.
● SPC-4E Disc Pelletized Supercalcine: 8 mm Dia.

Matrix/Waste Form Composite

Matrix Materials	Specimen Shape
Pb; Pb-10% Sn; Al-12% Si	28 mm d x 45 mm h
Ti-6% Al-4% v; TiO_2; ZrO_2	22 mm d x 28 mm h
Graphite	16 mm d x 64 mm h
High Lead Glass Alumino-Silicate Glass	22 mm d x 28 mm h
Portland Type II Cement Refractory Castables	28 mm d x 40 mm h

Table 2.30[82]

Phase Characterization Data For Matrix Waste Forms

Waste Material	Crystalline Phases	Volume Fraction	Density	Porosity
76-68 Glass	(Vitreous)	96-100%	2.98 g/cm^3	<1%
SPC-4E Supercalcine	$Ca(RE)_8(SiO_4)_6O_2$	35%	3.9 g/cm^3	25%
	$Ce,Zr...)O_2$	20		
	(Sr,Ba,Ca) MoO_4	15		
	$(RE)PO_4$	10		
	(Uncrystallized)	15		

Matrix Materials	Matrix Crystalline Phases	Volume Fraction Waste Load	Matrix Density (g/cm^3)	Matrix Porosity
Lead	Pb	64%	11.34	0
Ti-6% Al-4%V	α/γ Ti Metal Sol S	50	4.37	2%
7570 Glass	(Vitreous)	50	5.42	0
1720 Glass	(Vitreous)	50	2.52	0
Graphite	C	50	1.5	33%
HP-Ti$)_2$	Rutile	50	4.21	0
HP-ZrO_2	ZrO_2(Cubic)	50	6.03	2%
Alfrax-66	NA (Al_2O_3 Base)	64	2.42	30%
Cotronics-919	NA (MgO Base)	64	2.76	24%
Type II Portland Cement	$Ca(OH)_7$ Ca_3SiO_5	64	1.78	45%

Table 2.31[82]

Radionuclide Containment for Matrix Waste Forms

	Cast Matrix Monolith*	Hot Pressed Matrix Monolith**
Commercial Waste		
Glass (76-68)	3.35 Ci/cm^3	2.58 Ci/cm^3
Ceramic (SPC-4E)	9.93 Ci/cm^3	7.66 Ci/cm^3
Defense Waste		
Glass (TDS-211)	0.26 Ci/cm^3	0.20 Ci/cm^3
Ceramic (MB-1)	0.58 Ci/cm^3	0.46 Ci/cm^3

*64 vol % Waste Cores.
**50 vol % Waste Cores.

Table 2.32[83]

Multibarrier Waste Form Development, One Liter Demonstration

Inner Core	Coating	Matrix	Encapsulation
72-68 Glass 10 mm Marble	None	Pb-10% Sn	Vacuum Cast, 400°C
Supercalcine 7 mm	None	Al-12% Si	Vacuum Cast, 650°C
Supercalcine 7 mm	Glass Glaze, <1mm	Al-12% Si	Vacuum Cast, 650°C
Supercalcine 2 mm	CVD PyC - 40 μm Al_2O_3 - 60 μm	Cu	Gravity Sintered, 900°C - 8 hr

Table 2.33[87]

Process Related Cermet Characteristics

Waste loading	2-75 wt%
Waste volume reduction	1:1-100:1
Ceramic phase loading	20-50 wt%
Metal phase loading	50-80 wt%
Metal phase composition	70% Fe, 20% Ni, 5% Cu, 5% misc.

Cermet is reported to possess extremely high density, high thermal conductivity, and high impact resistance. The cermet alloy matrix is also highly resistant to corrosion. The range of values for the various cermet properties is given in Table 2.34. Cermet has been considered the prime candidate for a waste form for a space disposal option. Kobisk et al[87] have suggested immobilizing fresh waste into the cermet form for above-ground storage to cool, thus precluding the present practice of interim tank storage in a liquid slurry form.

Leach rates for SPC-4 supercalcine and 76-78 borosilicate glass encapsulated in various matrices are given in Table 2.35. These matrix encapsulated waste forms were tested at PNL using the MCC-1 test. Preliminary results show that 100% Pb matrix is optimum for glass marble and that graphite and hot-pressed TiO_2 and Ti-6% Al-4%V matrices are optimum for ceramic pellets. Non-metallic matrices such as concrete, castables, and hot-pressed glass are not acceptable due to their high permeability and matrix dissolution rates. Estimated matrix material corrosion rates, based on composite leach test using MCC-1, are compiled in Table 2.36. The results show that TiO_2 and Ti-6% Al-4%V have the lowest corrosion rates in deionized water at 90°C. Minimum matrix thicknesses required to provide 1000 year containment are calculated to be 5.1×10^{-12} cm for Ti-6% Al-4%V and 3.0×10^{-4} cm for TiO_2.

Thermal conductivities for 76-68 simulated waste glass and waste glass beads encapsulated in various metal matrices are given in Table 2.37. The results indicate that encapsulation of glass beads in metal matrices increases the thermal conductivity by a factor of 10 to 200.

Mechanical impact behavior of unencapsulated and encapsulated supercalcine and glass in metal matrices has also been tested.

Table 2.34[87]

Typical Cermet Property Ranges

Density	6.0-8.2 g/cc
Thermal conductivity	3-20 W/m · °C
Decay heat loading	0.02-0.2 W/cc
Oxidation	
8 hr - 500°C air	2 μm thick oxide layer
2 hr - 800°C air	5-7 μm thick oxide layer
Thermal shock (2 cm diameter cylinders)	
3 cycles: 900°C water quench	No damage detected metallographically
Leach rate	
Soxhlet test (72 hr)	7.1×10^{-6} $g/cm^2 \cdot d$, 0.024% Cs loss

Table 2.35

Matrix Encapsulated Waste Form Leach Rates

	Leach Rates (g/m^2-d)[a]					
				SPC-4E in		
Element	Glass 76-68	Glass 76-68 in 100% Pb	SPC-4E	Graphite	TiO_2	Ti6 Al-4V
Cs	0.82	0.02	0.26	<0.14	0.22	<0.351
Mo	0.11	0.03	1.30	0.09	6.90	5.00
Na	0.80	0.03	2.10	0.87	19.00	9.20
Si	0.78	0.01	0.93	0.07	0.12	0.07
Sr	0.71	<0.01	0.50	0.01	<0.01	0.46

[a] Static leach test: 90°C - 14 day, SA/V = 10 m^{-1}, deionized water.

Table 2.36

Estimated Matrix Material Corrosion Rates from Composite Leach Tests[a]

Matrix Material	Estimated Corrosion Rate	Thickness for 1000 yr Barrier
Ti - 6% Al - 4% V	$<5.11 \times 10^{-11}$ μm/yr	5.11×10^{-12} cm
TiO_2	$<3.03 \times 10^{-3}$	3.03×10^{-4}
Pb - 10% Sn	9.19	0.919
Al - 12% Si	18.1	1.81
1720 Glass	80.7	8.07
100% Pb	1259	125.9
7570 Glass	1279	127.9

[a] Static Leach Test: 90°C-14 day, SA/V = 10 m^{-1}, Deionized H_2O.

Table 2.37

Thermal Conductivity of Matrix Waste Forms

Material	Thermal Conductivity at 100°C (W/mK)
76-68 Simulated Waste Glass	0.75
Lead	34
50 vol% 6 mm Glass Beads in Pb	8.5
50 vol% 6 mm Glass Beads in Al - 12% Si	68
Al - 12% Si	190

2.5 Coated Particles

Coated particles represent a composite waste form consisting of a radionuclide-containing core coated with single or multiple layers of one or more inert materials. The inner core can be a glassy or a crystalline waste form. The individual waste form particles can be coated with ceramic materials such as Al_2O_3 or SiO_2; carbonaceous materials such as pyrolitic carbon (PyC), Cr_7C_3, or SiC; glass such as borosilicate or aluminosilicate glasses; or metal such as Ni, Si or Fe. These coated particles can be further protected by embedding them in a metal matrix. The resultant system is a waste form which provides improved leach and oxidation resistance and mechanical strength compared to a waste form without the coating.

Since chemical vapor deposition (CVD) has been demonstrated for coating fuel particles in a high-temperature, gas-cooled reactor (HTGR), the application of the existing CVD technology to coat waste forms was investigated at Batelle Columbus Laboratory (BCL), Oak Ridge National Laboratory (ORNL), and General Atomic Company (GAC).[88] Various coating materials produced by CVD in a fluidized bed have been evaluated at BCL. Materials successfully applied as coatings are listed in Table 2.38. One of the important considerations in the selection of candidate materials is low coating temperature, considering the potential volatility of Cs and Ru during processing.

Duplex coatings have also been studied at BCL. The inner coating and the overcoat for the various duplex coatings are given in Table 2.39. Based on preliminary work on duplex coatings, PyC and Al_2O_3 were identified as potential materials for further coating studies. PyC was selected as an inner coating because of its high leach resistance. The selection of Al_2O_3 as an overcoat over SiC or SiO_2 was based on its higher leach resistance than SiO_2 and the fact that SiC requires a deposition temperature of as high as 1400°C.[89] Process conditions for PyC and Al_2O_3 coating of supercalcine are given in Table 2.40. A PyC/Al_2O_3 duplex CVD coated supercalcine, consisting of a 50 μm thick Al_2O_3 overcoat and a 32 μm thick inner coating of PyC with an intermediate Al_2O_3 reaction zone between the two coatings, has been fabricated at BCL and tested at PNL. Besides the CVD coating procedure, thermal plasma spraying is being investigated at PNL using Ni/Cr, Al_2O_3; and Cr_7C_3 coatings on glass and supercalcine.[80]

The coated particle technology developed by GAC for their HTGR's has been applied to coat waste forms as well. In-house studies at GAC have focused on pyrolytic carbon and PyC/SiC coatings on supercalcine. Glass was not studied since the lowest coating temperature (1100°C) is sufficient to soften the glass. At 1100°C they found that there was a chemical interaction between the coating and supercalcine which caused permeability. Very recent work has resulted in a proprietary process in which the coating temperature has been reduced to 750°C. Using this, GAC believes that impermeable coatings can be deposited on supercalcine, SYNROC, and, possibly, glass.

Some of the major drawbacks of the high-temperature CVD coating process include[89]: (a) volatile components such as Cs and Ru are mobilized and trapped in the coating and subsequently leached out; (b) particle diameters are limited to 2 mm or less; and (c) waste forms are limited to ceramics

Table 2.38[88]

Coatings Applied in a Fluidized Bed
to Particles in the 200 μm Range

Coating	Reactants	Deposition Temperature, °C
Ni	$Ni(CO)_4$	170 to 230
Mo/MoC	$Mo(CO)_6$	350 to 450
C	C_2H_2	800 to 950
Fe	$Fe(CO)_5$	180 to 200
Si	$SiHCl_3+H_2$	500 to 800
Cr_7C_3	$Cr(C_9H_{12})_2$	500
SiC	$CH_3SiCl_3+H_2$	1100
Cr_2O_3	$CrO_2Cl_2+H_2O+H_2$	550 to 650
SiO_2	$SiCl_4+H_2O+H_2$	700 to 800
Al_2O_3	$AlCl_3+H_2O+H_2$	600 to 900

Table 2.39[88]

Duplex Coatings Applied in a Fluidized Bed
to Particles in the 200 μm Range

First Coating	Overcoat
Ni	Cr_7C_3
Cr_7C_3	Ni
Al_2O_3	C
Fe	Al_2O_3
Ni	Si
C	SiC
C	Al_2O_3

Table 2.40[88]

Conditions for PyC and Al_2O_3 Coating of Supercalcine

Coating	Core Diameter	Reactor	Temperature	Reactants	Coating Rate
PyC	1-5 mm	Fluidized Bed (ZrO_2 difuent)	1100° to 1200°C	C_2H_2	1-3 μm/min
Al_2O_3	1-2 mm	Vibrated Bed	1000° to 1100°C	$Al+HCl+CO_2+H_2$	4 μm/hr
Al_2O_3	3-5 mm	Drum Coater	1100°C	$Al+HCl+CO_2+H_2$	NA[b]
Al_2O_3[a]	1-2 mm	Vibrated Bed	550° to 1050°C	$Al+HCl+H_2O$	NA[b]

[a] Applied as intermediate coating between PyC and dense Al_2O_3 duplex coating.
[b] Not Available.

because glass melts at high temperatures. Because of these problems, low temperature CVD coating procedures are being investigated. In Austria, a study of the coating of simulated HLW calcine granules with pyrolytic carbon(PyC) or nickel has been reported by Neumann and Kofler.[81,91] Using acetylene (C_2H_2) as carbon deposition source the coating temperature was depressed from the usual 1000°C range to 325-525°C. Nickel carbonyl, $Ni(CO)_4$, was used as a catalyzer and coating thicknesses of about 100 μm were obtained. This low temperature deposition process is highly desirable since it reduces fission product losses from the calcine by volatilization. In addition to the pyrocarbon deposition work, a study of the deposition of nickel from the decomposition of $Ni(CO)_4$ was reported. "Acceptable" nickel coatings of approximately 45 m in thickness (a certain degree of coat cracking was observed) were also obtained from the thermal decomposition of $Ni(CO)_4$ at 200°C.

However, several questions arise concerning the "catalyzed" deposition of PyC. Since the process temperature for PyC deposition exceeds that for deposition of nickel from $Ni(CO)_4$, nickel may be codeposited with carbon. If so, the characteristics of the coating may be altered. Nickel could be in either a homogeneous solid solution or be dispersed heterogeneously through the carbon coating. Surface deposited nickel (or perhaps some nickel compound) may actually be the catalyst for C_2H_2 decomposition rather than $Ni(CO)_4$. If nickel is included in the pyrolytic carbon coating it is possible that it could detrimentally affect the leaching behavior. All the above uncertainties must be addressed in this type of coated particle work.

According to Oma[89], PNL has initiated the development of a PyC CVD coating procedure to coat large waste form particles (≈10 mm) at relatively low temperatures ranging from 400 to 500°C. Kilogram quantities of simulated waste glass marbles have been coated using this procedure. Coated and uncoated glass and supercalcine with various coating materials have been tested for leach resistance, thermal and radiation stability, and mechanical strength.[90]

At ORNL, the CVD fluidized bed coating process, developed for HTGR reactor fuel, is being applied for depositing coatings of PyC and SiC on gel-derived waste forms.[68,92] Spheres of SYNROC B and D (70% simulated SRP waste without Al removal + 30% additives), 70/30 (70% simulated SRP waste with Al removal + 30% SYNROC additives), 90/10 (90% simulated SRP waste with Al removal + 10% ZrO_2 additives), and a generic Cs-bearing waste form have all been sucessfully coated with PyC and SiC. Typical particle diameters and coating thicknesses are presented in Table 2.41. PyC coated SYNROC D has three coatings of PyC consisting of the inner dense layer, an intermediate, low density buffer layer, overlaid by an outer dense coating. The intermediate, low density carbon layer is designed to accommodate irradiation-induced volume changes in the waste and any gas generation. SiC coatings have also been applied to SYNROC B spheres at 1400 and 1500°C, temperatures at which the waste form kernel melted and penetrated the carbon buffer.

However, no reaction with the SiC coating was reported. Using a modified process, SiC coatings have been successfully deposited on 70/30, 90/10, SYNROC B and D spheres at temperatures in the range of 700 - 1000°C. The resultant coated particles have been tested for thermal stability and leach resistance.[68]

Leach test results for coated and uncoated particles reported by the ORNL group are given in Table 2.42, and displayed in Figure 2.6. Leach rates for various species of all coated waste forms are reported to be below the detection limits of ICP or atomic absorption.

Leach test results obtained at PNL for coated and uncoated SPC-4E pellets and TDS-211 glass marbles are given in Table 2.43. The results are based on MCC-1 leach tests on triplicate samples for 28 days at 90°C in deionized water. Extrapolated corrosion rates of metal coatings, based on MCC-1 test, reported by Oma et al[90] are given in Table 2.44. The lowest corrosion rate is reported for Cu coating deposited by thermal plasma spray. To ensure 1000 year containment, the minimum coating thicknesses required will vary from 4 μm for Cu deposited by plasma spray to 70 x 10^3 μm for Pb deposited by the wire gun process.

Table 2.41[92]

Typical Kernel Diameters and Coating Thicknesses

Waste Particle Type	Batch-Average Kernel Diameter, (μm) Typical	Batch-Average Kernel Diameter, (μm) Largest	Typical Coating Thickness (μm)
Synroc-B	600	890	110
Synroc-D	600	750	75
70/30	630		75
90/10	565	730	70
Cesium Waste Form	600		55

Table 2.42[92]

Leach Test Results for Coated and Uncoated Particles

Leach Rate [$g/(m^2 \cdot d)$]

Element	Detection Limit	Synroc-B Uncoated 3 d	PyC Coated Synroc-B 1 d	Uncoated Synroc-D 3 d	PyC Coated Synroc-D 3 or 7 d	Uncoated 70/30 3 d	Coated 70/30 3 d	Coated Cesium Waste Form 3 d
Fe	3×10^{-5}	3×10^{-4}	a	6×10^{-3}	a	7×10^{-3}	a	
Al	1×10^{-4}		a	2×10^{-2}	a	6×10^{-3}	a	
Mn	2×10^{-5}		a	1×10^{-3}	a	2×10^{-3}	a	
U	1×10^{-5}		a	4×10^{-3}	a	3×10^{-3}	a	
Ca	2×10^{-4}	2×10^{-2}	a	4×10^{-1}	a	5×10^{-2}	a	
Ni	4×10^{-5}		a	3×10^{-3}	a	2×10^{-3}	a	
Si	2×10^{-2}		a	7×10^{-2}	a		a	
Na	5×10^{-4}		a	1×10^{-2}	a	3×10^{-3}	a	
Zr	2×10^{-5}	9×10^{-5}	a	3×10^{-3}	a	2×10^{-4}	a	
Ti	5×10^{-6}	3×10^{-4}	a	2×10^{-4}	a	9×10^{-4}	a	
Ba	2×10^{-4}	4×10^{-3}	a		a		a	
Mo	1×10^{-3}	a	a		a		a	
Ce	4×10^{-4}	a	a	5×10^{-3}	a	4×10^{-3}	a	
Nd			a		a		a	
Sr	1×10^{-5}	4×10^{-4}	a	5×10^{-1}	a	8×10^{-2}	a	
Cs	1×10^{-3}							a

[a] Below detection limit.

Detection limit determined by averaging blanks submitted during test ($V_{sol}=20\ cm^3$, $t = 5\ d$, $SA = 75 \times 10^{-4}\ m^2$).

Leach test MCC-1; deionized H_2O; 90°C.

Table 2.43[90]

Leach Rates of Uncoated and Coated Supercalcine Pellets and Glass Marbles

Substrate	Coating(s)	Thickness (μm)	Process	Leach Rates ($g/m^2 \cdot d$)			
				Cs	Sr	Na	Si
SPC-4E Pellet	Uncoated	0	--	--	1.37	1.82	0.46
SPC-4E Pellet	Cr C /PyC/Cr C	1/20/4	CVD	--	0.15	0.30	0.05
TDS-211 Marble	Uncoated	0	--	23.4	2.6	18.8	12.8
"	Al	600	Plasma	0.02	<0.002	0.02	<0.0004
"	Al-6% Si	800	Wire	0.05	0.03	0.05	0.05
"	Pb	350	Wire	0.01	0.01	0.01	<0.0004
"	Sn alloy[a]	330	Wire	<0.003	<0.002	<0.0003	<0.0004
"	Zn	300	Wire	0.06	<0.002	0.12	<0.0004
"	Sn alloy/Zn	300/500	Wire	<0.003	<0.002	0.02	<0.0004

MCC-1 leach test on triplicate samples for 28 days at 90°C in deionized water. Surface area to volume ratio of 10 m^{-1}.

[a] Sn alloy composition: 88.75% Sn, 7.5% Sb, 3.5% Cu, 0.25% Pb.

Table 2.44[90]

Corrosion Rates of Metal Coatings[a]

Coating	Corrosion Rates (μm/year)
Cu Wire Gun	0.3
Cu Plasma Spray	0.004
Al Wire Gun	5
Al Plasma Spray	2
Pb Wire Gun	70
Sn Alloy Wire Gun	2
Zn Wire Gun	40

[a] Test: 14 days, 90°C, SA/V = 10 m^{-1}

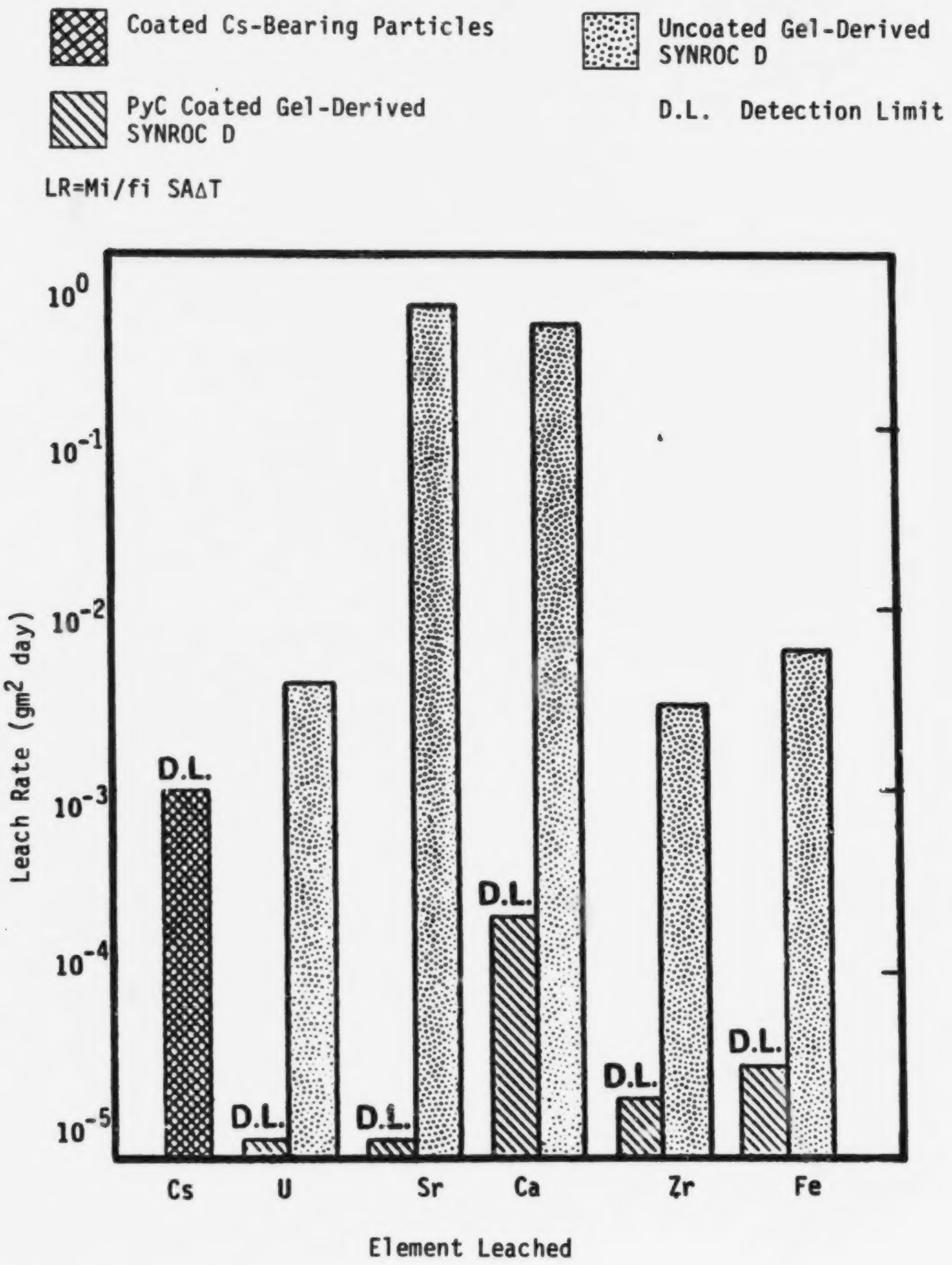

Figure 2.6 Leach rates of PyC coated gel-derived ceramic particles.[68]

BEST DOCUMENT AVAILABLE

2.6 Comparative Evaluation of Waste Forms

The most important factors considered in the evaluation of high level waste forms are

- Chemical Durability
- Thermal Properties
- Radiation Effects
- Mechanical Properties

Radiation stability of the various waste forms is discussed in Section 5. Waste form processing factors such as process safety and engineering practicality are not discussed in this report.

2.6.1 Chemical Durability

Chemical durability is the most important characteristic because it determines the nature, rate and extent of radionuclide release from a waste form, the source term for the entire high level waste repository system. Since the NRC criteria are expressed in terms of radionuclide containment and release over a period of time, the chemical durability data serve as a quantitative measure to identify those waste forms that are likely to meet independently the 1000 year containment criterion for the waste package and/or the 10^{-5}/yr controlled release criterion for the underground facility. In the sections below, we have attempted to evaluate, based on their leach rates, the waste forms that are the most leach resistant and also determine whether they have the potential to meet the NRC criteria.

2.6.1.1 Borosilicate Glass

The borosilicate waste glass evaluation is based on chemical durability data cited in Tables 2.5-2.7. At temperatures in the range of 70-150°C, most defense waste glasses have better leach resistance than the commercial glasses. Figure 2.7 displays the cumulative release of silicon versus time, based on MCC-1 28-day test, indicating that most defense waste glasses are approximately an order of magnitude more leach resistant than the commercial waste PNL 76-68 reference glass. Among the defense waste glasses, the SRL TDS-211 waste glass tested, however, exhibited increased silicon release. This can be attributed to its relatively lower silica content.

For most waste glasses, the fission products generally leach faster than the actinides. Depending on the experimental condition, the Cs leach rates can be higher or lower than the Sr leach rates, varying by not more than an order of magnitude.

An important parameter affecting the chemical durability of glass is temperature. For example, SRL Frit 131 exhibits a five-fold increase in

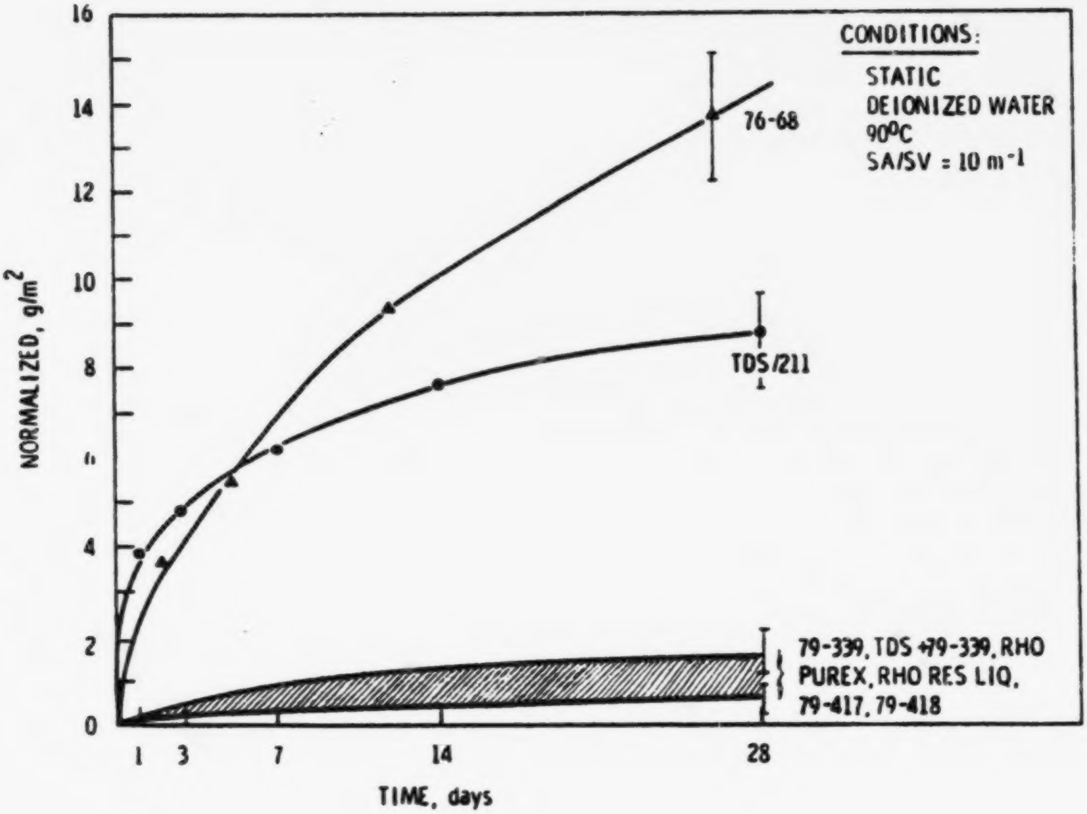

Figure 2.7 Cumulative silicon released vs. time at 90°C.[4]

BEST DOCUMENT AVAILABLE

leach rates with an increase in temperature from 25 to 90°C. Flow rates affect glass leach rates as well; an increase of one to two orders of magnitude in leach rates is observed at flow rates in the range of 2-70 m/y. With respect to the effect of solution chemistry, brine solutions generally result in lower leach rates when compared to DI water and silicate groundwaters. The solution pH is also important in that in the low and high pH regimes (pH = <5 and >9) the leach rates increase by up to two orders of magnitude.

2.6.1.2 Porous Glass Matrix (PGM)

Leach data for PGM High Alumina and PGM Composite core glasses at 70°C and under a range of flow conditions (Tables 2.9 and 2.10) show that at high and intermediate flow rates, the PGM core glasses are one to two orders of magnitude more leach resistant than the PNL 76-78 and SRL glasses. At low flow rates, representing nearly stagnant repository conditions, glass dissolution is controlled by silica solubility, the saturation pH of the system controlling the silica saturation levels. Since PGM core glasses do not exhibit a wide pH excursion and remain near neutral, their leach resistance is significantly greater than that of the other glasses.

Preliminary results of leach tests on PGM cladding glasses show that, at high flow rates, the leach rates are more than an order of magnitude lower than those for the core glasses. It was reported that the following time periods would be required to dissolve a 4 mm thick protective jacket of PGM cladding glass: 1.2×10^7 years at 70°C; and 1.2×10^4 years at 100°C.

Fully radioactive PGM composite core-clad glasses have been produced. Leach rates, based on core isotopes, are reported to be lower than 10^{-8} $g/m^2 \cdot d$. Estimated leach rates based on core exposure by fracture are 500 times lower than leach rates for bare core.

Estimates of fractional waste material loss, based on silica release at 70°C, from PGM High Alumina and PGM Composite core glasses and SRL and PNL 76-68 glasses as a function of flow rates, are given in Table 2.45.[18]

Table 2.45[18]

Fractional Waste Material Loss at 70°C(10^{-5}g/g·y)[a]

	Flow Rates (m/y)		
Core Glasses	70	2	0.1
PGM High Alumina	<0.36	0.09	-
PGM Composite	<1.00	0.17	0.16
SRL	50	11.4	>2.0
PNL 76-68	90	13.1	1.2

[a] Estimates based on silica release.

The results show that, at flow rates in the range of 2-70 m/y, the PGM core glasses exhibit material loss two to three orders of magnitude lower than the SRL and PNL glasses. Since the fractional material release is on the order of $<10^{-5}$/yr, it appears that PGM core glasses by themselves could meet the controlled release criterion, asssuming the silica dissolution rate to be comparable to that of the long-lived actinides. The above calculation is conservative because the high silica cladding will provide additional barrier. The high silica cladding glass is reported to exhibit at least an order of magnitude lower leach rate than the PGM core glasses. Since the cladding glass is free of radionuclides, the CUA workers estimate that a 4 mm thick protective jacket can provide containment of radionuclides in the core glass for time periods varying from 1.2×10^7 years at 20°C to 1.2×10^4 years at 100°C.[18] Based on their estimates, we believe that both NRC criteria of 1000 yr containment and controlled release of 10^{-5}/yr after the first 1000 years can be met by PGM core-clad composite.

2.6.1.3 Glass Ceramics

Based on their comparative leach tests, the Hahn Meitner Institute investigators reported that, compared to the glass systems, the glass ceramic waste forms exhibited no improvement in leach resistance.[51-54] Similar conclusions were reported by Rusin[56] for basalt glass and basalt glass ceramic. A PNL comparative test to study the leach resistance of a 76-68 glass, a celsian glass ceramic, and supercalcine SPC-5B shows no significant difference in their leach rates.

2.6.1.4 Crystalline Ceramics

The relative stabilities of reference glass, spent fuel, crystalline ceramic, and coated ceramic in silicate groundwaters and brine solutions under hydrothermal conditions are compiled in Tables 2.46 and 2.47.[93] The results clearly show the highly corrosive effect of brine on glass, spent fuel, and supercalcine ceramic. In contrast, the coated ceramic in contact with brine for a period of a month at 300°-400°C exhibited no release of even the most easily extractable elements such as Cs and Pb. In silicate groundwaters, the spent-fuel, glass, and supercalcine ceramic exhibited release of several elements. In addition, the glass matrix was completely altered. Coated ceramic and uncoated supercalcine ceramic exhibited no detectable alteration.

McCarthy et al.[93] presented results showing the hydrothermal reactivities of various waste forms such as supercalcine ceramics, duplex coated supercalcine pellets, SYNROC B and titanate ceramic in different types of solutions (Table 2.48). As mentioned above, the supercalcine ceramics in contact with brine solutions resulted in alteration of primary mineral phases such as pollucite and scheelite and release of substantial amounts of Cs and Sr. Monazite, however, one of the constituent minerals of supercalcine ceramic, was reported to remain unaltered. This observation is important in that monazite is the principal host mineral for the long-lived actinides and lanthanides. McCarthly et al.[94] have suggested monazite as a potentially ideal host for nuclear waste actinides. In groundwater and deionized water, supercalcine ceramic was found to be relatively inert with no degradation

Table 2.46[93]

Reactivity of Waste Forms in Silicate Groundwaters

Waste Form	Alteration of Solid	Elements in Solution
Spent Fuel (200°C)	Uranite (UO_2) Unaltered	Major Cs, Rb, Mo Trace U
Reference Glass (300°C)	Complete	Major Na, B, Mo, Cr, Minor Cs, Si, Ni, Rb, Ca Trace U, Ln, Sr, Ba
Current Crystalline Ceramic (300°C)	None(a)	Minor Na, Rb, Mo, Si Trace Cs, Sr, Ba, Ca
Coated Ceramic (400°C)	None	None

(a) Crystallinity of synthetic minerals enhanced, NCS phase crystallized.

Table 2.47[93]

Hydrothermal Reactivity Trends in Bittern Brine

Waste Form	Alteration of Solid	Elements in Solution
Spent fuel, 200°C	Not studied	Major* Cs, Sr, Ln,[†] Ba, Rb, U Minor* Mo
Reference glass (PNL-76-68), 200°C	Not crystallized Solid intact	Major Cs, Sr, Ln, B, Rb, Ba, Zn Minor U, Mo, Si, Ni Trace* Fe
Current crystalline ceramic (SPC-4), 300°C	Several minerals altered New phases formed Some are stable	Major Cs, Sr, Ln, Rb, Ba, Ni Minor Cr, Si Trace Fe
Coated ceramic 400°C	Some recrystallization of Al_2O_3 outer coating	No detectable Cs or Rb

*Major indicates > 10% of the amount originally in the solid; minor, 0.5 to 9.0%; and trace, < 0.5%.

[†] Ln is lanthanides (La, Ce, Pr, Nd, Sm, Gd, Y).

Table 2.48

Hydrothermal Stability Tests on Crystalline Waste Forms

Waste Form	Nature of the Test	Results
Supercalcine-Ceramics (SPC-2, SPC-4)	I. Groundwater typical of basalt and deionized water; 100, 200, 300°C/300 bars; 1-24 weeks	No degradation of primary containment phases, enhanced crystallization; only 0.5% of the Cs and 0.1% of the Sr in solution after 4 weeks
	II. Bittern Brine (Ca, Mg, K, Na Chlorides); 200, 300°C/300b; 1-4 weeks	Pollucite and scheelite phases altered; substantial Cs and Sr in solution
	III. Saturated Salt ("WIPP B") Brine; 250 and 350°C	Most Cs and a small amount of Sr (∼3%) in solution after 3 days at 350°C
Duplex Coated Supercalcine-Ceramic Pellets	Bittern Brine; 400°C/300b; 1-4 weeks	No sign of breach of coating; no detectable Cs in solution; Al_2O_3 outer coating recrystallizes
SYNROC B	I. Deionized water; 400-800°C/1000b, 1 day	No degradation of primary containment phases; no apparent loss of Cs or U from solids observable by electron microprobe
	II. Brine (10% NaCl); 400-800°C/1000b and 800, 900°C/5000b; 1 day	Same as above until 900°C where Cs extraction and alteration begins
Titanate-Ceramic	Various Brines	Rutile matrix resistant to degradation; dissolution behavior of primary containment phases not known

---

[a] All tests to date have been static tests in sealed noble metal capsules or sealed autoclaves.

of primary mineral phases. Slight amounts of Cs (0.5%) and Sr (0.1%), however, were released after 4 weeks of reaction time. For coated ceramic pellets, recrystallization of alumina outer coating was reported. However, no detectable release of Cs was observed. SYNROC B was found to be inert in deionized water under hydrothermal conditions. In brine solution, SYNROC B remained unaltered until 900°C at which Cs extraction and phase alteration began. Presumably, it is the hollandite phase, the mineral that hosts Cs, which undergoes alteration in SYNROC B. Reaction of Sandia titanate ceramic with various brine solutions under hydrothermal conditions produced no degradation of the rutile matrix. However, information on the dissolution behavior of the mineral phases is lacking.

Braithwaite and Johnstone reported results of matrix alteration and cation solubilization after leaching Sandia Copper borosilicate, a supercalcine, and a titanate ceramic (Table 2.49).[95] Overall the titanate ceramic exhibited better resistance to attack in terms of both matrix alteration and Cs release. In contrast, the glass showed maximum matrix alteration.

A. SYNROC

Comparision of leach rates of SYNROC C and borosilicate containing simulated high level commercial waste based on tests at 95°C conducted at the Australian National University show that SYNROC leach rates drop by more than an order of magnitude over a period of 20 days, while glass leach rates remain constant. Compared to glass, the long-term SYNROC leach rates are lower by two to three orders of magnitude.

Comparative leach testing of SYNROC and borosilicate glass containing the same simulated waste over a temperature range of 45-300°C has been conducted at the Australian Atomic Energy Commission.[96] To avoid saturation effects, a dynamic leach test method was used where the leachant was replenished daily to simulate groundwater circulation. Figure 2.8 shows cumulative Cs and Si, the most leachable elements, leached from SYNROC and two borosilicate glasses by deionized water at 100°C, indicating that the long-term cumulative release of Cs and Si from SYNROC is more than an order of magnitude less than that from PNL 76-68 glass. Secondly, with increasing time, the SYNROC leach rates drop off more rapidly than those of the glasses. The thermal dependence of initial leach rates of SYNROC and borosilicate glass is depicted in Figure 2.8.[96] The results show that although the leach rates for SYNROC and the glass increase with increasing temperature, the increase exhibited by SYNROC is markedly smaller than that for the glasses, with the difference in leach rates of SYNROC and the glasses becoming more pronounced at higher temperatures . Further, the SYNROC matrix elements such as Al, Ba, Ti, and Zr are reported to be very resistant to leaching.

Both crushed and monolith samples of SYNROC C and D formulations fabricated at LLL have been tested for leach resistance using MCC-4 test at 75°C (Table 2.27).[66] The leach rates generally decrease by more than an order of magnitude over a period of $\approx$30 days.

Table 2.49[95]

Matrix Alteration and Cs Solubility After Leaching of Copper Borosilicate Glass, Supercalcine, and Titanate Ceramic[a]

Leachant	Copper Borosilicate Glass		Supercalcine		Titanate Ceramic	
	% Altered	% Solubilized Cs	% Altered	% Solubilized Cs	% Altered	% Solubilized Cs
D. I. Water	75	12	12	4	10	4
NaCl Brine	13	1	17	14	2	5
Mg^{2+} Brine	50	5	4	7	2	4
Seawater	49	8	6	1	ND	ND

---

[a] At 250°C, 17.9 MPa, and 90 days

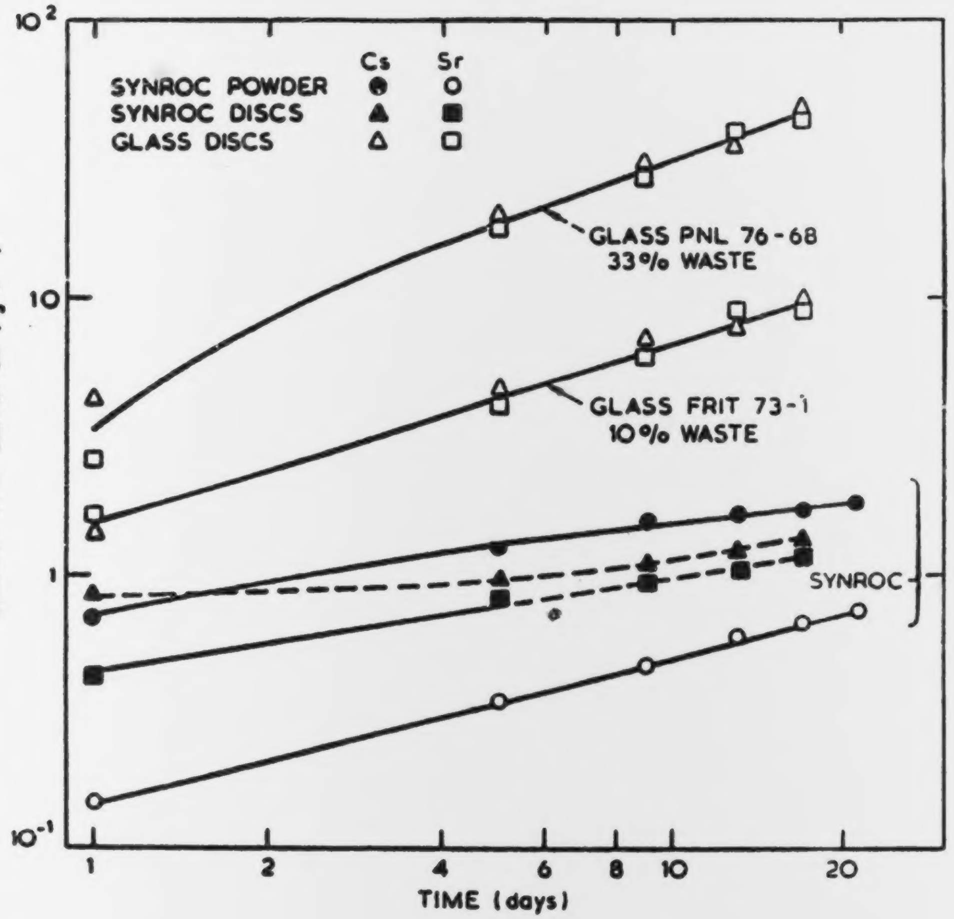

Figure 2.8 Cumulative quantities of cesium and strontium leached from SYNROC and borosilicate glasses.[96]

(Leachant: Deionized water replaced daily. Temperature: 100°C. For discs: Leachant volume/area = 0.1 m. For 100-150 mesh powders: Leachant volume/geometric surface area = 0.0017 m .)

BEST DOCUMENT AVAILABLE

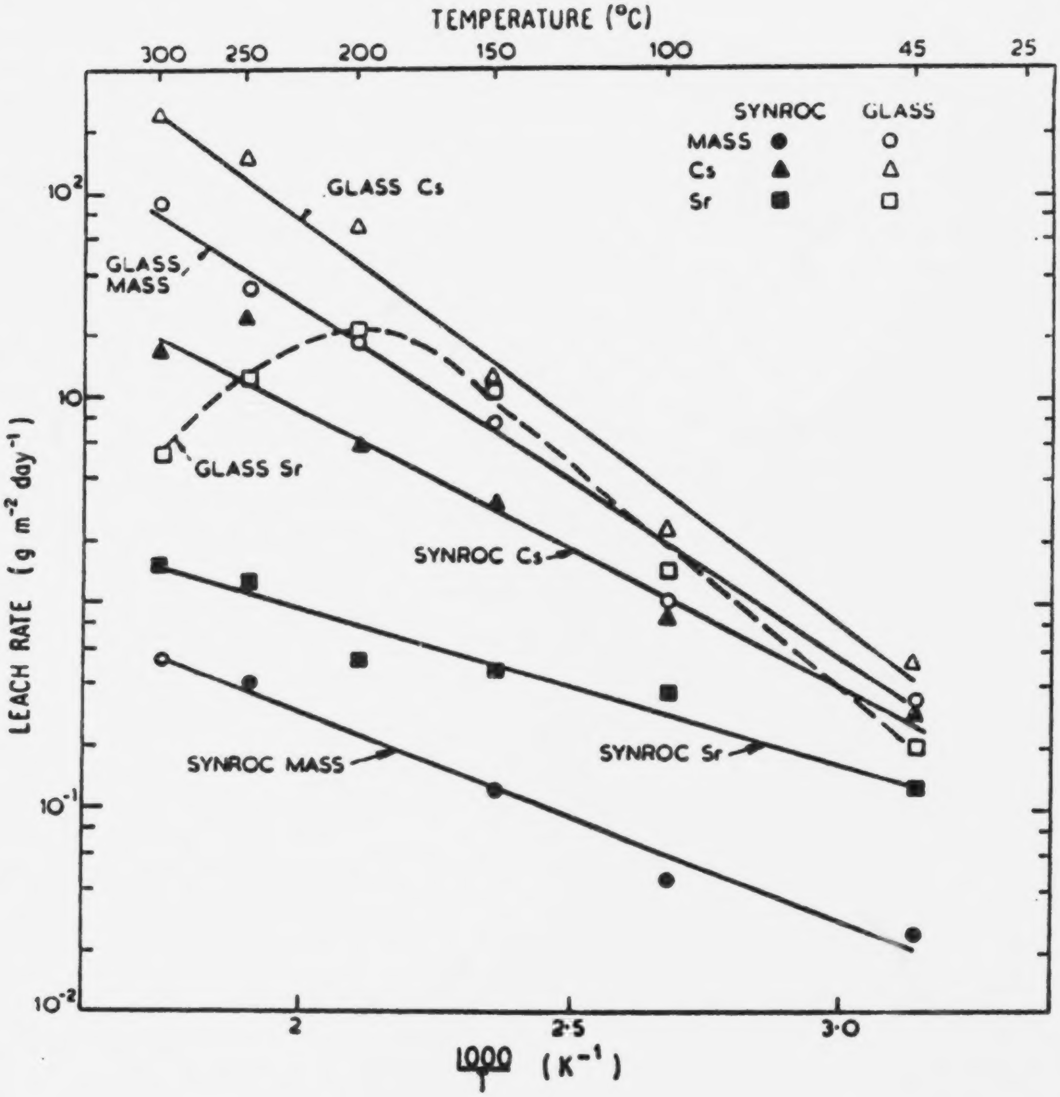

Figure 2.9 Effect of temperature on initial leach rate of SYNROC and borosilicate glass (PNL 73-1) containing 10 weight % simulated radwaste.[96]

(Leachant: deionized water. Leaching time: 1 day. Leachant volume/sample surface area = 0.1 m.)

BEST DOCUMENT AVAILABLE

Based on thermodynamic factors, there have been some questions raised about the stability of SYNROC minerals in natural waters. Nesbitt et al[97] have presented thermodynamic data showing that perovskite is relatively unstable in groundwaters equilibrated with basalts, gabbros, rhyolites, and granites (Figure 2.10). Because most groundwaters contain appreciable amounts of dissolved silica, Nesbitt et al. claim that sphene, a silico-calcium titanate ($CaTiSiO_5$), is the stable phase rather than perovskite, a silica free calcium titanate ($CaTiO_3$).

$$CaTiO_3 + SiO_2(aq) \rightleftarrows CaTiSiO_5$$

Furthermore, they argue that perovskite would be thermodynamically unstable in association with common rock forming siliceous minerals present in the backfill or the host rock. For example, kaolinite, a common clay mineral, can provide silica for perovskite transformation according to the reaction

$$CaTiO_3 + \tfrac{1}{2}Al_2Si_2O_5(OH)_4 + \tfrac{1}{2}H_2O \rightleftarrows CaTiSiO_5 + Al(OH)_3$$

Ringwood, in an earlier paper,[98] however, reported that reacting perovskite with silica spiked solutions under hydrothermal conditions did not result in any detectable transformation into a siliceous titanate phase such as sphene. Further research is required to study the thermodynamic and kinetic properties of SYNROC minerals.

Leach rates for gel-derived ORNL SYNROC B and D formulations, based on MCC-1 test for 3 days (Table 2.28), indicate that the leach rates for SNYROC D vary in the range of 10^{-1} to 10^{-4} $g/m^2 \cdot d$, while all elements leached from SYNROC B were below their analytical detection limits.

B. High Alumina Ceramic

Leach testing of High Alumina Ceramic and borosilicate glass using MCC-1 test (Table 2.7) shows that after 28 days no Cs, Sr, RE, Al, or Fe were detected in solution for alumina ceramic. Compared to glass, the high alumina ceramic leach rates are one to two orders of magnitude better for most elements tested. Na release has been attributed to the dissolution of nepheline in the ceramic. Leach rates of the constituent phases in the high alumina ceramic range from 10^{-1} $g/m^2 \cdot d$ for nepheline to 10^{-4} $g/m^2 \cdot d$ for the structural elements in magnetoplumbite.

2.6.1.5 Metal Matrices

Leach testing of SPC-4E supercalcine ceramic and 76-68 glass encapsulated in various matrices using MCC-1 test (Table 2.35) shows that 100% Pb matrix is optimum for glass marbles and that graphite and hot pressed TiO_2 and Ti-6% Al-4% V matrices are optimum for ceramic pellets. Nonmetallic matrices such as concrete and hot pressed glass are not acceptable due to their high permeability and matrix dissolution rates.

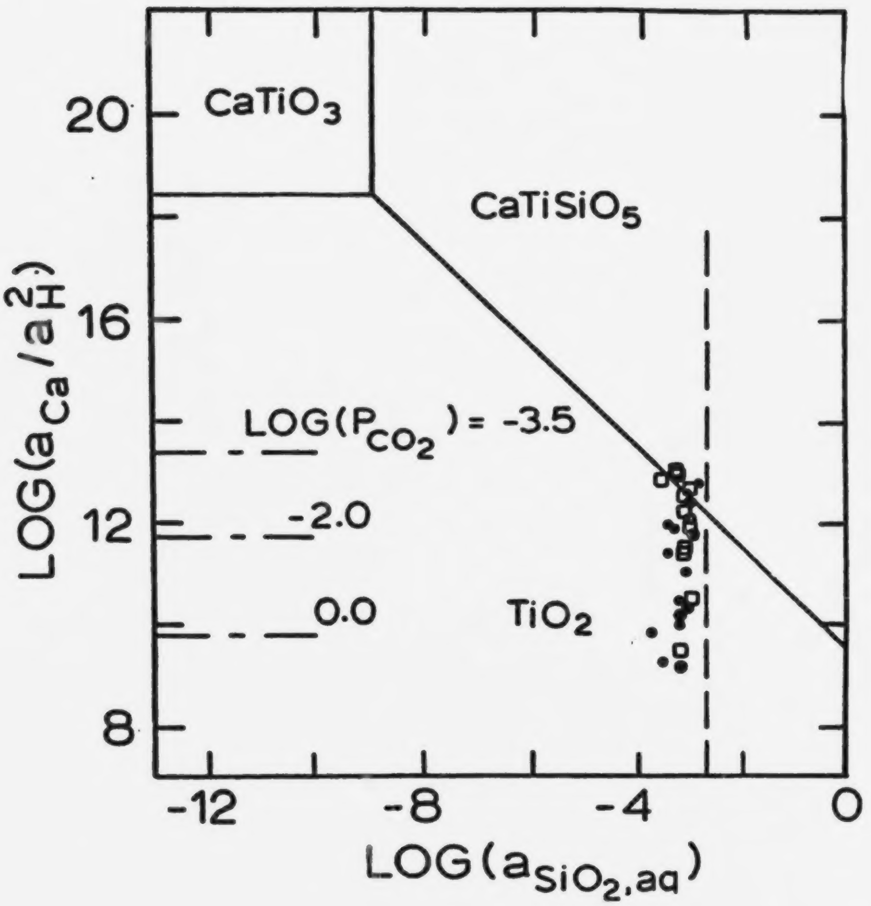

Figure 2.10 Stability fields of sphene, perovskite, and rutile in terms of H^+, Ca^{2+} and silica activities.[97]

BEST DOCUMENT AVAILABLE

Corrosion rates of the metals being considered as matrix materials show that TiO_2 and Ti-6% Al-4% V have the lowest corrosion rates in deionized water at 90°C. Minimum thicknesses required to provide 1000 yr containment are calculated to be 5×10^{12} cm for Ti alloy and 3×10^{-4} cm for TiO_2. These calculations are based on the assumption that the laboratory derived corrosion rates do not change over a period of 1000 years.

Work at Eurochemic in Mol, Belgium, has investigated the corrosion behavior of various lead alloys in salt solutions.[99] Samples of pure Pb and Pb-Sn alloys used in encapsulating glassy waste forms were allowed to react with distilled water and salt solutions prepared from ASSE II rock salt. The alloys were also exposed to dry ASSE II salt at temperatures of up to 250°C. In addition, the effect of the presence of oxygen, nitrogen and CO_2 in salt solutions on the corrosion rate was investigated. The experimental results of lead alloys-salt interactions are presented in Table 2.50. The corrosion rates are generally very low; on the order of μm/yr. Further experiments with other metals indicate that pure Al is as corrosion resistant as Pb when reacted with dry ASSE salt and its saturated aqueous solutions. Based on the corrosion rates reported in Table 2.50, we estimate minimum thicknesses of Pb or Pb alloys required for 1000 yr containment are on the order of millimeters.

Cermet matrix alloy has been reported to exhibit high resistance to oxidation corrosion. However, sufficient leach data are not available at this time to evaluate the chemical durability of cermet waste form.

2.6.1.6 Coated Particles

Leach test results of coated gel-derived ceramic spheres with multiple coatings of PyC (Table 2.42) show the release of all coated waste forms tested to be below the detection limits. For some of the waste forms tested, the waste loading was as high as 90% SRP sludge. ORNL has also developed a Cs-bearing coated particle which, upon testing, exhibited elemental release below detection. In addition, the ORNL group has succeeded in depositing SiC coating on 70/30 and 90/10, and on SYNROC waste forms at temperatures in the range of 700-1000°C. No leach data are available yet. Based on existing data, we believe that the chemical durability of coated particles developed at ORNL is far superior to that of other waste form.

Various coatings and coating techniques have been tested on supercalcine (SP-2, SPC-4) marbles at PNL.[100] Chemical Vapor Deposition (CVD) was used as the main coating technique since it had already been extensively developed as part of the HTGR fuel technology. These coatings were examined microscopically and were tested for leach resistance. Uncoated marbles, marbles with single coats of PyC or Al_2O_3, and marbles with duplex coatings of PyC and Al_2O_3 were tested (Table 2.51). Coating thicknesses were about 10 μm. The coated marbles clearly possessed superior leach resistance (an order of magnitude) with respect to the retention of Si, Ba, Sr, and Cs than did the uncoated marbles. The PyC coat was somewhat less effective than the Al_2O_3 or the duplex coats, particularly with respect to Cs and especially in 0.5 M NaCl leachant. This was attributed to Cs migration from the supercalcine

Table 2.50[99]

Corrosion Rates of Lead Alloys in Dry ASSE Salt and an Aqueous Solution Saturated With the ASSE Salt

Corrosion Condition	Temp. (°C)	Corrosion Period (Days)	Corrosion Rate (mm yr^{-1})					
			Pb 99.99	Pb 99.9 Cu	Pb-Sb	Pb 98.5	Pb-Sn 20	Pb-Sn 10
Dry ASSE II salt								
Composition (wt %) Cl (60); Na (39); SO_4 (1.2); Ca (0.4); Fe ($6x10^{-4}$); Mg (<0.1)	110	116-176	0.0008	0.0004	0.0004	0.0007	0.0001	--
Immersion in Saturated solution of ASSE salt								
a) Saturated with pure N_2 and under N_2 atmosphere	50	106	0.0004	--	--	0.0009	--	0.004
b) Saturated with air	50	92	--	--	--	0.016	--	0.013

Table 2.51[100]

Leaching Behavior of Coated Supercalcine Multibarrier Waste forms

		Element Leached, g/m^2[a,b]							
		Deionized Water				0.5 M NaCl			
Core	Coating	Si	Ba+Ca	Sr	Cs	Si	Ba+Ca	Si	Cs
CPC-2	None	0.59	0.52	0.22	0.112	0.60	0.77	0.27	0.032
SPC-2	PyC	0.004	0.017	0.01	0.14	0.014	0.071	0.011	0.068
SPC-4	None	0.46	0.16	0.12	0.19	0.42	0.44	0.20	0.045
SPC-4	Al 0	0.007	0.01	<0.001	0.011	0.014	0.051	0.001	0.012
SPC-4	PyC/Al 0	0.007	0.01	<0.001	<0.005	0.13	0.061	0.003	0.011

[a] Leach units not normalized by dividing by element weight fraction in waste form.
[b] Leaching Conditions: 90°C, 28 days, SA/SV = 10 m^{-1}.

marble into the PyC coating during coating deposition due to the high (1100-1200°C) deposition temperature. This conclusion is quite reasonable in light of the well known volatility of cesium. Efforts were made then to lower the deposition temperature. This was accomplished by using a nickel tetracarbonyl catalyst which allowed deposition at temperatures ranging from 325-515°C.

Recent data presented at the Alternative Waste Forms Technical Review Panel in Atlanta,[90] however, indicated that low temperature CVD coatings are porous and frangible. For example, although the low temperature CVD triple coat Cr_7C_3/PyC/Cr_7C_3 on supercalcine exhibits an improvement in leach resistance compared to the uncoated waste form (Table 2.43), it does not possess the durability or density of a high temperature PyC coating.

Metal coatings have been deposited on glass marbles using a thermal spray wire gun or a plasma process. The coating thicknesses range from 300 μm for Zn to 800 •m for Al-6% Si alloy. As shown in Table 2.43, Pb and Sn alloy single coatings and a Sn alloy/Zn double coating provide the best leach resistance in terms of Cs, Sr, Na, and Si release. Both Pb and Al coatings form a layer of alteration products. Estimated corrosion rates of metal coatings deposited by thermal spray wire gun or plasma process are given in Table 2.44. The lowest corrosion rates are reported for Cu, the plasma spray deposited coating having an approximately three orders of magnitude lower corrosion rate than that deposited by the wire gun process. This indicates that the process employed for depositing metal coatings is also important in that it affects its chemical durability. To obtain 1000 yr zero release containment, the minimum coating thicknesses required vary from 4 μm for Cu deposited by plasma spray to 70×10^3 μm for Pb coating deposited by the wire gun process.

2.6.2 Thermal Properties

Commercial high level wastes generate a considerable amount of heat, especially during the early stage of waste immobilization. In any evaluation of high level waste forms, the thermal properties should be considered. The temperature distribution in a waste form is a function of the type and age of the waste, the type of waste form and its geometry, the waste loading, the thermal conductivity of the waste form matrix, and the thermal characteristics of the encapsulating matrix. Similarly, the temperature distribution profile in a waste package would depend on the thermal characteristics of the package components and the overall package geometry. To illustrate the effect of radioactive decay over a period of time on heat distribution, the heat generated from a typical in-canister borosilicate glass having a waste loading of 25 wt% is displayed in Figure 2.11.

The important thermal properties of waste forms discussed below include phase stability and thermal conductivity.

2.6.2.1 Glasses

Borosilicate and phosphate glasses are known to devitrify within hours or days at temperatures above 500°C,[102] resulting in a significant increase in leach rates as shown in Figures 2.12-2.14.

Phase crystallization can be introduced during the vitrification process itself or from the self-heating during storage. Typical crystal phases observed are molybdates, platinum group metal oxides (as RuO_2), refractory oxides such as $(Ce,RE^{3+})_2O_{3-x}$ and complex silicate or phosphate phases (Figure 2.15). This will often lead to changes in leach rates either by direct change in leachability introduced by crystal phases or indirectly through microstructural change or stress generation. The change in leach rates, however, is not significant for borosilicate glasses (Figure 2.16). The variation is within an order of magnitude[4,34,102]; in some cases it is negligible.

Differential thermal and radiation expansion can lead to microfractures in glass, resulting in an increase in the exposed surface area. This increase in surface area can result in increased leachability of glass. However, data available at this time are not sufficient to quantitatively evaluate the effect of this process on glass leaching.

The thermal conductivities for waste glasses are on the order of 1 W/m·k. Lutze et al. reported that the thermal conductivities for celsian- and fresnoite-type glass ceramics are comparable to those for phosphate and

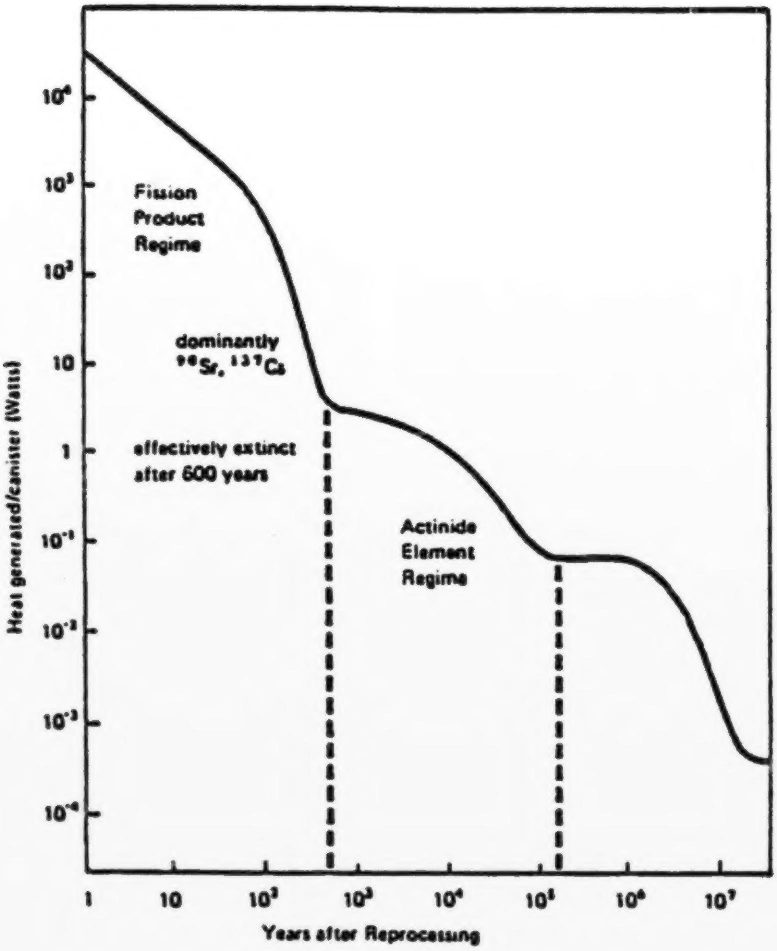

Figure 2.11 Heat Generated from a Typical In-Canister Borosilicate Glass Having a Waste Loading of 25% by weight.[101] Dimensions of Glass Cylinders are 300 cm (length) x 30 cm (diameter).

BEST DOCUMENT AVAILABLE

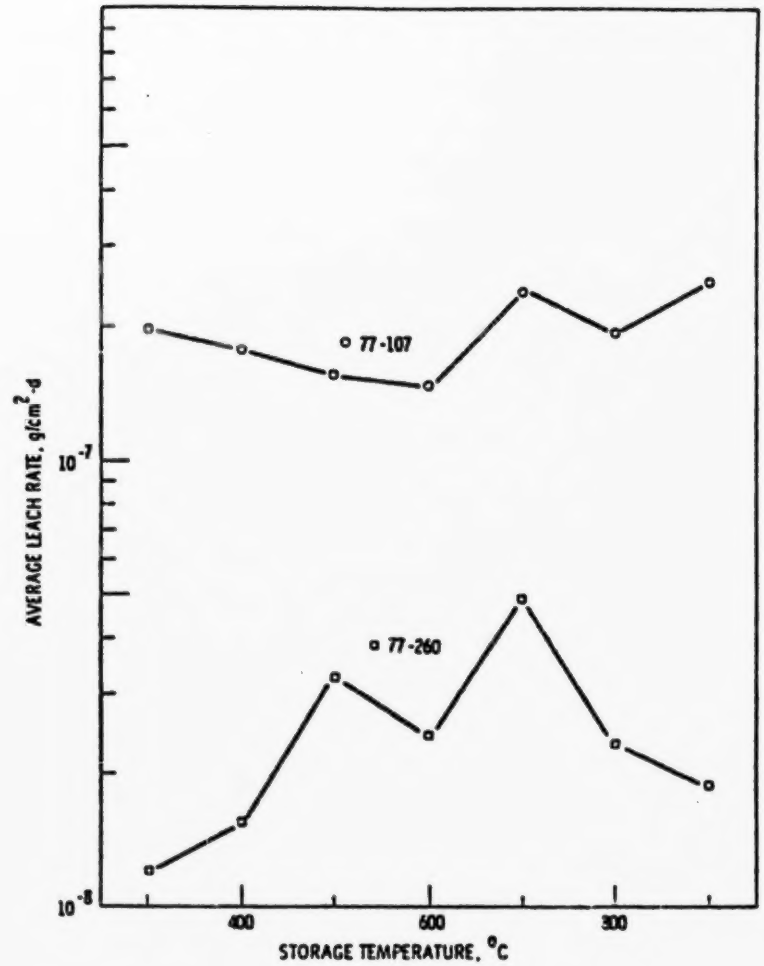

Figure 2.12 Long-term cesium leach rates of glasses PNL 77-107 and 77-260 as a function of temperature for a 2-month heat treatment.[102]

BEST DOCUMENT AVAILABLE

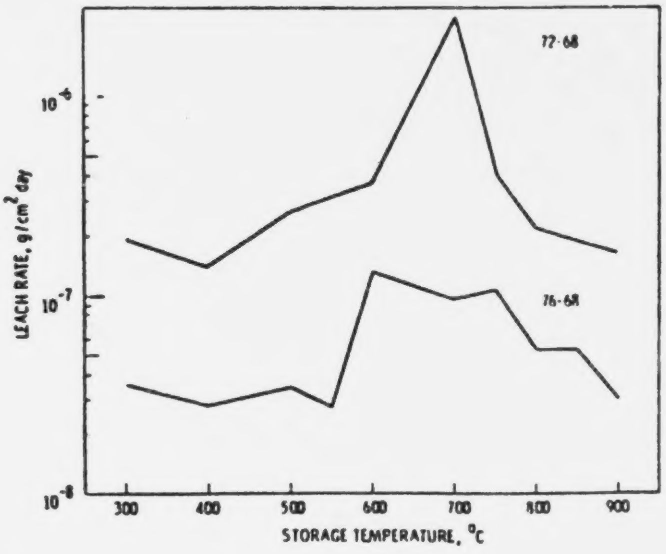

Figure 2.13 Long-term cesium leach rates of glasses PNL 72-68 and 76-68 as a function of temperature for a 2-month heat treatment.[102]

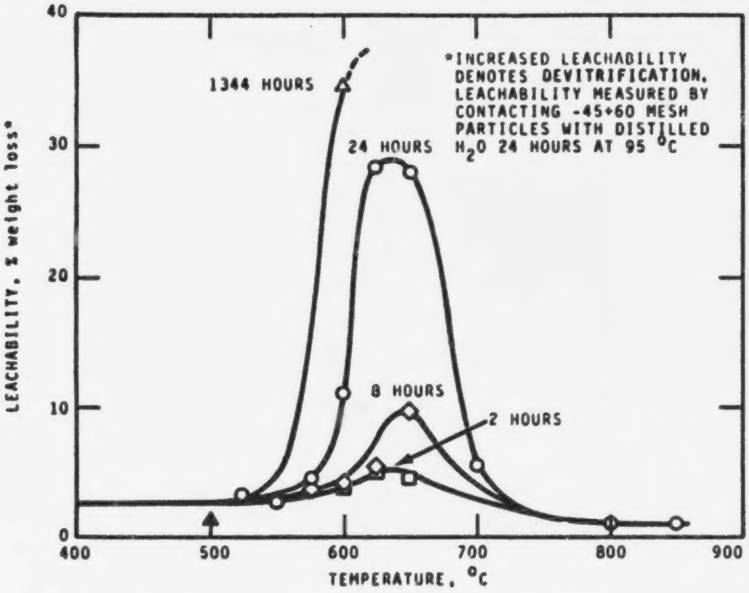

Figure 2.14 Leach rate of phosphate glass increases as heat treatment causes devitrification.[102]

BEST DOCUMENT AVAILABLE

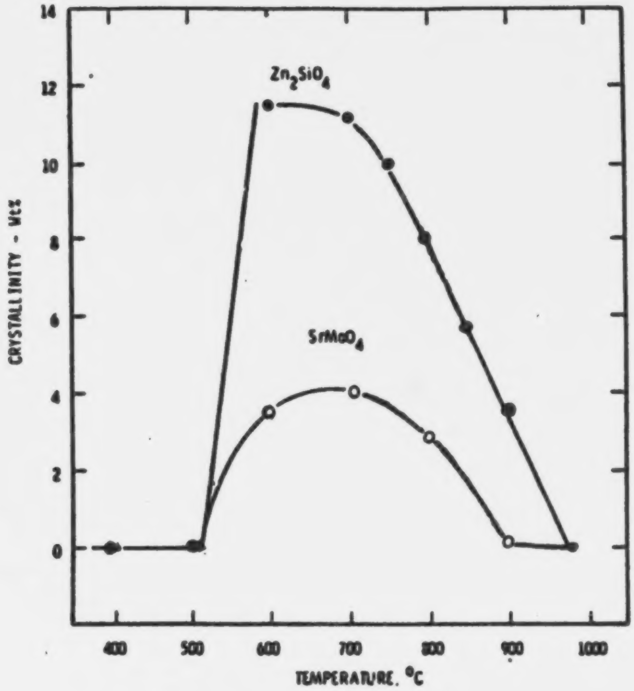

Figure 2.15 Ingrowth of Zn_2SiO_4 and $SrMoO_4$ as a function of temperature for glass PNL 72-68 heat-treated for 2 months.[102]

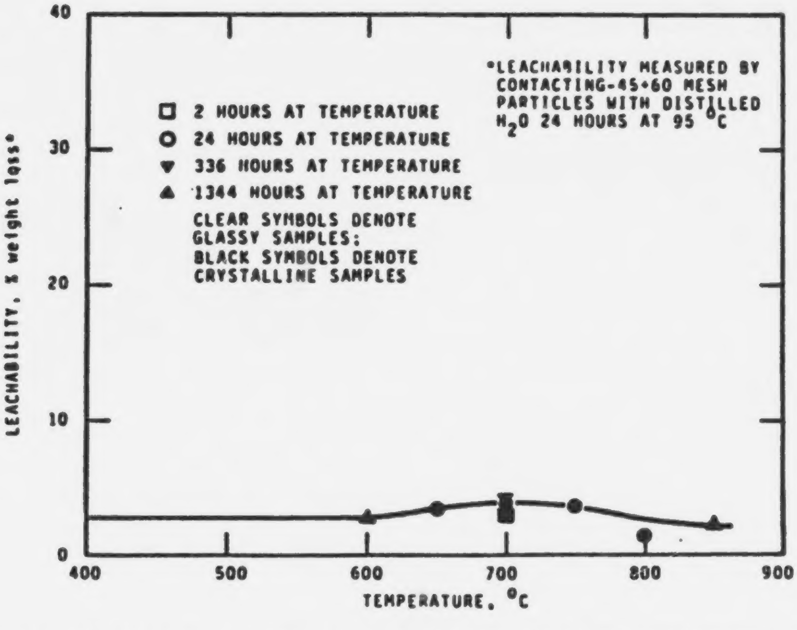

Figure 2.16 Glass leach rate as a function of heat treatment and temperature holding time for borosilicate glass IPM PW-4m: there is little change in leach rate as heat treatment devitrifies this borosilicate glass.[102]

BEST DOCUMENT AVAILABLE

borosilicate glasses. Data reported in Table 2.37 indicate that 76-78 simulated waste glass beads in a Pb matrix exhibited more than an order of magnitude improvement in conductivity while in Al-12% Si matrix the increase in conductivity approached two orders of magnitude. Geel et al. have reported significant improvement in the thermal conductivities of vitromets and cermets as a result of their metal encapsulation. A comparison of ΔT values for cylindrical vitromets 60 cm in diameter and borosilicate glass blocks 50 cm in diameter as a function of time after reactor discharge of fuel is depicted in Figure 2.17. Assuming the age of the waste to be 10 years after reactor discharge, vitromet shows an order of magnitude improvement in thermal conductivity, compared to glass.

In PGM glass, the glass core was reported to have a lower coefficient of thermal expansion than the cladding material. This can result in differential thermal expansion and affect the overall stability of the waste form. However, recent data indicate that PGM glasses have a very low coefficient of thermal expansion ($\alpha = 1.7\text{-}5 \times 10^{-6}/°C$) and are expected to be more resistant to radiation-induced thermal fracture than other glasses. Both the core-only and the core-clad composite are reported to have excellent thermal stability. No gas generation was observed upon heating the samples slowly and rapidly to 800°C under vacuum.[18]

2.6.2.2 Crystalline Ceramics

Crystalline waste forms are relatively stable at high temperature because they consist of refractory oxide, silicate, and titanate phases.

A summary of some important thermophysical properties of SYNROC is given in Table 2.52.[66] Compared to PNL 76-68 glass, the thermal properties of SYNROC C are reported to be far superior. However, no data are available on thermal cycling behavior of SYNROC.

For High Alumina Ceramic, no volume or phase change was reported upon thermal cycling of samples to 1200°C.[77] Because of its high thermal stability and thermal conductivity, the High Alumina ceramic is capable of high waste loading. In addition, since defense waste consists predominantly of inert materials and has low heat output, high defense waste loading can be incorporated in the ceramic. Figure 2.18 illustrates 100% Cs retention during fabrication of High Alumina ceramic by Hot Isostatic Pressing as compared with other processes where Cs is lost from the system.[77]

2.6.2.3 Metal Matrices and Coated Particles

In terms of thermal conducting properties, the metal encapsulated waste forms can be given the highest rating. As reported earlier, encapsulation of glass waste form in a Pb-10 Sn alloy or a 12 Al-Si matrix exhibits a one to two orders of magnitude improvement in thermal conductivity. A significant increase was also observed for supercalcine ceramic embedded in Al-12 Si or Cu matrix.

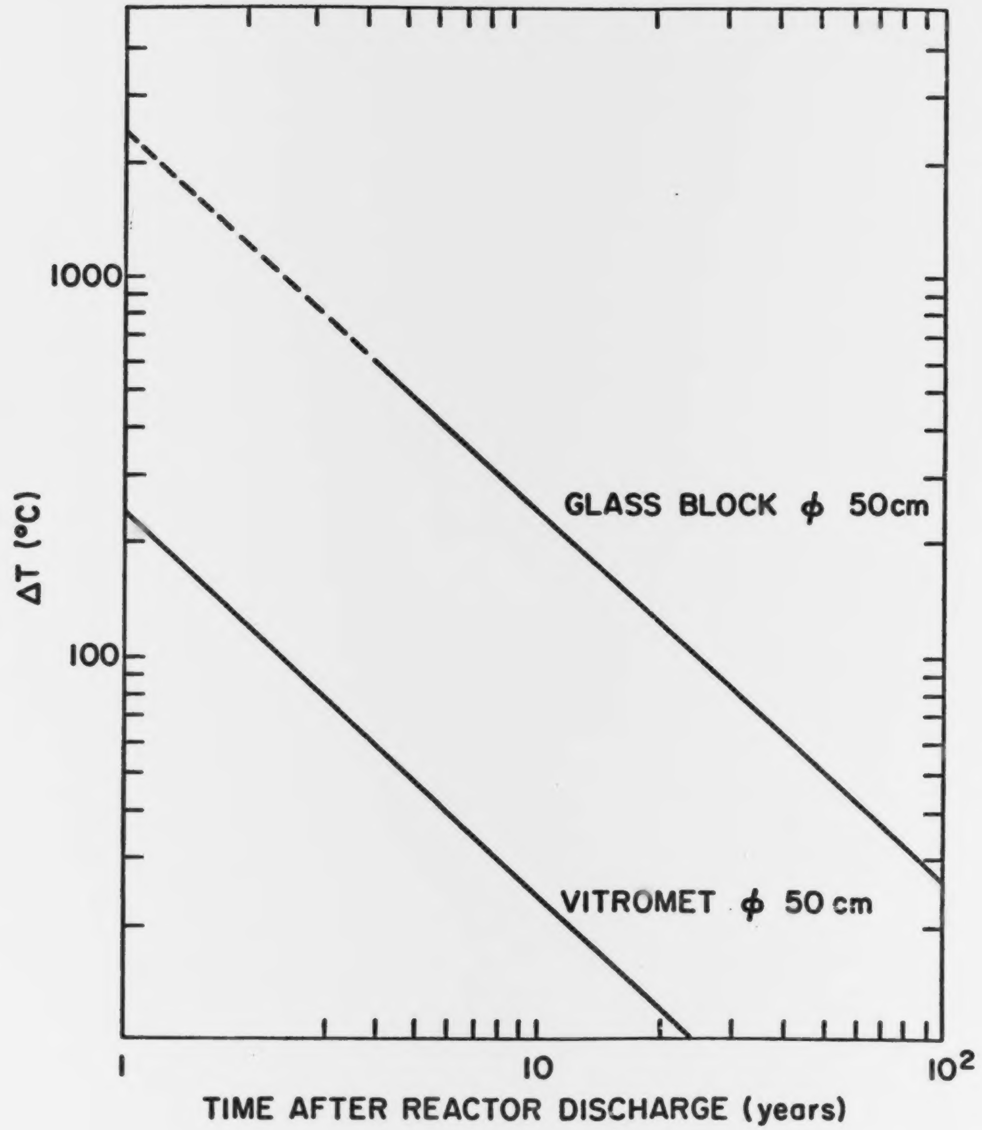

Figure 2.17 Temperature difference between centerline and wall of cylindrical glass blocks and vitromets of equal heat generation per metal length as a function of time after reactor discharge.

BEST DOCUMENT AVAILABLE

Table 2.52[66]

Summary of Some Important Thermophysical Properties of SYNROC

Property	SYNROC B	SYNROC C	SYNROC D
Thermal conductivity, 20°C (W/m·K)	3.8	3.0	1.7
Heat capacity, 20°C (J/gK)	0.61	--	--
Thermal diffusivity, 20°C (m^2/s)	1.5×10^{-6}	--	--
Thermal expansion coeff (20-950°C)[a]	1.0×10^{-5}	--	1.0×10^{-5}
(20-950°C)	1.1×10^{-5}	--	1.1×10^{-5}
Solidus temperature (°C)	--	1340	1270

[a] Linear thermal expansion coefficient; $\alpha = (L/L_0)/(\Delta L/\Delta T)$.

BEST DOCUMENT AVAILABLE

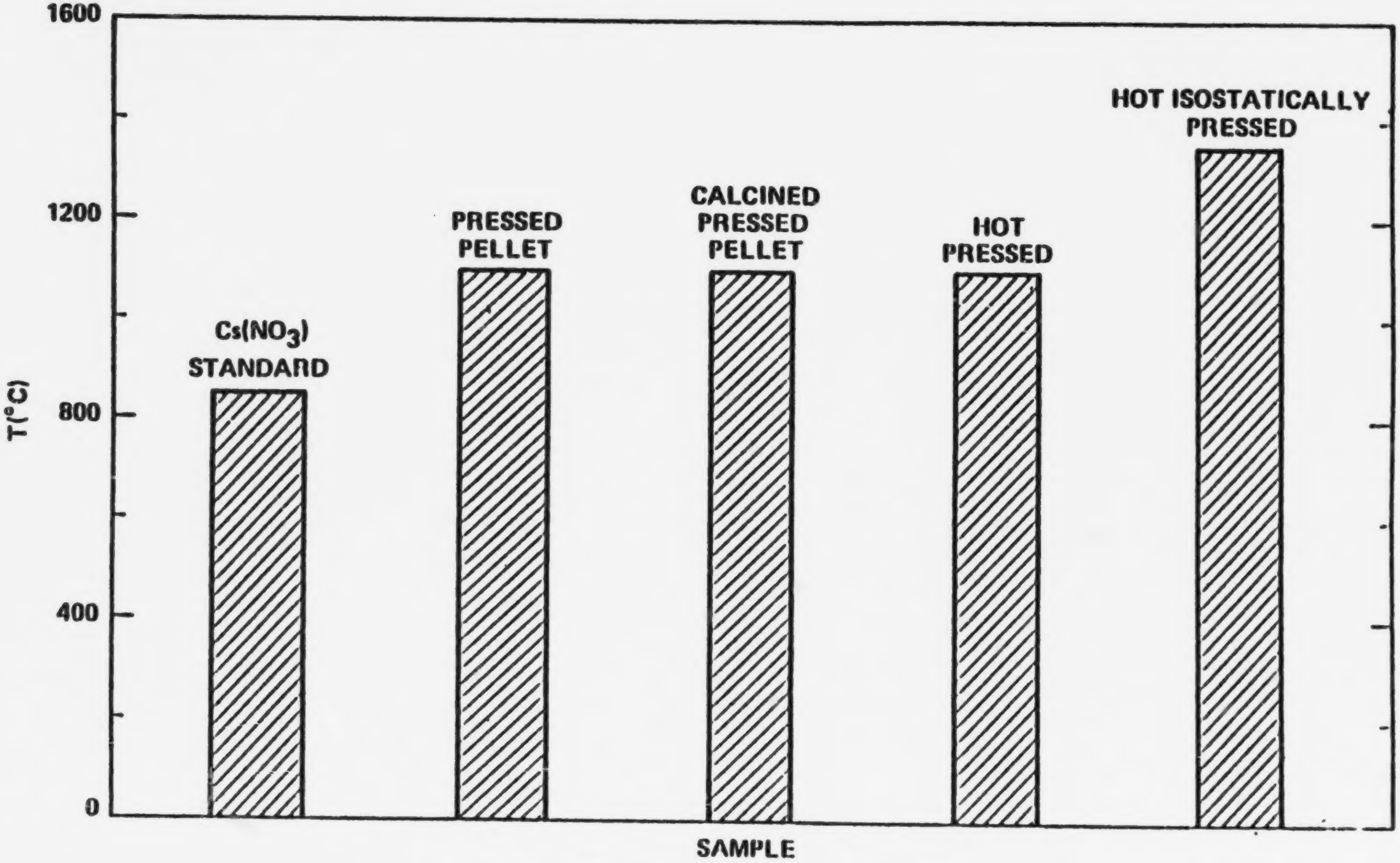

Figure 2.18 Cs^+ retention in tailored ceramic nuclear waste forms.[77]

Figure 2.19 shows the canister centerline temperatures for CVD-coated supercalcine ceramic embedded in various metal matrices.[103] Assuming a 60% volumetric waste loading of CVD-coated supercalcine embedded in a stainless steel matrix contained in a 30 cm diameter canister, the centerline temperature is 834°C. Using a sintered Cu matrix, the centerline temperature drops dramatically to 161°C. Encapsulation of the coated particles in a cast Al matrix results in a centerline temperature of 71°C.

The thermal properties of 76-68 glass and SPC-4E supercalcine ceramic encapsulated in various matrices are given in Table 2.53.[82]

Research at ORNL has shown that the thermal conductivity of simulated and actual waste cermets depends primarily on the density and on the ratio of metal-to-oxide phases present in the cermet. Thermal conductivities of simulated and real waste cermet pellets have been reported to lie between 3 and 20 W/m°C over a wide range of cermet densities and ceramic loading levels. Thermal cycling of 2 cm diameter cermet cylinders up to a temperature of 900°C, followed by quenching in water, shows no damage.[86,87]

2.6.3 Mechanical Properties

Although the mechanical properties of waste forms are not important with respect to the NRC criteria for the waste package or the underground facility, the waste forms should be consolidated and resistant to dispersion. Fracturing of the waste form under impact or static conditions can give rise to an increase in the exposed surface area which, upon contact with water, will result in a higher leach rate. Dynamic impact resistance tests are supposed to simulate accident conditions during transportation. In contrast, tensile strength tests provide information on the mechanical behavior of waste forms under respository conditions and over long time periods.

Impact data, compiled by Metz,[104] are given in Table 2.54. The dispersibility of a waste form, resulting from impact fracturing, is expressed as weight of fine particulate materials (<10 μm) lost relative to the initial weight of unfractured material. The increase in surface area, following impact fracture, can be as much as two orders of magnitude.

Recent laboratory data show that SRL 131 glass produced only 0.14 wt% respirable times less than 10 μm upon an impact energy of 10 joules/cm^3; this is far better than SYNROC, High silica glass, Pyrex, and FUETAP. Based on the amount of fines (<37 μm) generated, the mechanical impact behavior of metal matrix waste forms is given in Table 2.55.[82] The results show that encapsulation of supercalcine ceramic, PyC/Al_2O_3 coated supercalcine ceramic, and glass improves the impact resistance significantly. Fracture tests at ANL on high alumina ceramic yielded <0.06 wt% of less than 10 μm fines with 10 joules/cm^3 impact energy.

Tensile strengths for various waste forms are listed in Table 2.56.[104] The results show that 76-68 glass is relatively stronger than ceramic or glass ceramic waste forms.

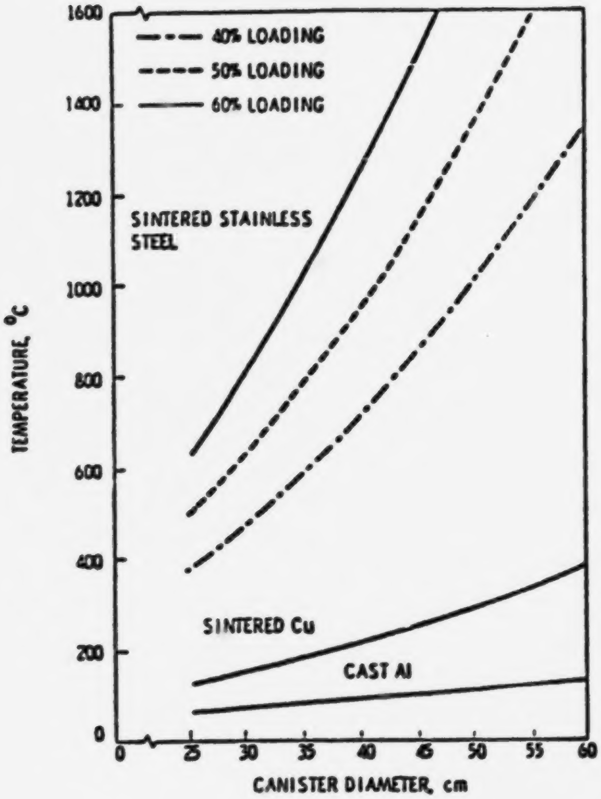

Figure 2.19 Canister centerline temperatures for CVD-coated supercalcine in various matrices.[103]

BEST DOCUMENT AVAILABLE

Table 2.53[82]

Thermal Properties of Glass and Supercalcine in Various Matrices

				SPC-4E in		
	Glass 76-68	76-68 in 100% Pb	SPC-4E	Ti-6Al-4V	TiO_2	Graphite
Formation Temp.	1050°C	400	1125°C	1100°C	1100°C	<800°C
Volatility Range	>800°C		>800°C			
Thermal Expansion	$9x10^{-6}$/°C	(N.A.)	$9.3x10^{-6}$/°C	$\sim 10x10^{-6}$	$7.6x10^{-6}$	1 to $5x10^{-6}$

BEST DOCUMENT AVAILABLE

Table 2.54[104]

Impact Data

Waste Type	Impact Energy/ Volume	Impact Velocity	Wt% Fines <10 μm	Surface Area Produced / Impact Energy	Surface Area Increase (ratio new/old)	Reference
Borosilicate (72-68)	Edge on impact at speed shown, canister + glass	7.6 m/sec	0.001		1.3 to 3	Smith and Ross 1975, pp. 76, 81
		36 m/sec	2		10 to 100	
ICM-11 PW-7-2 calcine	217 J/1.14 cm^3	4.88 m/sec	2.4	16 cm^2/J	574	Bunnell 1979
Borosilicate glass + sludge	78 J/3 cm^3	5 impacts 2 kg-0.8 m	0.0(a)	9.5 cm^2/J	58	Wallace and Kelley 1976
HAC concrete	94 J/5.86 cm^3	5 impacts 2 kg-0.8 m	1	7.3 cm^2/J	39	Wallace and Kelley 1976
HAC + 40% sludge	94 J/5.68 cm^3	5 impacts 2 kg-0.8 m	0.1	28.9 cm^2/J	154	Wallace and Kelley 1976
IP concrete	94 J/6.13 cm^3	5 impacts 2 kg-0.8 m	0.15	10.3 cm^2/J	55	Wallace and Kelley 1976
IP concrete + 40% sludge	94 J/5.65 cm^3	5 impacts 2 kg-0.8 m	0.4	19 cm^2/J	103	Wallace and Kelley 1976
Type III concrete + 40% sludge	94 J/5.80 cm^3	5 impacts 2 kg-0.8 m	0.53	25.3 cm^2/J	136	Wallace and Kelley 1976
SYNROC ceramic + 10% waste						Ramm and Ferenczy 1980
Sintered	127 J/1.53 cm^3	n.r.(b)	2.0	n.r.	n.r.	
Hot-pressed	217 J/1.53 cm^3	n.r.	1.1	n.r.	n.r.	

(a) No <10-μm particles were found.
(b) n.r. = not reported.

Table 2.55[82]

Mechanical Impact Behavior of Metal Matrix Forms

Material	Matrix	Waste Released* $g/cm^3 \times 10^{-4}$
Hot Pressed SPC	None	1600
PyC/Al_2O_3 Coated SPC	SST	200
Glass	None	120
Glass Marbles	Pb-10Sn	9

*Based on Fines <37 μm

Table 2.56[104]

Tensile Strength for Various Waste Forms

Waste Form	Tensile Strength, MPa
Cement + 10% PW-9 calcine powder	8.34
Cement + 10% SPC-5B	7.85
Supercalcine sintered ceramic SPC-5B	28.6
Sintered ceramic 50% frit + 50% PW-9	13.5
Sintered ceramic PW-9	8.80
Hot-pressed sintered ceramic PW-9	13.0
Glass ceramic 20% PW-9	34.3
Glass 76-68	51.4

2.7 TRU Waste Forms

An in-depth analysis and evaluation of the DOE research and development efforts on TRU Waste Forms has been completed.[105] The major conclusions and recommendations, as reported by Bida and MacKenzie in their Final Report[105], are presented in Sections 2.11 and 2.12.

2.8 Spent Fuel as a Waste Form

The possibility that spent fuel from commercial reactors may be a suitable permanent waste form is under consideration, and is a national policy.[106] A program for the characterization of spent fuel from Light Water Reactors has been established and will be completed in early 1987. The major issues which must be addressed are considered below:

2.8.1 Degradation of Spent Fuel Cladding

A number of mechanisms have been identified which could accelerate cladding degradation. Destructive and non-destructive testing of spent fuel is proceeding at Hanford Engineering and Development Laboratory (HEDL)[107] and computer modelling of such phenomena, particularly stress rupture, is also in progress.[108]

2.8.2 Cracking of Fuel Pellets

During irradiation, UO_2 fuel pellets can develop cracks which will affect the ultimate leach rate.

2.8.3 Fission Gas Release

Gaseous fission products such as krypton, xenon, and iodine can accumulate within the cladded fuel rods and deform the cladding. If the gases do escape through the ruptured cladding, their retention by other components of the waste package can not be assured at present. Both their gaseous state and their varied chemical reactivities differ from other fuel waste components and tailoring of backfills and overpacks will be necessary. No specific programs dedicated to this problem have yet been generated. The quantities of fission gas in some LWR typical reacter fuels is being determined at HEDL.

2.8.4 Leaching Studies

2.8.4.1 Spent Fuel Leaching

The possibility of permanent storage of spent fuel elements in an underground repository has necessitated studies of the leach rates of spent fuel as well as inactive uranium oxide. Although much less work has been concentrated on this subject than on waste glass leach rates, knowledge of spent fuel dissolution processes is rapidly approaching that for glasses.

Four groups in the western world are carrying out studies on UO_2 or spent fuel leaching in underground repository environments: Katayama and Bradley and Wang at PNL (WRIT project),[109, 110] Norris at LASL,[111] Vandergraaf and Johnson at Whiteshell (Canada),[112,113] and Eklund and Forsyth[114] in Sweden. The objectives of these studies are relatively similar:

1. Determine the absolute long term isotope release rate, particularly for important long lived (e.g., Pu, Cm) radionuclides in different fuels and for groundwaters with different oxygen concentrations.

2. Determine release rates of different radionuclides relative to uranium.

3. Determine the mechanisms of UO_2 oxidation and dissolution.

The dissolution rates of many more isotopes can be more readily followed for radioactive spent fuel than for other simulated waste form types. Typically, a static, unreplenished leaching procedure or the IAEA replenished procedure, have been used. Following each experiment, 10-15 radioisotopes are measured using alpha, beta, and gamma counting, combined with appropriate chemical separations. Although each group has used a different form of spent fuel, most of the general conclusions from each group are surprisingly similar. The major conclusions are given below:

1. Most isotope leach rates decrease by 1-2 orders of magnitude in the first few days of leaching at 25°C in aqueous solutions of 0.01 M $CaCl_2$, 0.03 M NaCl, .03 M $NaHCO_3$ or deionized water. A typical leach rate plot for deionized water is shown in Figure 2.20. Most leach rates continue to decrease by a further 1-2 orders of magnitude over the next 1000 days of leaching.

2. The more mobile fission products, such as ^{137}Cs and ^{125}Sb, are initially leached preferentially from the fuel; these isotopes have migrated to the exterior of the fuel element during irradiation. Actinide fission products are usually dissolved congruently.

3. Leaching in solutions of NaCl, $CaCl_2$, or $NaHCO_3$ appears to be significantly more rapid than in water. Only oxygen saturated solutions have been tested for spent fuel samples.

4. After 1000 days of leaching under 25°C static, aqueous conditions, the dissolution rate for most species reaches about the equivalent of 10^{-6} g of fuel/cm^2-day. In Table 2.57, quantitative leach rate data are given for a CANDU UO_2 fuel element sample[112] for different leach times, leachates and isotope or element determined. After 1000 days cesium is the only element which shows significantly greater proportional release from the UO_2 than the matrix element itself. Thus, since cesium activity will have decayed significantly during the proposed 1000 year total confinement period, in the post-thousand year period release of radionuclides from this type of waste form can not be expected to occur at a rate greater than $1x10^{-6}$ g UO_2/cm^2-day.

2.8.4.2 Dissolution Studies of UO_2

Concurrent with the above work on spent fuel, more fundamental studies on uranium oxide dissolution have also commenced. Some of the major aspects of this work are:

1. Gas phase oxidation studies of UO_2 - Single crystal UO_2 is oxidized at temperatures of 300°C to simulate long-term air storage of fuel. The structure of this oxidation film is important in understanding possible dissolution mechanisms. Work of this nature is taking place at PNL[112] and also in Canada.[113]

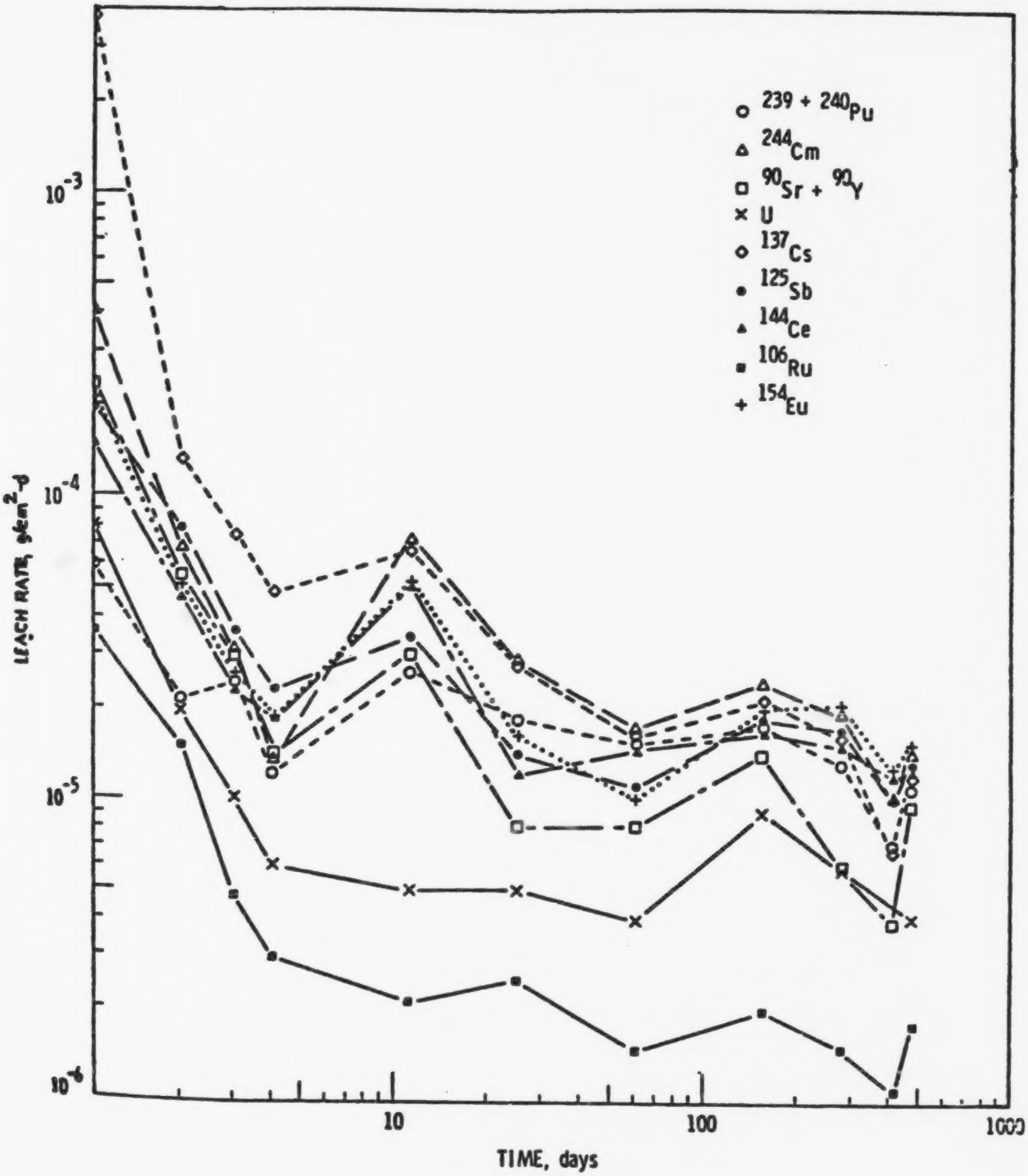

Figure 2.20 Leach rate of 28,000 MWd/MTU spent fuel in deionized water at 25°C based on selected elements.[112]

BEST DOCUMENT AVAILABLE

Table 2.57

UO_2 Matrix Dissolution Rates (10^{-6} g·cm^{-2}·d^{-1})[112]

Based On	Leaching Solution	Days Leaching		
		100	300	900
^{90}Sr	Distilled	86	24	0.75
	River	86	30	6.0
^{106}Ru	Distilled	7.0	3.0	---
	River	7.0	2.8	0.30
^{125}Sb	Distilled	18	24	1.0
	River	110	52	37
Cs Av.	Distilled	550	260	45
	River	1300	280	52
Rare Earth Av.	Distilled	5.4	16	0.38
	River	16	13	0.53
Actinide Av.	Distilled	---	27	1.4
	River	31	17	1.9
U*	Distilled	1.0	4.1	0.33
	River	12	8.0	2.0

* Dissolution rates obtained from U analyses in the leachates.

2. Autoclave Dissolution Studies of UO_2 - The dissolution mechanisms of polycrystalline UO_2 have been studied at elevated temperatures (up to 150°C) and in a variety of solutions (synthetic bicarbonate groundwater, salt brine, deionized water, etc.). Such experiments are being carried out at PNL,[110] LASL,[111] and at Whiteshell,[112,113] in Canada. Most experiments to date have been carried out with oxygen-saturated solutions.

   These experiments have shown that the dissolution of UO_2 is a function of temperature and is greatly assisted by oxygen. Initially, because of the high dissolution rate, the solution becomes quickly saturated with uranium ions near the UO_2 surface which reprecipitates on the surface as a UO_3 hydrate. However, as long as oxygen is available in solution, the dissolution of UO_2 continues at a high rate.

   Wang and Katayama[115] have proposed a dissolution mechanism, which is illustrated in Figure 2.21. This involves initial oxidation of a thin layer of UO_2 to U_4O_9, then dissolution of UO_2^{2+} ion, followed by reprecipitation, either at high temperature as a U^{6+} hydrate or at lower temperature as U^{+4} hydroxide.

   The effect of high radiation fields on this mechanism has been investigated. The presence of radiation-induced H_2O_2 enhances the oxidation-dissolution reaction, as well as the hydrolysis reaction. Since the formation of H_2O_2 is expected from water radiolysis, the dissolution mechanism for UO_2 may continue at the UO_2-solution interface, even when the solution has reducing or neutral conditions.

2.8.4.3 Electrochemical Studies

Although it is possible to study UO_2 dissolution under some reducing conditions in an autoclave, it is quite difficult to simulate the very low dissolved oxygen solutions typical of a flooded geologic repository after sealing. Therefore, many experimenters are turning to electrochemically assisted oxidation and dissolution techniques to understand the processes involved in the dissolution of UO_2 and fuel rods. Electrochemically assisted oxidation is capable of much greater control over both the solution Eh and the instantaneous measurement of the dissolution rate.

Studies to date have utilized single crystal UO_2, doped UO_2 pellets and spent fuel samples. Single crystal UO_2 is used to determine uranium dissolution from different crystal planes while controlled doping of pellets is used to investigate grain boundary effects. Solutions used have been distilled water, sodium bicarbonate, and WIPP brine with temperatures up to 70°C. With large quantities of dissolved oxygen, electrochemical studies give initial high dissolution rates of approximately $1x10^{-4}$ g/cm^2-day for uranium at 25°C[110] which at longer leaching times becomes much lower. This has led to the postulation of the following mechanisms:

1. In the early stages UO_2 oxidizes to a thin surface layer of U_4O_9 and subsequently goes into solution as a uranate.

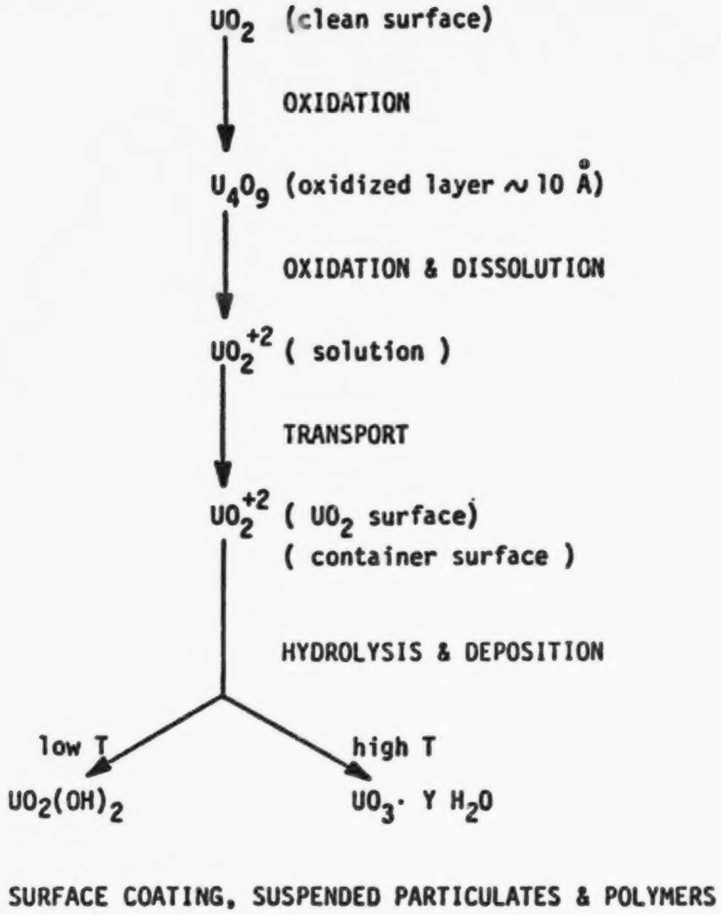
UO_2 (clean surface)
OXIDATION
U_4O_9 (oxidized layer ∼ 10 Å)
OXIDATION & DISSOLUTION
UO_2^{+2} (solution)
TRANSPORT
UO_2^{+2} (UO_2 surface)
(container surface)
HYDROLYSIS & DEPOSITION
low T
high T
$UO_2(OH)_2$
$UO_3 \cdot Y\ H_2O$
SURFACE COATING, SUSPENDED PARTICULATES & POLYMERS

Figure 2.21 Oxidation and dissolution mechanisms for a UO_2 surface.[115]

2. At longer periods and/or higher temperatures even higher valence uranium oxides will form on the surface. These form a porous film which nevertheless results in an overall decrease in the overall rate of uranium dissolution.

Surface techniques, combined with electrochemical methods, are important for elucidating the particular structure formed during dissolution. X-ray photoelectron spectroscopy has been used to follow the evolution of the U^{+4}/U^{+6} ratio on the surface film of a UO_2 electrode.[116]

The electrochemically assisted dissolution of spent fuel samples has begun to be investigated at PNL. Initial result show that the open circuit potential for a fuel element surface in any of the groundwater solutions is significantly higher than for UO_2 thus indicating that the spent fuel surface has been heavily oxidized during storage. Initial dissolution rates are determined to be approximately $1x10^{-5}$ g/cm^2-day.

2.9 Conclusions for HLW Forms

- Chemical vapor deposition (CVD) has been utilized for coating fuel particles in High Temperature Gas Cooled Reactors (HTGR). This existing CVD technology has been used to coat waste forms at Battelle Columbus Laboratory (BCL), Oak Ridge National Laboratory (ORNL), and General Atomic Company (GAC). Various coating materials produced by CVD in a fluidized bed have been evaluated at BCL.

- One of the important considerations in the selection of candidate materials is low coating temperature, considering the potential volatility of Cs and Ru during processing and that core materials will be limited to ceramics because glass melts at high temperatures. Because of these problems, low temperature CVD coating procedures are being investigated. In Austria, a study of the coating of simulated HLW calcine granules with pyrolytic carbon (PyC) or nickel has been carried out. Using acetylene (C_2H_2) as the carbon deposition source, the coating temperature was depressed from the usual 1000°C range to 325-525°C. Nickel carbonyl, $Ni(CO)_4$, was used as a catalyst and coating thicknesses of about 100 μm were obtained. This low temperature deposition process is highly desirable since it reduces fission product losses from the calcine by volatilization. In addition to the pyrocarbon deposition work, a study of the deposition of nickel from the decomposition of $Ni(CO)_4$ was reported. "Acceptable" nickel coatings approximately 45 μm in thickness (a certain degree of coat cracking was observed) were also obtained from the thermal decomposition of $Ni(CO)_4$ at 200°C.

- PNL has initiated the development of a PyC CVD coating procedure to coat large waste form particles (~10 mm) at relatively low temperatures ranging from 400 to 500°C. However, low temperature CVD coatings are reported to be porous and frangible. For example, although the low temperature CVD triple coat $Cr_7C_3/PyC/Cr_7C_3$ on supercalcine exhibits an improvement in leach resistance compared to the uncoated waste form, it does not possess the durability or density of a high temperature PyC coating.

- At PNL, metal coatings have been deposited on glass marbles using a thermal spray wire gun or a plasma process. The coating thicknesses range from 300 μm for Zn to 800 μm for Al-6% Si alloy. Pb and Sn alloy single coatings and a Sn alloy/Zn double coating provide the best leach resistance in terms of Cs, Sr, Na, and Si release. Both Pb and Al coatings form a layer of alteration products. The lowest corrosion rates are reported for Cu, the plasma spray deposited coating having an approximately three orders of magnitude lower corrosion rate than that deposited by the wire gun process. This indicates that the process employed for depositing metal coatings is also important in that it affects its chemical durability. To obtain 1000-year containment, the minimum coating thicknesses required will vary from 4 μm for Cu deposited by plasma spray to 70×10^3 μm for Pb coating deposited by the wire gun process.

- The coated particle technology developed by GAC for their HTGR's has been applied to coat waste forms as well. In-house studies at GAC have focused on pyrolytic carbon and PyC/SiC coatings on supercalcine. Glass was not studied since the lowest coating temperature (1100°C) is sufficient to soften the glass. At 1100°C they found that there was a chemical interaction between the coating and supercalcine which caused permeability. Very recent work has resulted in a proprietary process in which the coating temperature has been reduced to 750°C. Using this, GAC believes that impermeable coatings can be deposited on supercalcines, SYNROC, and, possibly, glass.

- At ORNL, the CVD fluidized bed coating process, developed for HTGR reactor fuel, is being applied for depositing coatings of PyC and SiC on gel derived waste forms. Spheres of SYNROC B and D (70% simulated SRP waste without Al removal + 30% additives), 70/30 (70% simulated SRP waste with Al removal + 30% SYNROC additives), 90/10 (90% simulated SRP waste with Al removal + 10% ZrO_2 additives), and a generic Cs-bearing waste form have all been successfully coated with PyC and SiC. Typical particle diameters and coating thicknesses are on the order of 600 μm and 75 μm, respectively. PyC coated SYNROC D has three coatings of PyC consisting of the inner dense layer, an intermediate low density buffer layer overlaid by an outer dense coating. The intermediate low density carbon layer is designed to accommodate irradiation induced volume changes in the waste and any gas generation. SiC coatings have also been applied to SYNROC B spheres at relatively low temperatures in the range of 700-1000°C.

- Leach test results for coated and uncoated particles reported by the ORNL group show that the leach rates for various species of all coated waste forms are below the detection limits of ICP or atomic absorption. No leach data, however, were reported for pyrolytic carbon. Using graphite leach data and assuming it to be similar to that of pyrolytic carbon, we estimated that in a period of 1000 years the carbon losses would be on the order of 7×10^{-6} and 7×10^{-3} cm at 99° and 250°C, respectively. Since typical pyrolytic carbon layer thicknesses total about 7.5×10^{-3} cm, it may be speculated that, under low flow non-saline conditions at 99°C, pyrolytic carbon coated particles have the potential to provide 1000-year containment of high level defense wastes. Until the carbon coatings are breached, this waste form could also meet the NRC controlled release criterion.

- Leach rates for SPC-4 supercalcine and 76-78 borosilicate glass encapsulated in various matrices have been reported by PNL. Preliminary results show that 100% Pb matrix is optimum for glass marbles, and that graphite and hot pressed TiO_2 and Ti-6% Al-4% V matrices are optimum for ceramic pellets. Non-metallic matrices such as concrete, castables, and hot pressed glass are not acceptable due to their high permeability and matrix dissolution rates. Estimated matrix material corrosion rates, based on composite leach tests using MCC-1, show that TiO_2 and Ti-6% Al-4% V have the lowest corrosion rates in deionized water at 90°C. Minimum matrix thicknesses required to provide 1000-year containment are calculated to be 5.1×10^{-12} cm for Ti-6% Al-4% V and 3.0 x 10^{-4} cm for TiO_2. In addition, the metal encapsulated waste forms exhibit good thermal conductivity and high impact resistance.

- Work at Eurochemic in Mol, Belgium, has investigated the corrosion behavior of various lead alloys in salt solutions. Samples of pure Pb and Pb-Sn alloys used in encapsulating glassy waste forms, were allowed to react with distilled water and salt solutions prepared from ASSE II rock salt. The alloys were also exposed to dry ASSE II salt at temperatures of up to 250°C. In addition, the effect of the presence of oxygen, nitrogen and CO_2 in salt solutions on the corrosion rate was investigated. The corrosion rates are generally very low; on the order of m/yr. Further experiments with other metals indicate that pure Al is as corrosion resistant as Pb when reacted with dry ASSE salt and its saturated aqueous solutions. Based on the reported corrosion rates, our estimates of minimum thicknesses of Pb or Pb alloys required for 1000-year containment are on the order of millimeters. Such thicknesses of encapsulating material such as Pb or Pb alloys should be able to protect the underlying waste form from groundwater attack for at least 1000 years.

- Cermet matrix alloy has been reported to exhibit high resistance to oxidation corrosion. However, sufficient leach data are not available at this time to evaluate the chemical durability of cermet waste form.

- Among the crystalline waste forms, a considerable amount of information has been generated on SYNROC during the last year. Comparison of leach rates of SYNROC C and borosilicate glass containing simulated high level commercial waste based on tests at 95°C conducted at the Australian National University show that SYNROC leach rates drop by more than an order of magnitude over a period of 20 days, while glass leach rates remain constant. Compared to glass, the long term SYNROC leach rates are lower by two to three orders of magnitude. Comparative leach testing of SYNROC and borosilicate glass containing the same simulated waste over a temperature range of 45-300°C has been conducted at the Australian Atomic Energy Commission. The results show that the long term cumulative release of Cs and Si from SYNROC is more than an order of magnitude less than that from PNL 76-68 glass. Secondly, with increasing time, the SYNROC leach rates drop off more rapidly than those of the glasses. Further, the results show that although the leach rates for SYNROC and the glass increase with increasing temperature, the increase exhibited by SYNROC is markedly smaller than that for the glasses, with the difference in leach rates of SYNROC and the glasses becoming more pronounced at higher temperatures. Further, that for the SYNROC matrix elements such as Al, Ba, Ti and Zr are reported to be very resistant to leaching.

- Both crushed and monolithic samples of SYNROC C and D formulations fabricated at LLL have been tested for leach resistance using MCC-4 tests at 75°C. The leach rates generally decrease by more than an order of magnitude over a period 30 days. Because of the presence of spinel phases, the SYNROC D formulation is reported to exhibit wide flexibility with respect to the compositional variations in SRP defense waste streams.

- At ORNL, the sol-gel technology developed for reactor fuel fabrication, has been successfully applied to SYNROC production. SYNROC microspheres and pellets of both B and D formulations, containing up to 70 wt % SRP sludge without Al removal, have been prepared. In addition, gel derived spheres of high waste loading (40 wt %) have been formed using simulated high Fe SRP waste as well as high Al SRP waste without Al removal.

- Leach rates for gel derived SYNROC B and D formulations, based on MCC-1 tests for three days, show that for SYNROC B all elements leached are below the analytical detection limits. In the case of SYNROC D, the leach rates vary in the range of 10^{-1} to 10^{-4} g/m^2-day. As discussed above, PyC coating of these waste forms yields elemental releases below detection limits.

- The high alumina ceramic is a relatively new development, designed to immobilize the high alumina SRP defense wastes. As a result, the available leach data are very preliminary. Comparison of leach rates of high alumina ceramic with 76-78 borosilicate glass shows that relative to glass, the ceramic leach rates are 10 to 100 times lower. Except U and Na, the elements measured are all below their analytical detection limits. Na release has been attributed to the dissolution of nepheline in the ceramic and is comparable to the Na release for glass. Thermal tests showed the ceramic to be stable up to a temperature of 1200°C. No Cs loss is reported during the fabrication of the high alumina ceramic.

- Borosilicate waste glass is one of the most developed waste forms and is being extensively studied in the DOE community as well as in foreign countries. The glass containing commercial HLW has larger amounts of fission products and actinides with a higher heat output compared to defense HLW glass.

- Most defense waste glasses have better leach resistance than the commercial glasses in the 70-150°C temperature range. Compared to PNL 76-68, most defense waste glasses are approximately an order of magnitude more leach resistant. One of the most important parameters affecting the chemical durability of glass is temperature. For example, SRL Frit 131 exhibits a five-fold increase in leach rates with an increase in temperature from 25 to 90°C. Flow rates affect glass leach rates as well; an increase of one to two orders of magnitude in leach rates is observed at flow rates in the range of 2-70 m/year. With respect to the effect of solution chemistry, brine solutions generally result in lower leach rates when compared to DI water and silicate groundwaters. The solution pH is also important in that in the low and high pH regimes (pH = <5 and >9) the leach rates increase by up to two orders of magnitude. Fission products leach generally faster than the actinides, the difference being sometimes more than an order of magnitude.

- Glass composition can also affect the chemical durability, although the change in leach rate may not be significant. No data on the effect of phase separation on the chemical durability have been reported. However, a study of commercial glass indicates that the heat treatment should be done carefully to avoid an easily leachable microstructure.

- Various vitrification processes and subsequent radiation, thermal and mechanical effects can induce glass cracking, resulting in an increase in reactive surface area. This increased area, in turn, will increase the fractional release rate.

- Mechanical degradation of waste forms under repository conditions and over long time periods can be evaluated in terms of their mechanical properties. The tensile strength of 76-68 glass is 51.4 MPa, which is slightly higher than for ceramic or glass ceramics waste forms. On the other hand, compression strength may not be important since the compression strength is greater than tensile strength by an order of magnitude. This could lead to frequent fracture of waste form by tensile stresses, not only by the application of a tensile force, but also by the development of tensile stresses at certain portions of waste form during general compression. Static fatigue is also known to be a very important mode of disintegration for glass in water. This is particulary important in repository conditions since cracks developed under static fatigue will increase the exposed surface area, leading to significant material release.

- With regard to glass weathering, ancient glasses may be indicative of long-term glass durability. Although the compositions of ancient glasses are quite different from the nuclear waste glasses, there is some evidence for over a 1000 yr durability.

- Recent work at Catholic University on the encapsulation of high level defense waste in a nonradioactive high silica glass sheath gave encouraging results. The thermal expansion of the core glass and sheath were matched successfully and, in a variety of leach tests, the leach rates were found to be significantly lower than those for noncoated glasses. Leach tests have been conducted under a range of conditions such as varying flow rates, solution matrices, temperatures, and time periods. For comparison purposes, PNL and SRL glasses have also been tested under identical conditions. The results show that, at high and intermediate flow rates, the PGM core glasses are one to two orders of magnitude more leach resistant than the PNL 76-78 and SRL glasses. At low flow rates, reflecting nearly stagnant repository conditions, the glass dissolution rates are controlled by silica saturation levels. Since PGM core glasses do not exhibit a wide pH excursion, their leach resistance is greater than that of the other glasses.

- Estimates of fractional waste material loss based on silica release at 70°C from PGM high alumina and PGM composite core glasses and SRL and PNL 76-68 as a function of flow rates indicate that, at flow rates in the range of 2-70 m/year, the PGM core glasses exhibit material loss two to three orders of magnitude lower than the SRL and PNL glasses. Since the fractional material release is on the order of $<10^{-5}$/year, we believe that PGM core glasses by themselves could meet the controlled release criterion, assuming the silica dissolution rate to be comparable to that of the long lived actinides. The above calculation is conservative because the high silica cladding will provide additional barrier. The high silica cladding glass is reported to exhibit at least an order of magnitude lower leach rate than the PGM core glasses. Since the cladding glass is free of radionuclides, the CUA workers report that a 4-mm thick protective jacket can provide containment of radionuclides in the core glass for time periods varying from 1.2×10^7 years at 20°C to 1.2×10^4 years at 100°C. Based on available information, we believe that PGM core-clad composite will meet both criteria of the 1000-year containment and the controlled release of 10^{-5}/year after the first 1000 years.

- PGM composite core clad glasses have been produced in fully radioactive form. Leach rates, based on core isotopes, are reported to be lower than 10^{-8} g/m^2-d. Estimated leach rates based on core exposure by fracture are 500 times lower than leach rates for bare core.

- Strictly based on limited chemical durability data, we believe that both ORNL coated particles and CUA porous glass composite have the potential to meet independently the NRC 1000-year containment and 10^{-5}/year controlled release criteria, assuming that the laboratory derived leach rates do not change significantly under realistic repository conditions and over repository time scales. Other waste forms such as SYNROC, gel derived ceramic microspheres, high alumina ceramic, and metal matrices also look promising and should be investigated further.

2.10 Recommendations for HLW Forms

Although some of the waste forms described above appear to have the potential to contribute independently to the overall performance of the waste package and/or the underground facility, further research is required before any one of these waste forms can be selected on the basis of its ability to meet the NRC criteria. Considering that the long term controlled release criterion applies specifically to the post-1000 yr fission product containment period, more emphasis should be placed on specific actinide release rates. Futhermore, the extent of actinide release appears to be controlled by the solubility of the waste form itself or by the newly precipitated actinide-bearing authigenic phases. In view of these factors, it is recommended that actinide leach rates be determined under a range of conditions such as varying flow rates, redox potential, pH and solution chemistries. Specific recommendations for research are outlined below:

Coated Particles

- Increased emphasis is required to fully characterize waste form coating procedures to ensure that optimum coating combinations and coating thicknesses be achieved. Current sizes of coated particles tend to be small. A study should be initiated to determine if larger sizes (1 cm) could be more desirable from a processing or dispersibility standpoint.

- HTGR fuel consists of fuel particles embedded in a carbon matrix to form a fuel stick. There should be an attempt to determine whether this would be an appropriate technology for waste encapsulation to prevent dispersibility, improve thermal conductivity, and increase leach resistance.

- Attempts should be made to develop the lowest possible deposition temperatures for barrier coatings so that volatilization of radionuclides during deposition is minimized. Although low temperature CVD PyC coating using nickel tetracarbonyl looks promising, several questions arise concerning the "catalyzed" deposition of PyC. Since the process temperature for PyC deposition exceeds that for deposition of nickel from $Ni(CO)_4$, nickel may be codeposited with carbon. If so, the characteristics of the coating may be altered. Nickel could be in either a homogeneous solid solution or be dispersed heterogeneously through the carbon coating. Surface deposited nickel (or perhaps some nickel compound) may actually be the catalyst for C_2H_2 decomposition rather that $Ni(CO)_4$. If nickel is included in the pyrolytic carbon coating it is possible that it could detrimentally affect the leaching behavior. All of the above uncertainities must be addressed in this type of coated particle work.

- Leach testing of candidate coated particles should be carried out in detail. Little long term information is currently available to confirm the dissolution rates of coatings such as PyC, Al_2O_3, and SiC. Although the ORNL gel-derived coated particles look promising in terms of their chemical durability, more work is needed to extensively characterize the coatings, the underlying core, and the core/coating and coating/coating interfaces. In addition, the work on low temperature deposition of SiC coating should be continued to determine the characteristics of the coating and its leach resistance.

- Radiation damage studies of the coated particles should also be conducted as described in Section 5.

Ceramic Waste Forms

- Although a considerable amount of information has been generated on SYNROC process and product, there is no experimental evidence to show that the SYNROC minerals are in thermodynamic equilibrium with each other and with the host titanate matrix, either at the processing temperature or at room temperature. This property is important in that it could affect the long-term stability and leach resistance of the waste form and requires careful investigation.

- We recommend that SYNROC process flexibility be tested. Specifically, the effects of increasing waste concentration and of compositional variations on the stability of the waste form need to be investigated. Further work is required to establish the maximum range of solid solutions, in terms of radionuclide compositional variability, for each SYNROC mineral. In other words, the extent to which the SYNROC minerals can accommodate the various fission products and actinide elements, without affecting their leach resistance and stability, is not known and requires experimental work. The SYNROC-D formulation, proposed for immobilizing defense wastes, possesses a more complex mineralogy considering the presence of spinel-like phases which immobilize the inert contaminants such as Fe, Al, and Mn. Further research is required to establish the precise mineralogical composition of SYNROC D and the properties of the individual phases.

- Other critical parameters such as variation in oxygen potential on the SYNROC mineral assemblage need to be investigated. This parameter is particularly important in producing large samples because of the probability of inhomogeneous oxygen distribution which could lead to the formation of a different mineral assemblage.

- Experiments on existing SYNROC samples should be carried out to determine the thermal stability of various SYNROC formulations. The sample can be thermally cycled several times, covering a wide range of temperature, say 25°C to 1100°C, in the subsolidus region. The changes in the initial mineral assemblage, occurring during the thermal cycle, can be monitored by high-temperature x-ray diffraction methods. Scanning electron and polarized light microscopy can be used to detect non-crystalline phases. The kinetic effect in such experiments can be assessed by carrying out time-temperature variation studies. This should provide quantitative information on the nature and extent of the reaction process. Detailed radionuclide distribution investigations of SYNROC minerals, before and after the above-mentioned experiments, may provide information on the thermal diffusion and resultant enrichment of radionuclides at mineral grain boundaries.

- In order to be able to predict the long-term stability of SYNROC, information is needed on the dissolution kinetics of SYNROC in terms of the matrix elements, the fission products, and the actinides. Such information, obtained from short-term experiments, can help to understand the mechanisms by which the SYNROC minerals undergo dissolution over a long time period. Further, experiments to study the dissolution kinetics and equilibria of individual SYNROC minerals under repository conditions should be carried out. Such information will help understand the long-term stability of SYNROC in terms of fission products and actinide release.

- Detailed characterization of reacted SYNROC material (that is, SYNROC after reaction with aqueous media) should be carried out to determine the nature and extent of alteration, the character of the alteration products, the relative resistance of SYNROC minerals to dissolution, the changes in grain boundary characteristics and radionuclide distributions within mineral phases.
- More data are required on high alumina ceramic, especially with respect to its process conditions and engineering practicality. Further leach tests should be conducted under a range of conditions such as varying flow rates, pH, temperature, etc. The observed Na and U release from nepheline and magnetoplumbite, respectively, should be further investigated. In addition, all the research outlined above for SYNROC should be carried out on the high alumina ceramic so that sufficient data are available to evaluate its chemical durability.

Glassy Waste Forms

- The available information on Porous Glass Matrix is generated by only one group of workers. Independent research is required to further test this process and the product. Further, the effects of high levels of radiation and of chemical transmutations on leaching behavior need investigation.
- Mechanisms controlling the flow rate dependence of PGM leach rates should be studied in order to predict its long-term performance.
- With respect to borosilicate glass, long-term leach tests should be performed, emphasizing studies of mechanisms involved in the dissolution process. Such leach data can then be used to extrapolate the dissolution behavior to long time periods. In addition, bench scale tests are desirable to avoid the difficulty of extrapolating small sample data to the size of a real waste package.
- It is necessary to identify the activation process in waste glass leaching. This will aid in the estimation of temperature sensitivity on leach rates justifying the use of accelerated leach test.
- Surface alteration zone and reprecipitation should be taken into consideration in the interpretation of leach data.
- More systematic study is necessary to quantify radiation and thermal induced cracking and its subsequent effect on total mass release.
- pH effect should be studied further, especially the change of pH shift due to a slight change in glass composition such as rare earth elements during leaching, and its subsequent effect on leachability.

- Regarding the long-term weathering effects, the study of ancient glasses is recommended to further assess the long term durability.

- The optimum microstructure for high leach resistance glass should be determined based on the principle of phase separation.

- The mechanical degradation of glass in repository conditions should be studied in detail, particularly the static fatigue behavior.

- More sophisticated and comprehensive modeling of glass corrosion processes is needed. Computerized code generation may be a necessary step in the assessment of the complex processes and in the area of long-term prediction of glass durability.

2.11 Conclusions for TRU Waste Forms

In addition to being conclusions, some of these points indicate areas that are obviously in need of additional effort if these waste forms are to meet the actinide release rate criterion of 10^{-5}/yr.

- An insufficient data base exists for all the TRU waste forms reviewed.

- In terms of the 10^{-5}/yr actinide release rate criterion, no TRU waste form under development has been shown to meet this requirement with any degree of confidence. In fact, the dearth of available information on the waste forms discussed leads us to conclude, at this time, that no credit can be taken by DOE for the waste form as an engineered barrier.

- In some cases, the TRU waste stream has not been adequately characterized.

- Few data are reported for waste forms containing actual waste.

- Inadequate information exists for the sensitivity of waste form properties to physical and chemical variations in the waste.

- Outside of the comparative assessment study at PNL, no standard test methods have been used in the evaluation of material properties.

- As concerns radiation damage, the available evidence indicates that effects due to alpha particle and recoil nucleus events are not expected to be a determining factor. However, this cannot be confirmed (determined) until the ranges of waste form composition and loadings are specified.

- The combination of certain TRU waste streams, e.g., incinerator ash and process sludges, with a HLW stream for processing into a single waste form appears to be a technically feasible strategy based on the available data.

2.12 Recommendations for TRU Waste Forms

The waste form-specific recommendations are too numerous and lengthy to be listed in this abbreviated section. Instead, some generic recommendations have been listed below.

- We recommend that the following waste forms be excluded from any further serious consideration as alternative TRU waste forms: (1) the existing TRU waste (2) Urea-formaldehyde resin, (3) Bitumen, and (4) Normal cast concrete. Reasons for making this recommendation are given below.

- The extent of the solubility of various actinides in glassy and crystalline phases appears to be well known only for borosilicate glass and monazite. This parameter is important because of anticipated variations in the actinide level in some TRU waste streams.

- Data on the phase characterization and actinide partitioning in the candidate waste forms are either scarce, incomplete, or lacking altogether. In the final analysis, these data must be obtained for production prototypic radioactive waste forms. The phases identified for lab-scale samples may not necessarily be representative of those present in large scale products.

- The role of various waste stream constituents in the formation of a durable product should be elucidated.

- In the area of radiation stability:

  (1) an improved understanding of the metamict state, and the metamict "transition", would increase our confidence in the isolation capabilities of crystalline TRU waste forms. Some effort should be directed toward investigating dose rate effects, and establishing the degree of equivalence between the metamict state in natural analogues and laboratory samples. Certainly, the effect of metamictization on leach behavior should be unambiguously determined.

  (2) The possibility of increased radiation damage susceptibility due to alteration under the repository environment (e.g., by incongruent leaching) should be evaluated.

- There is an obvious need for actinide leach data. In this area, we recommend:

  (1) use of standardized (MCC) tests with actual waste loaded samples,

  (2) use of waters equilibrated with repository rock and/or potential geologic environments,

(3) that the leach mechanisms for the various waste forms be understood for long term predictive capability,

(4) thorough investigation of the possibility that actinide leach rates are solubility limited at low groundwater flow rates, and

(5) if such is the case, then the concept of valence state control of the actinides in the candidate waste form should be pursued.

2.13 Conclusions and Recommendations for Spent Fuel are outlined below:

- As of this moment, there has been a more thorough scientific investigation of the leaching of spent fuel and UO_2 than any one of the other waste forms. Confirmatory data from several different sources are available on the release of a range of radionuclides that is more complete than for any other single glass or ceramic waste form. Also, because of the conducting nature of the fuel, fundamental electrochemical studies of the dissolution mechanisms have been possible; glasses and ceramics are, by contrast, almost impossible to characterize by such methods.
- Fission product distribution in the fuel as well as its mechanical properties are under investigation; this information is being obtained by earlier destructive and non-destructive tests of fuel burn-up efficiency.

2.14 References

1. J. M. Rusin, "A Review of High-Level Waste Form Properties," PNL-3035, 1980.
2. J. L. Crandall, "Development of Solid Radionuclide Waste Forms in the United States," in Scientific Basis for Nuclear Waste Management, Vol. 2, Plenum Press, New York, 1980.
3. Code of Federal Regulations, 10 CFR 60, "Technical Criteria for Regulating Geologic Disposal of High-Level Radioactive Waste," Advance Notice of Proposed Rule Making, Draft 14, 1980.
4. J. E. Mendel, J. H. Westsik, Jr. and D. E. Clark, "Chemical Durability," in A State-of-the-Art Review of Materials Properties of Nuclear Waste Forms, PNL-3802, 1981.
5. Management of Commercially Generated Radioactive Waste, DOE/EIS-0046H, Vol. 2, 1980.
6. L. Kahl, "The Chemical Durability of the HLLW-Borosilicate Glasses GP 98/12 and GP 98/26," in ORNL Conference on the Leachability of Radioactive Solids, Gatlinburg, TN, 1980.

7. Y. Sousselier, "Use of Glasses and Ceramics in the French Waste Management Program," in Ceramics in Nuclear Waste Management, Cincinnati, CONF-790420, 1979.

8. F. Lanza and E. Parnisari, "Evaluation of Long Term Leaching of Borosilicate Glasses," in Nuclear Science and Technology, ERU5947EN, 1978.

9. D. J. Cameron and G. G. Strathdee, "Materials Aspects of Nuclear Waste Disposal in Canada," in Ceramics in Nuclear Waste Management, Cincinnati, CONF-790420, 1979.

10. R. Terai, K. Eguchi and H. Yamanaka, "Characterization of Borosilicate Glasses Containing Simulated High Level Radioactive Wastes for PNC," in Ceramics in Nuclear Waste Management, Cincinnati, CONF-790420, 1979.

11. S. H. Sutherland and D. E. Bennett, "Defense High-Level Waste and Spent Fuel Characterization for Geologic Waste Repositories," SAND 79-0172, 1979.

12. L. M. Papouchado, "Use of Borosilicate Glass for Immobilization of Savannah River Plant Radioactive Waste," presented at the Alternate Waste Forms Peer Review Panel, Atlanta, 1981.

13. W. R. Cornman, "Composite Quarterly Technical Report, Long-Term HLW Technology," July-September 1980, DP-80-157-3, 1981.

14. L. Chick, et al., "Annual Report on the Development and Characterization of Solidified Forms for Nuclear Wastes, 1979," PNL-3465, 1980.

15. M. D. Dukes, "Multibarrier Storage of SRP Waste," in Scientific Basis for Nuclear Waste Management, Vol. 2, C. J. M. Northrup, Jr., Ed., Plenum Press, New York, 1980.

16. K. A. Boult, et al., "The Leaching of Radioactive Waste Storage Glasses," in Ceramics in Nuclear Waste Management, Cincinnati, CONF-790420, 1979.

17. W. Guber, et al., "Preparation and Characterization of Improved High Level Radiation Waste Borosilicate Glass," in Scientific Basis for Nuclear Waste Management, Vol. 1, G. J. McCarthy, Ed., Plenum Press, New York, 1978.

18. "The PGM Glass Process," presented at the Alternative Waste Form Peer Review Panel, Atlanta, 1981.

19. B. T. Kenna and K. D. Murphy, "Long-Term Soxhlet Leach Tests," in ORNL Conference on the Leachability of Radioactive Solids, Gatlinburg, TN, 1980.

20. J. R. Wiley, N. E. Bibler, M. D. Dukes and M. J. Plodimec, "Glass as a Matrix for SRP High-Level Defense Waste," DPST-79-294, 1980.

21. W. R. Corman, "Composite Quarterly Technical Report, Long-Term HLW Technology," October-December 1980, DP-80-157-4, 1981.

22. J. M. Rusin, "A Review of Glass Ceramic Waste Form," in Alternate Nuclear Waste Forms and Interactions in Geologic Media, CONF-8005107, 1980.

23. J. K. Bates, K. F. Flynn, L. J. Jardine and M. J. Steindler, "The Application of Neutron Activation Analysis to Leach Rate Studies," in ORNL Conference on the Leachability of Radioactive Solids, Gatlinburg, TN, 1980.

24. K. F. Flynn, L. J. Jardine and M. J. Steindler, "Resistance of HLW Materials to Dissolution in Aqueous Media," in Scientific Basis for Nuclear Waste Management, Vol. 2, C. J. M. Northrup, Jr., Ed., Plenum Press, New York, 1980.

25. H. C. Weed, et al., "Leaching Characteristics of Actinides From Simulated Reactor Waste, Part 2," in Scientific Basis for Nuclear Waste Management, Vol. 2, C. J. M. Northrup, Jr., Ed., Plenum Press, New York, 1980.

26. N. A. Chapman and D. Savage, "Dissolution of Borosilicate Glasses Under Repository Conditions of Pressure and Temperature," in Scientific Basis for Nuclear Waste Management, Vol. 2, C. J. M. Northrup, Jr., Ed., Plenum Press, New York, 1980.

27. R. A. Bonniand, et al., "Glasses as Materials Used in France for Management of HLW," in Ceramics in Nuclear Waste Management, Cincinnati, CONF-790420, 1979.

28. F. Lanza and E. Parnisari, "Evaluation of Long-Term Leaching of Borosilicate Glass in Pure Water," in Ceramics in Nuclear Waste Management, Cincinnati, CONF-790420, 1979.

29. D. D. Walker, J. R. Wiley, M. D. Dukes and J. H. LeRoy, "Leach Rate Studies on Glass Containing Actual Radioactive Waste," in ORNL Conference on the Leachability of Radioactive Solids, Gatlinburg, TN, 1980.

30. J. M. Perez, Jr. and J. H. Westik, Jr., "Effects of Cracks on Glass Leaching," in ORNL Conference on the Leachability of Radioactive Solids, Gatlinburg, TN, 1980.

31. L. L. Hench, D. E. Clark and E. L. Yen-Bower, "Corrosion of Glasses and Glass Ceramics," Nuclear and Chemical Waste Management 1 (1980).

32. T. M. Ahn and K. J. Swyler, "An Analysis of Radiation Induced Stress in HLW," BNL Memorandum, 1980.

33. J. W. Braithwaite, "Brine Chemistry Effects on the Durability of a Simulated Nuclear Waste Glass," in Scientific Basis for Nuclear Waste Management, Vol. 2, C. J. M. Northrup, Jr., Ed., Plenum Press, New York, 1980.

34. W. A. Ross, et al., "Annual Report on the Characterization of High-Level Waste Glasses," PNL-2625, 1978.

35. P. B. Adams, "Glass Containers for Ultrapure Solutions," in Ultrapurity, Marcel Dekker, Inc., New York, NY, 1972.

36. W. A. Ross and J. E. Mendel, "Annual Report on the Development and Characterization of Solidified Forms for HLW," PNL-3060, 1979.

37. J. L. McElroy, et al., "Quarterly Progress Report - Research and Development Activities -- HLW Immobilization Program, April 1 through June 30, 1979," PNL-3050-2, 1979.

38. M. Tomozana, "Phase Separation in Glass," in Treatise on Materials Science and Technology, Vol. 17, M. Tomozana and R. H. Doremus, Eds., Academic Press, New York, NY, 1979.

39. M. F. Kaplan, "Characterization of Weathered Glass by Analyzing Ancient Artifacts," in Scientific Basis for Nuclear Waste Management, Vol. 2, C. J. M. Northrup, Jr., Ed., Plenum Press, New York, 1980.

40. V. K. Sethi, R. M. Arons, J. P. Guha, J. T. Dusck and R. B. Poeppel, "ANL Program Review of High Level Waste Technology," Atlanta, GA, 1981.

41. T. H. Smith and W. A. Ross, "Impact Testing of Vitreous Simulated High-Level Waste in Canisters," BNWL-1903, 1975.

42. W. F. Merritt, "High Level Waste Glass: Field Leach Test," Nucl. Tech. 22 (1977).

43. A. R. Bancroft and J. D. Gramble, "Initiation of a Field Burial Test of the Disposal of Fission Products Incorporated in Glass," AECL-718, 1958.

44. A. Barkatt, E. N. Boulos, R. P. DePaula, O. H. El-Bayoumi, N. Lagakos, P. B. Macedo, C. N. Moynihan, S. M. Rekhson and J. H. Simmons, "Stability of Fixation Solids for High-Level Radioactive Wastes," in High-Level Radioactive Solid Waste Forms, Denver, NUREG/CP-0005, 1978.

45. P. B. Macedo, D. C. Train, J. H. Simmons, M. Saleh, A. Barkatt, C. J. Simmons, N. Lagakos and E. Dewitt, "Porous Glass Matrix Method for Encapsulating High-Level Nuclear Wastes," in Ceramics in Nuclear Waste Management, Cincinnati, CONF-790420, 1979.

46. J. H. Simmons, P. B. Macedo, A. Barkatt and T. A. Litovitz, "Fixation of Radioactive Waste in High Silica Glass," Nature 278, 729 (1979).

47. M. G. Drexhage and P. K. Gupta, "Strengthening of Glasses by Partial Leaching," J. Amer. Ceram. Soc. 63, 72 (1980).

48. M. G. Drexhage and P. K. Gupta, "Stresses Arising During the Leaching of a Two-Phase Glass," J. Amer. Ceram. Soc. 63, 196 (1980).

49. R. Dayal, K. J. Swyler and P. Soo, "NRC Nuclear Waste Management Technical Support in the Development of Nuclear Waste Form Criteria, Task 1: Waste Package Overview, Interim Report," BNL-NUREG-27961, 1980.

50. T. M. Ahn, R. Dayal and K. J. Swyler, "Chemical Durability and Structural Stability of Molecular Stuffed Glass -- An Evaluation," unpublished BNL Memorandum, 1980.

51. W. Lutze, J. Borchardt and A. K. De, "Characterization of Glass and Glass Ceramic Nuclear Waste Forms," in Scientific Basis for Nuclear Waste Management, Vol. 1, C. J. McCarthy, Ed., Plenum Press, New York, 1978.

52. W. Lutze, "Glassy and Crystalline High-Level Nuclear Waste Forms -- An Attempt at Critical Evaluation," in Ceramics in Nuclear Waste Management, Cincinnati, CONF-790420, 1979.

53. A. K. De, et al., "Development of Glass Ceramics for the Incorporation of Fission Products," Bull. Amer. Ceram. Soc. 55, 500 (1976).

54. A. K. De, B. Luckscheiter, G. Malow and E. Schiewer, "Fission Products in Glasses Part II: Development of Glass Ceramics," HMI-B218, Hahn-Meitner-Institute, Berlin, West Germany, 1977.

55. J. M. Rusin, J. W. Wald and R. O. Lokken, "Alternative Waste Forms -- A Comparative Study," presented at the Materials Research Society Meeting, Boston, MA, November 1979, PNL-SA-7782.

56. J. M. Rusin, "A Review of Glass Ceramic Waste Forms," in Alternate Nuclear Waste Forms and Interactions in Geologic Media, CONF-8005107, 1981.

57. N. Oguino, S. Masuda and N. Tsunoda, "Solidification of HLLW by Glass-Ceramic Process," in Ceramics in Nuclear Waste Management, Cincinnati, CONF-790420, 1979.

58. O. Kazuo, O. Takao, S. Masuda and N. Tsunoda, "Solidification of HLLW Into Sintered Ceramics," in Ceramics in Nuclear Waste Management, Cincinnati, CONF-790420, 1979.

59. G. J. McCarthy, "High-Level Waste Ceramics: Materials Considerations, Process Simulation and Product Characterization," Nucl. Tech. 32, 92 (1977).

60. R. Roy, "Rational Molecular Engineering of Ceramic Materials," J. Amer. Ceram. Soc. 60, 358 (1977).

61. W. A. Ross, J. M. Rusin and J. L. McElroy, "Processes for Production of Alternative Waste Forms," in Waste Management '79, Tucson, AZ, 1979.

62. A. E. Ringwood, S. E. Kesson, N. G. Ware, W. B. Hibberson and A. Major, "Immobilization of High Level Nuclear Reactor Wastes in SYNROC," Nature 278, 219 (1979).

63. J. D. Tewhey, C. L. Hoenig, H. W. Newkirk, R. B. Rozsa, D. G. Coles and F. J. Ryerson, "The Application of SYNROC to High Level Defense Wastes," in Alternate Nuclear Waste Forms and Interactions in Geologic Media, CONF-8005107, 1981.

64. W. B. Durham, C. L. Hoenig, F. J. Ryerson and J. D. Tewhey, "The Application of SYNROC to High Level U. S. Defense Wastes," in Waste Management '80, Vol. 2, M. E. Wacks and R. G. Post, Eds., 1980.

65. K. D. Reeve, D. M. Levins, E. J. Ramm, J. I. Woolfrey, W. J. Buykx and R. K. Ryan, "Progress in SYNROC Research and Development at Lucas Heights," in Waste Management '80, Vol. 2, M. E. Wacks and R. G. Post, Eds., 1980.

66. "Immobilization of High Level Defense Wastes in SYNROC: An Appraisal of Product Performance," presented at the Alternative Waste Form Peer Review Panel, Atlanta, 1981.

67. W. J. Lackey, P. Angelini, F. L. Layton, D. P. Stinton and J. S. Vavruska, "Sol-Gel Technology Applied to Glass and Crystalline Ceramics," in Waste Management '80, Vol. 2, M. E. Wacks and R. G. Post, Eds., 1980.

68. D. Angelini, W. D. Arnold, W. D. Bond, A. J. Caputo, L. Dole, W. J. Lackey, S. M. Robinson and D. P. Stinton, "Sol-Gel Coated Particle Waste Form for SRP Defense Waste Isolation," presented at the Alternative Waste Form Peer Review Panel, Atlanta, 1981.

69. V. K. Sethi, R. M. Arons, J. P. Guha, J. T. Dusek and R. B. Poeppel, "Fabrication, Characterization and Evaluation of SYNROC Waste Forms," presented at the Alternative Waste Form Peer Review Panel, Atlanta, 1981.

70. R. G. Dosch, "Ceramic Forms for Nuclear Waste," in Radioactive Waste in Geologic Storage, S. Fried, Ed., American Chemical Society Series 100, Washington, DC, 1979.

71. J. K. Johnson, T. J. Headley, P. F. Hlava, F. V. Stohl, "Characterization of a Titanate Based Ceramic for High Level Nuclear Waste Solidification," in Scientific Basis for Nuclear Waste Management, Vol. 1, C. J. McCarthy, Ed., Plenum Press, New York, 1978.

72. S. Forberg and T. Westermark, "A Radioactive Waste Solidification System Resulting in an Extremely Stable Product," in Scientific Basis for Nuclear Waste Management, Vol. 1, C. J. McCarthy, Ed., Plenum Press, New York, 1978.

73. R. G. Dosch, p. F. Hlava and T. J. Headley, "Titanate Waste Forms for High Level Waste," presented at the Annual Meeting of the Materials Research Society, Boston, MA, 1980.

74. D. E. D. Morgan, D. R. Clarke, C. M. Jantzen and A. B. Harker, "High Alumina Tailored Nuclear Waste Ceramics," J. Amer. Ceram. Soc. in press.

75. A. B. Harker, C. M. Jantzen, D. E. D. Morgan and D. R. Clarke, "Tailored Ceramic Nuclear Waste Forms: Preparation and Characterization," presented at the Annual Meeting of the Materials Research Society, Boston, MA, 1980.

76. H. Recht, "Status of Development of the Tailored Ceramic High Level Nuclear Waste Form," in Waste Management '81, M. E. Wacks and R. G. Post, Eds., 1981.

77. "Tailored Ceramics for Geologic Storage of High Level Nuclear Waste," presented at the Alternative Waste Form Peer Review Panel, Atlanta, 1981.

78. J. M. Rusin, J. W. Wald, R. O. Lokken and J. W. Shade, "Comparative Waste Forms Study," PNL-3516, 1980.

79. J. N. C. Geel and H. Eshrich, "New Developments on the Solidification of High Level Radioactive Wastes at Eurochemic," Trans. Amer. Nucl. Soc. 20, 671 (1975).

80. W. Heimerl, "Solidification of HLW Solutions With the Pamela Process," in Ceramics in Nuclear Waste Management, Cincinnati, CONF-790420, 1979.

81. W. Neumann, "Embedding Methods of Solidified Wastes in Metal Matrices," in Ceramics in Nuclear Waste Management, Cincinnati, CONF-790420, 1979.

82. J. W. Walt, J. M. Rusin and C. O. Burkwalter, "PNL Matrices Waste Forms," presented at the Alternative Waste Form Peer Review Panel, Atlanta, 1981.

83. J. M. Rusin, M. F. Browning and G. J. McCarthy, "Development of Multibarrier Nuclear Waste Forms," in Scientific Basis for Nuclear Waste Management, Vol. 1, C. J. McCarthy, Ed., Plenum Press, New York, 1978.

84. L. J. Jardine and M. J. Steindler, "Metal Encapsulation of Ceramic Nuclear Waste," in Scientific Basis for Nuclear Waste Management, Vol. 1, C. J. McCarthy, Ed., Plenum Press, New York, 1978.

85. W. S. Aaron, T. C. Quinby and E. H. Kobisk, "Development of Cermets for High Level Radioactive Waste Fixation," in Ceramics in Nuclear Waste Management, Cincinnati, CONF-790420, 1979.

86. E. H. Kobisk, W. S. Aaron, T. C. Quinby and D. W. Ramey, "High Level Waste Fixation in Cermet Form," in Alternate Nuclear Waste Forms and Interactions in Geologic Media, CONF-8005107, 1981.

87. W. S. Aaron, T. C. Quinby and E. H. Kobisk, "Development and Characterization of Cermet Forms for Radioactive Waste," in Scientific Basis for Nuclear Waste Management, Vol. 2, C. J. M. Northrup, Jr., Ed., Plenum Press, New York, 1980.

88. J. M. Rusin, J. W. Slade, R. W. Kidd and M. F. Browning, "Chemically Vapor Deposited Coatings for Multibarrier Containment of Nuclear Wastes," in Alternate Nuclear Waste Forms and Interactions in Geologic Media, CONF-8005107, 1981.

89. K. Oma, "Alternative Waste Form Development -- Low-Temperature Pyrolytic Carbon Coatings," in Waste Management '81, Tucson, AZ, 1981.

90. K. Oma, C. Q. Buckwalter and J. M. Rusin, "PNL Coated Particle Waste Forms," presented at the Alternative Waste Forms Peer Review Panel, Atlanta, 1981.

91. W. Neumann and O. Kofler, "Coating of Waste Containing Ceramic Granules," in Ceramics in Nuclear Waste Management, Cincinnati, CONF-790420, 1979.

92. W. J. Lackey, P. Angelini, W. D. Arnold, W. D. Bond, A. J. Caputo and D. P. Stinton, "Sol-Gel Derived Waste Forms," presented at the International Seminar on Chemistry and Process Engineering for High Level Liquid Waste Solidification, Jülich, West Germany, 1981.

93. G. J. McCarthy, W. B. White, S. Komarneni, B. E. Scheetz, W. P. Freeborn and D. K. Smith, "Hydrothermal Stability of Spent Fuel and High-Level Waste Ceramics in the Geological Repository Environment," in Ceramics in Nuclear Waste Management, Cincinnati, CONF-790420, 1979.

94. G. J. McCarthy, W. B. White and D. E. Pfoertsch, "Synthesis of Nuclear Waste Monazites, Ideal Actinide Hosts for Geologic Disposal," Materials Research Bulletin 13, 1239 (1978).

95. J. W. Braithwaite and J. K. Johnstone, "Chemical Durability and Characterization of Nuclear Waste Forms in a Hydrothermal Environment," in Ceramics in Nuclear Waste Management, Cincinnati, CONF-790420, 1979.

96. K. D. Reeve, D. M. Levins, E. J. Ramm, J. L. Woolfrey, W. J. Buykx, R. K. Ryan and J. F. Chapman, "The Development and Testing of SYNROC for High Level Radioactive Waste Fixation," Australian Atomic Energy Commission Research Establishment, New South Wales, Australia, 1981.

97. H. W. Nesbitt, G. M. Bancroft, W. S. Fyfe, S. N. Karkhanis, A. Nishijima and S. Shin, "Thermodynamic Stability and Kinetics of Perovskite Dissolution," Nature 289, 358 (1981).

98. A. E. Ringwood and S. E. Kesson, "Immobilization of High Level Wastes in SYNROC Titanate Ceramic," in Ceramics in Nuclear Waste Management, Cincinnati, CONF-790420, 1979.

99. J. Geel, H. Eshrich, F. Dobbels, P. Favre and H. Sterner, "Incorporation of Solid High Level Wastes Into Metal and Non-Metal Matrices," in High-Level Radioactive Solid Waste Forms, Denver, 1978.

100. L. A. Chick, G. L. McVay, G. B. Mellinger and F. P. Roberts, "Annual Report on the Development and Characterization of Solidified Waste Forms for Nuclear Wastes," PNL-3465, 1980.

101. A. E. Ringwood, "Safe Disposal of High Level Nuclear Reactor Wastes: A New Strategy," Australian National University Press, Canberra, 1978.

102. R. P. May and R. P. Turcotte, "Thermal Phase Stability," in A State-of-the-Art Review of Materials Properties of Nuclear Waste Forms, PNL-3802, 1981.

103. R. O. Lokken, "Multibarrier Waste Forms, Part III: Process Considerations," PNL-2668-3, 1979.

104. M. D. Merz, "Mechanical Properties," in A State-of-the-Art Review of Materials Properties of Nuclear Waste Forms, PNL-3802, 1981.

105. G. Bida and D. R. MacKenzie, "NRC Nuclear Waste Management Technical Support in the Development of Nuclear Waste Form Criteria: Task 2: Alternative TRU Technologies," BNL-NUREG-27715R, in press, 1981.

106. Fact Sheet on the President's Program on Radioactive Waste Management, Office of the White House Press Secretary, 1980.

107. R. B. Davis, "Data Report for the Nondestructive Examination of Turkey Point Spent Fuel Assemblies," HEDL-TC-1284, 1979.

108. R. E. Einzinger, "Preliminary Assessment of Fuel Rod Characteristics Pertinent to Spent Fuel Performance During Disposal," Hanford Engineering Development Laboratory Correspondence No. 8051315, 1980.

109. Y. B. Katayama, D. J. Bradley and C. O. Harvey, "Status Report on LWR Spent-Fuel Leach Tests, PNL-3473, 1980.

110. R. Wang, "Spent Fuel Special Studies Progress Report: Probable Mechanisms for Oxidation and Dissolution of Single-Crystal UO_2 Surfaces," PNL-3566, 1981.

111. A. E. Norris, "Status Report Concerning Empirical Measurements of Fission Product Release From Nuclear Reactor Spent Fuel," ONWI/79/ES-11-01200-11, 1979.

112. T. T. Vandergraaf, "Leaching of Irradiated UO_2 Fuel," Atomic Energy of Canada, Ltd. Technical Record, TR-100, 1980.

113. P. Taylor, E. A. Burgess and D. Owen, "Oxidation of UO_2," J. Nucl. Materials 88, 153 (1979).

114. U. B. Eklund and R. Forsyth, "Leaching of Irradiated UO_2 Fuel," KBS, Sweden, Report 70, 1978.

115. R. Wang and Y. B. Katayama, "Dissolution Mechanisms for UO_2 and Spent Fuel," in ORNL Conference on the Leachability of Radioactive Solids, Gatlinburg, TN, 1980.

116. S. Sunder, D. W. Shoesmith, M. G. Bailey, F. W. Stanchell and N. S. McIntyre, "X-Ray Photoelectron Spectroscopic Studies of the Electrochemical Oxidation of UO_2," J. Electroanal. Chem., in press.

3. EVALUATION OF CONTAINER MATERIALS

3.1 Introduction

The container in which the waste form is sealed must satisfy various basic requirements if it is to fulfill its role as a waste package component. These requirements were recently reviewed by Scott.[1] Current NRC criteria for the waste package require that there be containment of radioactivity for the first 1000 years after emplacement in a repository. Based on available data, it is anticipated that the container will be the principal means for meeting the 1000 year containment criterion.

Presently, work on container materials is not comprehensive and the choice of materials may be altered as more experimental data are accumulated. This is especially true for the U.S. effort since a large number of waste forms,[2,3] container materials,[4,5] backfill materials,[6] and host rocks[6] are under evaluation.

Because of the strength, fabricability and corrosion resistance, metallic materials are emphasized more than ceramic or polymeric materials for HLW containers. In the selection of a container metal, corrosion resistance is the most important factor. In order to conservatively evaluate radionuclide release scenarios, NRC is currently proposing that repositories be designed to withstand early flooding.[7] Because of this, a detailed evaluation of container corrosion must be made to determine those conditions which may cause a loss of container integrity and subsequent fission product release from the waste form. Both general and localized corrosion must be considered for the types of groundwaters that are likely to prevail.

The review described below will discuss container integrity within anticipated repository environments with the main emphasis on corrosion resistance. Domestic and foreign HLW container research programs are reviewed and discussed.

3.2 Candidate Metallic Container Materials

Table 3.1 lists tentative reference waste package materials being considered in foreign and domestic programs. An extensive effort in container development is currently in progress at Sandia National Laboratory and Battelle-Pacific Northwest Laboratory. The materials being evaluated fall into distinct categories (see Tables 3.12 and 3.23 for details):

- Carbon or low-alloy steels are principally used where high temperature corrosion and strength are not important. They are relatively inexpensive.

- Naval brass, 90-10 cupronickel and other copper alloys are of use where corrosion resistance, especially in saline environments, is important.

- The stainless steels which possess good mechanical strength, ductility and corrosion resistance in a wide range of environments.

Table 3.1

Candidate HLW Package Materials

Country	Waste Form	Container	Overpack/Backfill	Host Rock	Burial Depth (m)
Sweden[8]	borosilicate glass	3 mm stainless steel mold, 100 mm Pb liner, 6 mm Ti outer canister	80-90% quartz sand + 20-10% bentonite clay	granite	500
Britain[9]	borosilicate glass	Cu, Pb, Ti being evaluated		salt, clay, shale, or hard rock	
Germany[10]	borosilicate glass				
France[10,11]	borosilicate glass	stainless steel mold		granite or salt	
Canada[12]	borosilicate glass	Type 316L SS, Inconel 625, Ti		granite	
Japan[10]	borosilicate glass			granite, zeolite	
USSR[10,13]	phosphate or borosilicate glass				
USA[2,14]	borosilicate glass*	Ticode 12*		salt*	

*Reference materials--many other candidates being evaluated.

- Monel, Inconel, Incoloy, and Hastelloy are all high nickel materials and possess improved strength and corrosion resistance when compared to the normal austenitic stainless steels.

- Zirconium and titanium alloys possess moderate strength and excellent corrosion behavior, but are relatively expensive.

- MP35N is a cobalt based alloy with excellent strength and corrosion resistance.

3.3 Temperature of a Container

The temperature of the waste container is a function of time and waste loading. Claiborne et al.[15] calculated temperature profiles for a container in salt repository as a function of time after emplacement (Figure 3.1).

The maximum temperatures at container/backfill interfaces for different waste types and media formation are given in Table 3.2, calculated by Baithwaite and Molecke.[4] Values range between 70-300°C. They used a container spacing which resulted in a thermal loading of 150 kW/Acre, which is higher than those used by Claiborne et al. (60 kW/acre and 100 kW/acre).[15] In Swedish designs, the expected maximum temperature at the outer container surface is 80°C. However, the Swedish KBS study plans pre-burial aging of the waste to bring the temperature down.

3.4 Corrosion of Metallic Container Materials

Corrosion of metals can be divided into two main categories: dry and wet corrosion. Dry corrosion implies metal-gas reaction in the absence of an aqueous medium. An example of this at room temperature is the tarnishing of silver. At high temperatures, dry corrosion is usually called oxidation. The term wet corrosion refers to a corrosion reaction in the presence of an aqueous medium. An example of this at room temperature is the corrosion of steel structures in seawater. At high temperatures, the reaction between metals and molten salts is called hot corrosion.

In a HLW repository we can consider two corrosion periods: before flooding and after flooding. Before flooding, if the surface temperature of a container and the pressure in the repository are such that water vaporizes near the container, the corrosion of the container will be dry corrosion. If the temperature is so low that the water does not boil, then the corrosion of the container will be wet corrosion similar to most soil corrosion processes. After flooding, however, the corrosion of the container will be wet corrosion alone. There are many types of wet corrosion. Fontana[16] classified them into eight forms that cover practically all corrosion failures modes. They are:

1. Uniform, or general corrosion.
2. Galvanic, or two-metal corrosion.
3. Crevice corrosion.
4. Pitting corrosion.
5. Intergrannular corrosion.

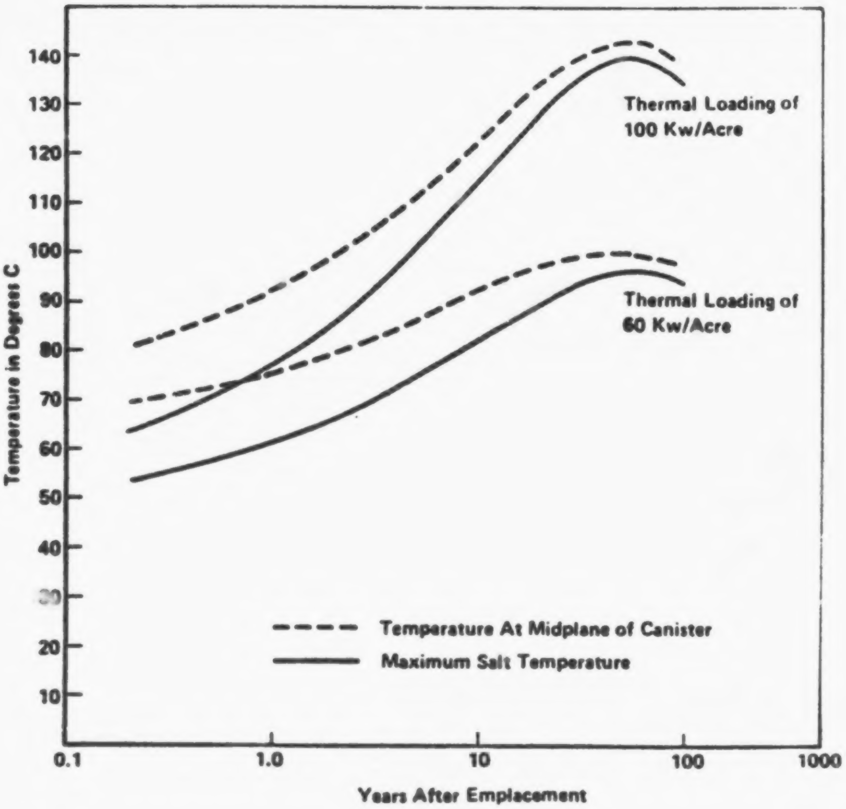

Figure 3.1 Calculated Temperature Profiles for Salt Repository.[15]

6. Selective leaching.
7. Erosion corrosion.
8. Stress corrosion cracking (SCC).

Hydrogen attack may be added to the above list. Under HLW repository conditions, erosion corrosion is not likely to occur. Three forms of corrosion, i.e., galvanic corrosion, intergranular corrosion, and selective leaching are unlikely to be important for the anticipated repository conditions and the classes of metals specified above. Thus, corrosion studies after flooding should focus on general corrosion, pitting corrosion, crevice corrosion, stress corrosion, and hydrogen effects.

In this section, the corrosion of metallic containers before and after flooding will be discussed separately for different prospective host rocks.

3.4.1 Corrosion Before Flooding

3.4.1.1 Bedded Salt Repository

Oak Ridge National Laboratory carried out a laboratory and an in-situ (Project Salt Vault) study to evaluate the behavior of waste isolation containers in a salt environment before flooding.

BEST DOCUMENT AVAILABLE

Table 3.2

Repository Isolation Environments for High Level Waste[4]

Geologic Formation and Waste Type	Maximum Interface Temperature	Lithostatic/ Hydrostatic Pressure	Chemistry
Bedded Salt:			
Spent Fuel	70-100°C	18 MPa	Dry NaCl
Defense HLW	70-100°C	18 MPa	Dry NaCl
Reprocessed HLW	250°C	18 MPa	Dry 98% NaCl, with dispersed 1/2% H_2O
Reprocessed HLW	150°C	18 MPa	With potential inundation due to localized intrusion of NaCl-$MgCl_2$ brine of hydrologic flow
Sub-seabed Sediments:			
Reprocessed HLW	200°C	55 MPa	Seawater saturated sediments (40% solids)
Basalt, Shale, Tuff:			
Reprocessed HLW	250-300°C	Atmospheric	Air and stream for about 100 years, then possibly inundated with ground water

*Assumes 37 watts/m^2 (150 kW/acre) canister spacing in repository; does not include radiolysis effects.

A wide range of materials, as shown in Table 3.3, was evaluated in the laboratory study, and the results given in Table 3.4.[17] In 720 h exposures the austenitic stainless steels (Type 304L, 310, and 347) showed similar corrosion rates. Titanium, high nickel, and high cobalt alloys were superior and carbon steel was inferior to stainless steels. All except titanium showed pitting attack.

In this laboratory study Type 304L welded specimens were buried in reagent grade NaCl containing various quantities of water, $CaSO_4$ and $MgCl_2$, and were heated for 30 day periods at 300°C in an autoclave. It was found that salt containing $MgCl_2$ tended to give the most aggressive general corrosion measured in terms of descaled weight losses. For most environments, pits of about 5 mils in depth were found. In the test with 98% NaCl - 2% H_2O the pits were about 10 mils deep.

In-situ tests (Project Salt Vault) were conducted in a salt mine in Lyons, Kansas, by the ORNL.[18,19] One heater with a Type 304L sheath was heated to a temperature of 200°C at the hottest location and reached 170-175°C in the unheated regions. Pitting was noticed over most of the surface and a large transgranular stress-corrosion crack was found in the unheated area. In contrast, the carbon steel heater sheath which was maintained for several months at 240°C suffered only general rusting. It is postulated that these general and localized corrosion processes are caused by the presence of water in the salt (up to approximately 0.5%) and Cl^- ion. The water was thought to condense in the cooler regions of the heater sheaths and cause the corrosion problems.

A recent series of tests was carried out on Type 304L, Cor-Ten A Steel, and ASTM-A-516 (Grade 70) carbon steel in salt from the Waste Isolation Pilot Plant (WIPP) site at Carlsbad, New Mexico.[20] The ASTM-A-516 steel is iron-based and contains about 0.3% C, 1% Mn, and 0.25% Si. After heating Type 304L stainless steel and Cor-Ten A for 10,000 h at 80°C and 225°C in unsealed capsules it was found that neither material showed much attack when examined visually. At high magnification, metallographically sectioned and polished specimens showed that at 225°C the Type 304L stainless steel had an oxide scale about 0.1 mil in thickness. The low alloy steel scale varied between 0.3-0.6 mil at the same temperature. For capsules which were sealed to prevent external water ingress, the Type 304L stainless steel specimens heated at 225°C for 5000 h showed no visible attack. The low-carbon steels had a black oxide film.

The main observation from these tests on materials exposed to Cl^- containing environments is that general corrosion is not severe for the temperatures likely to be encountered in a repository. However, localized pitting does occur in a very wide range of materials, with the possible exception of titanium based alloys. Maximum test periods in hot salt environments to date are 10,000 h but much longer term tests of 50,000 h duration are planned.[20]

Sandia National Laboratory tentatively plans to start a field test on a full-size, Sandia-fabricated, Ticode-12 overpack, surrounding a heater, emplaced in the Asse test facility in Germany in late 1981.[21] Tests with actual containers of reprocessed HLW at the WIPP facility are also planned for early 1986.[4]

BEST DOCUMENT AVAILABLE

Table 3.3

Nominal Compositions of Alloys Used in Salt Exposure Studies

Alloy	Fe	Cr	Ni	Co	Mo	Cu	Mn	Ti	W	Al	Nb	Ta	Si	C	S	N	H	V
Type 310 Stainless Steel	Bal	24-26	19-22	--	--	--	--	--	--	--	--	--	--	0.25[a]	--	--	--	--
Type 446 Stainless Steel	Bal	23-27	--	--	--	--	--	--	--	--	--	--	--	0.20[a]	--	0.25[a]	--	--
Type 304L Stainless Steel	68.4[c]	19	9.5	--	--	--	2.0	--	--	--	--	--	1.0	0.03[a]	--	--	--	--
Type 347 Stainless Steel	70[c]	18	11	--	--	--	--	--	--	--	10xC	--	--	0.08	--	--	--	--
LCNA[a,d,g]	32.0	21.4	40.0	--	3.0	1.8	0.6	10xC	--	0.1	--	--	0.4	0.05[a]	--	--	--	--
Hastelloy F	17	22	47	2.5[a]	6.5	--	1.7	--	0.6	--	--	--	1.0	--	--	--	--	--
Hastelloy C	5.5	15.5	54.6	2.5	16.0	--	1.0	--	3.8	--	--	--	1.0	0.08	0.006	--	--	0.30
Corronel 230	5.0[a]	35-37	Bal	--	--	1.0[a]	1.0[a]	1.0[a]	--	0.5[a]	--	--	0.6[a]	0.008[a]	--	--	--	--
Nichrome V	--	20	,80	--	--	--	--	--	--	--	--	--	--	--	--	--	--	--
Inconel	7.5	15.5	76.2	--	--	0.2	0.25	--	--	--	--	--	0.25	0.08	--	--	--	--
HAPO-BMI 20[b]	16	25	50	--	6	1	0.6	1.0	--	--	--	--	0.4	0.02	--	--	--	--
50 CR-50 Ni[e]	--	50	50	--	--	--	--	--	--	--	--	--	--	--	--	--	--	--
Titanium 45A[g]	0.25a	--	--	--	--	--	--	Bal	--	--	--	--	--	0.08[a]	--	0.005[a]	0.0015[f]	--
Haynes 25	3a	20	10	50	--	--	--	--	15	--	--	--	1.0a	0.10[a]	--	--	--	--

[a] Maximum.

[b] Experimental alloy developed by BMI and General Electric Company (Hanford Laboratory).

[c] Or specificed as "balance".

[d] Vacuum-melted, low-carbon variation of International Nickel Company trademarked alloy Ni-o-nel.

[e] Developed by Bureau of Ships, U.S. Dept. of the Navy. Specimen obtained from Canadian Pulp & Paper Institute.

[f] Maximum for sheet stock, Grades 35A to 75A.

[g] Alloys containing 0.2% Pt included in one or more tests as described in text.

Table 3.4

Corrosion of Various Metals Under Conditions Simulating Salt Mine Storage of Fixed Wastes[17]

	Type 304L Stainless Steel			Type 310 Stainless Steel			Hastelloy C			Haynes 25			Titanium 45A		Carbon Steel ASTM: A 108 Unwelded	
	200°C	300°C	500°C	200°C	300°C	500°C	200°C	300°C	500°C	200°C	300°C	500°C	200°C	300°C	200°C	300°C
Natural NaCl	0.6 (1.2)	0.4	0.5	0.4	0.2 (1.6)	0.1 (2.8)	0.1	0.1	0.1	<0.1	0.1	0.2	0.2	0	2.0 (1.6)	2.0 (1.8)
Reagent Grade NaCl	0.1	0.2	0.3	<0.1	0.1	0.5 (2.8)	<0.1	<0.1	0.1	0.1	0.1	0.1	0.1	0	1.1 (1.4)	1.6 (2.6)
99.5% NaCl-0.5% H_2O	0.2 (0.4)	0.5 (2.2)	0.6	0.2 (2.9)	0.3 (1.8)	0.4 (1.6)	0.1	0.1	0.	0.4	0.1 (3.2)	0.1	0.1	0.1	1.3 (1.8)	1.5 (2.6)
99.75% NaCl-0.25% $MgCl_2$	0.7 (2.0)	0.8	0.5	0.6 (2.1)	0.4 (1.5)	0.4 (2.4)	0.1	0.1	0.5	0.2 (2.7)	0.2	0.3	0.2	0.1	2.7 (etch)	3.5 (1.2)
95% NaCl-5% $CaSO_4$	0.1	0.6 (2.3)	0.4	<0.1 (1.5)	0.2 (2.2)	0.3 (1.6)	0.1	0.1	<0.1	0.	0.1 (3.2)	0.1	0.2	0.	1.0 (2.2)	1.9 (2.2)
94.5% NaCl-0.5% H_2O-0.25% $MgCl_2$-5% $CaSO_4$	0.8	0.4	0.7	0.4 (1.8)	0.3	0.2	0.2 (2.7)	0.1	0.1	0.1	0.1 (1.5)	0.1	0.1	0.1	3.3 (etch)	3.8 (2.2)

	Inconel		DMCR-8		Monel		Nickel		Ni-o-nel		Type 347 Stainless Steel		Unwelded Type 1100 Aluminum (200 Hr)	
	200°C	300°C	200°C	300°C	200°C	300°C	200°C	300°C	200°C	300°C	200°C	300°C	200°C	300°C
Natural NaCl	0.1 0.1	0.1	0.1	0.1	0.3	0.5	0.3	0.3	0.1	0.1 (5.8)	0.7	0.4 (2.3)	gain	gain (5.6)
Reagent Grade NaCl	<0.1 0.1	<0.1	0.	0.1	0.1	0.5 (5.8)	0.2	0.1	0.1 (3.9)	0.1 (2.3)	0.1 (3.8)	0.4 (8.0)	0.6 (2.4)	0.7 (3.3)
99.5% NaCl-0.5% H_2O	0.1 (3.2) 0.1	<0.1 (3.7)	0.1 (2.4)	0.1 (3.0)	1.0 (7.1)	0.1 (3.0)	0.1	0.1	0.6	0.3 (3.0)	0.5	0.7 (5.8)	0.2 (2.1)	gain (3.3)
99.75% NaCl-0.25% $MgCl_2$	0.2 (5.6) 0.1 (2.1)	0.2	0.2 (4.9)	0.9	0.9	0.9	0.3	0.6	0.9 (3.3)	0.3 (1.6)	0.7 (1.9)	1.0	gain	gain (3.6)
95% NaCl-5% $CaSO_4$	0.1 0.1 (1.9)	0.1	0.	0.1 (3.2)	0.1 (3.5)	0.1 (3.2)	0.1	0.1	<0.1	0.1 (3.7)	0.1 (2.2)	0.7 (2.3)	0.4 (3.0)	0.2 (2.7)
94.5% NaCl-0.5% H_2O-0.25% $MgCl_2$-5% $CaSO_4$	0.2 (2.8) 0.2 (2.6)	0.3 (2.5)	0.2 (3.7)	0.3 (2.3)	1.2 (2.7)	0.6 (2.0)	0.4	0.3 (6.0)	0.5 (3.0)	0.5 (4.2)	0.6 (3.0)	0.8	8.9 (4.0)	gain (4.0)

Exposure time = 720 hours except as indicated. All specimens were welded except as indicated. Rates in mils/yr. Numbers in parentheses indicate maximum pitting attack observed (total penetration in mils).

BEST DOCUMENT AVAILABLE

3.4.1.2 Clay Repository

Casteels et al.[22] recently reported work on metal-clay interactions. This is a Belgian effort which is part of the European radioactive waste management program. This study was on a potential repository site at a depth of 220 m at Mol, Belgium. Clay in these regions when heated to 50°C releases chlorides, sulfates, ammonia, and fluorides. At 105°C sulfur dioxide is also emitted. Released water is acidic. In laboratory tests and in-situ experiments the following general observations were made for metals heated to temperatures in the range 50-300°C in the presence of constituents released from the clay:

- Aluminum and its alloys form surface deposits of Na_2SO_4. Low pH values for surface moisture prevented passivation of the surface and pitting occurred.

- Carbon steel is attacked and FeO and FeS are formed. Chromium plating does not prevent corrosion since the plating has a fine network of cracks through which the corrodants pass.

- Type 304 stainless steel displayed deposits rich in the major alloying elements and S and Cl. Pitting was observed after the surface was cleaned. Types 304L and 316 stainless steel, although still pitted, were superior to Type 304.

- Ferritic AISI 430 stainless steel was corroded at 50°C and deep pits were found, together with intergranular attack. Areas of such attack were rich in Fe, Cr, S, Cl, and Si.

- Nickel-rich alloys such as Ni 200,* Inconel 600, and Incoloy 800 showed pitting and reaction layers containing S, Na, Si, and Cl. Hastelloy B and C, on the other hand, displayed little or no localized attack at 50°C although brittle sulfur-rich deposits were formed.

- Titanium and its alloys tended to form sulfur rich surface deposits but no localized attack was detected after 16 months' exposure.

3.4.2 Corrosion After Flooding

3.4.2.1 Groundwater Chemistry

Several different types of host rock have been considered for use in a HLW repository including rock salt, shale, basalt, tuff, and granite. Water chemistries will vary from location to location and also with depth. In principle, the deeper the location the smaller the quantity of oxygen and sulfate. Oxygen will be removed by oxidation processes in the rock and sulfate will be removed by sulfate-reducing bacteria.[23] Data compiled in reference 1 show groundwater chemistries for specific geologic sites. These are given in Tables 3.5 through 3.10. Note that Cl^-, F^- and SO^{-2} are usually present in all environments.

---

*Commercially pure nickel: 99.5 Ni-0.08 C. See Table 3.12 for compositions of other alloys.

Table 3.5

Compositions of Seawater (Seabed) and Brine (WIPP)[a]

Component	Concentration (ppm)		
	Seawater	Brine A[b]	Brine B[c]
Na^{+1}	10,651	42,000	115,000
K^{+1}	380	30,000	15
Mg^{+2}	1,272	35,000	10
Ca^{+2}	400	600	900
Sr^{+2}	13	5	15
Cl^{-1}	18,980	190,000	175,000
SO_4^{-2}	884	3,500	3,500
I^{-1}	0.05	10	10
HCO_3^{-1}	146	700	10
Br^{-1}	65	400	400
BO_3	---	1,200	10
pH[d]	8.1	6.5	6.5
Total dissolved solids	35 g/l	306 g/l	297 g/l

[a] Data taken from Reference 1.

[b] Brine A is thought to represent small brine inclusions in bedded-saltformations.

[c] Brine B is representative of dissolved bedded salt at depth of 800 m at the Waste Isolation Pilot Plant (WIPP) in New Mexico.

[d] These pH values are taken at room temperature; they decrease with increasing temperature (e.g., seawater solution quenched from 270°C measured 3.3 at room temperature).

Table 3.6

Shale Groundwater Chemistry[a]

Component	Composition (ppm)
HCO_3^{-1}	280
Ca^{+2}	79
CO_3^{-2}	0
Cl^{-1}	13
F^{-1}	0.6
Mg^{+2}	25
K^{+1}	6.6
Si	31
Na^{+1}	30
SO_4^{-2}	62
Fe^{+3}	0.03
Sr^{+2}	0.42
pH = 7.2	

[a] Data represent groundwater associated with argillite in the Eleana formation at the Nevada Test Site. Taken from Reference 1.

Table 3.7

Flood Basalt Groundwater Chemistry[a]

Component	Composition (ppm)
SO_4^{-2}	20.5
NO_3^{-1}	4.2
Cl^{-1}	3.1
HCO_3^{-1}	168.0
Na^{+1}	25.0
K^{+1}	5.4
Ca^{+2}	31.0
Mg^{+2}	7.1
pH = 7.9	

[a] Representative of Hanford, Washington flood basalt. Data taken from Reference 1.

Table 3.8

Groundwater Chemistry of Jackass Flats Tuffs[a]

Component	Composition (ppm)
Ba^{+2}	0.2
Ca^{+2}	13
Fe^{+2}	0
Li^{+1}	0.05
Mg^{+2}	2.0
K^{+1}	4.7
Na^{+1}	47
Sr^{+2}	0.06
HCO_3^{-1}	130
CO_3^{-2}	0
Cl^{-1}	7.7
F^{-1}	1.7
SO_4^{-2}	21
pH = 7.3-8.4	

[a] Data taken from Reference 1.

Table 3.9

Groundwater Chemistry of Sierra Nevada Granite[a]

Component	Composition (ppm)
Ca^{+2}	8.3
K^{+1}	1.5
Mg^{+2}	1.5
Na^{+1}	6.7
Si	12.5
SO_4^{-2}	2.7
Cl^{-1}	2.1
pH = 8	

[a] Data taken from Reference 1.

Table 3.10

Groundwater Chemistry of Swedish Granite[a]

Component	Composition (ppm)
Ca^{+2}	25-50
Mg^{+2}	5-20
Na^{+1}	10-100
K^{+1}	1-5
Fe (total)	1-20
Fe^{+2}	0.5-15
MN^{+2}	0.1-0.5
HCO_3^{-1}	60-400
CO_2	0-25
Cl^{-1}	5-50
SO_4^{-2}	1-15
NO_3^{-1}	0.1-0.5
PO_4^{-3}	0.01-0.1
F^{-1}	0.5-2
SiO_2	5-30
HS^{-1}	<0.1-1
NH_4	0.1-0.4
NO_2	<0.01-0.1
O_2	<0.01-0.07
$KMnO_4$	20-40
pH = 7.2-8.5	

---

[a] Data taken from Reference 1 represent depths of 450 m.

3.4.2.2 General Corrosion

A. Bedded Salt Repository

Corrosion behavior of many different metals in environments similar to that of a bedded salt repository have been studied in geothermal energy programs.[24-27] Some geothermal brines (e.g., Salton Sea Fluid) have high dissolved salt concentrations (up to 30%), and in this respect the brine is similar to the rocksalt brines specified in Table 3.5. The oxygen content of the Salton Sea brine was between 8-10 ppm and the pH was approximately 3.

Davis and Munir[26] investigated the corrosion behavior of several metals in synthetic Salton Sea brines, and the maximum corrosion rates are given in Table 3.11. At 95°C, the corrosion rate of pure Ni was 55 mdd,* while that of Monel 400 was 22 mdd. The corrosion rate of type 316 stainless steel was about half that of Monel. Mo, Nb, and Ti showed outstanding corrosion resistance, but Ti experienced severe pitting corrosion (15 mdd).

Similar work was conducted in the Salton Sea brine by Carter and McCawly[27] at temperatures of about 235°C. From the 15 day tests, it was found that nickel and titanium alloys, and high chromium stainless steels showed superior resistance to general corrosion. Corrosion rates were less than 0.1 mpy.** Low-carbon and low-alloy steel corroded much faster. Pitting and crevice corrosion were detected in some of the metals; this will be discussed in later sections.

Braithwaite and Molecke[4] exposed the U.S. candidate container materials, given in Table 3.12, to deoxygenated and oxygenated brines at 250°C for 28 and 14 days, respectively. The results are shown in Tables 3.13 and 3.14. General observations were compatible with those reported by previous workers,[26,29] i.e., low-carbon, and low alloy steels, lead and brass were inferior, while titanium and nickel-based alloys were very resistant to general corrosion. Austinetic stainless steels were intermediate in their corrosion behavior. These workers found that increasing the oxygen content, temperature and gamma irradiation tended to accelerate the general corrosion rate. It should be noted that the corrosion rate of copper in oxygenated brine was about 17 times higher than that in the deoxygenated brine. The effects of irradiation on corrosion properties will be discussed in a later section (5.3.2).

Sandia National Laboratory[5] studied the general corrosion of pure Ti, TiCode-12 and Ti-Pd (0.2% Pd). The effect of temperature on the corrosion rates in deoxygenated brine is shown in Table 3.15. Pure Ti showed inferior corrosion resistance to the alloys. The effect of dissolved oxygen on the corrosion rates at 250°C is shown in Table 3.16. The alloys showed better corrosion resistance in both sea water and brine. It should be noted that the corrosion rate of pure Ti increased to 3200 μm/yr from 14 μm/yr when 450 ppm

---

*mdd: mg/decimeter^2/day, 1 mdd = 10^{-5} g/cm^2/day.
**mil per year.

Table 3.11

Maximum Corrosion Rates and Macroscopic Appearance of Materials Tested in Salton Sea Brine[26]

Material	Maximum corrosion rate (mdd) (95% confidence level)			Maximum test duration (days)	Macroscopic appearance at maximum duration and $T = 368$ K
	368 K	333 K	296 K		
AISI 1010 steel	236.89	147.70	67.79	0.75	Nonadherent heavy black scale. Approx. 100% coverage.
304 SS	11.03	53.21	18.31	0.50	Very adherent light grey scale. Approx. 90% coverage (296 and 333 K approx. 5–10% coverage).
316 SS	9.81	9.20	8.59	2.00	Very slightly adherent gold tarnish along edges.
Monel 400	21.73	11.66	5.53	2.50	Nonadherent heavy grey-black scale. Approx. 80% coverage.
Nickel	55.25	29.42	6.37	2.00	Very adherent heavy grey scale. Approx. 100% coverage.
Molybdenum	0.57	–	–	7.00	Very adherent blue discoloration. Approx. 90% coverage.
Niobium	0.43	–	–	8.00	Very adherent light grey scale. Approx. 80% coverage.
Titanium	0.16	–	–	7.00	Very adherent gold tarnish. Approx. 80% coverage.

BEST DOCUMENT AVAILABLE

Table 3.12

Nominal Chemical Composition of U. S. Candidate Canister Materials[4]

Alloy	C	Mn	Si	Cr	Ni	Mo	Fe	Cu	Others
1018 Mild Steel	0.18	0.75	0.25	----	----	----	Bal	----	----
4130 Carbon Steel	0.3M*	0.5	0.3	1.0	----	0.2	Bal	----	----
Corten A Steel	0.1	0.4	0.5	1.0	----	----	Bal	----	0.02 Ti
2 1/4Cr-1Mo	0.2	0.8	0.3	2.2	----	1.0	Bal	----	----
Naval Brass	----	----	----	----	----	----	----	60.0	39.0 Zn, 1.0 Sn
90-10 Cupronickel	----	----	----	----	10.0	----	1.3	88.7	----
SS 304	0.08M	2.0M	1.0M	19.0	10.0	----	Bal	----	----
SS 316	0.08M	2.0M	1.0M	17.0	12.0	2.5	Bal	----	----
SS-Nitronic 50	0.06M	5.0	----	22.0	13.0	2.25	Bal	----	0.2 Nb, 0.2 V
SS 20-Cb3	0.07M	2.0M	1.0M	20.0	34.0	2.5	Bal	3.5	----
SS-Ebrite 26-1	0.01M	0.4M	0.4M	26.0	0.5M	1.0	Bal	0.2M	----
Monel 400	0.2	1.0	0.2	----	66.5	----	1.2	31.5	----
Incoloy 825	0.03	0.5	0.2	21.5	42.0	3.0	30.0	2.2	0.9 Ti
Inconel 600	0.04	0.20	0.20	15.5	76.0	----	8.0	----	----
Inconel 625	0.05	0.2	0.2	21.5	63.0	9.0	2.5	----	4.0 Nb, 0.2 Ti
Hastelloy C-276	----	----	----	15.0	59.0	17.0	5.0	----	4.0 W
Zircaloy 2	0.12	----	----	0.1	0.05	----	----	----	1.5 Sn, 98.2 Zr
Titanium, C.P.	----	----	----	----	----	----	----	----	99.5 Ti
Ticode 12	0.012	----	----	----	0.84	0.34	0.3	----	98.9 Ti
MP 35N	----	----	----	20.0	35.0	10.0	----	----	35.0 Co

*M denotes maximum

Table 3.13

Corrosion Rates of U. S. Candidate Alloys in Deoxygenated Solutions[4]

Alloy	Brine A (mm/yr)	Brine B (mm/yr)	Seawater (mm/yr)
(1018 Mild Steel, 25°)	0.03	0.03	----
(1018 Mild Steel, 70°)	0.07	0.036	----
1018 Mild Steel	1.7	0.07	0.4
Corten A Steel	0.9	0.05	0.2
2 1/4Cr-1Mo Steel	1.0**	0.1**	0.2
Lead	0.5	0.3	0.3
Copper	0.07	0.05	0.05
Naval Brass	1.0	----	1.0
90-10 Cupronickel	0.14	----	0.07
SS 304L	0.018	0.01	0.006
SS 316L	0.015	----	0.005
SS-Nitronic 50	0.008	----	0.003
SS-20Cb3	0.007	----	0.005
SS-Ebrite 26-1	0.016	----	0.005
Monel 400	0.03	----	0.1
Incoloy 825	0.006	----	0.004
Inconel 600	0.009	0.007	0.005
Inconel 625	0.005	0.001	0.012*
Hastelloy C-276	0.007	----	0.0015
Zircaloy 2	0.001	----	----
Titanium C.P.	0.014	----	0.012
TiCode-12	0.003	----	0.001

* pitting corrosion.
**crevice corrosion.

Table 3.14

Corrosion Rates of U. S. Candidate Alloys in Oxygenated Solutions
(250°C and P = 7 MPa, t = 14 days)
(O_2) = 600 ppm in Brine A and 1750 ppm in Seawater[4]

Alloy	Brine A (mm/yr)	Seawater (mm/yr)
1018 Mild Steel	7.0	11.0
Copper	1.2	5.0
Lead	1.2	1.0
90-10 Cupronickel	0.4	0.7
SS-Ebrite 26-1	0.24	----
SS-20Cb3	0.1**	----
Inconel 600	----	0.1
Hastelloy C-276	0.06*	0.2*
TiCode-12	0.0004	0.0006

* pitting and crevice corrosion.
**crevice corrosion.

Table 3.15

Effect of Temperature on the Uniform Corrosion Rate of Titanium Alloys in Deoxygenated Brine A[5]

Alloy	Corrosion Rate (μm/yr) 70°C	150°C	250°C
Ti-50A (pure Ti)	<.06	2.6	14.
TiCode-12	<.07	0.9	3.2
Ti-Pd	<.09	0.3	2.4

Table 3.16

Effect of Dissolved Oxygen on the Uniform Corrosion Rate of Titanium Alloys at 250°C[5]

	Corrosion Rate (μm/yr)			
	Seawater		Brine A	
Alloy	0 ppm O_2	500 ppm O_2	0 ppm O_2	450 ppm O_2
Ti-50A (pure Ti)	11.7	16.2	14	3200.
TiCode-12	1.10	0.60	3.2	1.8
Ti-Pd	1.14	0.62	2.4	0.4

O_2 was added to the deoxygenated brine. In contrast, the increased dissolved oxygen content reduced the corrosion rates of the alloys. It was suggested that alloying enhanced the tenacity and impermeability of the passivating oxide film.

Henrikson and Pourbaix[28] conducted corrosion tests on unalloyed Ti in Baltic Sea water on commission by KBS (Swedish Nuclear Safety Project). Sea water was used for the test, because it was believed that this was the most corrosive environment that would possibly come into contact with the waste containers. The material studied was ATi-24 which corresponds most closely to ASTM B265 Grade 1 with max 0.8% oxygen and 0.2% iron. Two different environments, (Table 3.17) and two different temperatures, 100 and 130°C, were used. Environment 1 denotes Baltic Sea water saturated with air, while environment 2 represents deoxygenated Baltic Sea water. Tables 3.18 and 3.19 show the results in environments 1 and 2, respectively. Three different positions of the samples were used as follows:

Position 1: in solution,

Position 2: solution/clay phase, i.e., with samples immersed halfway into buffer (clay),

Position 3: with samples embedded in clay.

The clay buffer was a mixture of 90% siliceous flux and 10% bentonite and was kneaded with 25 vol % solution. There was some uncertainty about the results for positions 2 and 3 samples because of the contamination by the clay.

Compared with Sandia's results on pure Ti, (Table 3.15), Henrikson and Pourbaix's corrosion rates are significantly lower probably because of the lower test temperatures. The corrosion rates in deaerated seawater were lower than those for the seawater saturated with air. It was concluded that a 6 mm thick Ti container will last tens of thousands of years with a maximum corrosion rate of 0.1 μm/yr.

PNL[29] exposed 22 different metals to $MgCl_2$-NaCl brine at 250°C for up to 72 days. The brine composition and the weight change measurements results are given in Tables 3.20 and 3.21, respectively. The weight loss for copper was about 1000 times that for Hastelloy C276, while titanium alloys showed negligible weight change. Inconels 600, 625, and Incoloy 800 and Zircaloy-2 were intermediate in behavior.

B. Basalt Repository

PNL[29] investigated the corrosion behavior of 22 metals in Hanford basalt groundwater at 250°C. Groundwater composition is given in Table 3.22 and the results of weight change measurements are shown in Table 3.23. The major difference between the first and second test was the oxygen content in the solution.

Table 3.17

Environmental Specifications[28]

Substance	Environment 1	Environment 2
Cl^- mg/l	ca 4000	ca 4000
F^- mg/l	10	10
O_2 mg/l	ca 8	<0.01
SO_4 mg/l	ca 560	ca 560
Na mg/l	ca 2500	ca 2500
Mg mg/l	ca 80	ca 80
Ca mg/l	ca 70	ca 80
pH	4.5	4.5

The corrosion environments are prepared from natural Baltic Sea water by adding NaF to the desired F^- content. The pH value was adjusted by adding dilute HCl.

Table 3.18

Corrosion Rates for Titanium in Environment 1;
Baltic Sea Water with 10 ppm F^-, pH 4.5, 8 ppm O_2[28]

Position	Sample Temp °C	Type	Corrosion Rate, m/yr After Day: 30	100	200	270	300
H_2O	100	K	0.05 (-)	0.04 <0.01 (-)	0.04	0.02	0.04
	130	K	0.03 (-)	0.03	≤0.01	≤0.01 ≤0.01 (-)	0.02
	100	KD	0.07	0.13	0.08	0.05	0.09
	130	KD	0.37	0.12	0.03	0.03	0.05
H_2O/clay	100	KD	0.50	0.11	0.05	0.05	0.05
	130	KD	0.27	0.29	0.16	0.22	0.16
	100	W					≤0.01 (-) 0.03
	130	W					0.05
Clay	100	KD	0.20	0.46 (-)	0.10	0.08	0.04
	130	KD	0.25	0.18	0.82	0.06	0.52
	100	W					0.02 (-)
	130	W					0.39

K = general corrosion sample 1.05 dm^2.
KD - sample with gap 0.90 dm^2 (crevice sample).
W = welded sample 0.90 dm^2.
(-) = decrease in weight.
If only one value is indicated it is an average value of 3 parallel samples. More than one value may occur if both a weight decrease and a weight increase are observed within this group of 3 samples.

Table 3.19

Corrosion Rates for Titanium Environment 2; Baltic Sea Water with 10 ppm F^-, pH 4.5, Less than 0.01 ppm O_2[28]

			Corrosion Rate, m/yr After Day:				
Position	Sample Temp °C	Type	30	100	200	270	300
H_2O	100	K	0.08	0.06	0.02	≤0.01	≤0.01
	130	K	0.05 (-)	0.04 (-)	0.02	0.02	≤0.01
	100	KD	0.53	0.04 (-)	0.09	0.06	0.07
	130	KD	0.30	0.02 (-)	0.09	0.04	0.06
H_2O/Clay	100	KD	0.55	0.03 (-)	0.04	0.06	0.05
	130	KD	0.63	0.04 (-)	0.09	0.07	0.07
	100	W					≤0.01 (-)
	130	W					0.04
Clay	100	KD	0.60	0.51 (-)	≤0.01 (-)	≤0.01	0.05
	130	KD	0.53	0.02 (-)	0.13	0.04	0.04
	100	W					≤0.01
	130	W					≤0.01

K = general corrosion sample 1.05 dm^2.
KD = sample with gap 0.90 dm^2 (crevice sample).
W = welded sample 0.90 dm^2.
(-) = decrease in weight
If only one value is indicated it is an average value of 3 parallel samples. More than one value may occur if both a weight decrease and a weight increase are observed within this group of 3 samples.

Table 3.20

Brine Solution Composition[29]

Ions	Makeup
Mg^{++}	24.98 g/L
Na^{++}	41.34 g/L
K^{+}	29.95 g/L
Ca^{++}	0.60 g/L
Li^{+}	20 mg/L
Rb^{+}	20 mg/L
Sr^{++}	5.3 mg/L
Cs^{+}	0.8 mg/L
Cl^{-}	191.3 g/L
SO_4--	3.51 g/L
BO_3	1.24 g/L
Br-	0.39 g/L
I-	10 mg/L
Fe^{++}	2 mg/L

Table 3.21

Corrosion of Samples in $MgCl_2$-NaCl Brine[a] at 250°C[29]

Sample	Weight Change First Period mg/dm^2[b]	Time, d	Weight Change Second Period mg/dm^2[b]	Time, d	Remarks
304 L S/S			-5	72	Bright HAZ[c]--
304 S/S			-5	72	Bright HAZ-- Black
316 S/S			-5	72	Bright HAZ-- Black
321 S/S			-5	72	Bright HAZ-- Black
405 S/S			-351	72	Broken, in HAZ-- Black
410 S/S			-354	72	Broken, in HAZ-- Black
Nickel 200	-486	58			
Inconel 600	12	58			
Inconel 625			-2	72	Track of Tarnish
Incoloy 800	-9	58			Light Tarnish
Copper-Nickel 70-30	-996	20			Spalling
Copper	-3,858	38			Spalling
Hastelloy-C276	-6	58			
Titanium-6AL-4V	+0.2	58			Light Black Tarnish
Titanium-Code 12	+0.9	58	0	72	Light Straw Tarnish
Titanium-50	+1.0	58	+10	72	Light Straw Tarnish
Zircaloy-2	+8.0	58	+10	72	Black
Cast-Iron 22-8	-7,713	20			Clean to Metal
Cast-Iron 22-8	-5,501	20			

(a) See Table 3.20.

(b) Weight change after cleaning in Na_2 EDTA solution with ultrasonics to remove deposited scale. Samples of copper, copper-nickel, and nickel were cleaned in 18% HCl (room temperature) 3 min. Cast iron cleaned in diammonium citrate plus phenylthiourea (85°C).

(c) HAZ: Heat-affected zone of weld.

BEST DOCUMENT AVAILABLE

Table 3.22

Synthetic Hanford Groundwater Formulations[29]

	August 1979 to May 1980		May 1980 to July 1980	
Ion	Make-up, mg/L	Effluent Analyses,(a) mg/L	Make-up, mg/L	Effluent Analyses,(a) mg/L
Al	0	10	0	6
Na	139	140	111	127
Mg	0.5	0.05	0.5	0.05
Ca	1.6	0.1	2.5	0.1
K	13	55	13	21
CO_3 (Total)	167	210	167	240
SiO_2	36	210	36	331
Cl^-	52	50	52	58
F^-	8	8	8	8
SO_4^{--}	0.8	--	0.8	5
O^2, ppm	<1	--	<0.05	--
pH	9.5	8.5	9.0	7.7
Conductivity, Mho	475	55	630	600

(a) Sample was cooled before sampling. The water passed through a bed of crushed basalt at 250°C in the autoclave, which increased the Al and Si, and decreased pH, Ca, and Mg.

Table 3.23

Corrosion of Samples in Simulated Hanford Groundwater(a) at 250°C[29]

	Weight Change First 3 Mo., mg/dm^2		Weight Change Second 3 Mo., mg/dm^2	
Material	Before Cleaning	After Cleaning(b)	Before Cleaning	After Cleaning(b)
304 L S/S	+11	-0.9	+4.8	-1.5
304 S/S	+14	-3.3	+7.4	-0.9
316 S/S	+6	-5.9	+15.0	-1.6
321 S/S	+14	-2.2	+4.4	-2.2
405 S/S	+15	-3.3	+2.7	-3.1
410 S/S	+28	-5.1	+18.0	-4.5
Inconel-600	+13	-3.3	+7.6	-4.2
Inconel-625	+43	-0.9	+8.0	-1.8
Incoloy-800	+24	0.0	+20.0	-1.3
Hastelloy-C-276	+14	-1.8	+14.0	-3.5
Nickel-200	+245	+168.0(c)	+20.0	-345.0
Titanium-Grade 2	+32	+0.4	+6.3	+1.8
Titanium-Grade 12	+17	+0.2	+5.2	-0.7
Titanium-6Al-4V	--	--	+39.0	+0.2
Zircaloy-2	+80	+23.0	+3.3	-11.0
Cast-Iron 180-7	+90	-415.0	+277.0	-442.0
Cast-Iron 22-8	+225	-345.0	+263.0	-476.0
Cast-Iron 142-12	+345	-180.0	-235.0	-422.0
Cast-Iron 166-3	+135	-180.0	+235.0	-422.0
Cast-Iron 136-4	+32	-411.0	+224.0	-530.0
Copper	--	--	+168.0	-171.0
Copper-Nickel-70-30	+58	-89.0	+268.0	-580.0

(a) See Table 3.21 for composition.

(b) Samples of Inconel, stainless teel, titanium, Zircaloy, Incoloy and Hastelloy only had the deposited film removed.

(c) Residual deposited film apparent.

(d) Samples of copper, copper-nickel, and cast iron had all deposited and most of the corrosion product film removed.

Stainless steels showed very small weight losses, but it was suggested that these materials will be subject to stress corrosion cracking when oxygen is added to the system to simulate radiation effects or air access to the repository. Titanium and its alloys showed a very good corrosion resistance, while copper showed a rather high corrosion rate (about 250 times higher weight loss than that of Ticode 12). In the experiment with a lower oxygen activity, lower corrosion rates were expected for most of the metals tested. However, the results show the opposite. More investigation is warranted.

As a part of the Basalt Waste Isolation Project (BWIP), PNL conducted a set of tests for Rockwell Hanford Operations.[30] The groundwater chemistry was a simulated Grande Ronde Basalt, the composition of which is given in Table 3.24. The weight changes at 250°C are shown in Table 3.25. The results from PNL Hanford Groundwater tests are also shown for comparison. For both experiments the oxygen contents in the solution were about the same (<50 ppb). The two sets of data do not closely agree with each other. The differences may be due to different solution chemistry or an artifact and should be studied further.

C. Clay Repository

Casteels et al.[22] exposed candidate container materials to water from an aquifer above the Boom clay layer and measured the resultant weight changes as a function of temperature and time. Tables 3.26 and 3.27 show the groundwater composition and the weight change results. As shown in Table 3.27 after 4 months at 98°C, no firm conclusions could be drawn, because the results do not show any clear trend.

The Commission of the European Communities[31] reported the results of corrosion tests on Pb and Pb alloys in which the wet atmosphere of an underground facility in a clay formation has been simulated. These metals are being evaluated as candidate filler materials for press compaction and encapsulation of fuel cladding wastes. Since lead and its alloys are also potential container materials, this work is pertinent to container materials evaluation. The experiments were conducted at 49°C for 15 days to four months and the results were reported as weight changes per unit area (mg/cm^2).

Using their results, the thickness changes after 1000 years were calculated, (Table 3.28). To convert the weight changes to thickness changes, the density of Pb($11.4\ g/cm^3$) was used for all Pb alloys since the compositions of the alloys were not specified in their report. For the thickness increases, the calculated values may not be correct, because the weight increases were caused by corrosion products for which the densities are not known. Therefore, the calculated values must be treated as approximations. For these calculations, the highest corrosion rate for each environment was used, and was linearly extrapolated to 1000 years.

As shown in Table 3.28, the groundwater environment gave the lowest corrosion rates; it was believed that the impurities in the groundwater form a

Table 3.24

Simulated Grande Ronde Basalt Groundwater[30]

Attribute	Desired	As Prepared*
pH (25°C)	9.92	9.86-9.99
Conductivity (mho)	--	1,056-1,254
Na^+ (mg/L)	250	270-295
K^+ (mg/L)	1.9	1.7-2.1
Ca^{+2} (mg/L)	1.3	0.9-1.0
Mg^{+2} (mg/L)	0.4	0.2-0.2
CO_3^{-2} (mg/L)	107	84-91
HCO_3 (mg/L)	--	8.7-24.4
Si	56.3	42-53
Cl^- (mg/L)	148	135-159
SO_4^{-2} (mg/L)	108	75-113
F^- (mg/L)	37	34-37

* Range of value for five batches.

Table 3.25

Weight Change of 250°C Screening Corrosion Test Specimens[30]

Material	60-Day Exposure, Simulated Grande Ronde Groundwater mdd	3-Month Exposure, PNL "Hanford" Groundwater mdd
Inconel 600	-0.035	-0.047
Hastelloy G	-0.064, -0.067	--*
Inconel 625	-0.072	-0.02
Titanium Grade 2	+0.077, 0.0	+0.02
Titanium, Grade 12	-0.027, -0.054	-0.01
Ferallium, 25-5	-0.74, -0.75	--*
Hastelloy C-276	-0.022	-0.04
Cupronickel, 90/10	-0.24	--*
Cupronickel, 70/30	--*	-6.45
Zircaloy-4	+0.072	--*
Zircaloy-2	--*	-0.12
Inconel 825	-0.08	--*

* Alloy not included in test.

Table 3.26

Analysis of Groundwater used in Corrosion Tests[22]

SiO_2	8.05	mg SiO_2/1
Na	63.4	mg Na/1
K	7.4	mg K/1
Mg	3.57	mg Mg/1
Ca	21.3	mg Ca/1
Pb	<1	μg Pb/1
fluorides	817	μg F-/1
phosphates	53	μg PO_4^{---}/1
free CO_2	6	mg CO_2/1
carbonates	188	mg CO_3^{--}/1
organic species	3.7	mg O_2/1
chlorides	35.5	mg Cl^-/1
sulphates	<0.5	μg SO_4^{--}/1
nitrates	5.95	μg NO_3^-/1
Fe	189	μg Fe/1
Cu	<10	μg Cu/1
Sn	<10	μg Sn/1
pH	7.35	--

Table 3.27

Corrosion of Candidate Container Materials in Groundwater as a Function of Temperature and Time (Expressed in mg/cm^2)[22]

	Temperature and Time		
Alloy	49°C 4 Months	49°C 9 Months	98°C 4 Months
AISI 304	0	-0.10	+0.12
	0	-0.04	+0.10
AISI 304L	0	-0.04	+0.08
	-0.02	-0.04	+0.22
AISI 316	0	-0.08	+0.70
	0	-0.08	+0.10
AISI 316L	0	-0.08	+0.10
	0	-0.02	+0.08
AISI 430	0	+0.08	+0.10
	-0.02	-0.06	+0.08
1803 T	0	-0.08	+0.10
	0	-0.04	+0.10
Inconel 600	-0.02	-0.18	+0.02
	0	-0.14	+0.06
Incoloy 800	-0.08	-0.30	+0.04
	+0.02	-0.08	+0.06
Ni-200	-0.02	-0.16	+0.04
	-0.08	-0.18	+0.08
1803 Mot	+0.14	+0.22	+1.0
	+0.76	+0.02	+0.08
Carbon steel	destroyed	destroyed	not exposed
	destroyed	destroyed	not exposed
Chromised steel	-6.46	-7.64	+0.08
	-5.28	-6.18	+0.04
Hastelloy C	+0.02	-0.12	+1.08
	-0.04	-0.12	+0.20
Hastelloy B	-0.08	-0.28	+0.20
	-0.02	-0.18	+0.16
Inconel 625	-0.06	-0.16	+0.32
	-0.02	-0.12	+0.20
URB904L	-0.04	-0.12	+0.20
	-0.20	-0.08	+0.24
AISI 304L	-0.02	-0.08	+0.20
	0	-0.08	+0.28
IMI	-0.02	-0.08	+0.28
	-0.10	-0.14	+0.44
Ti	-0.02	-0.14	+0.24
	0	-0.02	+0.24
Ti-Al-Sn 52	-0.04	-0.04	+0.20
	-0.02	-0.14	+0.61
Ti-Al-V 6-4	-0.04	-0.10	+1.76
	-0.04	-0.10	+2.12
AISI 304L	-0.04	-0.14	+0.20
	-0.01	-0.06	+0.30

0 = weight change less than ±0.005 mg/cm^2.

Table 3.28

Estimated Thickness Changes (cm) of Lead Alloys after Exposure to Different Environments at 49°C for 1000 Years*

		Demineralized Water		
Alloy	Groundwater	Saturated with Air	Absence of Air	Humid Clay Atmosphere
Pb	-0.08	-38.81	-2.85	+0.04
Pb-Zr-Mg	+0.40	-39.68	-2.51	+0.08
Pb-Te	-0.15	-76.31	-5.01	+0.04
Pb-Sb	-0.04	-35.77	+0.82	+0.04
Pb-Ag	+0.10	-14.43	-16.66	+1.68

*Positive sign (+) denotes thickness increase and vice versa.

protective layer or act as corrosion inhibitors. However, the amounts and species of impurities were not given. In demineralized water saturated with air, the corrosion rates are unacceptably high. However, for natural clay groundwaters Pb appears to show high potential for use in a HLW container system.

D. Granite Repository

In the Swedish plan, waste packages will be placed in vertical boreholes 500 m below ground in igneous granite rock. KBS, an organization set up by the Swedish power industry, proposed three alternative container types:

- A titanium container with a wall-thickness of 6 mm and 100 mm thick lead lining, KBS I Plan, was proposed for reprocessed and vitrified waste. The waste form will be enclosed in a 3 mm thick casing of chromium-nickel steel (24% Cr, 12-13% Ni, and 0.15% C) before being placed in a container. The general corrosion of titanium under the prevailing conditions was estimated to be less than 0.25 m/year and the risk of localized corrosion was judged to be small.[32] However, because of the risk of delayed fracture* of Ti, although small, the main corrosion resistance was evaluated to be from the lead lining.[32]

- A copper (OFHC)** container with at least 200 mm thick walls, KBS II Plan, was proposed for unprocessed spent fuel rods. The penetration rate was calculated and it was concluded that a copper container with a wall thickness of 200 mm would last hundreds of thousands of years[32] (see Section 3.4.2.3).

- The third type is designed to use α-alumina sintered under hot isostatic pressure.

E. Summary

Based on the data reviewed above, the following metals were judged by BNL to perform satisfactorily in terms of general corrosion:

Bedded Salt Repository	Basalt Repository
Ticode-12	Copper
Ti, C.P.	Lead
Ti-Pd	Ticode-12
Stainless Steel	Ti-Pd
Nickel Alloys	Ti, C.P.
Zircaloy-2	Stainless Steel
	Nickel Alloys
	Zircaloy-2

Evaluations of these materials for iron-uniform corrosion (pitting, crevice corrosion, and SCC) and hydrogen effects are given below.

---

*This will be discussed in detail in section 3.4.2.6.

**Oxygen free high conductivity.

The approximate thickness changes after 1000 years for some of the above mentioned metals were estimated mainly from Sandia and PNL's data, and are shown in Table 3.29. Simple linear extrapolations were used assuming a single corrosion mechanism, i.e., uniform corrosion. PNL's weight change results were converted to perforation rates for this calculation. It should be noted that this calculation shows a rough estimation since most of the rates were from one single data point experiments. This table should therefore be used for comparisons only. It can be seen that copper and lead show very poor performance in oxygenated brine solution and seawater. Pure Ti also shows very poor corrosion resistance in oxygenated brine solution.

3.4.2.3 Pitting Corrosion

Pitting is a form of localized attack that is particularly dangerous since rapid penetration of thick metal sections can occur. The small pits are anodic and the bulk of the passivated (oxidized) surface is cathodic. Because of the large size of the cathode it is understandable how the concentrated electrochemical reaction at the pit sites can lead to the accelerated attack.

A number of theories have been proposed to explain the initiation of pits using both kinetic and thermodynamic approaches. Shreir[33] and Szklarsaka-Smialowska[34] reviewed and discussed these theories in their publications.

For the propagations of pits, a mechanism by Fontana[35] is widely accepted. This mechanism is based on the migration of chloride ions (Cl^-) to the pit and hydrolysis of the metal chloride which results in a pH drop in the pit.

For carbon or low alloy steels the "Pourbaix" diagram[36] in Figure 3.2 serves as a guide in defining electrochemical/pH conditions for which pitting will occur in chloride solutions. The electrode potential E_H* is the potential difference between the metal and the solution with respect to a hydrogen standard electrode. Note that pitting occurs in neutral and slightly alkaline solutions. Local measurements within the pits, given by the short thick line, show that highly acidic conditions are present. If the chloride solution is highly alkaline, passivation occurs and corrosion is negligible. For very acidic conditions, general corrosion occurs.

Pitting behavior of several candidate metals is briefly reviewed below.

A. Stainless Steels

Parr and Hanson[37] tested stainless steel in seawater and marine atmospheric environments for 8 years. Martensitic (Type 410), ferritic (Type 430), and austenitic (Type 300 series) stainless steels were all pitted to some extent (Tables 3.30 and 3.31). Generally, Type 316 stainless steels are more resistant to pitting corrosion than other types. Linear extrapolation of the maximum pit depth for Type 316 to 1000 years leads to a value of about 80 cm. Note that this was an in-situ experiment, which means the testing temperatures were about 25-30°C (Panama Canal Zone).

---

*E_H is not the same as E_h (oxidation potential) that is used by geologists.

Table 3.29

Estimated Thickness Changes of Metals after 1000 Years at 250°C (Thickness Changes in mm)*

	Brine	Basalt Groundwater	Seawater	O_2 Content	Reference
TiCode-12	3	--	1	Deoxygenated	4
	0.4	--	0.6	600 ppm	4
	--	--	--	1750 ppm	4
	--	0.06	--	<0.05 ppm	29
Pure Ti (Grade 2)	14	--	12	Deoxygenated	4
	3200	--	--	450 ppm	5
	--	--	16.2	500 ppm	5
Ti-Pd	2.4	--	1.14	Deoxygenated	5
	0.4	--	--	450 ppm	5
	--	--	0.62	500 ppm	5
Cu	7	--	5	Deoxygenated	4
	1200	--	--	600 ppm	4
	--	--	5000	1750 ppm	4
	420	--	--	<1 ppm	29
	--	8	--	<0.05 ppm	29
Pb	500	--	300	Deoxygenated	4
	1200	--	--	600 ppm	4
	--	--	1000	1750 ppm	4
316 L S/S	15	--	5	Deoxygenated	4
316 S/S	0.3	0.3	--	<1 ppm	29
	--	0.1	--	<0.05 ppm	29
Hastelloy C-276	7	--	1.5	Deoxygenated	4
	60**	--	--	600 ppm	4
	--	--	200**	1750 ppm	4
	0.4	0.08	--	<1 ppm	29
	--	0.16	--	<0.05 ppm	29

* It was assumed that the corrosion mechanism does not change for 1000 years.

**Pitting and crevice corrosion.

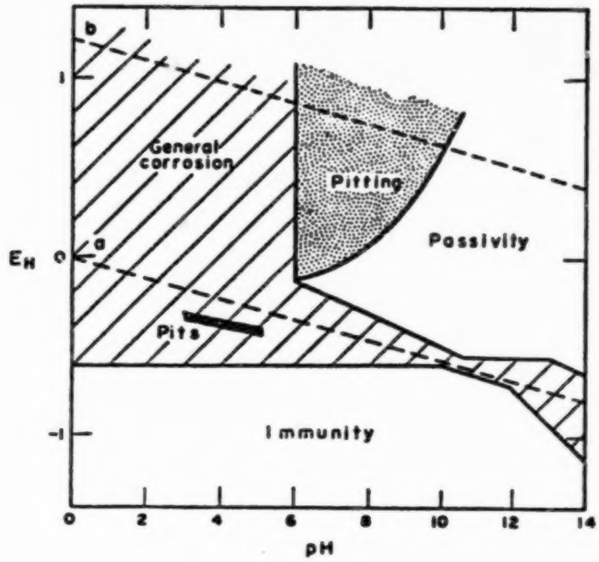

Figure 3.2 Potential/pH diagram for iron in chloride solutions (10^{-2}-10^{-3} mol Cl) at room temperature (according to Pourbaix).[36]

BEST DOCUMENT AVAILABLE

Table 3.30

Pitting in Stainless Steels After Eight Years' Immersion in Seawater[37]

AISI	Weight loss, g/dm^2				Average depth of 20 deepest pits(c), mils				Deepest pit(d), mils				Type of corrosion attack
type	1 yr	2 yr	4 yr	8 yr	1 yr	2 yr	4 yr	8 yr	1 yr	2 yr	4 yr	8 yr	
410	5.99	9.56	15.87	28.09	61 (11)	64 (11)	148	161	260 (P)	264 (P)	260 (P)	259 (P)	Localized, concentration cell pitting
302	2.93	4.43	7.06	10.89	70 (12)	74	107	140	261 (P)	238	286 (P)	236	Random pitting
316	1.18	0.65	0.54	4.08	44 (7)	52	48	154	245 (P)	82	93	245 (P)	Random pitting
321	2.32	3.44	6.55	10.22	64 (8)	120	175	193	270 (P)	206	273 (P)	272 (P)	Random pitting

(a) Data from U. S. Naval Research Laboratory

(b) Test location was 1½ miles from the shoreline near Fort Amados in the Panama Canal Zone.

(c) Numbers in parentheses are the total number of pits averaged when less than 20 were available.

(d) (P) indicates complete perforation.

Table 3.31

Pitting in Stainless Steels After Eight Years' Exposure to a Seashore Atmosphere [37]

AISI	Weight loss, g/dm^2				Type of
type	1 yr	2 yr	4 yr	8 yr	corrosion attack
410	0.08	0.11	0.11	0.08	Some localized pitting
430	0.05	0.07	0.07	0.07	Some localized pitting
301	0.00	0.00	0.01	0.01	No visible attack
316	0.00	0.00	0.00	0.00	No visible attack
321	0.01	0.00	0.01	0.01	No visible attack

(a) Data from U. S. Naval Research Laboratory

(b) Test location was the roof of the Washington Hotel, 55 ft above sea level and 300 ft from the harbor at Cristobal, Panama Canal Zone.

BEST DOCUMENT AVAILABLE

A group of stainless steels was evaluated at higher temperatures (68-121°C) by Lawson et al.[38] for potential use as tubing in a desalination plant. 400 series stainless steel showed poor pitting resistance. Type 316 and 317 showed better pitting resistance than Type 304. The maximum pit depth for Type 316 after 18 months at 113-121°C was 20 mils. Simple linear extrapolation of this result to 1000 years leads to a pit depth of 35 cm. The higher pitting rate at lower temperature was probably caused by the different oxygen content. Lawson et al. used deaerated seawater for which the final oxygen content was 25 ppb.

Braithwaite and Molecke[4] did not observe pitting corrosion of Type 316L in deoxygenated brine solution and seawater at 250°C. This is perhaps because of the short experiment duration (28 days) compared to Lawson et al.'s 18 months. Usually an initiation time is required for stainless steel to develop pitting corrosion. The extrapolation of general corrosion rates of Type 316 stainless steels reported by Braithwaite and Molecke to 1000 years leads to metal loss values of only 1.5 cm and 0.5 cm at 250°C in brine solution and seawater, respectively. However, it can be seen that no stainless steel container of reasonable thickness can achieve 1000 year containment in flooded bedded salt repository environment due to pitting corrosion.

Most pitting corrosion is caused by chloride and chlorine containing ions. Figure 3.3 shows the effect of chloride concentration on pit initation in Types 316L* and 317L* stainless steel and Hastelloy G.[39] As shown in Tables 3.6-3.10, chloride ion (Cl^-) contents range from 3 to 50 ppm in repository groundwaters (basalt, granite, etc.). In this Cl^- concentration range, pitting for Type 316L and 317L stainless steel is not likely. However this could be confirmed by long-term experiments (e.g., 1-2 years) for a prototypic groundwater if these metals become serious candidate metals in a basalt repository, for instance.

B. Copper

Pitting corrosion of copper in fresh water has been extensively studied due to the wide usage of copper plumbing. Campbell[40] categorized pitting corrosion of copper into Type I and Type II.

Type I pitting usually occurs in cold water pipes of hard well waters. The pits are fairly large and usually contains crystalline cuprous oxide and cuprous chloride beneath hard green mounds of calcium carbonate and basic copper carbonate. A schematic diagram is shown in Figure 3.4.[36] This type of pitting can cause perforation in only one or two years.[40]

Type II pitting is associated with certain soft water and hot water pipes (60°C). Deep pits of small cross section contain cuprous oxide and are capped by small black or greenish-black mounds of cuprous oxide and basic copper sulfate.

---

*Compositions; Type 316L: 0.08 %C, 2.00 %Mn., 16-18 %Cr, 10-14 %Ni, 2-3%Mo, bal. Fe.
Type 317L: 0.08 %C, 2.00 %Mn, 18-20 %Cr, 11-15 %Ni, 3-4 %Mo, bal. Fe.

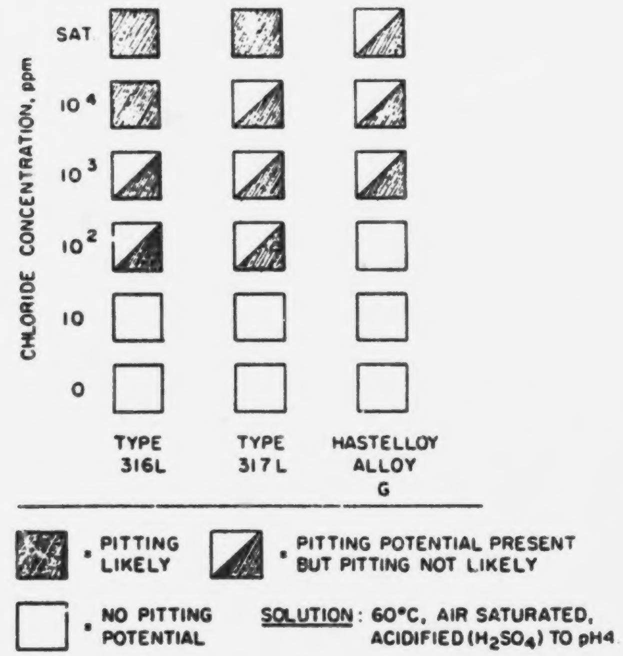

Figure 3.3 Effect of chloride concentration on pit initiation in Types 316L and 317L stainless steel and Hastelloy G.[39]

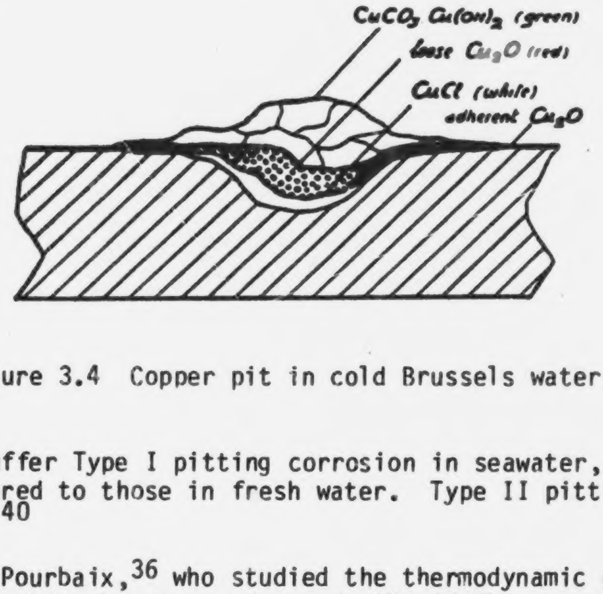

CuCO3 Cu(OH)2 (green)
loose Cu2O (red)
CuCl (white)
adherent Cu2O

Figure 3.4 Copper pit in cold Brussels water.[36]

Copper can suffer Type I pitting corrosion in seawater, but pits are wide and shallow, compared to those in fresh water. Type II pitting in seawater has not been reported.[40]

According to Pourbaix,[36] who studied the thermodynamic equilibria for copper in chloride, bicarbonate, and mixed chloride/bicarbonate solutions,

BEST DOCUMENT AVAILABLE

pitting corrosion occurs only and always when the general electrode potential rises to a critical value (+170 mV/SCE). Such potentials can be reached by coupling the copper to a more noble metal or to carbon.[40]

Evans[41] discussed the pitting corrosion of copper as follows: "Especially in fresh waters, pitting is most likely to occur when the main surface is one on which the cathodic reaction (normally reduction of oxygen) can proceed readily, since this will increase the current at the small anode. Unfortunately copper pipes sometimes carry on their interior surface carbonaceous films (often almost invisible) derived from lubricant used in the drawing processes; such a film can provide an efficient cathode. Alternatively, they sometimes carry a special type of oxide-film which also acts as an efficient cathode. Every endeavour is now made at the tube works to control the furnace atmosphere and thus avoid the production of either carbonaceous or oxide layer; but if either layer should exist on the pipes when put into service with certain waters, pitting is liable to develop."

In evaluating the Swedish KBS II plan, Mattsson[32] representing a group of Swedish scientists argued that copper container corrosion for the first 1000 years will be determined by the supply of oxygen to the container surface.

From the estimated amount of oxygen entrapped when the repository is closed, they calculated the average penetration to be 0.02 mm after 1000 years. The maximum pit depth of 0.5 mm was obtained by multiplying the average penetration by a pitting factor* of 25, which was based on Denison and Romanoff's[43] 14 year field test results on soil corrosion of copper. In this calculation, they estimated the oxygen supplied from the groundwater, or formed by radiolysis, to be negligible.

On the other hand, PNL's experiments conducted in basalt groundwater with an oxygen concentration of less than 50 ppb showed an estimated average penetration of 8 mm after 1000 years (see Table 3.29). Multiplying the pitting factor of 25 with this value gives 200 mm. This value is far larger than that calculated by the Swedes. BNL believes that the estimated pit depths from the PNL study are likely to be more accurate since they were obtained from experiments which closely simulated repository conditions.

C. Titanium and its Alloys

Based on existing information, it appears that titanium and its alloys are resistant to pitting. Braithwaite et al.[5] did not report any such attack in their work on titanium, Ticode 12, and Ti-Pd when exposed to high temperature salt brine and seawater. However, there is some information which shows that both pitting and crevice corrosion can occur in titanium for high temperature NaCl solutions[44] (Figure 3.5). Pitting is enhanced by acidic conditions as well as increasing temperatures and chloride levels. In Salton Sea brine severe pitting was found in titanium at 95°C as mentioned earlier (Section 3.4.2.2).

The effect of temperature on pitting potential of commercially pure titanium is shown in Figure 3.6.[45] When the temperature is increased from room

---

*Ratio of deepest metal penetration to average metal penetration as determined by weight loss of the specimen.[42]

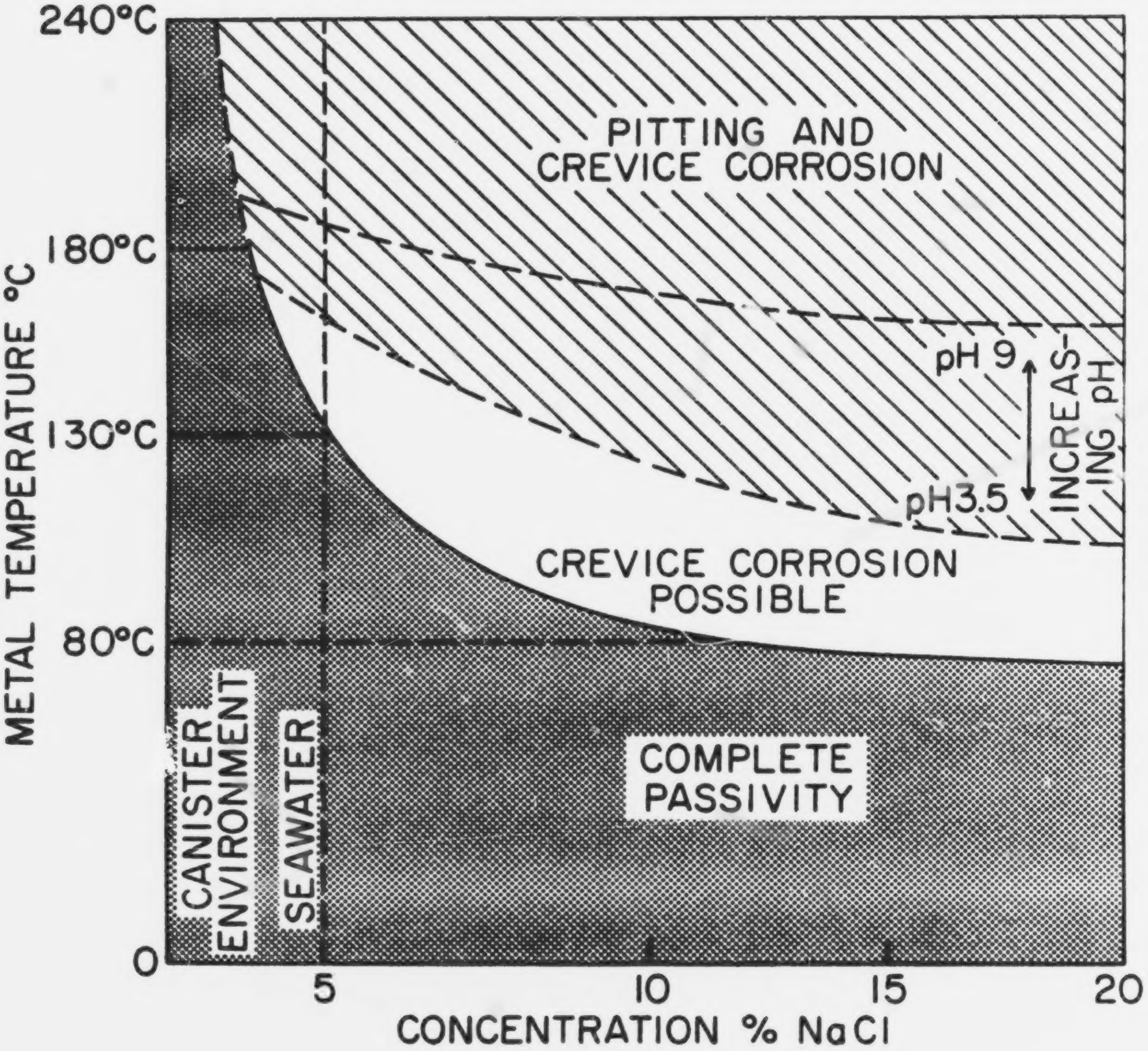

Figure 3.5 Influence of temperature, chloride content and pH value on crevice corrosion and pitting of unalloyed titanium.[44]

BEST DOCUMENT AVAILABLE

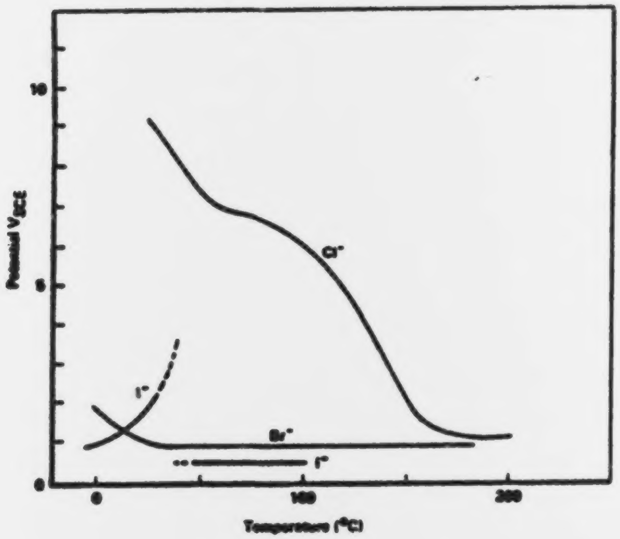

Figure 3.6 Effect of temperature on pitting potential of CP titanium in 0.6 to 1 M halide solutions.[45]

BEST DOCUMENT AVAILABLE

temperature to 200°C, the pitting potential in chloride solution decreases from 9 V to 1 V. The pitting potential in bromide is considerably lower than that in chloride solution, exhibiting no change with increasing temperature. It should be noted that small amounts of I^{-1} and Br^{-1} (about 10 and 400 ppm, respectively) exist in brine solutions (Table 3.5).

Swedish scientists[32] reported that pitting or crevice corrosion may occur in warm chloride solutions. However, they concluded that these types of corrosion are not to be expected in the Swedish granite HLW repository because the repository temperature will not exceed 80°C and the chloride content will not reach 0.04%. We believe that the Swedish data should be used only as a guide for U.S. plans because the conditions in the Swedish and U.S. granite repositories are not the same.

D. Lead

Lead and its alloys are usually resistant to pitting. However, the general corrosion rate of lead is high in some environments that do not form protective films. For instance, the corrosion rate in aerated distilled water is approximately 90 mmd.[42]

E. Nickel Alloys

Niederberger et al.[46] tested Ni-Cr-Mo alloys in seawater. Hastelloy C and Inconel 625 did not show pitting, while Incoloy 825 showed pitting rate of 25 mils/yr based on a maximum pit depth. However, Tables 3.12 and 3.13 show that Inconel 625 and Hastelloy C-276 will pit.

3.4.2.4 Crevice Corrosion

Crevice corrosion may occur if a metal surface is shielded in such a way that areas of limited access to corrosive solutions are present. Because of this, replenishment of certain substances is restricted--hence the name crevice (or cranny) corrosion.[23] This is a type of localized corrosion which shares much in common with pitting and SCC.[34] Crevice corrosion occurs in easily passivating alloys such as stainless steels, titanium, and aluminum. In certain situations, corrosion products in the crevice are more voluminous than the metal lost and they may create stresses large enough to seriously deform the metal.[23] Although this particular form of corrosion may not represent a major problem for a container in a well-designed repository, it is conceivable that overpack or backfill materials adjacent to the metal surface could form numerous pockets of void spaces where crevice corrosion could occur.

A. Stainless Steel

Crevice corrosion is found in ferritic stainless steels.[47] Using a special potentiostatic polarization technique, attack was found for a range of 25% Cr - Mo alloys (Table 3.32). For a constant Mo level, increasing the Cr content gave higher crevice corrosion resistance. For a constant Cr level, increased Mo content also enhanced resistance. Temperature increases enhanced crevice corrosion.

Austenitic 18% Cr - Mo stainless steels were investigated by Bringham[48] for susceptibility to crevice attack in 10% $FeCl_3$ after 24 h exposures. The

Table 3.32

Results of Controlled Potential Crevice Corrosion Test in 1 N NaCl Cell on Ferritic Stainless Steels[47]

Steel Type	Presence of Crevice Corrosion at Indicated Test Temperature				
	21 to 22°C	30°C	40°C	50°C	60°C
20 Cr - 2 Mo	yes	--	--	--	--
22.5 Cr - 2 Mo	yes	--	--	--	--
25 Cr	yes	--	--	--	--
26 Cr - Mo	no	yes	yes	--	--
25 Cr - 2 Mo	no	yes	yes	--	--
28 Cr - 2 Mo	no	no	no	yes	--
25 Cr - 3.5 Mo	no	no	no	yes	--
25 Cr - 5 Mo	no	no	no	no	yes

temperature was increased until crevice attack occurred. He found that the crevice corrosion temperature (CCT) was defined by the relationship:

$$CCT(°C) = -(45 \pm 5) + 11 \times \% \, Mo$$

Thus, a Type 304 stainless steel containing no Mo could exhibit crevice corrosion at $T > 45°C$, where Type 316 containing 2.5% Mo would be susceptible to attack at a temperature above about 73°C. Ellis and LaQue[49] observed significant crevice corrosion of stainless steel in seawater. Peterson et al.[50] also reported intensive crevice corrosion of Type 304 stainless steel in seawater.

B. Titanium and its Alloys

Gleekman[51] and Sheppard et al.[52] reported that severe crevice corrosion of Ti occurs in NaCl and Cl^- environments. Turnbull[53] found that some crevice corrosion occurred in neutral brine but not in alkaline environments ($pH > 12$). Bohlman and Posey[54] found crevice attack in synthetic seawater and also in NaCl solutions. No crevice corrosion was noticed for temperatures below 100°C. Greiss[55] found that at 150°C crevice corrosion occurred in 1 M NaCl solution. The mechanism was connected with the formation of a highly acidic solution within the crevice ($pH \sim 1$). Not only did NaCl induce attack but iodide, bromide, and sulfate solutions also cause crevice corrosion. Shimose and Takamura[56] also showed that crevice corrosion could occur in hot concentrated magnesium and ammonium chloride solutions. Figure 3.5 summarizes crevice corrosion conditions for titanium in NaCl solutions.

Additions of Mo, Ni or Pd were found to enhance the resistance of titanium to attack. TiCode-12 (Ti-0.3 Mo-0.8 Ni) and Ti-Pd alloy (0.2 Pd) have better corrosion resistances than pure Ti. TiCode-12 is particularly resistant to crevice corrosion in hot brines.[57] Figure 3.7 shows crevice corrosion of TiCode-12 and pure Ti (grade 2) in saturated NaCl solution.

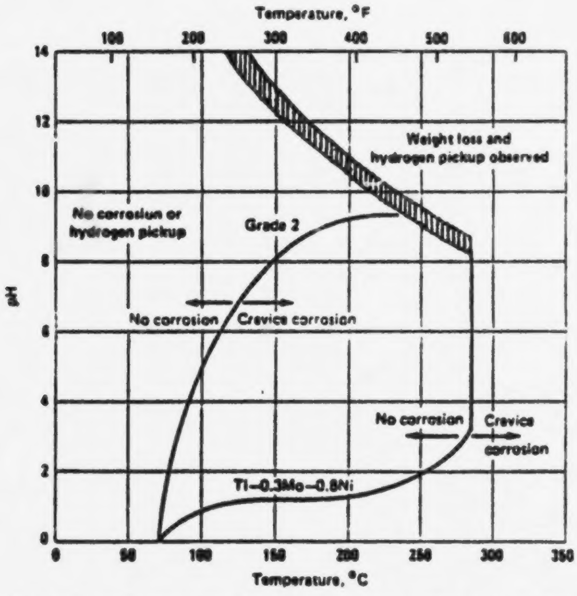

Shaded band represents transition zone between active and passive behavior.

Figure 3.7 Crevice corrosion of TiCode-12 (Ti-0.3 Mo-0.8 Ni) and pure Ti (Grade 2) in saturated NaCl solutions.[57]

Braithwaite et al.[5] studied the crevice corrosion of pure Ti, TiCode-12 and Ti-Pd in brine solutions at 250°C. Pure titanium showed severe crevice corrosion, while TiCode-12 and Ti-Pd did not. Even at 300°C and a dissolved oxygen concentration of 250 ppm, TiCode-12 did not exhibit any crevice corrosion. It should be noted that the increased dissolved oxygen content, while causing very severe crevice attack in titanium, actually reduced the general corrosion rates of the titanium alloys (see page 143).

PNL[29] also studied the crevice corrosion of pure Ti and TiCode-12, and the results are shown in Table 3.33. Not much information was given in this paper, and no clear trend can be seen in their results. It is interesting to notice that most TiCode-12 samples gained more weight than pure Ti in pre-cleaning weight-change measurements.

BEST DOCUMENT AVAILABLE

Table 3.33

Titanium Crevice Specimens Exposed in Hanford Groundwater at 250°C[29]

Material in Stacking Order	Weight Changes, mg/dm²(a) Before Cleaning	Weight Changes, mg/dm²(a) After Cleaning	Hydrogen Analyses, ppm
Bolt 1			
Ti-50A	+0.8	-0.8	--
Ti-12	+0.8	+0.8	--
Ti-50A	+0.8	0.0	33
Ti-12	+1.6	+0.8	32
Ti-12	+2.4	+0.8	30
Teflon	--	--	--
Ti-50A	+0.8	0.0	--
Ti-12	+3.2	+0.8	--
Bolt 2			
Ti-50A	+2.4	-0.8	--
Ti-12	+22.0	+4.0	32
Cast-Iron 146-4	+81.0	-260.0	--
Ti-12	+28.0	+4.0	31
Ti-50A	+22.0	+7.0	35
Cast-Iron 136-4	+4.0	-212.0	--
Ti-50A	+27.0	+7.0	34
Ti-12	+4.0	-0.8	32
Unexposed Samples			
Ti-12	--	--	23
Ti-50A	--	--	34

(a) Weight changes approximately +/-0.6 mg/dm².

In conclusion, TiCode-12 and Ti-Pd are apparently very resistant to crevice corrosion. However, more studies should be conducted to establish the range of environments under which crevice corrosion occurs. These ranges of conditions should then be compared with anticipated repository conditions to determine the potential for crevice corrosion of Ti and Ti alloy in a realistic repository situation.

C. Lead

In the case of lead, a simple experiment by Evans showed that crevice corrosion could occur at room temperature in a KCl solution.[23] A lenticular glass was placed on a specimen immersed in the solution. In the crevice area introduced, oxygen was difficult to replenish and this led to anodic attack. Lead chloride formed and interacted with KOH formed in the better aerated cathodic regions to give a brown annulus of $Pb(OH)_2$. More studies on crevice corrosion of lead are needed because of the possibility of lead being used as a shielding material inside the outer container. The KBS II plan is considering 100 mm lead inside a titanium overpack, with the expected corrosion resistance being provided by the lead rather than the titanium. In this case, the crevice corrosion of lead should be studied seriously, because crevices exist between the lead liner and the titanium container (Figure 3.8).

D. Copper

Information on crevice corrosion of Cu is sparse. However, very recent experiments at Brookhaven National Laboratory* showed crevice corrosion of copper in brine solution at 150°C. This work is in progress at the time of writing.

E. Nickel Alloys

Niederberger[46] reported pits (depths of 1-26 mils) formed in crevice areas when Incoloy 825 was exposed to flowing seawater for 2 years. In the same experiment, Inconel 625 and Hastelloy C did not show crevice corrosion. However, it was reported by others that Inconel 625 showed 11 mil pits beneath a Teflon washer after 6 years exposure to seawater.[58] Hastelloy C and Inconel 625 have shown some crevice corrosion under gaskets of pipe flanges handling hot seawater.[59] Welded Hastelloy C showed intergranular corrosion in hot seawater and Hastelloy C-276 is preferred for welded structures.[60]

3.4.2.5 Stress Corrosion Cracking (SCC)

If a passivated (oxidized) surface film is locally fractured, electrochemical reactions are likely to occur in which the underlying metal surface becomes an anode and the oxidized surface layer becomes cathodic. Rapid dissolution of these localized anodic regions may then occur in the presence of a

---

*Preliminary experiment, HLW Corrosion Research Group, Nuclear Waste Management Division.

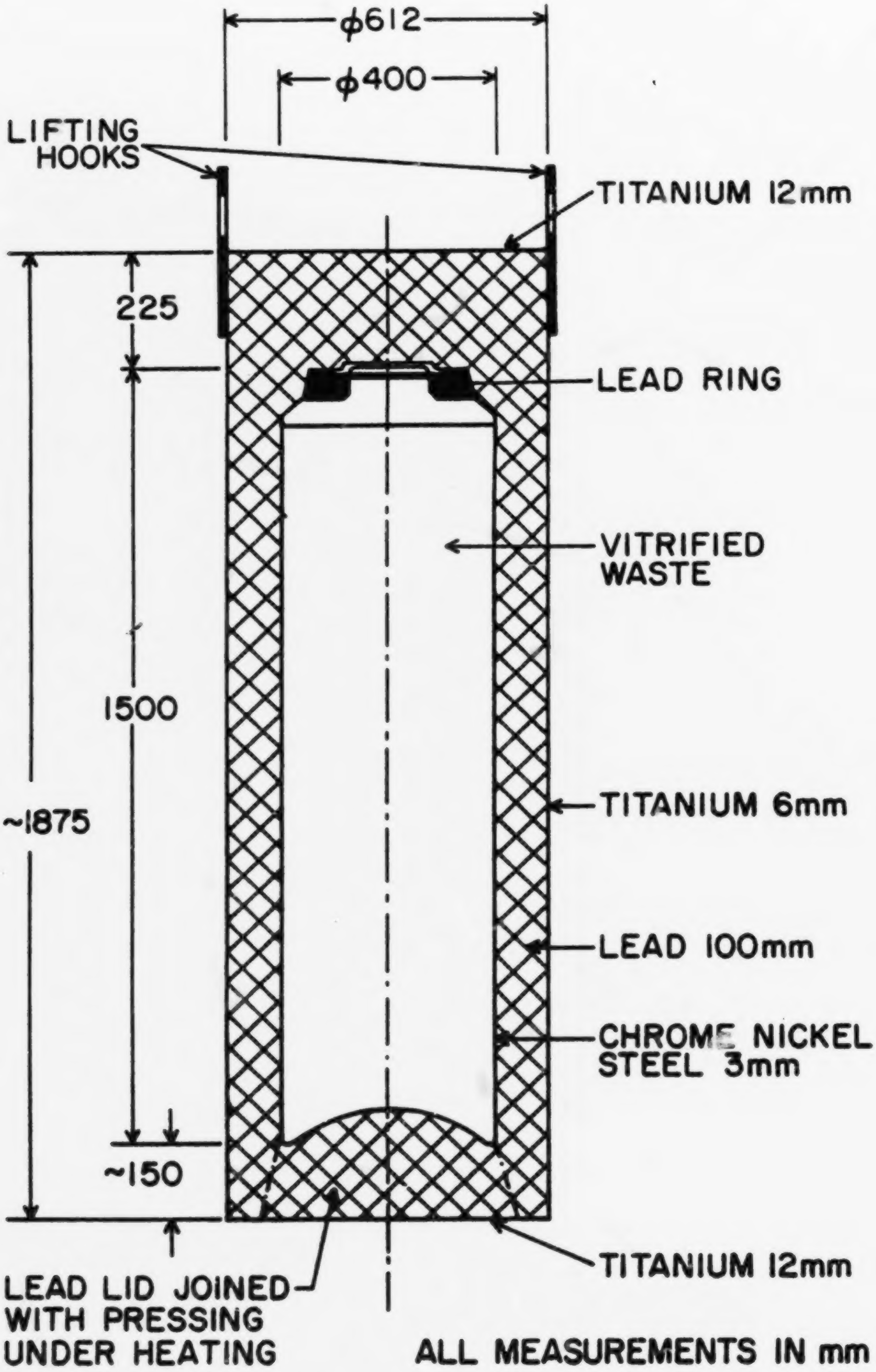
ϕ612
ϕ400
LIFTING HOOKS
TITANIUM 12mm
225
LEAD RING
VITRIFIED WASTE
1500
~1875
TITANIUM 6mm
LEAD 100mm
CHROME NICKEL STEEL 3mm
~150
TITANIUM 12mm
LEAD LID JOINED WITH PRESSING UNDER HEATING
ALL MEASUREMENTS IN mm

Figure 3.8 Swedish lead-titanium canister design.

BEST DOCUMENT AVAILABLE

stress, and cracks may propagate rapidly through large thicknesses of metal. This phenomenon is known as stress corrosion cracking (SCC). The mode of crack propagation may be transgranular (across the grain) or intergranular (along grain boundaries), or it may be a combination of both. Among the more aggressive environments are aqueous solutions containing Cl^- ions. In the following discussion, halide SCC will be discussed with particular emphasis on temperature and chloride levels which are likely to be representative of repository conditions.

A. Stainless Steels

In $MgCl_2$ solutions, boiling at approximately 140°C (containing about 40% solute), ferritic stainless steels with about 17% Cr were found to be highly resistant to SCC if Ni and Cu were absent as alloying elements.[61,62] The high resistance of ferritic material to chloride SCC was also found in earlier work by Scheil.[63,64]

If, however, this same class of 17% Cr stainless steels is quenched from a high temperature to impart high strength (martensitic stainless steel) cracking could be induced in a 5% NaCl solution at room temperature.[65] Failure rates were minimized if approximately 5% delta ferrite phase was present in the microstructure.

Austenitic stainless steels containing iron and approximately 18% Cr and 8% Ni, are an extremely important class of engineering materials because of their good general corrosion resistance, excellent fabricability and mechanical properties. In terms of chloride induced SCC, however, they possess many limitations. Concentrations of $FeCl_3$ as low as 0.5 ppm may cause failure for high stress levels and high temperatures (350°C) if the material is in a "sensitized" condition; i.e., the material has been preheated to a temperature where chromium carbides are precipitated at grain boundaries. In this condition the chromium depleted zones adjacent to the carbides are low in corrosion resistance and offer easy pathways for rapid intergranular attack.

Figure 3.9 shows the effects of temperature and chloride level on the time-for-cracking of Type 304 stainless steel in an aqueous NaCl solution[66]. The specimens were stressed by bending strips into the form of a "U bend". The important point to note is that failure will occur for chloride concentrations between 10-1800 ppm if the tests are of sufficient duration. Short term laboratory tests, lasting for days or weeks, may be totally inadequate in the prediction of stress assisted failure.

Oxygen also plays an important role in the SCC of austenitic stainless steels. In Figure 3.10 the conjoint action of oxygen/chloride levels is shown for Type 304 stainless steel.[67] High oxygen and chloride contents in the solution promote early failure. Work cited by Braithwaite and Molecke[4] indicate that oxygen in water in the range of parts per billion could enhance chloride SCC.

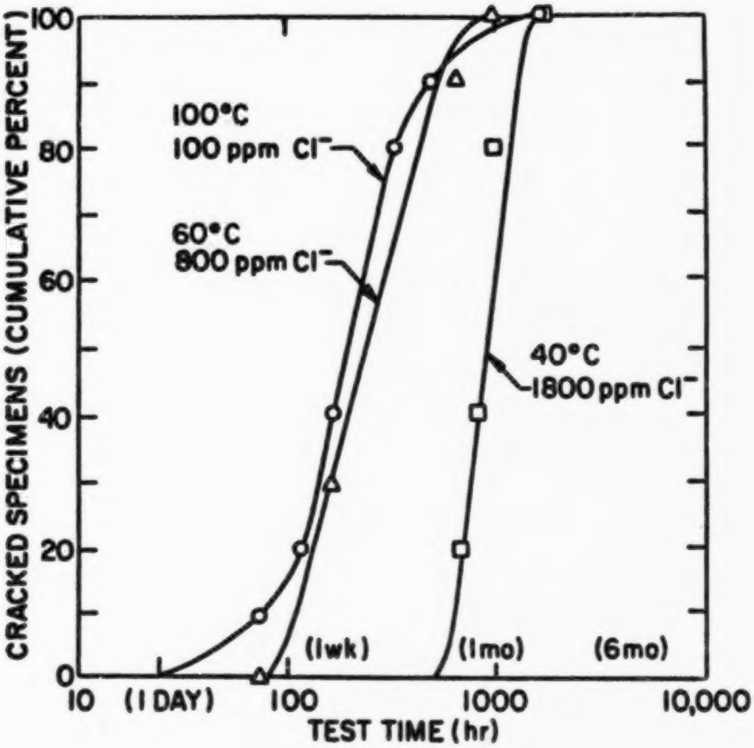

Figure 3.9 Effect of temperature and chloride level on the time-for-cracking of type 304 stainless steel in aqueous NaCl solution.[66]

BEST DOCUMENT AVAILABLE

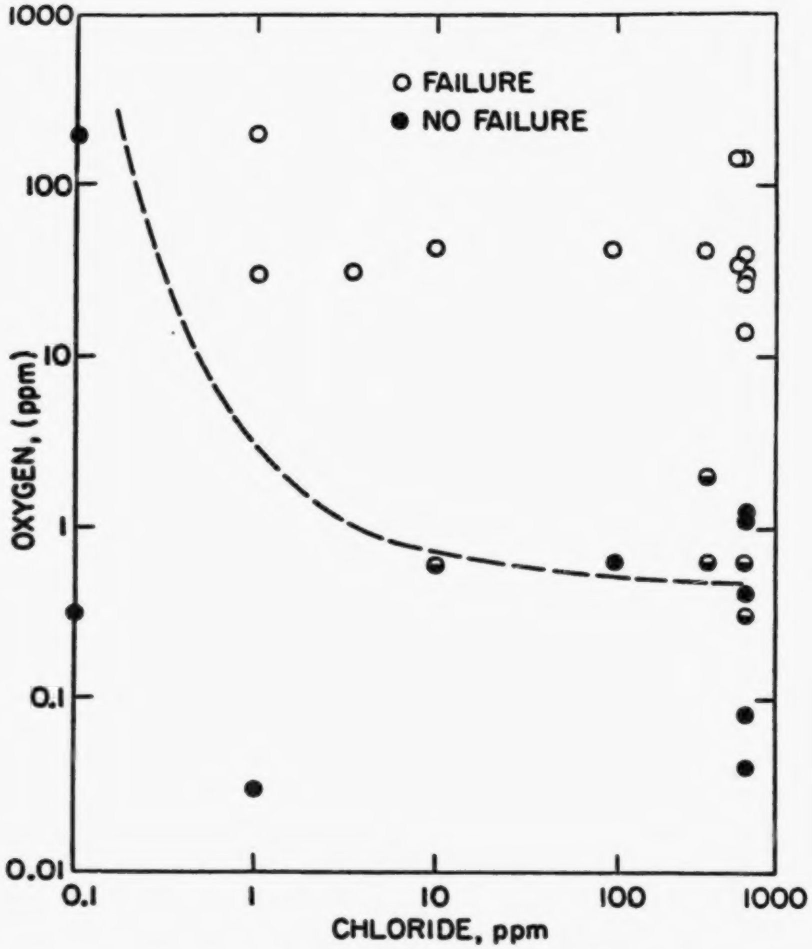

Figure 3.10 Relationship between chloride and oxygen content of alkaline-phosphate treated boiler water and susceptibility to stress corrosion of austenitic stainless steel exposed to the steam phase with intermittent wetting.[67]

BEST DOCUMENT AVAILABLE

Another important factor determining the severity of SCC in chloride solutions concerns the metallic cation involved. Warren[66] showed that for Type 304 stainless steel exposed to water at 100°C, containing 100 ppm of chloride, the cations could be ranked in the order of increasing corrosivity as Na^+, Ca^{2+}, Fe^{3+}, and Mg^{2+}. Since most brine inclusions in salt repositories contain large concentrations of Mg^{2+} (Table 3.5), it must be anticipated that Mg^{2+} will be significantly more damaging than Na^+.

Increasing exposure temperature is also known to accelerate the SCC of austenitic stainless steels in chloride solutions.[66] For small changes in temperature (from 60° to 100°C) the failure time in U bend samples of Type 304 stainless steel may be reduced by over an order of magnitude. Several investigators have shown that the following relationship is valid for SCC failure times in chloride solutions.[68,70]

$$t_f = A \exp (B/T)$$

in which t_f = time to failure
T = absolute temperature
A,B = system constants

Stresses and residual strains are the most important factors in SCC. Since neither variable can be eliminated in a waste container their effects must be quantified. Birchon and Booth[71] found that for prestrained Types 304 and 321 stainless steels (Type 321 stainless steel contains approximately 0.5% Ti to minimize intergranular carbide precipitation) there exists a strain limit below which failure will not occur in the steam phase above aerated solutions containing 5 ppm chloride. These strains are extremely low and will be unavoidable in practice. A similar type of behavior was found for a range of austenitic stainless steels which were stressed and exposed to boiling 42% $MgCl_2$ solution.[72] Type 304L, a candidate for use as a waste container behaves similarly to regular Type 304. A well defined threshold stress does not exist for fracture times of up to 750 h. The stress required to cause failure in this time is about 60 MPa, which is significantly below the range of stresses which will normally be experienced in a container. Nevertheless, it would be judicious to reduce the stresses in the container to a value as low as practicable.

Type 304L stainless steel has also been found to catastrophically fail by SCC in dilute chloride solutions at 49°C during a 2-year period of service in a feedwater deaerator system.[73] the feedwater chloride content was about 160 ppm but the overall chloride level at the steel surface was probably much less. After careful analysis it was concluded that stresses induced by thermal gradients caused the failure. Although the stress levels could not be accurately estimated, considerable plastic deformation was thought to be present.

Initially, Type 304L was selected in order to reduce the amount of chromium carbide precipitation at grain boundaries during high temperature in-can melting processes for high level waste glass encapsulation, and during sealing of the container by welding. By reducing the amount of chromium depletion adjacent to the grain boundaries, it was hoped that intergranular attack could be avoided.

However, the data in Figure 3.11 indicate that the sensitization of the boundaries in austenitic stainless steel is not completely avoided by lowering the carbon level.[74] It is seen from the iso-corrosion curves that if the materials are exposed to temperatures in the range of 500-850°C for extended times, even very low carbon material (0.01% C) is susceptible to intergranular attack when subsequently exposed to the "Strauss" solution, i.e., boiling acidified $CuSO_4$ solution. Any high temperature exposure of Type 304L must, therefore, be limited if sensitization induced attack is to be avoided in a repository environment. More detailed descriptions of SCC of austenitic steels in chloride and other environments are given in references 75 and 76.

B. Copper and Copper Alloys

Copper is being considered in the Swedish program (KBS I Plan) as a container material for spent fuel[8] and cupronickel (90% Cu - 10% Ni) and naval brass (60% Cu, 39% Zn, and 1% Sn) were evaluated as container alloys in the U.S. program.[4] Stress corrosion cracking, particularly of brasses, usually occurs over very extended periods of time in mildly corrosive atmospheres containing small quantities of nitrogen compounds, sulfur compounds, carbon dioxide, and chlorides.[77] Ammonium ion is the most damaging species for copper base materials.[77]

Uhlig[78] reported that commercial Tough Pitch, oxygen-free high conductivity and electrolytically refined copper are immune to stress-corrosion cracking. However, it was reported that phosphorus-deoxidized copper containing small amounts of P (as little as 0.004%) is susceptible to SCC. Recently, the KBS I Plan was evaluated by the National Academy of Sciences.[79] Their discussion on the SCC of pure Cu in a granite repository is quoted: "...The immunity of high-purity metals to SCC is a long-held belief, but several recent papers have presented evidence that high-purity copper under some conditions can undergo SCC (Pugh et al., 1966; Escalante and Kruger, 1971; Suzuke and Hisamatsu, 1974, Pednekar et al., 1979). The conditions are rather specific, and tensile stress must be present. Dissolved materials described as capable of causing stress corrosion of copper include cupric ammonia ion, cupric acetate, nitrate, and other solutes, some in concentrations less than 0.1 N but higher than 0.01 N. These agents in such concentrations are extremely unlikely in a repository environment unless an incursion of seawater should introduce nitrogen compounds. Although the KBS is not strictly accurate, the Subcommittee agrees that cracking should not occur in a repository environment..."

Table 3.7 shows that Hanford basalt groundwater contains 4.2 ppm (7×10^{-5} N) of NO_3^{-1}. This concentration is far below the concentration range mentioned above, and it is unlikely that copper will suffer SCC in the Hanford basalt groundwater. However, long term testing under prototypic repository conditions is required to confirm this. It should be noted that BNL does not recommend copper for bedded salt repository because of the high uniform corrosion rate in a brine solution.

BEST DOCUMENT AVAILABLE

BEST DOCUMENT AVAILABLE

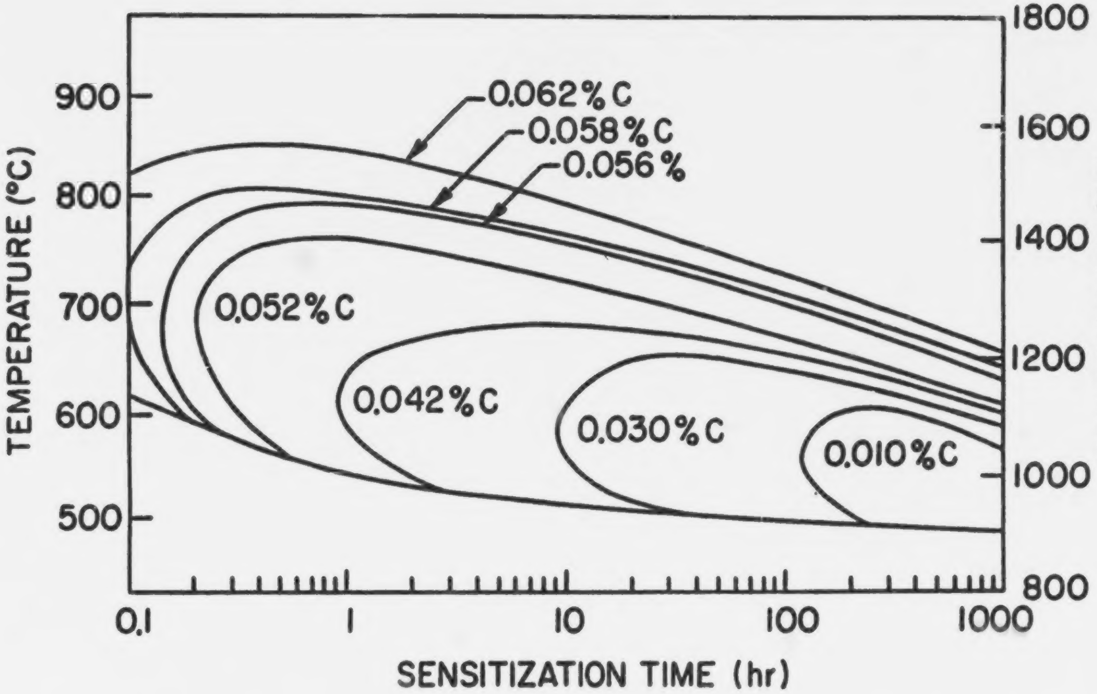

Figure 3.11 Onset of sensitization in 18-8 stainless steels as a function of carbon as determined by the Strauss test.[74]

C. Titanium and Zirconium Alloys

Titanium and its alloys generally possess excellent resistance to stress corrosion cracking. Nevertheless, it has been reported that cracking in salt environments can occur in many alloys but almost invaribly at temperatures in excess of about 275°C.[80] This is not within the temperature range anticipated inside a salt repository. However, certain situations were identified for which SCC could be induced in prenotched samples which were loaded under static cantilever conditions and exposed to seawater at room temperature.[81] The specimens had either machined notches with a root radius of 50 μm (0.002 in.) or they had cracks formed by fatigue. Table 3.34 shows that in the seawater environment, commercial purity Ti, Ti-7Al-2Cb-1Ta, Ti-7Al-3Cb, and Ti-6Al-2.5Sn showed large losses in strength. In Table 3.35 a wider range of titanium alloys was classified into groups which were either susceptible or non-susceptible to seawater induced SCC.[81]

Other workers, however, have found behavior which is contradictory to that described above. Powell and Scully,[82] for example, found that in slow strain rate mechanical testing at room temperature, transgranular SCC was found in Ti-5Al-2.5Sn alloy exposed to 3% NaCl but titanium failed in a ductile fashion. Details of the fracture surface characteristics are given in Table 3.36. For the alloy the fracture surface was characterized by brittle cleavage steps but, in the titanium, dimples indicative of ductile behavior were found. In 0.1 ppm Cl^- solutions, the alloy became more resistant to SCC as the pH was increased from 6 to 13.

Sanderson and Scully exposed titanium and several alloys to a boiling $MgCl_2$ solution at 154°C.[83] The alloys were susceptible to cracking but the titanium suffered only pitting. They found that in some alpha phase alloys, hydrides formed on the surfaces of the material can promote transgranular failure. In the absence of hydride, the cracking tends to be predominantly intergranular.

Very recent slow strain rate test data by Braithwaite et al.[5] are available for 3 titanium alloys (Table 3.37). At 250°C, tests in air, dry salt, and saturated brine gave ductilities (reductions in cross-sectional area, R.A.) which lie within a tight scatter band. Although the existence of an environmental effect is debatable, it is clear that ductility differences are likely to be small. Experiments were also conducted on hydrogen charged and gamma irradiated alloys. Braithwaite et al. concluded that with the possible exception of one test neither factor affected the bulk ductility. However, when samples were sectioned and examined metallographically, a TiCode-12 specimen tested in brine at 250°C was found to have a less ductile quasi-cleavage fracture surface extending to a depth of 50 m below the exposed surface. Specimens exposed to brine during irradiation also showed embrittled surface layers. Further investigation is under way.

Swedish scientists[32] concluded that stress corrosion cracking and corrosion fatigue may be excluded, as the stresses and notches required for such attack can be easily avoided.

Table 3.34

Effect of Seawater on the Fracture Strength of Titanium and Some Alloys[81]

	Nominal Fracture Strength in Air			Nominal Fracture Strength in Seawater		
	Slow Notch-Bend Test	Static Load Cantilever Test		Static Load Cantilever Test		
Titanium Alloy	Ksi	Ksi	Min*	Ksi	Min*	Sensitive by Fracture Appearance**
Ti Commercially Pure Rs-70	182	157	45	64	3	yes
7 Al-2 Cb-1 Ta	222	183	8	70	5	yes
7 Al-3 Cb	193	166	70	125	3	yes
6 Al-2.5 Sn	233	181	40	110	3	yes
6.5 Al-5 Zr-1 V	222	186	180	186	200	no
6 Al-2 Sn-1 Mo-1 V	209	196	9	180	1430	no
6 Al-2 Sn-3 V-1 Mo	211	115	1845	120	342	no

* Time to failure under static load.

Table 3.35

Classification of Titanium Alloys Susceptible to Stress Corrosion Cracking in Seawater[81]

Sensitive Alloys	Insensitive Alloys
Commercially Pure Titanium (RS-70)[b]	Ti-7 Al-2.5 Mo[a]
Ti-7 Al-3 Cb[c]	Ti-6 Al-2 Mo[c]
Ti-7 Al-3 Cb[c]	Ti-6 Al-2 Sn-1 Mo-1 V[a]
Ti-6 Al-2.5 Sn[a]	Ti-6.5 Al-5 Zr-1 V[a]
Ti-5 Al-2.5 Sn[a]	Ti-6 Al-4 V[a]
Ti-6 Al-3 Cb-2 Sn[b]	Ti-6 Al-2 Sn-1 Mo-3 V[c]
Ti-7 Al-3 Cb-2 Sn[b]	Ti-5 Al-2 Sn-2 Mo-2 V[c]
Ti-8 Al-3 Cb-2 Sn[b]	

[a] Alloy was tested in the mill-annealed condition.
[b] Alloy was tested in the beta-annealed condition.
[c] Alloy was tested in the as-rolled condition.

Table 3.36

Fracture Characteristics of Titanium and Titanium-5 Al-2.5 Sn Alloy in Various Chloride Media at Room Temperature[82]

Type of Test		
Instron Tensile Test	Ti	Ti-5 Al-2.5 Sn
3% NaCl	D	C(1)
H_2O 0.1 ppm C , pH 6	--	C
H_2O 0.1 ppm C , pH 11.6	--	C
H_2O 0.1 ppm C , pH 13	--	D
10 N HCl	--	C
MeOH/HCl	D	C
U-bend, MeOH/HCl	G	C
U-bend, MeOH	G	C
Unstressed specimen exposed to MeOH/HCl; fractured in air	G	G(2)
Instron, 3% NaCl + cathodic polarization	--	D
Instron, 3% NaCl + anodic polarization	--	D
Instron, 10 N HCl + cathodic polarization	--	D

All Instron experiments on the alloy were performed with crosshead speeds that caused cleavage failure under freely corroding conditions in aqueous 3% NaCl solutions.

(1) C = cleavage, D = dimple; G = grain boundary separation.

(2) Small amount of C.

Table 3.37

Nominal chemical Compositions of Titanium Alloys Studied in Sandia Container Corrosion Program[5]

Alloy	ASTM Grade	C	N	O	H	Fe	Pd	Ni	Mo	Ti
Ti-50A	2	.10M*	.03M	.25M	.015M	.3M	--	--	--	Bal.
TiPd	7	.10M	.03M	.25M	.015M	.3M	.12/.25	--	--	Bal.
TiCode-12	12	.08M	.03M	.25M	.015M	.3M	--	.6/.9	.2/.4	Bal.

*M denotes maximum.

With respect to zirconium, it appears to show basically similar SCC behavior to titanium. Generally it is thought to be immune to SCC but, like titanium (Table 3.36), certain environments containing methanol will cause failure. A comparison between the two metals when exposed to methanol/chloride mixtures is given in Table 3.38.[84]

Based on the above discussions it may be stated that although titanium and zirconium alloys posses excellent overall SCC resistance, much more work needs to be performed before either material can be fully qualified as a container material capable of withstanding failure for at least 1000 years.

PNL[29] has studied the stress corrosion cracking of pure Ti and TiCode-12 in Hanford basalt groundwater at 250°C for 89 days. There was no significant evidence of SCC; however, because of the experimental inaccuracies, no firm conclusions were reached.

D. High Nickel Alloys

Voluminous data exist on the SCC of high nickel alloys in chloride environments. Review articles are given in references 75 and 76. For a range of Fe-Cr-Ni wires tested in boiling 42% $MgCl_2$ solutions it was found that the nickel content was an important factor in the failure process. With the exception of very low nickel alloys it was found that the time to failure increased dramatically with the amount of nickel (Figure 3.12). Alloys with more than about 40% nickel did not fail after 800 h test periods.[85] Data on specific alloys are given in Table 3.39[86] for U bend specimens exposed at temperatures between 30-260°C in a range of different chloride media. Environment 8 is relevant to repository conditions. Clearly, increasing nickel content reduces the possibility of chloride-induced stress corrosion. For some high-nickel materials, such as Inconel 718 (52% Ni, 19% Cr, 5% Nb, 3% Mo, 0.8% Ti, 0.5% Al, 1.0% max. Co, balance in Fe), some highly stressed material exposed to boiling $MgCl_2$ at 154°C may resist failure for up to 100,000 min. (70 days).[75] Hence, short term tests must be avoided and a large number of specimens should be evaluated to obtain statistical failure data.

Table 3.38

Effect of Alcohol/Chloride Environment on the Stress Corrosion Cracking of Titanium and Zirconium After Stressing for 470 h at Room Temperature[84]

Environment	Titanium		Zirconium	
	Reaction	(Minutes)	Reaction	(Minutes)
Methanol	No Crack	--	Cracked	28000
Ethanol	No Crack	--	No Crack	--
N-Butanol	No Crack	--	No Crack	--
Methanol + 0.4% HCl	Cracked	65	Cracked	60
Ethanol + 0.4% HCl	No Crack	--	Cracked	600
N-Butanol + 0.4% HCl	No Crack	--	No Crack	--
Methanol + 0.4% HCl + 3% H_2O	No Crack	--	Cracked	1200
Methanol + 1% H_2SO_4	Cracked	1440	Cracked	1440
Methanol + 1% H_2PO_4	No Crack	--	No Crack	--
Methanol + 1% $(COOH)_2$	No Crack	--	No Crack	--
Methanol +1% HCOOH	No Crack	--	Cracked	9000

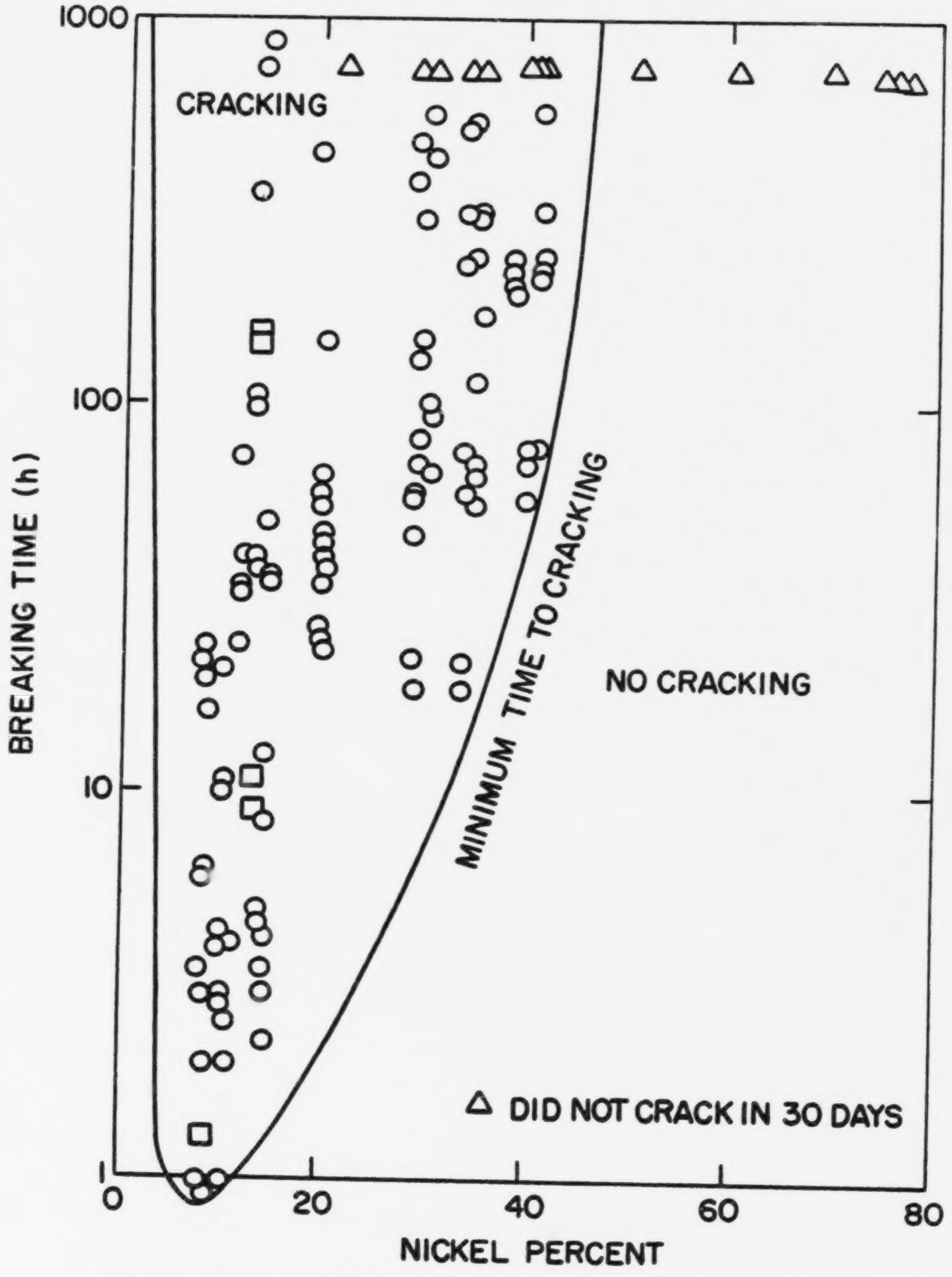

Figure 3.12 Effect of increasing the nickel content on the susceptibility of Fe-Cr-Ni wires in boiling 42% $MgCl_2$.[85]

BEST DOCUMENT AVAILABLE

Table 3.39

Results of Chloride Stress Corrosion Tests for Materials with Different Nickel Contents[86]

Environment	Test Time (Days)	Temp. (°C)	Average Time-to-Failure (Days) Type 304 S/S	Type 310 S/S	Inc. 800	Inc. 600
1. 35% NaCl - 0.5% CH_3OOH + H_2S	30	30	5	NF	NF	NF
2. 50% H_2SO_4 - 3% NaCl	30	30	1	NF	NF	NF
3. NaCl, Wick Test	30	100	3	16	--	NF
4. Saturated NaCl, pH = 4	30	109	12	NF	NF	NF
5. 36% $CaCl_2$	30	110	5	--	NF	--
6. 42% $MgCl_2$	10	154	1	1	4.5	NF
7. 85% $ZnCl_2$	10	180	1	1	3.5	NF
8. Aerated Water + 875 ppm NaCl*	56	260	--	--	56	NF

NF = No failure at end of test;-- = Not tested, * = Autoclave tests, weekly inspection of specimens.

Some of the U.S. high nickel candidate container alloys listed in Table 3.12 have been previously evaluated for resistance to a 3.5% NaCl solution with a pH between 6.8-7.2.[87] In particular, iron based 20Cb-3 and Multiphase MP35N containing 35% Ni and 35% Co were compared in their SCC behavior to a range of other engineering alloys. The materials were exposed at ambient temperature to the solution under alternate wetting and drying conditions. It was found that MP35N and 20-Cb3 were highly resistant to failure, as were Inconel 718 and Unitemp L-605. On the other hand, martensitic stainless steels and 18% Ni maraging steels were susceptible to SCC for specific test conditions. The 4130 carbon steel (also a U.S. candidate container alloy) was susceptible to both general corrosion and SCC.

An important factor which must also be considered in many high nickel alloys is the possibility of sensitization phenomena such as those occurring in austenitic stainless steels. Of the U.S. canister candidate alloys (Table 3.11) Inconel 600 could be sensitized during high temperature exposure in the course of welding or stress-relieving heat treatments.[88]

E. Lead

Lead is an important candidate container material in the Swedish[8] and U.S. program. A literature survey on this material did not reveal any corrosive environment in which SCC occurred.

F. Stress Corrosion Cracking in Non-Chloride Environments

Environments found in salt repositories are possibly the most aggressive that are to be found in candidate host rocks because of their high aqueous chloride concentrations. Groundwaters listed in Tables 3.5 through 3.10 are low in impurity content and, due to the low oxygen contents at great depths below the surface of the earth, it is possible that stress corrosion from the species present will be uncommon. However, if container temperatures are such that water reaching the container wall begins to boil, it is possible that this could give rise to a solute concentration mechanism. Much higher values of water impurities could then prevail in the vicinity of the metal surface. In addition, if an overpack or backfill material is in contact with the container, crevice regions would be formed in which accelerated corrosion could be induced. In concentrated solutions, groundwater constituents such as nitrates,[77] sulfates,[89] and fluorides[90] are known to induce SCC failure in steels. Caustic solutions (NaOH) are also a common source of SCC in austenitic stainless steels.[67,75] Although repository groundwaters do not contain significant quantities of caustic, small quantities are generated by localized corrosion of metal in chloride solutions.[23] Whether this can contribute to the failure process is not clear.

3.4.2.6 Hydrogen Effects

The source of hydrogen in repositories is likely to be a natural consequence of aqueous corrosion, but it may also be generated by the radiolysis of water by gamma irradiation (see Section 5.3.2).

Hydrogen induced cracking is not rare. Many cases of hydrogen induced failure in oil-well brines or in natural gas containing hydrogen sulfide have been reported.[91] Cracking of steel springs during pickling or after electroplating has also been observed.[91]

Fontana[92] classified hydrogen effects into four categories:

1. hydrogen blistering,
2. hydrogen embrittlement,
3. decarburization,
4. hydrogen attack.

Of these, decarburization and hydrogen attack are high-temperature processes. Decarburization refers to the removal of carbon from steel by moist hydrogen at high temperature, which lowers the tensile strength of steel.[92] Hydrogen attack results from the interaction between dissolved hydrogen and components (or impurities) of an alloy at high temperature. Examples are disintegration of oxygen containing copper in the presence of hydrogen (>400°C),[91] and methane (CH_4) bubble formation in carbon steel (>300°C).[93] These two forms of hydrogen effects are not likely to be the problems in HLW repositories.

Hydrogen blistering is caused by the diffusion of hydrogen atoms into a void, as shown in schematic illustration in Figure 3.13. The equilibrium pressure of molecular hydrogen in contact with atomic hydrogen is several hundred thousand atmospheres, which is sufficient to rupture any known engineering material.[92] Metals reported to show hydrogen blistering include steels, OFHC Cu,* Ni, Al, and Mg.

The exact mechanism of hydrogen embrittlement is not known. It is believed that hydrogen embrittlement for titanium and other hydride-forming metals is caused by the formation of brittle hydrides. For other metals that show hydrogen embrittlement, another proposed mechanism is that adsorbed hydrogen reduces the surface energy of the metal at imperfections at the crack tip and makes the cracking easier.[94]

Fidelle et al.[95] summarized the mechanisms of hydrogen embrittlement as shown in Table 3.40.

There usually exists a delay time for the hydrogen embrittlement after the stress is applied. Delay in fracture results because of the time required for hydrogen to diffuse to specific areas near a crack nucleus until the concentration reaches a damaging level.[91] Figure 3.14 shows the relationship between delayed fracture times and minimum stress for cracking of 6.4% C steel as a function of hydrogen content.

Hydrogen embrittlement has been identified for candidate materials such as Types 304 and 304L stainless steel[96,97] and titanium.[98] A complete review on the effects of hydrogen on properties of iron and steel was published by Hirth[99] recently.

In evaluating the KBS I Swedish plan (6 mm Ti container with 100 mm Pb lining), Mattsson[32] considered the delayed failure of Ti as follows: "... the risk of delayed fracture is also judged to be very small, but this type of failure cannot be fully excluded. So, to be very conservative, the titanium sheath has not been ascribed any appreciable life..." This statement shows that delayed failure caused by hydrogen is the main concern over the service life of Ti or Ti alloy containers. Appendix B analyzes some of the concerns of a Swedish Panel member who believes delayed failure in titanium is a problem.

The delayed fracture of pure titanium and its alloys has been studied by many researchers.[100-103] Recently Archbold and Palonis[104] reviewed this subject extensively under the sponsorship of DOE. The most important parameters regarding the dalayed fracture are hydrogen content, temperature and applied stress. It is generally believed that hydrogen tends to migrate to regions of high stress intensity when applied stress and/or residual stress exist. A brittle hydride phase will precipitate when the hydrogen content at the high stress intensity region exceeds the solubility limit, and this will facilitate cracking.

---

*Oxygen free high conductivity copper.

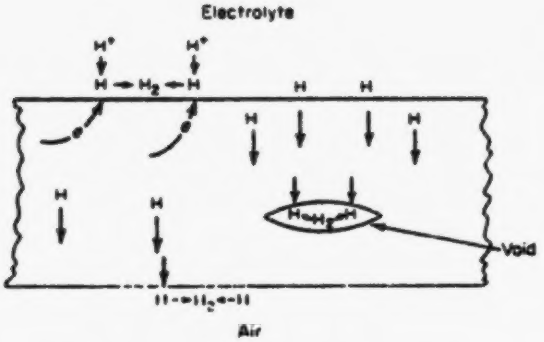
Electrolyte
H+
H+
H → H2 ← H
H
H
H
H
H
H
H
H → H2 ← H
Void
H → H2 ← H
Air

Figure 3.13 Schematic illustration showing the mechanism of hydrogen blistering.[92]

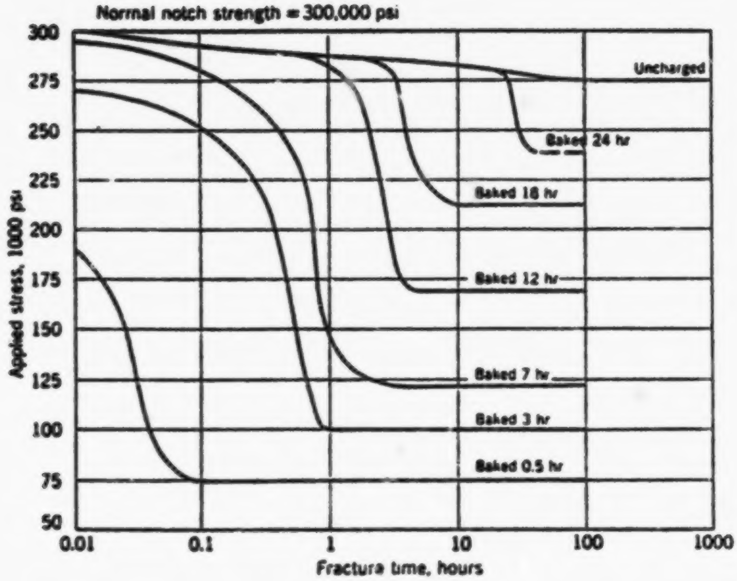

Figure 3.14 Delayed fracture times and minimum stress for cracking of 0.4% C steel as a function of hydrogen content. Specimen initially charged cathodically, baked at 150°C for varying times to reduce hydrogen content (Johnson et al.[91])

BEST DOCUMENT AVAILABLE

Table 3.40

General Mechanisms of Hydrogen-Enhanced Cracking of Metals (Modified from Fidelle, Brouduer and Clauss)[95]

	Behavior of Hydrogen	State of Embrittling Hydrogen	Examples of Affected Metals
Embrittlement by hydrides.	Hydrogen reacts with elements in the metal matrix producing hydride precipitates.	MH_x hydride platelets at the grain boundaries or dispersed within the grains.	Alloys of MgZr, MgTh, certain steels?
	Hydrogen reacts with the metal matrix itself producing hydrides.		α-Ti, Zr, Hf, U, Pu, Th, ... Rare earths, alkaline metals, Cr, Mn, Ni, Pd, V, Nb, Ta, ...
"True" hydrogen-enhancement of cracking.	Adsorbed hydrogen reduces the surface energy of the metal and facilitates cracking.	Surface-adsorbed hydrogen.	V, Nb, Ta charged with O or N, steels, Al alloys, solders Mg, W, Mo? U-Mo alloys?
	Hydrogen affects the chemical bonds of the metal atoms, producing decohesion at a lower stress.	Hydrogen dissolved in the metal.	Fe, steels, α-Ti, β-Ti, Ni, ... Mg-Al-ZnMn and Mg-Li alloys, V, Nb, Ta, ... Mo, W?
	Hydrogen interacts with crystal defects (dislocations, vacancies, etc.).		

Hydrogen embrittlement of Ti may be classified into two different types, impact embrittlement and low-strain-rate embrittlement.[100] Impact embrittlement is caused by the hydride phase already existing in the alloy before stress is applied. When the alloy is annealed in a hydrogen contaminated environment and cooled, hydride forms because of the decreased solubility. Impact embrittlement is generally observed in α alloys with hcp structure. Low-strain-rate embrittlement is observed during straining at low rates. Above mentioned strain induced hydride formation at the crack tip is generally believed to cause this. Hydrogen contaminated α / β alloys usually show this, but they do not show impact embrittlement.[100]

Hydrogen solubility in α phase Ti alloys is believed to be lower than that in β phase.[104] In pure Ti (α phase) hydride forms at hydrogen concentrations above about 20 ppm at room temperature. This solubility difference between phase and α/ β phase alloys probably causes the different types of hydrogen embrittlement.

Although information on hydrogen embrittlement on pure Ti and other α / β alloys is available, the experimental data for TiCode-12 are sparse. Hydrogen embrittlement of Ti and TiCode-12 should be studied in conjunction with radiation effects since these metals are the primary candidate materials for HLW containers.

3.5 Assessment of Container Durability from Archeological Data

The NRC criterion that a high level waste package contain the radioactivity for the first 1000 years after emplacement can be met if the container maintains its integrity over this period of time. Unfortunately, no laboratory test can hope to simulate this time frame, and accelerated tests present problems in extrapolation of data to the long term. One way in which long term corrosion behavior can be estimated for metals centers is the examination of archeological metal artifacts, some of which have been exposed to atmospheric and subterranean environments for millenia. Although these alone will not prove that a container can exist for 1000 years without failure, such studies can indicate whether the development of metal container technology is likely to be a fruitful procedure.

A recent paper by Johnson and Francis[105] summarizes some available archeological data (Table 3.41). Noble metals such as gold, silver, and copper have existed for millenia under environmental conditions of air and water and have not been destroyed. Tylecote 106 has shown that lead and copper base metals have survived in seawater for periods of up to, and beyond, 1000 years without destruction. Most readers are also aware of situations in which gold and silver coins have been recovered from Spanish galleons submerged in the ocean for hundreds of years and also Roman coins which have been buried for almost 2000 years in moist soils in Europe. Meteorites composed of Fe - Ni alloys have also existed on the earth's surface for geological times and still maintained their integrity.[105] Evans[41] also cites a case in which iron nails buried about AD 79 at Perthshire, Scotland, in clean beaten earth under oxygen-free conditions were recently retrieved. Most were unrusted 1870 years later, although some showed

Table 3.41

Examples of Metal Archeological Artifacts[105]

Artifact	Location	Date-BC	Remarks
Copper beads	Catal Huyuk (Turkey)	7000-6500	
Copper pin	Sialk (Iran)	4500	Worked; relatively good condition
Gold jewelry	Varna (Bulgaria)	3500	
Smelted copper	Near Ur (Iraq)	3400	
Sumer bronze objects	Brak (Syria)	3000	
Copper tools	Egypt	2900	First copper found in tombs.
Silver vase on copper stand	Lagash (Iraq)	2800	
Tin bracelet	Thermi (Lesbos)	2700-2500	Oldest tin artifact.
Iron dagger, bracelet, head rest, miniature tools	King Tutankhamen tomb	1350	May be oldest man-made iron articles.
		Date-AD	
Iron pillar	Delhi, India	400	

general corrosion and others deep pitting.[23] He also describes American studies of pilings driven into the earth which created a closely compressed soil around the metal. Although air was probably restricted, it would be anticipated that sulfate-reducing bacteria could release free oxygen and initiate a corrosion process. Since little corrosion was detected it was concluded that for the situation evaluated the effect of sulfate-reducing bacteria was very small.

All of the above studies, then, may be taken as encouraging signs that a high integrity container can be designed for the geologic isolation of high level waste. At least, the evidence indicates that in oxygen deficient dry regions, many classes of metals and alloys can be used successfully for long term container designs. In the absence of definitive corrosion data it will be necessary to design very conservatively and greatly overestimate the required container wall thickness. In addition, combinations of many metals may be used for multi-layered structures so that all of the main corrosive species can be combated by a particular metal component. The effects of irradiation and internal corrosion from the waste form must, of course, also be addressed since they could have a large influence over periods of hundreds of years. Nevertheless, the development of a 1000 year container does not appear to be an insuperable problem.

3.6 Non-Metallic Materials

Several studies have been carried out on non-metallic container materials in order to avoid the type of localized corrosin problems that can destroy the integrity of metals. Braithwaite and Molecke[4] drew attention to a program at Battelle Pacific Northwest Laboratory which was evaluating ceramic and polymer coatings on titanium-based and nickel-based alloys. For unreprocessed spent fuel the Swedes are considering the use of a high purity alumina canister prepared by sintering under isostatic pressure.[32] They anticipate that it will have a wall thickness of 10 cm and be essentially free of pores and grain boundary impurities. It will be sealed by sintering a cap onto the structure.

Some recent work on a Corning glass-ceramic (Code 9617) for storage of spent fuel showed it to have a corrosion rate of 0.013 cm/1000 years when stored in a granite repository at an initial temperature of 110°C.[107] This work was part of the Swedish program to develop a long life container. PNL[108] conducted leach tests on 16 ceramic materials in demineralized water, a synthetic Hanford groundwater, and a synthetic brine solution. Based on the experimental results, other necessary properties and cost considerations, they recommended graphite as a primary choice and alumina as the second choice.

In summary, non-metallic containers are likely to be highly resistant to corrosion, but there is the distinct possibility that fracture could easily occur from rock overburdens and/or seismic activity. The lack of impact resistance may also be a problem during transportation. Further studies in this area are warranted.

3.7 Strength and Ductility Requirements for Containers

These properties have an important bearing on the integrity of waste containers since transportation accidents and repository overburdens can cause low ductility materials to fracture. Containers will be subjected to high thermal stress during in-can melting procedures and during welding. Metallic materials usually have the strength and ductility needed, while ceramic materials generally have low impact resistance. For these reasons, more emphasis is put on metallic materials in selecting optimum container materials.

For the material selection and the engineering design after the material selection, mechanical properties such as tensile strength and fracture toughness should be studied.

PNL[109] conducted the following tests on pure Ti and TiCode-12:

tensile tests,

fatigue-crack-growth rate tests (air),

fracture toughness (static),

dynamic fracture toughness and impact toughness,

stress corrosion cracking.

For the experimental methods used, refer to Task 4 report.[110] Some of the conclusions from this study are quoted as follows:

1. The mechanical properties of Grade 2 titanium (pure Ti) are better than those of Grade 12 titanium (TiCode-12), except for the tensile and yield strengths. These properties include fatigue-crack-growth rate, environmental fatigue-crack-growth rate, fracture toughness, impact toughness, and dynamic fracture toughness.

2. Both alloys have lower toughness and crack-growth resistance in the longitudinal orientation than in the transverse orientation.

In the PNL study the testing of fatigue properties was not fully justified. They indicated that more materials will be tested depending on the materials selection from corrosion resistance study. We recommend that realistic containers should be fabricated with several prospective materials and the mechanical strength tests including impact testing should be conducted to evaluate the materials behavior.

3.8 Weldability and Fabricability of Containers

A highly corrosion resistant container material is of little value if it cannot be efficiently fabricated into the required shapes and sizes. If a metal cannot be sealed by regular welding techniques, or if welds are likely to possess poor integrity in repository environments, it will limit a material's usefulness.

Recently in their report, Archbold and Polonis[104] reviewed literature on the weldability of titanium and its alloys. Welding of Ti and Ti-alloy has not been as easy as other common metals such as carbon steel. Some problems are encountered in the welding procedure.[104] The absorption of oxygen, nitrogen, carbon, and hydrogen by weldments causes severe embrittlement of the welds. The presence of an oxide layer on the base metal is a potential embrittlement source. Thus, to eliminate these problems, all welding is performed in a vacuum or in an argon atmosphere, and the oxide layer is removed by an auto-vacuuming procedure[111] or by cold working.

In the Heat Affected Zone, for pure Ti, a large amount of brittle α' martensite will be found, and proper annealing treatments after welding is needed.[104] They concluded that the weldability of unalloyed Ti, near α and even α/β alloys is satisfactory if the proper procedures are followed. The weldability and weld structures of the candidate titanium alloys (pure Ti, TiCode-12) should be studied more extensively in connection with the HLW container investigations.

3.9 Conclusions

- In the sections above, HLW container research and other programs have been reviewed and discussed. General conclusions and specific recommendations are presented in the following sections.

- In the U.S., a range of metallic container materials has been screen-tested by Sandia National Laboratory and Pacific Northwest Laboratory (PNL). Sandia and PNL have been evaluating the candidate metals mainly under bedded salt repository and basalt repository conditions, respectively.

- Sandia selected pure titanium, Ticode-12 and Ti-Pd based on the screen-test results, and conducted further studies on these metals. Pure titanium showed crevice corrosion at 250°C in brine solutions. As a result, Sandia concluded that pure titanium is unacceptable as a container material. Further investigation of Ticode-12 is under way.

- PNL has not yet selected any metals for further studies after the screen-tests on corrosion properties of candidate metals. It is believed that their corrosion study is still in progress. However, a separate program at PNL studied the mechanical properties of pure Ti and TiCode-12, which were chosen on the basis of Sandia's results. The general mechanical properties of pure Ti were superior to those of TiCode-12.

- As for the overseas programs, the Swedish plans give the only completed designs, which were considered sound by American and Swedish scientists. A titanium container with a wall thickness of 6 mm and 100 mm thick lead lining, KBS I Plan, has been proposed for reprocessed and vitrified waste. For unprocessed spent fuel rods, a copper container with at least 200 mm thick walls, KBS II Plan, has been proposed. Since the

Swedish material selection and design are based on a granite repository, these proposed waste packages should not be considered ideal for U.S. design. In fact, BNL does not recommend copper or lead for a bedded salt repository because of their high general corrosion rates in brine solutions.

- So far, TiCode-12 is the only material that has been recommended by Sandia to meet the 1000 year containment criterion in a bedded salt repository. BNL believes that this material will probably meet the criterion if it is shown that hydrogen effects will not be a serious problem. The Sandia recommendation is based on the expected maximum container surface temperature of 250°C. However, if the thermal loading in the repository is adjusted such that the surface temperature is far below 250°C (e.g., 100°C), it is possible that more materials will qualify. In short, it should be better to have alternatives than having only one recommended metal. For these reasons, other metals besides TiCode-12 were studied and discussed in this Report. It is very clear from the experimental data reviewed that salt represents a much more aggressive environment than granite, basalt, or shale, etc. Hence from the standpoint of container corrosion, hard rock repositories are to be desired.

- One major problem which needs to be addressed is the assessment of container integrity over periods of hundreds or thousands of years. Analyses of metallic artifacts from archeological excavations are helpful since it clearly reveals that under certain conditions, some of which are more aggressive than those in anticipated repository environments, many metals remain essentially intact after subterranean or subsea burial for hundreds or thousands of years. Even iron has been shown to remain without serious corrosion after 1500-2400 years in selected environments. Based on their proven long term corrosion resistance it seems reasonable that these metals, either singly or in combination, and in sufficient thicknesses to decrease stress levels and to increase the time for corrosion penetration, could withstand breaching by the low oxygen groundwaters to be found in hard rock repositories for at least a 1000 year period. If so, the NRC containment criterion for this time span can be met. Synergistic effects from the waste form or backfill materials, however, could conceivably influence container corrosion rates and these will have to be evaluated before the lifetime of the container can be estimated and experimentally verified. Nevertheless, a 1000 year container appears to be clearly achievable.

3.10 Recommendations

- From the standpoint of container corrosion, hard rock repository environments are recommended.

- Candidate container materials should be tested for extended times (ideally for periods up to the time of repository operations) to determine whether localized attack such as pitting, crevice corrosion, and stress corrosion cracking can occur. Such long term tests do not appear to be included in current DOE efforts.

- Additional less expensive materials than Ti and its alloys or copper should also be evaluated for corrosion resistance since they may be required to provide sufficient strength to minimize compressive stresses on the waste form in the repository.

- The corrosion of welded material must be studied together with the base materials. Weld structures are often very different from base metal and as such could be more susceptible to failure. Evaluation of SCC, pitting, and corrosion of welds of all the candidate metals listed above should be carried out.

- The radiolysis of groundwaters by gamma irradiation can cause hydrogen interaction with metals which could cause loss of ductility. These effects must be studied for candidate materials.

- Interactions between the container materials and the waste form, filler materials and backfill materials should be studied. Groundwaters passing through the backfill could suffer a change in impurity concentration. Conceivably, this could have an effect on the corrosion behavior of the container; hence, evaluation is warranted.

- The backfill materials will be in contact with the container and could give rise to the formation of numerous crevice regions in which groundwater could remain in a stagnant condition. The possible occurrence of crevice corrosion should be determined by conducting corrosion tests on stressed and unstressed samples which are placed in intimate contact with candidate backfill materials. Long duration tests are required to determine if such a corrosion mechanism is likely.

- Multiple container designs with suitable filler materials should be studied since it can lead to prolonged life because of the necessity to repeat the induction and propagation of different forms of corrosion that could occur. In addition, several different metals could be selected, each to combat different corrosive species in the groundwaters. Sacrificial metals could also be induced.

- Due to the interest in extraordinarily corrosion resistant materials, accelerated tests might be inevitable. New accelerated test methods and new ways to interpret the data from the accelerated tests should be developed so that the extrapolation of the test results to non-accelerated condition and to geologic time can be justified. Ideally, both accelerated and non-accelerated tests should be conducted simultaneously to be able to correlate accelerated test results with actual corrosion behavior.

- Mechanical strength tests including impact testing should be conducted on containers fabricated with candidate materials to evaluate the material's behavior.

3.11 References

1. T. E. Scott, "Issues Relevant to Nuclear Waste Canister Materials", in Corrosion/80, NACE, Paper #210, Proc. of Conference held March 1980, Chicago.

2. L. A. Casey (Ed.), "High Level Radioactive Solid Waste Forms", NUREG/CP-0005, 1978.[1]

3. "The Evaluation and Review of Alternate Waste Forms for Immobilization of High Level Radioactive Wastes", DOE/TIC-10228, August 1979. Available from Office of Nuclear Waste Management, DOE, Washington, DC.

4. J. W. Braithwaite and M. A. Molecke, "Nuclear Waste Canister Corrosion Studies Pertinent to Geologic Isolation", Nuc. and Chem. Waste, 1, 1980.

5. J. W. Braithwaite, N. J. Magnani, and J. W. Munford, "Titanium Alloy Corrosion in Nuclear Waste Environments", in Corrosion/80, NACE, Paper #213, Proc. of Conference held March 1980, Chicago.

6. Scientific Basis for Nuclear Waste Management, Proc. of Int'l. Conf. Sponsored by Materials Research Society, held in Boston, MA, November 1979, to be published.

7. Code of Federal Regulations, 10CFR60, "Disposal of High Level Radioactive Wastes in Geologic Repositories", (Proposed), Advance notice of proposed rulemaking.

8. P. E. Ahlstrom, "Treatment of High Level Waste and Spent Fuel for Final Disposal--The Proposed KBS Plan", in Waste Management '79, R. G. Post (Ed.), Published by Univ. of Arizona and Arizona Atomic Energy Commission, 1979, pp. 245-262.

9. L. E. J. Roberts, "Radioactive Waste: Policy and Perspectives"; lecture delivered to the British Nuclear Energy Society, London, November 1978.

10. "Report to the President by the Interagency Review Group on Nuclear Waste Management", TID-28817 (Draft), October 1978, Appendix G.[1]

11. C. G. Sombret, R. A. Bonniaud, and A. F. Jouan, "Status of the French AVM Vitrification Facility", in Waste Management '79, R. G. Post (Ed.), Published by Univ. of Arizona and Arizona Atomic Energy Commission, 1979, pp 263-294.

---

[1] Available from the National Technical Information Service, Springfield, VA 12161.

12. D. J. Cameron and G. G. Strathdee, "Materials Aspects of Nuclear Waste Disposal in Canada", in *Ceramics in Nuclear Waste Management*, Published by U.S. Tech. Information Center, DOE, 1979, pp. 4-8.[1]

13. N. E. Brezneva, A. A. Minaev, and S. N. Oziraner, "Vitrification of High Sodium-Aluminum Wastes", in *Scientific Basis for Nuclear Waste Management, Vol. 1*, Plenum Press, NY, 1979, pp 43-50.

14. "Management of Commercially Generated Radioactive Waste, Vol. 1", DOE/EIS-0046D, April 1979. Available from Office of Nuclear Waste Isolation", Battelle Columbus Laboratory, Columbus, OH.

15. H. C. Claiborne, L. D. Rickertsen, and R. H. Graham, *Expected Environments in High Level Nuclear Waste and Spent Fuel Repositories in Salt*, ORNL/TM-7201, Oak Ridge National Laboratory, Oak Ridge, TN, August 1980.

16. M. G. Fontana and N. D. Greene, *Corrosion Engineering*, Second Edition, McGraw-Hill Book Company, 1978.

17. W. E. Clark, D. N. Hess, P. D. Neumann, L. Rice, and J. L. English, "Laboratory Development of Processes for Fixation of High Level Radioactive Wastes in Glassy Solids (4) Corrosion Studies on Candidate Materials of Construction", ORNL-3816, August 1967.

18. T. M. Kegley, Jr. and F. M. Empson, "Examination of Modified Pillar and Simulated Waste Container Test Heaters", ORNL-TM-2422, January 1969.

19. R. L. Bradshaw and W. C. McClain (Eds.), "Project Salt Vault: A Demonstration of the Disposal of High Activity Solidified Wastes in Underground Salt Mines", ORNL-4555, April 1971.

20. W. N. Rankin, "Canister Compatibility with Carlsbad Salt", in *Corrosion/80*, NACE, Paper #212, Proc. of Conference held March 1980, Chicago.

21. M. Molecke and L. Abrego, "Status of Sandia HLW Canister/Overpack Program Studies", SAND 80-2191C, UC-70, Sandia National Laboratory, December 1980.

22. F. Casteels, H. Tas, J. Naets, M. Brabers, and J. Kelchtermans, "Corrosion of Canister Materials in a Clay Environment", *Scientific Basis for Nuclear Waste Management*, Proc. of Int'l. Conf. Sponsored by Materials Research Society, held in Boston, MA, November 1979, to be published.

23. U. R. Evans, *An Introduction to Metallic Corrosion*, E. Arnold (Publishers), Ltd., London 1975.

24. B. C. Syrett, D. D. MacDonald, and H. Shih, "Pitting Resistance of Engineering Materials in Geothermal Brines,--I. Low Salinity Brine", Corrosion, 3, *36*, 1980.

25. D. W. Shannon, "The Role of Chemical Components in Geothermal Brines on Corrosion", Paper 57, presented at Corrosion '78, NACE, Houston, TX, March 1978.

26. R. B. Davis and Z. A. Munir, "Corrosion Susceptibilities of Various Metals and Alloys in Synthetic Geothermal Brines", J. Mat. Sci., 12, 1977, pp. 1909-1913.

27. J. P. Carter and F. X. McCawley, "In-Situ Corrosion Tests in Salton Sea Geothermal Brine Environments", J. Met., 3, 1978, pp. 11-15.

28. S. Henrikson and M. Pourbaix, "Corrosion Testing of Unalloyed Titanium in Simulated Disposal Environments for Reprocessed Nuclear Waste", KBS Technical Report, KBS-tr-96, Karnsbarnslesakerhet Fack, Stockholm, April 1978.

29. R. W. Westerman, "Investigation of Metallic, Ceramic, and Polymeric Materials for Engineered Barrier Applications in Nuclear-Waste Packages", PNL-3864, UC-70, Pacific Northwest Laboratory, p. 47, October 1980.

30. W. J. Anderson, "Corrosion Tests of Canister and Overpack Materials in Simulated Basalt Groundwater", presented at the ANS Topical Meeting on Waste Management '81, Tucson, AZ, February 1981.

31. Commission of the European Communities, Nuclear Science and Technology, Second Annual Progress Report, p. 7, 1978.

32. E. Mattsson, "Corrosion Resistance of Canisters for Final Disposal of Spent Nuclear Fuel", in Scientific Basis for Nuclear Waste Management, Vol. 1, Plenum Press, NY, 1978, pp. 271-281.

33. L. L. Shreir, Corrosion, Metal/Environment Reactions, L. L. Shreir, Ed., Vol. 1, p. 182, Newness-Butterworths, Boston, MA, 1976.

34. S. Szklarska-Smialowska, "Various Forms of Corrosion in Iron and Steel: Common Features and Differences", Brit. Corrosion J., 10, 1975, pp. 11-16.

35. M. G. Fontana and N. D. Greene, Corrosion Engineering, Second Edition p. 51, McGraw-Hill Book Company, 1978.

36. M. Pourbaix, "The Electrochemical Basis for Localized Corrosion", Localized Corrosion, NACE-3, Ed., Staehle et al., NACE, p. 15, 1974.

37. J. G. Parr and A. Hanson, An Introduction to Stainless Steel, American Soc. for Metals, OH, 1965.

38. H. H. Lawson, S. E. Doughty, and R. T. Jones, "Evaluating Materials Performance in a 3000 - GPD Stainless Steel Desalination Test Plant", Materials Performance, 13, 1974, pp. 11-16.

39. A. J. Sedriks, Corrosion of Stainless Steel, p. 82, John Wiley and Sons, NY, 1979.

40. H. Campbell, "Pitting Corrosion of Copper and its Alloys", Localized Corrosion, NACE-3, Eds. Staehle et al., NACE, p. 625, 1974.

41. U. R. Evans, The Corrosion and Oxidation of Metals, p. 125, St. Martin's Press Inc., NY, 1960.

42. H. H. Ulig, Corrosion and Corrosion Control, Second Edition, p. 14, John Wiley and Sons, Inc., 1971.

43. J. A. Denison and M. Romanoff, "Solid Corrosion Studies, 1946 and 1948: Copper Alloys, Lead and Zinc", J. Res. NBS, 44:259, 1950.

44. "Titanium Heat Exchangers for Service in Sea Water, Brine, and other Aqueous Environments", Titanium Inf. Bull. from IMI, Birmingham, 1976.

45. T. R. Beck, "Pitting Attack of Titanium Alloys", Localized Corrosion, NACE-3, Eds, Staehle et al., NACE, p. 646, 1974.

46. R. E. Niederberger, R. J. Ferrara, and F. A. Plummer, Mater. Protection and Performance, 9(8), 18 (1970), cited by ref. 59 on pg. 310.

47. E. A. Lizlovs, "Crevice Corrosion of some High Purity Ferritic Stainless Steels", in Localized Corrosion-Cause of Metal Failure, ASTM Spec. Tech. Public. No. 516, 1972, pp. 201-209.

48. R. J. Bringham, "Temperature as a Crevice Corrosion Criterion", Corrosion, 30, 1974, pp. 396-398.

49. O. B. Ellis and F. L. LaQue, Corrosion, 7, 11, 362 (1950).

50. M. M. Peterson, Z. I. Lennox, and R. E. Groever, Materials Protection, 9, 1, 23 (1970).

51. L. W. Gleekman, Chem. Eng. 70, 1963, pp. 217-224.

52. R. S. Sheppard, D. R. Hise, P. G. Gegner, and W. L. Wilson, Corrosion, 18, 1962, pp. 211t-218t.

53. J. M. Turbull, Corrosion 16, 1960, pp. 11-16.

54. E. G. Bohlmann and F. A. Posey, Proceeding of the First Int'l. Symposium in Water Desalination, Washington, DC, Vol. 1, pp. 306-325.

55. J. C. Greiss, "Crevice Corrosion of Titanium in Aqueous Salt Solutions", Corrosion, 24, 1968, p. 96.

56. T. Shimose and A. Takamura, J. Jap. Inst. Metals, 29, 1965, pp 416-421.

57. Metals Handbook, Vol. 3, Ninth Edition ASM, Metals Park, OH, 1980, p. 381.

58. Huntington Alloys, Inc., "Huntington Alloys - Resistance to Corrosion," Bulletin S-37, 1970.

59. W. Z. Friend, *Corrosion of Nickel and Nickel-Base Alloys*, John Wiley and Sons, NY, 1980, p. 312.

60. F. W. Fink and W. K. Boyd, "Corrosion of Metals in Marine Environments," DMIC Report 245, Defense Metals Information Center, Battelle Memorial Inst., 1970.

61. A. P. Bond, J. D. Marshall, and H. J. Dundas, "Resistance of Ferritic Stainless Steels to Stress Corrosion Cracking", in *Stress Corrosion Testing*, ASTM Spec. Tech. Public. No. 425, Amer. Soc. for Testing and Mat., 1967, pp. 116-126.

62. A. P. Bond and H. J. Dundas, "Effects of Composition on the Stress Corrosion Cracking of Ferritic Stainless Steels".

63. M. A. Scheil, "Some Observations of Stress Corrosion Cracking in Austenitic Stainless Alloys", *Symposium on Stress Corrosion Cracking of Metals*, Amer. Soc. for Testing and Mat., 1945, pp. 395-410.

64. M. A. Scheil, et al., "First Report on Stress Corrosion cracking of Stainless Steel in Chloride Solutions", Supp., J. of the Amer. Welding Soc., October 1943, pp. 4935-5045.

65. P. Lillys and A. E. Nehrenberg, "Effect of Tempering Temperature on Stress Corrosion Cracking and Hydrogen Embrittlement of Martensitic Stainless Steels", Trans. A.S.M., 48, 1956, pp. 327-355.

66. D. Warren, "Chloride Bearing Cooling Water and the Stress Corrosion Cracking of Austenitic Stainless Steel", *Proc. of the 15th Industrial Waste Conference*, Purdue Univ., 1960, pp. 420-438.

67. W. L. Williams, "Chlorides and Caustic Stress Corrosion of Austenitic Stainless Steels in Hot Water and Steam", Corrosion, 13, 1957, p. 539t.

68. H. Kohl, "A Contribution to the Examination of Stress Corrosion Cracking of Austenitic Stainless Steels in Magnesium Chloride", Corrosion, 23, 1967, p. 39.

69. T. P. Hoar and J. G. Hines, "The Stress Corrosion Cracking of Austenitic Stainless Steels", J. Iron and Steel Inst., 182, 1956, p. 124.

70. A. S. Couper, "Testing Austenitic Stainless Steels for Modern Refinery Applications", Materials Protection, 8, 1968, p. 17.

71. D. Birchon and G. C. Boothe, *Stress Corrosion Cracking and Embrittlement*, D. W. Robertson (Ed.), J. Wiley and Sons, 1956, p. 32.

72. E. E. Denhard, "Effect of Composition and Heat Treatment on the Stress Corrosion Cracking of Austenitic Stainless Steels", Corrosion, 16, 1960, p. 359t.

73. J. M. A. Van Der Horst, "Corrosion Cracking of Stainless Steels by Thermal Gradient Stresses", Corrosion Science, 11, 1971, pp. 885-887.

74. C. M. Rosendahl, "Welding of Austenitic Stainless Steel", Svet-Saren Esab., No. 1-2, 1969.

75. R. M. Latanision and R. W. Staehle, "Stress Corrosion Cracking of Iron-Nickel-Chromium Alloys", in Fundamental Aspects of Stress Corrosion Cracking, NACE, 1969, pp. 214-296.

76. R. W. Staehle, J. J. Royuela, T. L. Raredon, E. Serrate, C. R. Morin, and R. V. Farrar, "Effect of Alloy Composition on Stress Corrosion Cracking of Fe-Cr-Ni Base Alloys", Corrosion, 26, 1970, pp. 451-486.

77. H. L. Logan, The Stress Corrosion of Metals, J. Wiley and Sons, NY, 1966, Chapter 5.

78. H. H. Uhlig, Corrosion and Corrosion Control, Second Edition, p. 323, John Wiley and Sons, Inc., 1971.

79. A Review of the Swedish KBS-II Plan for Disposal of Spent Nuclear Fuel, National Academy of Sciences, Washington, DC, 1980.

80. Stress Corrosion Cracking of Titanium, ASTM Spec. Tech. Public. No. 397, 1966, Amer. Soc. for Testing and Materials, Philadelphia.

81. I. R. Lane, Jr., J. L. Cavallaro, and A. G. S. Morton, "Seawater Embrittlement of Titanium", ibid., pp. 246-258.

82. D. T. Powell and J. C. Scully, "Stress Corrosion Cracking of Alpha Titanium Alloys at Room Temperature", Corrosion, 24, 1968, pp. 151-158.

83. G. Sanderson and J. C. Scully, "Stress Corrosion of Titanium Alloys in Aqueous Magnesium Chloride Solution at 154°C, Corrosion, 24, 1968, pp. 75-81.

84. K. Mori, A. Takamura, and S. Takaaki, "Stress Corrosion Cracking of Ti and Zr in HCl-Methanol Solutions", Corrosion, 22, 1966, p. 29.

85. H. R. Copson, Principal Metallurgy of Stress Corrosion Fracture, Interscience, NY, 1959.

86. A. J. Sedriks, "Comparative Stress Corrosion Cracking Behavior of Austenitic Iron-Base and Nickel-Base Alloys", Corrosion, 31, 1975, p. 339.

87. E. E. Nelson, "Stress Corrosion Cracking of Several High Strength Ferrous and Nickel Alloys", NASA TM X-64626, November 1971.[1]

88. R. G. Aspden, G. Economy, F. W. Pement, and I. L. Wilson, "Relationship Between Magnetic Properties, Sensitization, and Corrosion of Incoloy Alloy 800", Metall. Trans., 3, 1972, pp. 2691-2697.

89. D. A. Vermilyea, "Stress Corrosion Cracking of Iron and Nickel Base Alloys in Sulfate Solutions at 289°C, Corrosion 29, 1973, pp. 442-448.

90. C. T. Ward, D. L. Mathis, and R. W. Staehle, "Intergranular Attack of Sensitized Austenitic Stainless Steel by Water Containing Fluoride Ions", Corrosion, 25, 1969, pp. 394-396.

91. H. H. Uhlig, Corrosion and Corrosion Control, Second Edition, p. 42 John Wiley and Sons, Inc., 1971.

92. M. G. Fontana and N. D. Greene, Corrosion Engineering, Second Edition, p. 111, McGraw-Hill Book Company, 1978.

93. P. G. Shewman, "Hydrogen Attack of Carbon Steel", Proceedings of an Int'l. Conf. on Effect of Hydrogen on Behavior of Materials, Jackson Lake Lodge, Moran, WY, Sept. 1975, Eds. A. W. Thomson and Z. M. Bernstein, Metallurgical Society of AIME.

94. N. Petch and P. Stables, Nature, 169, 842 (1952).

95. J. P. Fiddelle, R. Broudeur, and A. Clauss, "Influence of Gaseous Additions on the Effects of Hydrogen Isotopes on Metals", in Hydrogen in Metals, Published by AEC Research Center, Bruyeres-le-Chatel, France, 1969, pp. 324-354.

96. A. A. Seys, M. J. Brabers, and A. A. Van Haute, "Analysis of the Influence of Hydrogen on Pitting Corrosion and Stress Corrosion of Austenitic Stainless Steel in Chloride Environment", Corrosion, 30, 1974, pp. 47-52.

97. M. L. Holzworth, "Hydrogen Embrittlement of Type 304L Stainless Steel", Corrosion, 25, 1969, pp. 107-115.

98. L. C. Corrington, "The Influence of Surface Condition and Environment on the Hydriding of Titanium", Corrosion, 35, 1979, pp. 378-382.

99. J. P. Hirth, "Effects of Hydrogen on the Properties of Iron and Steel", Metal. Trans. A, 11A, June 1980, p. 861.

100. D. N. Williams, "The Hydrogen Embrittlement of Ti Alloys", J. Inst. Metals, 9, pp. 147, 1963.

101. H. G. Nelson, D. P. Williams, and J. E. Stein, "Environmental Hydrogen Embrittlement of an Alpha/Beta Titanium Alloy: Effect of Microstructure", Met. Trans. 3, p. 469, 1972.

102. D. A. Meyn, "Effect of Hydrogen on Fracture and Inert-Environment Sustained Load Cracking Resistance of Alpha/Beta Titanium Alloys", Met. Trans., 5, p. 2405, 1974.

103. N. R. Moody and W. W. Gerberich, "Hydrogen Induced Slow Crack Growth in Ti-6Al-6V-2Sn", Met. Trans., 11A, p. 973, 1980.

104. T. F. Archbold and D. H. Polonis, "Assessment of Delayed Failure Modes in Titanium and Titanium Alloys", Final Report, prepared for PNL, Metallurgical Engineering Division, Univ. of Washington, September 1980.

105. A. B. Johnson and B. Francis, "A Perspective of Metal Durability from Ancient Metal Behavior", in Corrosion '80, NACE, Paper #211, Proc. of Conference held March 1980, Chicago.

106. R. F. Tylecote, Durable Materials for Seawater: Archeological Evidence, Brit. Nuc. Fuel Ltd., Report BNFL 314(R), 1977, cited in ref. 105.

107. J. D. Sundquist, "Preliminary Corrosion Test of a Glass-Ceramic Candidate for a Nuclear Waste Canister", in Scientific Basis for Nuclear Waste Management, Vol. 1, Plenum Press, NY, 1979, pp. 389-396.

108. R. W. Westerman, "Investigation of Metallic, Ceramic, and Polymeric Materials for Engineered Barrier Applications in Nuclear-Waste Packages", PNL 3864, UC-70, Pacific Northwest Laboratory, p. 63, October 1980.

109. ibid., p. 17.

110. T. M. Ahn, et al., "NRC Nuclear Waste Management Technical Support in the Development of Nuclear Waste Form Criteria", Task 4 Report, October 1981, (in press).

111. K. H. Holko, "Hot Press and Roll Welding of Ti-6Al-4V with Auto-Vacuum Cleaning", Welding Research Supplement, 39, 1974, pp. 219-S-224-S, cited in ref. 104.

4. EVALUATION OF BACKFILL MATERIALS

Any evaluation of high level radioactive waste packages for the isolation of nuclear wastes in deep, geologic disposal systems must also include an investigation of the effectiveness of backfill barriers. These barriers can not only provide a redundant barrier to radionuclide migration should the waste package be breached, but also can augment the effectiveness of the waste package itself by controlling groundwater flow and conditioning the groundwater so as to reduce the likelihood and rate of waste container corrosion. Furthermore, the current U.S. DOE definition of the waste package includes the backfill as a component while the NRC definition considers only discrete backfill an integral part of the waste package (see Section 1). Thus, this component may be crucial in demonstrating compliance to the proposed NRC regulatory performance criteria for the waste package and/or an underground facility. For these reasons, the properties and the potential of the backfill for nuclear waste isolation must be thoroughly understood.

4.1 Backfill Purposes and Properties

Several groups of researchers have considered the purpose and properties that backfill materials should have to be effective redundant barriers in nuclear waste disposal.[1,2,3,4] Basically, the purposes of backfill are twofold: (1) to assist or enhance the ability of the waste package (as defined by the NRC here and for the rest of this section) to isolate radioactive wastes and (2) to function independently as a barrier to radionuclide migration should failure of the waste package occur. It is envisioned that a backfill can fulfill the first purpose by controlling groundwater ingress and modifying the near-field groundwater chemistry so that the likelihood of waste container corrosion would be reduced. The backfill can fulfill its role as an independent barrier to radionuclide migration by possessing high radionuclide "sorptive" properties, by reducing near field groundwater flow rates thereby mitigating radionuclide transport away from the repository, and by controlling groundwater pH and Eh to keep multivalent radionuclides in their most favorable valence state for sorption.

In order to accomplish the functions outlined above, the backfill must possess appropriate properties. Table 4.1 lists the various functions of a backfill and the properties which they exhibit. It is these properties that are the focus of the research devoted to backfill performance which will be reviewed here. It should be pointed out that these properties are often interdependent, as illustrated in Table 4.1. This should be kept in mind during the following discussion. For example, the reduction of groundwater flow to the waste package and the reduction of radionuclide transport are both dependent upon the permeability of the backfill.

Attributes not explicitly mentioned in Table 4.1 deal with the stability of the backfill in the repository environment. Wheelwright has pointed out that a backfill is required to withstand mechanical stress, high radiation field, above ambient temperature, groundwater flow, and the influence of various groundwater constituents for up to 10^6 years and still be able to function adequately[2]. In this context, backfill must be thermally stable and have adequate thermal conductivity during the thermal period of waste

Table 4.1

Functions and Properties of Backfill Materials

Waste Package Augmentation		
Water Flow Control Support	**Near Field Chemistry Control**	**Mechanical**
Low Permeability	pH Buffering Capacity	Bearing Capacity
High Swelling Pressure Pressure	Eh Buffering Capacity	Swelling
Low Porosity		Shear Strength
		Plasticity
Radionuclide Retardation		
Radionuclide Sorption Control	**Water Flow Control**	**Near Field Chemistry**
Ion Exchange Capacity	Low Permeability	pH Buffering Capacity
Chemisorption	High Swelling Pressure	Eh Buffering Capacity
Precipitation	Low Porosity	

disposal. The backfill must be stable under hydrothermal conditions and be able to withstand alternating wet-dry cycles, which can be expected during early repository flooding, and not crack or fissure thereby allowing groundwater access to the waste package. The backfill should also maintain its physical integrity and radionuclide sorptive properties in the radiation fields to which it will probably be exposed. Finally, the backfill should be compatible with both the host rock and the waste container.

4.2 Candidate Backfill Materials

Given the various functions of backfill, it is no surprise that many materials of divergent characteristics have been suggested for use in nuclear waste repositories. A list of candidate backfill materials is given below in Table 4.2 and while this list is not all inclusive, the principal backfill components have been covered. In light of the multiple demands placed upon backfill, a blend of two or more of the materials will be required to create an effective barrier, each component performing a particular function such as those given in Table 4.1.

In order to create a backfill barrier with low permeability, high swelling pressure, and plasticity, researchers have looked to the expandable clays such as the smectites. Because of their low permeability and their ability to seal fissures, smectites are perhaps the crucial elements in current backfill designs. In addition, the use of clay minerals in backfill provides an additional benefit because their relatively high ion-exchange capacities aid in radionuclide sorption and retardation. Other swelling materials, such as MgO, have also been investigated in the Canadian disposal program.[5] Upon wetting, MgO hydrates and swells by up to 70% over its original volume. The hydrate, brucite, is said to be nearly impervious to water flow.

Various materials have been considered in order to enhance the ion-exchange capacities of the backfill, mainly zeolites because of their high ion-exchange capacities[6,7,8,9] although some clay minerals have also been considered.[2,3,4,10] A list of the cation exchange capacities of some clays and zeolites is given in Table 4.3. Clearly, based upon their ion-exchange capacities, zeolites could be a very useful component in a backfill mixture. Zeolites have even been considered for use as the sole component of a backfill in the Swedish KBS program because of their superior sorptive charactistics.[9] However, preliminary research into the geologic behavior of zeolites indicated that they may tend to cement and can undergo transformation to feldspars, a mineral with particularly low sorptive capacity, under certain conditions of pressure and temperature which could exist in deep geologic burial.[13,14] For these reasons, the Swedes opted for their current compacted bentonite clay reference material. The aforementioned research focused only on a few zeolites such as analcite, phillipsite, chabazite, and clinoptilolite. Recent research into the hydrothermal stability of zeolites has shown favorable results for mordenite zeolite. Since zeolites, as a group, are composed of minerals of a wide range of compositions and properties, any final conclusion as to the efficacy of their use in backfill should be withheld until more complete data are available.

The use of ferrous iron containing minerals has been suggested to buffer

Table 4.2

Candidate Backfill Materials*

Clay Minerals

Bentonite (2,7,16)
Montmorillonite (3,17)
Illite (7)
Kaolinite (17)
Hectorite (17)
Attapulgite (3)

Zeolites

Mordenite (6,8,9)
Clinoptilolite (7,8)
Chabasite (8,9)
Phillipsite(8,9)
Synthetics (7,8)

Rock Materials

Salt, ONWI (18)
Basalt, BWIP (2,7)
Tuff, PNL, LASL (7,17)
Granite, Canada (19)

Ferrous Iron Minerals (3,20-22

Bornite
Pyrite
Biotite
Olivine
Vivianite
Chalcopyrite
Chlorite
Garnet
Magnetite
Siderite

Chemisorbing Minerals(3,20,21,22)

Apatite
Monazite
Vivianite
Calcite
Dolomite
Barite
Gypsum
Cinnabar
Chalcocite
Galena

Other Materials

Quartz (7,16)
Activated Charcoal (6)
Synthetic Titanate (6)
Powdered Metals (23)
Graphite (23)
Magnesium Oxide (5)

---

*References are given in parentheses.

Table 4.3

Cation Exchange Capacities of Some Clay Minerals and Zeolites[11,12]

Mineral	Exchange Capacity* meq/g
Kaolinite	0.02 - 0.10
Illites	0.11 - 0.42
Montmorillonites	0.57 - 1.5
Micaceous clays	0.03 - 1.5
Chabazite	5(3.9)*
Clinoptilolite	2.6(2.2)*
Zeolite X	6.4(4.7)*
Zeolite Y	5.0(3.7)*

*Value in parentheses is exchange capacity of hydrated zeolite.

the near field redox conditions.[3,4,15] A minor component with respect to quantity in backfill design, a reduced iron mineral would be very important in providing the conditions where container corrosion could be minimized and also where the multivalent actinides and technetium could be maintained in their reduced, most sorbable form.[16,24] Under reducing conditions, some of these radionuclide species tend to form insoluble compounds such as oxides or hydroxides, undergo coprecipitation, or are incorporated into mineral lattices.[25] Due to the long half lives of the actinides, such control and immobilization would be invaluable to the effectiveness of backfill as a barrier to the migration of all waste radionuclides. On the other hand, the benefit of minimizing container corrosion is obvious. The mineral generally considered by the Swedes for this purpose has been vivianite, a ferrous phosphate, though, as can be seen from Table 4.2, other minerals could perhaps be used.

The use of quartz sand as a major component in backfill has been considered within the context of the Swedish KBS program among others.[4,9,23,26] While the Swedes have deemed that highly compacted bentonite is an adequate backfill for use in the disposal of spent reactor fuel rods, the thermal output of HLW poses a special problem. As a result, a modified backfill composed of from 80-90% quartz with the balance bentonite, has been proposed in order for the backfill to possess sufficient thermal conductivity. As a secondary benefit, the use of quartz adds to the mechanical strength of the fill. Clearly, this is a compromise solution because while the lower percentage of clay still lends an adequate degree of plasticity to the backfill, its sorptive capacity is significantly diminished.

Recently, the use of crushed host rock material for backfill or as a component in a backfill has been advocated by various researchers.[2,7,17-19] The use of crushed host rock has certain advantages in that is is easily available, inexpensive and will not react unfavorably with the surrounding repository rock. Like quartz, the thermal conductivity of crushed host rock will also allow for adequate cooling of the waste package during the thermal period of waste disposal. The use of crushed salt could be justified for the above reasons but because of its low radionuclide sorptive characteristics, it would not contribute to radionuclide retardation. Use of crushed tuff or basalt, in contrast, would at least provide some degree of radionuclide sorption. The sorptive properties of tuff have been extensively studied at Los Alamos and Sandia National Laboratories and indicate good radionuclide retention for many nuclear waste species.[27] This is especially true for the zeolitized tuff. Use of crushed basalt as backfill in a basalt repository also has promise since basalt has been shown to have "fairly high" cationic radionuclide sorptive properties and, under hydrothermal conditions (100°-300°), has been known to alter to clay mineral-like alteration products having high sorption capacity for cationic species.

Other backfill components have also been considered. For example, Nowak,[6] in research on backfill design for salt repositories, has examined the efficiency of activated charcoals, synthetic mordenite and sodium titanite for sorbing anionic radionuclides and Cs^+ and Sr^{2+}. Research on the use of powdered metals and/or powdered graphite has been proposed in the PNL Backfill Development Program.[2,8] Use of such materials, it is said, would avoid deleterious interactions between the container and the backfill, would provide for good thermal conductivity, and could aid in maintaining reducing conditions in the vicinity of the waste package.

4.3 Backfill Evaluation

Some proposed backfill designs are given in Table 4.4. Basically, each design incorporates an expandable clay, usually bentonite, as a principal component for plasticity, swelling properties and low permeability. Quartz or crushed host rock are included in some for mechanical strength and thermal conductivity and depending upon the design, various accessory components are added for either sorption of particular radionuclides or control of the redox environment. In general, most backfills are designed to possess the previously discussed required properties within a single layer around the waste package. A departure from this line of thought can be found within the BWIP program where different properties are ascribed to separate engineered elements of a barrier system around the waste package.[25] This approach would provide a useful alternative if an extra degree of redundancy was necessary or if some incompatability of backfill components had to be remedied. At the time of this writing, with the exception of the Swedish KBS program, comprehensive research on backfills has not been conducted. The following sections consider the research which has been done on the properties of backfills and upon the efforts that have been made to relate backfill performance to regulatory criteria.

4.3.1 Swelling Properties and Permeability

Research on the mechanical properties of backfill has focused primarily upon those of the bentonite clays themselves. Pusch,[10,26,28] within the context of the Swedish KBS program, studied the swelling properties and permeability of highly compacted Na-bentonite clays with respect to bulk density (Figures 4.1 and 4.2). His findings indicated that a maximum swelling pressure of 10MPa could be achieved (at a bulk density of 2.1 tons/m^3) and that at equilibrium, this would decrease to 5MPa. Backfill with such swelling nature would, according to Pusch, provide adequate sealing of the canister from groundwater, would accommodate host rock stresses without fissuring and could also fill cracks in the repository wall to a certain extent. In addition, permeabilities of 5×10^{-13}-10^{-14}m/s were achieved, so low that any radionuclide transport from the repository, presuming breach of containment, would occur through the backfill strictly by means of molecular diffusion.

While these properties are functions of bulk density, they are also somewhat dependent upon such factors as water content and composition, particle orientation, and the type and quantity of adsorbed cations. Recent work by Beall et al.[29] on the swelling properties of montmorillonite has indicated that swelling volume (and thus swelling pressure) is a function of the cation form of the clay (see Figure 4.3). The swelling volume of the calcium form of montmorillonite is less than that of the sodium form by a factor of 2.5. This phenomenon could be a potential means of failure for a montmorillonite based backfill. For example, the sodium form of montmorillonite is generally considered to be the clay used in backfills. In the repository, the clay would have time to equilibrate with the local groundwater and would exchange its sodium cations for calcium and magnesium cations. This, in turn, could result in shrinkage of the clay and perhaps cause fissuring which would allow greater

Table 4.4

Some Proposed Backfill Designs

KBS[26]

Compacted Bentonite*

10-20% Bentonite + Quartz**

AECL[19]

10-20% Bentonite + Crushed Granite +
Quartz Sand

BWIP[3]

Bentonite
Crushed Basalt
Zeolite
Quartz Sand
Apatite
Azurite
Ultramarine
Bournonite
Chalcopyrite
Pyrite

Beall and Allard[4]

60-70% Quartz +
15-20% Montmorillonite +
2-5% Apatite or Monazite +
2-5% Barite +
2-5% Chalcocite +
2-5% Fe^{2+} Mineral +
2-5% Illite or Attapulgite

Nowak[6]

30% Bentonite + 70% Charcoal

30% Bentonite + 20% Charcoal +
40% Mordenite +
10% Na-Titanate

PNL[23]

10% Bentonite + Quartz + Sand +
Zeolites +
Powdered Metal or Graphite

---

* Spent Fuel
**Reprocessed Waste

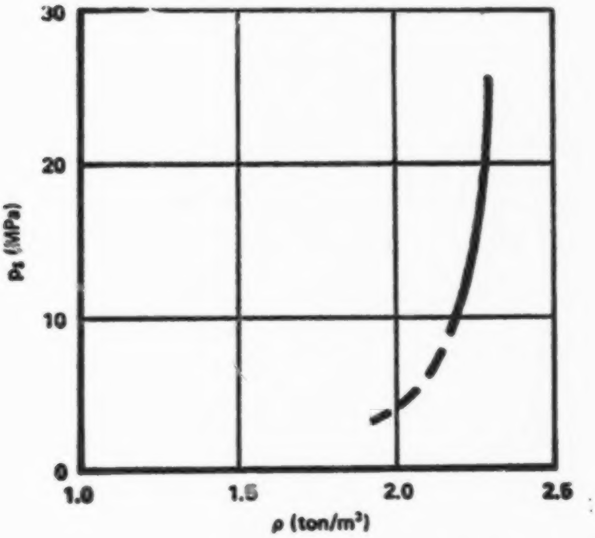

Figure 4.1. Swelling pressure as a function of bulk density for sodium bentonite at 100% saturation.[10,26,28]

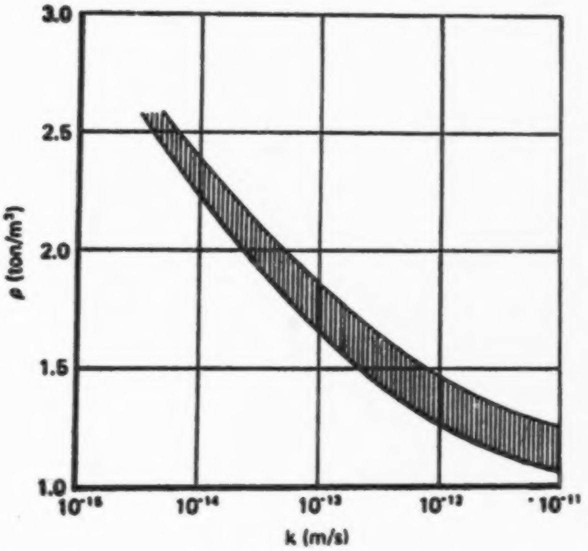

Figure 4.2. Range of empirically derived coefficients of permeability of sodium bentonite as a function of bulk density.[10,26,28]

BEST DOCUMENT AVAILABLE

BEST DOCUMENT AVAILABLE

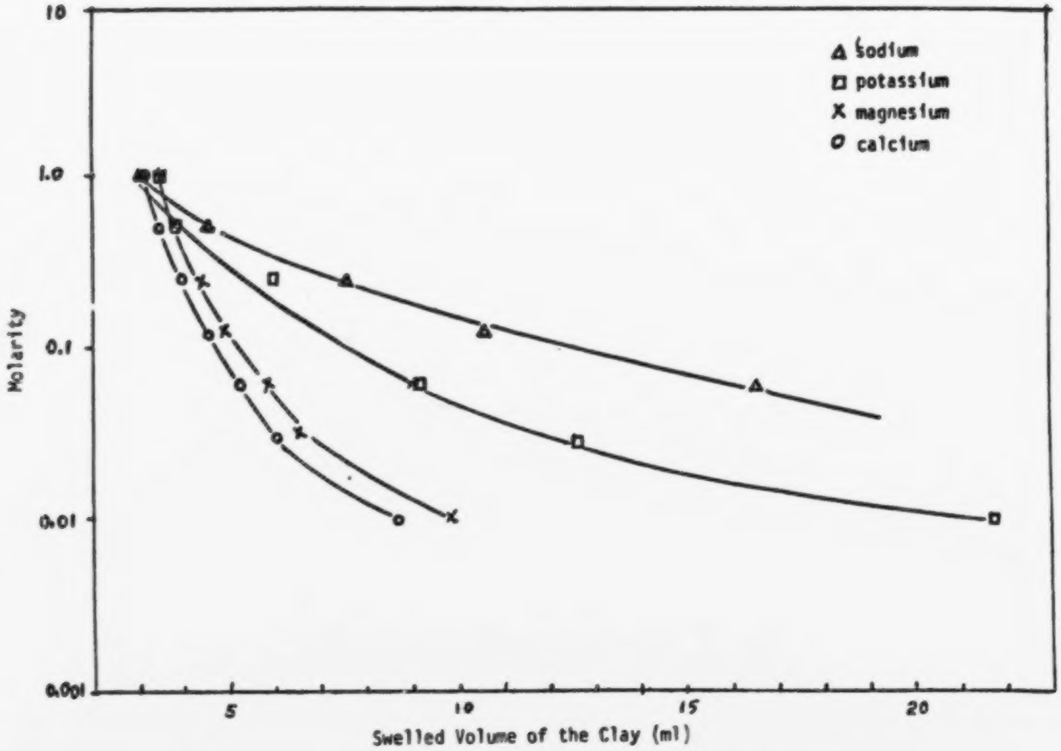

Figure 4.3. The influence of various cations upon the swelling volume of montmorillonite clay.[29]

groundwater access to the waste package. Another potential problem, with the montmorillonite and clay minerals, in general, is their anisotropic character. This also could influence the performance of clay backfill in a repository. Given the importance of swelling clays in all of the proposed backfill designs, these problems and the properties of the clays in general need to be more fully researched. Also, given that most backfill designs consider the use of substantial quantities of other materials (quartz, zeolites, accessory minerals, etc.), data on the influence of these components upon the overall barrier performance are needed. Presumably, the swelling and permeability characteristics of the clay would be diminished. Little work has been done on this topic.

4.3.2 Thermal Conductivity and Stability

Unless pre-burial cooling is employed in the radioactive waste disposal scheme, backfill materials are likely to encounter reasonably high temperatures (up to 300°C). An important parameter in this respect is the thermal conductivity of the backfill barrier mass. The backfill must have adequate thermal conductivity so as to conduct heat from the waste package and maintain its own temperature at levels low enough to minimize any potential structural damage or alteration which could cause failure of one or more of its functions. Recent work by Radhakrishna[30] determined the thermal conductivities of various potential backfill mixtures some of which are given in Table 4.5. Other work currently under way concerns the effects of temperature and pressure on the permeability, strength, and swelling characteristics of the fill.

Preliminary results indicated that illite based backfill mixtures had the best overall thermal conductivity followed by kaolinite backfills and then bentonite based backfills. The thermal conductivity of all the mixtures tested decreased with increasing clay content and temperature and increased significantly up to a "critical" backfill moisture content after which only slight increase was observed. Radhakrishna[30] concluded that any of the mixtures would be adequate, though the illite backfill was the best. Further, the fact that thermal conductivity is a function of moisture content has important implications regarding the disposal of HLW. The dependence of thermal conductivity versus moisture content of an illite-quartz backfill is given in Figure 4.4. Note that the thermal conductivity of the backfill falls off rapidly below a moisture content of about 1% in this case. During the thermal period of HLW disposal, the backfill would presumably be subjected to dehydration. If dehydration took place to the extent that the moisture content fell below the 1% level, the backfill would become thermally less efficient during the time when the highest thermal conductivity would be desirable.

Work performed by Komarneni and Roy[31] to investigate the hydrothermal stability of backfill materials indicated that clay minerals, especially vermiculite, exhibited layer collapse with a significant decrease in exchange capacity. More recent work at Pennsylvania State University[32] studied the effect of hydrothermal treatment on the structure and the sorption capacity of several backfill materials. At 200°C, only the vermiculites and phillipsite showed detectable alterations. At 300°C, only two montmorillonites and mordenite did not exhibit any detectable structural changes. These results are directly illustrated by changes in the sorptive capacities of the minerals as can be seen in Table 4.6. The sorptive properties of the altered minerals

Table 4.5

Thermal Conductivity of Candidate Buffer/Backfills[30]

Mix Composition	Moisture Content Range (%)	Dry Density Range (kg/m³)	Thermal Conductivity in Moist Condition W/°C.m	Thermal Conductivity in Dry Condition W/°C.m
sand + bentonite (15% clay)	6-17	1100 - 1770	1.3 - 2.8	0.7 - 1.0
sand + bentonite (25% clay)	5-16	1200 - 1760	1.2 - 2.7	0.6 - 0.9
sand + bentonite (50% clay)	15-29	1330 - 1400	1.2 - 2.0	0.5 - 0.6
silica + bentonite (10% clay)	6-10	1850 - 2000	2.0 - 3.0	0.4 - 0.7
silica + bentonite (25% clay)				
silica + bentonite (50% clay)				
silica + illite (15% clay)	4-9	2050 - 2175	3.0 - 4.0	1.5 - 1.7
silica + kaolinite (15% clay)	4-9	2000 - 2200	2.5 - 3.5	1.8 - 2.0
silica + zeolite (15% zeolite)	5-12	1725 - 1850	0.8 - 3.5	1.8 - 2.0
granite + bentonite (15% clay)	5-19	1750 - 2000	1.3 - 2.6	0.8 - 1.0
granite + bentonite (25% clay)	6-12	1620 - 1710	1.0 - 1.5	0.6 - 0.8
granite + bentonite (50% clay)	12-17	1500 - 1550	0.8 - 1.0	0.5 - 0.6
granite + illite (15% clay)	6-10	1890 - 2200	2.4 - 3.4	1.4 - 1.8
granite + illite (25% clay)	7-12	1600 - 2050	1.4 - 2.4	0.8 - 1.0
granite + illite (50% clay)	9-15	1850 - 1980	1.8 - 2.4	0.9 - 1.0
granite + kaolinite (15% clay)	6-10	1900 - 2050	2.2 - 3.0	1.7 - 2.0
granite + kaolinite (25% clay)	9-12	1850 - 1980	1.7 - 2.5	0.9 - 1.2
granite + kaolinite (50% clay)	9-15	1770 - 1860	2.1 - 2.2	1.0 - 1.2

BEST DOCUMENT AVAILABLE

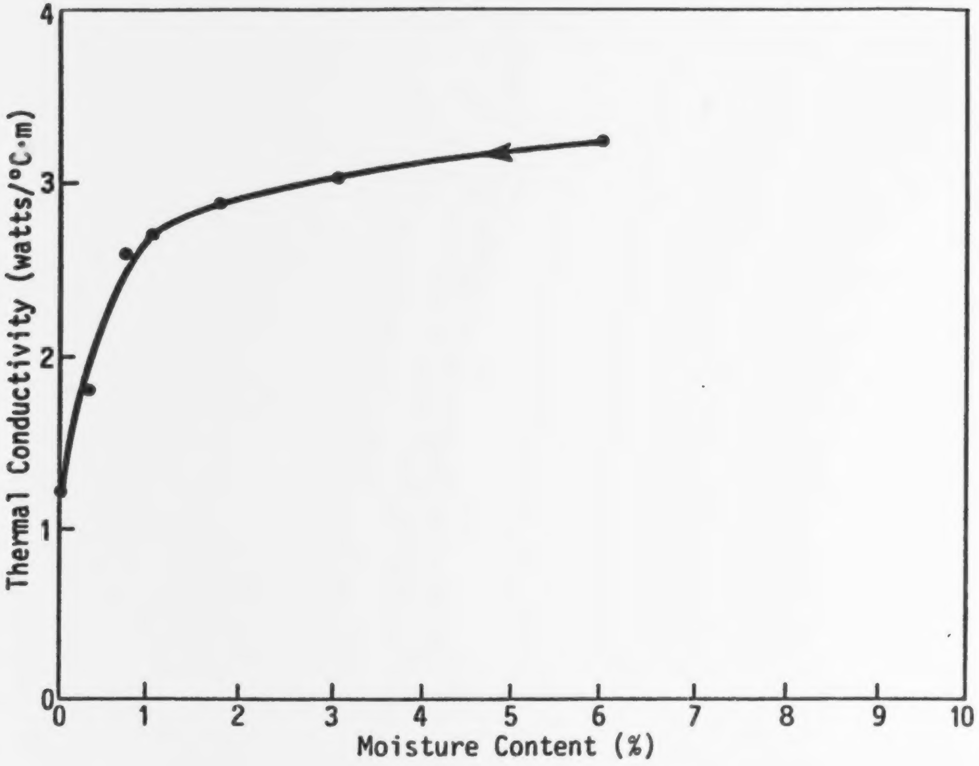

Figure 4.4. Thermal conductivity of an 85% graded silica - 15% illite backfill as a function of moisture content.[22]

BEST DOCUMENT AVAILABLE

Table 4.6

Effect of Hydrothermal Treatment on Cesium Sorption by Candidate Overpack Materials[32]

Sample Name, State	Cesium Sorption, K_d (ml/g)		
	Untreated	200°C, 30 MPa, 28 days	300°C, 30 MPa, 28 days
Montmorillonites			
Sodium-montmorillonite, Wyoming	150 ± 20[a]	140 ± 10	170 ± 20
Calcium-montmorillonite, Texas	190 ± 20	200 ± 20	160 ± 20
Calcium-montmorillonite, Arizona	590 ± 60	510 ± 50	280 ± 30
Vermiculites			
Poole vermiculite, South Carolina	2600 ± 300	60 ± 10	90 ± 10
Williams vermiculite, South Carolina	2900 ± 300	100 ± 10	60 ± 10
Zeolites			
Phillipsite, California	3900 ± 400	3200 ± 300	70 ± 10
Chabazite, Arizona	4600 ± 500	4800 ± 500	2800 ± 300
Erionite, California	8100 ± 800	6900 ± 700	1000 ± 100
Erionite, Oregon	4300 ± 400	---	3600 ± 400
Clinoptilolite, California	2900 ± 300	3200 ± 300	2600 ± 300
Clinoptilolite, Idaho	3800 ± 400	3500 ± 400	3200 ± 300
Mordenite, Arizona	4600 ± 500	4200 ± 400	4500 ± 500
Mordenite, Nevada	4100 ± 400	5100 ± 500	4800 ± 500

[a] The ± denotes 90% confidence limit on the mean.

decreased as a result of hydrothermal treatment, in some cases drastically. Based strictly upon the thermal stability of these minerals, the authors felt that the two montmorillonites and the mordenite would be preferable as a backfill.

Wood and Schultz[3] argue that "there is no convincing evidence that montmorillonite will be altered above 100°C." They base this conclusion on experimentation[33] that indicated that inter-layer water is lost reversibly up to 300° and that structural water is not lost until temperatures of 450°C are reached. They suggest, then, that the montmorillonite structure should be thermally stable up to 300°C and presumably retain its properties. This would seem to be confirmed by the results of Komarneni and Roy[32] presented above. Weaver,[34] however, argues that montmorillonite alteration to chlorites and illites can occur at temperatures as low as 40°C. Such alteration would not only affect the swelling behavior of the clay, but decrease its ability to control flow rates and alter its sorptive capacity. Wood and Schulz[3] counter by pointing out that such alterations to illite, for instance, would require the presence of potassium which, in the case of basalt repositories, is at very low concentrations in the groundwater. Hence, they argue montmorillonite alteration would be "unlikely" to occur. The presence and concentration of groundwater constituents is a very significant issue with respect to mineral clay alterations. For instance, alteration to chlorite could occur in the presence of magnesium and iron. It should be recalled that the experiments of Komarneni and Roy[32] were conducted using deionized water and non-prototypic repository groundwater. Further experimentation along these lines using more reasonable simulations of repository conditions (i.e. -simulated or actual groundwater) could go a long way to help resolve the dispute over backfill stability.

During the thermal period of high level waste disposal, the possibility exists that the backfill could be subjected to alternate wet/dry cycles. Under such circumstances, there is potential for the backfill to crack or fissure, permitting groundwater access to the waste package. Little information is available on this topic. Sethi et al.[35] conducted wet/dry cycling experiments on three montmorillonitic clays at 75°, 100° and 150° in basaltic and granitic groundwater. Preliminary results indicated that, while X-ray diffraction studies did not show significant structural alteration, the gel strength, liquid limit, and the flow index of the Na-montmorillonite clays decreased with increasing wet/dry cycling (Figure 4.5). In contrast, in the Ca^{2+}-Mg^{2+} montmorillonite clays these properties increased with the number of wet-dry cycles. These results were taken to indicate that microcracking may occur in the Na^+-montmorillonites should these conditions exist. This has direct significance for the montmorillonite based backfills since, in general, the proposed mixtures utilize the sodium form of the clay. These results, while preliminary, along with the findings of Beall et al.[29] reported earlier suggest that efforts should be directed towards tailoring the cation composition of the clays used in backfills to the specific groundwater in which they will be utilized.

4.3.3 Backfill Sorptive Properties

Research on the radionuclide sorption properties of potential backfill materials is important since this interaction represents the most significant

BEST DOCUMENT AVAILABLE

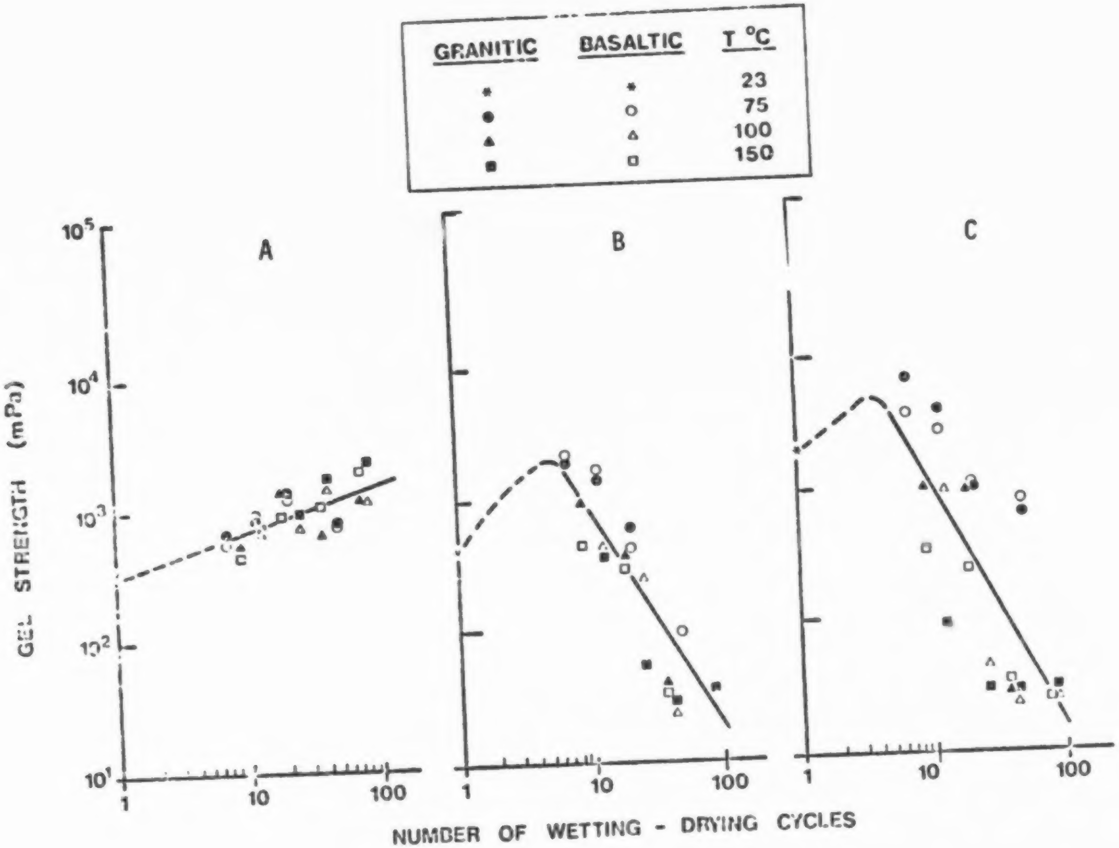

Figure 4.5. Gel strength as a function of the number of wet/dry cycles for montmorillonitic clays: A = Ca-mg montmorillonite; B = Na-montomorillonite #1; C = Na-montmorillonite #2.[35]

means of radionuclide retardation aside from the control of groundwater transport by highly impermeable clay minerals. The standard means used to evaluate the sorption of radionuclides by a solid is the determination of the system K_d value or equilibrium distribution coefficient. This coefficient is a measure of the partitioning of a radionuclide between the solid and liquid phase of the system. Many experimental variables can influence the K_d of a system and a list of some of these is given in Table 4.7. Several works are available which treat these variables with respect to their influence upon sorption[24,36-38] and no such evaluation will be attempted here. Table 4.7 is intended to illustrate factors which must be kept in mind both when experimentally determining these coefficients and when attempting to evaluate the performance of backfills on their basis. Also, classically speaking, sorption of radionuclides should only include reversible mechanisms such as ion-exchange or adsorption. However, frequently, the experimental conditions used in determining sorption coefficients have not been adequately controlled so as to exclude irreversible interactions such as precipitation or chemisorption. Such possible effects must also be understood. Because of the wide range of repository conditions which influence sorption, no attempt will be made to comprehensively present all available backfill/radionuclide sorption data. The data given in this section have been selected on the basis of their ability to illustrate significant aspects of backfill sorption research.

Table 4.7

Variables Influencing Distribution Coefficients

Temperature	Solid Composition
Groundwater Concentration	Redox Conditions
Groundwater Composition	pH
Solid-Solution Ratio	Tracer Concentration
Equilibration Time	Particle Surface Area
Corrosion Products	Radiation Effects

The distribution coefficients for secondary mineral smectite clay in basaltic groundwater at 60°C (ambient temperature of potential repository host rock) are given in Table 4.8.[3,38,39] Not surprisingly, in light of its good cation exchange capacity, the smectite tested here possessed good sorptive properties for the radionuclide cations ^{85}Sr, ^{137}Cs, ^{226}Ra, and ^{241}Pu under these conditions. Significantly, however, the sorption of toxic radionuclides such as ^{75}Se, ^{99}Tc, and ^{125}I was very poor as was the sorption of the actinide ^{237}Np. These results are in general agreement with the findings of other backfill researchers such as Allard et al.[16] in similar environments and serve to point out that while, overall, montmorillonite clays are good radionuclide sorbents, they do have deficiencies with respect to the full range of radionuclides which they would be required to face in a repository.

Since the anionic species of I, Tc, Se, Np and Pu are not sorbed by most backfill materials, the use of chemisorbing minerals has been recommended. Strickert, et al.[20], in experiments with various minerals containing reduced

Table 4.8

K_d Values for Secondary Smectite in Basaltic Groundwater* at 600°C[3,39]

Radionuclide	K_d', ml/g		Contact Time (Days)
	1 g/10 ml**	1 g/80 ml**	
^{75}Se	1.1 ± 0.8	7.1 ± 4.7	14
	0	4.2 ± 3.9	37
^{85}Sr	772 ± 580	906 ± 46	14
	449 ± 167	997 ± 14	37
^{99}TC	0	0	14
	0	0	37
^{125}I	0	0	14
	0	0	37
^{137}Cs	22,200 ± 18,500	15,300 ± 4,300	14
	1,701 ± 1,099	17,000 ± 1,000	37
^{226}Ra	212 ± 17	1,220 ± 180	14
	90 ± 7	613 ± 79	37
^{237}Np	14 ± 2	63 ± 5	14
	17 ± 4	66 ± 21	37
^{238}U	25 ± 13	349 ± 79	14
^{241}Am	4,700 ± 2,500	16,200 ± 1,400	14
	7,275 ± 3,100	20,000 ± 7,400	37
^{241}Pu	767 ± 288	2,200 ± 1,144	14
	1,536 ± 750	611 ± 270	37

*Synthetic groundwater composition

Constituents	Concentration (mg/ℓ)
Na^+	30.7
K^+	9.0
Ca^{+2}	6.5
Mg^{+2}	1.0
Cl^-	14.4
HCO_3	81.5
SO_4^{-2}	11.1
SiO_2	25
	pH=8.0

**Experimental solid-to-water ratio.

metals such as Cu^+ and Fe^{2+}, succeeded in demonstrating nearly complete removal of certain anions from solution. An example of their results is given in Table 4.9. Presumably, the technetium is first reduced and then sorbed though the precise mechanism has not been experimentally determined. Iodide, on the other hand, is apparently precipitated as transition metal iodides. This is probably what also occurs to the iodine in iodate after it is reduced, like technetium. In view of the toxic hazard posed by these long lived waste elements, use of such materials in backfill provides an attractive option for retarding their migration.

Nowak[6,40] has pursued the question of the overall adequacy of smectites with respect to their performance in various groundwaters, particularly salt brines characteristic of the WIPP site. He found that bentonite clays did not reasonably sorb the anionic radionuclides and further demonstrated that, in brine, bentonite did not adequately sorb Cs^+ or Sr^{2+}. Because of these results, Nowak was led to investigate the performance of activated charcoal, synthetic mordenite, and sodium titanate as alternatives. Somes of the results are presented in Table 4.10. Significant sorption was observed for TcO_4^- and I^- on activated charcoals while Sr^{2+} sorbed well on sodium titanate and Cs^+ sorbed well on synthetic mordenite. Such results imply that the tailoring of backfill compositions to sorb effectively in the various environments proposed for nuclear waste disposal is essential.

As mentioned earlier, research has also focused upon the use of zeolites to improve the sorbing qualities of backfill barriers. Komarneni and Roy[8] examined the sorption of Cs^+, Sr^{2+}, Rb^+ and Ba^{2+} (PW-4b waste simulant) on clays, natural and synthetic zeolites and on various mixtures of these minerals. The fixation of the sorbed radionuclides was also tested by means of a $NaCl-CaCl_2$ groundwater simulant extraction. As can be seen in Table 4.11, the natural zeolites sorbed and fixed greater quantities of radionuclides than did the clay minerals with respect to all the ions tested. In general, the synthetic zeolites also outperformed the clay minerals but, because of their more uniform pore characteristics, the synthetic zeolites were more selective as to the ions they sorbed and fixed most effectively. Mixtures of natural zeolites and vermiculite were also tested along with mixtures of natural and synthetic zeolites. Such mixtures exhibited superior sorption and fixation characteristics versus those of individual minerals in most instances. However, poorer sorption and fixation was usually observed for one of the ions tested. Komarneni and Roy[8] found that the best overall performance was obtained by utilizing mixtures of natural zeolites as sorbents (see Table 4.12). Such mixtures provided the best compromise with respect to the sorption and fixation of the suite of ions involved. Most important, synergistic effects were observed where mixtures of zeolites sorbed and fixed greater quantities of ions than would have been expected on the basis of the performance of the individual component minerals. The results of this research are pertinent to radioactive waste disposal primarily in light of the synergistic effects observed with mixtures of sorbents. Since most backfills as now conceived consider multi-component barriers, such synergism could provide increased radionuclide retardation capacities. As yet, however, this research stands as the only work in which multi-component backfills have been tested for their properties. It would appear, then, that due to the signifi-

Table 4.9

Fraction of Radiotracers Sorbed on Various Sulfides[20]

Sorbent	TcO_4^-	I^-	IO_3^-
CdS[a]	0.03	0.97	
Cu_2S	0.99+	0.99+	0.99+
CuS	0.04±0.02	0.99+	0.99+
FeS	0.99+		0.14
HgS[a]	0.02	0.70	
PbS	0.46±0.20	0.94±0.05	0.95±0.04
ZnS[a]	0.08	0.10	

[a] Only one measurement made.

Table 4.10

Sorption Characteristics of Potential Backfill Components for Salt Repositories[40]

Species	Sorbent	Brine*	$K_d$ml/g
TcO_4	Charcoal #1	A	380
TcO_4	Charcoal #1	B	300
I^-	Charcoal #1	A	35
I^-	Charcoal #2	A	53
I^-	Charcoal #3	A	18
Sr^{2+}	Sodium Titanate	A	125
Sr^{2+}	Sodium Titante	1% A	100,000
Sr^{2+}	Sodium Titanate	B	540
Cs^+	Synthetic Mordenite	A	27
Cs^+	Synthetic Mordenite	1% A	12,000
Cs^+	Synthetic Mordenite	B	74
Cs^+	Illite	B	115

*WIPP A = A
WIPP B = B

BEST DOCUMENT AVAILABLE

Table 4.11

Sorption Characteristics of Various Minerals for Certain Fission Product Ions[8]

Zeolite Type	Cs^+			Rb^+			Sr^{2+}			Ba^{2+}		
	Sorption[1] Coefficient	% Sorbed[2]	% Fixed[2]	Sorption[1] Coefficient	% Sorbed[2]	% Fixed[2]	Sorption[1] Coefficient	% Sorbed[2]	% Fixed[2]	Sorption[1] Coefficient	% Sorbed[2]	% Fixed[2]
Natural Zeolites (200 mesh)												
Clinoptilolite, AZ	5100	96	78	3600	93	72	1300	83	22	27,000	99^+	-
Clinoptilolite, ID	5100	96	78	4100	94	77	2000	89	67	69,000	99^+	-
Mordenite, AZ	7500	97	89	1100	81	49	130	35	18	1200	83	-
Mordenite, NV	5600	96	85	1100	81	56	75	23	16	1300	84	-
Erionite, OR	4000	94	84	4300	95	60	110	31	2	960	79	-
Erionite, CA	14,000	98	89	4100	94	71	770	75	7	130000	99^+	-
Chabazite, AZ	9800	97	85	1700	87	59	280	53	0	3200	93	-
Phillipsite, CA	8000	97	96	6800	96	90	190	43	0	170000	99^+	-
Synthetic Zeolites (600 mesh)												
Linde, 3A	190	43	16	30	11	0	64000	99^+	87		100	-
Linde, 4A	800	76	53	220	47	19	220,000	99^+	70		100	-
Linde, 5A	2300	90	62	250	50	21	3600	94	28	2400	99	-
Clay Minerals												
Montmorillonite, AZ (200 mesh)	770	76	25	310	55	12	260	51	0	560	70	-
Vermiculite, SC (60 mesh)	1400	85	.55	120	32	17	530	68	0	450	64	-
Shale (200 mesh)												
Conasauga Shale, TN	96	28	6	81	24	11	57	18	0	-	-	-

1. Calculated from sorption data given by Komarneni and Roy.
2. Calculated with respect to the concentration of the ion in the unreacted solution.

Table 4.12

Sorption Characteristics of Various Mineral Mixtures for Certain Fission Product Ions[8]

Sample Mixtures	Cs^+			Rb^+			Sr^{2+}			Ba^{2+}		
	Sorption Coefficient	% Sorbed	% Fixed	Sorption Coefficient	% Sorbed	% Fixed	Sorption Coefficient	% Sorbed	% Fixed	Sorption Coefficient	% Sorbed	% Fixed
1:1 Mixtures with Vermiculite, SC												
Clinoptilolite, AZ	2300	90	58	1800	88	68	360	59	15	21000	99	-
Chabazite, AZ	3000	92	79	780	76	54	390	61	0	2300	90	-
Phillipsite, CA	3600	93	86	3600	94	88	300	55	0	110,000	99^+	-
Linde, 3A**	1300	84	74	130	34	27	790	76	24	-	100	-
Linde, 4A**	1600	87	63	520	67	40	44000	99^+	25	-	100	-
Linde, 5A	1400	85	62	160	40	25	64000	99^+	14	16000	99	-
Montmorillonite, AZ**	1100	81	50	190	43	6	3900	94	0	490	66	-
Conasauga Shale, TN**	1300	84	56	120	32	18	40	14	0	370	60	-
1:1 Mixtures of Natural and Synthetic Zeolites												
Phillipsite CA + Linde 3A	1300	84	63	550	69	48	220,000	99^+	38	-	100	-
Phillipsite CA + Linde 4A	4300	95	79	6800	96	84	220,000	99^+	44	-	100	-
Phillipsite CA + Linde 5A	4900	95	80	7400	97	86	5400	96	11	79000	99^+	-
Chabazite, AZ + Linde 3A	1300	84	60	310	56	20	220,000	99^+	47	-	100	-
Chabazite, AZ + Linde 4A	4900	95	79	1200	83	48	220,000	99^+	59	-	100	-
Chabazite, AZ + Linde 5A	4500	95	79	880	78	45	4200	94	9	12000	98	-
Clinoptilolite AZ + Linde 3A	900	78	52	260	51	19	220,000	99^+	47	91000	99^+	-
Clinoptilolite AZ + Linde 4A	3100	93	72	2700	92	62	220,000	99^+	62	51000	99^+	-
Clinoptilolite AZ + Linde 5A	3100	93	72	1600	86	59	4700	95	14	15000	98	-

BEST DOCUMENT AVAILABLE

cance of such effects further research is needed in this area.

4.3.4 Radionuclide Diffusivity and Retention

The measurement of K_d values in the laboratory is a useful tool but does not represent the dynamic situation which will be present in the repository. Evaluation of backfills under such dynamic conditions would be appropriate to better establish their performance.[41]

One step in this direction has been taken by the researchers in the Swedish KBS waste disposal program. Neretnieks and Skagius[42,43] and Allard and Kipatsi[44] experimentally determined the diffusivities of various radionuclides and other species in compacted bentonite and bentonite/quartz backfills in order to be able to infer radionuclide transport rates in these barriers. Their results are given in Table 4.13. This type of information is particularly meaningful in cases where molecular diffusion is expected to be the primary mechanism of radionuclide transport, a situation that has been suggested to exist in backfills based on expanding clays where low permeability is achieved upon clay hydration.[3,6]

The influence of tortuosity upon the migration of radionuclides through backfill can be seen by comparing the diffusivities for strontium and cesium in Table 4.13 with typical bulk solution diffusivities. It should be noted that, in general, empirical diffusivities normally reflect the effect of both tortuosity and sorption. In this instance, however, these values were adjusted by Neretnieks and Skagius for the effect of sorption and, therefore, are indicative of the effects of tortuosity only. Typical values of diffusivity in bulk solution are on the order of 10^{-9} to 10^{-10} m^2/s,[45] an order of magnitude greater than those for cesium and strontium in Table 4.13. The differences between these values show the value of low permeability materials in retarding radionuclide migration in backfill. Similarly, the effect of sorption can also be illustrated. Diffusivities for silver in bentonite/quartz backfill were not adjusted for sorption and are nearly three orders of magnitude less than those for bulk solution diffusivity. Thus, from this type of comparison, the rate of movement of radionuclides through backfill can be inferred. As will be demonstrated later in this section, diffusivity data can be utilized to calculate radionuclide breakthrough times through backfill and thus be directly applied to proposed NRC waste package performance criteria.

Given that a backfill possesses the required attributes and can survive in the repository environment, the ultimate measure of its performance is its contribution to achieving the NRC performance criteria of complete radionuclide containment for 1000 years and, after that, to control radionuclide release to 10^{-5} parts per year.

The first efforts at calculating the retention time of radionuclides in a backfill barrier were made by Neretnieks[9] though these were not directed towards regulatory criteria. Neretnieks[9] calculated the retention times of various radionuclides in a one meter thick bentonite backfill given that only diffusive transport took place. The results, given in Table 4.14, show that ^{90}Sr, ^{137}Cs, and ^{241}Am would decay to insignificant levels ($C/Co = 10^{-9}$) within the barrier. With the exception of the anionic radionclides

Table 4.13

Experimentally Determined Diffusivities of Various Dissolved Species in Backfill

Species	Diffusivity (m^2/s)	Medium	Groundwater	T(°C)	Density (g/cm^3)	Ref.
Sr^{2+}	3.3×10^{-11}[a]	Compacted Bentonite	Granitic	50	2.1	43
Cs^{+}	5.4×10^{-11}[a]	Compacted Bentonite	Granitic	50	2.1	43
CH_4	3.9×10^{-11}	Compacted Bentonite	Distilled	50	2.1	42
H_2	1.8×10^{-11}	Compacted Bentonite	Distilled	50	2.1	42
^{110m}Ag	8×10^{-13}	Bentonite Quartz	Brine	85	Not given	44
^{110m}Ag	7×10^{-13}	Bentonite Quartz	Brine	25	Not given	44
^{110m}Ag	7×10^{-13}	Bentonite Quartz	Granitic	85	Not given	44
^{110m}Ag	6×10^{-13}	Bentonite Quartz	Granitic	25	Not given	44

[a] Adjusted for sorption effects.

Table 4.14[9,46]

Radionuclide Retardation Factors and Retention Times for the One Meter Thick Backfill Barriers[a]

Nuclide	Half-life (yr)	Compacted Bentonite Retardation Factor	Compacted Bentonite Retention[b] Time (yr)	10% Bentonite 90% Quartz Retention[c] Time (yr)	Clinoptilolite Retention[c] Time (yr)
^{90}Sr	2.77×10^1	600	1.3×10^4[d]	30	600 - 1400
^{99}Tc	2.12×10^5	1	22	1	1
^{129}I	1.7×10^7	1	22	1	1
^{137}Cs	3.0×10^1	400	9×10^3	20 - 30	2200 - 5200
^{226}Ra	1.602×10^3	800	1.8×10^4	40 - 50	600 - 1400[e]
^{229}Th	7.34×10^3	1000	2×10^4	50 - 300	Unknown
^{237}Np	2.14×10^6	200	4.4×10^3	10	"
^{239}Pu	2.44×10^4	1200	2.6×10^4	60 - 80	"
^{240}Pu	6.58×10^3	1200	2.6×10^4	60 - 80	"
^{241}Am	4.33×10^2	4000	9×10^4	200 - 4000	1000 - 30000[f]
^{243}Am	7.95×10^3	4000	9×10^4	200 - 4000	1000 - 30000

[a] Granitic Groundwater

[b] Flow Rate ≈ 1.4×10^{-7} cm/s

[c] Flow Rate ≈ 3×10^{-6} cm/s

[d] Underlined values indicate radionuclide decay to below 10^{-9} of the original activity

[e] Based on analogy to Sr

[f] Based on analogy to Eu

^{99}Tc and ^{125}I, all the radionuclides studied would be retained within the barrier for greater than about 4000 years. Using radionuclide retardation factors, retention times have also been estimated for one-meter thick barriers of 10% clay-90% quartz and of clinoptilolite (Table 4.14).[45] While these barriers are also incapable of retaining the toxic anions for any reasonable period of time, the other radionuclides, with the exception of ^{137}Cs and ^{234}Np, are retained within the barriers for greater than 1000 years. These values can be viewed as an important quantitative measure of the potential of backfills to aid in compliance with regulatory criteria.

Neretnieks' approach has been further refined by Nowak[6,40] who applied mass balance principles to modeling radionuclide migration through backfill barriers. From the solutions of mass-balance differential equations, Nowak[6,40] calculated the breakthrough times of various radionuclides through backfills of different composition. Knowing the barrier thickness, using empirically determined retardation factors, and assuming a diffusion coefficient of $1x10^{-9}$ m^2/s, Nowak arrived at the retention times given in Table 4.15. These results essentially represent a confirmation of Neretnieks' findings but under more rigorous conditions and also demonstrate the effectiveness of tailoring backfills for particular environments, in this case salt brine. It is necessary, however, to point out that Nowak, in using this approach to evaluate backfill performance, defined that radionuclide breakthrough occurred when the radionuclide concentration outside the backfill reached 1% of the source term radionuclide concentration. Defining breakthrough at this level is probably not realistic in light of the NRC performance criteria. It is a simple matter to recalculate the breakthrough times using other definitions of radionuclide breakthrough. For example, the retention times of Nowak's[40] bentonite/mordenite/charcoal/titanate backfill are given in Table 4.16 for breakthrough defined at $^C/Co = 10^{-4}$. These data represent a more realistic and conservative evaluation of backfill performance. Such calculation could be performed for any desired definition of radionuclide breakthrough.

Also, Nowak estimated radionuclide diffusivity in backfill and used this value in the calculation of radionuclide retention time. Experimentally determined diffusivities such as those give in Table 4.13 could be used in such calculations. These values can be easily determined under reasonable repository conditions and would add to the accuracy of the performance calculation.[47]

We have used a mass balance approach similar to that of Nowak in order to evaluate the effectiveness of a hypothetical zeolite backfill with respect to both the proposed NRC containment and controlled release rate criteria (Appendix B). The assumptions, calculation and detailed conclusion are given therein. Briefly, the radionuclide retention and controlled release characteristics of a zeolite backfill were studied parametrically with respect to bed thickness, time, sorption coefficient, groundwater velocity and release scenario. A 3-ft thick zeolite backfill was found to be capable of retaining the activity released from a glass waste form for a period of 1000 years. The controlled release criterion was found to be met by a 3-ft to 10-ft thick bed of zeolites. These finding serve to indicate the value of backfill with respect to waste package compliance with proposed NRC criteria. The fact that this model is more sophisticated than those previously described adds significance to these conclusions and also serves to demonstrate the utility of this

Table 4.15

Calculated Retention Times for Various Backfill Compositions Assuming Diffusion Controlled Transport[6,40]

Backfill Composition	Thickness (m)	Retention Time (Years)					
		Pu	Am	Cs	Sr	I	TcO_4
Compacted Bentonite[a,c]	0.3	1×10^4	1×10^4	1×10^3	1×10^3	-	-
Compacted Bentonite[a,c]	1.0	1×10^5	1×10^5	1×10^4	1×10^4	-	-
70% Bentonite[b] 30% Charcoal	1.0	5×10^4	2×10^4	-	-	1×10^3	1×10^4
30% Bentonite[b] 40% Mordenite 20% Charcoal 10% Na-Titanate	1.0	5×10^4	2×10^4	6×10^2	7×10^2	4×10^2	4×10^3

Effective porosity = 0.1

Breakthrough = C/Co = .01 (1%)

Calculated from: $$C/Co = \mathrm{erfc}\left\{\frac{h}{1.7\sqrt{\frac{D}{R}\, t_b}}\right\}$$

where h = barrier thickness
D = diffusion coefficient (1×10^{-5} cm^2/s)
R = retardation factor
t_b = breakthrough time

[a] Groundwater not specified

[b] WIPP A Brine

[c] On basis of estimated retardation factors for actinides and fission products.

Table 4.16

Estimated Radionuclide Retention Times in One-Meter Thick Backfill Bed*[40]

	Retention Time (years)					
Breakthrough	Pu	Am	Cs	Sr	I	TcO_4
$C/Co = 10^{-2}$	5×10^4	2×10^4	6×10^2	7×10^2	4×10^2	4×10^3
$C/Co = 10^{-4}$	2×10^4	5×10^3	2×10^2	3×10^2	1×10^2	2×10^3

---

*30% Bentonite
40% Mordenite
20% Charcoal
10% Titanate

approach in waste package evaluation.

This type of quantitative data, the results from these approaches, represents the information necessary to evaluate backfills in terms of the proposed NRC performance criteria. However, more refinement of these models is needed, particularly with respect to the data used in them. Better data concerning the diffusive and sorptive properties of radionuclide/backfill systems must be supplied especially in multi-component backfill systems. Backfill research must be conducted with ultimate application of the results to NRC performance criteria in mind. Where feasible, experimentation should be carried out in order to validate the results calculated from models such as those discussed above.

4.4 Conclusions and Recommendations

- Although a considerable amount of data has been generated on backfill research, few of the reported investigations deal directly with the proposed NRC 1000 year containment and/or 10^{-5}/yr radionuclide controlled release criteria. These performance objectives have to be addressed if the backfill is required to perform as an effective barrier to the migration of released radionuclides in a repository.

- Most researchers have considered the use of a montmorillonite clay as the primary component of a backfill barrier. The swelling nature of the clay would limit groundwater access to the waste container thereby delaying the onset of corrosion. Reduced water flow near the waste package would also restrict radionuclide migration to diffusional transport. Some preliminary research has been initiated with regards to the parameters which control the swelling nature of these clays. The cation form of the clay and the composition of the groundwater are important factors.

- The use of multi-component backfills to achieve the properties necessary to effectively carry out the multiple functions of the backfill is currently envisioned. These accessory components are most commonly added in order to aid in the sorption or fixation of highly mobile radionuclide species such as TcO_4, I^-, IO_3 and SeO_4^{2-}. Mostly, these components are thought to be minerals containing reduced metals such as ferrous phosphate, vivianite. Minerals such as iodides or sulfides to precipitate these anionic species are also being considered. Sorption data are available which indicate the effectiveness of such minerals for this purpose. Furthermore, reduced metal minerals can act to buffer the near field redox conditions thereby reducing canister corrosion and maintaining multivalent radionuclides, particularly the actinides, in their reduced, most sorbable form. The effectiveness of these accessory components still must be tested in the presence of other intended backfill components.

- Research concerning the sorptive properties of mixtures of zeolites and clays has been performed and preliminary results indicate that synergistic effects can enhance sorption.

- A critical factor in the use of backfills in HLW repositories is that of thermal stability. Thermodynamic stability calculations have not proved conclusive in this area. Research on the thermal stability of clays and zeolites in hydrothermal conditions has indicated that some clays and zeolites may be unsuitable for HLW repositories due to their degredation at high temperatures. Some montmorillonite clays and mordenite zeolites, however, performed well under such conditions.

- The tailoring of backfills to specific repository environments has been done on a preliminary scale. In WIPP brine, sorption of fission products and anionic radionuclide species was found to be inadequate. Synthetic mordenite zeolite, sodium titanate, and activated charcoal were found to provide the needed radionuclide sorptive properties for the backfill in the salt environment. Crushed host rocks, especially basalt, tuff, and salt are also being considered.

- The use of quartz or crushed host rock as a component of backfills has also been examined. The use of quartz increases the thermal conductivity of the backfill and thus can enhance the survivability of the backfill and the waste package. The presence of quartz also adds to the mechanical strength of the backfill. Use of crushed host rock results in the same benefits as accrued with quartz. Further, crushed host rock is readily available and inexpensive. Some host rock types, particularly zeolitized tuffs and basalt provide added sorptive capacity to backfills.

4.5 Recommendations

While a range of experimental data is available concerning the properties of various candidate backfills, much more work must be done to sufficiently characterize these factors to allow for the quantitative evaluation of backfill performance with respect to proposed NRC criteria.

- Further research is necessary concerning the swelling nature of montmorillonite clays since this aspect appears to be crucial to backfill performance. The influence of clay cation content and groundwater composition along with pH, Eh, radiation and temperature effects on the swelling properties of clay should be investigated. Dehydration, wet-dry cycling, anisotropy, and the presence of accessory minerals also merit attention.

- The use of accessory components in backfills needs more adequate study. While current information is promising, near field pH and Eh control has not been conclusively demonstrated even on a laboratory scale. This is particularly significant with respect to a reduction of container corrosion.

- The thermal and hydrothermal behavior of backfill components has not yet been clearly resolved. This is particularly important for the disposal of commercial HLW. The effect of various repository environments and the presence of accessory components need to be considered for evaluating backfill stability.

- Since the use of multi-component backfills is highly probable, more research is necessary on potential synergistic interactions. Very little work exists in this area and on the basis of what research has been conducted, such interactions can have a significant impact on the overall performance of the backfill.

- More effort must be expended towards generating data needed for backfill evaluation with respect to proposed NRC performance criteria. Data concerning radionuclide diffusion and sorption in backfills under various repository conditions should be collected in order to calculate radionuclide specific retention times and release rates for comparison to the proposed NRC performance criteria.

- The potential use of backfill to control groundwater flow rates and patterns should be investigated. Specifically, the use of synthetic zeolites for backfill to control groundwater flow and radionuclide migration requires investigation.

4.6 References

1. C. Klingsberg and J. Duguid, "Status of Technology for Isolating High Level Radioactive Wastes in Geologic Repositories," DOE/TIC-11207 (Draft) 1980.

2. E. J. Wheelwright "Development of Backfill Material," Nuclear Waste Management Quarterly Project Report, April through June 1980 (A. M. Platt and J. A. Powell, Eds.) Pacific Northwest Laboratory, PNL-3000-6, September 1980.

3. M. I. Wood and W. W. Schultz, "Engineered Barrier Development for a Nuclear Waste Repository in Basalt," (M. J. Smith, Ed.), Rockwell International Corp., RHO-BWI-ST-7, May 1980.

4. G. W. Beall and B. Allard, "Chemical Aspects Governing the Choice of Backfill Materials for Nuclear Waste Repositories," Nuclear Technology, in Press, presented at American Chemical Society Second Chemical Congress Meeting, Las Vegas, Nevada, August 25-29, 1980.

5. G. W. Bird, "Possible Buffer Materials for Use in a Nuclear Waste Vault," Whiteshell Nuclear Research Establishment, Atomic Energy of Canada Limited, TR-72, May 1979.

6. E. J. Nowak, "Backfill Barriers for Nuclear Waste Repositories in Salt," Sandia National Laboratory, SAND 81-0377A, March 1981.

7. E. J. Wheelwright, "PNL Backfill Development Project," Pacific Northwest Laboratory, PNL-SA-9477, presented at "Research and Development Needs Relating to Backfill," sponsored by the National Bureau of Standards, Gaithersburg, Maryland, April 13-14, 1981.

8. S. Komarneni and R. Roy, "Super Overpack: Tailor-made Mixtures of Zeolites and Clays," in Scientific Basis for Nuclear Waste Management, Vol. 2, (C. J. Northrup, Ed.), Plenum Press, 1980.

9. I. Neretnieks, "Retardation of Escaping Radionuclides from a Final Repository," KAERNBRAENSLESAEKERHET, KBS-TR-30, 1977.

10. R. Pusch, "Required Physical and Mechanical Properties of Buffer Masses," KAERNBRAENSLESAEKERHET, KBS-TR-33, 1977.

11. C. B. Amphlett, Inorganic Ion Exchangers, Elsevier, New York, p. 17, 1964.

12. D. W. Breck, Zeolite Molecular Sieves - Structure Chemistry and Use, Wiley Interscience, New York, p. 537, 1974.

13. A. Jacobsson, "A Short Review of the Formation, Stability and Cementing Properties of Natural Zeolites," KAERNBRAENSLESAEKERHET, KBS-TR-27, 1977.

14. D. S. Coombs, A. J. Ellis, and W. S. Frye, "The Zeolite Facies, with Comments on the Interpretation of Hydrothermal Syntheses," Geochimica et Cosmochimica Acta, 17, 53-107, 1959.

15. National Academy of Sciences, "A Review of the Swedish KBS II Plan for Disposal of Spent Nuclear Fuel," 1980.

16. B. Allard, H. Kipatsi and J. Rydberg, "Sorption of Long-lived Radionuclides in Clay and Rock," KAERNBRAENSLESAEKERHET, KBS-TR-55, 1977.

17. E. J. Nowak, "The Backfill as an Engineered Barrier for Nuclear Waste Management," in Scientific Basis for Nuclear Waste Management, 2, (C. J. Northrup, Ed.), Plenum Press, 1980.

18. R. A. Wagner, "Preliminary Investigation of the Thermal and Structural Influence of Crushed Salt Backfill on Repository Disposal Rooms," Office of Nuclear Waste Isolation, ONWI-138, August 1980.

19. Acres Consulting Services Limited, "Irradiated Nuclear Fuel and Immobilized Waste Vaults: Backfilling System," Atomic Energy of Canada Limited Technical Record, TR-66, 1980.

20. R. Strickert, A. M. Friedman and S. Fried, "The Sorption of Technetium and Iodine Radioisotopes by Various Minerals," Nuclear Technology, 49, 253-266, 1980.

21. S. M. Fried, A. M. Friedman, and A. Cohen, "The Migration of Long-lived Radioactive Processing Wastes in Selected Rocks-Annual Report to the Office of Waste Handling," Argonne National Laboratory, ANL-78-46, 1978.

22. G. W. Bird and J. J. Lopata, "Solution Interaction of Nuclear Waste Anions with Selected Geologic Materials," in Scientific Basis for Nuclear Waste Management, Vol. 1, (G. W. McCarthy, Ed.), Plenum Press, 1979.

23. E. J. Wheelwright, "Development of Backfill Material," in Nuclear Waste Management Quarterly Project Report July through August 1980 (T. D. Chikalla and J. A. Powell, Eds.), Pacific Northwest Laboratory, PNL-3000-7, November 1980.

24. R. G. Strickert, "Sorption of Redox Sensitive Elements-Critical Analysis," Pacific Northwest Laboratory, PNL-3432, 1980.

25. W. E. Coons, E. L. Moore, M. J. Smith, and J. D. Kaser, "The Functions of an Engineered Barrier System for a Nuclear Waste Repository in Basalt," Rockwell International Corp., RHO-BWIP-LD-23, January 1980.

26. R. Pusch, "Highly Compacted Sodium Bentonite for Isolated Rock Deposited Radioactive Waste Products," Nuclear Technology 45, 153-157, 1979.

27. J. K. Johnstone and K. Wolfsberg (Eds.), "Evaluation of Tuff as a Medium for a Nuclear Waste Repository: Interim Status on the Properties of Tuff," Sandia National Laboratory, SAND 80-1464, July 1980.

28. R. Pusch, "Properties of Bentonite-Based Buffer Material," KAERNBRAENSLESAEKERHET, KBS-TR-32, 1978.

29. G. W. Beall, A. G. Lamkin, and K. L. Kelly, "Critical Factors Affecting the Use of Montmorillonite as a Nuclear Backfill Material", presented at "Research and Development Needs Relating to Backfill," sponsored by the National Bureau of Standards, Gaithersburg, Maryland, April 13-14, 1981.

30. H. S. Radhakrishna, "Evaluation of Thermal Properties of Buffer Materials for a Deep Underground Nuclear Waste Disposal Vault," presented at "Research and Development Needs Relating to Backfill," sponsored by the National Bureau of Standards, Gaithersburg, Maryland, April 13-14, 1981.

31. S. Komarneni and D. M. Roy, "Hydrothermal Effects on Cesium Sorption and Fixation by Clay Minerals and Shales," Clay and Clay Minerals, 28, 142-148, 1981.

32. S. Komarneni and R. Roy, "Hydrothermal Transformation in Candidate Overpack Materials and Their Effects on Cesium and Strontium Sorption," Nuclear Technology 54, 118-122 (1981).

33. W. A. Deer, R. A. Howie, and J. Zussman, Rock-Forming Minerals, Vol 1-5, Longman, Greens and Co., London, England, 1967.

34. C. E. Weaver, "Geothermal Alteration of Clay Minerals and Shales: Diagenesis," Office of Nuclear Waste Isolation, ONWI-21, 1979.

35. A. J. Sethi, G. W. Bird, and R. N. Yong, "Effect of Hydrothermal and Cyclic Wetting-Drying Treatment on Properties and Characteristics of Montmorillonitic Clays," presented at "Research and Development Needs Relating to Backfill," sponsored by the National Bureau of Standards, Gaithersberg, Maryland, April 13-14, 1981.

36. R. G. Dosch, "Assessment of Potential Radionuclide Transport in Site-Specific Geologic Formations," Sandia National Laboratory, SAND 79-2468, August 1980.

37. E. J. Nowak, "Radionuclide Sorption and Migration Studies of Getters for Backfill Barriers," Sandia National Laboratory, SAND 79-1110, July 1980.

38. C. D. Winslow, "The Sorption of Cesium and Strontium from Concentrated Brines by Backfill Barrier Materials," Sandia National Laboratory, SAND 80-2046, March 1981.

39. L. L. Ames and J. E. McGarrah, "Geomedia-Radionuclide Distribution Coefficients, Fiscal Year 1979 Annual Report," Pacific Northwest Laboratory, PNL-3146, 1979.

40. E. J. Nowak, "Composite Backfill Materials for Radioactive Waste Isolation by Deep Burial in Salt," Sandia National Laboratory, SAND-80-1377C, January 1981.

41. T. M. Ahn, K. S. Czyscinski, E. M. Franz, C. J. Klamut, B.S. Lee, N.S. McIntyre, K. J. Swyler, and R. J. Wilke, "NRC Nuclear Waste Management Technical Support in the Development of Nuclear Waste Form Criteria, Task 4: Test Development Review," Brookhaven National Laboratory, BNL-NUREG-29700, Informal Report, June 1981.

42. I. Neretnieks and C. Skagius, "Diffusivity Measurements of Methane and Hydrogen in Wet Compacted Clay," KAERNBRAENSLESAEKERHET, KBS-TR-86, 1978.

43. I. Neretnieks and C. Skagius, "Diffusivity Measurements in Wet Clay for Sr^{++}, Cs^{+}, and Na-Lignosulfonate," KAERNBRAENSLESAEKERHET, KBS-TR-87, 1978.

44. B. Allard and H. Kipatsi, "Measurement of the Rate of Diffusion of Silver in a Clay-Sand Mixture," KAERNBRAENSLESAEKERHET, KBS-TR-53, 1977.

45. R. Berner, Principles of Chemical Sedimentology, McGraw-Hill Book Co., New York, 1971.

46. I. Neretnieks, "Transport of Oxidants and Radionuclides Through a Clay Barrier," KAERNBRAENSLESAEKERHET, KBS-TR-79, 1978.

47. T. M. Ahn, R. Dayal, and R. J. Wilke, "Evaluation of Synthetic Zeolites as Backfill in a HLW Repository," Appendix to a letter from D. G. Schweitzer (BNL) to E. A. Wick (NRC), 11/12/80.

5. RADIATION EFFECTS ON WASTE PACKAGE COMPONENTS

All the components of a waste package may be exposed to radiation. The waste form will, of course, receive a heavy radiation dose from the decay of incorporated radionuclides. Other waste package components will be subjected to a gamma flux which depends upon the waste form loading, and upon the internal shielding properties within the waste package. In this Section, we assess the effects of radiation, insofar as they are known, on the properties of suggested waste package components. Emphasis is placed on those properties which most directly affect the ability of the waste package to retain radionuclides. In those cases where direct measurements have not been carried out, some information may be derived from generic studies or by analogy. We begin with a brief general discussion of radiation effects; this is intended to serve as a background for the specific considerations which follow.

5.1 General Considerations

In the waste package, we are concerned with six types of "radiation": gamma rays, beta particles, alpha particles, alpha-recoil nuclei, energetic (spontaneous) fission fragments and neutrons. The first two originate primarily from the decay of fission products within the waste form, while the alpha particles and recoil nuclei are produced in the decay chains of transuranic elements (TRU). Less frequently, some of these elements may decay by spontaneous fission, producing highly energetic (90 MeV) fission fragments, as well as fast neutrons.

The manner in which irradiation interacts with matter depends on the mass, charge and energy of the bombarding particle (or photon). There are basically two primary processes by which radiation deposits its energy in matter: knock-on events, in which atoms are displaced by elastic collision with incident particles, and ionization; which involves a radiation induced displacement of electronic charge. In general, a particle may deposit some of its energy by either process, the relative fraction depending on the parameters listed below (Table 5.1).

Estimates such as those presented in Table 5.1 have led the majority of studies to emphasize the role of atomic displacements due to alpha-recoil nuclei when considering radiation effects in the waste form. For these considerations the natural radiation dose unit is the DPA (displacements per atom) given as the number of displaced atoms produced by irradiation per atom of irradiated material. It is commonly held that typical high level waste forms will receive a local alpha recoil dose corresponding to approximately 1 DPA over their useful lifetimes.[5-8] Fortunately, most of the displaced atoms often are not stable and ultimately return to equilibrium sites in the material. To a large extent, then, the amount of radiation damage which results from atomic displacements due to elastic collisions with energetic particles will depend upon those processes which ultimately stabilize the displaced atoms. These frequently involve aggregate formation and exhibit

Table 5.1

Radiation Environment in HLW Waste Glass

		Dose/cm^3		Knock-on Displacements/ cm^3		Ionization (Rad)		
Radiation	Atomic Displacement per delay Event[c]	10^3 Year[a]	10^6 Year[b]	10^3 Year	10^6 Year[b]	10^3 Year[a]	10^6 Year	Range (mm)
Fission Fragment	10^5	$8x10^{12}$	$2x10^{13}$	$8x10^{17}$	$2x10^{18}$	10^8	10^8	$2x10^{-2}$
Alpha Recoil	1500	$1.5x10^{19}$	$7x10^{19}$	$2.2x10^{22}$	$1x10^{23}$	--	--	$2x10^{-5}$
Alpha Particle	140	$1.5x10^{19}$	$7x10^{19}$	$2.1x10^{21}$	$1x10^{22}$	$5x10^{11}$	$2x10^{12}$	$2.5x10^{-2}$
Beta Particle	0.13	$2.3x10^{20}$	$2.5x10^{20}$	$3x10^{19}$	$3x10^{19}$	$5x10^{11}$	$5.4x10^{11}$	1
Gamma Ray	--	--	--	10^{18}	10^{18}	$3.4x10^{11}$	$3.4x10^{11}$	10^3

[a] Based on waste from LWR fuel 33,000 MWd/MT, cooled 5 years before reprocessing. 170 kg solidifed glass/MT. Data from ref. 3 and 4. The alpha decay values may depend on the fuel cycle--see Table 5.2.

[b] Million year data scaled from Figure 2 in reference 3.

[c] Data from Ref. 1 and 2.

a characteristic temperature dependance--void formation in irradiated metals is a familiar example.[9] Excellent reviews of the subject in ceramics have been given by Hobbs[10,11] and by Clinard.[5,12] Among those effects which may result from displacement damage are the following:

- Swelling - Due either to lattice dilation by point defects or to void formation.
- Anisotropic Grain Growth - Due to anisotropic strains produced in swelling.
- Dislocation Growth - Due to strains or to aggregate formation.
- Gas Formation - Due both to helium buildup resulting from stopped alpha particles and, presumably, to clustering of displaced anions.[1,10]
- Amorphization - Crystalline materials may gradually disorder until they become x-ray amorphous. This is termed metamictization in naturally radioactive minerals.[13]
- Compaction - Glassy materials may increase in density upon irradiation.[14]

Attempts have been made to phenomenologically characterize the radiation resistance of materials in terms of generic features such as crystal structure or ionic bonding character, but a unified viewpoint has not yet emerged. This is not surprising since the radiation damage formation may involve a delicate balance between competing processes. For example, Primak has suggested that in glasses as many as four different mechanisms may contribute simultaneously to the net swelling or compaction.[14] Moreover, resistance to one type of radiation does not necessarily imply resistance to another type. In addition, there is evidence which suggests that displacement damage formation may be modified by ionization effects.[15,16] Accordingly, generalizations at this point are of limited value.

Ionization is the principal energy loss mechanism for beta particles and gamma rays in matter and this energy is deposited fairly uniformly. Accordingly, in those cases where the effects of ionizating radiation are of primary importance, the natural dose unit is the rad,* rather than the DPA. It should also be noted that alpha particles and fission fragments deposit a significant fraction of their energy by ionization.

Ionization does not produce atomic displacements directly; however, in insulating materials, ionization may result in local electronic charge configurations which are highly unstable. Relaxation of these unstable configurations may be sufficiently vigorous to rupture molecular bonds or produce atomic displacements in the solid state. We will term these effects as "internal radiolysis", when referring to atomic displacements in solids.**

---

* One rad = energy deposition of 100 ergs/gram.

**This may also be known as "ionization damage".

Local charge instabilities are not produced by irradiation in metals. Consequently, metals are completely resistant to bulk damage by ionization. In many refractory oxides ionization may modify local charge states but rarely, if ever, generates atomic displacements. In certain halides and silicates, however, displaced atoms may be produced directly by ionizing radiation without the need for elastic collisions of the type discussed earlier.[10,11] The mechanism for alkali and alkaline earth halides is fairly well understood.[11] This is not the case, however, in silicate materials. The amorphization of quartz under ionizing radiation[10,17,18] is thought to involve a local radiolysis of the SiO_4 tetrahedra, in which the bonding is [illegible] covalent.[10] The extent to which amorphization of other waste forms occurs under ionizing radiation is uncertain; a substantial [illegible] dose (estimated as $2x10^{13}$ rads) is required to promote amorphization in quartz.[18]

In insulating materials, electronic charge displacement by ionzing radiation can lead to several effects of practical importance even in the absence of internal radiolysis. In particular:

- Changes in the local charge state of atoms or defects. This may affect the mobility of certain atomic species, or the production efficiency of displacement damage.[12,14,15,16,19]

- Buildup of local space charges. This may be of importance at metal-insulator interfaces, if substantial electric fields can develop. Ionizing radiation could produce discharge tracks in certain cases.[20] This effect may be offset by enhancement of electrical conductivity during irradiation.

Under conditions anticipated in the waste form (see Table 5.1) it is likely that this ionization effect will be swamped by displacement damage due to alpha recoils provided that ionization does not affect the efficiency of displacement damage formation. There is some evidence that this is not the case. For example, Arnold et al. have observed that volume expansion induced by ion implantation in alumina can be "annealed" or recovered upon irradiating the sample with electrons.[15,16] On this basis it appears possible that the expansions due to internal alpha recoils might be moderated by simultaneous ionizing radiation.[15,21] In glasses containing short lived alpha-emitters, saturation of radiation damage effects is frequently observed, leading to the suggestion that radiation induced annealing occurs simultaneously with radiation damage formation.[22] We feel that this annealing may be promoted to a certain extent by the emitted alpha particle, which loses roughly 80% of its energy by ionization; this suggestion has been advanced by others as well,[8] and, if valid, may explain some recent results which suggest an anomalously high degree of surface damage in ion-implanted glasses. To maintain critical perspective, however, we must point out that to a certain extent, the initial production of atomic displacements by elastic collisions may be enhanced by ionization.[12]

Since the overall formation of radiation damage involves a balance between defect formation and annealing, it is difficult to make general statements about the net effect of ionization on displacement damage formation. However, the possible synergistic effects of simultaneous heavy particle and ionizing radiation do not appear to have been explicitly considered in radiation damage studies on candidate waste form materials. This heavy flux of ionizing radiation due to beta decay of fission fragments will, of course, persist for a relatively short time scale in comparison to that required for the buildup of internal alpha decay. Beta decay is essentially complete in a time during which the alpha decay dose reaches roughly 10% of its million-year value (Table 5.1). Consequently, one would probably not expect significant annealing of the alpha displacement damage by ionizing radiation from fission fragments unless these somehow precondition the material. It is interesting, however, that even in the absence of ionizing radiation, measurements on candidate waste forms doped with alpha-emitters commonly indicate the onset of saturating effects at roughly 10% of the total alpha dose anticipated after one million years.[3,4] In any event, the available data imply that the silicate tetrahedron may be somewhat less durable than certain other crystal structures in that atomic rearrangements can be promoted by ionizing radiation alone. In the rest of this section we will discuss the effect of those processes mentioned above on specific waste package components.

5.2 Radiation Effects in Waste Forms

The most important property of a waste form is its leach resistance. Effects such as swelling, metamictization, devitrification, etc., while interesting in their own right, are significant in the current context only insofar as they affect the ability of a waste form to retain radionuclides. There is at present a great deal of flexibility in waste form design (see Section 2). The true significance of potential radiation effects in the waste form must be considered in terms of specific waste package designs. A general assessment of this sort is not yet possible. Indeed, in a number of candidate waste form materials, the influence of effects such as metamictization upon leachability has not been determined. Recently, however, several excellent general reviews have appeared.[3,4,23,24] Under these circumstances, we shall document the available radiation information and, where possible, infer the practical consequences. We begin with glass waste forms, which have received the most study.

5.2.1 Glassy Waste Forms

A number of investigations have been carried out on the effect of radiation damage on borosilicate waste glasses. For the most part, these involve efforts to simulate the effects of internal alpha decay.[1,4,6,8,25-33] The conditions which these experiments attempt to match are set down in Table 5.2. In this table we have also included estimated doses for defense HLW glass and for SYNROC HLW. It is apparent that grossly accelerated testing is involved if alpha recoil damage effects are to be studied in the laboratory time frame. The most commonly employed form of simulation is to dope the candidate waste form with short lived alpha-emitters.[1,3,4,6,23-30] Other techniques include external heavy particle bombardment, neutron irradiation or internal fission.[2,8,30-34] All the methods necessarily involve unrealistic dose rates. Less emphasis has been placed on the effects of beta and gamma irradiation in actual waste glasses, but this area is receiving increased

Table 5.2

Cumulative Alpha-Decay Dose in Glasses and SYNROC (α-Decays/g[†])

	High Level Waste Glass[6]				
	UO_2 Fuel Waste	Pu Recycle Fuel Waste			
Time Since Fabrication (Years)	(x 10^{17})	Pu Fraction Only (x 10^{17})	Average of Entire[a] Mixed-Oxide Case (x 10^{17})	SYNROC[7] Zirconolite (x 10^{17})	Defense[8] HLW Glass (x 10^{17})
2	1.1	15.4	4.71	--	--
6	1.9	26	7.9	--	--
10	2.5	38	11.3	--	4×10^{-3}
10^2	7.1	109	32.6	5	--
10^3	14.6	174	54.5	11	4×10^{-2}
10^4	29.5	333	105	22	--
10^5	61.3	601	196	42	4×10^{-1}
10^6	195	815	350	150	5×10^{-1}

[†] We estimate that an alpha dose of 10^{19} α/g corresponds to roughly 1 DPA.

[a] Assumes a reactor core containing 25 % Pu fuel.

attention. Ionization may affect both the radionuclide host phase, and the properties of barrier or leachant media. The common means of studying these effects is to irradiate the sample externally with gamma rays or fast electrons and determine the irradiation-induced changes in physical properties. The conditions relevant to these measurements are shown in Table 5.1.

Recently, studies of the effects of atomic transmutations on glassy and crystalline materials have also been reported. The various glassy systems are discussed below in terms of the radiation effects which have been investigated.

5.2.1.1 Swelling

Silicate glasses may either expand or compact under irradiation. The effect is illustrated for a number of different glasses in Figure 5.1. Zinc borosilicate waste glasses (72-68) compact under irradiation in both amorphous and devitrified form; the effect appears to saturate with α-dose at a volume contraction of about 1%. Both lead silicate (P-G) and European borosilicate (E-G) (high silica) waste glasses swell due to internal alpha decay. The figure suggests that certain intermediate glass compositions may exist which exhibit essentially no irradiation induced volume change, and this indeed appears to be the case. Simulated waste glass PNL 77-260 (a copper-titanium borosilicate incorporating gadolinium rich waste) shows less than .10% volume change after an internal alpha dose of $\sim 2 \times 10^{18}$ α/g.[26]

Alpha audioradiography demonstrates that for suitable concentrations actinides can be homogeneously distributed in waste glasses.[25,26,35] Since the waste glasses themselves are ordinarily fairly homogeneous under favorable conditions (see Section 2) differential swelling or compaction effects due to radiation should be minimal. If, however, the material devitrifies or is inherently inhomogeneous (as for example in the porous glass systems[36]) the situation may be quite different.

Weber et al. have studied the effect of devitrification on the radiation stability of 77-260 glasses doped with curium.[26] Devitrification produced crystalline gadolinium-apatite and cubic titanate phases which tended to precipitate curium from the residual glass. The apatite phase became x-ray amorphous (metamict) with increasing radiation doses, and an overall swelling of about 1% was observed for the devitrified glass at $\sim 5 \times 10^{18}$ alpha decays/cm^3 Both the swelling and the formation of surface microcracks are due to the differential expansion of the apatite phase with respect to the residual glass.

Weber and co-workers report that, for a number of glasses, the swelling data can be empirically fitted to an expression of the form

$$\Delta\rho = A(1-e^{-BD}) \qquad (1)$$

where D is the dose (in alpha decays per cm^3), $\Delta\rho$ the density change and A

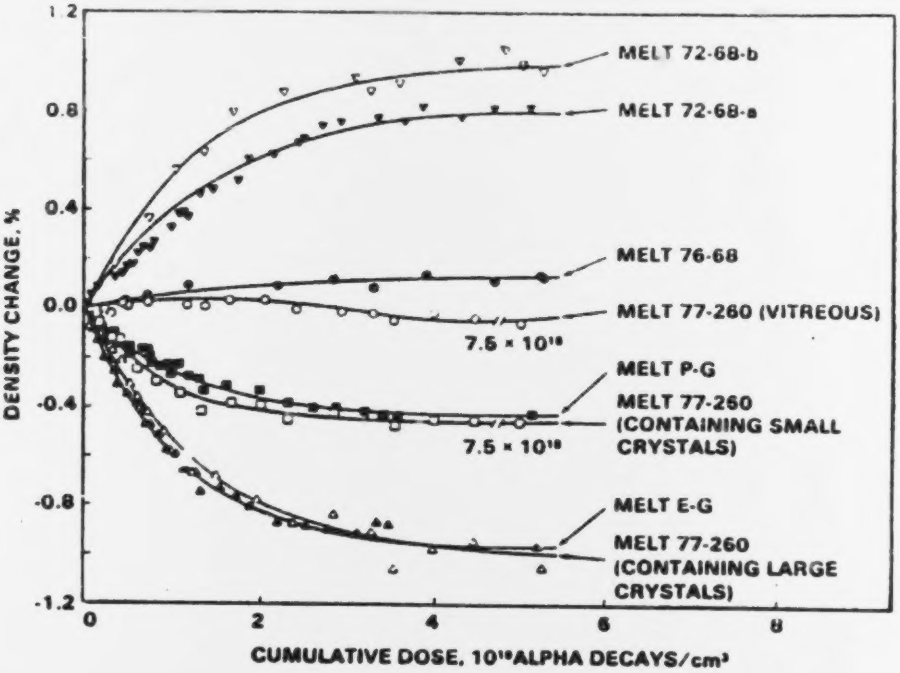

Figure 5.1 Volume changes in glass due to alpha-decay. from Roberts, Turcotte, and Weber, Ref.4.

and B are fitting parameters. A is thus the predicted density change at saturation, and B is the reciprocal "saturation dose". Typically, A ranges between ±0.01 while B^{-1} is of order 10^{18}-10^{19} alpha·decays/cm^3. This saturation dose corresponds to a storage time of 1000 to 100,000 years for commercial HLW glass and is greater than the 10^6 year dose for defense current HLW (Table 5.2). No direct information is available on how A and B vary with dose rate or temperature.

Ionizing radiation may also produce volume changes in glasses. For fused silica, the volume compaction depends on impurity content; typically doses near 10^{11} rad are required to produce swelling of 0.1%.[37] Recently, Shelby[38] has studied density changes produced by gamma irradiation of commercial borosilicate glasses. He finds that for some formulations, volume compactions near 1% can be produced by an irradiation dose of 10^{10} rad (Figure 5.2). The data do not indicate saturation up to 10^{10} rad. Extrapolation of these data to repository doses (Table 5.1) indicates a compaction approaching 10%.

Only limited data are available on ionization involved volume changes in simulated waste glasses. These commonly do not report any significant effects.[1,6] A detailed study of ionization radiation effects on the physical properties of borosilicate waste glasses is currently under way at the Savannah River Laboratory.[39]

BEST DOCUMENT AVAILABLE

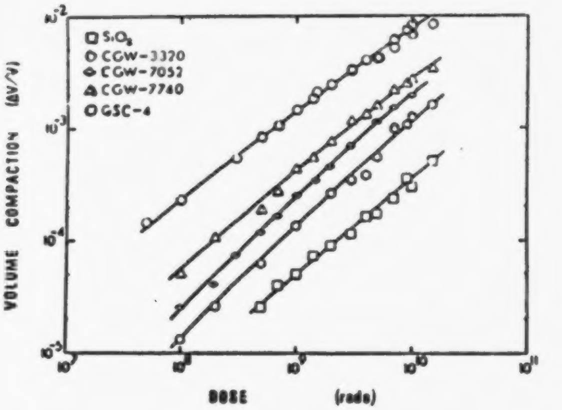

Figure 5.2 Effect of gamma radiation on glass density.

Irradiation induced volume changes may produce internal stresses within the waste form or generate stresses in inert barriers or containers. For sufficient stress levels fracture could result. Microfracture has been observed in both vitreous and partially devitrified simulated waste glasses following internal alpha decay.[26,28] It is not difficult to imagine that differential radiation-induced volume changes could be accommodated quite well in many systems by proper design. The point is that the consequences of such changes should be explicitly evaluated in any waste package design. This does not seem to have been done very often. Mendel has stated that typical waste containers should be able to accommodate a 1% radiation induced volume expansion of a glassy waste form.[40] Our own first order, highly simplified analysis of the possible consequences of radiation-induced stresses in waste package components, suggests that further more detailed consideration is indeed warranted in some cases.

Radiation-induced stresses in glass are being explicity considered in an NRC sponsored program at Iowa State University.[41] The objective of these investigations is to develop a means of predicting stress, fracture, and exposed surface areas in waste glass systems. At this time it is probably fair to say that precise prediction may be a formidable problem, involving a detailed investigation of the correlation between models and experiments. An analytic model for radiation induced stresses in glasses has also been developed in this program. Briefly, the model applies to situations where radiation induced volume changes occur in the presence of a thermal gradient in the waste glasses. The radiation induced volume changes are taken to vary with temperature (by virtue of relaxation processes) leading to differential stresses. Since thermal gradients in the waste form are expected to exist over (and in fact are intimately connected with) the period of intense beta-gamma decay, the present model would apply primarily to beta-gamma damage. On the other hand, significant volume changes could occur under isothermal conditions due to alpha-decay damage. This would be the situation prevailing after about the first 1000 years. In this region, it would

BEST DOCUMENT AVAILABLE

probably be necessary to consider certain effects not included in the present calculation, such as inhomogeneity in either the matrix (devitrification products, etc.) or the radionuclide distribution.

5.2.1.2 Leach Resistance

A number of studies have been carried out both in this country and abroad on the effects of radiation on the leach resistance of glasses. The majority of these studies have involved samples doped with alpha emitters. Typical results are tabulated in Table 5.3. These data indicate that the effect of internal alpha decay on leachability is rather small--changes are commonly less than a factor of two. It is particularly interesting that the devitrified waste glass 77-260, which exhibited amorphization of the devitrified phase and surface cracking, sensibly retains its leach resistance.

Recently, leaching measurements have been carried out on glass surfaces which have been implanted with heavy ions to simulate alpha recoil damage. Fused silica and high silica glass are found to be reasonably durable under the implantation, which was 10^{13} 200 keV lead ions/cm^2. The implanted layer in borosilicate glass, however, was rapidly etched away in saline solutions at 100°C. The most recent results obtained under heavy ion bombardments show a strong dependence on both leaching conditions and on sample type. Certain glasses show a strongly enhanced etching in NaCl brine at 100°C following implantation doses above a "threshold" value, while others do not. Similarly, the results in DIW at 100°C may show only a modest leachability increase (approximately three times) in contrast to that seen with brine, (approximately 50 times, Table 5.4). The relevance of these results to the situation in actual waste forms is still a subject of debate. Further comment on the equivalence between external heavy ion bombardment and internal alpha decay is given in the Task 4 Report; resolution of this issue falls most naturally in the province of test development.

A major difficulty in comparing results obtained with internal alpha decay and external ion bombardment is establishing equivalent doses. The French workers define a threshold dose of 5×10^{12} ions/cm^2 at which tracks begin to overlap.[32] They take this to correspond to an internal alpha decay dose of 2×10^{18} α-decays/g. Assuming a density of 3 for a waste glass this converts to an alpha decay dose of 6×10^{18} alpha decays/cm^3. There are, however, other criteria for determining equivalent doses for external ion bombardment and internal alpha decay as shown below (Table 5.5).

According to Table 5.3, the first three criteria have clearly been achieved by internal doping in a number of cases. These do not show any dramatic increases in leach rate. The last two criteria appears to have been achieved for internal alpha decay in at least two cases without serious consequences. In short, where comparison is at least plausible, data obtained with internally doped samples contradict the ion-implantation results. It may be argued that the effects observed in the ion-implantation results would become observable upon higher doses of internal alpha decay. However, for alpha-decay doses near 2×10^{18} α/gm^3 in glass, saturation effects are clearly evident in parameters such as volume change and stored energy.

Table 5.3

Leach Rates for Some Glasses Doped With Alpha Emitters

Dose (α/cm^3)	HLW 98[a]	189[b]	PNL 76-68		PNL 77-260[e]	PNL 77-260[e] Devitrified
Unirradiated		2×10^{-3}	8×10^{-6}[c]			
2.7×10^{16}	3×10^{-6}					
2×10^{17}			2×10^{-5}	6×10^{-5} [d]		
2.7×10^{17}		1.6×10^{-3}				
3×10^{17}					3×10^{-4}	3×10^{-9}
1×10^{18}	9×10^{-7}		1.5×10^{-5}			
2.3×10^{18}			1.1×10^{-5}		3×10^{-4}	5.7×10^{-4}
3.5×10^{18}	7×10^{-7}					
4×10^{18}				1×10^{-4}		
4.6×10^{18}					2.5×10^{-4}	5.5×10^{-4}
5.3×10^{18}		2.4×10^{-3}				
8×10^{18}		2.3×10^{-3}				
10×10^{18}				1.2×10^{-6}		

[a] Based on 241 Am; Ref. 25.
[b] Based on weight loss; Ref. 27.
[c] Based on potassium; Ref. 6.
[d] Based on soxhlet test; Ref. 29.
[e] Based on weight loss; Ref. 26.
All rates in g/cm^2-day.

Table 5.4

Sensitivity of Various Glasses to α-Recoil Aging As Simulated by Ion-Implantation[33]

	Composition (wt%)					Vo	ΔV	K
	SiO_2	Al_2O_3	B_2O_3	Na_2O	Other oxides	$g.cm^{-2}.d^{-1}$	$g.cm^{-2}.d^{-1}$	
4681	56	-	29	10	Li_2O:5	≤ $2.3\ 10^{-3}$	$9.5\ 10^{-3}$	> 3
4680	38	-	15	6	ZnO:30 K_2O:6 CaO:2 BaO:2	$2.9\ 10^{-4}$	$4.5\ 10^{-3}$	16
4678	64		12	24		$\sim 1.10^{-4}$	$1.9\ 10^{-3}$	20
ASA 15 N°7	67	5		16	SWO:12	$4.6\ 10^{-5}$	$1.2\ 10^{-3}$	27
BONI	48	5	15	18.5	SWO:13.5	$1.5\ 10^{-5}$	$8.2\ 10^{-4}$	53
4679	-	25	15	21	P_2O_5:38	$3.3\ 10^{-5}$	$4.3\ 10^{-4}$	14
Soda lime	75	1		11	CaO:9 MgO:2	≤ 5.10^{-6}	$1.4\ 10^{-4}$	> 28
SON 69 16	54	-	13.5	13	CaO:5, SWO:19.5	9.10^{-4}	$7.\ 10^{-5}$	1
4677	50	-	20	12	Fe_2O_3:17		$5.8\ 10^{-5}$	
PIVER 40-16	50	13	16	16	SWO:5		$2.4\ 10^{-5}$	
Pure silica	100	-	-	-	-		$1.4\ 10^{-7}$	

ASA 15 N° 7, PIVER 40-16 and SON 69 16 15 C_3 are simulated radwaste glasses prepared at Marcoule, the last one being the only one relevant to PWR wastes. BONI is a laboratory simulated radwaste glass prepared at ISPRA. Glasses 4677 to 4681 have been manufactured by Centre de Recherches St Gobain, Aubervilliers (France) for investigating the influence of glass composition on α-recoil aging.

SWO : simulated mixture of waste oxides.

The Vo and ΔV values refer to both a lead ion fluence of $10^{13}.cm^{-2}$ and to our standard NaCl solution ($250g.1^{-1}$, T~100°C, P~1bar).

Vo = Initial Leach Rate; ΔV = Change in Leach Rate due to Implantation; $K = \Delta V/V_0$

Table 5.5

Dosimetry Equivalence between External Ion Bombardment and Internal Alpha Decay*

Criterion	"Threshold" Ion Implantation	Equivalent Alpha Delay Dose (Recoil)
Implantation Density	$5x10^{12}/cm^2$	$1x10^{18}/cm^3$
Displacements per Unit Volume	$5x10^{12}/cm^2$	$2x10^{18}/cm^3$
No. Tracks per Unit area in Bulk	$5x10^{12}/cm^2$	$4x10^{18}/cm^3$
Dran, et al.[31]	$5x10^{12}/cm^2$	$\sim 6x10^{18}/cm^3$
No. Tracks per Unit Area at Surface	$5x10^{12}/cm^2$	$8x10^{18}/cm^3$

*Assumes a range of 500 Å for the implanted ions and 250Å for the alpha recoils. The general relationship is $F = \rho \cdot R/2$ where F is the particle flux/unit area (in bulk), ρ is the density of internal decays which generate the particles and R is the particle range.

BEST DOCUMENT AVAILABLE

While these parameters do not directly measure chemical durability, the general trend suggests that if damage tracks are indeed formed and ultimately overlap, the overlap has already begun at 2×10^{18} decays/cm^3. Direct comparison between the ion-implantation and internal alpha-decay results is further complicated by the fact that little leach data are available for internally doped samples in hot brine solutions.

Measurements are currently under way at PNL and SRL on the effect of gamma radiation on leachability. These data, unlike some previous gamma ray measurements, are being obtained on samples leached during irradiation. Initial results are given in Table 5.6 for 76-68 waste glass. Data are also shown for supercalcine. The fractional leach rates are given in terms of the amount of material released after leaching for 304 h under gamma irradiation at 90°C. The total dose is roughly 10^{-3} of that expected in the actual waste form. Under the test conditions gamma irradiation produced only a relatively modest (about 2X) increase in the glass leach rate as determined by weight loss. The release rates for cations such as sodium and calcium were more noticeably affected.

Table 5.6

Fractional Leach Rates For Glass and Supercalcine Without Gamma-Irradiation (Modified From McVay[42])

	7668 Glass		Supercalcine	
Element	γ-irradiation (cm hr)	no irradiation (cm hr)	γ -irradiation (cm hr)	no irradiation (cm hr)
Si	2.27 x 10	6.53 x 10	1.48 x 10	3.24 x 10
B	2.80 x 10	9.50 x 10	--	--
Ca	3.14 x 10	4.41 x 10	1.38 x 10	4.10 x 10
Sr	2.15 x 10	4.89 x 10	2.15 x 10	1.97 x 10
Ba	1.38 x 10	1.16 x 10	1.54 x 10	3.05 x 10
Na	6.64 x 10	1.22 x 10	2.26 x 10	9.50 x 10
Cs	1.83 x 10	1.27 x 10	7.15 x 10	5.05 x 10
Mo	2.58 x 20	2.67 x 10	3.51 x 10	5.33 x 10
Ni	2.53 x 10	--	2.93 x 10	--

All samples were leached for 209.5 hours in deionized water at ~90°C;
V/SA ratio = 10/1
Radiation dose rate = 2.4×10^6 R/hr; Total dose = 7.4×10^8 R.

Under the experimental conditions either solution radiolysis or radiation effects in the glass may contribute to the enhanced release rate.

For glasses, more recent data indicate that the enhanced leaching is due to radiolysis effects on leachant chemistry. Both the PNL and the SRL studies show that nitric acid, formed by water radiolysis in the presence of atmospheric nitrogen, can significantly enhance leach rates by lowering the leachant pH (Table 5.7). In the measurements on PNL 76-68 glass, it does not appear that acid formation in the presense of air can account for all the irradiation enhanced leaching; elements such as Zn and Fe, which are incorporated in passivating layers, may be most sensitive to acid conditions. Conversely, in SRL glass, at a dose rate of 1.5 x 10^6 R/hr, no effect on leach rates is observed until the pH drops (at approximately 10^9 R) due to acid formation. At higher dose rates, 5 x 10^6 R/hr, radiation enhanced leaching is observed in SRL glass exclusive of acid formation--the effect is a modest 60% increase. Evidently, the importance of factors other than irradiation induced pH changes depends on the radiation dose rate, and possibly depends on sample type. At repository dose rates, these effects could be less significant than those measured here. Dose rate and temperature data are presently becoming available in the PNL experiments. Measurements have also been carried out on alpha-and beta-radiolysis effects on SRP glass leaching. Thus far, no significant effects have been found.[39]

5.2.1.3 Helium Buildup

Helium is formed by electron capture when alpha particles are stopped in matter. The consequences of this effect have been considered by a number of authors.[1,25,28,44,45] In crystalline materials, helium bubbles have been observed to form along grain boundaries, affecting mechanical properties;[5] vitreous glasses, however, will not suffer from this effect. The amount of helium produced in the waste form can be estimated from data such as that in Table 5.2. Depending upon the waste loading, values after 10^5-10^6 years may be between 0.1 and 1 atomic percent. Were this helium released, it could pressurize the container. In tightly packed containers, this pressure could be substantial. This can, of course, be ameliorated either by helium diffusion or leakage through retaining barriers, by providing a suitable expansion volume, in the container, or by retention of the helium within the radionuclide host.

Helium diffusion rates in glass depend strongly on temperature and apparently decrease as radiation damage builds up.[44,45] The available evidence suggests that helium largely remains in the glass under the accelerated testing conditions where radiation effects on swelling and leach rates were studied.[3,6,7,23,31] These experiments gave no evidence of significant helium related effects on the mechanical properties of the glasses.[6,25,26,28] The time scale of these experiments, of course, is of the order of years rather than centuries. It is possible that at the low alpha decay rates encountered in actual waste forms, the situation might be somewhat different - the helium formation rate would become more nearly commensurate with the helium diffusion rate and significant buildup of helium within the waste glass would not occur. Malow and Andersen have recently estimated mean square displacements between

Table 5.7

Effect of Gamma Irradiation on Glass Leaching

	PNL 76 68 Glass 5 Day Leach+			SRL Defense HLW Glass[39] Periodic Sampling	
Gamma Dose Rate (R/hr)	2.4×10^6	2.4×10^6	0	1.5×10^6	5.8×10^6
Leachant	DIW (50°C)	DIW (50°C) Air Excluded	HNO_3	DIW (<45°C)	Buffered DIW (50°C)
pH (Initial/ Final)	5.7/3.3	5.7/6.5	3.5/3.9	6.5/4.0	6.8/6.8
	Increase in Leach Rate:				
Element					
Si	6 x	6 x	2.2 x	Unchanged for doses <10^9 rad; following pH drop, uniform 2 x increase occurs.	1.6 x
B	4 x	3.4 x	2.6 x		1.6 x
Na	6 x	4.6 x	3 x		1.6 x
Cs	4 x	1.8 x	1.8 x	--	--
Sr	7 x	3.5 x	3.5 x	--	--
Zn	33 x	13 x	14.5 x	--	--
Fe	>130 x	>3 x	>60 x	--	--

+The PNL reviews give total amount released in a 5-day leach. We take this to be proportional to the leach rate to obtain the factors given in Table 5.7.

3 and 10 cm for helium diffusion in glass waste forms, after 10^6 years.[45] Thus, for glass waste forms of the size commonly proposed, most of the helium would be expected to remain in the glass. Surface to volume ratios and cracks would be important, however.

5.2.1.4 Stored Energy

When atoms or electrons are displaced from their equilibrium positions in a solid by radiation, the internal energy of the system is raised. In a number of cases, the system can be largely restored to its equilibrium configuration by (thermal) annealing. This process is exothermic and the energy which is given off is termed stored energy. Historically, stored energy has been of practical interest in radiation effects studies because of the possibility that its catastrophic release might damage critical components. It is now generally agreed that this will not be a problem in waste glasses. More recently, stored energy has become a commonly accepted parameter for use in intercomparison of radiation effects.[8]

Stored energy measurements have been carried out on most of the waste glasses currently under study. The data indicate a remarkable degree of similarity (Table 5.8): stored energy shows saturation behavior at an internal alpha dose near 10^{18} alphas per gram for a wide variety of materials (Figure 5.3). The saturation behavior is also implicit under neutron irradiation, heavy ion bombardment and internal fission. These latter irradiations are conducted at vastly different radiation dose rates than the internal alpha decay; however, the saturation behavior seems to persist and, when the radiation doses are normalized to estimated DPA, saturation commonly begins at about 0.1 DPA. It is at about this dose, which we take as equivalent to $\sim 10^{18}$ α/g, that saturation behavior in the radiation induced swelling is also observed (Figure 5.1). Taken together, these data suggest it is only the first ten percent* of the internal alpha decays which may significantly affect the waste glass. These decays will occur during the first 1000 years. Following this, more subtle changes in internal structure may take place, and of course helium buildup will continue. The similarity of stored energy and swelling data obtained with different dose rates and varieties of radiation further suggests that it is the number of displaced atoms and not the radiation dose rate which is a determining factor in the damage formation.[8] This result supports the validity of accelerated testing with doped samples. These speculative arguments, however, require further confirmation.

5.2.1.5 Transmutations

The effects of transmutations due to beta decay of fission fragments in HLW forms are being studied.[50] Samples containing ^{133}Cs have been neutron irradiated to convert the ^{133}Cs to ^{134}Cs, which transmutes to ^{134}Ba with a two-year half life. Immediately following irradiation, samples were annealed to remove neutron damage. Density measurements are being periodically carried out as the transmutations build up. Thus far, about 3% of the total Cs has transmuted to Ba. For simulated waste glass, high Cs glass, high silica glass, high alumina glass, pollucite and supercalcine, preliminary results show no significant effect of transmutations on waste form stability.

---

*Referred to the million-year dose.

Table 5.8

Saturation Behavior in Stored Energy Buildup

Material	Saturation Stored Energy (cal/g)	Saturation Alpha Dose (α/g)	(DPA)	Remarks
72-68 Glass (E)	30	4×10^{18}	0.4†	46
Lead Glass	21	1.2×10^{18}	0.12†	46
European Glass	30	1.2×10^{18}	0.12†	46
HLW 98 Glass	83	1×10^{18}	0.1†	25
76-260 Glass	25	1×10^{18}	0.1†	26
76-260 Devit.	20	1×10^{18}	0.1†	26
SPC-2 Supercalcine	10	5×10^{17}	0.05†	47
BONI Glass	18		0.1	Internal Fission[8]
BONI Glass (I)	35		0.1	Heavy Particle Irradiation[8]
72-68 Glass (I)	23			Neutron Irradiation[48]

† Our estimate, using 1 DPA = 10^{19} α/g.
All saturation values are approximate; (E) indicates that the actual saturation level was not precisely observed; (I) indicates that the data density is insufficient to rigorously confirm saturation.

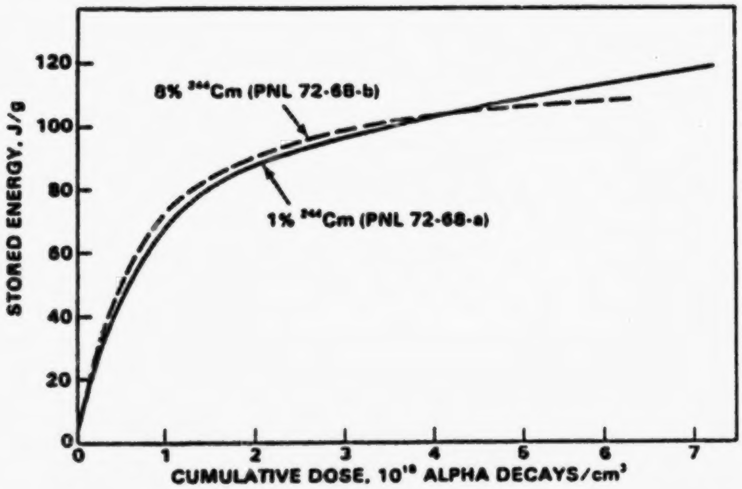

Figure 5.3 Effect of dose rate on stored energy in ^{244}Cm-doped PNL 72-68 HLW glass. Adapted from Turcotte and Roberts, in Ref. 49.

BEST DOCUMENT AVAILABLE

5.2.1.6 Other Effects

In addition to those mentioned above, certain other radiation effects are known to occur in glasses which may affect their suitability as HLW waste forms. Among these are irradiation enhanced diffusion, changes in oxidation states and transmutation of incorporated HLW elements. Charge states can be altered by ionizing radiation. Sodium, for example, often appears in glasses as a local charge compensator (near a trivalent element for example). Should the charge state of this element be modified by ionization effects, the sodium can diffuse away.[14] This may be considered one form of radiation enhanced diffusion;[19] it is possible that this effect may be operating in the leaching studies conducted during gamma irradiation (Table 5.6).

Cerium is a well known example of an element which can change its charge state in glass under ionizing radiation.[51] This element will, of course, be present in HLW waste streams. In glasses, the structural consequences of such an irradiation induced change in ionization state are probably not very serious. The situation must be re-examined for crystalline waste forms.[52] In either case, the effect of ionization on actinide mobility at repository temperatures should be determined.

5.2.2 Crystalline Waste Forms

These comprise the various ceramic systems such as SYNROC, supercalcines, high alumina-tailored ceramics and titanates. As is the case for glassy systems, a number of multibarrier modifications of basic ceramic waste forms have been proposed. The multibarrier systems and hybrid systems (e.g., glass-ceramics) will be considered separately. Here we deal with radiation effects on the fundamental ceramic phases which contain the radionuclides. In most cases there is at present very little radiation damage information available on the actual materials. That which does exist largely concerns metamictization and swelling. While we are confident that the situation will improve in the very near future at this point we must rely to a certain extent on information obtained from generic materials or natural analogues.

Such information can in no way be considered a complete measure of the radiation damage response of actual ceramic waste forms. In particular, the proposed ceramic waste forms share one feature which distinguishes them from waste glasses: the radionuclides in ceramic waste forms will by design be inhomogeneously partitioned among the various phases present in the ceramic. As a result, the distribution of radiation dose within ceramic waste forms is inherently inhomogeneous, and the potential exists for degradation of the waste form by differential radiation damage effects (such as localized swelling and cracking[26]). Under these conditions, it is premature to rigorously infer the radiation stability of a ceramic waste form by studying the behavior of a few component phases.[7] With this in mind, the available data are assessed below.

5.2.2.1 Metamictization

Certain component phases of proposed ceramic waste forms, or their natural analogs, are known to become metamict (or x-ray amorphous) after heavy internal alpha-decay doses. These include the zirconolite phase of SYNROC,[7] the apatite phase of supercalcines and the rare earth titanates in glass ceramics and devitrified glasses. Ringwood[7] has examined natural radioactive zirconolites which have been exposed to heavy internal alpha decay doses (Table 5.9). He finds that samples which have received doses of roughly 10^{18} α/g are largely crystalline, although there is some disorder on the cation sublattice. With increasing dose, disorder increases and metamictization is complete in samples with estimated doses of 2×10^{19} α/g. These samples, and others which have received even greater doses, are said to be completely unaltered, and to have retained essentially all the lead decay products after prolonged weathering under geological conditions.

Metamictization in the apatite phase of supercalcine SPC-2 has been observed at an alpha dose of $\sim4.2\times10^{18}$ α/cm^3 in doped samples.[50] The tetragonal and fluorite supercalcine phases were sensibly unaffected. However, the partitioning of the curium was apparently such that the fluorite phase was largely undoped. Consequently the reported α/g values for the apatite phase may be somewhat low, if curium was concentrated in this phase. We have mentioned earlier the reported metamictization of the apatite phase in devitrified borosilicate glasses.

The gadolinium titanate phase (pyrochlore structure) in celsian glass ceramic becomes metamict following 3.2×10^{18} alpha decays/cm^3 in doped samples. For the same structure in devitrified glass metamictization is not observed at doses in excess of 5×10^{18} alpha decays/cm^3. Also the pure compound analog of the apatite structure in SPC-2 is not completely metamict for doses greater than 6×10^{18} α/cm^3. It is not clear whether the apparent variation in sample-to-sample durability actually reflects fluctuations in the local dose or indicates that the radiation resistance of a given phase is sensitive to trace impurities or process conditions.[50]

The fluorite structure (PuO_2, UO_2) is evidently quite stable against internal alpha decay; others such as zircon (thorite structure) and perovskite may be easily damaged (Figure 5.4). Monazite (huttonite structure) also appears to be quite durable in natural analogs and is being considered as a host for TRU elements.[55] (See the Task 2 Report for further discussion.)

Structural damage in crystalline host phase materials has also been studied under external irradiation, including alpha particles, neutrons and heavy ions.[2,33,50,59] Studies have also been carried out using internal fission to produce damage. The fission is induced by neutral irradiating, uranium doped samples. Internal fission doses in excess of $10^{15}/cm^3$ are required to produce the metamict state in silicates (zircon; huttonite) phosphates (monazite) and titanates (zirconolites). This dose is several orders of magnitude greater than that anticipated for spontaneous fission. Oxides such as MgO, α-alumina, Fe_2O_3 and PuO_2 do not exhibit structural effects for internal fission doses $>10^{15}/cm^3$. Several of these phases may appear in alumina/silica-tailored HLW ceramics.[60] Phases such as pollucite or scheelite are not expected to incorporate actinides, and have been examined only peripherally by internal fission.[2]

The quantitative correspondence between the damage produced by internal alpha decay and by external ion bombardment or internal fission is difficult to establish. The trend has been to calculate the number of collision-induced

Table 5.9

Structural Damage in Ceramics for Internal Alpha Decay and Internal Fission

Material	Metamict Dose Alpha Decays/cm^3 x 10^{-18}	Metamict Dose Internal Fissions/cm^3 x 10^{-14}	Ref.
Zircon	45+	60	53,2
Monazite	N.D.(200)+	20	54,2
Huttonite	--	20	2
Zirconolite	80+	60	7,2
SPC-2 (Apatite phase)	4.2	--	50
Devit Glass (Apatite phase)	1.5	--	50
Glass Ceramic (Pyrochlore phase)	3.2	--	50
Devit Glass (Pyrochlore phase)	N.D.(5)	--	50
PuO_2, UO_2 (Fluorite)	N.D.(50)	N.D. (10^7)	56,57,2
Perovskite	--	N.D. (100)	58
$CmAlO_3$ (Perovskite)	11	--	58

+Data from natural analogs.
N.D.= None detected for a dose of ( ).
Assumed densities: Zirconolite, 4.0; zircon,4.5, Monazite,5.0; $CmAlO_3$, 7.0.

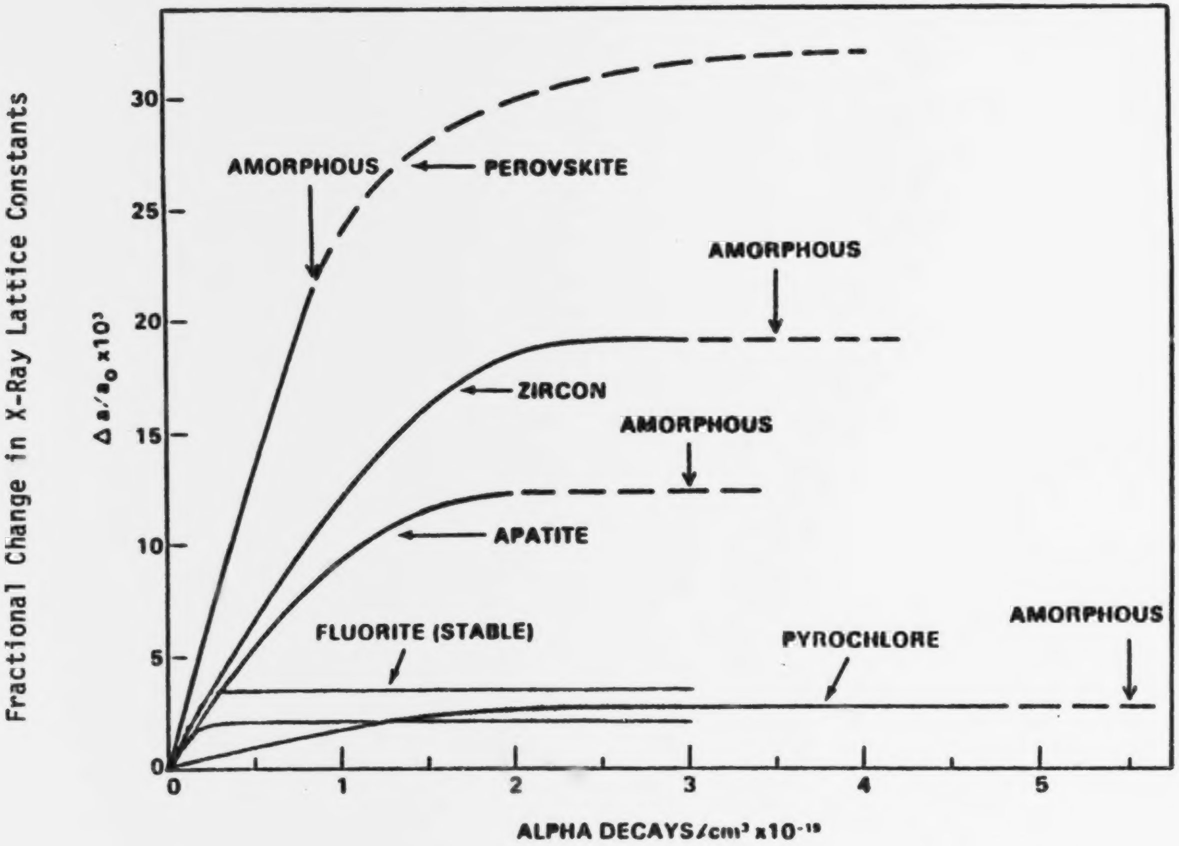

Figure 5.4 Effects of internal alpha decay on various crystal structures. From Weber, Wald, and Gray, reference 55.

BEST DOCUMENT AVAILABLE

atomic displacements produced by each technique and compare results at equivalent displacement doses (DPA). On this basis the relative efficiency for damage formation may vary substantially for different irradiations. For example, Weber finds that 5 MeV alpha particles, on a DPA basis, produce swelling with about twice the efficiency of alpha-recoil in UO_2.[56] Vance and Pillay have cited evidence indicating that, in zircon, fission fragments may produce damage with an efficiency which is 1000 times greater than that for alpha-recoils on a collision induced DPA basis.[2] They suggest that ionization induced displacement may account for the increased efficiency. Further, they conclude that internal fission is qualitatively not a good simulation for internal alpha decay. The relative durability of natural analog monazite phases suggested under internal alpha decay is not reflected in the internal fission experiments (Table 5.9).

Presently, little direct information is available on ionization effects in crystalline waste forms at repository doses. The possibility that ionizing radiation might produce atomic displacements in some crystalline waste forms (internal radiolysis) has been discussed by Hobbs.[10] A number of systems incorporating the silicate tetrahedron are known to undergo internal radiolysis[61] (Table 5.10); the silicate tetrahedron is a common structural unit in waste form materials. The susceptibility to internal radiolysis varies dramatically from material to material. Defect concentrations in alkali halides may approach as much as 1% following a dose of 10^{10} rad. A dose estimated at 10^{13} rad is required to promote metamictization in quartz.[18] A large number of materials such as alkaline earth oxides show no evidence of internal radiolysis. Hobbs has outlined the general characteristics which may favor susceptibility to internal radiolysis.[61] The requisite data are not available to apply these considerations to structures like perovskite.

5.2.2.2 Swelling

Radiation may cause ceramics to swell; radiation induced compaction is uncommon in crystalline ceramics. In refractory oxides such as Al_2O_3 a substantial dose of heavy particle irradiation (of order 1 DPA) is required to produce swellings of one or two percent.[5] In other materials no swelling is observed even at these doses. On the other hand, certain ceramics of interest as candidate waste forms exhibit swelling at much lower radiation doses. It is likely that this reflects differences in the swelling mechanism.

Several multiphase waste forms and actinide host phases have been studied by doping with short lived actinide isotopes.[57] Changes in density, stored energy and lattice constant are monitored as a function of accumulated alpha dose. These property changes can in general be fit to a saturating exponential relationship similar to equation (1):[57]

$$X = A\,[1 - \exp(-BD)] \qquad (2)$$

where D is the dose, A and B material constants and X the property being measured. Generally, saturation is observed at about 5×10^{18} alpha decays-/cm^3 (this corresponds to a storage time of about 10^3-10^4 years for HLW; current defense waste will not achieve this dose in 10^6 years).

Table 5.10

Inorganic Solids in Which Internal Radiolysis is Known to Occur
(Tabulated by Hobbs, Ref. 61)

---

alkali halides (LiF, LiCl, LiBr, LiI, NaF, NaCl, NaBr, NaI, NF, KCl, KBr, KI, RbF, RbCl, RbBr, RbI, CsF, CsCl, CsBr, CsI)

alkaline earth halides (CaF_2, SrF_2, BaF_2, MgF_2)

silver halides (AgCl, AgBr, AgI)

cadmium halides (CdI_2)

lanthanum halides (LaF_3)

lead halides (PbI_2)

perovskite halides ($NaMgF_3$, $KMgF_3$)

silicas (quartz cristobalite, fused silica)

silicates (alkali feldspars, some amphiboles, mica)

ice (H_2O)

alkali hydrides (LiH)

alkali azides (LiN_3, NaN_3, KN_3)

sulfides (MoS_2)

carbonates ($CaCO_3$)

alkali perchlorates (NH_4ClO_3,$NaClO_3$,$KClO_3$)

alkali bromates ($NaBrO_3$)

Generally, for multi-phase waste forms such as partially devitrified glass, celsian glass ceramic and SPC-2 supercalcine, the overall volume dilation at saturation is about 1%. On the other hand, the dilation for individual radionuclide bearing host phases may be much larger. Apatite structures in partially devitrified glass and SPC-2 increase 3-4% by volume and become X-ray amorphous at saturation (see Table 5.9). This difference between the various phases in multi-phase form may lead to cracking, as pointed out earlier. Phases with the fluorite structure (e.g., PuO_2) exhibit minimal swelling. Figure 5.4 gives some comparative swelling data obtained under internal alpha decay.

The data for the (supercalcine) apatite phase (Figure 5.4) were obtained with curium doped samples. It is noteworthy that, as in devitrified glasses, the apatite phase exhibits a pronounced swelling. The tetragonal and fluorite phases of the supercalcine were then less noticeably affected. However, as in the devitrified glass, preferential partitioning of the ^{244}Cm occurred in the apatite and (presumably) tetragonal phases. Thus, it is difficult to be certain of alpha decay doses within the individual phases. It is probable that the fluorite phase was not significantly irradiated. (This observation, incidentally, illustrates the fact that it is not always a trivial matter to realistically simulate radiation damage within an inhomogeneous waste form).

In certain cases, as shown in the table, saturation of the radiation induced swelling has been observed. For the supercalcine, overall swelling saturates at about 1.5×10^{18} α/g, and the total swelling is ~1.5%. This is less than the swelling of the apatite phase, estimated at 3%, but volumetric considerations suggest that other phases may contribute to the overall swelling as well. The apatite concentration in supercalcine is estimated at 12.5%.[7] In other cases, notably zircon, saturation is not in evidence. Zircon continues to swell linearly with α-dose to a volume increase of 12% at about 8×10^{18} α/g. Zircons are observed to become metamict at about the same α-dose as Ringwood finds in zirconolite (Table 5.9). It is important to determine if the swelling in zirconolite is similar to that in zircon.

In natural zirconolite, a density change of ~3% at 10^{19} α/g is inferred from annealing data; this may not indicate a true radiation effect.[7] Recently, neutron irradiation damage measurements have been reported for synthetic barium hollandite, perovskite, zirconolite, and SYNROC B and SYNROC C.[62,63,64] The equivalence between neutrons and internal alpha decays was assumed to be on a DPA basis: (6.5×10^{19} n/cm^2 = 0.18 DPA). Swelling was observed in all cases (Table 5.11).

IN SYNROC B at 3×10^{18} α/gm, this dimensional change is commensurate with the observed density decrease; for perovskite and hollandite, it is not. Extensive microcracking was observed in the perovskite and hollandite, possibly accounting for much of an increase in observed porosity. Only isolated microcracks were observed in SYNROC B. The volume expansion in hollandite and perovskite can be directly related to lattice parameter changes; the samples did not become metamict. The expansion for neutron irradiated prototype SYNROC B is probably not typical of that which would occur in a waste form. The colli-

Table 5.11

Density Changes in Neutron Irradiated SYNROC and SYNROC Minerals

Equivalent Alpha Decay* Dose ($(\alpha/g) \times 10^{18}$)	Percent Volume Expansion[62,63]				
	Hollandite**	Perovskite***	Zirconolite	SYNROC B***	SYNROC C
2.5	--	--	1.7	1.4	17-2.2
3.0	1.4	2.6	--	1.7	--
4.5	0.9	2.2	--	3.5	
30	1.9	3.4	--	5.5	

* Assuming 6.5×10^{19} n/cm^2 = 0.18 DPA = 2×10^{18} α/g in Ref. 64.
**In all cases, the hollandite dose exceeds the 10^6 year expected value.[64]
***For perovskite and SYNROC B, 30×10^{18} α/gm $\sim 10^5$ year dose.[64]

sion mean free path for neutrons in these materials is typically several centimeters, resulting in a spatially homogeneous irradiation dose. Consequently, neutron irradiation cannot hope to reflect the local inhomogeneities in radiation damage which may occur in SYNROC waste forms. Three of the four perovskite specimens irradiated to $\sim 30 \times 10^{18}$ α/g split cleanly across a diameter during or after irradiation; all other specimens were intact.[63]

The mechanism by which these effects occur is obviously a question of some importance. In principle, swelling may occur either through growth of voids and aggregate defects, or by accumulation of point defects which dilate the lattice.[5,10,61] Aluminum oxide swells by void formation, which requires relatively long range atomic diffusion and exhibits a characteristic peak swelling temperature. The swelling mechanism for many of the candidate waste form materials at ambient temperature is not known. For SYNROC it apparently involves a "lattice" dilation under neutron irradiation. Experience with silicate systems suggests that swelling in zirconolites or apatites might involve a relatively localized reorientation of local bonding polyhedra to a more random configuration, rather than long range atomic diffusion and aggregate formation. This process might be fairly sensitive to the local lattice structure. Haaker and Ewing have pointed out that materials with the monazite structure may, as a class, be more resistant to radiation than those with zircon-like phases.[65,66]

The saturating exponential dependence observed in the swelling curves of a number of these materials can at least be rationalized by a simple model assuming first order annealing kinetics during irradiation.[56] The actual mechanism of annealing is of some concern, since it may govern radiation dose rate dependence. In particular it is important to determine the extent to which the mechanism is thermal or athermal (i.e. radiation-induced). This information is not currently available.

5.2.2.3 Leach Resistance

There is hardly any information available on the extent to which radiation induced effects such as metamictization and swelling will affect leach rates. One expects that extensive microfracturing, for example, would enhance leaching. The only evidence we have obtained so far, however, is indirect and contradicts assumptions: in devitrified glass,[26] radiation induced metamictization and swelling of the devitrified gadolinium apatite phase evidently did not enhance leach rates under the test conditions. Nor, surprisingly, did mirocfracture. Ringwood reports that heavily damaged ($>10^{20}\ \alpha/g$) natural radioactive zirconolites and perovskites have remained unaltered and retained essentially all the lead decay products under severe weathering conditions.

Leaching measurements have been carried out on natural perovskites and zirconolites which have received internal alpha decay doses estimated between 1 to $8\times10^{18}\ \alpha/g$.[64] These do not show a clear correlation between leach rate and radiation dose; the total dose range is very limited. Generally, leach rates at 90°C and 200°C were less than 10^{-6} g/cm^2-day after 10 days of leaching, indicating that the irradiated samples are chemically durable. Leaching measurements are planned on neutron and helium bombarded samples.[63] At PSU, leaching studies are under way on metamict single phase samples produced by internal fission.[2]

Leaching studies have been carried out on supercalcine waste forms under gamma irradiation. Results are given in Table 5.6. The data indicate a fairly substantial enhancement of leach rates for the cations calcium and sodium. Other elements are more modestly affected.

5.2.2.4 Helium Buildup

No information has been collected on actual waste form materials. High helium permeability may enhance the radiation stability of materials in certain cases, particularly those which swell by void growth. Helium may collect in the voids and stabilize them, permitting further growth;[5,12] helium buildup along grain boundaries (or dislocations) could result in both a loss of mechanical strength and affect swelling behavior.[5,10,12] The extent to which these may occur in ceramic waste forms has yet to be assessed. Natural zirconolites several million years old have been found which are said to have retained roughly 36% of the total helium generated by alpha decay.[7] While this fact has been used to argue for the radiation durability of SYNROC, in view of the points discussed above, it is not clear that helium retention is necessarily favorable. One must evaluate its effect on the waste form.

5.2.2.5 Transmutations

Beta-gamma transmutation effects in crystalline forms are under investigation in the PNL study cited earlier. As yet, only preliminary data are available. These indicate nothing untoward. In crystals, the equilibrium co-ordination number is sensitive both to ionic charge and ionic radius. Both of these change rather drastically in the beta decay of ^{137}Cs and ^{90}Sr; when transmutations occur, the equilibrium state of the crystalline material will be modified. (This inevitable alteration of the equilibrium state is not always included in discussions emphasizing the thermodynamic stability of crystalline phases in comparison to glasses). For example, metamictization of cerium containing materials has been suggested to result from the slow oxidation of Ce^{3+} to Ce^{4+}, in the complete absence of any radiation effects.[52] As pointed out above, glasses may be more forgiving in this regard. They are not in equilibrium to begin with, and possess internal degrees of freedom which might allow some compensation for transmutations.

5.2.2.6 Other Effects

As we have mentioned, the oxidation state of matrix materials and radionuclides can be changed by ionizing radiation. Consequently, it seems to us that the effects of transmutation cannot be realistically assessed unless the simultaneous effects of ionizing radiation are also considered. For example, local charge redistributions brought about by ionizing radiation might relax the effect of beta transmutations to the extent that the system, while not in equilibrium, could be practically metastable. We feel that this speculation deserves further consideration. It is also interesting that in the supercalcine system, the chemistry of the apatite phase is determined to depend upon the oxidation state of cerium.[67] It is possible that the formation and stability of this phase might be influenced by radiation. Again, no data are available.

5.2.3 Glass-Ceramic Waste Forms

Glass-ceramic waste forms are here taken to include materials such as VCP15 and celsian glass-ceramic. In these systems differential radiation damage effects are to be anticipated, since the radionuclides are presumed to be largely contained in the crystalline phases. There is as yet little information available on the radiation effects to be anticipated in these systems. Were it possible to distribute radionuclides more homogeneously throughout the system, one might conceive of a situation in which the radiation induced swelling of the crystalline phases is counterbalanced (largely) by glass compaction. Barring this, it seems that differential swelling and cracking under irradiation, as in devitrified borosilicate glasses, remains a real possibility.

Radiation enhanced devitrification should also be considered. The information here is sketchy and there appear to be no extensive investigations of radiation effects on devitrification kinetics. However, we know of no case where radiation has unambiguously provided devitrification in a glass. The studies cited above, including thermal analysis for stored energy release, make no mention of a radiation enhanced devitrification for doped waste glasses, and in some cases radiation is said to reduce crystallinity.

5.2.4 Multibarrier Waste Forms

Multibarrier waste forms are those in which the radionuclide host is either encapsulated in some kind of coating, embedded in a matrix material, or both. In all proposed forms of which we are aware, the radionuclide host is either a ceramic or glassy material of the type discussed previously. The fundamental radiation effects within these host forms will not be modified by the additional barriers in multibarrier schemes. In considering radiation effects on multibarrier forms, then, the central concern is whether radiation effects will either degrade the barriers or render the radionuclide host and coating incompatible. We are aware of only one multibarrier form where the radiation damage effects have been investigated -pyrolytic carbon coated particles which are intended to serve as fuel for gas cooled reactors.[68] We will proceed, then, by examining radiation effects on coatings and matrix materials, and on possible interactions between the radionuclide host and the barriers.

5.2.4.1 Radiation Effects on Coating Materials

Among the materials which have been proposed for coating or encapsulating radionuclide hosts in multibarrier waste forms are pyrolytic carbon, nickel, aluminum oxide and, in the porous glass scheme, high silica glass. In all cases, the proposed coating thicknesses are hundreds of times greater than the range of an alpha-recoil nucleus.[36,47,68] Radiation damage from recoil nuclei ejected from the waste form, if it occurs at all, will be sensibly limited to the first few hundred angstroms of the inner coating surface. Similarly, while alpha particles may penetrate further, there is no danger of the coating being penetrated by damage tracks. From geometric arguments we can get a rough idea of the maximum implantation flux of alpha recoils which would occur at the inner surfaces of coatings on radionuclide host phases. This is of order of $10^{13}/\text{cm}^2$ after about 10^6 years for typical waste loadings. Within the implanted layer, both the particle concentration and energy deposition will fall off rapidly with penetration depth.

Radiation damage studies on pyrolytic carbon have been carried out for a number of years in conjunction with gas cooled reactor development. These measurements, of course, address conditions anticipated in reactor operation, rather than HLW waste form applications. Commonly, these involve irradiation to fluences of 10^{21}-10^{22} neutrons/cm^2.[69] Early measurements were carried out to study the so-called "spearhead" attack of inner pyrolytic surfaces which was attributed to energetic fission fragments.[70] References to this effect have not appeared in the recent literature. Neutron irradiation is found to cause anisotropic dimensional changes in pyrocarbons. The susceptibility of pyrocarbon layers to radiation damage depends sensitively upon material parameters such as density and anisotropy. These in turn are governed by the deposition process. Spearhead attack is said to be controlled either by incorporating a highly porous sacrificial inner layer, or by deposition of high density coatings. This may involve high deposition temperatures. Cracking due to neutron bombardment is minimized in coatings which are both dense and highly isotropic.

We feel that reactor conditions are likely to represent a more severe test for particle coatings than those anticipated in HLW applications. Thus, the fact that PyC coatings can operate under reactor conditions is strong testimony for their suitability in HLW forms. Since, however, the radiation resistance of PyC is sensitive to processing steps it is possible that certain coatings, such as those deposited at low temperature to reduce the release of volatile HLW components,[68] may be less radiation hard; some examination here is warranted. In addition, factors such as the effect of temperature on damage formation must be understood, since different temperatures are involved in reactor and waste repository applications. In view of the large volume changes which may occur in waste forms such as SYNROC, a porous sacrificial layer may be an absolute requirement in some cases. Porous layers able to accommodate a swelling of 6% or more can be readily achieved by present technology.

Metals such as nickel or lead will probably be largely unaffected by radiation damage at the levels anticipated in waste form barriers or matrices. (See Section 5.3 for a more complete discussion.) In terms of radiation resistance these should be considered superior. Insulating coatings such as aluminum oxide or high silica glass are expected to be durable under the anticipated conditions also. Silica appears durable under modest ion implantation.[31] It is probable that if these coatings can withstand the thermal stresses inherent in manufacture, damage to the inner surface should cause no great harm; indeed some stresses might be relieved. Since, however, aluminum oxide and glass are subject to brittle fracture, a more careful assessment is warranted.

5.2.5 TRU Waste Forms

Traditional waste forms intended to fix TRU elements have been identified in Section 2.7.2 and in the Task 2 Report. These include organics such as bitumen and urea-formaldehyde resins, and several concrete formulations. Since TRU elements are present in HLW, the high level waste forms discussed earlier must also be considered potential candidates for TRU retention. In fact, as pointed out in the Task 2 Report, after the first 1000 years, HLW waste forms sensibly become TRU waste forms.

Insofar as radiation effects are concerned, the essential difference between TRU and HLW waste form requirements is that the TRU waste forms will not be exposed to the substantial beta-gamma flux due to fission fragment decay. As mentioned earlier, the recoil nucleus in alpha decay efficiently produces displaced atoms. The alpha particle, although it carries far more energy, dissipates nearly all of this energy by ionization as shown in Table 5.12. No attempt has been made in Table 5.12 to depict actual loadings, since these are for the most part undetermined at present. The object is to illustrate relative efficiencies for different fundamental processes.

5.2.5.1 Traditional Waste Forms

The traditional waste forms discussed in the Task 2 report include organics and concretes. The organics are not considered acceptable candidates for long term disposal. Concretes contain water which is subject to

Table 5.12

Radiation Conditions in TRU Waste Forms

Radiation	Effect	Efficiency*
Recoil Nucleus	Displacement	$10^3\ \frac{\text{Displaced Atoms}}{\text{Decay}}$
Alpha Particle	Displacement	$10^2\ \frac{\text{Displaced Atoms}}{\text{Decay}}$
	Ionization	10^{18} α/g ↔ 8×10^{10} rad
	Helium Buildup	10^{18} α/g ↔ 100 ppm He

*Typical value ranges for glasses and ceramics.

α-radiolysis. In addition, the TRU waste itself may contain molecules or molecular ions which undergo radiation induced decomposition. Consequently, radiolytic gas production in concretes has been investigated as well as radiation effects on structural and chemical durability.

Stone has reported measurements of gamma-irradiation on the compressive strength and strontium leachability of concretes containing simulated SRP sludges.[71] Gamma irradiation to 10^{10} rads apparently decreases long term strontium leachability: In every case strontium leachability after six weeks' leaching was lower in irradiated specimens than in unirradiated control samples. The reduction factor was as much as 20. No data were presented for the effects of irradiation on TRU leachabilities. The compressive strength of samples following irradiation was not significantly different from that of samples exposed only to heat at the irradiation temperature.

Radiolytic gas production in concretes has been discussed in the Task 2 report. With respect to the waste form, a critical parameter is the recombination rate for radiolysis products.[72] There is apparently some control over this parameter; radiolysis yields may be reduced through the use of additives which act as scavengers. FUETAP concretes, for example, are said to show recombination rates which are more than ten times those observed in neat cement. Not surprisingly, saturation pressures observed in radiolytic gas formation in concretes may depend upon radiation dose rate. Moreover, at a given ionization dose rate, gamma radiolysis is not equivalent to alpha radiolysis. Bibler has reported that steady state conditions are not achieved in alpha-radiolysis of concretes containing simulated SRP waste for radiolytic gas pressures up to 200 psig.[73] At equivalent dose rates, steady state pressures of 50 psig are predicted for gamma radiolysis. The total dose in the α-radiolysis measurements was $\sim 1.5 \times 10^9$ rad. This corresponds to an α-decay dose of 2×10^{16} α/g (see Table 5.12). For TRU waste forms loaded at the same TRU level as HLW forms, this dose would be reached quite rapidly (see Table 5.2). This radiolytic gas production is a potentially serious drawback to the use of ordinary concretes as TRU forms.

5.2.5.2 Newly Developed Waste Forms

The non-traditional or newly-developed waste forms which might be of use include the various glassy, crystalline and multibarrier HLW waste forms whose radiation resistance was discussed earlier. If these are to be used as TRU forms, the radiation durability requirements may be relaxed in that the TRU modifications will not have to withstand the substantial beta-gamma dose from fission fragments.

In non-traditional forms, major questions with respect to radiation effects are the anticipated TRU loading, and the composition of the TRU waste. Since, in many HLW forms the long term effects of α-decay at the loadings proposed in HLW are not yet established one cannot scale the results to anticipated TRU loadings even if these loadings were known. The newly-developed waste forms are intrinsically much less susceptible to radiolytic gas production than the traditional TRU forms containing organics or hydrated water. While some evidence has been cited for the formation of oxygen bubbles in waste glass by electron bombardment,[1,10] it is probably safe to say that radiolytic gas production in the newly-developed waste forms mentioned above will be a relatively minor problem in comparison to that encountered in traditional TRU forms. An important consideration here is the makeup of the waste itself. If the TRU stream incorporates species which are subject to radiolytic decomposition, these will probably swamp "radiolysis" effects associated with the radionuclide host. Multibarrier waste forms may provide more latitude in coping with such effects. No direct evidence exists at this point. A more extensive discussion of the radiation stability of newly-developed TRU wasteforms is given in the Task 2 Report prepared under this contract.

5.2.6 Spent Fuel

Spent fuel has received consideration as a waste form. Radiation effects will influence the durability of both the fuel itself and of the cladding. Here we briefly assess the effect of radiation on the ability of fuel elements to retain radionuclides under respository conditions. Spent fuel will have received a substantial radiation dose at elevated temperatures prior to any anticipated service as a waste form. Due to this large "zero point" dose, one might speculate that the incremental effects of any additional radiation exposure following removal from the reactor would be relatively minor, if no steps are taken to recover the radiation damage prior to utilization as a waste form. However, further consideration is required since repository and reactor conditions differ substantially. This point is taken up below.

5.2.6.1 Radiation Effects in Fuel Pellets

Recent reviews on the properties of spent fuel have been given by Houston and by Holland and Brusis.[74,75] The distribution of chemical species and radionuclides in a fuel element following reactor service is complex and inhomogeneous. We do not know how this distribution would be affected during long term irradiation at repository conditions. In reference 75 it is concluded that the lattice structure of UO_2 is unaffected by irradiation at temperatures encountered in reactor operations (> 500°C). Evidence[76] was, however, cited for irradiation induced lattice structural damage at temperatures below 400°C. Presumably, damage of this sort (rather than the creep and grain growth encountered in reactor operations) might occur due to alpha-decays at repository temperatures. We are not aware of any direct measurements.

Recently, Wang and Katayama[77] have carried out leach tests on UO_2 during irradiation to simulate conditions in spent fuel. They find that surface dissolution in reducing solutions is enhanced by radiation. The effect is attributed to formation of oxidants such as O_2 and H_2O_2 by water radiolysis, and to a "radiation activated UO_2 surface". Based on the existing data they feel that this oxidation process caused by radiation may be a problem if spent fuel becomes an alternative waste form.

5.2.6.2 Radiation Effects on the Cladding

In all probability, bulk radiation effects in the cladding under repository conditions would be insignificant in comparison to those produced during reactor service. For waste forms the effects of radiation on corrosive media and on fuel-cladding interactions should be evaluated under repository conditions if the cladding is to be given any credit as a barrier.

5.3 Radiation Effects on Waste Containers

Practically all the proposed waste containers are metals. As such they are sensibly immune to ionization damage. As is the case in multibarrier waste forms, only the inner container surface which is in essentially intimate contact will experience displacement damage due to ejected alpha recoils or alpha particles. Thus, bulk damage in the metal could result only from atomic displacements caused by beta or gamma irradiation. This point is briefly considered below. Other effects of potential significance include gamma radiolysis effects at the outer canister surface, helium buildup and radiation damage to protective oxide films. These are also discussed in this section.

5.3.1 Displacement Damage

While little direct evidence is available, we do not anticipate that atomic displacements produced in metal waste containers by beta or gamma irradiation from the waste form will have a significant effect on the bulk metal properties. The displacement doses are simply too low. As indicated in Table 5.1, gamma rays and beta particles are not at all efficient in displacing atoms by elastic collisions, and ionization effects do not produce atomic displacements in metals. Typically, swelling and void formation in metals become observable for displacement doses of about 1-10 DPA.[9] The anticipated displacement dose in waste canisters due to beta-gamma irradiation is orders of magnitude below this. In fact, due to threshold effects, no atomic displacements would be produced in lead canister components by Cs^{137} gamma rays. Measurements on alloys such as Cu_3Au and α-brass have shown that small decreases in resistivity can be produced by gamma irradiation, presumably by increased ordering due to radiation enhanced diffusion.[79] We do not feel that these effects will be of practical significance in radioactive waste canisters, particularly where pure metals are employed and/or internal shielding is used. There is evidence that slight dislocation pinning can result from ^{60}Co gamma irradiation in metals; if sufficiently extensive, this could lead to embrittlement. Tests could easily be carried out on candidate container materials gamma irradiated to repository doses to rigorously confirm their anticipated durability under ionizing radiation.

Displacement doses at the inner canister surface due to alpha recoil are expected to be small as compared to those at which swelling becomes important. The inner surface of the canister may be considered as having received a relatively modest heavy ion implantation: no significant effects are anticipated.

5.3.2 Radiolysis

Radiolysis can indirectly affect waste canisters in at least two ways - by altering the chemistry of corrosive solutions, and by generating gases which may embrittle the material. Corrosive agents or gases might also be produced in the radiation-induced decomposition of overpack materials or geomedia - each case requires individual assessment. In any event, if the canister remains unbreached, it is the gamma irradiation field which exists beyond the outer wall of the canister which will determine the extent of radiolysis product formation (or of radiation effects in overpack or geomedia).

The magnitude of the external gamma ray field will be governed by the waste form loading, and by the internal shielding properties of the waste form and canister. These can be significant. Shielding properties of typical materials are tabulated below (Table 5.13).

Table 5.13

Shielding Properties of Waste Canister Materials[80]

	Transmission for Cs-137 Gamma Rays			
Thickness (cm)	Lead	Copper	Iron	Concrete
2.5	7×10^{-2}	5.6×10^{-1}	6×10	
5.0	5.5×10^{-2}	1.6×10^{-1}	2×10	6×10
7.5	3×10^{-4}	4×10^{-2}	6×10	
10.0	$^{*}2 \times 10^{-5}$	1×10^{-2}	2×10	4×10
12.5		3.6×10^{-4}	7×10	
15.0		6.2×10^{-4}	1.5×10	2.3×10
17.5		3×10^{-4}	8×10	
20.0		$^{*}1 \times 10^{-4}$	3×10	6×10
25.0				
30.0				3×10
40.0				
50.0				1.6×10

*Proposed in Swedish designs.

The Swedish canister designs incorporate substantial thicknesses of copper and/or lead (see Section 3). While we have not yet assessed waste loading or geometric effects in detail, it is probably safe to assume that material immediately adjacent to the Swedish canisters will be exposed to a radiation dose of less than one megarad. This dose will, of course, be almost entirely due to fission fragment decay, and will be administered during the first few hundred years.

Conversely, in the early monolithic borosilicate glass/steel canister designs considered in this country, high external radiation levels were anticipated. Table 5.14 gives estimated external gamma doses for borosilicate glass waste forms/stainless steel can combinations. Midplane values are given for ten year aged waste. In more recent designs, the waste form loading has been reduced. In these systems, if no additional shielding is employed, gamma radiation effects external to the canister might become significant.

Table 5.14

External Radiation Conditions for Glass Waste Forms

	HLW[a]	Spent Fuel[b]	PNL[b] (1 kW)	SRP[c] Glass
Initial dose rate (rad/hr)				
Edge of can	9×10^4	1.5×10^4		3×10^4
1 m from can (in air)			4×10^3	
Dose at edge of can (rad)				
20 years after burial	1.15×10^{10}			
300 years after burial	2.9×10^{10}			

[a] Illustrative values from Reference 85 for borosilicate glass/stainless steel canisters in rock salt. Values are at the midplane, for 10 year aged waste.

[b] Based on data reported for engineering scale fully loaded waste forms produced in 1979 at PNL by in-can melting.[87] Loadings are about 2 curies/gm.

[c] Calculated value for 2' diam. x 10' tall SRP waste glass cylinders; neglects   and   radiation, which would be blocked by the container.[39]

5.3.2.1 Radiation Corrosion

A large number of studies have been carried out on radiation effects on corrosion. While heavy particle bombardment may damage both metals and protective oxide layers,[81] it is generally held that the important corrosion related effects of gamma radiation are associated with solution radiolysis. Two factors, in general, determine the concentration of gamma radiolysis products anticipated under given conditions: the primary formation rate (which is usually proportional to dose rate), and the rate of scavenging or back reactions. Competition between these processes determines equilibrium levels.[82] Recently, experiments have been carried out in which gamma radiation has been shown to affect the solubility and transport of corrosion products.[83] The susceptibility of Type 304 stainless steel to stress corrosion cracking in high temperature water is said to be decreased by increased buildup of uniform corrosion layers under gamma irradiation[84]

Very few direct evaluations have been carried out on radiation corrosion under repository conditions. Rock salt appears to represent the most aggressive environment of current repository media with respect to radiation corrosion.[85] Ordinarily, steady state radiolysis product concentrations are low unless scavengers are present to prevent back reactions. In rock salt brines (bitterns) bromine acts as an effective scavenger which stabilizes radiolytic hydrogen and other species.[86] In other ground waters this effect would presumably be unimportant.

Jenks has considered the radiolysis (and hydrolysis) of rock salt brines.[85,86] His early estimates of product formation rates are given in Table 5.15. These values are based on early (1972) glass waste form designs; presumably, radiolysis and thermally induced brine migration to the waste canister would occur more slowly when contemporary waste loadings are considered. Due to the encapsulation properties of rock salt, the hydrogen will be largely retained in solution, at concentrations less than 1M. At higher concentrations dissolved hydrogen pressures will cause brine cavity expansion - gas will be released into the resulting voids. It is interesting that chlorates and perchlorates were anticipated, in view of their explosive potential. These are not expected to reach harmful levels at repository temperatures.[86] However, see below. In a later report, Jenks estimates that in thirty years, brine inclusions adjacent to the container may contain radiolytic hydrogen concentrations of up to 26 moles/kg for HLW. Over one hundred years as much as 12 liters of brine could flow to the region surrounding the container.[85] The hydrogen pressure will depend on the extent of sealing and pressure in around the container. We are not aware of any special hydrogen pressure estimates for a particular scenario; however, steam pressures as high as 900 psi have been estimated for certain cases.

Jenks has estimated corrosion rates for carbon steel spent fuel canisters in a salt repository.[88] He concludes that rapid localized corrosion is a strong possibility, unless special precautions are taken.

Table 5.15[86]

Summary of Conclusions Regarding Identities of Species Appearing Around a Waste Can and Regarding Maximum Rate of Appearance[48]

Species	Source	Max. rate of appearance and max. period after burial (mole/yr)	(yr)	Balancing oxidized species	Remarks
H_2	Radiolysis product within encapsulated brine	4	< 1	O_2, chlorates, bromates	Comparable rates for 2 and 5 Kw cans.
H_2	Radiolysis of solution around can	.8 followed by .3	.1 .5	O_2, Cl_2, Br_2, ClO_2^-, ClO_3^-, BrO_3^-	For 2 Kw cans. Insignificant period of time with 5 Kw cans because of rapid heat up.
H_2	Corrosion of can (50 mils/yr)	400	< 1		Assumed brine inflow rate of 7 ℓ/yr with all H_2O reacting with can.
HCl	Hydrolysis of $MgCl_3$	20	< 1		Assumed brine inflow rate of 7 ℓ/yr, 3$\underline{M}$ $MgCl_3$ within brine, and 50% hydrolysis of $MgCl_2$.
HNO_3	Radiolysis of moist mixtures of N_2 and O_2	.50	<.1		Likely that all N_2 will have been expelled at < .1yr after burial.
O_2 and other oxidized species	Radiolysis				To balance radiolytic H_2.

Braithwaite and co-workers have studied the corrosive behavior of several alloys in rock salt brines during gamma irradiation.[89] At dose rates of 10^7 rad/hr they find a substantial increase in corrosion rate for 1018 steel (75x) and an even larger effect for 304L stainless steel (>100x). At "dose rates more typical of wastes" (presumably $\sim 10^5$ rad/hr) the corrosion rate of 1018 steel is doubled, while that in stainless steel is just detectably increased. TiCode-12 is evidently more resistant - at 10^7 rad/hr the corrosion rate only doubled. It is also noteworthy that over half the sealed quartz sample tubes were either attacked or exploded during exposure. The increased metallic corrosion is attributed to the formation of radiolysis products; some of the chemical species produced either in the radiolysis or corrosion process evidently can recombine explosively.[89]

5.3.2.2 Hydrogen Embrittlement

In the Swedish HLW canister design, estimated equilibrium concentrations of oxygen, hydrogen, and hydrogen peroxide are all less than 10 ppB. The risk of hydrogen embrittlement is considered small under these conditions.[90] In the TiCode-12 samples subjected to irradiated brine, brittle fracture was observed in the near surface regions (5-10μ). It has not yet been established to what extent this effect is due to irradiation.[89] As mentioned earlier, Jenks has estimated that radiolytic hydrogen concentrations and pressures in encapsulated voids around waste canisters in salt repositories may be large. The potential would appear to exist for hydrogen embrittlement. Magnani and Braithwaite[90] have described slow strain rate SCC tests on TiCode-12 samples which had previoulsy been gamma-irradiated while partly immersed in salt brine. The total dose was 8 $\times 10^9$ rad at a dose rate of $\sim 1\times10^7$ rad/hr. While overall ductility was not significantly affected by irradiating, a narrow ($\sim 10\mu$) band of material at the surface showed brittle failure, indicating stress corrosion cracking. The importance of radiolytic hydrogen in promoting the effect is being investigated. Under irradiation conditions similar to those for TiCode-12, 304 SS specimens cracked under internal stress and could not be subsequently tested. Overall, Magnani and Braithwaite feel that alteration of the environment by radiation may be the most important factor in evaluating the lifetime of a waste canister.

5.3.3 Other Effects

It is possible that the waste canister could become internally pressurized by helium buildup, or internally stressed by radiation induced swelling of the waste form. It has been suggested that waste canisters should be designed so as to accommodate waste form swelling of 2%, where glass waste forms are used.[14] It seems that this criterion would probably include sufficient latitude to accommodate helium release; we are, however, not yet in a position to comment critically on the ability of various canisters to meet this requirement. In lead containing forms, it is likely that stress could be relieved by creep, if some free volume is available.

Helium embrittlement is known to occur in metals such as copper and stainless steel.[92] This effect is thought to involve the formation of bubbles under stress at high temperature. While our assessment is continuing, we do not presently foresee any particular difficulties due to helium buildup under repository conditions. Significant local helium concentrations, in the metal, if they arise at all, should not build up until the temperature has dropped substantially below those where embrittlement is commonly encountered. In view of the long times available for diffusion, however, some further consideration may be necessary in certain cases.

Russian investigators have reported the buildup of radiation-induced sublimates on the inside of canisters containing glass waste forms, and on the inner surface of metal foils encapsulating glasses under gamma irradiation.[93] Similar effects are said to occur on waste form surfaces, leaving a less durable surface layer. The Russian workers feel that these effects result from a radiation-chemical reaction in the presence of air. This might be termed gas phase radiolytic attack. We are attempting to determine if similar effects have been observed elsewhere. It is claimed that to prevent this effect, contact with air must be limited. Radiolysis of moist air may produce nitric acid, as indicated in section 5.2.

5.4 Radiation Effects on Overpack Materials

Assessment of the effects of radiation on overpack materials is still under way. Only limited data are available for most materials. The subject of radiation effects on sorptive properties seems to have received some detailed study in Russia. Spitsyn and co-workers[94] report that the sorptive characteristics of quartz grains in minerals can be modified to some extent by heavy doses of electron irradiation. In other experiments, sorptive capacities of aluminosilicates are said to be increased slightly by ionizing radiation.

The significance of the Russian work is not clear at present. Perhaps of equal importance is the suggestion that the charge state of migrating plutonium might be affected by radiation.[95,96] Also, since some of the overpack materials contain molecular subgroups or hydrated water, the possibility of damage due to internal radiolysis requires some consideration. Internal radiolysis can occur in other systems such as concretes which contain hydrated water.

Recently some interest has risen in radiation damage effects on ion-exchange media with respect to reactor cleanup operations. Early data also exist on zeolites. Some radiation effects data are summarized in Table 5.16 for ion-exchange media with possible applications as backfill components. For the most part, the zeolite materials seem fairly durable for beta-gamma doses up to those anticipated in repositories.

The limited information indicates that, indeed, internal radiolysis and/or gas generation may be a consideration depending on radiation dose and moisture content. One possible effect of radiation on sorptive properties is intriguing. The available information suggests that, due to irradiation or decay heating, the pore structure of heavily loaded zeolites may collapse and tend to fix sorbed radionuclides.[99,106] In effect, since the (beta-gamma) irradiation and heating is produced by the radionuclides themselves, they become "self-trapped". Whether or not the effect is useful (if in fact it occurs at all) will depend on whether the radionuclides are sorbed before

Table 5.16

Radiation Effects in Inorganic Ion-Exchange Media

Material	Irradiation	Effect	Comment
Sodium Titanate	2×10^{8} rad gamma	50% decrease in exchange capacity	Possibly degraded by heating[97]
Zirconium Arseno-phosphate	1×10^{9} rad gamma	Slight increase in exchange capacity	Ref. 98
Zeolite A	10 KCi ^{90}Sr for 2 Years	Fixation of strontium	Dehydrated at 600°C after loading[99]
Zeolite A	2×10^{7} R gamma	Gas Uptake or catalyzed Water formation	Deyhdrated before irradiation[99]
Zeolite A	1×10^{11} rad (90 Sr)	35 PSIG of radiolytic gas	Dried to 7% H_2O;[99] T = 500°C
Zeolite 13X	7×10^{19} n/cm^{2}	Lattice collapse	Ref. 100
Clinoptilo-lite	8.4×10^{9} rad gamma	None detected	X-Ray Diffraction; distribution co-efficient; D.T.A.[102]
IE-95 (Chabazite)	1×10^{10} rad gamma	None detected	X-Ray diffraction; distribution co-efficient [101]
IE-95	1.5×10^{9} rad gamma,	Gas generation	Drip-dry samples[103,104]
IE-95	5×10^{9} rad beta	Gas generation	"
Zeolites: AW-500 Zeolon 900, etc.	Processing and shipping; exposures to 10^{10} rad or more		Some column plugging and some evidence for Cs fixation. No hazardous degradation reported.[105,108]

or after the period of intense beta-gamma flux. The internal dose will also depend on the distribution of sorbed radionuclides. Local doses could be quite high if radionuclides are concentrated in the sorption process. Consequently, if the container remains intact during the period of intense beta-gamma decay, it is the sorption properties of externally gamma-irradiated backfill which will be important. (For the bulk of the backfill, under these conditions, the total gamma dose will most probably be lower than that ($>10^{10}$ rad) for which structural changes are inferred in some zeolites.) If the container is rapidly breached, it is the effect of internal irradiation on backfill elution properties which must be emphasized. Both conditions, as well as the possibility of gas evolution, require more detailed consideration.

5.5 Radiation Effects in Geomedia

Unless the canister and waste form are breached, radiation effects in host rock adjacent to waste canisters will be entirely due to gamma irradiation. The radiation exposure will depend on the waste form loading, and on the shielding properties of canister and overpack. (See Tables 5.13 and 5.14.) Geomedia which have been considered as potential hosts for HLW repositories include rock salt, basalt, granite, and shale. Radiation damage formation has been studied in some detail for synthetic NaCl and natural rock salt; much less is known about radiation effects in other geomedia. Accordingly, we begin our discussions by considering radiation effects in rock salt.

5.5.1 Rock Salt

Among the geomedia which may constitute part of a waste package, rock salt is probably unique in its radiation damage susceptibility. Internal ionization can easily produce displacements on the anion sublattice, without the need for elastic collisions with energetic particles. The required energy to displace an anion has been estimated at 15 eV.[107] Consequently, substantial displacement doses can be produced by gamma irradiation.[†] In addition, rock salt contains about 0.5% brine. We have discussed brine radiolysis in Section 5.3.2; it is also known that the process by which brine inclusions migrate involves dissolution of the host rock salt. Radiation damage products in the rock salt can then be dissolved in the migrating brine and transported to the waste canister.

5.5.1.1 Radiation Damage Formation

Buildup and release of stored energy in irradiated rock salt has been studied in some detail.[108] It was concluded that while values of 30 cal/gm might be anticipated in rock salt near waste canisters under certain conditions this in itself posed no particular hazard for repository operations.

Electron microscope studies on thin NaCl foils by Hobbs and co-workers have disclosed an important radiation damage process which probably accounts for most of the stored energy.[11] High defect concentration may be stabilized by aggregation. In NaCl, the charged vacancy aggregates are equivalent to colloidal sodium particles while the interstitial aggregates are dislocation loops and, presumably, clusters of molecular chlorine. The aggregate defect production exhibits a characteristic peak formation temperature. The electron microscope studies indicate that colloidal sodium concentrations of ∿1-2% can be achieved at ∿10^{10} rad without saturation.

[†] In Table 5.1, if the waste form were rock salt, rather than glass, the number of displaced atoms due to gamma irradiation would be $10^{24}/cm^3$.

More recent measurements have established that the general behavior observed in the electron microscope irradiations holds for "bulk" single crystals of natural rock salts from different locations.[109] The qualitative aspects of radiation induced colloidal sodium formation in natural rock salts are remarkably similar; quantitative differences may be largely confined to an initial period during which the salt receives only a few percent of its ultimate radiation dose. This suggestion, however, requires direct verification by experiments at high radiation dose as does the question of radiation damage saturation.

Substantial colloid formation occurs only within a restricted temperature range, peaked near 150°C. On theoretical grounds[107] the peak formation temperature should decrease at lower dose rates, but the scaling is not yet established. (It is important that this be done, since maximum repository dose rates may be one hundred to one thousand times lower than those used in the laboratory). Colloid formation is enhanced in samples which are plastically deformed and then electron irradiated near the peak formation temperature. Should the rock salt in the waste repository plastically deform, a similar enhancement would be expected. It is possible that this effect is significant only in the early stages of colloid formation, but further study is warranted. Taken together the results outlined above indicate that for repository temperatures near 150°C, substantial concentrations of colloidal metallic sodium, together with dislocation loops and chlorine in an as yet undetermined form, should be anticipated in rock salt surrounding unshielded HLW canisters. The precise amounts generated will depend upon the prevailing temperature strain and dose rate conditions. Concentrations of 0.1 to 1% could occur for a dose of 10^{10} rad.[109]

5.5.1.2 Effects on Material Properties

One of the advantages of rock salt as a repository medium is the ease with which it plastically deforms in response to an applied stress. Dislocations and point defects introduced by irradiation may harden the rock salt.[110] The effect of irradiation on the yield point of NaCl rock salts is shown in Table 5.17. Hardening of material around the waste canister could affect consolidation or retrievability. The radiation hardening is pronounced for single crystal NaCl. Other factors apparently dominate the mechanical strength of bulk rock salt.

When irradiated rock salt is dissolved in water, gaseous hydrogen and hypochlorite ion are produced.[113] Direct measurement has shown that the amounts generated may be estimated by simply considering the aqueous dissolution of metallic sodium or molecular chlorine, in amounts commensurate with the radiation damage levels. The dissolution reactions may be viewed schematically as:

Table 5.17

Effect of Radiation on the Yield Strength of Rock Salt

Dose (rad)	Yield Stress (psi)[a]	Yield Stress (kg/cm^2)[b]
0	2300 ± 300	10
10^7	2700 ± 250	120
5×10^7		175
10^8	3400 ± 250	
5×10^8	2700 ± 200	

[a] Natural rock salt, bedded parallel.[111]
[b] Single crystal NaCl, <100> strain.[112]

$$Na + H_2O \rightarrow 1/2\ H_2 + Na^+ + OH^-$$

and

$$Cl_2 + H_2O \rightarrow Cl^- + H^+ + HOCl$$

$$HOCl \rightarrow H^+ + OCl^-$$

Thus, in terms of solution chemistry, irradiated rock salt can be pictured as containing atomic sodium and molecular chlorine "in storage". The amounts of hydrogen and hypochlorous acid released upon dissolution will depend upon the extent of the radiation damage in the rock salt. Quantitative estimates are being collected.

5.5.2 Other Host Rocks

As is the case for overpack materials, extensive radiation damage information is not available for host rocks other than salt. Jenks has reviewed the situation in 1975.[17] Our own evaluation is ongoing and will not be discussed in detail. We have mentioned previously that quartz can become amorphous under heavy doses of ionizing radiation. We do not, however, expect these doses to be approached in repository host rock. The same could be true of feldspars, but here again more precise information is required. Limestone is composed of carbonates such as calcite and dolomite. Ionizing radiation is known to produce charge defects in these materials. Further, there is some suggestion that the carbonate ion can undergo radiation induced decomposition into CO and O_2. Based on our present experience, we do not anticipate any particular difficulty with radiation effects in most hard rock hosts.

5.6 Summary and Conclusions

In this section, the available radiation effects data for individual waste package components are summarized. This information is then considered in light of current NRC draft "strawman" criteria for waste package performance. The ability of currently available technology to provide the radiation effect information required for licensing under these criteria is assessed;

outstanding key issues are identified and recommendations made to expedite the development of information required for licensing.

Almost without exception, the radiation effects test procedures which are currently available share three features in common: first, they emphasize or evaluate the change in a physical property as a function of radiation dose; second, the irradiations are carried out at dose rates which are orders of magnitude greater than those anticipated in the repository; finally, almost all of these tests have been applied to isolated specimens of prototypical waste rather than to specimens incorporated in the actual waste package.

5.6.1 Radiation Durability of Waste Forms

Most of the test procedures which are currently available have been developed to evaluate the effects of radiation on waste form properties--density, phase stability, and leach rate. The effects associated with internal alpha decay have received greatest attention. Internal alpha decay in the manufactured waste form has been simulated by doping waste forms materials with short lived actinides, by external heavy particle or neutron bombardment and internal fission. The different simulation techniques may yield different results. Ionizing radiation effects on the waste form and on corrosive media are studied with external gamma or electron irradiation. Recently, techniques have been developed for evaluating the effect of beta transmutations in the waste form. Additional techniques such as thermal analysis and electron microscopy exist which can be employed in mechanistic considerations. In all, a fairly broad spectrum of tests exists for the waste form. One standard test has been produced (MCC-6) which evaluates the effect of internal alpha decay in the waste form. We agree with the priorities evident in this choice as a starting point for standardized test development.

- Glasses

Thus far, waste glasses appear to sensibly retain their chemical durability as alpha decays build up in actinide doped samples. Either positive or negative density changes may occur which, in homogeneous materials, can lead to radiation-induced stresses and microcracking. In glasses, density changes can be quite small; it is apparently possible to effect a balance between swelling and compaction effects. Radiation damage produced by different sources saturates in a manner which may imply that radiation dose rate effects are not important, but no direct information exists. In silicate glasses saturation effects are quite commonly observed in radiation damage formation, due to internal alpha decay. The typical "saturation dose" is about 10^{18} α/g, very roughly 10% of the million year dose anticipated in the waste form. One might speculate that beyond this point (i.e., for times greater than about 1000 years) the cumulative effect of additional alpha decays is largely negligible. This suggestion, however, requires further study--it is not clear, for example, that one can ignore 90% of the helium buildup.

When the effects of internal alpha decay are simulated by external heavy-ion bombardment, some glasses are said to undergo a dramatic (>20X) enhancement in leach rate under certain conditions. These results are in contrast to those reported for actinide doped samples. This issue is presently under study in DOE laboratories; its resolution is of central importance in evaluating the long radiation durability of waste glass.

In glasses comparative measurements suggest that damage formation by internal alpha decays is, for the most part, governed by the number of atomic displacements (DPA) and not the dose rate. This implies that accelerated testing at high dose rates by doping with short lived alpha-emitters provides a valid simulation of effects to be anticipated under repository conditions. Examination of the effects of ionizing radiation from beta decays on displacement damage formation is warranted, however. The silicate tetrahedral structure may be particularly susceptible to ionization effects; the role of ionization on damage annealing should also be determined.

Thus far transmutation studies do not report any significant beta-transmutation effects in glassy or crystalline phases. These limited experiments are still at an early stage and should be extended to include temperature conditions anticipated in repositories.

- Ceramics

All ceramic materials which have been proposed for waste forms share one common feature: radionuclides are selectively partitioned among different phases; differential radiation damage effects such as local swelling and fracture may result. This has been observed in SYNROC. SYNROC, supercalcines and high alumina ceramics all possess phases which are susceptible to radiation-induced metamictization and swelling. In contrast to glasses all ceramic phases exhibit swelling under irradiation, as opposed to compaction. In some cases the swelling may be substantial in comparison to glasses.

In ceramic waste forms, one cannot generalize about saturation effects in radiation damage without some better understanding of the mechanism. Swelling and stored energy appear to saturate in supercalcines in a manner similar to that in glasses. Materials such as zircon may swell linearly to 12% without reaching saturation. Certain swelling mechanisms involving void formation are strongly temperature dependent. These mechanisms typically involve thermally activated diffusion of displaced atoms as a rate limiting step in damage formation. It appears that void swelling may not be operative in most candidate waste form materials at the temperatures involved in present studies. The apparent absence of the dose rate effects characteristic of diffusion limited processes in radiation damage formation is another indicator. In view of the fact that most radiation studies have evidently been carried out near room temperature, however, the possibility of increased radiation damage formation at temperatures near 200°C requires further consideration.

It has been suggested or asserted that metamict ceramic waste form phases will lose their leach resistance. At this point, almost no direct information is available. Certain inferential evidence contradicts this claim. Naturally metamict zircon apparently retains its uranium but loses the daughter product lead; metamict zirconolite is said to retain both. Limited measurements suggest that the leach rate of devitrified borosilicate glass is not significantly affected as the devitrified phase becomes metamict. Leaching measurements carried out on natural analogs of SYNROC minerals suggest chemical durability under irradiation. Experiments in which radiation effects on leach rates have been directly evaluated in actinide-doped crystalline phases are only just beginning. More explicit information on the leach resistance of irradiation induced metamict phases in ceramic waste forms is needed promptly. Recent data suggest that some crystalline phases may be more chemically durable than glasses under external heavy-ion implantation.

In ceramic materials, a non-equilibrium condition results when radionuclides are modified by transmutations. It has been suggested that, in the process of achieving a new equilibrium configuration drastic effects may occur. Various arguments have been made regarding the stability of waste forms against transmutation damage; however, only limited data are available. It has been argued that SYNROC may be less liable to fission fragment transmutation damage than supercalcine if radionuclide partitioning is properly controlled. Glasses by virtue of their non-equilibrium nature may be more forgiving still. We feel however, any assessment of transmutation effects should give due consideration to the charge transfer processes which can occur under ionizing radiation. These effects might offset the effects of beta transmutation to some extent, or change the oxidation state of critical components such as cerium in supercalcines.

An enhanced leachability for small cations evidently occurs in supercalcine under gamma irradiation; the effect could be more pronounced than in glass. The effect of ionizing radiation on leach rates in ceramic waste forms has not yet been experimentally assessed to any great extent.

- Multibarrier Waste Forms

Materials presently considered for particle coatings or matrix materials in multibarrier waste forms are for the most part highly radiation resistant. Major advantages of multibarrier forms from the viewpoint of radiation effects include the ability to include porous or sacrificial surfaces, as in coated particles and to control the internal beta-gamma dose (and thermal loading) by the use of heavy metal matrices or varying the concentration of matrix particles. This provides an important design degree of freedom in waste packages since these changes can be effected without varying the loading (or chemistry) of the radionuclide host phases. Differential swelling or compaction in the barrier or host phases under irradiation appears to be the most significant radiation effect in terms of its potential to cause barrier failure. Differential stresses of this sort should be minimized in waste forms such as coated particles, where the host phase is not fully dense. More compacted systems such as porous glass may require careful evaluation of radiation-induced stresses. No standard evaluation procedures are currently available.

5.6.2 Radiation Durability of Containers

Only a very limited testing experience exists for container materials under simulated repository conditions. Available tests consider, but do not discriminate between, corrosion effects associated with leachant radiolysis and embrittlement by radiolytically produced gases. Development of more extensive test facilities is currently under way. This area is receiving increased attention.

We do not expect that the bulk properties of metal containers will be significantly modified by irradiation alone under repository conditions. The corrosion rate of mild steel, stainless steel, and TiCode-12 in salt brines is increased during gamma irradiation (presumably by the formation of radiolysis products in solution). The magnitude of the increase depends upon radiation dose rate. TiCode-12 is evidently more durable under irradiation.

In the Swedish HLW canister design, estimated equilibrium concentrations of oxygen, hydrogen, and hydrogen peroxide are all less than 10 ppB. The risk of hydrogen embrittlement is considered small under these conditions. In the TiCode-12 samples subjected to irradiated brine, brittle fracture was observed in the near surface regions (5-10 μ). It has not yet been established to what extent this effect is due to irradiation. As mentioned earlier, Jenks has estimated that radiolytic hydrogen concentrations and pressures in encapsulated voids around waste canisters in salt repositories may be large. The potential would appear to exist for hydrogen embrittlement; direct evaluations will be required. These should specifically consider the accuracy with which the hydrogen environment in a rock salt repository can be predicted.

In container systems without heavy interior shielding, radiation effects on the container environment are expected to be a major factor in determining container lifetime.

5.6.3 Radiation Durability of Backfill

For backfill materials, all radiation effect information is inferential. Thus far, and perhaps based on this inferential evidence, no tests appear to have been planned or carried out in this country specifically to evaluate the effects of radiation on backfill performance under repository conditions. We do not in general feel that the inferential evidence which is currently available provides an adequate data base to rule out the need for such design-specific evaluation. For example, it is difficult to completely dry zeolites. It seems likely that backfill materials may contain a few percent moisture upon emplacement. Should this moisture be driven off by decay heating or irradiation both the mechanical properties of the zeolite and the environment of the container could be affected. The effect of radiation on the tendency of zeolites to alter under hydrothermal conditions is also largely unknown.

5.6.4 Performance Assessment

At this point, there is no direct evidence to indicate that radiation effects alone will disqualify a particular waste package from further consideration under current licensing criteria. Additional information, however, remains to be developed before compliance with these criteria can be critically evaluated.

In terms of resistance to swelling and structural changes due to internal alpha decay glasses appear superior to certain crystalline phases. Consequently, homogeneous glasses are evidently less susceptible to differential stresses and microcracking due to TRU radionuclide partitioning. On the other hand, there is some evidence to suggest that glasses might be structurally damaged by ionizing radiation, which may have consequences for systems incorporating inert glass barriers. As yet, there is no clear evidence for enhanced leaching due to microcracking of radionuclide host phases. The available data are extremely limited and apply almost entirely to glass.

Leach rates may be affected by solution radiolysis. In laboratory experiments, glass leach rates may increase by factors from two to six under gamma irradiation; for some elements, the increase can be greater. Limited data indicate that crystalline phases also exhibit this effect.

At this point the only evidence for a truly dramatic radiation induced enhancement of leach rates is based on an experimental technique (external ion bombardment) whose relevance to repository conditions can be seriously questioned. These results suggest that, in terms of resistance to leaching or chemical etching, crystalline phases may be more durable than glasses under internal alpha decay. Again, almost all of the leach data on internal alpha decay apply to glass, and simulate storage times of 10^4 years or less.

TiCode-12 is evidently more resistant than stainless steel to radiation corrosion in salt brines; however, TiCode-12 could be embrittled by radiolytic hydrogen.

Inferential evidence derived from other applications suggests that some zeolite backfill materials such as chabazites will be durable under the radiation doses anticipated in repositories. However, radiation doses have not been administered to these materials under conditions anticipated in repositories.

In short, in terms of radiation effects, certain materials and designs appear potentially more attractive than others. Degrees of freedom exist in any waste package design which can be employed to minimize the impact of radiation effects:

- Gamma radiation effects on corrosion can be reduced by internal radiation shielding within the container.

- Radiolysis effects on leachants will be reduced in direct relation to the time that the container remains intact.

- The significance of volume changes due to internal alpha decay can be reduced by encapsulating partially dense radionuclide host phases in inert barrier phases.

- Radiolytic hydrogen production can be reduced by promoting recombination reactions (say by removing scavengers for OH such as bromine) or choice of repository.

These degrees of freedom provide a "fall-back" position. However, it is not yet clear exactly when and if such steps will be required to achieve compliance with licensing criteria; nor is it clear exactly how to determine when such steps will be needed. In some cases preliminary conclusions can be drawn. For example, after one million years the anticipated alpha dose for defense HLW glass will have just about reached a value where structural radiation effects typically become observable.* The conclusion is that, given the validity of testing techniques, alpha-decay effects will be negligible in (current) defense HLW glass.

In other cases, a fair amount of work remains to be done before the sensitivity of a particular waste package design to radiation effects can be rigorously assessed. In the next section we have identified several key areas where we believe additional information is required in support of such an assessment. In nearly all of these areas work is either imminent or currently under way; a substantial amount of progress has been made since our earlier report under this Task.

5.6.5 Outstanding Questions and Recommendations for Further Study

With regard to radiation effects on the waste package the outstanding issues fall into two categories. In one, additional scoping and comparative tests are required to determine the relative practical significance of certain postulated effects. In the second category, additional information is required to connect scoping and comparative test data into the absolute performance assessment required for licensing under current criteria. This category falls more naturally within the scope of test development. Extensive discussion is provided in the Task 4 Report issued under this contract. With respect to scoping and comparative tests, the following key issues can be identified.

- External vs Internal Irradiation - We believe, with the MCC, that internal doping with short lived actinides should be the recommended method for simulating the alpha decay of TRU elements in waste forms. However, while the degree of quantitative correspondence between internal alpha decay and heavy ion implantation is difficult to establish, an issue has been raised which warrants further attention: whether or not highly etchable damage tracks can be formed by alpha-recoil nuclei in waste glasses. We do not know of any direct observations of alpha-recoil tracks in glasses. However, such etchable tracks have been reported in minerals and their implications for radioactive waste storage discussed.[114]

  We feel that the apparent difference between chemical durability results obtained with ion-implanted samples and with internally doped samples must be understood if the durability of HLW glass under internal alpha decay is to be rigorously established. This will require a detailed characterization and comparison of the radiation damage produced by each technique, under standard test conditions, in glassy and in crystalline samples.

---

*This dose is at least an order of magnitude lower than the "critical" or "threshold" dose reported in the ion implantation experiments.

The DOE has responded to this issue in a timely manner. We understand that work along these lines is presently under way at ANL, Sandia, and SRL. We only suggest that particular emphasis be placed on any (microscopic) evidence for track formation, and venture the speculation that alpha particle effects might account for some of the observed differences. This could be the case if, through some process perhaps involving ionization, longer range alpha particles cause irradiation annealing of localized alpha recoil tracks before track overlap begins.

- Effects of Internal Alpha Decay on Crystalline Phases - Leaching tests should be carried out on crystalline phases doped with short lived actinides. More information is required here as soon as possible. This information should be used to directly assess the chemical durability of metamict phases. Comparing the properties of the metamict forms produced in a given material by different types of irradiation and in natural analogs would aid in qualifying laboratory test procedures and in understanding the metamict "state" itself.

- Effects of Ionizing Radiation - Efforts should continue toward identifying those cases where the waste form may be susceptible to ionization damage. These efforts should include (1) determining the effect of ionizing radiation alone at repository doses (10^{12} rad) and (2) determining if the formation of alpha decay damage will be affected by a prior dose of beta-gamma radiation. Inert barrier phases as well as radionuclide host phases will be exposed to ionizing radiation. The effect of ionizing radiation on the structure and solubility of such phases must also be evaluated. Recent evidence suggests that ionizing radiation effects on glass barriers may warrant particular consideration.

  A good start has been made on glass leaching under gamma irradiation. Similar measurements should be carried out on crystalline waste forms. Again, we are able to report that work in several of these areas is currently under way in DOE laboratories. Ionizing radiation effects will also be the topic of an MCC workshop in the near future.

- Radiation Induced Stresses - From the repository design viewpoint, the most important structural effect of radiation may involve density changes (and attendant generations of internal stresses).

  Testing will be required to evaluate the possibility and consequences of radiation induced microfracture in radionuclide host phases or inert barriers. This will require a knowledge of radiation induced expansion coefficients and the details of the anticipated radionuclide distribution. Uniform irradiation (e.g. neutron bombardment) will not provide an acceptable simulation for critically evaluating microfracture in inhomogeneous waste forms.

Thus far, little emphasis has been placed on evaluating the practical consequences of irradiation induced stress for systems other than glassy waste forms. Prompt scoping assessments are warranted for other waste form types. There is presently no prescription for evaluating such effects in multibarrier waste forms. We recommend that measurements be carried out to realistically assess the amount of structural damage anticipated in manufactured waste forms due to radiation induced strains. Here emphasis should probably be placed on multiphase forms such as SYNROC, and on multibarrier forms such as porous glass with a high silica barrier. These measurements should also explicitly determine the effect of microfracture on leach rate.

- Evolution of Waste Form Properties - Thus far laboratory evaluations of radiation effects have been almost entirely carried out on as-manufactured waste forms or host phases. In fact, most of the alpha decays in actual waste forms will build up subsequent to the initial 1000-year period after emplacement. During the first 1000 years, the waste form will have received a substantial beta-gamma dose, undergone internal beta transmutations and prolonged heating, and possibly, have been altered by incongruent dissolution or other effects in the repository environment. (Leaching data indicate that TRU elements may be retained in layers which are altered by incongruent dissolution.) Thus, waste form materials which are called on to withstand the majority of internal alpha decays will have a different radiation history, chemical composition and, possibly, surface structure from most samples currently used in laboratory tests. We recommend that scoping measurements be carried out to determine if such "preconditioning" effects will (synergistically) affect long term durability under internal alpha decay.

- Radiation Corrosion - In view of the major role anticipated for the container in meeting the short-term containment criterion, more scoping information on the effect of radiation on container availability under simulated repository conditions is required promptly. These measurements should occur on solution radiolysis and hydrogen embrittlement effects. We understand that the increased effort in this area will begin at PNL toward the end of FY 81.

We expect that, under repository conditions, the dominant mechanism in radiation corrosion will involve formation of gamma radiolysis products. The identity and concentration of radiolysis products anticipated in various repository environments should be specified as promptly and accurately as possible. These estimates should be made as a function of gamma radiation dose and dose rate; a good start has been made for salt repositories. Experiments may be required to support calculations. These anticipated radiolysis products could then be incorporated into scoping tests to provide a first-order simulation of radiation effects. One major question which must be addressed before radiation/corrosion effects can be estimated for repository conditions is the dependence of test results on radiation dose rate. In particular, it is essential to understand how the corrosion rate, or time to failure, depends on dose rate. Research should continue to determine how to (conservatively) relate corrosion data at laboratory dose rates to anticipated results at repository dose rates. It should also be determined if the mechanism of hydrogen uptake will be influenced by the presence of radiation or corrosion products in titanium alloys.

- Backfill Properties - Scoping tests should be initiated to determine the effect of gamma radiation and/or decay heating on the sorption-desorption properties of candidate backfill materials under repository conditions. Radiolytic gas production should also be evaluated for backfill/groundwater combinations and the effect of solution radiolysis on sorptive behavior assessed. Some encouraging radiation information on zeolites is currently available from other programs, but it is not entirely clear how to relate this to conditions peculiar to waste repositories. For example, the effect of irradiation on susceptibility to alteration in the geologic environment should be determined for candidate materials. We are informed that the effects of gamma radiation on backfill properties is to be addressed in the DOE backfill development program, which is still in its early stages.

5.6.6 Conclusions

At this point, there is no conclusive evidence to indicate that radiation effects alone will disqualify a particular waste package from further considerations. Outstanding questions of potentially major significance currently exist. In general, DOE has moved to address these issues in a manner which, in scope and in context, reflects a serious commitment towards the understanding of radiation effects on waste package components. Progress over the last year has been significant; in certain areas, further study is warranted.

Overall, it presently appears that the DOE program will ultimately produce the information required to determine which waste package components and designs exhibit the greatest radiation durability on a comparative basis. As discussed in the Task 4 test development review, additional steps may be required to confirm that this information will provide a conservative assessment of performance under repository conditions.

5.7 References

1. A. R. Hall, et al., "Development and Radiation Stability of Glasses for Highly Radioactive Wastes", in Management of Radioactive Wastes From the Nuclear Fuel Cycle, 2, (IAEA, Vienna, 1976) p.3.

2. E. R. Vance and K. K. S. Pillay, Pennsylvania State University, "Structural Damage From Fission Fragment Irradiation in Crystalline Nuclear Waste Phases, " DOE Subcontractor Report DOE/ET/41900-5, (1980).

3. F. P. Roberts, R. P. Turcotte and W. J. Weber, Pacific Northwest Laboratory, "Materials Characterization Center Workshop on the Irradiation Effects in Nuclear Waste Forms - Summary Report, " Pacific Northwest Laboratory Report, PNL 3588/UC-70, (January, 1981).

4. J. E. Mendel, et al., Pacific Northwest Laboratory, " A State of The Art Review of Material Properties of Nuclear Waste Forms, PNL 3802, April, 1981.

5. F. W. Clinard, Jr. and G. F. Hurley, "Effects of Irradiation on Structural Properties of Crystalline Ceramics", p. 300, in Ceramics in Nuclear Waste Management, USDOE Conference Proceedings, CONF-790420, May 1979.

6. J. E. Mendel, et al., Pacific Northwest Laboratory, "Annual Report on the Characterization of High Level Waste Glasses", BNWL-2252, June 1977.

7. A. E. Ringwood, V. M. Oversby, and W. Sinclair, "The Effects of Radiation Damage on SYNROC", p. 273-280, in Scientific Basis for Nuclear Waste Management, Vol II, C. M. Northrup Jr, Ed. (Plenum Press, N.Y. 1980).

8. M. Antonini, F. Lanza, and A. Manara, "Simulations of Radiation Damage in Glass", p. 289, in Ceramics in Nuclear Waste Management, USDOE Conference Proceedings, CONF-790420, May 1979.

9. W. G. Johnston, et al., "The Effect of Metallurgical Variables on Void Swelling", in Radiation Damage in Metals, N. L. Peterson and S. D. Harkness, Eds., (American Society for Metals, Metals Park, Ohio, 1976) pp. 227-266.

10. L. W. Hobbs, "Application of Transmission Electron Microscopy to Radiation Damage in Ceramics", J. Am. Ceram. Soc. 62, p. 267-278 (1979).

11. L. W. Hobbs, "Point Defect Stabilization in Ionic Crystals at High Defect Concentrations", J. Physique Collog. 37: C7-3 (1976).

12. F. W. Clinard, Jr., "Radiation Damage in Ceramics", p. 147, in Ceramic and Glass Radioactive Waste Forms, USERDA Conference Proceedings, CONF-770102, 1977.

13. R. F. Haaker and R. C. Ewing, "The Metamict State Radiation Damage in Crystalline Materials", p. 310, in Ceramics in Nuclear Waste Management, USDOE Conference Proceedings, CONF-790420, May 1979.

14. W. Primak, "Notes on Radiation Effects on Glasses Pertinent to Solid Storage of Radioactive Wastes", p.157, in Ceramic and Glass Radioactive Waste Forms, USERDA Conference Proceedings, CONF-770102, 1977.

15. G. W. Arnold, G. B. Krefft, and C. B. Morris, "Atomic Displacement and Ionization Effects on the Optical Absorption and Structural Properties on Ion-Implanted Al_2O_3", Applied Phys. Lett. 25, 540 (1974).

16. G. B. Krefft, "Ionization-Stimulated Annealing Effects on Displacement Damage in Magnesium Oxide", J. Vac. Sci. Technol. 4, 533, (1977)

17. G. H. Jenks, Oak Ridge National Laboratory, "Gamma-Radiation Effects in Geologic Formations of Interest in Waste Disposal: A Review and Analysis of Available Information and Suggestions for Additional Experimentation", ORNL-TM-4827, September 1975.

18. G. Das and T. E. Mitchell, "Electron Radiation Damage in Quartz", Radiation Effects 23, 49 (1972).

19. W. Primak, "Postirradiation Alkali Migration", J. Electrochem Soc. 127, 1002, (1775).

20. P. V. Murphy and B. Gross, "Polarization of Dielectrics by Nuclear Radiation II: Gamma-Ray-Induced Polarization", J. Applied Physics 35 171, (1961).

21. A. N. Goland, "Radiation Damage of Non-Metallic Solids" in Radiation Damage in Metals, H. L. Peterson and S. D. Harkness, Eds. (American Society for Metals, Metals Park, Ohio, 1976) pp. 366-393.

22. American Physical Society Study Group on Nuclear Fuel Cycles and Waste Management (L. C. Hebel, Chairman), "Report to the American Physical Society", Rev. Mod. Phys. 50, S130, (1978).

23. P. H. Permar, and W. R. McDonell, "Significance of Radiation Effects in Solid Radioactive Waste", in ASTM Proceedings 10th Symposium on Effects of Radiation on Materials, ASTM STP-000 (1980).

24. D. W. Kneff, "Radiation Effects Simulation in High Level Nuclear Waste Forms: A Literature Review", Supporting Document No. 364T1000001, Energy Systems Group, Rockwell International, Canoga Park, California, 1980.

25. K. Scheffler and U. Reige, Kernforschungszentrum Karlsruhe, "Investigation on the Long Term Radiation Stability of Borosilicate Glasses Against Alpha-Emmiters", Report No. KFK 2422, April 1977.

26. W. J. Weber, et al., "Radiation Effects in Vitreous and Devitrified Simulated Waste Glass", p. 294, in Ceramics in Nuclear Waste Management, USDOE Conference Proceedings, CONF-790420, May 1979.

27. K. A. Boult, et al., "The Leaching of Radioactive Waste Storage Glass", p. 248, in Ceramics in Nuclear Waste Management, USDOE Conference Proceedings, CONF-790420, May 1979.

28. N. E. Bibler and J. A. Kelley, Savannah River Laboratory, "Effects of Internal Alpha Radiation on Borosilicate Glass Containing Savannah River Plant Waste", DP-1482, May 1978.

29. F. P. Roberts, "Irradiation Effects on Borosilicate Glasses", Presentation, 10th ASTM International Symposium on Effects of Radiation on Materials, Savannah, Georgia, June 3-5, 1980.

30. F. P. Roberts, G. H. Jenks, and C. D. Bopp, Pacific Northwest Laboratory, "Radiation Effects in Solidified High-Level Wastes - Part I, Stored Energy", BNWL 1944, January 1976.

31. J. C. Dran, V. Langevin, M. Maurette, and J. C. Petit, "A Microscopic Approach for the Simulation of Radioactive Waste Storage in Glass", in Scientific Basis for Nuclear Waste Management, Vol II, C.M. Northrop Jr., Ed. (Plenum Press, N. Y., 1980) p. 135-140.

32. J. C. Dran, M. Maurette and J. C. Petit, "Radioactive Waste Storage Materials: Their Alpha Recoil Aging", Science, 209, p. 1518-19, 1980.

33. J. C. Dran, M. Maurette, B. V. Assent and J. C. Petit, "Ion Implantation Effect on the Leach Resistance of Glasses and Minerals: Implications for Radioactive Waste Storage", Abstracts, Symposium D; Scientific Basis for Nuclear Waste Management, Annual Meeting, Materials Research Society, Boston, November, 1980.

34. E. H. Hirsch, "A New Irradiation Effect and its Implications for the Disposal of High-Level Radioactive Waste", Science, 209, p. 1520-22.

35. C. T. Walker and U. Riege, "Compatability of Actinides With HLW Borosilicate Glass", p. 198, in Ceramics in Nuclear Waste Management, USDOE Conference Proceedings, CONF-790420, May 1979.

36. P. B. Macedo, et al., "Porous Glass Matrix Method for Encapsulating High-Level Nuclear Wastes", p. 321, in Ceramics in Nuclear Waste Management, USDOE Conference Proceedings, CONF-790420, May 1979.

37. W. Primak and R. Kampworth, "The Radiation Compaction of Vitreous Silica", Journal of Applied Physics. 39, 5651, 1968.

38. J. E. Shelby, "Effect of Radiation on the Physical Properties of Borosilicate Glasses", Journal of Applied Physics, 51, 2561-65, 1980.

39. D. D. Walker, M. D. Dukes, M. J. Plodinec and N. E. Bibler, "Effect of Radiation on Leaching of Borosilicate Glass Containing Defense High-Level Nuclear Waste", Abstracts, Symposium on Chemical Consideration for Important Radioactive Waste Species, 181st National Meeting of the American Chemical Society, Atlanta, March 1981.

40. J. E. Mendel, "The Storage and Disposal of Radioactive Waste as Glass in Canister", Pacific Northwest Laboratory Report PNL-2764, 1978.

41. D. M. Martin, Iowa State University, "Thermal Stresses in Waste-Disposal Systems - Annual Report for the Period Ending 30 September, 1979, NRC Contractor Report NRC-04-789-268, 1980.

42. G. McVay, "Gamma-Irradiation Effects on Leaching", p. 83, in Proceedings of the Task 2 Workshop, Waste Isolation Safety Assessment Program, USDOE Report PNL-SA-7992, May 1979.

43. G. L. McVay, W. J. Weber and L. R. Pederson, "Effects of Radiation on the Leaching Behavior of Nuclear Waste Forms", Abstracts, ORNL Conference on the Leachability of Radioactive Solids, Gatlinburg, Tennessee, December 1980.

44. R. P. Turcotte, Pacific Northwest Laboratories, "Radiation Effects in Solidified High Level Waste, Part 2, Helium Behavior", BNWL-2051, May 1976.

45. G. Malow and H. Andersen, "Helium Formation From Alpha Decay and Its Significance for Radioactive Waste Glasses", in Scientific Basis for Nuclear Waste Management, Vol I, G. J. McCarthy, Ed. (Plenum Press, N.Y., 1979), p. 109-115.

46. W. A. Ross, et al., Pacific Northwest Laboratory, "Annual Report on the Characterization of High Level Waste Glasses", PNL 2625, June 1978.

47. J. M Rusin, W. J. Gray and J. W. Wald, Pacific Northwest Laboratories, "Multibarrier Waste Forms, Part II: Characterization and Evaluation", PNL-2668-2, August, 1979.

48. F. P. Roberts, G. H. Jenks, and C. B. Bopp, Pacific Northwest Laboratory, "Radiation Effects in Solidified High-Level Waste - Part I, Stored Energy", BNWL 1944, January 1976.

49. R. P. Turcotte and F. P. Roberts, "Phase Behavior and Radiation Effects in High-Level Waste Glass", p. 65, in Ceramic and Glass Radioactive Waste Forms, USERDA Conference Proceedings, CONF 770102, 1977.

50. W. J. Weber, J. W. Wald and W. J. Gray, "Radiation Effects in Crystalline High-Level Nuclear Waste Solids", Abstracts-Symposium D: Scientific Basis for Nuclear Waste Management, Annual Meeting, Materials Research Society, Boston, November, 1980.

51. J. S. Stroud, "Color Centers in a Cerium Containing Silicate Glass", J. Chem. Phys. 37, p. 836-841, 1961.

52. P. B. Macedo, et al., "Stability of Fixation Solids for High-Level Radioactive Wastes", p. 81, in High Level Radioactive Soilid Waste Forms, USNRC Conference Proceedings, NUREG/CP-0005, December 1978.

53. H. D. Holland and D. Gottfried, "The Effect of Nuclear Radiation on the Structure of Zircon", Acta Cryst. 8, 291, 1955.

54. K. M. Ghouse, "Refinement of the Crystal Structure of Heat-Treated Monazite Crystal", Indian J. Pure. Appl. Phys. 6, 256, 1968.

55. L. A. Boatner et al., "Monazite and Other Canthanide Orthophosphates as Alternate Actinide Waste Forms", in *Scientific Basis for Nuclear Waste Management*, Vol II, p. 289-296, C. M . Northrop Jr., Ed. (Plenum Press, N.Y., 1980).

56. W. J. Weber, Pacific Northwest Laboratory, "Ingrowth of Lattice Defects in Alpha-Irradiated UO_2 Single Crystals", Pacific Northwest Laboratory Report, PNL-SA-8574, August, 1980. (To appear in *J. Nuclear Materials*.)

57. W. J. Weber and R. P. Turcotte, "Radiation Damage in Nuclear Waste Ceramics", Presented at the Fall Meeting of American Ceramic Society, San Francisco, California, October 26-29, 1980.

58. W. C. Mosley, "Self-Radiation Damage in Curium-244 Oxide and Aluminate", J. Amer. Cer. Soc. *54*, p. 475, 1971.

59. L. Cartz, F. G. Karioris, R. E. Fournelle, A. Gowda, K. Ramasami and M. Limoges, "Metamictization by Heavy Ion Bambardment of Alpha-Quartz, Zircon, Monazite and Nitride Structures", *Abstracts-Symposium D: Scientific Basis for Nuclear Waste Management*, Annual Meeting, Materials Research Society, Boston, November, 1980.

60. Rockwell International Energy Systems Group, "Tailored Ceramics for Geologic Storage of High Level Nuclear Waste", Presented to the Alternate Waste Form Peer Review Panel, Atlanta, Georgia, May 18, 1981.

61. L. W. Hobbs, "Radiation Effects in Analysis of Inorganic Specimens by TEM", in *Introduction to Analytical Electron Microscopy*, eds. J. J. Hren, J. T. Goldstein, and D. C. Joy, (Plenum Press, New York, 1979) p. 437.

62. K. D. Reeve and J. L. Woolfrey, "Accelerated Irradiation Testing of SYNROC Using Fast Neutrons - I. First Results on Barium Hollandite, Perovskite and Undoped SYNROC B", J. Austr. Ceram. Soc. *10*, 1980.

63. K. D. Reeve, et al., "The Development and Testing of SYNROC for High Level Radioactive Waste Fixation", Presented at *Waste Management '81*, American Nuclear Society/Univ. of Arizona/USDOE Conference, February 1981, Proceedings in press.

64. Lawrence Livermore Laboratory Presentation, "Immobilization of High Level Defense Wastes in SYNROC: An Appraisal of Product Performance", Presented to the Alternate Waste Form Peer Review Panel, Atlanta, Georgia, May 18, 1981.

65. R. F. Haaker and R. C. Ewing, University of New Mexico, "Naturally Occurring Crystalline Phases: Analogs for Radioactive Waste Forms", Pacific Northwest Laboratory Report, PNL-3505, January, 1981.

66. R. C. Ewing, "Radiation Damage in Natural Materials: Implications for Radioactive Waste Forms", Abstracts, *Alternate Nuclear Waste Forms and Interactions in Geologic Media - A Workshop*, Sponsored by ORNL and USDOE, Gatlinburg, TN, May 13-15, 1980. Available from ORNL.

67. G. J. McCarthy, J. G. Depim, and D. E. Pfoertsch, "Crystalline Chemistry of Materials in Current Supercalcine Ceramics", p. 315, in Ceramics in Nuclear Waste Management, USDOE Conference Proceedings, CONF-790420, May 1979.

68. W. Neumann and O. Kofler, "Coating of Waste Containing Ceramic Granules", p. 150, in Ceramics in Nuclear Waste Management, USDOE Conference Proceedings, CONF-790420, May 1979.

69. D. J. Clough, et al., "Irradiation Damage Study of Pyrolytically Deposited Carbon Coatings", p. 505, in Radiation Damage in Reactor Materials, IAEA Conference Proceedings, STI/PUB/230, Vienna, 1969.

70. R. A. U. Huddle, K. Mayr and K. W. Jones, "Influence of Fabrication Parameters on the Incidence of Spearhead Attack in Coated Particle Fuel", p. 481, in Radiation Damage in Reactor Materials, IAEA Conference Proceedings, STI/PUB/230, Vienna, 1969.

71. J. A. Stone, Savannah River Laboratory, "Evaluation of Concrete as a Matrix for Solidification of Savannah River Plant Waste", DP-1448, June, 1977.

72. S. Katz, "The Reaction of Hydrogen and Oxygen in the Presence of Concretes Incorporating Simulated Radioactive Waste", in Scientific Basis for Nuclear Waste Management, Vol 2, C. M. Northrup Jr., Ed. (Plenum Press, N.Y., 1980), p. 577-584.

73. N. E. Bibler, "Radiolytic Gas Production From Concrete Containing Savannah River Plant Waste", Savannah River Laboratory Report, DP-1464, January, 1978.

74. M. D. Houston, "Properties of Spent Fuel", p. 561, in High-Level Radioactive Solid Waste Forms, USNRC NUREG/CP-0005, December 1978.

75. H. D. Holland and L. H. Brusis, "Uranium Oxides in Ores and Spent Fuels", p. 597, in High-Level Radioactive Solid Waste Forms, USNRC Conference Proceedings, NUREG/CP-0005, December 1978.

76. J. Belle, "Uranium Dioxide: Properties and Nuclear Application", TID-7546, 1961.

77. R. Wang and U. B. Katayama, "Probable Leaching Mechanisms for Spent Fuel", Abstracts, Alternate Nuclear Waste Forms and Interactions in Geologic Media - A Workshop, Sponsored by ORNL and USDOE, Gatlinburg, TN, May 13-15, 1980. Available from Oak Ridge National Laboratory.

78. N. Q. Lam and S. J. Rothman, "Radiation Enhanced Diffusion in Metals and Alloys", in Radiation Damage in Metals, H. L. Peterson and S. D. Harkness, Eds., (American Society for Metals, Metals Park, Ohio, 1976), p. 125-156.

79. J. C. Bourgoin and J. W. Corbett, "Enhanced Diffusion Mechanisms", Radiation Effects, 36, p. 157-188, 1972.

80. Radiological Health Handbook, U. S. Department of Health, Education and Welfare, Publication #PB 121784R, September, 1960.

81. A. V. Byalobzheskii, "Radiation Corrosion", U. S. Atomic Energy Commission Translation, AEC-Tr 7096, 1970.

82. W. G. Burnes and P. B. Moore, "Water Radiolysis and its Effect Upon In-reactor Zircaloy Corrosion", Radiation Effects, 30: 233, 1976.

83. K. Isisigure, et al., "Effect of Gamma Radiation on the Release of Corrosion Products from Carbon Steel and Stainless Steel in High Temperature Water", Nuclear Technology, 49, 1980.

84. N. Fujita, M. Akiyama and T. Tamura, "Stress Corrosion Cracking of Type 304 Stainless Steel in High Temperature Water Under Gamma Ray Irradiation", Corrosion, 37, p. 335, 1981.

85. G. H. Jenks, "Review of Information on the Radiation Chemistry of Materials Around Waste Canisters in Salt and Assessment of the Need for Additional Experimentation", Oak Ridge National Laboratory Report, ORNL-5607, March, 1980.

86. G. H. Jenks, Oak Ridge National Laboratory, "Radiolysis and Hdyrolysis in Salt-Mine-Brines", ORNL-TM-3717, March 1972.

87. W. F. Bonner, D. E. Knowlton, W. J. Bjorklund and M. S. Hanson, "Engineering Scale Vitrification of Commercial High-Level Waste", Presented at Waste Management '80 - The State of Waste Disposal Technolgoy, Mill Tailings and Risk Analysis Models, Symposium Sponsored by the University of Arizona and the USDOE, Tuscon, Arizona, March 10-14, 1980 (Proceedings in Press).

88. G. H. Jenks, Oak Ridge National Laboratory, "Effect of Gaseous Radionuclides on the Design and Operation of Repositories for Spent LWR in Rock Salt", ORNL-5578, December 1979.

89. J. W. Braithwaite and M. A. Molecke, "Nuclear Waste Canister Corrosion Studies Pertinent to Geologic Isolation", Nuclear and Chemical Waste 1, 2, 1980. Available from Pergamon Press.

90. P. E. Ahlstrom, "Ceramic and Pure-Metal Canisters in Buffer Material", p. 285, in High-Level Solid Radioactive Waste Forms, USNRC Conference Proceedings, NUREG/CP-0005, December 1978.

91. M. J. Magnani and J. W. Braithwaite, "Corrosion Resistant Metallic Canisters for Nuclear Waste Isolation", in Scientific Basis for Radioactive Waste Management, Vol II, C. M. Northrup Jr., Ed. (Plenum Press, N.Y.), p. 377-384.

92. E. E. Bloom, "Irradiation Strengthening and Embrittlement", p. 295, in Radiation Damage in Metals, N. L. Peterson and S. D. Harkness, Eds., (American Society for Metals, Metals Park, Ohio, 1976).

93. A. S. Nikiforov, et al., "Thermal Chemical and Radiation Stability of Vitreous Radioactive Wastes", in Scientific Basis for Radioactive Waste Management, Vol I, G. J. McCarthy, Ed., (Plenum Press, N.Y., 1979), pp. 117-121.

94. V. I. Spitsyn, et al., "Influence of Radiation of the System Liquid Radioactive Wastes - Geologic Formation", in Scientific Basis for Nuclear Waste Management, Vol I, G. J. McCarthy, Ed., (Plenum Press, N.Y., 1979), p. 249-256.

95. S. Fried et al., "The Effect of Radiation on the Oxidation States of Plutonium in Various Aqueous Solutions", Abstracts, Symposium G - Scientific Basis for Nuclear Waste Management, Materials Research Society Annual Meeting, Boston, MA, November 1979. Proceedings in press.

96. D. Rai, R. J. Serne and D. A. Moore, Soil Sci. Soc. Am. J., 44, p. 490-495, 1980.

97. B. T. Kenna, Sandia Laboratory, "Radiation Stability of Sodium Titanate Ion Exchange Materials", SAND79-0199, February, 1980.

98. N. J. Singh and S. M. Tandon, "Zirconium Orthophosphate as an Ion Exchanger", J. Radioanal. Chem., 49, p. 195, 1979.

99. B. W. Mercer and W. C. Schmidt, "Storage of Long-Lived Fission Products on Alumino-Silicate Zeolites", in Proceedings of the Symposium on the Solidfication and Long-Term Storage of Highly Radioactive Waste, USAEC Report LONG-660208, p. 207, February, 1966.

100. L. V. C. Rhees and C. J. Williams, "Neutron Irradiation of Molecular Sieve 13X", Proc. Roy. Soc. A 290, p. 1481, 1965.

101. R. Fullerton, General Electric Company, Hanford Atomic Products Operation, "The Effect of Gamma Radiation on Clinoptilolite", General Electric Company Report, HW-69256, April, 1961.

102. R. M. Wallace, SRL, to K. Swyler, BNL, Private Communication, March 27, 1981.

103. K. K. S. Pillay, Pennsylvania State University, "Radiation Effects on Ion Exchangers Used in Radioactive Waste Management", NE/RWM-80-3, October, 1980.

104. K. Swyler, R. E. Barletta and R. E. Davis, "Review of Recent Studies of the Radiation Induced Behavior of Ion Exchange Media", Brookhaven National Laboratory Report, BNL-NUREG-28682, November 1980.

105. R. E. Brooksbank, ORNL, to S. W. Ahrends, DOE, Oak Ridge Operations, December 12, 1980. A. P. Malinauska, ORNL, to S. W. Ahrends, DOE Oak Ridge Operations, February 19, 1981 - Private Communication with Copies Provided to USNRC.

106. D. Campbell, ORNL, to K. Swyler, BNL, Private Communication, March 27, 1981.

107. U. Jain and A. B. Lidiard, "The Growth of Colloidal Centres in Irradiated Alkali Halides", Phil. Mag. 35, p. 245, 1977.

108. G. H. Jenks and C. D. Bopp, Oak Ridge National Laboratory, "Storage and Release of Radiation Energy in Salt in Radioactive Waste Repositories", ORNL 5058, October 1977.

109. K. J. Swyler, R. W. Klaffky and P. W. Levy, "Recent Studies on Radiation Damage Formation in Synthetic NaCl and Natural Rock Salt for Radioactive Waste Disposal Applications", in Scientific Basis for Radioactive Waste Management, Vol II, C. J. Northrup, Jr., Ed. (Plenum, N. Y., 1980), p. 553-560.

110. G. W. Arnold, "Radiation Hardening of Rock Salt", Abstracts, Symposium D, Scientific Basis for Nuclear Waste Management, Materials Research Society, Boston, MA, November 1980.

111. B. D. Gunter and F. L. Parker, Oak Ridge National Laboratory, "The Physical Properties of Rock Salt as Influenced by Gamma Rays", ORNL-3027, March, 1961.

112. F. Aguillo-Lopez and P. W. Levy, "Effects of Gamma-Ray Irradiation on the Mechanical Properties of NaCl Single Crystals", Proc. Brit. Ceram. Soc. 1, p. 183, 1964.

113. G. H. Jenks, E. Sonder, C. D. Bopp and J. R. Walton, "Reaction Products and Stored Energy Released From Irradiated Sodium Chloride by Dissolution and Heating", J. Phys. Chem. 79, p. 871, 1975.

114. R. L. Fleischer, "Isotope Disequilibrium of Uranium: Alpha Recoil Damage and Preferential Solution Effects", Science 207, p. 979-981, 1980.

6. IDENTIFICATION OF VARIABLES AFFECTING RADIONUCLIDE RELEASE FROM THE WASTE PACKAGE

In establishing licensing criteria for a HLW repository, NRC is considering the following basic performance objectives for a waste package:[1,2]

- Presuming that early flooding of the repository will occur the waste package should limit the release of radionuclides to near zero for the first 1000 years after emplacement, and as long as reasonably achievable thereafter.
- The maximum annual rate of radioactivity release from the underground facility at any time after package failure should not exceed $1/10^5$ of the package inventory 1000 years after decommissioning.
- The repository design should allow the option to retrieve the wastes throughout the operating period and for 50 years thereafter.

Many variables exist within the waste package/repository environment and some are critically important in determining whether the above criteria can be met. In the sections below, we will identify some of the principal variables which must be well understood if a satisfactory package design is to be developed; i.e., one which can be confidently expected to meet predetermined limits for radionuclide release. The waste package components themselves are important variables and their performance, in turn, is influenced by the environmental conditions characteristic of a specific repository site. The two sets of variables are interrelated in that the waste package characteristics can affect the ambient environmental conditions. Therefore, in order to develop a satisfactory waste package, i.e., one which can be expected to meet the NRC 1000 yr and the 10^{-5}/yr controlled release criteria, the waste package components and the repository environmental conditions and the interdependence of these two sets of variables must be well characterized and understood.

6.1 Waste Package Components

The overall performance of a waste package in a given environmental setting is determined, to a large extent, by the design and the characteristics of its major components and behavior of these components over a period of time spanning the life of the repository. The package components discussed below include: the waste form, the container, and the backfill.

6.1.1 Waste Form

The waste form is the primary medium for waste encapsulation. Selection of the appropriate waste form is important because it represents the radionuclide source term for the entire geologic waste isolation system. For example, some of the newly developed waste forms such as the porous glass matrix and coated particles are highly inert to dissolution and appear to have the potential to satisfy the NRC controlled release criterion.[3] A detailed evaluation of the various waste forms and their potential for meeting the NRC criteria is presented in Section 2 of this Report.

Perhaps the most important characteristics of a waste form are its composition, in terms of the fission products and actinides, and the resultant heat content and radiation level. The waste form composition, in turn, is determined by the type of waste, the waste loading relative to the inert matrix elements of the waste form, aging of the waste prior to immobilization, and delayed emplacement of the waste form in a container. All these factors will determine the thermal and radiation environment of the waste form which, in turn, can affect the chemical and mechanical durability of a waste form (see Sections 2 and 5 for details). The waste form composition and solution chemistry can influence waste form leaching. The importance of temperature as a variable is realized when temperature dependences of the waste form solubility and leachability are considered. The overall dissolution processes and mechanisms can be affected by temperature.

The rates of radionuclide release and the mechanisms by which waste form dissolution occurs over long time periods determine, to a large extent, the rate and extent of radionuclide release from a waste package. Waste form dissolution under repository conditions is represented in most cases by parabolic kinetics, reflecting diffusion controlled radionuclide release, and is believed to indicate that the leaching process slows down over a period of time presumably due to the buildup and growth of residual material which serves to protect the underlying unreacted material from further attack by groundwater.[4] The leach rate will be influenced by the type of waste form and its thermal and radiation environment. Other rate controlling variables include local repository conditions such as pH, Eh, and composition of groundwater, and flow rate. Leaching of most waste forms is increased at both high and low pH. The overall dissolution process and waste form solubility are both dependent on groundwater pH. In addition, the use of a large sample having a small surface-to-volume ratio for a waste form, will effectively decrease the rate of radionuclide release. However, large samples would be more susceptible to decay heating induced thermal cracking of the waste form, thereby resulting in an increase in the effective surface area and radionuclide release. Some of the repository variables such as pH, Eh, groundwater composition, and flow rate can be modified by using the appropriate mixture of materials and geometry for backfill.

Assuming early flooding of the repository and a zero flow static situation, the waste form leach rate becomes less important as compared to its solubility for several radionuclides. The concentrations of Np, Am, U, and Pu are reported to be solubility limited by the precipitation of their oxide or other solid phases.[5,6] For crystalline waste forms, the extent of radionuclide release will be constrained by the equilibrium solubility of the individual minerals. Repository conditions such as temperature, redox potential, pH, and composition of groundwater can all be controlled to decrease the solubility of the waste form, thus resulting in a lower release of radionuclides. The concentration levels of other radionuclides such as Tc, Se, and I are also solubility limited, the pH and Eh being the most important variables affecting the precipitation of their respective solid phases.[3] It should be mentioned, however, that addition of fresh groundwater to the saturated system will presumably result in an adjustment of the saturation equilibrium, giving rise to further release of radionuclides from the waste form or dissolution of the freshly precipitated minerals until a new saturation equilibrium is reached between the radionuclides in solution and the solid phases. Therefore, the groundwater flow rate is a critical variable with respect to waste form dissolution and radionuclide precipitation.

6.1.2 Container

The container in which the waste form is sealed must satisfy various basic requirements if it is to fulfill its role as a principal barrier of the waste package designed to contain wastes for a period of up to 1000 years. Because of this, container corrosion and the conditions which determine the rate and extent of the corrosion process must be identified (see Section 3 of this Report for further details).

An important factor is the minimization of container corrosion by selecting the appropriate repository environment. Several different types of host rocks have been considered in a HLW repository including rock salt, shale, basalt, tuff, and granite. Since the groundwater composition is controlled by the type of host rock, water chemistries will vary from one rock type to another and also from location to location for the same rock type. For example, the very high chloride levels, especially the presence of $MgCl_2$ in salt brines, are likely to be more damaging to metallic containers so that factor must be weighed against the anticipated higher water levels but less corrosive environment in hard rock repositories.

Lower oxygen contents are usually reported in groundwaters found deep below the surface. This has a most important bearing on the probability of the metal containers failing by localized pitting, crevice corrosion, and stress corrosion cracking. Therefore, the repository depth is an important consideration with respect to minimizing container corrosion. The oxygen content of groundwater can also be controlled by tailoring overpack/backfill with Fe^{2+} minerals.

Both temperature and radiation effects, which can be controlled by adjusting the loading and delayed emplacement of the waste form, could alter the nature and extent of the corrosion process in metals. Elevated temperatures greatly accelerate localized corrosion of the metal containers. The radiolysis of groundwater by gamma radiation can cause hydrogen generation and interaction with metals which could result in loss of ductility. Corrosion of container materials can be enhanced by radiolysis of rock salt brines.

As a controllable variable, the container design can be an important variable in assuring that a waste package will last for a period of up to 1000 years. Radiation and radiolytic effects on the container can be controlled by internal shielding of the container with a lead lining. This strategy has been adopted by the Swedes in their KBS program.[7] A sealed waste container could become internally pressurized or stressed by radiation induced helium buildup or by swelling of the waste form (see Section 5 for details). Therefore, containers should be designed to accommodate such anticipated changes, resulting from radiation and thermal effects. For example, the use of a can-in-a-can container system consisting of several containers of two different materials such as Ti and Pb is advantageous as compared with a single wall container because of the nature of localized corrosion processes. The length of time for pit or crack initiation in a metal is often much greater than the penetration rate. Therefore, in a multiple walled container system the time required for failure to occur will be much greater than that in a thick, single walled container.

6.1.3 Backfill

The primary functions of backfill in an HLW repository are to control groundwater ingress in order to minimize the possibility of container corrosion and to retard radionuclide migration should failure of the container occur. There are a number of variables which could affect the properties of backfill. To ensure that backfill will function as an effective barrier in a HLW repository, the variables that are likely to affect the backfill performance must be identified and, if possible, controlled. A detailed evaluation of backfill in a HLW repository is given in Section 4 of this Report.

Since backfill is expected to perform as a barrier for the entire life of a repository, the candidate backfill materials should be stable over long time periods, especially during the first 1000 years when hydrothermal conditions may prevail. This can be achieved by selecting the most stable materials for backfill or by avoiding hydrothermal conditions by the use of a waste form with a low waste loading.

In the event of a container breach, backfill is the main barrier to radionuclide migration. Hence, it is important to ensure that radionuclide transport occurs principally by diffusional and sorption processes rather than by advection.[8,9] This can be achieved by the use of a highly sorptive backfill having low permeability. Selection of a repository where groundwater flow approaches a static situation will also provide slow diffusional transport of radionuclides.

In order to minimize container corrosion and immobilize the migrating radionuclide anionic species such as TcO_4^-, I^-, and SeO_4^{2-}, the backfill should be tailored to provide the appropriate redox conditions. This can be achieved by the use of Fe^{2+} minerals in backfill as proposed by the Swedes in the KBS study[7] or by the use of other non-aluminosilicate minerals.[10] Recent studies show that activated charcoal is an extremely efficient sorbent for I^- and TcO_4^-.[11] This material could be admixed with backfill to retard the migration of these radionuclides.

Certain zeolites are reported to fix sorbed radionuclides irreversibly.[12,13] Selection of appropriate material to immobilize released radionuclides by fixation would be extremely useful in containing the waste ions within the spatial extent of the backfill boundary.

Expandable materials, which swell upon hydration with a resultant decrease in permeability, such as montmorillonites[14,15] and brucite[10] are being considered for backfill to control water ingress. The swelling behavior of montmorillonites is a function of the nature of the interlayer cation.[16] For example, Ca-montmorillonite swells less than the Na form by a factor of 2.5. Location of a repository in a salt formation would ensure that the backfill is saturated with Na^+ ions, thus providing the maximum swelling, as desired, to reduce the effective permeability.

Compatibility of backfill with the surrounding host rock can be achieved by the use of crushed host rock material for backfill. The BWIP program is considering the use of crushed basalt as backfill for a repository located in basalt.[17] The presence of Fe^{2+} minerals such as olivine in the basalt is reported to maintain the concentration of dissolved oxygen at low levels, thus minimizing the probability of canister corrosion.

As controllable variables, the groundwater composition and concentration, pH and Eh, temperature and radiation effects, and the rate of water flow will also influence sorption of released radionuclides by backfill.

Gas generation in backfill by radiolysis or other factors should be controlled to minimize its effect on the performance of backfill and its subsequent deformation.

With respect to backfill design, increased thickness of low permeability backfill will provide enhanced capability for the minimization of water ingress and increase the diffusional path length for the released radionuclides, thereby maximizing its radionuclide retardation effectiveness. Synthetic materials such as zeolites and/or titanates of regularly shaped small particles can be used, through prior selection of the mass, volume, shape, and packing densities, to predetermine and control the groundwater flow rates and patterns into and through the engineered underground facility for varying aquifer pressures and flow rates. Such a modification of the hydrodynamics of an underground facility could be advantageous in that rapid radionuclide transport by advection would be minimized, resulting in diffusion-controlled transport. The feasibility of using such backfill materials and design has been evaluated in terms of the NRC radionuclide release criteria (see Appendix A).

6.1.4 Waste Package

It must, of course, be realized that the "best" waste form, the "best" container, the "best" overpack/backfill system and the "best" host rock when used in combination do not necessarily constitute the most effective system for minimizing the release of radionuclides. It is possible that synergistic effects exist between adjacent components which could compromise the overall effectiveness of the waste package.[18] If, however, a container/ backfill system could be designed such that the probability of water contacting the waste form is reduced to near zero for an indefinite time, then the characteristics of the waste form become unimportant. Hence, it can be seen that the selection of an effective combination of waste form components is the most important variable to be considered in limiting the release of radioactivity from the waste package.

6.2 Repository Conditions

Knowledge of the environmental conditions anticipated in high level waste repositories is of particular importance to the testing and overall performance of waste package components. In the past, it was difficult to even estimate some repository conditions due to the fact that repository design was in its early stages. At this point in time, however, repository designs have evolved from which reasonable calculations of the near field thermal environment can be made. In addition, research has proceeded concerning the geochemical environment of repositories, especially that of a basalt repository. In the sections below, available data and calculations concerning repository conditions are presented.

6.2.1 Repository Thermal Environment

Some information concerning thermal characteristics of proposed repository designs in salt, basalt, tuff, granite, and shale is presented in Table 6.1. From this information along with other design specifications, the reference peak near field temperatures have been calculated (Table 6.2). It is worth noting that, on the whole, these peak temperatures are below those calculated (>300°C) in the past.

Table 6.1

Thermal Characteristics of Reference Repositories[19]

Characteristic		Salt	Basalt	Tuff	Granite	Shale
Canister Thermal Loading (KW)*	SF	0.55	1.65 or 0.55	0.55	0.55	0.55
	CHLW	2.16	N.A.	2.16	1.0	1.0
	DHLW	0.31	N.A.	N.A.	0.31	0.31
Areal Thermal Loading (KW/ACRE)	SF	25	12.3	25	20	10
	CHLW	25	N.A.	25	25	10
	DHLW	11.6	N.A.	N.A.	13.5	10
Repository Depth (m)	SF	600	1000	800	1000	600
	CHLW	600	N.A.	800	1000	600
	DHLW	600	N.A.	N.A.	1000	600
Ambient Repository Temperature (°C)		34	57	35	20	38

Table 6.2

Reference Peak Near Field Temperatures (°C)[19]

Host Rock	Location	SF	CHLW	DHLW
Salt	Host Rock	140	160	80
	Canister Wall	145	260	90
	Waste[(a)]	175	320	100
Basalt	Host Rock	145 (165)[(b)]	--	--
	Canister Wall	255 (170)[(b)]	--	--
	Waste[(a)]	275 (185)[(b)]	--	--
Tuff	Host Rock	190	215	--
	Canister Wall	195	235	--
	Waste[(a)]	230	275	--
Granite	Host Rock	150	165	105
	Canister Wall	170	205	115
	Waste[(a)]	190	225	120
Shale	Host Rock	125	140	125
	Canister Wall	140	210	135
	Waste[(a)]	165	235	140

(a) Maximum centerline temperature for CHLW and DHLW; maximum cladding temperature for SF.

(b) Results for 3 PWR elements per canister waste package configuration. Results for 1 PWR element per canister waste package configuration are shown in parentheses.

6.2.2 Basalt Repository

The most thorough overall effort at characterizing a repository environment has been that conducted at Hanford for a basalt repository as part of the BWIP effort. Relevant data are given in Table 6.3. Perhaps of great importance is that the BWIP effort has succeeded in establishing the mechanism and equilibrium by which the important geochemical parameters such as pH and Eh are controlled in a basalt repository. Unfortunately, at this time, this type of information is unavailable for other potential repository host rocks.

6.2.3 Groundwater Flow Rates

In addition to the above information, some data are available concerning groundwater flow rates in various host rocks (Table 6.4). This information is most important with respect to container corrosion, waste form solubility and leach rate, and migration of released radionuclides through backfill to the surrounding host rock.

Table 6.3

Basalt Repository Conditions[20]

Repository Depth:	1000 m
Ambient Repository Temperature:	57°C (60-70°C)[a]
Range of Expected Temperatures:	60-300°C[b]
Range of Expected Pressures:	100-300 bars[c]
Ambient pH:	9.4-9.9 (@65°C)
Range of Expected pH:	3 to 9.4-9.9[d]
Range of Expected Eh:	-0.45 to -0.55 V[e]

[a] Dependent upon precise repository depth.

[b] Based upon a 2:1 ratio of BWR to PWR and a thermal loading of 25 W/m^2.

[c] Dependent upon final design and local stratigraphy

[d] Controlled by equilibrium between precipitation of clays and hydrolysis of silicates.

[e] Controlled by magnetite/siderite/pyrite mineral suite; oxic conditions anticipated for "hundreds" of years after repository closure.

6.2.4 Groundwater Chemistry

The composition of groundwater is a variable that can be controlled by the selection of appropriate host rock and location of the repository. For example, by siting a repository in a salt environment, the very high chloride levels in salt brine are likely to be much more damaging to metallic containers and most waste forms than the less corrosive groundwaters in hard rock repositories. Furthermore, the anticipated lower oxygen levels of groundwater in a basalt repository would be advantageous with respect to minimizing container corrosion and inducing precipitation of anionic radionuclide species of Tc, I, and Se. Groundwater compositions for the various rock types are given in Section 3 of this Report.

Table 6.4

Hydrologic Parameters for Host Rock Types[21]
(Based on Generic Stratigraphic Sections)

Rock Type	Generic Hydraulic Conductivity, cm/sec.	Range, cm/sec.
SALT:		
Glacial Till	$6.8x10^{-6}$	$1x10^{-7}$-$1x10^{-3}$
Calcerous Shale (partly sandy)	$1.2x10^{-5}$	$1x10^{-10}$-$1x10^{-1}$
Sandstone and Dolomite	$8.1x10^{-5}$	$1x10^{-10}$-$1x10^{-2}$
Shale; Partly Calcerous with some Anhydrite	$1.2x10^{-5}$	$1x10^{-10}$-$1x10^{-3}$
Cherty Limestone Dolomite with some Anhydrite	$5.8x10^{-5}$	$5x10^{-8}$-$1x10^{-3}$
Dolomite	$4.6x10^{-5}$	$5x10^{-8}$-$1x10^{-2}$
Salt		$2x10^{-21}$-$1x10^{-8}$
Interbedded Dolomite-Shale	$5.8x10^{-6}$	$1x10^{-10}$-$1x10^{-3}$
Shale	$7.1x10^{-7}$	$1x10^{-10}$-$1x10^{-3}$
GRANITE:		
Continuous Granitic Rock		$5x10^{-8}$-$5x10^{-4}$
SHALE:		
Sand and Gravel	$5.9x10^{-2}$	0.001-0.1
Interbedded Sandstone, Coal, Shale	$1.2x10^{-3}$	$5.x10^{-7}$-$4x10^{-3}$
Sandstone	$3.5x10^{-4}$	$1x10^{-10}$-$1x10^{-2}$
Shale	$7.1x10^{-7}$	$1x10^{-10}$-$1x10^{-3}$
Limestone	$4.7x10^{-5}$	$5x10^{-8}$-$1x10^{-2}$
BASALT:		
Gravel, Sand, Silt	$3x10^{-3}$	
High Density Basalt	$1x10^{-7}$	
Low-Medium Density Basalt	$1x10^{-6}$	
Low Density Basalt-Tuff	$3.5x10^{-6}$	
Tuffaceous Sandstone	$1x10^{-4}$	
Sandstone	$5x10^{-5}$	
Sandstone with Clay	$1x10^{-4}$	
High Density Basalt (depth >450 m)	$5x10^{-8}$	$3.5x10^{-9}$-$1.1x10^{6}$
CRYSTALLINE ROCK:		
Impermeable Zone	$1.4x10^{-12}$	
TUFF		$1x10^{-7}$-$1x10^{-3}$

6.3 References

1. Code of Federal Regulations, 10 CFR 60, "Technical Criteria for Regulating Geological Disposal of High-Level Radioactive Wastes," advance notice of proposed rule making, May 13, 1980.

2. L. A. White, M. J. Bell, and D. M. Rohrer, "Regulation of Geologic Repositories for the Disposal of High Level Radioactive Wastes," in Scientific Basis for Nuclear Waste Management, (C. J. M. Northrup, Jr., ed.), Proc. of Conf. held in Boston, November 1979, Materials Research Society.

3. R. Dayal, K. J. Swyler, and P. Soo, "NRC Nuclear Waste Management Technical Support in the Development of Nuclear Waste Form Criteria: Waste Package Overview," Interim Report, Brookhaven National Laboratory, June 1980.

4. L. L. Hench, "Physical Chemistry of Glass Surfaces," in Proceedings of the XIth International Congress on Glass, 1977.

5. D. Rai and R. G. Strickert, "Maximum Concentration of Actinides in Geologic Media," American Nuclear Society, Washington, D.C., 1980.

6. D. Rai, R. J. Serne, and J. L. Swanson, "Solution Species of Plutonium in the Environment," Journal Environmental Quality, Vol. 4, 1980.

7. National Academy of Sciences, "A Review of the Swedish KBS-II Plan for Disposal of Spent Nuclear Fuel," 1980.

8. T. M. Ahn, R. Dayal, and R. J. Wilke, "Evaluation of Backfill as a Barrier to Radionuclide Migration in an HLW Repository," unpublished Brookhaven National Laboratory Memorandum, 1980.

9. E. J. Nowak, "The Backfill Barrier as a Component in a Multiple Barrier Nuclear Waste Isolation System," Sandia National Laboratory, SAND79-1109, 1980.

10. G. W. Bird, "Possible Buffer Materials for Use in a Nuclear Waste Vault," Whiteshell Nuclear Research Establishment, Atomic Energy of Canada, Ltd., 1979.

11. E. J. Nowak, "Backfill Barriers for Nuclear Waste Repositories in Salt," Sandia National Laboratory, SANDI81-0377A, 1981.

12. S. Komarneni and R. Roy, "SUPEROVERPACK: Tailor-made Mixtures of Zeolites and Clays," Presented at Materials Research Society Annual Meeting, Massachusetts, 1979.

13. R. Roy and S. Komarneni, "Design of Overpack (Backfill) Materials," Paper presented at the National Bureau of Standards Sponsored Workshop on Research and Development Needs Relating to Backfill, Gaithersburg, Maryland, April 1981.

14. R. Pusch, "Required Physical and Mechanical Properties of Buffer Masses," KAERNBRAENSLESAEKERHET KBS-TR-33, 1977.

15. E. J. Nowak, "The Backfill as an Engineered Barrier for Nuclear Waste Management," in Scientific Basis for Nuclear Waste Management, (C. J. M. Northrup, Jr., ed.), Materials Research Society Annual Meeting, Boston, Massachusetts, 1979.

16. G. Beall, A. G. Lamkin, and K. L. Kelley, "Critical Factors Affecting the Use of Montmorillonite as a Nuclear Backfill Material," Paper presented at the National Bureau of Standards Sponsored Workshop on Research and Development Needs Relating to Backfill, Gaithersburg, Maryland, April 1981.

17. M. I. Wood and W. W. Schulz, "Engineered Barrier Development for a Nuclear Waste Repository in Basalt," Rockwell International Corporation, RHO-BWI-ST-7, 1980.

18. J. W. Shade and D. J. Bradley, "Initial Waste Package Interaction Tests: Status Report," PNL-3559, 1980.

19. Office of Nuclear Waste Isolation, "Proceedings of the 1980 National Waste Terminal Storage Program Information Meeting," ONWI-212, 1980.

20. Rockwell Hanford Operations, Rockwell International, "Engineered Barrier Development for a Nuclear Waste Repository Located in Basalt -- An Integration of Current Knowledge," RHO-BWI-ST-7.

21. U. S. Department of Energy, "Technology for Commercial Radioactive Waste Management," Vol. 4, DOE/ET-0028, 1979.

7. EVALUATION OF REGULATORY CRITERIA FOR HIGH-LEVEL WASTE, SPENT FUEL, AND TRU WASTE

The four main performance criteria specified by the NRC in 10 CFR 60* have been outlined in Section 1 of this report. They are:

(a) For the waste package there shall be containment of all radionuclides for the first 1000 years after decommissioning of the geologic repository operations area and as long thereafter as is reasonably achievable, assuming expected events and processes and that some of the waste dissolves soon after decommissioning.

(b) Starting 1000 years after decommissioning of the geologic repository operations area, the radionuclides present in HLW will be released from the underground facility at an annual rate that is as low as reasonably achievable and is in no case greater than an annual rate of one part in one hundred thousand of the total activity present in HLW within the underground facility 1000 years after decommissioning assuming expected processes and events.

(c) Starting at decommissioning radionuclides present in TRU waste will be released at a rate that is as low as reasonably achievable and is in no case greater than one part in one hundred thousand of the total activity present in TRU waste within the underground facility at the time of decommissioning assuming expected processes and events.

(d) The repository area shall be designed so that radioactive waste stored there can be retrieved for a period of 50 years after termination of waste emplacement operations, if the geologic repository operations area has not been decommissioned. If during this period a decision is made to retrieve the wastes the Department shall insure that wastes could be retrieved in compliance with 10 CFR (Part 20) and in about the same period of time as that during which they were emplaced.

These requirements have been a source of debate since they were first published in the Federal Register in May, 1980.* A short discussion is given below on their relevance as regulatory criteria.

7.1 Containment of Radionuclides for a Specific Time Period

During the reprocessing of spent fuel for the commercial power industry, uranium and plutonium will be removed and the uranium enriched in U-235 and new fuel fabricated. The plutonium may also be incorporated into either light water reactor or fast breeder reactor fuel. In the defense program the plutonium is used for warhead manufacture. In the naval reactor program the uranium is recovered and reenriched but the small amounts of plutonium are usually disposed of with the waste products.[1] Because of such factors there are significant differences in the composition of commercial and defense waste and spent fuel. In addition, defense waste is much cooler because of the long periods of time that it has been stored.

---

*Since the writing of this report a more recent version of 10 CFR 60 has been issued (July 1981).

Figure 7.1 shows the radionuclide activity of defense waste for times extending to one-million years.[2] For spent PWR fuel, decay curves are shown in Figure 7.2.[3] It may be seen that the rate of radionuclide decay is relatively rapid up to above 600-800 years, after which an inflection is reached. For defense waste the inflection extends beyond 10^4 years before additional major reductions in activity occur. In the case of spent fuel, it extends to about 2000-3000 years. In the 600-800 year period, then, the major fission products (Cs, Sr) have decayed in activity and heat content by about three orders of magnitude. Since the major fission product species are effectively extinct after about 800 years, and long-lived isotopes such as I-129 and Tc-99 are relatively low in concentration, a natural conservative containment time for the radionuclide inventory in a high-level or spent-fuel waste package would be 1000 years. Containment for a much longer period, say 10^4 years, would not yield any significant additional benefit in terms of decreased heat content or reduction in toxicological effects arising from fission-product species. On this basis the minimum 1000 year NRC containment criterion appears to be sound and defensible.

In the case of TRU waste, the long-lived nature of these radionuclides make 1000 year containment an unnecessary criterion since no significant decay occurs in this time frame (see Figures 7.1 and 7.2). Containment times of about 10^5 years will be needed for spent TRU waste in order to decrease the activity by one order of magnitude (Figure 7.2). At this time there does not appear to be a practical way to develop a data base that can reasonably demonstrate containment for such extended times.

7.2 Controlled Release of Radionuclides

White et al.[4] recently carried out a simple study on the effect of radionuclide decay rates on the rate of release of the radionuclides from an underground facility. Assuming a constant release rate (RR) they define a release time RT = 1/RR. Thus, an element with an annual release rate of 1 part in 10^6 per year will be totally lost from the underground facility in 10^6 years provided that it does not exhibit radioactive decay. If an element does show decay then a certain proportion will decay in-situ so that less will be released from the engineered system. The following equation was derived, relating the fractional release (FR) of a radionuclide having a half life of $t_{1/2}$:

$$FR = \frac{1.443}{RT/t_{1/2}} \left[1-e^{-0.693\,(RT/t_{1/2})}\right].$$

Assuming release times of 10^5, 10^6, and 10^7 years, White et al. obtained fractional release values for selected radionuclides (Table 7.1). For a

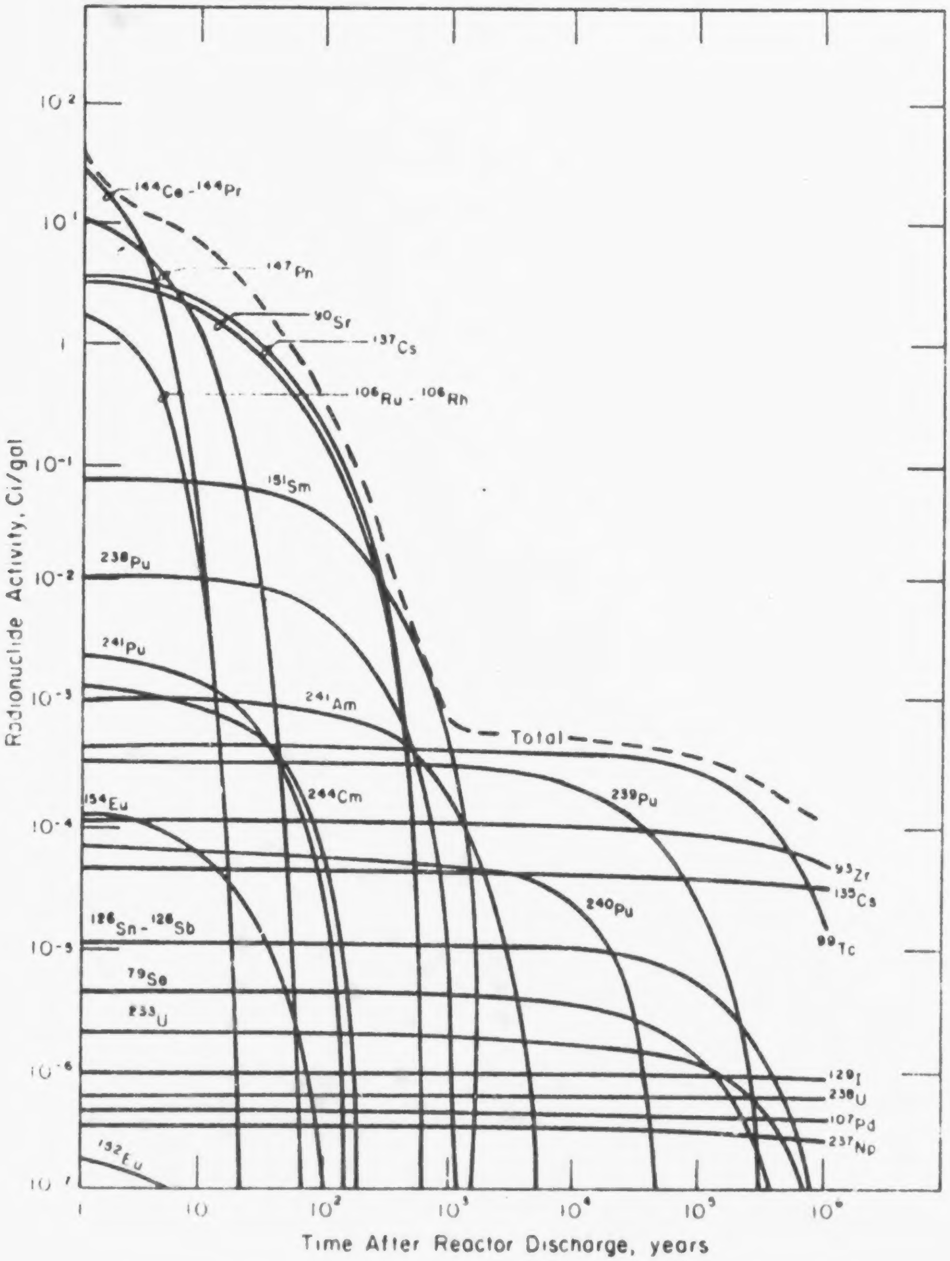

Figure 7.1 Radionuclide composition of SRP waste (1 to 10^6 years after irradiation).

BEST DOCUMENT AVAILABLE

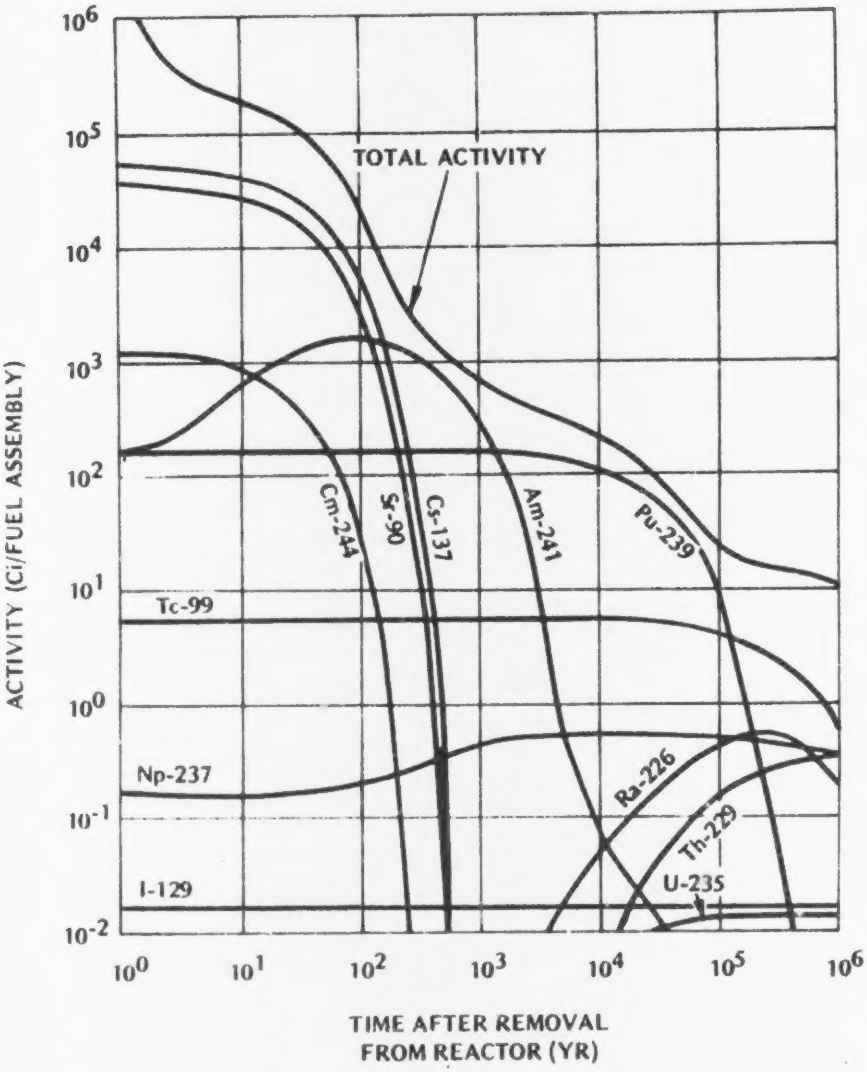

Figure 7.2 Radioactive decay of PWR spent fuel.

BEST DOCUMENT AVAILABLE

Table 7.1

Relationship Between Release Time and Total Releases from the Engineering Repository

Release Time = 10^5 Years

Nuclide	Half-Life	Fraction Release
^{14}C	5.7×10^3y	0.08
^{240}Pu	6.6×10^3y	0.10
^{239}Pu	2.4×10^4y	0.27
^{99}Tc	2.1×10^5y	0.88
^{129}I	1.7×10^7y	1.0

Release Time = 10^6 Years

Nuclide	Half-Life	Fraction Release
^{14}C	5.7×10^3y	0.008
^{240}Pu	6.6×10^3y	0.010
^{239}Pu	2.4×10^4y	0.035
^{99}Tc	2.1×10^5y	0.29
^{129}I	1.7×10^7y	0.98

Release Time = 10^7 Years

Nuclide	Half-Life	Fraction Release
^{14}C	5.7×10^3y	0.0008
^{240}Pu	6.6×10^3y	0.0010
^{239}Pu	2.4×10^4y	0.0035
^{99}Tc	2.1×10^5y	0.030
^{129}I	1.7×10^7y	0.82

release time of 10^5 years, Tc-99 and I-129 decay so slowly that essentially all of the inventory is released in this time. For a release time of 10^7 years, however, the Tc-99 shows significant in-situ decay and only 3% is released. In the case of I-129, the decay rate is such that 82% of the initial inventory is released. For C-14, Pu-139, and Pu-140 the decay rates are fast compared to I-129 and even for a release time of 10^5 years the vast majority of these elements decays in-situ and relatively little is released from the underground facility. Problems may be encountered with Tc-99 since a release time of about 10^6 years is needed to minimize the fractional release value. This becomes an important factor since this element is one of the more abundant radionuclides in the post 1000 year period. Iodine-129 has such a long half-life that a release time of 10^7 years has only a small impact on the fractional release value.

On the basis of the above discussion it appears that the behavior of Tc-99 is sufficiently important for it to be given prime consideration. The quantities present in high level waste suggest that an overall annual release rate of 1 part in 10^6 would be a reasonably conservative value. This is an order of magnitude less than the value specified by NRC (see above). At this time, however, the choice of an annual release rate of 1 part in 10^5 or 1 part in 10^6 is tentative since the eventual release rate will have to conform to an EPA standard which is currently being developed. This standard is expected to be radionuclide specific since the toxicological effects vary from radionuclide to radionuclide. Nevertheless, the NRC criterion of an annual release rate of 1 part in 10^5 for high level and transuranic wastes is useful as an interim criterion to be addressed in the DOE waste package effort, even though it is less defensible than a 1 part in 10^6 value.

7.3 Retrievability of Waste

A basic requirement in the design of a waste package and underground facility is retrievability, i.e., the ability to remove waste if the performance of the engineered system is judged to have been compromised. The requirement, stated above, is for all of the waste to be retrievable for the operational period of the repository and for 50 years thereafter. A further requirement is that the time for retrieval be similar to that for emplacement.

The need for retrievability stems from the following considerations:

- Continued research into the behavior of the engineered system may reveal design flaws which could adversely affect the radionuclide release rate. In such a case the waste should be removed and repackaged.

- Monitoring of the waste could indicate that package failure has occurred. This would require recovery of the package.

- Flooding may occur; although the package must be designed to address this situation, an analysis of the event may lead to retrieval.

- Retrieval may also be required for a variety of other reasons such as fires in the facility, discovery of toxic or flammable gas generation in TRU waste, a decision to reprocess spent fuel (if this type of waste is emplaced), and sabotage, etc.

Although the retrieval period of 50 years is basically arbitrary it does appear to have some justification if calculations by Cohen are considered.[5] Detailed descriptions of his assumptions and calculations are not given but his studies show that the host rock temperature, in the vicinity of a glass waste form, should reach a maximum after about 40 years. Thereafter, the temperature and the thermal gradient would decrease. A 50 year retrievability option should, therefore, span the period during which the host rock closest to the waste package passes through the period when thermally-induced stressing and fracture are more likely. On the basis of host rock heating it, therefore, appears that retrievability for 50 years after waste emplacement has been completed is desirable. However, as discussed above, there may be other considerations which could give rise to unacceptable waste package or repository behavior after the formal 50 year retrieval period. Since these are extremely difficult to predict at this time there does not appear to be a plausible reason for considering a larger retrieval period. We, therefore, feel that the 50 year retrievability criterion is currently a reasonable minimum requirement.

7.4 Conclusions

In the sections above the applicability and usefulness of the NRC performance requirements on the waste package and engineered system have been briefly discussed. The following general conclusions have been drawn:

- Consideration of fission-product decay in HLW shows that the 1000-yr containment period is sound and defensible. There is little additional benefit to be gained by much longer containment periods, such as 10^4 years. For TRU waste, a similar containment time is unimportant since no significant decreases in activity levels occur in 1000 years.

- With respect to the controlled-release criterion for the waste package, the NRC annual release requirement of 1 part in 10^5 is basically sound for most radionuclides. However, the very long half-life of Tc-99 makes a 1 part in 10^6 release rate more desirable in order to allow a significant proportion of this radionuclide to decay *in situ*.

- The 50-yr retrievability requirement in 10 CFR 60 is basically arbitrary. However, there is some indication that the temperature in the host rock will peak within this time frame. Therefore, the most severe thermal effects should be decreasing after the formal retrieval period. At this time, it seems that the NRC 50-yr retrieval criterion is a reasonable minimum requirement.

7.5 Recommendations

The NRC performance requirements discussed above are reasonable and defensible as interim criteria. It is recommended that they be taken into consideration by DOE in the design of waste packages and engineered systems.

Upon completion of the EPA standard, a reevaluation of these criteria should be undertaken by NRC to determine if any modifications are required.

7.6 References

1. M. Willrich and R. K. Lester, Radioactive Waste Management and Regulations, The Free Press, New York, (1977), p. 10.

2. "Long-Term Management of Defense High-Level Radioactive Wastes", DOE/EIS-0023, November 1979, p. IV-7.

3. "The Disposal of Spent Nuclear Fuel", ONWI-59, December 1979, p. 17.

4. L. A. White, M. J. Bell, and D. M. Rohrer, "Regulation of Geologic Repositories for the Disposal of High-Level Radioactive Wastes", in Scientific Basis for Nuclear Waste Management, vol. 2, Plenum Press, New York, (1980), p. 5-19.

5. B. L. Cohen, "The Disposal of Radioactive Wastes from Fission Reactors," Scientific American, 236, (1977), pp. 21-31.

8. REASONABLY ACHIEVABLE WASTE PACKAGES

At this time the specification of waste package designs for high level and TRU wastes, and spent fuel, which will have reasonable assurance of meeting NRC containment and release criteria cannot be made with certainty - the reason being the lack of comprehensive data on interactions of waste package components and the absence of validated models which will predict the migration of radionuclides from the waste form through the individual engineered barriers. However, it is possible to specify those package components which, based on currently available data, appear to show the best potential for waste isolation over extended periods of time. Below are discussed various waste forms, container systems, and overpack/backfill barriers which we feel show most promise. To fully qualify a waste package made up of combinations of these components, or others, whole package tests (with unbreached and artificially breached configurations) need to be carried out to check synergistic effects. Using data obtained, validated models for radionuclide transport will be required to extrapolate to relevant time frames.

8.1 Waste Forms

Very recent work carried out at ORNL on SYNROC and other ceramic particles coated with pyrolytic carbon show excellent behavior in MCC-1 leach tests (see Section 2). A porous inner layer of carbon is designed to accommodate irradiation-induced volume changes in the waste and any gas generation. Outer layers of dense carbon and SiC act as barriers to radionuclide migration. The technology for this type of waste form was developed in General Atomic Company and ORNL High Temperature Gas Cooled Reactor (HTGR) fuel effort. In this situation, the coated fuel particles experience extremely high temperatures (1000°C) for several years with excellent containment of fuel and fission product elements. One might, therefore, expect orders of magnitude increased containment times for high level and transuranic wastes if these are coated in a manner similar to HTGR fuel particles.

The ORNL leach data show non-detectable levels of radionuclides in the leach solution (Section 2). However, dissolution of the pyrolytic carbon will occur and eventually lead to exposure of the waste particle to groundwater. Some data by Chick et al[1] allow an estimate to be made of the time to corrode through the outer carbon coatings. In deionized static water at 99°C, a general leach rate for graphite was found to be 5×10^{-11} g/cm^2-d. At 250°C the rate was 5×10^{-8} g/cm^2-d. These rates were based on 1 day tests and should be viewed with caution. However, it is possible that they represent maximum rates since one usually expects the leach rate to decrease with time. By assuming that the density of graphite is 2.2 g/cm^2, and the graphite and pyrolytic carbon exhibit similar general leach rates, the rate of loss of a carbon coating may be shown to be about 2×10^{-8} cm/d at 250°C and 2×10^{-11} cm/d at 99°C. In 1000 years the carbon losses, assuming a linear rate with time, would be, respectively, 7×10^{-3} and 7×10^{-6} cm. Since typical pyrolytic carbon layer thicknesses total about 75 microns (7.5×10^{-3} cm) it may be speculated that, under low-flow hard rock groundwater conditions at 99°C, pyrolytic carbon-coated particles have the potential to give 1000 year containment of high level and TRU waste. Until the carbon coatings are breached, this waste form will also meet the NRC criterion of a maximum annual release of 1 part in 10^5.

More comprehensive tests should, however, be conducted to verify this under more prototypic test conditions.

Recent work at Catholic University on the encapsulation of high level waste in a nonradioactive high silica glass sheath gave encouraging results (see Section 2). The thermal expansion of the core glass and sheath were matched successfully and, in a variety of leach tests, the leach rates were found to be significantly lower than those for noncoated glasses. This type of concept would obviously be one that should receive high priority in the national program for high-integrity waste forms. Encapsulation of TRU waste in a similar system might also be desirable since calculations indicate that a 4 mm sheath exposed to groundwater at 70°C could take about 10^5 years to dissolve. In this period, significant decay of the transuranic elements will occur.

In the case of spent fuel, leaching data are discussed in Section 2. If the spent fuel is encapsulated in a castable metal, such as lead, the containment of the radionuclides will be significantly enhanced. In deoxygenated static brine at 250°C, it was shown that a general corrosion rate, based on a 28-day exposure, was 0.3-0.5 mm/d.[3] For 1000 year containment under similar conditions, assuming a linear rate, 30-50 cm of lead would be needed. In the case of copper it was found that 5-7 cm would be required. It appears, therefore, that the development of such sophisticated spent fuel waste forms is unwarranted on the basis of cost and the potential resource value of the encapsulating metals. It should prove to be much more cost effective to emphasize other waste package components, such as containers and backfills, in demonstrating compliance with regulatory criteria.

8.2 Containers

Significant progress has been made in the evaluation of metallic containers for waste isolation in Sweden and the U.S. (see Section 3). The Swedish work addresses granitic host rocks, whereas the U.S. efforts are primarily focused on salt and basalt environments. The general consensus at this time is that titanium and its alloys, such as TiCode-12 (Ti, 0.8% Ni, 0.35% Mo, and 0.1% Fe) offer the most cost effective way to combat general and localized corrosion. In the Sandia Labortory program,[2] TiCode-12 was shown to be greatly superior to unalloyed titanium in terms of general corrosion in brine at 250°C. Most of the U.S. effort is, therefore, on TiCode-12 which is the reference container material. If the temperature of the container is maintained below 250°C, it is postulated that titanium and TiCode-12 will be immune to pitting and crevice attack in brine.[2] In granitic water, the Swedes believe that the maximum temperature should be 80°C.[3]

Other metals which appear to perform well in anticipated hard rock groundwaters include lead and copper (see Section 2). The Swedes have studied these is some detail together with titanium.[4] For vitrified waste the Swedish container design incorporates a lead liner 100 mm in thickness. By making the assumptions that all of the oxygen within the bore hole, in which the container is emplaced, migrates to a single pit in the container surface, it was calculated that it would take about 4500 years to perforate the liner.

Calculations for the time to perforate a 200 mm copper container for spent fuel in the Swedish program indicate that the container would remain unbreached for hundreds of thousands of years.[43]

The Swedish work on titanium as a thin sheath to cover the lead liner for vitrified waste identified an uncertainty in the behavior of this metal in the presence of gamma irradiation from the waste.[3] Although nine of the ten-man Swedish panel believe that it would not present a significant problem, Professor G. Wranglen believes that hydrogen could cause "delayed failure" in which hydrogen could migrate to metallurgical discontinuities in stressed titanium and cause crack propagation and failure. Wranglen also was less optimistic than the other panel members on the estimated lifetime of the lead liner used in the vitrified waste container system. A BNL evaluation of Wranglen's opinion has been carried out previously and is reproduced in Appendix B of this report. Basically, the findings indicate that his comments are not generally supported by information from the literature. Our evaluation of the Pb-Ti container design to be used in the Swedish effort is similar to that of the nine majority members of the panel, i.e., the container has the potential to remain intact for at least several thousands of years.

Appendix B illustrates a BNL modification of the Swedish container design for hard rock groundwaters which incorporates two titanium (or TiCode-12) shells separated by a lead barrier. If the outer titanium shell is breached by a hydrogen-embrittlement mechanism, this material will presumably continue to act as a sink for radiolytic hydrogen. The inner titanium shell should not then be susceptible to hydrogen-induced failure. The lead component of the system will be a major additional barrier and corrode preferentially with respect to titanium. In the long-term, the corrosion direction of the lead will be parallel to the container surface, thereby leading to an enhanced time for the container system to be breached.

Alternative systems may be developed to increase the life of a container. Since the time to initiate localized corrosion is often much longer than the time to propagate the mechanism to a breached-container condition, a concept of multiple containers may be used. Containers within containers should give a much longer life compared to a single container of equivalent thickness. The space between adjacent containers could be filled with water migration retardants and oxygen getters so that corrosion of the inner containers becomes more difficult with time. Although such a system offers a potential for greatly increasing container life it should be investigated experimentally to confirm the design to be used.

8.3 Overpack/Backfill Systems

Of the components of a waste package the overpack/backfill system offers potential for meeting the NRC criteria for 1000 year containment and long-term controlled release of radionuclides (Appendix A). The discussion of backfill, in a HLW repository in Section 4 of this study, shows that the technology is relatively well understood compared to other package components. Although there is a need for more comprehensive experimental data on sorption behavior of geologic materials used for backfills, the analytical tools needed to predict containment and controlled release rates over extended times appear to be sufficiently well developed to design a viable system. Based on the evaluation given in Section 4 it seems that synthetic zeolites could independently give 1000 year containment and an annual controlled release value of less than 1 part in 10^5 for high level and TRU wastes and, also, spent fuel.

8.4 Achievable Limits for Engineered Barriers

In Section 6 of this report we have identified the principal variables which must be well understood if a satisfactory package design is to be developed; that is, one which can be confidently expected to meet predetermined limits for radionuclide release. A quantitative evaluation of the feasibility of using highly sorptive materials such as synthetic zeolites as backfill in a HLW repository is presented in Appendix A. In the evaluation in Appendix A, we have shown that, under a given set of conditions, backfill can perform satisfactorily over long time periods to meet both the 1000 yr containment criterion for the waste package and the 10^{-5}/yr controlled release criterion for an underground facility. In the following section, we adopt a conservative approach and show that the NRC criteria could be greatly exceeded and reasonably achieved as follows:

Backfill: Based on Table 3 in Appendix A, we can confidently say that a 10 ft-thick backfill, consisting of highly sorptive materials such as synthetic zeolites, can provide an annual controlled release of 2 parts per 10^6 from an underground facility. This is based on the assumptions outlined for model 2 in Appendix A.

Waste Form: In terms of the zero release criterion, we believe that some of the newly developed waste forms could provide radionuclide containment for periods much greater than the 1000 years required by NRC for a waste package. For example, as discussed in Section 8.1, a typical PyC layer of 70 μm thickness in a coated particle, which has a rate of loss of carbon of 2×10^{-11} cm/d at 99°C, can provide total containment of radionuclides for tens of thousands of years. Similarly, PGM glass consisting of a 4 mm thick radionuclide-free protective jacket can provide containment of all radionuclides in the core glass for time periods varying from 10^7 years at 20°C to 10^4 at 100°C (Section 2.6.1.2). These examples illustrate that the NRC criteria are likely to be well within achievable limits.

8.5 Retrievability of Waste

In the NRC draft criteria for the regulation of high level waste disposal activities published in 10 CFR 60, May 13, 1980, it is stated:

> "The Department shall design and construct the geologic repository operations area to permit retrieval of all waste packages, mechanically intact, if retrieval operations begin within 50 years after all of the waste has been emplaced and if the geologic repository has not been decommissioned. The design of the geologic repository operations area shall provide for retrievability of the waste within a period of time that is about the same time as that in which it is emplaced."

Consider, first, the need to maintain package integrity. This is primarily required to facilitate safe retrieval through the minimization of radionuclide dispersal in the repository. For high integrity packages such as those which will be used for high level waste and spent fuel (if this is emplaced), their design for 1000 year containment should ensure that integrity will be maintained for a maximum emplacement time of 110 years (this assumes a 30 yr emplacement time, 50 yr retrievability period, and an additional 30 yr retrieval time). Therefore, from a design integrity standpoint there should be no problem with retrieving such types of waste. A different situation could arise for TRU waste since NRC criteria do not stipulate a 1000 year minimum containment time. Thus, a high integrity container is not mandatory. If a container for TRU waste is designed to facilitate only the emplacement strategy without due regard to corrosion and mechanical stresses during the maximum emplacement time of about 110 years, it may not retain sufficient strength to withstand retrieval operations. Caution must, therefore, be exercised in the design of a suitable retrieval package for TRU waste.

The second consideration regarding the retrieval time may also have an important implication concerning the safety of the repository during the emplacement period. In order to ensure that the water is retrieved in about the same time as it takes for emplacement, it would probably be necessary to leave access tunnels open. For a salt repository without backfilled tunnels there is likely to be significant creep of the host rock which could affect package integrity. In a hard rock repository, creep would be a minor consideration but collapse of the tunnels could occur. In addition, maintaining an open tunnel system causes an increased possibility for sabotage and an easy pathway for radionuclide release.

In summary, it appears that, technically, the NRC criterion for a 50 year retrievability period is achievable. However, additional study is required regarding the most practical and safe way to implement it.

8.6 Conclusions

In addressing the achievability of the NRC's radionuclide release and retrievability criteria it appears that viable options are available. Confirmatory research and evaluations are required, however, before they can be confidently implemented. The following conclusions may be drawn:

- Components for high level waste packages which independently have the potential for 1000 year containment of radionuclides include (a) ORNL-type carbon-coated particles, (b) Catholic University type waste glass coated with nonradioactive high-silica glass, (c) the BNL modification of the Swedish container, i.e., a Ti-Pb-Ti multilayered structure, (d) a multicontainer system with each pair of adjacent containers separated by oxygen getter materials and, (e) a backfill system based on a suitable thickness of synthetic zeolites.

- For spent fuel packages, the above-mentioned container and backfill concepts should also be appropriate for 1000 year containment.

- For high level and TRU waste, and spent fuel the only package component which has the potential to meet the annual release rate of 1 part in 10^5 is a backfill based on synthetic zeolites. For high level and TRU wastes, carbon-coated particles and waste glass coated with nonradioactive high-silica glass may also be effective in meeting the controlled release criterion for some extended time period. However, the coatings could be lost after long-term exposure to groundwater so that meeting the criterion for an indefinite period may not be an achievable goal.

- There will be greatly increased assurance of meeting the containment and release rate criteria if the above waste forms, container systems, and backfill are used together in an integrated package. However, additional testing to evaluate interactive effects needs to be carried out. Models to assess the release of radionuclides through such packages need to be developed and verified.

- An evaluation of achievable limits for engineered barriers indicates that the NRC criteria of 1000-yr containment for the waste package and of 10^{-5}/yr for the underground facility are readily achievable by the engineered barriers independently. In some cases, more conservative criteria can be met.

- There do not appear to be any insurmountable technical difficulties in meeting the 50 year retrievability criterion. However, various options need to be evaluated to specify a system which will optimize safety, effective waste isolation, and speed of retrieval.

8.7 References

1. L. Chick et al., "Annual Report on the Development and Characterization of Solidified Forms for Nuclear Wastes, 1979," PNL-3465, 1980.

2. J. W. Braithwaite and M. A. Molecke, "Nuclear Waste Canister Corrosion Studies Pertinent to Geologic Isolation," Nuc. and Chem. Waste Management 1, 1980, pp. 37-50.

3. E. Mattson, "Corrosion Resistance of Canisters for Final Disposal of Spent Fuel," in *Scientific Basis for Nuclear Waste Management*, Plenum Press, N.Y., Vol. 1, 1979, pp. 271-181.

APPENDIX A

EVALUATION OF BACKFILL AS A BARRIER TO RADIONUCLIDE MIGRATION IN A HIGH LEVEL WASTE REPOSITORY

T. M. Ahn, R. Dayal, and R. J. Wilke

Department of Nuclear Energy
Brookhaven National Laboratory
Upton, NY 11973

SUMMARY

The feasibility of using highly sorptive synthetic minerals such as zeolites or titanates as backfill in a HLW repository has been evaluated in terms of the NRC 1,000 yr containment and 10^{-5}/yr controlled release criteria. The results indicate that for groundwater velocities below 1 ft/yr, diffusion and sorption are the dominant processes controlling radionuclide migration in backfill systems. A 3-ft-thick bed of synthetic zeolite backfill can provide total containment of activity released continuously from a 55-gallon glass monolith for a period of up to 1,000 years. For longer time periods of up to 10^6 years, the controlled release rate of 10^{-5}/yr can be met by a >10-ft-thick bed of zeolite backfill, assuming the glass monolith to be the source term. In the absence of the waste form as an engineered barrier, a bed thickess of 3 to 10 ft is required to satisfy the controlled release criterion for a period of up to 10^5 years. With a bed thickness of 200 ft, synthetic zeolites can be used as backfill to provide containment of the total U.S. waste inventory (10^9 Ci), if it were placed in one repository, for periods up to 10^6 years. Zeolites are known to exhibit radionuclide-specific sorption properties. We believe that the range of sorption coefficients (10^3-10^4 ml/g) considered in the calculations will cover the various zeolite-radionuclide systems. We wish to emphasize that the above estimates are conservative since diffusion occurs radially and we have only considered uni-dimensional transport in our models. In addition, radioactive decay of the nuclides has not been considered in the calculations.

We also wish to note that in this report we have not dealt with radiation and thermal stability of backfill materials. Zeolites have been used to clean radioactivity from water systems and have been loaded to as high as 75,000 curies per MTHM. Although we believe that zeolites should be structurally stable to low radiation loadings (approx 1,000 curies per cubic foot) and that radiolysis effects should not be important at these levels of radiation, very little work exists in this area. In addition, we have not addressed the retention of long-lived anionic species such as SeO^{2-}, I^-, and TcO_4^-. It appears that other materials will have to be added to backfill to maximize its effectiveness for retention of all radionuclides of interest.

INTRODUCTION

The operational life of a geologic high level waste (HLW) repository after decommissioning can be divided into two time periods: (1) the period (<1,000 yr) during which the short lived fission products dominate the hazard posed by the wastes, and (2) the long term period (>1,000 yr) during which the hazard is dominated by the very long lived isotopes including the actinides.[1] In view of these considerations, the Nuclear Regulatory Commission (NRC) has adopted a strategy for regulating and licensing the disposal of high level radioactive wastes in geologic repositories which requires that the engineered systems of the underground facility meet the following criteria:(2)

(a) Containment of all radionuclides in HLW for at least the first 1,000 years after decommissioning of the geologic repository, assuming expected events and processes. This containment shall result from properties of the waste package.

(b) Starting 1,000 years after decommissioning of the geologic repository, the radionuclides present in HLW will be released from the engineered system to the geologic setting at an annual rate that is no case greater than one part in one hundred thousand of the total activity present within the underground facility at that time, assuming expected processes and events.

(c) For transuranic waste (TRU), the engineered system shall be designed so that following decommissioning of the geologic repository the annual release rate from the underground facility into the geologic setting is at most one part in one hundred thousand of the total activity present in the underground facility at any time following decommissioning.

Most of the current Department of Energy (DOE) programs in high level waste research are investigating the waste form and container as potential components of a waste package in meeting the containment requirements outlined above. In this report, we have attempted to evaluate the effectiveness of using synthetic zeolites and titanates as potential backfill materials in an HLW repository. It should be pointed out that a DOE waste package is defined to include everything that is placed in the waste repository emplacement hole, i.e., the waste form, filled container, overpack, sleeve, and backfill. The NRC waste package includes discrete backfill(3) in contrast to non-discrete backfill in DOE definition. Since the 1,000 yr criterion applies specifically to the waste package and the 10^{-5}/yr controlled release criterion refers to the engineered system, we have evaluated the effectiveness of backfill in meeting both performance requirements: discrete backfill for 1,000 yr containment and non-discrete backfill for controlled release.

Zeolites and Titanates as Backfill

Although backfill in an HLW repository has been identified to provide several functions, the most important role is to retard migration of radionuclides in groundwater that has reached the waste in the event of a container breach. It is primarily this property that we have considered in our evaluation of synthetic zeolites and titanates for backfill. In addition to providing a high potential for required retention of radionuclides, synthetic backfill materials of regularly shaped small spheres can be used, through prior selection of the mass, volume, shape, and packing densities, to predetermine and control the groundwater flow rates and patterns into and through the engineered underground facility for varying aquifer pressures and flow rates. Such a modification of the hydrodynamics of an engineered facility could be advantageous in that rapid radionuclide transport by advection would be minimized, resulting in diffusion-controlled transport.

Existing technology, widely used in purification systems for water reactors, has demonstrated that synthetic materials including a wide range of zeolites can be used to quantitatively hold up fission products and actinides. A most prominent example of zeolite application to waste management is the use of IONSIV-IE95 and Zeolon 900 in the Submerged Demineralized System (SDS) to be used to decontaminate water from the Three Mile Island Unit 2 Nuclear Power Plant.(4) Another such example is the storage of krypton-85 in sodalite zeolite.(5) Recently, Nowak(6) and Winslow(7) at Sandia Laboratories and Komarneni and Roy(8) at Pennsylvania State University have examined the sorption properties of zeolites as potential backfill material for use in a HLW repository. Pennsylvania State is also investigating the use of mixtures of zeolites and clay minerals for backfill material around a waste package and the fixation properties of sorbed radionuclides of various zeolite minerals.(9)

Sodium titanate materials have been developed at Sandia Laboratories for quantitative removal of fission products and actinides from commercial liquid wastes.(10,11) Subsequent pressure sintering of the loaded material results in a dense ceramic waste form resistant to leaching. Based on the high decontamination factors observed in HLW studies, the Sandia titanate materials are also being investigated for the decontamination of defense liquid wastes stored at the Hanford site in Washington.

In this report, we have attempted to evaluate the feasibility of using highly sorptive materials such as synthetic zeolites and titanates as backfill in a HLW repository. The effectivenss of such a barrier with respect to radionuclide retention has been assessed in terms of the NRC release criteria discussed above.

Radionuclide Transport Processes

To evaluate the migration of radionuclides in an ion exchange backfill barrier, we have to first consider the dominant transport mechanisms. The principal mechanisms controlling the nature and extent of radionuclide transport in sorptive materials are ion exchange, sorption, diffusion, precipitation, advection, and other irreversible reactions. Ion exchange and sorption processes are essentially reversible (at least over short time periods), resulting in a net retardation in the diffusion-controlled ion migration. The extent of retardation will be primarily determined by the sorption kinetics and equilibria of solid-fluid interactions. Non-reactive ions such as tritium, however, do not exhibit interactions with particle surfaces. In this case, ion exchange and sorption processes are not significant and, consequently, the migration is primarily controlled by diffusion and advection.

Precipitation of dissolved radionuclides as authigenic minerals will decrease the rate of radionuclide migration. Formation of new minerals, immobilizing radionuclides released from the waste form, as a result of quaternary interactions involving waste/backfill/host rock with hydrothermal fluids has been documented.(12) However, such data are not available for the various backfill materials. Therefore, precipitation, as a retardation process, will not be considered in this report.

Similarly, irreversible reactions such as fixation of sorbed ions with aging of the sorbent can also decrease the rate of radionuclide migration. Recently, it was reported that synthetic zeolites, used for decontamination purposes at Hanford, were found to fix certain radionuclides irreversibly in a period of less than five years.(13) Although this mechanism could be potentially effective in retarding radionuclides in a bed of synthetic zeolites, the available data are insufficient at this time for this mechanism to be considered in our transport model.

At a recent Waste Rock Interaction Technology Meeting in Seattle, a paper was presented describing the role of fine suspended particulates in transporting radionuclides.(14) This process could serve as a potentially important mechanism for radionuclide migration in argillaceous backfill materials which commonly contain extremely small particulates. However, in the case of synthetic materials, the particle size distribution would be very narrow, giving rise to a relatively uniform particle size. Therefore, we believe that this mechanism will not contribute significantly to an increase in the rate of radionuclide migration in backfill systems. However, the significance of this process as a transport mechanism for radionuclides should be investigated.

The principal transport mechanisms which we have considered for evaluating zeolite backfill are diffusion, sorption, and advection. Since groundwater flow rate is relatively low in a realistic repository situation, dispersion associated with advection is considered to be negligible. An example of radionuclide transport by advection, diffusion, and a combination of advection, diffusion, and sorption processes is displayed in Figure 1.(15) As shown in Figure 1, pure diffusion corresponds to radionuclide migration as a result of interstitial concentration gradient for non-reactive ions such as tritium. For reactive ions such as Cs^+ and Sr^{2+} and assuming bulk fluid flow to be negligible, the transport is primarily determined by diffusion and sorption, where the sorption equilibrium coefficient determines the extent of ion retardation as compared with diffusional transport for non-reactive ions. For systems having high a groundwater flow velocity, advection becomes the dominant transport process as compared with diffusion (Figure 1). Dispersion effects, resulting from the variation in bulk fluid flow velocities between the particles, could give rise to a broadening of the advective front.

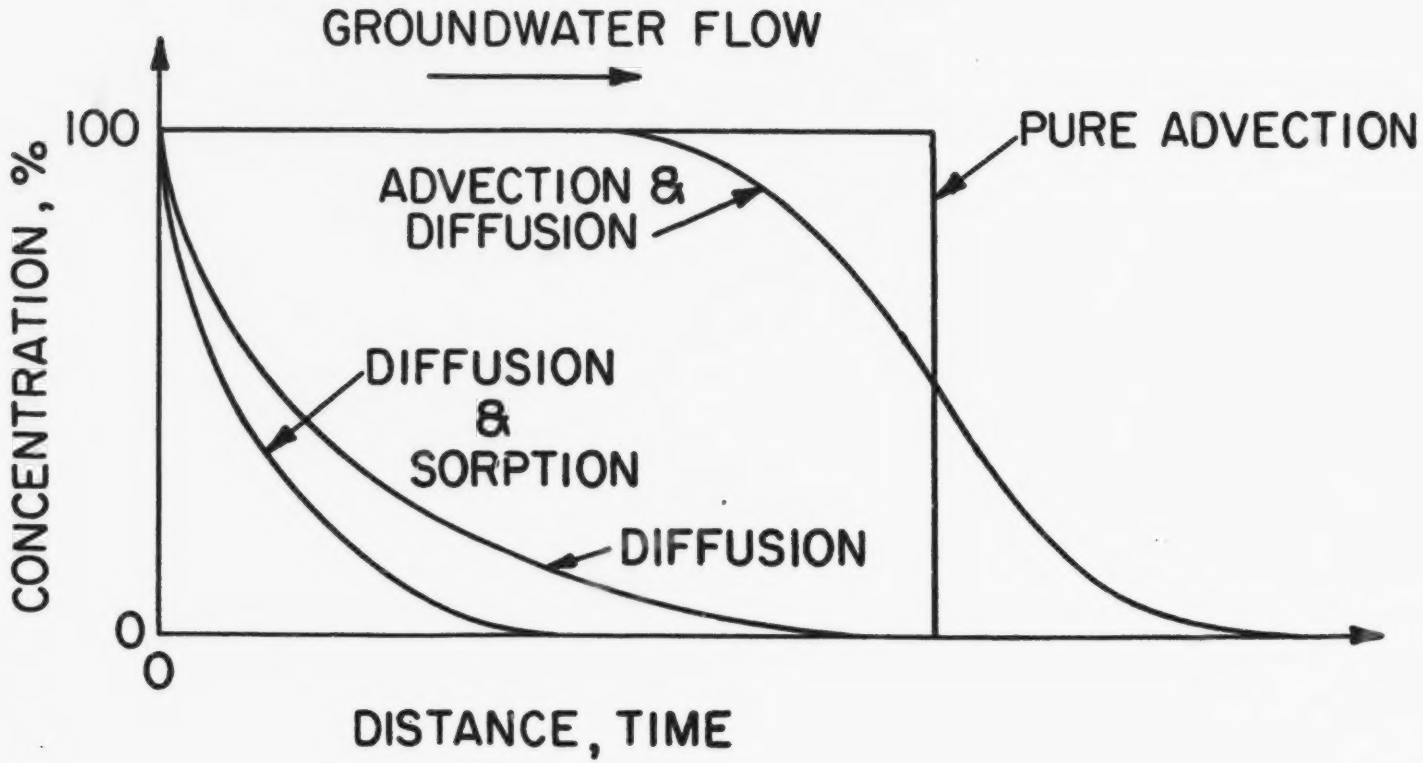

Figure 1. Principal radionuclide transport processes in sorptive backfill material [after Neretnieks(15)].

BEST DOCUMENT AVAILABLE

MODEL CALCULATIONS

We have developed one-dimensional models that describe quantitatively the transport of radionuclides in a backfill bed. A range of values are considered for groundwater flow rate, sorption coefficient, bed thickness, and transit time.

Table 1

Parameters Considered in Radionuclide Transport Calculations

Backfill Bed Thickness (ft): 1, 3, 10, 100
Transit Time (years): 1,000, 10,000, 100,000, 1,000,000
Sorption Coefficient (mL/g): 1, 10, 100, 1,000, 10,000
Ion Diffusion Coefficient (cm^2/sec)(6): 10^{-5}
Groundwater Velocity (ft/yr)(16,17,18): 0, 1
Bed Porosity(19): 0.34
Bed Density (g/cm^3)(20): 0.423

Phenomenological Model 1

In model 1, the details of which are given in Appendix 1, we have assumed a waste glass, having a constant leach rate over a long period of time, to be the source term. A constant concentration is maintained at x=0, the interface between the waste glass and backfill. In other words, it is assumed that the radionuclide source is non-depleting, time invariant. The transport mechanisms considered are diffusion, sorption, and advection. The groundwater velocity is assumed to be constant with time and uniform throughout the bed. The dispersion term, resulting from localized velocity variations around the particles, is assumed to be negligible. Finally, radioactive decay of the source term and precipitation and fixation of the radionuclide are not considered.

Nowak(6) simplified a material balance equation around a differential volume element in the backfill bed. His formulation is directly applicable to the present analysis. It consists of a linear partial differential equation with three terms: (1) the rates of accumulation (or depletion) of sorbing species in the liquid and on the solid, (2) the net transport of liquid phase species by advection, and (3) the net transport of liquid phase species by ion diffusion. The groundwater flow in a repository must be considered and could serve as a potentially important transport process, especially for non-reactive radionuclides.

Using model 1, the results were calculated for a range of conditions and the concentration-bed thickness profiles for various transit times are displayed in Figure 2. In Figure 2a, for a sorption coefficient of 1,000 mL/g and a water velocity of 1 ft/yr, the 1,000 year and 10,000 year profiles show that for rela-

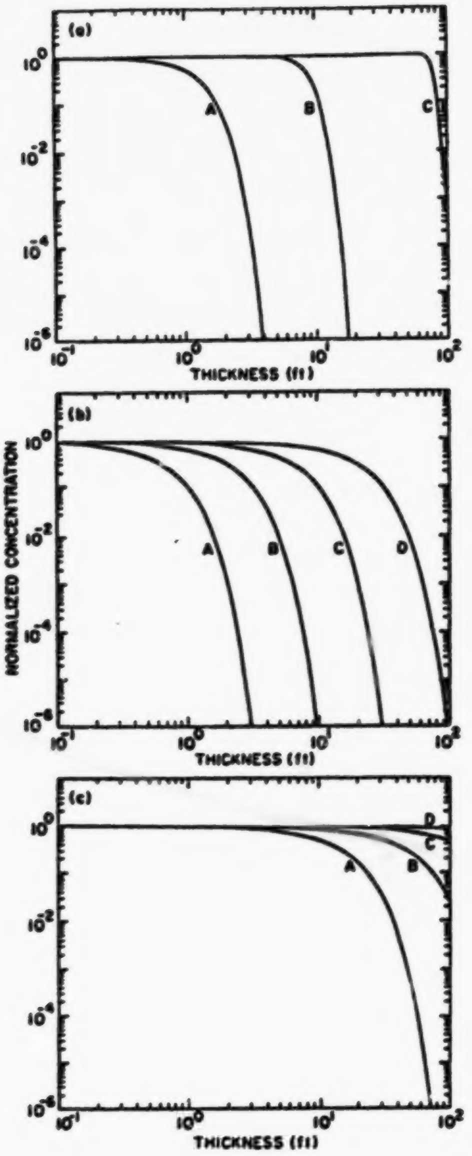

Figure 2. Concentration vs bed thickness profiles for various transit times based on model 1: (a) K_d = 1000 mL/g, V_g = 1 ft/yr; (b) K_d = 1000 mL/g, V_g = 0 ft/yr; (c) K_d = 1 mL/g, V_g = 0 ft/yr, A = 10^3 yr, B = 10^4 yr, C = 10^5 yr, D = 10^6 yr.

BEST DOCUMENT AVAILABLE

tively short time periods diffusion plus sorption are the rate controlling processes, with the initial concentration dropping by a factor of $>10^6$ within 20 feet of backfill thickness. However, for longer time periods of up to 100,000 years and greater, transport associated with bulk fluid flow becomes dominant, even for reactive ions having a sorption coefficient of 1,000 mL/g. In the absence of bulk fluid flow, the advective term becomes zero. As shown in Figure 2b, the transport is dominated by diffusion and sorption. These findings are in general agreement with those reported recently by Nowak.(21) For materials having negligible sorptive capacity such as quartz, and in a zero groundwater flow stationary system, radionuclide transport is determined by pure diffusion via interstitial water (Figure 2c), emphasizing the importance of sorption as a retardation process in the transport of radionuclides through a backfill barrier.

Phenomenological Model 2

In this model, we exclude the waste form as an engineered barrier which maintained constant concentration at the interface of the glass and backfill by continuous congruent leaching over a period of time. Instead, at zero time (t=0), the total concentration of the radioactive waste is hypothesized to enter into the backfill instantaneously along the x direction as a sharp step increase (more precisely as a delta function) in its liquid phase concentration c from zero to a constant value C_0. We derived a mathematical expression using the appropriate initial and boundary conditions as given in Appendix 2. The calculated results were obtained using the same range of parameters given in Table 1. The assumption of an instantaneous pulse at time=0 and continuously depleting over a period of time for the source term in model 2 means that no reliance is placed on the waste form as an engineered barrier. Concentration-bed thickness profiles for various transit times, based on model 2 using the parameters given in Table 1, are given in Figure 3.

Evaluation of NRC Criteria

Although the concentration-bed thickness profiles generated using models 1 and 2 (Figure 2 and 3) are useful in terms of identifying the processes that control radionuclide migration in a sorptive backfill system and in determining their relative magnitudes, quantitative information is required to address the performance objectives set by NRC. For this purpose, we assumed the source term to be a glass monolith having a volume of 55 gallons. Assuming 30% waste loading in the glass, an activity of approximately 4.2 Ci/cm^3 of glass monolith is calculated. The age of the waste is assumed to be approximately 1.5 years old.(21) The average glass leach rate is considered to be 10^{-3} g/cm^2-yr.

Based on assumed leach rates for the waste glass, surface areas of the glass monolith and the total amounts of radioactivity released from the source for the periods 10^3 and 10^6 years as estimated from the profiles shown in Figure 2, we estimated the total amount released from a 3-ft-thick backfill, having a range of sorptive capacities, in a period of 1,000 years at the groundwater flow velocity of 1 ft/yr. As shown in Table 2, a 3-ft-thick bed of backfill materials, such as zeolites having a sorption coefficient of 10^4 mL/g,

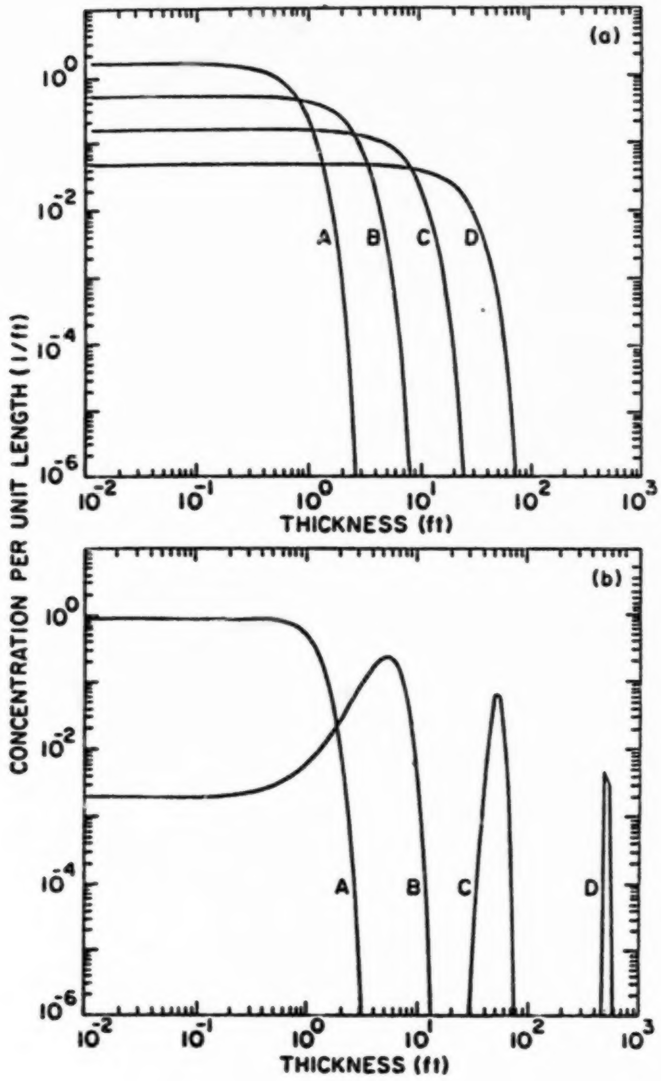

Figure 3. Concentration vs bed thickness profiles for various transit times based on model 2: (a) K_d = 1000 mL/g, V_g = 0 ft/yr; (b) K_d = 100 mL/yr, V_g = 1 ft/yr; A = 10^3 yr, B = 10^4 yr, C = 10^5, D = 10^6 yr.

BEST DOCUMENT AVAILABLE

Table 2

Total Release of Radioactivity From a 3-ft-Thick Backfill in 10^3 Years (Model 1)

Backfill Sorption Coefficient Kd (mL/g)	Total Amount Released From Backfill (Ci)	
	SA = 3.6×10^{4} (cm^2)	SA = 3.6×10^{6} (cm^2)
100	4×10^{4}	4×10^{6}[a]
1,000	4×10^{0}	4×10^{2}
10,000	5×10^{-46}	5×10^{-44}

[a] Artificial number indicating total inventory release.
V_g= 1 ft/yr; backfill thickness = 3 ft; leach rate (LR) = 10^{-3} g/cm^2-yr; C_0 = LR x SA x transit time/area under the concentration curves (SA = surface area of the glass monolith).

Table 3

Fractional Release Rate From a 10-ft-and a 100-ft-Thick Backfill in 10^6 Years (Model 1)

Backfill Sorption Coefficient Kd (mL/g)	Fractional Release Rate From Backfill (/yr)			
	SA = 3.6×10^{4}(cm^2)		SA = 3.6×10^{6}(cm^2)	
	10-ft	100-ft	10-ft	100-ft
100	6.8×10^{-5}	6.7×10^{-5}	6.8×10^{-3}	6.7×10^{-3}
1,000	6.7×10^{-5}	6.0×10^{-5}	6.7×10^{-3}	6.0×10^{-3}
10,000	6.0×10^{-5}	3.6×10^{-9}	6.0×10^{-3}	3.6×10^{-7}

V_g = 1 ft/yr; leach rate (LR) = 10^{-3} g/cm^2-yr; SA = surface area of the glass monolith.

will contain practically all the inventory released from the waste for a period of up to 1,000 years. This implies that a discrete zeolite backfill will satisfy the NRC 1,000 year containment criterion. Table 3 shows calculated results of fractional controlled release rate from a 10- and a 100-ft-thick backfill bed over a period 10^6 years. In these calculations, the assumptions made for the source term and backfill are the same as those described in Table 2. Assuming a leach rate of less than 10^{-3} g/cm^2-yr and a surface area of the glass monolith to be 3.6×10^4 cm^2, the NRC controlled release criterion can be met using a >10-ft-thick non-discrete zeolite backfill bed for periods of up to 10^6 years. These calculations show the significance of a waste form having a low leach rate with respect to meeting the controlled release criterion. In such a situation, the sole purpose of the backfill would be to control water ingress in order to minimize the probability of container corrosion. It must be emphasized that bulk fluid flow, based on a groundwater velocity of 1 ft/yr, also contributes to radionuclide transport. In a realistic repository situation, the flow velocities are much smaller than that assumed in our calculations. In that case, the transport would be predominantly diffusion-controlled, resulting in a more effective containment by the backfill barrier.

Using model 2 and making the same assumptions for the source term and backfill barrier, we obtained estimates of the total amount of activity released from a 3-ft-thick backfill barrier in a period of 10^3 years. As shown in Table 4, the calculated values indicate that the 1,000 year containment criterion will be met by a 3-ft-thick bed of backfill with sorption coefficients in the range of 10^4 mL/g. Also included in Table 4 are values for fractional amounts of activity released from the backfill barrier in 1,000 years.

Using the same model and considering a time period of 10^5 years and bed thicknesses of 3 ft and 10 ft, we obtained estimates of fractional release per year from the backfill bed (Table 5). The results show that for backfill materials having sorption coefficients in the range of 10^4 mL/g, the annual fractional releases from 3-ft-and 10-ft-thick beds are 10^{-5}/yr and 10^{-6}/yr, respectively. This indicates that the controlled release criterion of 10^{-5}/yr will be met by highly sorptive backfill materials such as synthetic zeolites and/or titanates for long periods of time.

Model Calculation for Total U.S. Waste Inventory

In order to demonstrate the effectiveness of backfill as a barrier to radionuclide migration, we assumed the source term to be the total U.S. waste inventory and calculated the total thickness of backfill that would be required to provide controlled release rate over a period of 10^6 years.

Using models 1 and 2, we used a value of 10^9 Ci(23) for the total waste inventory in the U.S.(12) and 100- and 200-ft for bed thicknesses. The calculated estimates of radionuclide release are compiled in Tables 6 and 7. Table 6, based on model 1, shows that the annual release from 200-ft-thick backfill, having a sorption coefficient of 10^4 mL/g, is on the order of

Table 4

Fractional and Total Release From a 3-ft-Thick Backfill in 10^3 Years (Model 2)

Backfill Sorption Coefficient Kd (mL/g)	Fractional Release	Total Release (Ci)
100	9.97×10^{-1}	8.80×10^5
1,000	3.25×10^{-4}	2.90×10^2
10,000	5.93×10^{-50}	5.20×10^{-44}

V_g = 1 ft/yr, backfill thickness = 3 ft.

Table 5

Fractional Release Rate From a 3-ft-Thick Backfill and a 10-ft-Thick Backfill in 10^5 Years (Model 2)

Backfill Sorption Coefficient Kd (mL/g)	Fractional Release Per Year (/yr)	
	3-ft	10-ft
100	$>10^{-5}$	$>10^{-5}$
1,000	$>10^{-5}$	$>10^{-5}$
10,000	9.97×10^{-6}	1.85×10^{-6}

V_g = 1 ft/yr.

Table 6

Annual Release From a 200-ft-Thick Backfill for 10^6 Years, Assuming the Source Term to be Total U.S. HLW Inventory (Model 1)

Backfill Sorption Coefficient Kd (mL/g)	Annual Release From Backfill (Ci/yr)	
	SA = 2.4×10^5 (cm^2)	SA = 2.4×10^7 (cm^2)
100	4×10^2	4×10^4
1,000	3×10^2	3×10^4
10,000	3×10^{-80}	3×10^{-78}

V_g = 1 ft/yr; backfill thickness = 200 ft; leach rate (LR) = 10^{-3} g/cm^2-yr; SA = surface area of all glass monoliths considered.

Table 7

Annual Release From a 200-ft-Thick Backfill for 10^6 Years, Assuming the Source Term to be Total U.S. HLW Inventory (Model 2)

Backfill Sorption Coefficient Kd (mL/g)	Annual Release From Backfill (Ci/yr)
100	10^3
1,000	10^3
10,000	10^{-79}

V_g = 1 ft/yr.

10^{-80} Ci/yr. This indicates that total containment will be achieved during this period.

Table 7, based on model 2, also shows that a 200-ft-thick bed of backfill ($K_d=10^4$ mL/g) will provide total containment. A bed thickness of 100 ft, however, is not sufficient to obtain the desired containment.

CONCLUSIONS

For groundwater velocities below 1 ft/yr, diffusion and sorption are the dominant processes controlling radionuclide migration in highly sorptive backfill materials such as synthetic zeolites. A 3-ft-thick bed of synthetic zeolite backfill can provide total containment of activity released continuously from a 55-gallon glass monolith for a period of up to 1,000 years. For longer time periods of up to 10^6 years, the controlled release rate of 10^{-5}/yr can be met by a >10-ft-thick bed of zeolite backfill, assuming the glass monolith to be the source term. In the absence of the waste form as an engineered barrier, a bed thickness of 3 to 10 ft is required to satisfy the controlled release criterion for a period of up to 10^5 years. With a bed thickness of 200 ft, synthetic zeolites can be used as backfill to provide containment of total U.S. waste inventory (10^9 Ci), if it were placed in one repository, for periods of up to 10^6 years.

ACKNOWLEDGMENTS

We thank D. G. Schweitzer for initiating this study and C. Sastre for his assistance in computer work. E. J. Nowak, A. Okubo, and G. W. Beall reviewed the manuscript. We thank them for their constructive comments. We are also grateful to Grace Searles, Katherine Becker, Sharon Moore, and Cathy Van Noy for typing and preparation of the manuscript.

REFERENCES

1. R. Dayal, K. J. Swyler, and P. Soo, NRC Nuclear Waste Management Technical Support in the Development of Nuclear Waste Form Criteria, BNL Report, BNL-NUREG-27961 (1980), Chaps. 4 and 5.
2. Code of Federal Regulations, 10 CFR 60, "Disposal of High-Level Radioactive Wastes in Geologic Repositories," (Proposed Rule), Advance Notice of Proposed Rule Making, Federal Register, May 13, 1980.
3. Code of Federal Regulations, 10 CFR 60, "Disposal of High Level Radioactive Wastes in Geologic Repositories", (Proposed Rule), Advance Notice of Proposed Rule Making, Federal Register, July 8, 1981.
4. E.D. Collins, J.E. Bigelow, D.O. Campbell, L.J. King, and J.B. Knauer, "Evaluation of the Submerged Demineralizer System (SDS) Flowsheet for Decontamination of High-Activity-Level Water at the Three Mile Island Unit 2 Nuclear Power Station," ORNL Report, ORNL-TM-7448 (1980).

5. R.W. Benedict, A.B. Christensen, J.A. Del Debbio, J.H. Keller, and D.A. Kneckt, "Technical Feasibility of Krypton-85 Storage in Sodalite," in *The Scientific Basis for Nuclear Waste Management* - Vol. 2, Plenum Press, N.Y. (1980).

6. E.J. Nowak, "The Backfill as an Engineered Barrier for Nuclear Waste Management," Sandia Report, SAND 79-0990C (1979).

7. C. D. Winslow, "The Sorption of Cesium and Strontium From Concentrated Brines by Backfill Barrier Materials," Sandia Report, SAND 80-2046 (1981).

8. S. Komarneni and R. Roy, "SUPEROVERPACK: Tailor-made Mixtures of Zeolites and Clays," Presented at Materials Research Society Annual Meeting, Massachusetts, 1979.

9. R. Roy and S. Komarneni, "Design of Overpack (Backfill) Materials," Paper presented at the National Bureau of Standards Sponsored Workshop on Research and Development Needs Relating to Backfill, Gaithersburg, Maryland, April 1981.

10. R. G. Dosch, "The Uses of Titanates in Decontamination of Defense Waste," Sandia Report, SAND 78-0710 (1978).

11. R. G. Dosch, "Application of Titanates, Niobates, and Tantalates to Neutralized Defense Waste Decontamination-Materials Properties, Physical Forms, and Regeneration Techniques," Draft Sandia Report, SAND 80-1212 (1980).

12. B. E. Scheetz, S. Komarneni, D. K. Smith, and C. A. F. Anderson, "Hydrothermal Interaction of a Ceramic Waste Form With Basalt," in *Alternate Nuclear Waste Forms and Interactions in Geologic Media*, Proceedings of the a Workshop held in Gatlinburg, Tennessee, May 1980.

13. R. E. Barletta, personal communication.

14. G.G. Eichholz, "Subsurface Migration of Radioactive Waste Materials by Particulate Transport," Abstract of paper presented at Waste Rock Interaction Technology Meeting, 13-15 October (1980), Seattle, Washington.

15. I. Neretnieks, "Retardation of Escaping Nuclides From a Final Depository," KBS-TR-30, (1977).

16. R.K. Kibbe and A.L. Boch, Technical Support for GEIS: "Radioactive Waste Isolation in Geologic Formations, Vol. *21*, Groundwater Movement and Nuclide Transport," Y 10 WI/FM-36/21 (1978).

17. L.D. Ramspott, "Waste Isolation Project: FY-78", UCRL-50050-78

18. I. Neretnieks, "Transport of Oxidants and Radionuclides Through a Clay Barrier," KBS-TR-79, (1978).

19. D.W. Breck, Zeolite Molecular Sieves, J. Wiley & Sons, N.Y. (1974), Chap. 9.

20. R.C. Weast, Handbook of Chemistry and Physics, CRC Press, 56th Ed. (1975).

21. E. J. Nowak, "The Backfill Barrier as a Component in a Multiple Barrier Nuclear Waste Isolation System," Sandia National Laboratories, SAND 79-1109, 1980.

22. Management of Commercially Generated Radioactive Waste, DOE Report, DOE/EIS-0046-D, Volume 2, Appendices (1979).

23. D. Majumdar and J. P. Indusi, "Inventory of HLW in the U.S.," BNL-NUREG-27817 (1980).

APPENDIX 1

The simplified equation of the differential mass balance is

$$\frac{\delta c(x,t)}{\delta t} + \frac{V_g}{R_f} \frac{\delta c(x,t)}{\delta x} - \frac{D_f}{\sqrt{2}\, R_f} \frac{\delta^2 c(x,t)}{\delta x^2} = 0 \qquad (1)$$

where

R_f = $\left(1 + \frac{\rho_b K_d}{\varepsilon} \right)$, the retardation factor

x = the distance from the interface of the glass and the zeolite along the direction of flow and longitudinal diffusion

t = time

$c(x,t)$ = liquid phase concentration, quantity of sorbing species per unit volume of liquid at distance along flow direction x and time t

ε = effective porosity of bed (fraction of bed volume containing flowing liquid)

V_g = average interstitial velocity of flowing water

$D_f/\sqrt{2}$ = coefficient of longitudinal fluid diffusion with a tortuosity factor to account for the tortuous diffusion path through the porous bed

ρ_b = the bulk packing density of solid sorbent, mass of solid per unit bed volume

K_d = the distribution coefficient for a linear sorption isotherm. The ratio of quantity of sorbed species per unit mass of solids to quantity of mobile species in the liquid phase per unit volume of liquid.

The boundary condition is

$c(x = 0, t > 0) = C_o$.

The initial condition is

$c(x > 0, t = 0) = 0$.

Define

$$U(x,t) = c(x,t) \cdot \exp\left[\frac{-V_g\, x}{\sqrt{2}\, D_f}\right] \cdot \exp\left[\frac{V_g^2 \cdot t}{2\sqrt{2} \cdot D_f \cdot R_f}\right]$$

Then, Equation (1) is reduced to a heat equation of U(x,t) as function of x and t. With the rearrangement of boundary and initial conditions, the Fourier transform is applied to the heat equation, and the subsequent convolution gives the following solution

$$c(x,t)/C_e = 1 - \frac{1}{2}\left[\operatorname{erfc}\left\{\frac{V_g \cdot \sqrt{t}}{2^{3/4}\sqrt{D_f \cdot R_f}} - \frac{\sqrt{R_f} \cdot x}{2^{3/4}\sqrt{D_f \cdot t}}\right\} - \exp\left\{\frac{\sqrt{2}\, V_g \cdot x}{D_f}\right\} \cdot \operatorname{erfc}\left\{\frac{V_g \cdot \sqrt{t}}{2^{3/4}\sqrt{D_f \cdot R_f}} + \frac{\sqrt{R_f} \cdot x}{2^{3/4}\sqrt{D_f \cdot t}}\right\}\right] \qquad (2)$$

where

erfc(y) = 1 - erf(y) and erf(y) is error function of y.

The integration from x = backfill thickness to infinity is done numerically for the total release from backfill.

APPENDIX 2

The same differential equation is used as in model 1. The new constraint instead of the boundary condition is

$$\int_0^\infty C(x>0,\ t>0)dx = C_{total}$$

and the new initial condition is

$$C(x > 0,\ t = 0) = C_{total}\ \delta(x)$$

where $\delta(x)$ is a delta function of x and C_{total} is a total quantity of sorbing species.

The transformation technique may not be plausible in this case for the closed form solution. However, since we know the response of step function from Appendix 1, the response of the delta function should be the derivative of the response of the step function with respect to x: the derivative of Equation (2) of Appendix 1. Further, we need the integral from x equals the backfill thickness to infinity, which is equivalent to the response function of Appendix 1 (Equation 2).

APPENDIX B

[redacted]

APPENDIX B

bnl
aui

BROOKHAVEN NATIONAL LABORATORY
ASSOCIATED UNIVERSITIES, INC.

Upton, New York 11973

(516) 345
FTS 666
4094

Department of Nuclear Energy

August 28, 1980

Mr. Everett A. Wick
High Level Waste Licensing Management Branch
Division of Waste Management
Mail Stop SS 965
U. S. Nuclear Regulatory Commission
Washington, DC 20555

Subject: Analysis of the Swedish Lead-Titanium Container Design

Dear Mr. Wick:

We have received your requests to carry out the following work:

1. Review of draft memorandum by R. Boyle (NRC) on the economic impact of using copper containers for spent fuel isolation -- request received 8/21/80.

2. Estimate the containment period that would be provided by the Pb-Ti container proposed by KBS, with particular interest being assigned to the minority opinion in the KBS report -- request received 8/25/80.

3. Suggest other materials that could be used instead of Cu or Pb-Ti with estimates of the amounts of these materials which would be needed -- request received 8/25/80.

Our comments are given below:

REVIEW OF MEMORANDUM ON COPPER CONTAINERS

We have reviewed the calculations which estimated the amount and cost of using copper for containing spent fuel and find them correct except for minor errors in arithmetic and typing. The only perturbation would occur if DOE decided to disassemble the spent fuel bundles prior to encapsulation in order to reduce the volume. They are evaluating this and other options (ONWI-39).

CONTAINMENT PERIOD FOR A Pb-Ti CONTAINER

Below are listed some of the main arguments presented by the minority member (Professor G. Wranglen) of the 10-man Swedish panel of experts which evaluated the penetration times for the Pb-Ti container. The majority opinion is detailed in Appendix 1 of this letter. Appendix 2 contains the minority view by Professor G. Wranglen. Our comments follow each of Wranglen's statements.

Statement 1 (page 20 in Appendix 2)

> "If the titanium canister is penetrated as a result of corrosion or other reasons, the exposed lead will be attacked locally. Lead displays a relatively great tendency toward pit corrosion, certainly less than that of steel (including chromium steel), but far greater than that of copper. Romanoff's data (Ref. 8, p. 20, 89) are presented in Table 2. On the lead canister, the attack is intensified by the electrochemical effects from the titanium jacket.
>
> Table 2. Pit corrosion on pure lead exposed in a reducing (oxygen-poor clay* for 2-11 Years. Test surface about 0.1 m^2. Average temperature 21°C.
>
> | Exposure Time in Years | Max. Carrier Pit Depth Total, mm | Pit Corrosion Rate in mm/Year |
> |---|---|---|
> | 2.1 | 0.95 | 0.45 |
> | 4.0 | 0.92 | 0.23 |
> | 9.0 | 2.15 | 0.24 |
> | 11.2 | 2.50 | 0.22 |
>
> *Lake Charles clay with the following data:
>
> | | Soluble Constituents | | | | | | |
> |---|---|---|---|---|---|---|---|
> | pH | Na$^+$ | Ca | Mg$^+$ | HCO_3^- | Cl^- | SO_4^{2-} | |
> | 7.1 | 717 | 138 | 56 | 490 | 565 | 1460 | mg/kg |
>
> The concentrations were determined in lake water, but are reported in mg per kg of clay. While the 2-year specimens have a larger value, the other samples taken 4, 9, and 11 years after disposal, display an almost constant value for the pit corrosion rate of 0.23 mm/year. If we calculated with 0.2 mm/year, we find a service life of 500 years for a 100 mm lead jacket."

Comment 1

The 500-year breaching time of the container is based on the assumption of a linear pitting rate and that all of the available oxygen in the repository structure migrates to one location forming a hemispherical pit. We believe that a linear pitting rate, though apparently supported by Wranglen's Table 2 above, is unlikely to hold for a period of hundreds of years. When heavy corrosion products are formed in the pit the migration of oxygen through them becomes more difficult which is well established in the field of corrosion. From the 11.2-year data in Table 2 the pit depth is only 2.5 mm. This is an extremely small distance compared to the 100-mm wall thickness of the lead. Hence, as time proceeds the large thickness of corrosion products would be expected to significantly decrease the pitting rate.

Another very important fact is that the Swedish panel's assumption of a single pit is virtually impossible for a container with the surface area of the Swedish design. Statistically, if a pit forms in one location it will also form in many other locations. Hence, if 100 pits were to form in the lead, then the penetration time based on Wranglen's own linear rate model would be 100 x 500 = 50,000 years.

Statement 2 (page 13 in Appendix 2)

> With respect to pitting in lead Wranglen states that "...since Ramonoff's data[7] pertain to pit corrosion above, while in the case of the canister, that is, after the titanium jacket has been penetrated, we are dealing with pit corrosion intensified by electrochemical corrosion."

Comment 2

Wranglen's statement is speculative. In Appendix 1, page 5, Pettersson more scientifically analyzes the problem citing supporting data. He concludes that anticipated electrochemical interactions between the Pb and Ti cannot lead to a more accelerated pitting rate than that for the reference case where Ti is passive.

Statement 3 (page 19 in Appendix 2)

> "..........to this risk of so-called brittle failure in welds. Concerning this, lecturer Fred Nilsson writes in a KBS report the following in his summary "The critical point of these canisters is thought to be welds in the outer titanium shell, where the risk of direct failure is not negligible[14]."

> With respect to these failure risks and with the "totally safe" criterion, the titanium canister, should, therefore, be given a short service life, essentially = 0, in comparison with the lead lining."

Comment 3

Unalloyed titanium and alpha alloys are considered to be readily weldable*. Difficulties may arise only in alpha-beta phase alloys*. The latter are not used in the Swedish design. The possible problem Wranglen refers to concerns high stresses remaining in the welds after sealing. However, one must note that in the fabrication of any container structure, each weld design and weld procedure is routinely evaluated, tested, and qualified. Options to remove residual stresses are available, including post weld heating. Clearly, potential weld problems will be satisfactorily resolved through standard qualification procedures.

Statement 4 (page 15 in Appendix 2)

> "The conditions under which crevice corrosion has been observed previously on titanium in laboratory tests are illustrated in Fig. 4 and Fig. 5[12] (reproduced below). With the combination of temperature and salt content prevailing at the surface of the canister, no local corrosion has yet been observed on titanium. According to Fig. 5, however, crevice corrosion has been observed at Cl^- levels as low as 100 ppm at a pH of 3 and 150°C."

Comment 4

Wranglen's last statement that crevice corrosion has been observed at Cl^- levels as low as 100 ppm at a pH of 3 and 150°C is irrelevant. The pH of the groundwater adjacent to the Swedish container is 8.5 (see Pettersson's comments in Appendix 1) and the maximum temperature is 80°C. From Wranglen's Figure 4 the anticipated "pure" water anticipated in the Swedish repository would probably not cause crevice corrosion. Even if relic seawater could reach the container, as Wranglen suggests, it would only give crevice corrosion at temperatures in excess of 130°C. However, such seawater would very likely be highly diluted by fresh groundwater so that the minimum temperature for crevice corrosion would probably be much higher than 130°C.

---

*Metals Handbook, Vol. 1, "Welding and Brazing," ASM, 1971, p. 375.

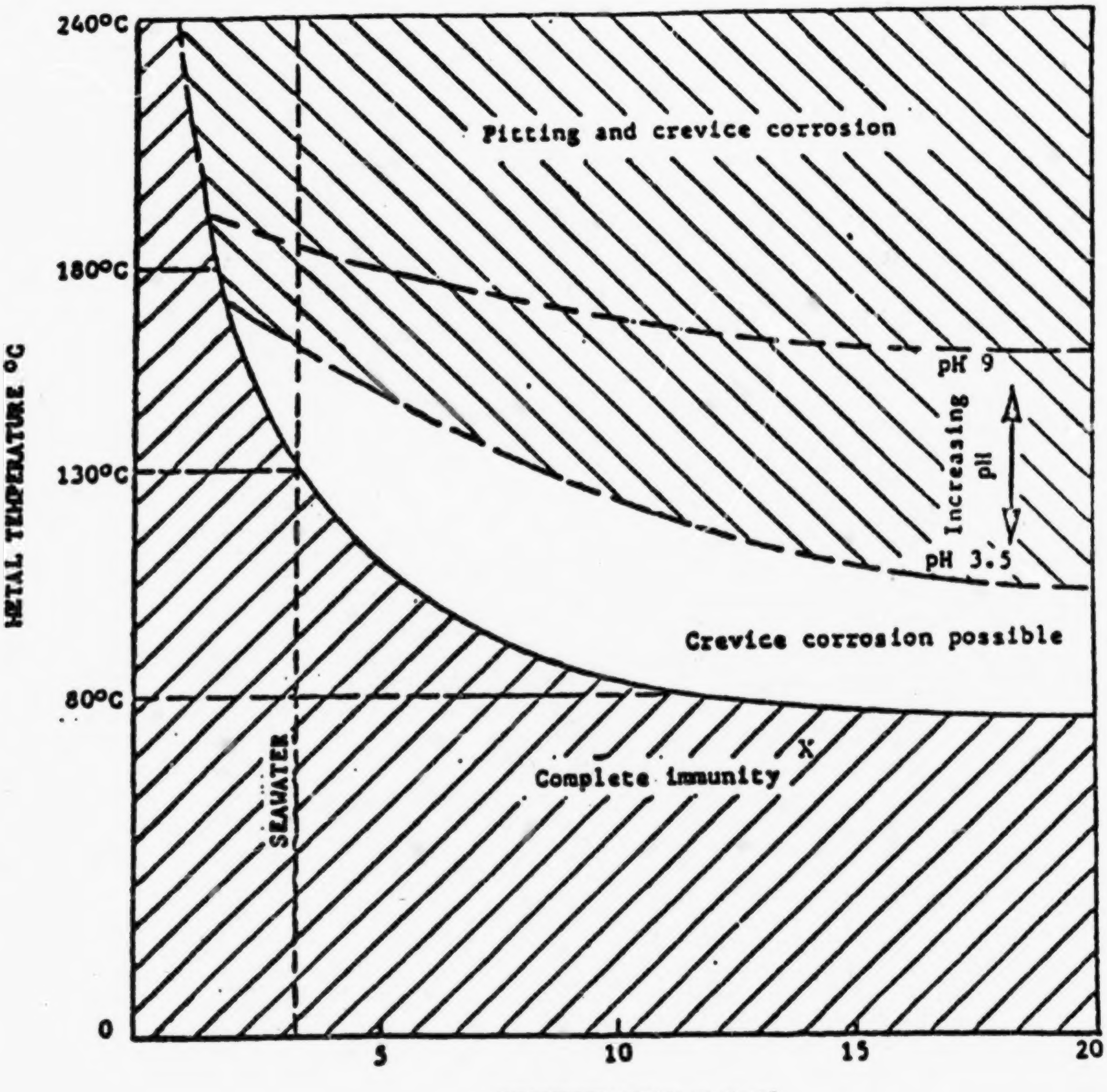

ˣBör stå: Complete passivity

KEY

▨	Complete immunity from crevice or pitting corrosion	☐	Crevice corrosion possibility irrespective of solution pH	▧	High probability of pitting attack and crevice corrosion according to solution pH

Fig.4. Effect of temperature, concentration, and pH on crevice corrosion and point corrosion of unalloyed titanium in seawater and concentrated chloride solutions in laboratory tests. In practice, crevice corrosion has been observed under asbestos packings in deaerated seawater at 120°C.

BEST DOCUMENT AVAILABLE

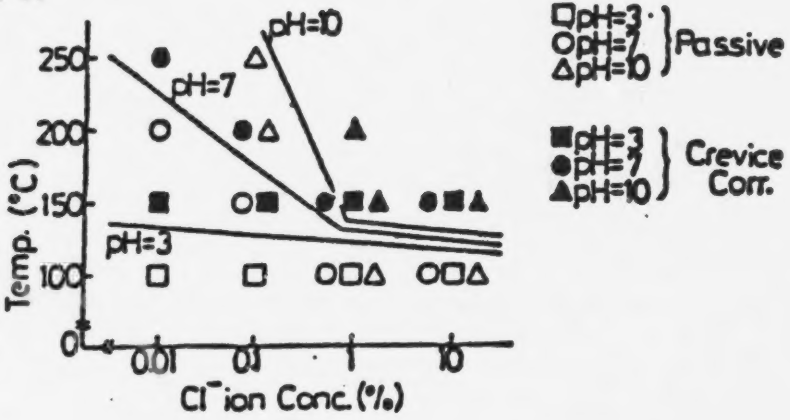

Fig. 5. Range for crevice corrosion and acidity at different pH, Cl Concentrations, and temperatures [9].

Statement 5 (page 16 in Appendix 2)

> "In practice, for example, through-corrosion of a 3-mm titanium plate has been observed under an asbestos packing in deaerated seawater at an operating temperature of 200-250°F (93-121°C) and an operating time of 8 months, despite the fact that the oxygen content was as low as 0.01 - 0.005 ppm. On one occasion, the oxygen content rose to 0.08 ppm, while the temperature during 40 hours went up to 300°F (149°C)[13]. This example showed that the low oxygen contents which are present in the long-term state of the disposal facility are sufficient to induce local corrosion on the titanium canister."

Comment 5

The data cited by Wranglen may be irrelevant. First, seawater is not the reference groundwater for any repository. Second, the asbestos itself could be responsible for the corrosion. Some information on aluminum, for example, cautions against contact with wet asbestos.*

---

*Corrosion Resistant Materials Handbook, 3rd Edition, Noyes Data Corp., 1976, p. 420.

Statement 6 (page 13 of Appendix 2)

> "Note that titanium is sensitive not only to oxidation but also to hydrogen absorption, something which, among other things, leads to crack formation as a result of so-called delayed fracture. Experiences with sister metal zirconium have shown that even in a reactor environment which is extremely pure with respect to freedom from impurities in the surrounding water, one can obtain not only various local corrosion attacks (breakaway, nodular oxidation, sunburst), but also delayed failure after relatively short exposure times."

Comment 6

The statement that delayed failure can occur in Ti and Zr is not true if data from the literature are the basis of this statement. Neither the Swedish panel (including Wranglen), nor experts writing in the literature, nor we, can find any evidence for delayed failure in unalloyed Ti and Zr. Delayed failure has only been shown in a few instances in alloys containing both the hexagonal close packed alpha phase and the body centered cubic beta phase.[1-5]. The mechanism is reasonably well established and concerns the rapid migration of hydrogen through the beta phase to the tip of a crack or imperfection where it concentrates as a "cloud" possibly forming hydrides. The stresses at the crack tip attract the hydrogen until eventually local conditions are such that the crack advances along an alpha-beta interface, and the process then repeats itself. In pure alpha phase Ti hydrogen diffuses much more slowly so that this, also, would decrease the possibility of achieving a sufficiently high hydrogen concentration at the crack tip to cause propagation.

Only highly stressed cracks, apparently, attract enough hydrogen to give delayed failure in this way. Paton believes that in unalloyed Ti which is soft, the stresses at the crack tip are relaxed by local deformation so that sufficient hydrogen is never accumulated to propagate a crack,[1] i.e. Ti cannot suffer delayed failure. In related work, Weinstein and Holtz studied Zr and some of its alloys. Under aggressive conditions of up to 500 ppm of hydrogen they could not detect any evidence for delayed failure.

Even if delayed failure was conceptually possible in Ti this would not necessarily be a major problem since many workers have identified that there is a well defined stress level below which failure cannot occur. The effect is similar to that observed in a regular fatigue curve. Hence, by careful design it should be possible to keep stresses in the Ti container sufficiently low to eliminate this problem. The general Swedish philosophy to reduce hydrogen levels in the titanium to less than 20 ppm, and to prevent radiolysis effects (which would produce H_2 in groundwater) by using the thick Pb inner container will also minimize any possibility of delayed failure.

In short, we believe that delayed failure in Ti may be near impossible, which is in accord with the majority of the Swedish panel. Wranglen's comments on delayed failure occurring in Zr are, to the best of our knowledge, incorrect. He may have been referring to delayed failure in a single lot of Zircaloy-2 (Zr - 1.5 Sn - 0.12 Fe - 0.1 Cr - 0.05 Ni).[6] However, very high stresses equal to 70% of the tensile strength were used, and the results could not be repeated by the same workers. Nevertheless, Zircaloy-2 is a complex alloy with several secondary phases. It is not representative of unalloyed Zr behavior.

Conclusions

The comments of Professor Wranglen on delayed failure, crevice corrosion, pitting and failures in Ti welds are not usually supported by the literature. In many cases he cites data on materials and conditions which are vastly different from the reference case. We find his comments on the rapid penetration of the Pb-Ti container to be highly speculative and very likely incorrect. Our opinion is that both the Ti and the Pb container components are likely to have extremely high resistance to penetration by corrosion and mechanical failure and that a reasonable estimate for the corrosion resistant lifetime of such a container would be several thousand years. In this respect our judgement is similar to that of the nine majority members of the Swedish panel.

ALTERNATE MATERIALS FOR CONTAINERS

With respect to the specification of new designs and materials to supersede the KBS container we cannot give details within the time available for such a study. Such work would need detailed information on the host rock, the overpack/backfill, shielding required, geometric layout in the repository, etc. However, some qualitative information would be appropriate. Since the Swedish Pb-Ti container has been designed by a group of experts we may assume that 10 cm of Pb is of the magnitude sufficient for shielding spent fuel assemblies even though this container was specifically designed for vitrified waste. More detailed thermal shielding, and structural evaluations will be needed in a detailed study for spent fuel. We feel that a Pb-Ti container would, basically, be a sound proposition. The arguments for this are similar to those given by the KBS group, i.e. good corrosion resistance, mechanical properties, shielding, etc. In view of the concern expressed by Wranglen we suggest that a simple modification be made to such a container to give much greater assurance of containment. Figure 1 below describes this design which comprises two titanium shells separated by a closely contacting layer of cast Pb. The Ti shells are welded shut at opposite ends so that if failure in the welds does occur there is a tortuous path for the groundwater to follow before it can reach the second failed weld and attack the main Pb mass in which the fuel is encapsulated.

Suppose that pitting failure does occur in the outer Ti shell as shown in Figure 2. Wranglen suggests that the pit will then proceed inwardly at a linear rate consuming Pb as it moves. However, in this design, the second Ti shell will prevent this from occurring. Corrosion can still occur, but the Pb between the two Ti shells will be a sacrificial surface and it will corrode along a path parallel to the container surface. The main Pb matrix will be essentially unaffected even if the second Ti shell is breached at a location close to the first failure point since it would be far easier to corrode the Pb between the shells because of its greater accessibility. Such a container design would greatly decrease the penetration rate when compared to the reference Swedish design. Laminated containers are, therefore, a highly desirable design since repeated initiation of a crack or pit will be required at each interface. By introducing sacrificial layers the direction of corrosion can be redirected laterally. Many different materials can be selected for each container, each having the ability to combat corrosion from a particular corrodent in the groundwater.

At present we feel there is great potential for long term corrosion resistance (several thousand years) in multilayered containers made of conventional materials such as stainless steels, carbon steels, Pb-Sn alloys, copper, titanium, etc. For instance, we believe a container composed of several hundred layers of three materials such as (1) Pb-Sn, (2) carbon steel, (3) stainless steel, which alternate periodically may well provide corrosion resistance in a repository for many thousands of years. We believe a wall thickness of 1 to 2-inches may be more than adequate.

Generally, we would continue to recommend Ti as an outer shell for any normal metal container because of its proven excellent resistance to corrosion. Zirconium could be a good alternate. It may be possible to use much cheaper corrosion resistant materials if cathodic protection is used. In this procedure a large sacrificial mass of another metal is placed adjacent to the container and they are connected by electrically conducting wires. If the metal is more anodic than the outer container shell, then the container is protected at the expense of the sacrificial mass.

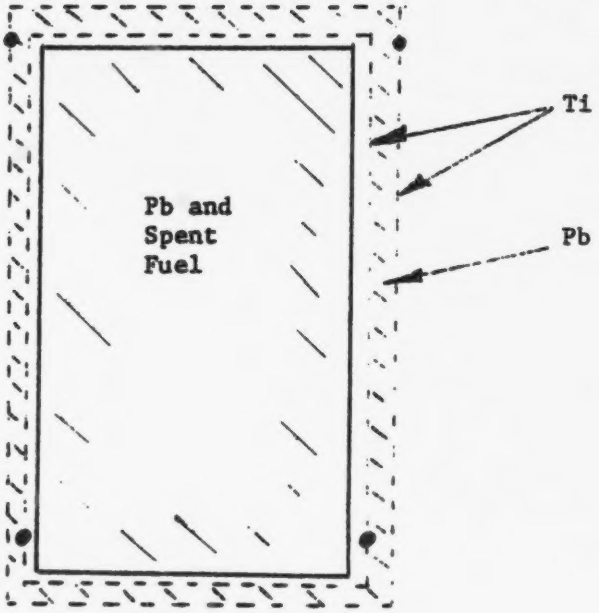
Ti
Pb and
Spent
Fuel
Pb

● = Circumferential Weld

Figure 1. General design of a laminated Pb-Ti container.

BEST DOCUMENT AVAILABLE

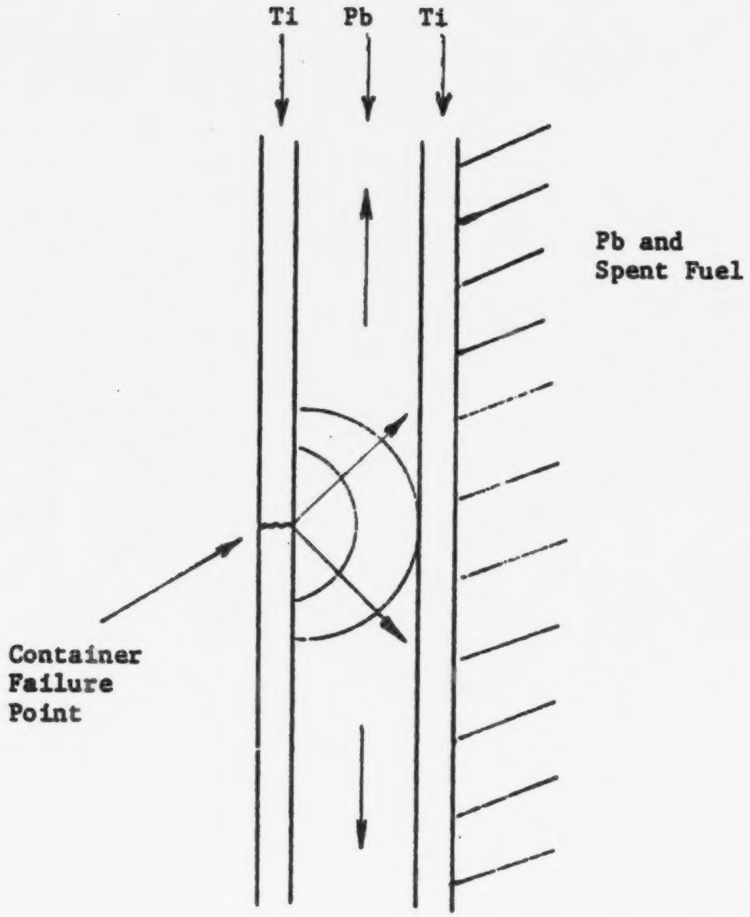
Ti
Pb
Ti
Pb and
Spent Fuel
Container
Failure
Point

Figure 2. Schematic of corrosion processes in a laminated Pb-Ti container.

BEST DOCUMENT AVAILABLE

REFERENCES

1. N. E. Paton and J. C. Williams, "Effect of Hydrogen on Titanium and Its Alloys" in Hydrogen in Metals, ASM, 1974, p. 409.
2. D. N. Williams, "The Hydrogen Embrittlement of Titanium Alloys," J. Inst. Metals, 91, 185 (1962).
3. D. A. Meyn, "Effect of Hydrogen on Fracture and Inert Environment Sustained Load Cracking Resistance of α-β Titanium Alloys," Met. Trans., 5, 319 (1974).
4. N. R. Moody and W. W. Gerberich, "Hydrogen Induced Slow Crack Growth in Ti-6Al-6V-2Sn," Met. Trans., 11A, 973 (1980).
5. D. Weinstein and F. C. Holtz, "Susceptibility of Zirconium and Zirconium Alloys in Delayed Failure Hydrogen Embrittlement," Trans. ASM, 57, 284 (1964).
6. G. Ostberg, "Some Observations on the Ductility of Zirconium Alloys With Special Reference to the Effect of Hydrogen," J. Inst. Met., 93, 223 (1964).

Sincerely yours,

Peter Soo

Peter Soo
Nuclear Waste Management Division

PS:gfs
Attachments (Appendices 1 and 2 being sent under separate cover)
cc: D. G. Schweitzer

APPENDIX 1

Studsvik Arbetsrapport

Technical Report

May 23, 1979

Report No. MZ-78/116

SUPPLEMENTARY VIEWS ON DELAYED FAILURE OF TITANIUM

Kjell Pettersson

AB ATOMENERGI

Sweden

[redacted]

SUPPLEMENTARY VIEWS ON DELAYED FAILURE IN TITANIUM

by

Kjell Pettersson

SUMMARY:

Since the earlier recommendation that the hydrogen content be limited to 20 ppm in cannisters for waste storage in order to avoid delayed failure was judged to be insufficient, the possibility is discussed of having a criterion based on a maximal permissible stress intensity factor. Due to a poor experimental foundation, the latter was set at 2 $\text{MPa}\sqrt{\text{m}}$*. If the maximum stress per cannister is 120 MPa, it can then be guaranteed to resist disintegration through delayed failure if the largest crack-like defect is 0.2 mm in diameter. On the other hand, it is impossible to guarantee that no local failures will occur in the cannister due to internal stresses in welds.*

1. Introduction

The earlier study on the risks of delayed failure in unalloyed titanium [1] led to the conclusion that if the hydrogen content of 20 ppm maximum is permitted, the risk of delayed failure due to the mechanism discussed in the report is nonexistent. The study was criticized from many different aspects. Among other things, criticism was directed at the fact that many of the numerical data for the calculations are guesses and that the data base may also be uncertain in other respects. It is thus important to recall that the evaluation had the result that in order to preclude the risk of delayed failure, one should make certain that hydrides cannot be precipitated out at all. As a result, the only critical number is the solubility of hydrogen in titanium. This is based on only one study [2], which also appears to be the only one performed during the past twenty years. This is an uncertainty factor even though the study reported appears to be fairly responsible. A better foundation would be desirable.

BEST DOCUMENT AVAILABLE

A more serious criticism of the evaluation was advanced by K. Videm and B. Cox [3]. The criticism is based on a report on subcritical crack propagation in two-phase titanium alloys where such crack propagation was observed at a hydrogen content as low as 7 ppm, which is clearly below the solubility limit [4]. It was also noted that the model for delayed failure used in the evaluation yields a crack propagation rate 1000 times too low for the two-phase alloy with 7 ppm of hydrogen. Videm and Cox draw the conclusion from this that the judgment made may possibly be incorrect, and that instead, by analogy with what was done in Canada regarding pressure pipes and reactors, one should show that defects and stresses in the titanium cannister are so small that the initiation of cracks cannot occur.

2. *Delayed Failure in One and Two-Phase Alloys*

It should be pointed out that delayed failure has never been observed in unalloyed type titanium. As a matter of fact, there is only a single report on subcritical crack propagation in α-titanium, i.e., in an alloy with 4% Al and 100 ppm H [5]. This, of course, is not sufficient to preclude the risk of delayed failure in unalloyed titanium, which is also the reason why the earlier analysis was performed.

In α-β-alloys, however, delayed failure is a well-known phenomenon. The explanation as to why the hydrogen in the material is believed to cause delayed failure is quite simply that with increase in hydrogen content, the material becomes more susceptible to delayed failure. The study reported by Videm and Cox with cracking at 7 ppm hydrogen deviates from

BEST DOCUMENT AVAILABLE

this pattern; with increasing hydrogen content, the alloy became less susceptible, and therefore, one can question whether in this case it was delayed failure due to hydrogen. If it were not, in such cases there is an additional (unknown) mechanism for subcritical crack propagation in Ti which, of course, is cause for concern. This is an additional factor indicating that one should make certain that the stresses and defects are at a level sufficiently low that cracking cannot occur.

3. *Crack Propagation Velocity -- Stress Intensity Factor*

The state of stress at the point of a crack can be characterized by a so-called stress intensity factor denoted by K. It is frequently the magnitude of this factor which determines the crack propagation velocity in the case of subcritical crack propagation. For delayed failure in zirconium alloys, in Canada, it was found that at stress intensities below 6 $MPa\sqrt{m}$, no crack propagation at all occurs. The rules for the permissible stresses and defects in pressure pipes in CANDU reactors were then based on this.

By examining the literature on delayed failure in titanium alloys, it should be possible, in principle, to arrive at a similar limit for it. One such study shows that there is no crack propagation at all at a K value below 12 $MP\sqrt{m}$. On the other hand, all these experiments are of a short-term character. The test times are rarely longer than a few weeks. No extrapolation for longer times and lower stress intensities is possible. However, it is significant that for the lowest stress intensity factors, generally, the crack propagation velocity is strongly dependent on K.

BEST DOCUMENT AVAILABLE

For a similar variant of subcritical crack propagation, stress corrosion cracking, it is often true for low K values that

(eq 1)

$$da/dt = DK^n$$

da/dt = crack propagation velocity

n = constant = 4-10

C = constant

The data provide no basis for setting any limit for K below which subcritical crack propagation will not occur. On the basis of equation 1 and the relatively high value of K at which crack propagation was observed, however, one can make it probable that the crack propagation velocity is extremely low, e.g., at $K = 2$ MPa$\sqrt{m}$.

With this value as the starting point, a recommendation for the largest permissible defects could be given. Such a recommendation should then be observed by the manufacturer, starting with the stresses to which the cannister is exposed. At a maximum stress of 120 MPa, the largest permissible defect is 0.2 mm according to the formula for half the crack length.

$$a = \frac{1}{\pi}\left(\frac{K}{\sigma}\right)^2 = \frac{1}{\pi}\left(\frac{2}{120}\right)^2 = 0.1 \text{ mm} \qquad \text{(eq 2)}$$

The weld properties constitute a special problem. In the worst case, they can go up to the elastic limit of the material. Since it is simultaneously most probable that crack-like defects can be found in the

BEST DOCUMENT AVAILABLE

weld, it is extremely difficult to guarantee crack freedom in titanium cannisters unless the internal stresses of the welds can be reduced in some way, e.g., by a special welding technique or by stress relieving annealing or both. It should also be noted that the internal welding stresses by themselves cannot cause extensive failure of the cannister, since the average value of these stresses summed up over a large area must be 0. However, it cannot be excluded that the internal welding stresses may initiate a defect up to a certain size so that it will later grow under the influence of the nominal stress on the cannister. Therefore, it is important that the tensile stresses on the cannister be as low as possible and of as brief duration as possible. The present design appears to satisfy these requirements. Moreover, the cannister is expected, with time, to be exposed to an external overpressure which is favorable.

4. *Conclusions*

It is possible (but not necessarily correct) that the previously reported recommendation that the hydrogen content be limited to 20 ppm in order to avoid delayed failure is insufficient. One finds no reason to reject the recommendation. However, it may be supplemented by a calculation of the dependence of the crack propagation velocity on the stress intensity factor so that one can guarantee that the cannister will contain such small defects that it cannot crack at the low stresses to which it is exposed. From an inadequate experimental foundation, $K = 2\ \mathrm{MPa}\sqrt{m}$

BEST DOCUMENT AVAILABLE

is proposed as a limit for the permissible stress intensity factor below which freedom from cracking due to delayed failure is guaranteed. With this limit, one can guarantee that the cannister will hold together during its lifetime. On the other hand, one cannot guarantee that the cannister will not be penetrated at the welds.

Finally, it should be emphasized that this is a very conservative evaluation based on the current level of knowledge. It is highly probable, and all operating experiences indicate, that delayed failure is not a problem with unalloyed titanium.

REFERENCES

1. Pettersson, K., Evaluation of the risk of delayed failure in titanium, KBS-26 (AE-MZ-82).

2. Paton, N.E., Hickman, B.S. and Leslie, D.H., Behavior of hydrogen in α-phase Ti-Al alloys. Met Transactions 2 (1971) pp. 2791-96.

3. Videm, K. and Cox, B., Discussion of the Scandpower's study of the KBS Report on Corrosion. Mote pa SKI 1978-04-10.

4. Williams, D.N., Effects of hydrogen in titanium alloys on sub-critical crack growth under sustained load. Mat Sci Eng 24 (1976) pp. 53-63.

5. Paton, N.E. and Williams, J.C., Effect of hydrogen on titanium and its alloys. Hydrogen in Metals, ed I.M. Bernstein and A.W. Thompson, American Society for Metals, 1974.

BEST DOCUMENT AVAILABLE

Corrosion of the Lead Lining

By: Göran Eklund, Institute for Metal Research, May 1978

A corrosion of the lead lining can, of course, not occur until the titanium casing has been penetrated in some way and the lead metal exposed to the environment. The penetration of the titanium casing can occur in two different ways: It can either be damaged purely mechanically, or the titanium casing can be penetrated as a result of pit corrosion or crevice corrosion.

Lead can corrode under two different conditions, on the one hand, when the titanium casing is passive, and on the other, when both the titanium and the lead are in the active state.

Preliminary Assumptions

The lead-titanium cannister, according to the assumptions, is placed in the disposal hole as shown in Fig. 1, whose dimensions are shown in the figure also. The disposal hole and tunnel are filled with a sand-bentonite mixture with a porosity of about 40%. At the time of disposal of the cannister itself, water is added to the sand-bentonite mixture (1). Since corrosion is dependent on the quantity of oxidizers supplied to the surface of the cannister, the calculations below were based on the available quantity of air oxygen, i.e., that air oxygen which can be locked in when the depository [storage space] is sealed. There are no reasons to take other oxidizers into account, such as the oxygen from the groundwater, radiolysis oxygen, or the sulfide ions supplied by the

BEST DOCUMENT AVAILABLE

groundwater or formed through bacterial activity, in consideration of the relatively limited service life (thousands of years) involved in this case.

Available Quantity of Oxidizers

After the sealing, the depository will contain oxygen from the air in the pores of the sand-bentonite mixture. When the water from the surrounding rocks penetrates the filling material or is supplied intentionally, one can conservatively estimate that all of the air will be dissolved in the penetrating water and become available to maintain a corrosion process. In reality, the water will probably displace the air so that the quantity of dissolved air oxygen in the water is considerably smaller than that assumed below.

The Disposal Hole

The volume of the sand-bentonite mixture in the disposal hole is 3.4 m^3. After the water is added to the sand-bentonite mixture at the time of disposal of the cannister, the water in the pores of the filler will become saturated with air of atmospheric pressure. The oxygen content in this water will therefore lie at 10 ppm at the maximum. This means that $3.4 \cdot 0.40 = 1.36$ m^3 of water is available in the disposal hole, corresponding to 13.6 g of O_2 or 0.42 mole of O_2.

The Tunnel System

When the cannisters are placed in disposal holes 4 m from one another, a tunnel part of 4 m corresponds to every cannister. The volume of the

BEST DOCUMENT AVAILABLE

tunnel is 43.7 m^3, which contains $43.7 \cdot 0.40 \cdot 0.21 = 3.67$ m^3 of O_2 or 164 moles of O_2.

Corrosion of the Lead Cannister

As stated above, one can distinguish two different cases of corrosion. The corrosion of the lead jacket when the titanium casing is passive, and simultaneously, corrosion when both titanium and lead are present in the active state. Below, it was assumed that the most unfavorable case would occur, i.e., a local attack at *one* single point.

Corrosion of Lead When Titanium Casing is Passive

This form of corrosion can occur when the titanium casing is punctured mechanically or when a penetrating corrosion pit in the titanium casing is passivated.

The attack on the lead cannister, if it occurs, can be assumed to have the form of a corrosion pit which grows in a hemispherical manner. When the thickness of the lead casing is determined, one can calculate the quantity of lead which must be dissolved before the stainless steel casing around the vitrified waste product will be exposed at a point. Assuming a hemispherical attack, this means that 2.1 dm^3 of lead must be dissolved, corresponding to 23.9 kg of lead.

The total quantity of lead which can go into solution is determined by the quantity of oxidizers at the time of disposal and the quantity supplied to the surface of the cannister with time. If the quantity of lead is calculated to correspond to the total oxygen content in the system, regardless of the time required to dissolve this quantity, one finds:

[redacted]

BEST DOCUMENT AVAILABLE

Oxygen from	mol O_2	kg Pb
Disposal hole	0.5	0.2
Tunnel	164	67.9

The total quantity of lead, 68.1 kg, more than exceeds the 23.9 kg that is required for the penetration of the cannister. The question is thus how long a time it will take to penetrate the cannister?

Calculation of the Surface Life

The calculations involved did not take into consideration the corrosion rate. The corrosion rate is determined by the supply of oxygen per unit time to the cannister surface, and if the permeability in the sand-bentonite mixture is low, the oxygen can be transferred only through diffusion. At this point, we assume that all oxygen in the disposal hole will be consumed immediately, corresponding to 0.2 kg of Pb. If the tunnel system is considered to be an infinite oxygen source containing 3.75 moles of O_2/m^{-3}, from which the oxygen can diffuse down through the disposal hole to the upper surface of the cannister, i.e., a distance of 2.9 m, according to Fig. (1), one can calculate how long a time it will take to dissolve that quantity of lead that is required for a breakthrough.

BEST DOCUMENT AVAILABLE

$$J = - D\frac{\Delta c}{\Delta \alpha}\cdot A$$

$$D = 4\cdot 10^{-10}\ m^{2}s^{-1}$$

$$\Delta = 3.75\ mol\ m^{-3}$$

$$\Delta\alpha = 2.9\ m$$

$$A = 0.78\ m^{2}$$

The oxygen flow is therefore $4.03\cdot 10^{-10}$ mole/sec^{-1} and corresponding to $1.67\cdot 10^{-7}$ g of Pb/sec^{-1} or 5.26 g/year^{-1}, signifying that penetration can only occur after 4500 years.

The calculation above is based on the fact that *only on* hemispherical attack occurs. Many simultaneous attacks, of course, signify that the time to penetration will increase. The reason why a hemispherical attack is assumed is that in a corrosion pit where all of the hemispherical surface is active, the ohmic voltage drop tends to regulate the dissolution rate at each point. This means that the growth will be hemispherical from the penetration hole.

The precipitation of poorly soluble compounds on parts of the walls of the corrosion pits can influence the direction of growth for a certain time, but with time, the precipitates will eventually fill up and plug the corrosion pit, thus impeding the transportation processes and reducing the rate of attack.

Corrosion When Both Lead and Titanium are in the Active State

When titanium corrodes through pit corrosion or crevice corrosion, the pH and potential in the active range are strongly shifted from the potential and pH which prevail on the passive titanium surface. On the passive

BEST DOCUMENT AVAILABLE

titanium surface, the pH is about 8.5 because of the buffering effect of the bentonite. According to AE [2], the potential lies at around 200 mV when 8 ppm of oxygen is present in the water, and at about 24 mV when the oxygen content is 15 ppb, i.e., somewhere within the shaded region in Fig. 2. The potential of the active titanium metal and the pH of the anode solution will lie within the range marked by Ti^{3+}, Ti^{2+} in the figure.

In order for the corrosion of lead and titanium to take place simultaneously, the potential in the active range must be higher than -400 mV and the pH lower than 0; otherwise, the lead will become cathodically shielded by the corroding titanium metal, as indicated in Fig. 2. Tests by Schlain [3], Fig. 3, indicate that corroding titanium assumes a potential of around -400 mV in a strong hydrochloric acid solution. This signifies that a situation such as that above may possibly arise.

When corrosion of titanium begins, reduction of oxygen gas must constitute the cathode process. The cathode process can subsequently pass into hydrogen gas generation, as a result of which, the reaction will become self-sustaining. An exposed lead surface can then begin to corrode if potential and pH are in the suitable range. This corrosion is determined by the cathodic reduction of oxygen gas on the surface of the cannister. If part of the hydrogen reduction required to maintain the titanium reaction is used for the dissolution of the lead, the pH will rise in the range and the titanium will be passivated. Under no conditions can such corrosion of lead occur more rapidly than would correspond to the supply of oxygen gas to the surface of the cannister. Local corrosion, according to the above,

BEST DOCUMENT AVAILABLE

therefore cannot lead to more rapid through-corrosion than in case A.

Summary

With respect to the conditions discussed above, it can be estimated *conservatively* that the lead capsule will be penetrated only after 4500 years.

If the improbable situation should arise that lead and titanium are simultaneously in the active state, everything suggests that the time for penetration will be considerably longer.

However, it must be pointed out in particular that the surface life of the titanium casing in all cases was set at *zero*. In reality, the service life of the titanium casing is probably at least 1000 years, which should be added to the service life above.

REFERENCES

1. The final stage of the nuclear fuel cycle. Vitrified wastes from Reprocessing. III Anläggningar, KBS.
2. Experiments in electrochemical corrosion between titanium and lead. KBS-uppdrag ur 209 AE MC 244 780/27.
3. Schlain, D., Rep. Invest. US Bur. Min. No. 4965 (1953).

BEST DOCUMENT AVAILABLE

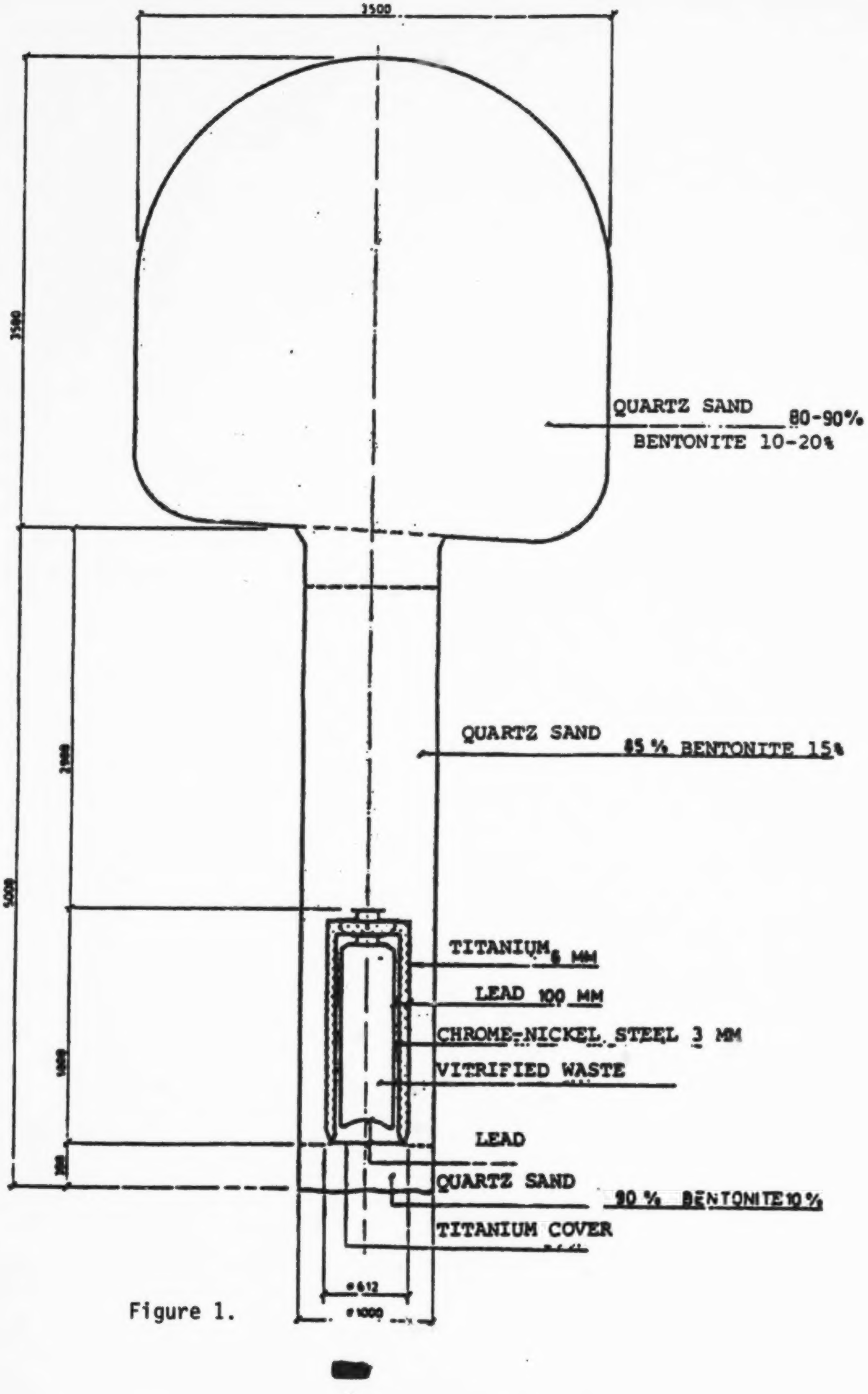
3500
3500
5000
2000
1000
QUARTZ SAND 80-90%
BENTONITE 10-20%
QUARTZ SAND 85 % BENTONITE 15%
TITANIUM 6 MM
LEAD 100 MM
CHROME-NICKEL STEEL 3 MM
VITRIFIED WASTE
LEAD
QUARTZ SAND 90 % BENTONITE 10 %
TITANIUM COVER
ø612
ø1000

Figure 1.

376

BEST DOCUMENT AVAILABLE

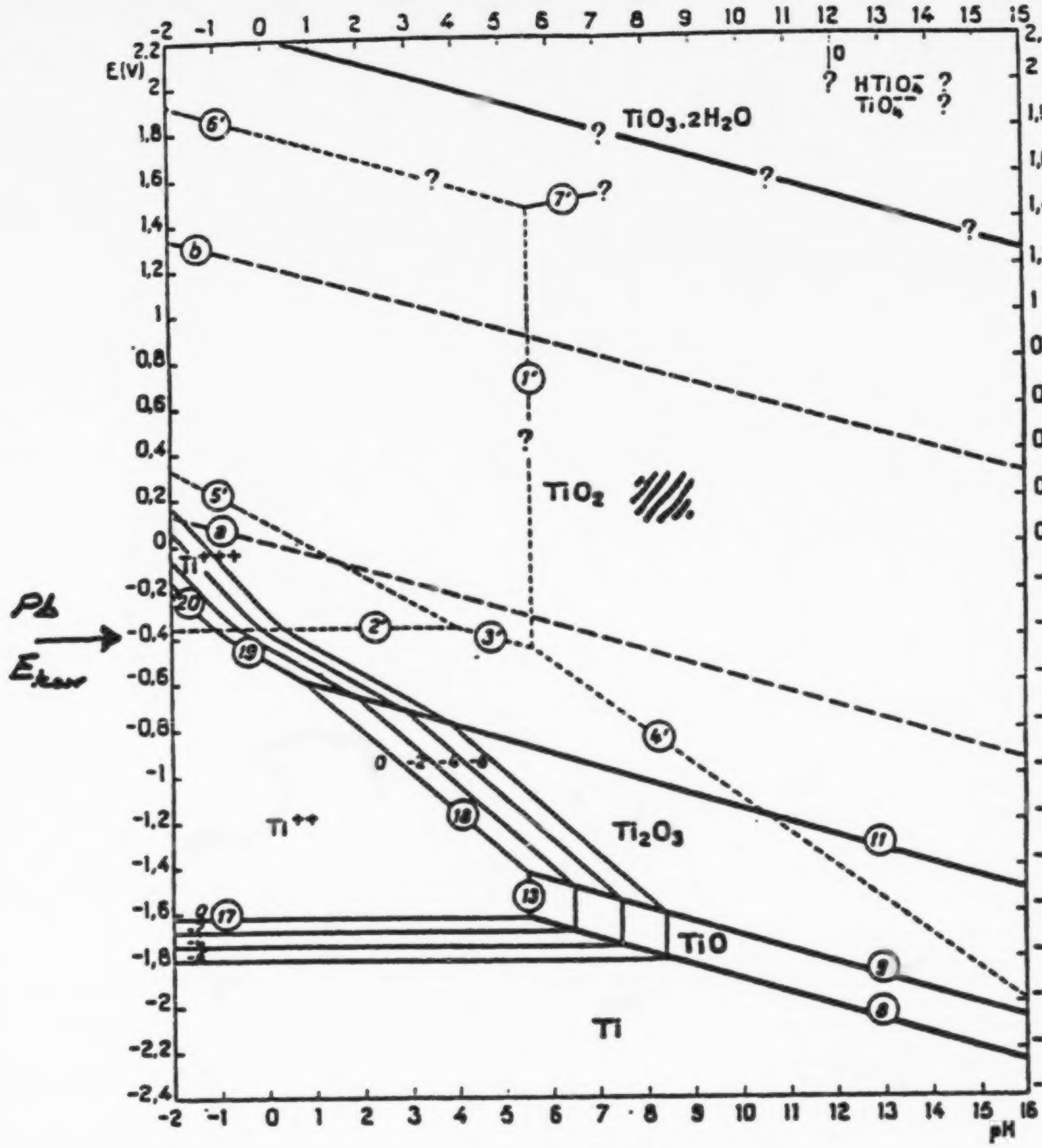

Figure 2.

Fig. 2. Potential-pH-equilibrium diagram for titanium-water at 25°C (Pourbaix).

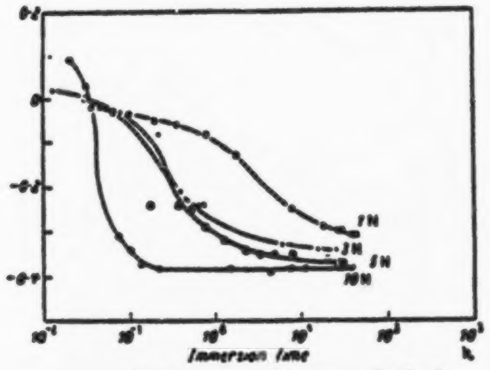

Electrode-potential/time curves for titanium immersed in hydrochloric acid solutions of various strengths at 25° C in a helium atmosphere (after SCHLAIN³)

Figure 3.

BEST DOCUMENT AVAILABLE

APPENDIX 2

SEPARATE OPINION

by

Professor Gosta Wranglen, Kungl.
Technical Academy, Stockholm 70

concerning

LEAD-LINED TITANIUM CANNISTERS FOR REPROCESSED AND VITRIFIED NUCLEAR FUEL WASTES -- EVALUATION FROM THE CORROSION STANDPOINT
(Report from the Reference Group of the Corrosion Institute for Cannister Material for Nuclear Fuel Waste).

SUMMARY:

1. *According to a well-established guiding principle in the international debate on nuclear fuel waste, the long-term danger of the waste, i.e., after the decay of the fission products, should not be permitted to exceed the danger of the uranium ore from which the waste originally came. On these grounds, French and American investigators have found it to be "absolutely necessary" to further separate plutonium from conventional highly-active wastes from reprocessing in which 99.5% of the plutonium in the fuel used has already been removed so that only 0.01-0.05% of the original amount of plutonium remains.*

2. *Disposal of conventional highly-active wastes should, according to the same investigators, require service lives of the cannister material of 100,000s or millions of years.*

3. *The lead-titanium cannister proposed by KBS could guarantee a service life of only a few hundred years, which is ascribed to the lead lining. With the criterion "completely safe", in other words, the service life of the titanium jacket must be set equal to 0, especially with respect to the risk of so-called delayed fracture and brittle fracture in wells.*

4. *The lead-titanium cannister therefore seems to be inferior to a copper cannister with comparable radiation shielding effect, since the latter could be predicted to have a service life of a few thousand years.*

5. *It is incumbent on us of the now-living generations to dispose of our own long-lived radioactive wastes of the plutonium and other transuranium types. It appears that this could be done be reprocessing of spent nuclear fuel after separation of the transuraniums and the use of the latter as new fuel in breeder reactors. Besides preserving an invaluable energy resource in*

BEST DOCUMENT AVAILABLE

this way, the storage problem is thereby limited to the storage of fusion products for a relatively short time, 500 - 1000 years. For this purpose, a copper cannister appears to be better suited than a lead-titanium cannister.

1. *Service Life Requirement for Cannisters*

No precise requirements for a certain service life for cannister material for nuclear fuel wastes has been reported as a guide for the judgment of the reference group. However, such a service life requirement can be derived from a principle which has long been the guiding one in the international debate on nuclear waste. This means *that the danger of the waste in the long term, i.e. after the decay of the fusion products, should not be permitted to exceed the danger of the uranium ore from which the waste originally came.* This is chiefly a question of vitrified wastes with a low transuranium content stemming from conventional reprocessing, supplemented by subsequent separation of the transuranium elements. Swedish nuclear power engineers [1, 2], among them the leader of the encapsulation group within the KBS project, have also adhered to this principle. Such a safety requirement based on a comparison with uranium ore has the great advantage of being well defined and unequivocal, something which cannot, however, be said about the risk analysis (or safety analysis) practiced within the KBS project, which was previously used in the American Space Program, as well as for nuclear reactors. The risk analysis is of value when one is making a comparison between similar systems or designs during relatively short events. To make estimates of absolute risks for the long periods of time in question here is obviously very difficult. The result has been found

BEST DOCUMENT AVAILABLE

to vary by several powers of ten, depending on the initial assumptions, as follows from a comparison between the results in references 3 and 4.

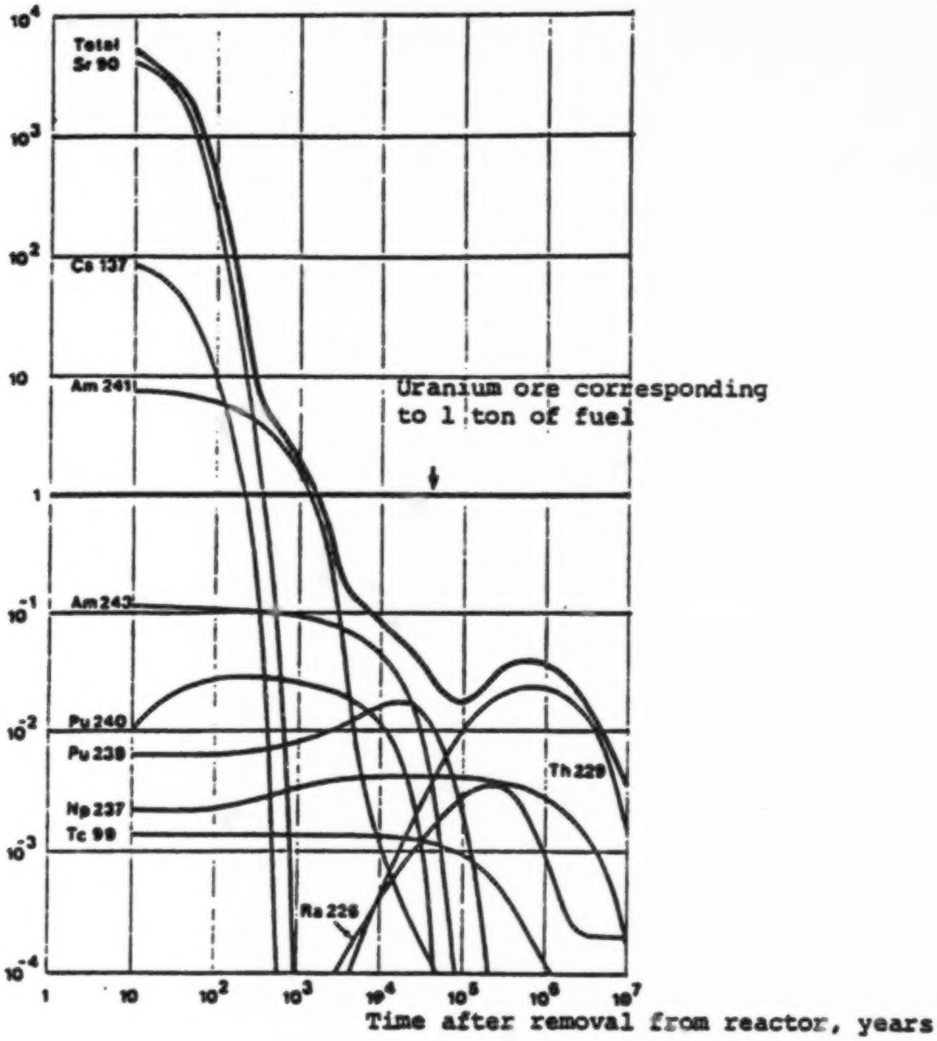

Figs. 3 - 9. Potential danger index for different nuclides in highly active wastes from one ton of spent fuel as related to the quantity of uranium ore corresponding to one ton of fuel. The real danger is also influenced by the routes of spread of the substances to man (see chapter 6). The fuel has a burn off of 33000 MWd (t)/tU, a power denisty of 34.4 MW(t)/tU and an enrichment of 3.1% uranium-235.

BEST DOCUMENT AVAILABLE

A comparison between the danger of highly-active waste from conventional reprocessing and uranium in ore is shown in Fig. 1, which was taken from a KBS report [3], which shows how the danger index for the highly-active waste declines with time, where the index for one ton of uranium in ore was selected as unity. From this figure, one can get the idea that the danger of the highly-active waste has already declined to the level of the ore after 1500-2000 years. However, this is misleading, since we are calculating with 100% uranium ore, while most uranium deposits contain only 0.2-0.3% uranium, and, for example, Ranstad ore contains only 0.03% uranium. By a comparison between highly active waste and 100% ore, one is taking into account only the concentration of radioactivity in time due to the nuclear energy activity, but not the concentration of activity in space, which is a result of most of the enrichment processes in the production of the fuel.

The significance of the concentration of the radioactivity in space is strongly emphasized in a recently published work by French geologists [4], from which the following may be cited: "The effect of the geological disposal is to concentrate 3530 tons of naturally radioactive material in approximately 0.26 tons of glass. An enormous dilution is necessary in order to meet the safety requirements. Thus, for example, 1/30 of the groundwater reserves of France are necessary in order to dilute the collected quantity of waste that will be produced in the country up to the year 2000. -- The high concentration of radioactive material in a disposal facility makes any comparison with natural radioactivity unacceptable until hundreds of thousands of years have passed, at which time the radioactive decay will have reduced this concentration to the natural level of the soil."

[redacted]

BEST DOCUMENT AVAILABLE

In other foreign calculations of the danger index for waste and ore, consideration has also been given to the great dilution of uranium in the ore. An example of this is given in Fig. 2 in accordance with Bond, Clayborne and Leuze [5]. While the danger index for the highly active wastes, calculated at the volume of water of maximum permissible concentration per volume of waste, declined to the danger index for 100% uranium ore after 5000 years, on the other hand, it appears that the danger index for the waste never, not even after dilution with the tenfold quantity of glass, declines to the danger index of 0.2% uranium ore. Since an effective encapsulation cannot be guaranteed for all future time, the authors conclude from this that it is necessary to separate the heavy nuclides U, Np, Pu, Am and Cm from the wastes. With the requirement that the danger index for undiluted waste, after the decay of the fusion products, may not exceed the danger index for 3% uranium ore, one finds the following degrees of separation:

99.9% for uranium, americium and curium,

95.0% for neptunium,

99.95% for plutonium.

Similar results were arrived at in a French study published two years ago [6]. From the leaching rate of French waste glass, combined with the maximum permissible concentration (MPC) for various nuclides, an acceptable danger index was calculated for waste glass, which amounted to $3 \cdot 10^6$ $m^3 H_2O/m^3$ of glass. As Fig. 3 shows, conventional waste glass declines to this value only after 10^7 years. From this, the conclusion is again

BEST DOCUMENT AVAILABLE

drawn that it is necessary to separate the transuranium elements from the highly active waste so that the above-named limit is reached after only 1000 years, which is a reasonable service life for an effective encapsulation. The following degrees of separation were calculated:

99.5% for americium and curium

95.0% for neptunium

99.99% for plutonium.

In both these studies, therefore, the conclusion was drawn that the disposal of conventional highly active waste glass is impossible, since the cannister material does not have a sufficient service life. The alternative thus becomes to separate the long-lived nuclides, above all, the transuranium elements. Such a separation is called "absolutely necessary" in the French report.

It is noteworthy that none of these reports are cited and taken into consideration in the Swedish study on the final storage of vitrified waste from reprocessing [3]. The French study in particular, which is published by the French Atomic Energy Commission Researchers in its own journal, should be of interest to Sweden with respect to the existing reprocessing agreement, which means that French waste glass will be finally disposed of in Sweden.

Besides the Swedish Nuclear Power Engineers mentioned in the introduction [1,2], the final disposal of separated highly active wastes with low transuranium contents was also spoken in favor of by Professor Gerholm [7].

[redacted]

BEST DOCUMENT AVAILABLE

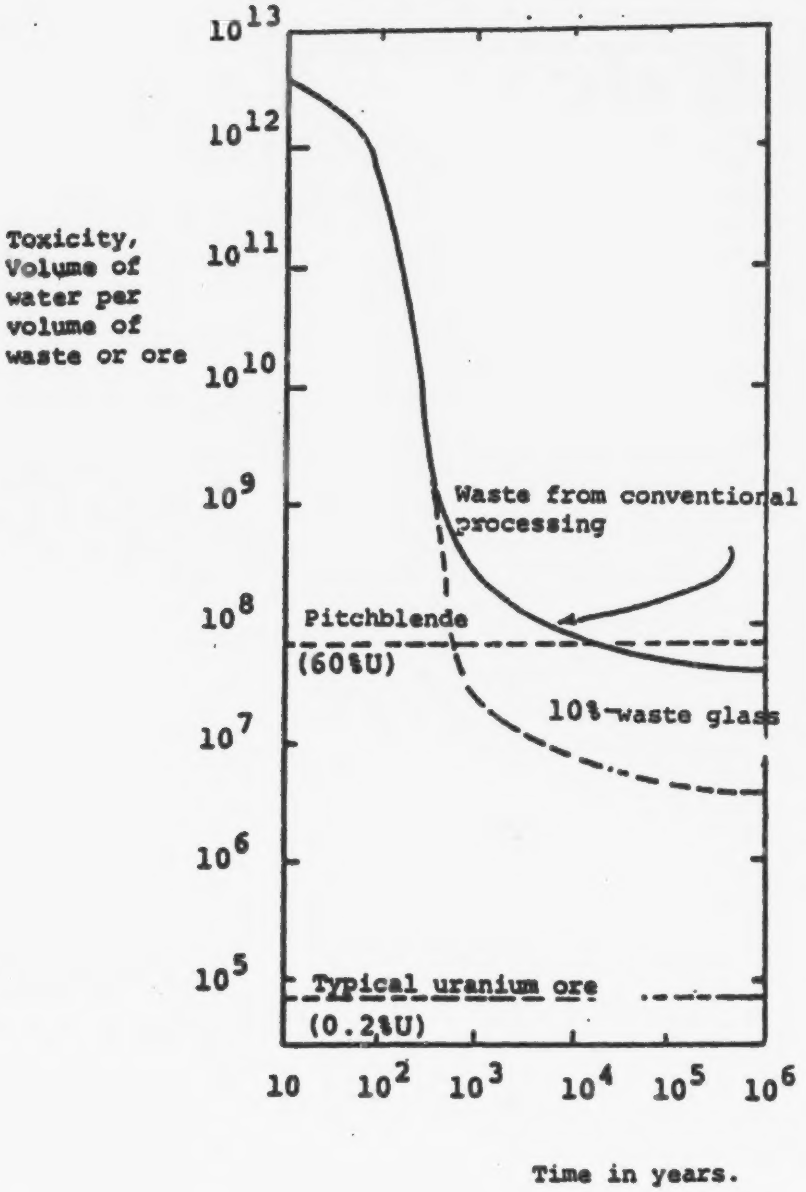

Fig. 2. Toxicity of highly active waste in comparison with uranium ore according to W.D. Bond, H.C. Claiborne, and R.E. Leuze, Nuclear Technology 24 (1974), 362.

[redacted]

BEST DOCUMENT AVAILABLE

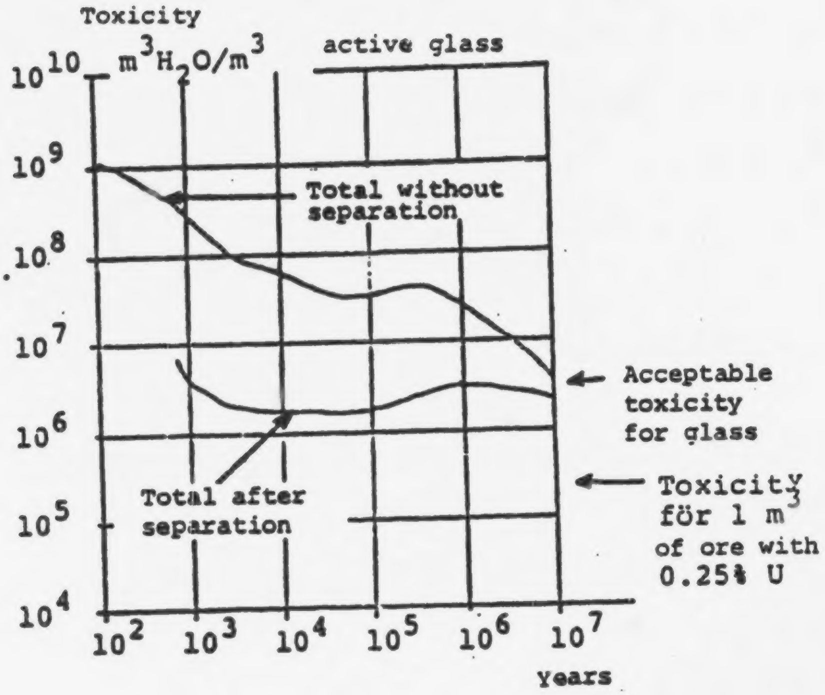

Fig. 3. Toxicity index for highly active waste glass in comparison with uranium ore according to B. Guillaume, B.I.S.T., CEA, No. 217, September 1976, p. 31.

2. *Proposals Studied*

The most important element in the encapsulation of reprocessed nuclear fuel wastes proposed by the KBS project originally was a 6-mm thick titanium jacket. From the outset, it was clear that this would be rapidly destroyed as a result of the radiolysis effect envisioned by the AKA Study [9]. In order to reduce this to a negligible level, it was proposed to start with an "internal radiation shield" consisting of a steel cylinder with a wall thickness of 25 cm (1). In consideration of, among others, the risk of hydrogen embrittlement of the titanium capsule as a result of the evolution

BEST DOCUMENT AVAILABLE

of hydrogen gas in the titanium jacket, the steel lining in it was soon replaced with a 10 cm lead lining. The proposal studied therefore consisted of a lead cylinder with a wall thickness of 10 cm, surrounded by a titanium jacket with a thickness of 6 mm.

Paradoxically enough, in the course of the investigation, it was found that the titanium jacket, particularly with respect to the risk of so-called delayed fracture and fracture in welds, and under consideration of the "totally safe" requirement of the conditional law, must be expected to have a very short service life, which can be neglected in comparison with the life of the lead lining, which can be estimated at a few hundred years.

3. *The Dependence of Corrosion on Time*

As regards general corrosion, the service life of a metallic cannister material can be predicted with certain resistance requirements under the assumption that the average corrosion rate varies linearly with time, as in the case of a cracking oxide layer, or parabolically, as with the case of the remaining layer of corrosion products. However, one finds that general corrosion on the cannister materials proposed can be neglected. As is almost always the case, the service life is limited by the local corrosion attack and by the stress corrosion, hydrogen embrittlement, crevice corrosion and pit corrosion. While crevice corrosion and hydrogen embrittlement are in the foreground in the case of titanium, the picture for lead is dominated by pit corrosion, intensified by electrochemical corrosion. To predict the rate of different types of local corrosion on metals over long

BEST DOCUMENT AVAILABLE

periods is extremely difficult and, strictly speaking, impossible. On the one hand, often long incubation times occur before an attack occurs, and on the other, the rate of attack can vary with time within broad limits. As regards corrosion in the soil, this difficulty has been repeatedly emphasized by Romanoff in his standard work in the field (Ref. 8, p. 9, 15, 73).

Regarding pit corrosion in particular, Romanoff states (Ref. 8, p. 38) that in the case of corrosion in the soil, it can vary with time according to

$$P = k \cdot t^n$$

where P = the depth in the deepest corrosion pit

t = the time in years

and k and n are constants, where it is true for steel that

$n \sim 0.1$ in well ventilated soils

$n \sim 0.9$ in insignificantly aerated soils.

Insignificantly aerated soils are primarily dense clays. These are characterized by such a low oxygen content that the iron present exists primarily in divalent form. Such soils are often designated as reducing. The highest value of n, 0.92 (which is too low in consideration of the corrosion of the last sample), Romanoff obtained (Ref. 8, p. 39) in a sun-dried clay (clay adobe), which was designated as "extremely impermeable". In agreement with that which has been stated, the pit corrosion rate usually increases with depth below the soil surface (Ref. 8, 70).

The experimental values one must start with pertain to exposure in different surface soils at a few meters depth for about ten years time. Reasons can be cited why the pit corrosion rate by itself should be lower

BEST DOCUMENT AVAILABLE

and decrease more rapidly on cannisters in a disposal facility than in the experiment in the surface soils, as a result of the very low rate of oxygen supply. However, these effects are compensated for by the considerably higher temperature as well as by the large cathode/anode ratio for the cannister. In the introductory step of the disposal, the oxygen content in the surrounding water is also the same as in the surface water (10 ppm = 10 mg/liter). An oxygen content far above the natural one (about 0.1 ppm) could exist in the vicinity of the cannister in a few hundred or thousands of years. To this the radiolysis effect must be added, which produces an Fe^{3+} content corresponding to 0.4 ppm of oxygen. Note that the radiolytic oxidizers are produced *in situ*, i.e., on the cannister surface itself and do not need to be transported there by diffusion.

To the extent that the pit corrosion rate decreases with time, this is based on plugging of the corrosion pits with poorly soluble corrosion products, before these succeed in diffusing out into the environment. Since both solubility and diffusion rates increase with temperature, the possibility of plugging is lower at a high temperature.

Because of the large surface of the cannisters, even small contents of oxygen or other oxidizers are of significance for local corrosion on metal cannister material, assuming that the corrosion is cathodically governed, i.e., limited by the quality of oxygen, etc. diffusing per unit time to the cathode surface = the cannister surface. For electrochemical corrosion on a base metal X in contact with a noble metal Y, the law states that the attack is proportional to the sum surfaces ($A_X + A_Y$). This case is directly

BEST DOCUMENT AVAILABLE

applicable to the lead cannister after the breakthrough of the titanium jacket. Table 1 illustrates how a low oxygen content can be compensated for by a large surface.

Table 1. Compensating Surface Enlargement at Low Oxygen Contents.

Oxygen Concentration			Compensating surface enlargement
M	Meq/liter	ppm	
$2.5\cdot10^{-4}$	1	10[a]	-
10^{-5}	0.04	0.4[b]	25
$2.5\cdot10^{-6}$	0.01	0.1[c]	100
10^{-6}	0.004	0.04	250

a) Corresponding to surface water + disposal facility at the time of closing.

b) Corresponding to radiolytically formed trivalent iron.

c) Corresponding to the disposal facility in the steady state.

The lead-titanium cannister has a surface of about 300 dm^2, while the experimental value for pit corrosion on lead in clay according to [7] concerns specimens with a surface of 3 dm^2. The surface enlargement for the Pb-Ti cannister is therefore 300/3 = 100.

For cannisters in a disposal facility, one should, therefore, as a first approximation, calculate on the assumption that the depth of a corrosion pit increases linearly with time. To estimate the pit corrosion rate and, with it, the service live of the lead cannister, one therefore uses the experimental value for the pit corrosion rate in clay, assuming that the growth is linear. This appears to be all the more justified, since

BEST DOCUMENT AVAILABLE

Romanoff's data [7] pertain to pit corrosion alone, while in the case of the cannister, that is, after the titanium jacket has been penetrated, we are dealing with pit corrosion intensified by electrochemical corrosion.

4. Titanium

4a) Thermodynamic Instability

As stated earlier [9], titanium belongs to the metals which should be excluded a priori due to thermodynamic instability. The extraordinary corrosion resistance of titanium in many environments is based exclusively on the presence of a dense, poorly soluble, and impermeable, so-called passivating oxide film. However, this oxide film can be broken down locally with time, at which point the attack takes place much more rapidly due to the thermodynamically strongly non-noble character of the metal. Note that titanium is sensitive not only to oxidation but also to hydrogen absorption, something which, among other things, leads to crack formation as a result of so-called delayed fracture. Experiences with sister metal zirconium have shown that even in a reactor environment which is extremely pure with respect to freedom from impurities in the surrounding water, one can obtain not only various local corrosion attacks (breakaway, nodular oxidation, sunburst), but also delayed failure after relatively short exposure times.

4b) Crevice Corrosion

When titanium was first corrosion tested in the laboratory as a construction material, no signs of local corrosion could be observed. At first, it was believed that titanium represented a material which was unsusceptible to the great weakness of stainless steel, i.e. crevice corrosion. Later on,

BEST DOCUMENT AVAILABLE

when operational experiences were collected, it was found, however, that this belief was not correct. Crevice corrosion began occurring on titanium also, at first in acid (hydrolyzable) chloride solutions such as $AlCl_3$ and $ZnCl_3$, and later also in NaCl solutions. However, the attack does not take place as easily as on stainless steels. Today it is known that crevice corrosion on titanium is facilitated by

1. Low oxygen levels which can occur locally, e.g., in crevices and under packings, especially if the flow rate in the main mass is low.
2. High salt levels (especially chlorides but also sulfates).
3. High temperatures.
4. Low pH values in the main mass. In the crevice, the pH becomes lower than in the main mass as a result of hydrolysis. On titanium, pH values around 1 have been measured in crevices while the pH value in the main mass was neutral.

Crevice corrosion on titanium, as on other metals, is based on the formation of an oxygen concentration cell between the crevice surface and the free surface [10, 11]. In the initial step, the titanium surface in the crevice is activated due to the fact that the passivating oxide film there is dissolved and dispersed, essentially according to a reaction of the type.

$$TiO_2 \text{ (film)} + Cl^- \rightarrow \text{soluble Ti compound} \rightarrow TiO_2 \text{ (finely divided)} + Cl^-$$

It is natural that this activation would be facilitated by the conditions cited above, where

BEST DOCUMENT AVAILABLE

1. A low oxygen content in the crevice counteracts passivation,
2. A high chloride content raises the reaction rate,
3. A high temperature raises the reaction rate,
4. A low pH increases the solubility of the TiO_2 film.

When the oxide film in the crevice is dissolved, active titanium metal is exposed, and the reaction proceeds with the development of hydrogen gas. This means that the titanium can become locally embrittled as a result of hydride formation, even before the crevice corrosion attack has penetrated the metal.

The conditions under which crevice corrosion has been observed previously on titanium in laboratory tests are illustrated in Fig. 4 and Fig. 5 [12]. With the combination of temperature and salt content prevailing at the surface of the cannister, no local corrosion has yet been observed on titanium. According to Fig. 5, however, crevice corrosion has been observed at Cl^- levels as low as 100 ppm at a pH of 3 and 150°C.

According to R. Blomqvist (AE-TPM-RB-437), 9% waste glass disposed of 40 years after removal from the reactor gives the following maximum temperatures at the surface of the titanium cannister:

In dry sand	130°C, which is reached 1 year after disposal
In dry zeolite	110°C, which is reached 1 year after disposal
In wet sand	63°C, which is reached 12 years after disposal
In wet zeolite	73°C, which is reached 10 years after disposal.

In order to avoid salt enrichment on the surface of the titanium cannister during the disposal step, the buffer material is continuously

BEST DOCUMENT AVAILABLE

moistened with desalinated water during this step. After the sealing of the installation, the desalinated water is eventually displaced by groundwater with an assumed maximum chloride content of 100 mg Cl^-/liter. The sealing should take place a few years after the last cannisters are deposited.

Despite low salt contents and relatively low temperatures, the risk of crevice corrosion could not be considered to be excluded during the long storage time. Local activation due to the breakdown of the TiO_2 film could occur even at lower temperatures and lower salt contents than shown in Fig. 4, but they would require a considerably longer time. In practice, for example, through-corrosion of a 3 mm titanium plate has been observed under an asbestos packing in deaerated seawater at an operating temperature of 200-250°F (93-121°C) and an operating time of 8 months, despite the fact that the oxygen content was as low as 0.01 - 0.05 ppm. On one occasion, the oxygen content rose to 0.08 ppm, while the temperature during 40 hours went up to 300°F (149°C) [13]. This example showed that the low oxygen contents which are present in the long-term state of the disposal facility are sufficient to induce local corrosion on the titanium cannister. In the initial step, the oxygen contents are about 100 times higher. In fact, not only the laboratory tests, as the diagram shows, but also the existing operating experiences can be considered as accelerated tests, where one works with a higher chloride content and a higher temperature than in the case of disposal, while conversely, the oxygen content was far lower than in the initial step of disposal. As these accelerated tests led to crevice corrosion, one should, until proven differently, assume that such corrosion

BEST DOCUMENT AVAILABLE

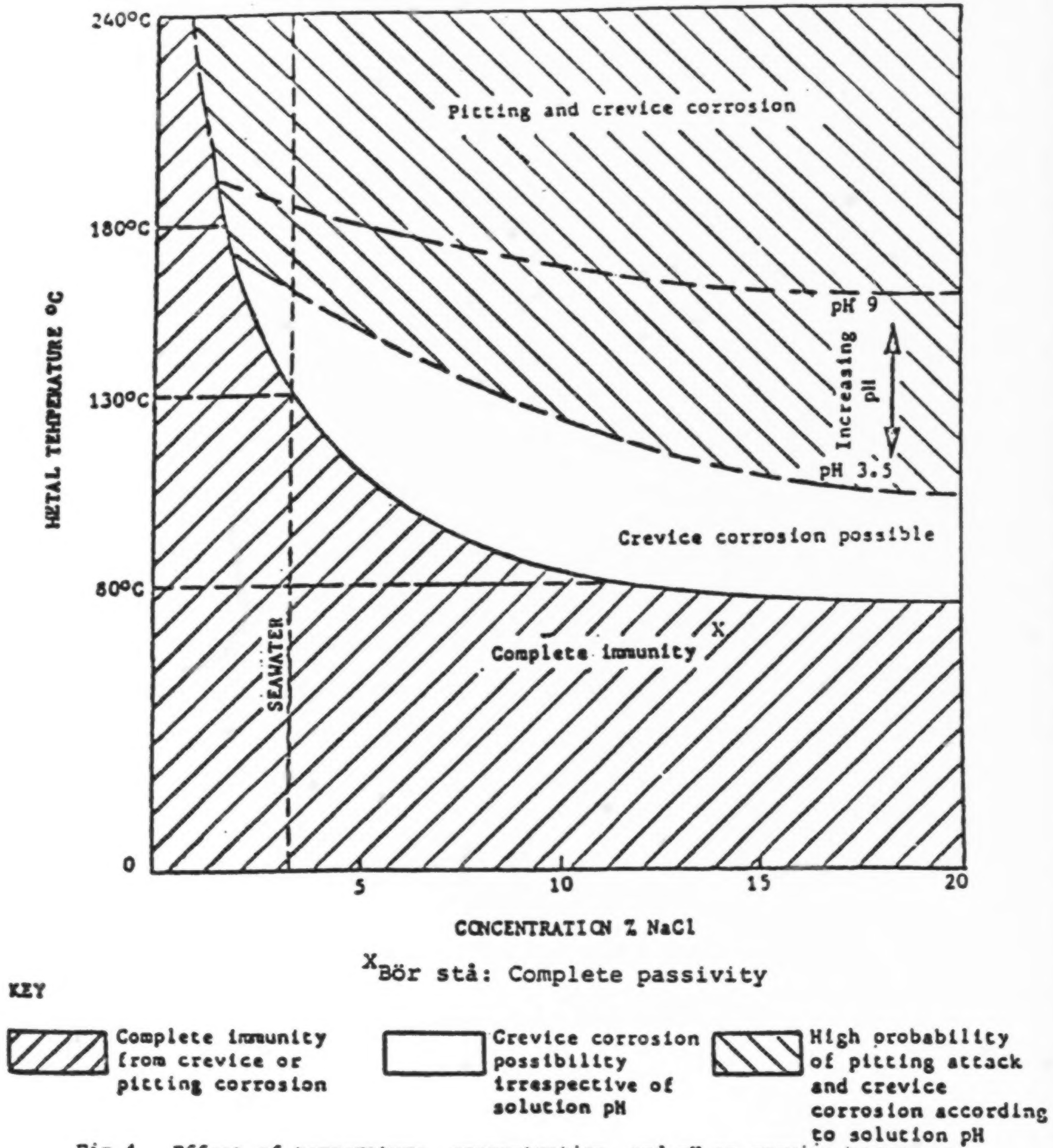

^{X}Bör stå: Complete passivity

Fig.4. Effect of temperature, concentration, and pH on crevice corrosion and point corrosion of unalloyed titanium in seawater and concentrated chloride solutions in laboratory tests. In practice, crevice corrosion has been observed under asbestos packings in deaerated seawater at 120°C.

BEST DOCUMENT AVAILABLE

can also occur in the case of disposal with respect to the incomparably longer times, and in the introductory step, perhaps during several hundred years, a higher oxygen content also. Other conditions which can favor crevice corrosion on titanium cannisters are the following:

1. The leaking in of Baltic seawater (about 3000 ppm Cl^-) or fossil seawater (about 20000 ppm Cl^-) with far higher salt contents than normal deep groundwater (about 100 ppm Cl^-).
2. The possible occurrence of high chloride contents which, at the low pH values occurring in the crevice, strongly increase the attack on the titanium. As a result, the propagation stage in the crevice corrosion process is promoted. Direct contact between titanium cannister and chloride-containing mineral rains would be extremely dangerous.
3. The relatively large surface area of the cannister (about 3 m^2), which increases the probability of the occurrence of impurities and defects (e.g., in the welds), which increase the cathode/anode ratio.
4. The large number of cannisters, which increases the probability of corrosion-inducing defects.
5. The low flow rate around the titanium cannister which impedes the evening out of the concentration differences.

Finally, we must refer to certain experiences with zirconium which greatly resembles titanium in the chemical respect. On Zircaloy in the reactor environment, which is characterized by high chemical purity, various types of local corrosion attacks have been observed after times which, in relation to the service lives required for a cannister, are very brief.

BEST DOCUMENT AVAILABLE

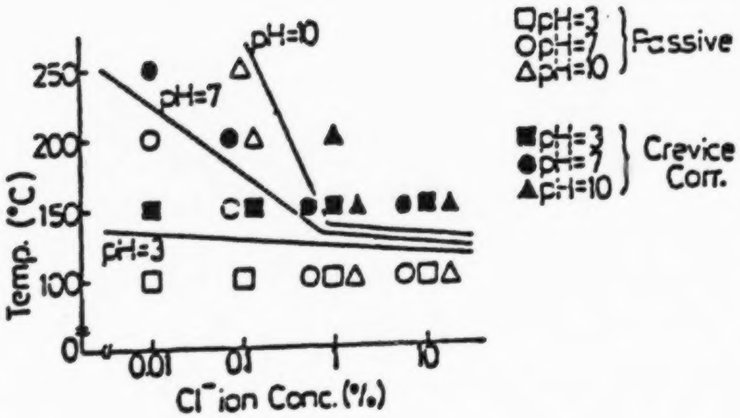

Fig. 5. Range of crevice corrosion and passivity at different pH, Cl concentrations, and temperatures.

To predict the time until a crevice corrosion attack occurs is, of course, impossible. Perhaps one can nope that this will take some 100 years. However, this is of subordinate significance, since the titanium jacket may have been destroyed long before this through so-called delayed failure or failure in the welds.

4c) Crack Formation

In the main statement of the reference group, it was asserted that the risk of so-called *delayed fracture* cannot be excluded, in which case the titanium casing can be penetrated after a relatively short time. Add to this the risk of so-called *brittle failure in welds*. Concerning this, lecturer Fred Nilsson writes in a KBS report the following in his summary: "The critical point of these cannisters is thought to be welds in the outer titanium shell, where the risk of direct failure is not negligible" [14].

[redacted]

BEST DOCUMENT AVAILABLE

With respect to these failure risks and with the "totally safe" criterion, the titanium cannister, should, therefore, be given a short service life, essentially = 0, in comparison with the lead lining.

5. *Corrosion of Lead*

If the titanium cannister is penetrated as a result of corrosion or other reasons, the exposed lead will be attacked locally. Lead displays a relatively great tendency toward pit corrosion, certainly less than that of steel (including chromium steel), but far greater than that of copper. Romanoff's data (Ref. 8, p. 20, 89) are presented in Table 2. On the lead cannister, the attack is intensified by the electrochemical effects from the titanium jacket.

Table 2. Pit Corrosion on Pure Lead Exposed in a Reducing (Oxygen-Poor) Clay for 2-11 years. Test surface about 0.1 m^2. Average temperature 21 C.*

Exposure Time in years	Max. carrier pit depth total, mm	Pit corrosion Rate in mm/yr.
2.1	0.95	0.45
4.0	0.92	0.23
9.0	2.15	0.24
11.2	2.50	0.22

* Lake Charles clay with the following data:

Soluble Constituents

pH	Na^+	Ca	Mg^+	HCO_3^-	Cl^-	SO_4^{2-}	
7.1	717	138	56	490	565	1460	mg/kg

BEST DOCUMENT AVAILABLE

The concentrations were determined in lake water, but are reported in mg per kg of clay. While the two-year specimens have a larger value, the other samples taken 4, 9, and 11 years after disposal, display an almost constant value for the pit corrosion rate of 0.23 mm/year. If we calculate with 0.2 mm/year, we find a service life of 500 years for a 100 mm lead jacket.

Another estimate of the service life of the lead jacket after penetration of the titanium jacket can be made by starting with the quantity of oxygen which is found in the pore water of the buffering material at the time of sealing. According to a study performed within the reference group [15], this quantity of oxygen is sufficient to oxidize about 70 kg of lead, while its rate of supply to the cannister through diffusion corresponds to an errosion of about 0.5 cm^3 of lead per year. Assuming a hemispherical corrosion pit, the author estimates a service life of 4300 years. The assumption of a hemispherical corrosion pit is optimistic, however. If instead one assumes a spool-shaped or pear-shaped corrosion pit, a common form on stainless steel, for example, and then approximates it with a cylinder, one obtains the following set up:

Hole Area	Hole Diameter	Service Life
1 cm^2	1.13 cm	20
3 cm^2	1.95 cm	60
10 cm^2	3.57 cm	200
30 cm^2	6.18 cm	600

BEST DOCUMENT AVAILABLE

It appears plausible that the 10-cm thick lead capsule will be penetrated by a hole with a few cm diameter after the breakthrough of the titanium jacket.

6. *Conclusions*

According to the estimate of the service life of the titanium jacket given above (0 years) and that of the lead lining (a few hundred years), one finds a service life for the titanium-lead cannister of only a few hundred years. According to the requirements established in the French [4, 6] and American [5] studies mentioned in the introduction, this is in no way satisfactory for conventional highly active waste, but only for separate waste, e.g., according to the French standards.

Under all conditions, a lead-titanium cannister is clearly inferior to a copper cannister with corresponding radiation shielding effect. The lead-titanium alternative should therefore be rejected in favor of the copper alternative, which, with an estimated service life of a few thousand years, appears to be the most promising for reprocessed and separated nuclear fuel waste with very low levels of plutonium and other transuranium elements.

REFERENCES

1. P. Isberg, Svensk Kärnkraft, Swedish Nuclear Power 1976, p. 95.

2. K. Hannerz, Radioactive Wastes of Nuclear Power, 2nd Edition, *ASEA*-ATOM, p. 7.

3. The final step of the nuclear fuel cycle. Vitrified waste from reprocessing, part IV, Safety Analysis, Fig. 3-9, p. 29.

BEST DOCUMENT AVAILABLE

4. G. de Marsily, E. Ledoux, A. Barbreau and J. Margat, Nuclear waste disposal: Can the geologist guarantee isolation? *Science 197*, No. 4303, p. 519, Aug. 5, 1977.

5. W.D. Bond, H.C. Claiborne, and R.E. Leuze, Methods for the removal of actinides from high-level wastes, Nuclear Technology 24 (1974) 362.

6. G. Guillaume, Problems posed by the presence of the transuranium element in the reprocessing wastes of nuclear fuel, *Bulletin d'Information Scientifiques et Techniaqes*, No. 217, Sept. 1976, p. 31, Commissariat à l'Énergie Atomique.

7. T.R. Gerholm, Why Nuclear Power? KREAB, Stockholm 1974.

8. M. Romanoff, Underground Corrosion, *National Bureau of Standards Circular No. 579* (1957)

9. G. Wranglen, Nuclear Power Wastes and Corrosion, Minority Report on the AKA-study, 22.10.1976.

10. T.R. Beck, Localized Corrosion, NACE 1974, p. 694.

11. J.B. Cotton, Localized Corrosion, NACE 1974, p. 676.

12. S. Henriksson, Study concerning the suitability of titanium as a corrosion-resistant material for encapsuling nuclear fuel wastes, (AE-Report MS 132), 77-07-24.

13. F.W. Fink, E.L. White and W.K. Boyd, Research and Development Progress Report No. 255, U.S. Department of the Interior, December, 1966.

14. Fred Nilsson, Some views on mechanical safety of cannisters for nuclear fuel waste, KBS Teknisk Report No. 66.

15. G. Eklund, Corrosion of the Lead Lining, Appendix to the Report of the Reference Group.

BEST DOCUMENT AVAILABLE

LIST OF KBS TECHNICAL REPORTS

01 Source strengths in spent fuel and highly active waste from PWR calculated with ORIGEN
Nils Kjellbert
AB Atomenergi 77-04-05

02 PM regarding the coefficient of heat conduction of soil material
Sven Knutsson
Roland Pusch
Hogskolan and Lulea 77-04-15

03 Disposal of highly active waste in drill holes with buffering substance
Arvid Jacobsson
Roland Pusch
Hugskolan and Lulea 77-05-27

04 Disposal of highly active wastes in tunnels with buffering substance
Arvid Jacobsson
Roland Pusch
Hogskolan and Lulea 77-06-01

05 Orientative temperature calculations for final storage in rock of radioactive wastes, Report 1
Roland Blomqvist
AB Atomenergi 77-03-17

06 Groundwater movements around a repository, Phase 1, State of the art and detailed study plan
Ulf Lindblom
Hagconsult AB 77-02-28

07 Residual effect studies for KBS
Part 1 Review of Literature
Part 2 Calculations
Kim Ekberg
Nils Kjelbert
Goran Olsson
AB Atomenergi 77-04-19

08 Leaching out of French, English and Canadian glass with highly active wastes
Goran Blomqvist
AB Atomenergi 77-05-20

BEST DOCUMENT AVAILABLE

09 Diffusion of soluble materials in a fluid filling a porous medium
Hans Haggblom
AB Atomenergi 77-03-24

10 Translation and development of the BNWL-Geosphere Model
Bertil GrundfeltKemakta Konsult AB 77-02-05

11 Study of the suitability of titanium as a corrosion resistant casing for nuclear fuel waste
Sture Henriksson
AB Atomenergi 77-04-18

12 Evaluation of properties and functions of concrete in relation with the final disposal of nuclear fuel waste in rocks
Sven G Bergstrom
Goran Fagerlund
Lars Romben
Cement - och Betonginstitutet 77-06-22

13 Leaching out of spent nuclear fuel (irradiated uranium oxide) during direct disposal
Ragnar Gelin
AB Atomenergi 77-06-08

14 Influence of cementation on the deformation properties of bentonite/quartz buffer substance
Roland Pusch
Hugskolan and Lulea 77-06-20

15 Orientative temperature calculations for final storage in rock of radioactive waste
Rapport 2
Roland Blomquist
AB Atomenergi 77-05-17

16 Review of foreign risk analyses and plans and projects concerning final disposal
Ake Hultgren
AB Atomenergi August 1977

17 The gravity field in Fennoscandia and postglacial crustal movements
Arne Bjerhammar
Stockholm August 1977

BEST DOCUMENT AVAILABLE

18 Movements and instability in the Swedish foundation rock
Nils-Axel Murner
Stockholm University August 1977

19 Studies of neotectonic activity in central and northern Sweden, aerial map review and geophysical interpretation of recent displacements
Robert Lagerback
Herbert Henkel
Sveriges Geologiska Undersokning September 1977

20 Analysis of Southern Sweden, Western and Northern Scania
Kennert Roshoff
Erik Lagerlund
Lundis University and Hogskolan Lulea September 1977

21 Earthquakes of Sweden 1891 -1957, 1963 - 1972
Ota Kulhanek
Rutger Wahlstrom
Uppsala University September 1977

22 The influence of rock movement on the stress/strain situation in tunnels or bore holes with radioactive cannisters embedded in a bentonite/quartz buffer mass
Roland Pusch
Hogskolan and Lulea 1977-08-22

23 Water uptake in a bentonite buffer mass
A model study
Roland Pusch
Hogskolan and Lulea 1977-08-22

24 Calculation of leaching out of certain fission products and actinides from a cylinder of French glass
Guran Blomqvist
AB Atomenergi 1977-07-27

25 Blekinge coastal, gneiss, geology and hydrogeology
Ingemar Larsson KTH
Tom Lundgren SGI
Ulf Wiklander SGU
Stockholm, August 1977

26 Evaluation of the risk of delayed failure in titanium
Kjell Pettersson
AB Atomenergi 1977-08-25

BEST DOCUMENT AVAILABLE

27 A short review of the formation, stability and cementing
properties of natural zeolites
Arvid Jacobsson
Hogskolan and Lulea 1977-10-03

28 Heat conduction tests on buffering substance of bentonite/pitesilt
Sven Knutsson
Hogskolan and Lulea 1977-09-20

29 Deformations in jointed rock
Ove Stephansson
Hogskolan and Lulea 1977-09-28

30 Retardation of escaping nuclides from a final depository
Ivars Neretnieks
Kungliga Tekniska Hogskolan Stockholm 1977-09-14

31 Evaluation of corrosion resistance of material intended for
encapsuling nuclear fuel waste. Status report 1977-09-27 as
a supplementary statement.

32 Long term mineralogical properties of bentonite/quartz
buffer substance
Preliminary Report November 1977
Second report February 1978
Roland Pusch
Arvid Jacobsson
Hogskolan and Lulea

33 Required physical and mechanical properties of buffer masses
Roland Pusch
Hogskolan Lulea 1977-10-19

34 Manufacture of lead-titanium cannister
Folke Sandelin AB
VSB
ASEA-Kabel
Institute for Metallforskning
Stockholm November 1977

35 Project for the handling and storage of vitrified high-level
waste
Saint Gobain Techniques Nouvelles October, 1977.

36 Composition of groundwater at great depth in granitic bed
rock
Jan Rennerfelt
Orrje & Co., Stockholm 1977-11-07

BEST DOCUMENT AVAILABLE

37 Handling of buffer material of bentonite and quartz
Hans Fagerstrom, VBB
Bjorn Landahl, Stabilator
Stockholm October 1977

38 Shaping of rock storage facilities
Arne Finne, KBS
Alf Engelbrektson, VBB
Stockholm December 1977

39 Construction studies, direct disposal
ASEA-ATOM
VBB
Vasteras

40 Ecological transport and radiation doses from ground-water-borne radioactive substances
Ronny Bergman
Ulla Bergstrom
Sverker Evans
AB Atomenergi

41 Safety and radiation shielding in the nuclear power field. Laws, standards and grounds for evaluation.
Christina Gyllander
Siegfried F. Johnson
Stig Rolandson
AB Atomenergi and ASEA-ATOM

42 Safety in the handling, storage and transportation of spent nuclear fuel and vitrified highly active waste
Ann Margret Ericsson
Kemakta November 1977

43 Transportation of radioactive substances with groundwater from a rock storage site
Bertil Grundfelt
Kemakta November 1977

44 Resistance of borosilicate glass
Tibor Lakatos
Glasteknisk Utveckling AB

45 Calculation of temperature in a single story final disposal site in rock for vitrified radioactive waste, Report 3
Roland Blomquist
AB Atomenergi 1977-10-19

BEST DOCUMENT AVAILABLE

46 Temperature calculations for spent fuel
Taivo Tarandi
VBB

47 Theoretical studies of groundwater movements. Preliminary report October 1977
Final Report February 1978
Lars Y Nilsson
John Stokes
Roger Thunvik
Institute for kulturteknik KTH

48 The mechanical properties of the rock in Stripa, Krakemala, Finnsjon and Blekinge
Graham Swan
Hogskolan and Lulea 1977-09-14

49 Rock stress measurements in strip mines
Hans Carlsson
Hogskolan and Lulea 1977-08-29

50 Leaching studies with highly active French glass in Studsvik
Goran Blomqvist
AB Atomenergi November 1977

51 Seismotechtonic risk modelling for nuclear waste disposal in the Swedish bedrock
F Ringdal
H Gjoystdal
E S Hysebye
Royal Norwegian Council for scientific and industrial research

52 Calculations of nuclide migration in rock and porous media, penetrated by water
H Haggblom
AB Atomenergi 1977-09-14

53 Measurement of diffusion rate for silver in clay-sand mixture
Bert Allard
Heino Kipatsi
Chalmers tekniska hogskola 1977-10-15

BEST DOCUMENT AVAILABLE

54:01 Geological and geotechnical conditions
Håkan Stille
Anthony Burgess
Ulf E Lindblom
Hagconsult AB september 1977

54:02 Thermal analyses
Part 1 Conduction heat transfer
Part 2 Advective heat transfer
Joe L Ratigan
Hagconsult AB september 1977

54:03 Regional groundwater flow analyses
Part 1 Initial conditions
Part 2 Long term residual conditions
Anthony Burgess
Hagconsult AB oktober 1977

54:04 Rock mechanics analyses
Joe L Ratigan
Hagconsult AB september 1977

54:05 Repository domain groundwater flow analyses
Part 1 Permeability perturbations
Part 2 Inflow to repository
Part 3 Thermally induced flow
Joe L Ratigan
Anthony S Burgess
Edward L Skiba
Robin Charlwood

54:06 Final report
Ulf Lindblom et al
Hagconsult AB oktober 1977

55 Sorption of long-lived radio nuclides in clay and rock.
Part 1 Determination of the distribution coefficients.
Part 2 Review of literature.
Bert Allard
Heimo Kipatsi
Jan Rydberg
Chalmers tekniska hogskola 1977-10-10

56 Radiolysis of filling material
Bert Allard
Heino Kipatsi
Jan Rydberg
Chalmers tkniska hogskola 1977-10-15

BEST DOCUMENT AVAILABLE

57 Radiation doses during emergencies in sea transporation of nuclear fuel.
Anders Appelgren
Ulla Bergstrom
Lennart Devell
AB Atomenergi 1978-01-09

58 Radiation risks and maximum permissible radiation doses for man.
Gunnar Walinder
FOA 4 November 1977

59 Tectonic linaments in the Baltic from Gavle to Simrishamn
Tom Floden
Stockholm University 1977-12-15

60 Preliminary work for choice of location, bedrock studies
Soren Scherman

Bedrock water conditions in the Northeastern part of the sea of Finland
Carl-Erik Klockars
Ove Persson
Sveriges Geologiska Undersokning January 1978

61 Permeability determinations
Anders Hult
Gunnar Gidlund
Ulf Thoregren
Geophysical drill hole measurements
Kurt-Ake Magnusson
Oscar Duran
Sveriges Geologiska Undersokning January 1978

62 Analyses and age determination of groundwater at great depths
Gunnar Gidlund
Sveriges Geologiska Undersokning 1978-02-14

63 Geological and hydrogeological soil documentation from the Stripa experimental station
Andrei Olkiewicz
Kenth Hansson
Karl-Erik Almen
Gunnar Gidlund
Sveriges Geologiska Undersokning February, 1978

BEST DOCUMENT AVAILABLE

64 Stress measurements in the Scandinavian bedrock -- preconditions, results and interpretation
Sten G A Bergman
Stockholm November 1977

65 Safety Analysis of encapsulating processes
Goran Carleson
AB Atomenergi 1978-01-27

66 Some views on mechanical safety of cannisters for nuclear fuel waste
Fred Nilsson
Kungl Tekniska Hogskolan Stockholm February 1978

67 Corrosion between titanium and lead and measurement of the corrosion potential of titanium under γ radiation.
Sture Henrikson
Stefan Poturaj
Matha Asberg
Derek Lewis
AB Atomenergi January-February 1978

68 Degradation mechanisms for basin storage and handling of spent nuclear reactor fuel
Gunnar Vesterlund
Torsten Olsson
ASEA-ATOM 1978-01-18

69 A three-dimensional method for calculating the hydraulic gradient in porous and cracked media
Hans Haggblom
AB Atomenergi 1978-01-26

70 Leaching of irradiated UO_2 fuel
Ulla-Britt Eklund
Ronald Forsyth
AB Atomenergi 1978-02-24

71 Rock crack sealing with bentonite
Roland Pusch
Hogskolan and Lulea 1977-11-16

72 Heat conduction tests on buffering substance of compacted bentonite
Sven Knutsson
Hogskolan and Lulea 1977-11-18

BEST DOCUMENT AVAILABLE

73 Self-injection of highly compacted bentonite into rock joints
Roland Pusch
Hogskolan and Lulea 1978-02-25

74 Highly compacted Na bentonite as buffer substance
Roland Pusch
Hogskolan and Lulea 1978-02-25

75 Small-scale bentonite injection test on rock
Roland Pusch
Hogskolan and Lulea 1978-03-02

76 Experimental determination of the stress/strain situation in a sheared tunnel model with cannister
Roland Pusch
Hogskolan and Lulea 1978-03-02

77 Nuclide migration from a rock storage site for spent fuel
Bertil Grundfelt
Kemakta konsult AB, Stockholm

78 Evaluation of radiolysis in groundwater
Hilbert Christenssen
AB Atomenergi 1978-02-17

79 Transport of oxidants and radionuclides through a clay barrier
Ivars Neretnieks
Kungl Tekniska Hogskolan Stockholm 1978-02-20

80 Diffusion of poorly soluble nuclides out of cannisters after cannister failure
Karin Andersson
Ivars Neretnieks
Kungl Tekniska Hogskolan Stockholm 1978-03-07

81 Manufacture of copper cannisters
Kare Hannerz
Stefan Sehlstedt
Bengt Lonnerberg
Liberth Karlson
Gunnar Nilsson
ASEA, ASEA-ATOM

82 Handling and final disposal of active metal parts
Bengt Lonnerberg
Alf Engelbrektsson
Ivars Neretnieks
ASEA-ATOM, VBB, KTH

BEST DOCUMENT AVAILABLE

83 Handling cannisters with spent fuel in final storage
Alf Engelbrektsson
VBB Stockholm April 1978

84 Manufacture and handling of bentonite blocks
Alf Engelbrektsson
Ulf Odebo
ASEA, VBB

85 Calculation of kryp rate of a lead casing containing a glass body under the influence of gravity
Anders Samuelsson

Variation of kryp properties of a lead casing as a result of mechanical damage
Goram Eklund
Institute for Metallforskning September 1977 - April 1978

86 Diffusivity measurements of methane and hydrogen in wet clay
Ivars Neretnieks
Christina Skagius
Kungl Tekniska Högskolan Stockholm 1978-01-09

87 Diffusivity measurements in wet clay Na-lignosulfonate, Sr^{2+}, Cs^{+}
Ivars Neretnieks
Christina Skagius
Kungl Tekniska Hogskolan Stockholm 1978-03-16

88 Groundwater chemistry at depth in granites and gneisses
Gunnar Jacks
Kungl Tekniska Hogskolan Stockholm April 1978

89 Effect of glaciation on a disposal site situated in bedrock
500 m below the surface. Roland Pusch Högskolan i Lulea March 16, 1978.

90 Copper as a casing material for non-reprocessed nuclear fuel waste -- evaluation from the standpoint of corrosion
Status Report 1978-03-31
Korrosionsinstitutet och dess referensgrupp

91 Short term variations in the pressure level of the groundwater
Lars Y Nilsson
Kungliga Tekniska Hogskolan, Stockholm September 1977

92 Thermal expansion of granitoid rock variety
Ove Stephansson
Hogskolan and Lulea April 1978

BEST DOCUMENT AVAILABLE

93 Preliminary corrosion studies of glass ceramic code 9617 and a sealing frit for nuclear waste cannisters
I D Sundquist
Corning Glass Works 78-03-14

94 Waste flows in the reprocessing process
Birgitta Andersson
Ann-Margret Ericsson
Kemakta mars 1978

95 Separation of C-14 during the reprocessing process.
Sven Brandberg
Ann-Margret Ericsson
Kemakta mars 1978

96 Corrosion testing of unalloyed titanium in simulated disposal environments for reprocessed nuclear fuel waste
Sture Henrikson
Marian de Pourbaix
AB Atomenergi 1978-04-24

97 Colloid chemical aspects of the "confined bentonite concept"
Jean C Le Bell
Ytkemiska Institute 1978-05-07

98 Sorption of long-lived radionuclides in clay and rock, Part 2.
Bert Allard
Heino Kipatsi
Borje Torstenfelt
Chalmers Tekniska Hogskola 1978-04-02

99 Effect of rock movements and other external loads of integrity of copper cannisters
Alf Engelbrektson
VBB

100 Doses and dose recording from groundwater-borne material in direct storage of spent nuclear fuel
Ronny Bergman
Ulla Bergstrom
Sverker Evans
AB Atomenergi

101 Leaching out of Ni-59 from a rock storage site
Ivars Neretnieks
Kungl Tekniska Hogskolan Stockholm

BEST DOCUMENT AVAILABL

102 Method for bending irradiated fuel rods
Torsten Olsson
ASEA-ATOM 1978-03-29

103

104 Finite element analysis of bentonite-fill rock storage sites
Ove Stephansson
Kenneth Maki
Tommy Groth
Per Johansson
Hogskolan and Lulea

105 Neutron induced activity in fuel element parts
Nils A Kjellbert
AB Atomenergi

106 Radiation level in radiant energy given off to water outside cannisters in final storage site
Klas Lundgren
ASEA-ATOM

107 Lead-lined titanium cannisters for reprocessed and vitrified nuclear fuel waste - evaluation from the corrosion standpoint
Slutrapport
1978-05-25

BEST DOCUMENT AVAILABLE

NRC FORM 335
(7-77)

U.S. NUCLEAR REGULATORY COMMISSION
BIBLIOGRAPHIC DATA SHEET

1. REPORT NUMBER *(Assigned by DDC)*
NUREG/CR-2333, Vol. 1
BNL-NUREG-51458

4. TITLE AND SUBTITLE *(Add Volume No., if appropriate)*
Nuclear Waste Management Technical Support in the
Development of Nuclear Waste Form Criteria for the NRC
Task 1: Waste Package Overview

2. *(Leave blank)*

3. RECIPIENT'S ACCESSION NO.

7. AUTHOR(S)
R. Dayal, B.S. Lee, R.J. Wilke, K.J. Swyler,
P. Soo, T.M. Ahn, N.S. McIntyre, E. Veakis

5. DATE REPORT COMPLETED

MONTH	YEAR
September	1981

9. PERFORMING ORGANIZATION NAME AND MAILING ADDRESS *(Include Zip Code)*
Department of Nuclear Energy
Brookhaven National Laboratory
Upton, NY 11973

DATE REPORT ISSUED

MONTH	YEAR
February	1982

6. *(Leave blank)*

8. *(Leave blank)*

12. SPONSORING ORGANIZATION NAME AND MAILING ADDRESS *(Include Zip Code)*
Division of Waste Management
Office of Nuclear Material Safety and Safeguards
United States Nuclear Regulatory Commission
Washington, DC 20555

10. PROJECT/TASK/WORK UNIT NO.

11. CONTRACT NO.
NRC FIN A3158

13. TYPE OF REPORT
Final Report

PERIOD COVERED *(Inclusive dates)*
October 1979 to September 1981

15. SUPPLEMENTARY NOTES

14. *(Leave blank)*

16. ABSTRACT *(200 words or less)*

This report assesses the current state of waste package development for high-level waste, transuranic waste, and spent fuel in the U.S. and abroad. Recent and on-going research on various waste forms, container materials and backfills are reviewed and those which are likely to perform most satisfactorily in the repository environment are identified. Radiation effects on the waste package components have been reviewed and the magnitude of these effects has been identified. Areas requiring further research have been identified. The important variables affecting radionuclide release from the waste package have been described and an evaluation of regulatory criteria for high-level waste and spent fuel is presented. Finally, for spent fuel, high-level, and TRU waste, an attempt is made to describe and identify components which could be used to construct a waste package having potential to meet NRC performance requirements.

17. KEY WORDS AND DOCUMENT ANALYSIS

17a DESCRIPTORS

17b IDENTIFIERS/OPEN-ENDED TERMS

18. AVAILABILITY STATEMENT
Unlimited

19. SECURITY CLASS *(This report)*
Unclassified

20. SECURITY CLASS *(This page)*
Unclassified

21. NO. OF PAGES

22. PRICE
$

NRC FORM 335 (7-77)

U.S. GOVERNMENT PRINTING OFFICE: [illegible]